

Advances in Biochemical Engineering/Biotechnology 179
Series Editors: Thomas Scheper · Roland Ulber

Janina Bahnemann
Alexander Grünberger *Editors*

Microfluidics in Biotechnology

 Springer

179

Advances in Biochemical Engineering/Biotechnology

Series Editors

Thomas Scheper, Hannover, Germany
Roland Ulber, Kaiserslautern, Germany

Editorial Board Members

Shimshon Belkin, Jerusalem, Israel
Thomas Bley, Dresden, Germany
Jörg Bohlmann, Vancouver, Canada
Man Bock Gu, Seoul, Korea (Republic of)
Wei Shou Hu, Minneapolis, MN, USA
Bo Mattiasson, Lund, Sweden
Lisbeth Olsson, Göteborg, Sweden
Harald Seitz, Potsdam, Germany
Ana Catarina Silva, Porto, Portugal
An-Ping Zeng, Hamburg, Germany
Jian-Jiang Zhong, Shanghai, Minhang, China
Weichang Zhou, Shanghai, China

Aims and Scope

This book series reviews current trends in modern biotechnology and biochemical engineering. Its aim is to cover all aspects of these interdisciplinary disciplines, where knowledge, methods and expertise are required from chemistry, biochemistry, microbiology, molecular biology, chemical engineering and computer science.

Volumes are organized topically and provide a comprehensive discussion of developments in the field over the past 3–5 years. The series also discusses new discoveries and applications. Special volumes are dedicated to selected topics which focus on new biotechnological products and new processes for their synthesis and purification.

In general, volumes are edited by well-known guest editors. The series editor and publisher will, however, always be pleased to receive suggestions and supplementary information. Manuscripts are accepted in English.

In references, *Advances in Biochemical Engineering/Biotechnology* is abbreviated as *Adv. Biochem. Engin./Biotechnol.* and cited as a journal.

Janina Bahnemann • Alexander Grünberger
Editors

Microfluidics in Biotechnology

With contributions by

J. Aranda Hernandez · S. Arshavsky-Graham ·
J. Bahnemann · J. M. Bolivar · S. Buchheim ·
M. P. Cardoso Marques · A. Dietzel · C. Dusny · P. Ertl ·
L. J. Frey · A. Grünberger · D. Helmer · S. Hengoju ·
C. Heuer · S. Kakava · A.-K. Klein · F. Kotz · R. Krull ·
A. Lorente-Arevalo · D. K. W. Man · I. Maschmeyer ·
B. E. Rapp · M. A. Rosenbaum · M. Rothbauer · E. Segal ·
N. Szita · M. Tovar · M. Viefhues · T. Wang · S. Winkler ·
X. Xie · C. Yu

 Springer

Editors

Janina Bahnemann
Institute of Physics
University of Augsburg
Augsburg, Germany

Alexander Grünberger
Multiscale Bioengineering, Faculty of
Technology
Bielefeld University
Bielefeld, Germany

ISSN 0724-6145

ISSN 1616-8542 (electronic)

Advances in Biochemical Engineering/Biotechnology

ISBN 978-3-031-04187-7

ISBN 978-3-031-04188-4 (eBook)

<https://doi.org/10.1007/978-3-031-04188-4>

© Springer Nature Switzerland AG 2022

This work is subject to copyright. All rights are reserved by the Publisher, whether the whole or part of the material is concerned, specifically the rights of translation, reprinting, reuse of illustrations, recitation, broadcasting, reproduction on microfilms or in any other physical way, and transmission or information storage and retrieval, electronic adaptation, computer software, or by similar or dissimilar methodology now known or hereafter developed.

The use of general descriptive names, registered names, trademarks, service marks, etc. in this publication does not imply, even in the absence of a specific statement, that such names are exempt from the relevant protective laws and regulations and therefore free for general use.

The publisher, the authors and the editors are safe to assume that the advice and information in this book are believed to be true and accurate at the date of publication. Neither the publisher nor the authors or the editors give a warranty, expressed or implied, with respect to the material contained herein or for any errors or omissions that may have been made. The publisher remains neutral with regard to jurisdictional claims in published maps and institutional affiliations.

This Springer imprint is published by the registered company Springer Nature Switzerland AG
The registered company address is: Gewerbestrasse 11, 6330 Cham, Switzerland

Preface: Microfluidics in Biotechnology

In modern biotechnology, microorganisms, plants, and animals (or parts thereof) are frequently leveraged to produce or refine high value products, recycle waste, and develop novel strategies for improving our health and wellbeing. Although biotechnological processes (which include the production of beer, wine, and cheese) have a long and storied tradition dating back for thousands of years, new biotechnological tools have recently emerged which allow researchers and industry to address challenges in food security, health, environmental pollution, and medicine in an unprecedented manner. Modern biotechnology is a truly multidisciplinary field, combining many diverse disciplines – including (molecular) biology, microbiology, biochemistry, genetics, and informatics, as well as process engineering.

Advances across many different biotechnological fields have led to more efficient production of high-value products and have resulted in the generation of novel biopharmaceuticals – including antibiotics, recombinant proteins, and vaccines. Progress in this area is being further accelerated by the associated advancement of innovative technologies, ranging from molecular biological tools such as CRISPR/Cas to novel fabrication techniques such as 3D (bio-)printing with never-before-reached spatial resolutions.

One particularly important trend of the last two decades is the miniaturization of biological workflows and devices. This has enabled parallel handling of samples and screening for desired characteristics of biotechnologically relevant molecular features (e.g., host cells and enzymes). In recent years, microfluidic systems have captured growing interest for their biotechnological applications, such as screening and analytical tools. The handling and manipulating liquids and/or gases in very small volumes has been dubbed microfluidics, and such systems offer the possibility of combining a wide variety of process steps within a very small space, rendering possible highly miniaturized continuous workflows. Microfluidic systems are particularly interesting for their potential analytical purposes, since many analytical steps can be automated and run in sequence. The production and integration of such microfluidic analysis systems can thus significantly help contribute to an improved understanding of bioprocesses and enable optimal experimental control.

This volume of “Advances in Biochemical Engineering/Biotechnology” addresses the growing synergy between the fields of microfluidics and modern biotechnology. In total, it contains 15 contributions written by world-leading experts in these fields. We have chosen to include articles that specifically explore this dynamic intersection between these two booming areas of science, and the chapters cover a wide range of microfluidic applications across different biotechnological fields. Our aim herein is to provide students, researchers, and practitioners with further motivation to continue to apply microfluidic systems within the field of biotechnology.

Chapter 1 provides an overview of the status quo and outlines current challenges and perspectives of microfluidic systems for applications in biotechnology. Chapters 2 and 3 introduce the reader to some fundamental concepts that help to define the field of microfluidics: In Chap. 2, Klein and Dietzel give an overview of the scientific laws that govern microfluidic systems, and the reader is introduced to the basic concept of microfabrication. This introduction is further extended in Chap. 3, where Rapp and colleagues summarize the latest developments in advanced microfabrication techniques, with a focus on various 3D printing technologies.

In the next part of the book, selected emerging applications of microfluidics in biotechnology are described. In Chap. 4, Frey and Krull highlight the importance of microbioreactors for the cultivation and characterization of industrially relevant microorganisms. They discuss how these microsystems might be leveraged as future screening and characterization tools for strain development and optimization in industrial biotechnology. Szita and colleagues then provide an overview of the microfluidics systems used for analysis and cultivation of cell culture systems that find important applications in medical biotechnology. Examples are provided to demonstrate the versatility and potential for culturing adherent and suspension cell lines, as well as the potential for studying cellular differentiation strategies.

Rosenbaum and coworkers introduce the emerging field of droplet microfluidics as a future screening tool for a wide variety of biotechnologically relevant topics. For example, they demonstrate its potential for screening environmental samples to look for novel industrially or medically relevant metabolites.

Christian Dusny discusses the emerging field of microfluidic single-cell analysis and cultivation, highlighting different methods and studies on how to characterize the cellular behavior of single cells with a focus on growth, substrate uptake, and production. The following chapter features a contribution by Martina Viefhues, who provides an overview on different analytical methods that can be used to detect and analyze metabolites and characterize cells on a small scale.

Thereafter, Boliviar and coworkers describe the use and application of microfluidic systems in the field of biocatalysis. They systematically show how microfluidic flow systems (in combination with free or immobilized enzymes) can be utilized as a future technology in fundamental and applied biocatalysis. In Chap. 10, Graham and Segal give an overview on lab-on-a-chip devices for application in medical biotechnology, giving particular focus to point-of-care medical diagnostics.

In the next chapter, Xie and colleagues highlight the field of microfluidics for environmental applications. Examples of this new and emerging field are shown and

discussed in terms of their potential for detection and analysis of environmentally relevant compounds and contaminants – for example, multi-resistant bacteria represent a particularly difficult challenge that medical science will need to confront in the coming decades. Klein and Dietzel also discuss the potential of microfluidic systems for performing antimicrobial susceptibility testing (AST).

Maschmeyer and Kakava provide an overview of organ-on-a-chip systems which are currently transforming diagnostic assays and will eventually replace animal testing in the future. They survey these systems, highlight recent proof-of-concepts, and discuss how these can be used and integrated for future toxicity testing of novel drugs in the near future. In the following chapter, Rothbauer and Ertl discuss emerging trends in biosensor development for organ-on-a-chip systems, paying particular attention to various techniques that will likely contribute to organ-on-a-chip systems becoming ready-to-use systems in the future.

In the final chapter, Bahnemann and coworkers provide an overview and discuss future prospects for the application and integration of microfluidic systems within the general field of biotechnology. They emphasize how exciting technological advances and progress in emerging technologies will likely bring these two fields even closer together and consider how the application of microfluidics could significantly shape and transform the field of biotechnology in the coming years.

In summary, these fifteen review chapters highlight some current trends in how microfluidic systems are increasingly being used to address key issues within modern biotechnology. There is no doubt that microfluidic systems will find their niches within various biotechnological applications – and now is the time to integrate these systems into biotechnology workflows. The promise of this technology is so great that it will ultimately likely be less about what we *can* do with microfluidics than what we *want* to do with it.

We are very grateful to the series editor of this book series for being so supportive of putting out a volume on this topic and approaching us to edit it, as well as for many fruitful substantive discussions on the content herein. Our deep gratitude also goes out to all the contributing authors, who took our initial ideas and developed them into the invaluable contributions presented herein. Finally, we thank the team of Springer Nature and its various contractors, who guided and supported us through the process of drafting, editing, and publishing this book.

We sincerely hope that readers will gain new insights, find suitable tools for their applications, and get inspired to reflect even more deeply on how biotechnological issues can benefit from novel microfluidic methods and technologies. Finally, we hope that all readers *enjoy* reading all of this material as much as we enjoyed writing, editing, and reviewing it!

Augsburg, Germany
Bielefeld, Germany

Janina Bahnemann
Alexander Grünberger

Contents

Microfluidics in Biotechnology: Overview and Status Quo	1
Janina Bahnemann and Alexander Grünberger	
A Primer on Microfluidics: From Basic Principles to Microfabrication	17
Ann-Kathrin Klein and Andreas Dietzel	
Emerging Technologies and Materials for High-Resolution 3D Printing of Microfluidic Chips	37
Frederik Kotz, Dorothea Helmer, and Bastian E. Rapp	
Microbioreactors for Process Development and Cell-Based Screening Studies	67
Lasse Jannis Frey and Rainer Krull	
Microfluidic Devices as Process Development Tools for Cellular Therapy Manufacturing	101
Jorge Aranda Hernandez, Christopher Heuer, Janina Bahnemann, and Nicolas Szita	
Droplet Microfluidics for Microbial Biotechnology	129
Sundar Hengoju, Miguel Tovar, DeDe Kwun Wai Man, Stefanie Buchheim, and Miriam A. Rosenbaum	
Microfluidic Single-Cell Analytics	159
Christian Dusny	
Analytics in Microfluidic Systems	191
Martina Viefhues	
Biocatalysis in Continuous-Flow Microfluidic Reactors	211
Marco P. Cardoso Marques, Alvaro Lorente-Arevalo, and Juan M. Bolivar	
Lab-on-a-Chip Devices for Point-of-Care Medical Diagnostics	247
Sofia Arshavsky-Graham and Ester Segal	

Microfluidics for Environmental Applications 267
Ting Wang, Cecilia Yu, and Xing Xie

Microfluidic Systems for Antimicrobial Susceptibility Testing 291
Ann-Kathrin Klein and Andreas Dietzel

Organ-on-a-Chip 311
Ilka Maschmeyer and Sofia Kakava

Emerging Biosensor Trends in Organ-on-a-Chip 343
Mario Rothbauer and Peter Ertl

Microfluidics in Biotechnology: Quo Vadis 355
Steffen Winkler, Alexander Grünberger, and Janina Bahnemann

Microfluidics in Biotechnology: Overview and Status Quo



Janina Bahnemann and Alexander Grünberger

Contents

1	Introduction	2
1.1	Biotechnology	2
1.2	Microfluidics	3
1.3	The Vision of a Microfluidic “Lab-on-a-Chip”	4
2	Microfluidics in Biotechnology	6
2.1	History and Milestones	6
2.2	Application Areas	8
3	Analytics and Screening	8
4	Cell Cultivation and Processing	11
4.1	Single-Cell Analysis and “Omics”	12
4.2	Chances and Challenges	12
5	Conclusion	13
	References	13

Abstract Microfluidics has emerged as a powerful tool, enabling biotechnological processes to be performed on a microscale where certain physical processes (such as laminar flow, surface-to-volume ratio, and surface interactions) become dominant factors. At the same time, volumes and assay times are also reduced in microscale – which can substantially lower experimental costs. A decade ago, most microfluidic systems were only used for proof-of-concept studies; today, a wide array of microfluidic systems have been deployed to tackle various biotechnological research questions – especially regarding the analysis, screening, and understanding of cellular systems. Examples cover all biotechnological areas, from diagnostic

J. Bahnemann (✉)

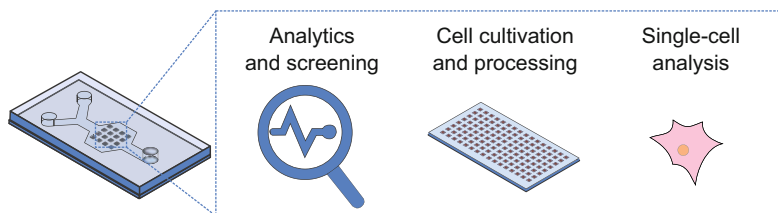
Institute of Technical Chemistry, Leibniz University Hannover, Hannover, Germany
e-mail: jbahnemann@iftc.uni-hannover.de

A. Grünberger (✉)

Multiscale Bioengineering, Faculty of Technology, Bielefeld University, Bielefeld, Germany
e-mail: alexander.gruenberger@uni-bielefeld.de

applications in the field of medical biotechnology to the screening of potentially useful cells in the field of industrial biotechnology. As part of this review, we provide a brief introduction to microfluidics technology (including the vision of Lab-on-a-chip (LOC) systems) and survey some of the most notable applications of microfluidic technology in biotechnology to date.

Graphical Abstract



Keywords Biomicrofluidics, Biotechnology, Lab-on-a-chip, Microfluidics, Microsystems integration, Point-of-care diagnostic, Single-cell analysis

1 Introduction

1.1 Biotechnology

In modern biotechnology, microorganisms, plants, and animals (or parts thereof) are used to produce or refine high-value products, recycle waste, and/or develop new strategies to improve our health and well-being [1]. Biotechnological processes – which include the production of beer, wine, and cheese – have a long and storied tradition that dates back for millennia; yet it is only in recent decades that they have been purposely honed to enable researchers and industry to specifically address food safety, health, environmental pollution, and medical challenges [2]. Nevertheless, the quickly developing field of biotechnology has already helped to revolutionize the industrial, agricultural, and medical sectors by improving both the quantity and quality of various relevant products that are produced for human consumption [3]. Indeed, the number of commercially-produced biotechnological products has been continuously increasing for decades now and shows no sign of slowing down [4]. Biotechnology has been specifically identified as a key discipline within what has been dubbed the emerging “Bio-Economy”, and it will undoubtedly continue to play an essential role in supporting economic growth, employment, energy supply, and a new generation of bio-products in the years to come [4, 5].

The rate of progress evidenced within this field has also been substantially accelerating in recent years, thanks to a host of innovative emerging technologies that range from molecular biological tools (such as CRISPR/Cas) [6, 7] to novel

fabrication techniques (such as 3D bio-printing with unprecedented spatial resolution) [8, 9]. A particularly important trend over the past two decades – and the specific focus of this review – is the miniaturization of biotechnological workflows and functional devices.

1.2 Microfluidics

Microfluidics is defined as the science and technology of handling and manipulating liquids and gasses on a very small scale [10]. Small scale here refers to the μm – mm scale, which corresponds to volumes within the fL – μL range (Fig. 1a). At these scales, the relative effects of various physical processes (such as osmotic movement, electrophoretic motility, and surface interactions) become significantly enhanced. Indeed, the physical factors governing fluid behavior at the microscale are very distinctive and quite different from those at the macroscale. For example, in

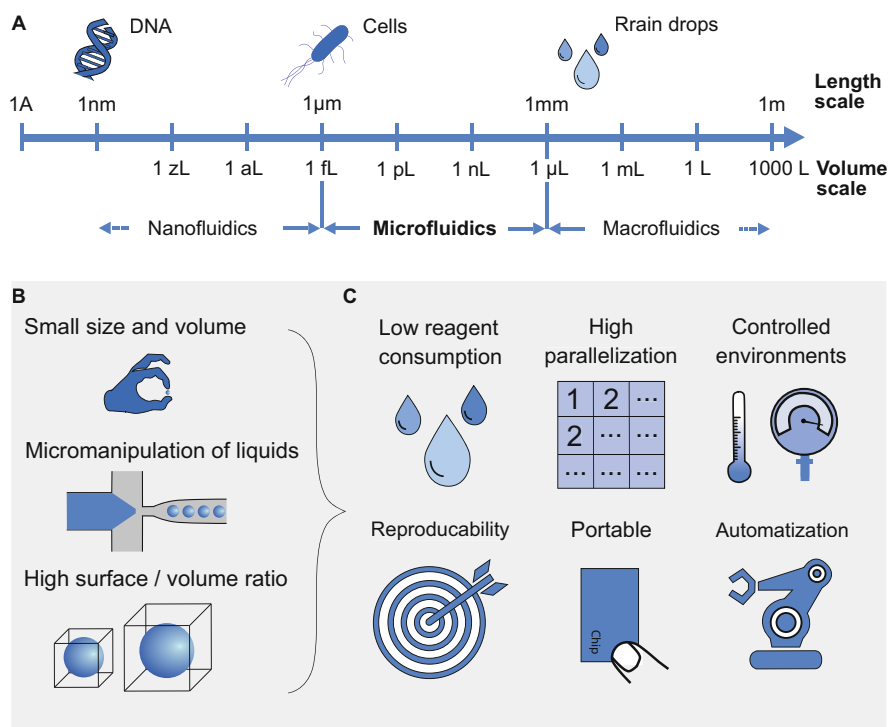


Fig. 1 Introduction and advantages of microfluidics. (a) Size dimensions of different scales, showing the typical length of volume scale for microfluidics; (b) General characteristics of microfluidic systems, resulting from miniaturization; and (c) Advantages of microfluidics, resulting from the general characteristics shown in (b)

microscale, fluid flow is characterized by low Reynolds numbers (<1), and, as a result, fluid flow is almost completely laminar and lacks turbulence [11]. This leads to an interesting phenomenon in which different fluids can flow parallel to each other within a given microchannel without any chaotic mixing transpiring. Such mixing occurs only through diffusion at the interface of these liquid layers – which allows for the predictable transport of molecules through the microchannels. Fluids in microchannels are also characterized by a high Péclet number, which is the ratio of the rate of advective transport to the rate of diffusive transport. This property enables parallel-flowing fluids to flow in tandem with one another longer than they typically would in higher volumes without mixing [11].

These properties allow researchers working with microfluidic systems to utilize very small volumes of materials, and also simultaneously achieve very precise liquid handling and high surface-to-volume ratios within those systems (Fig. 1b). These technical features also lead to several different advantages which make microfluidic systems very useful for the development of future biotechnological toolboxes – perhaps most importantly, a low rate of reagent consumption, and a high degree of potential for parallelizing flows (Fig. 1c). The low rate of reagent consumption is of particular importance in cases where expensive components (e.g., reagents or difficult to purify enzymes) are a major experimental cost center, which frequently occurs in the field of medical biotechnology – for example, in the design of new biocatalysts [12] or in the analysis of antibiotics [13]. Additionally, the small volume of sample required is advantageous where reagents are hazardous. Due to low working volumes and the ability to parallelize reaction sites, microfluidic systems are particularly well-suited for high-throughput applications such as screening experiments [14] and experiments designed to generate statistically meaningful data [15].

One further advantage of these systems is the ability for researchers to exercise precise control over the mass transfer within them. Combined with suitable analytical tools, this enables researchers to perform experiments and assays with a high spatio-temporal resolution at precisely defined micro-environments [16]. Well-defined handling and precise environmental control lay the foundation for a high rate of reproducibility of experimental procedures – a critical goal in all research endeavors. Other advantages are the portability of the devices [17, 18] due to their small size and increased potential for automatization [18]. In sum, these factors create unique synergies which can significantly reduce assay times (and thus help to promote experimental efficiency) while simultaneously facilitating considerable cost savings.

1.3 The Vision of a Microfluidic “Lab-on-a-Chip”

Microfluidic systems are typically channel systems (with a channel diameter of <1 mm) that can combine a wide variety of process steps in a very small space. These are frequently referred to as “Lab-on-a-chip” (LOC) systems (Fig. 2)

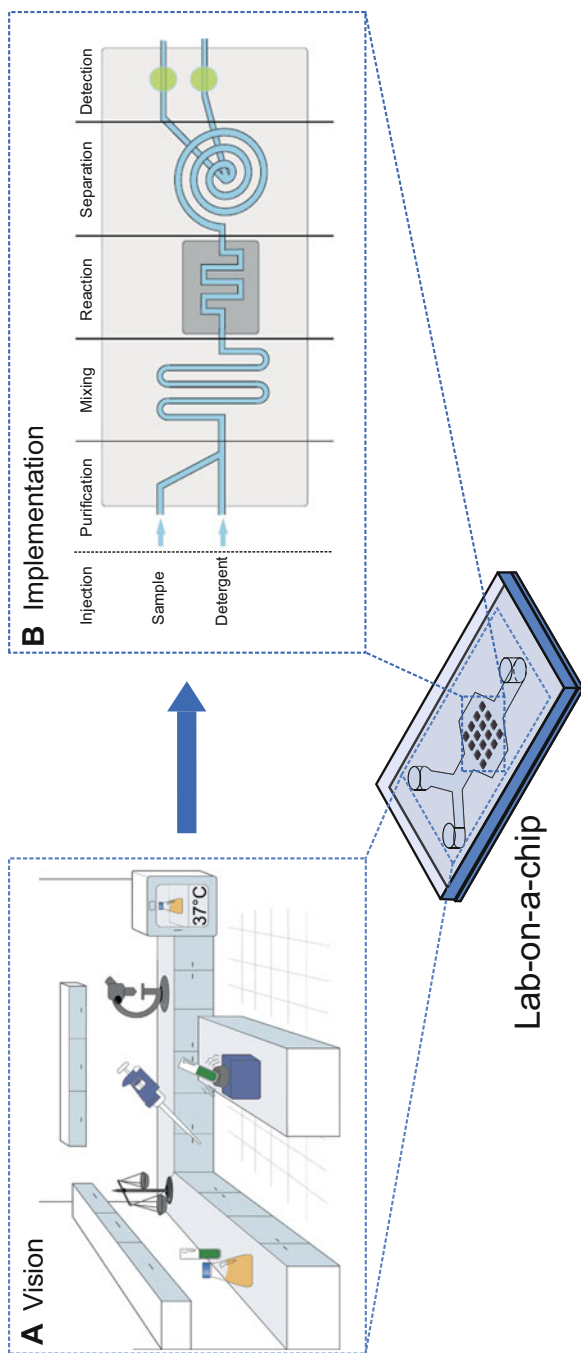


Fig. 2 Vision and structure of a Lab-on-a-chip (LOC). (a) The ultimate goal of LOC systems is to achieve the functional miniaturization of existing macro-level experimental protocols and workflows into a single microfluidic chip system, and (b) sketch of an LOC system, consisting of several functional units: Sample and detergent inlets, purification and mixing units, a reaction unit (temperature-controlled if necessary), and a separation and detection unit

[19, 20]. The ultimate goal of the LOC vision is to transfer entire functionalities or workflows that would typically be performed via a macroscopic laboratory onto a single microchip (Fig. 2a). From a biotechnological perspective, this can range from relatively straightforward applications like sample purification or the cultivation of cells to more diverse analytical procedures such as those used to assess and observe molecules or cells of interest. A typical LOC system consists of a network of microchannels, inlets for injecting fluids/detergents and samples, micropumps and microvalves (for fluid manipulation within the chip), and outlets (for removing fluids) (Fig. 2b). LOCs can potentially consist of purification and mixing units as well as reaction, separation, and detection units [21, 22]. These various units can respectively perform a wide variety of tasks during an analysis run and can also be leveraged to work in tandem depending on the purpose or operation to be performed. Most of the current devices reported in the literature contain only some of these operational units, however, and perform only certain selected steps within a larger biotechnological workflow.

2 Microfluidics in Biotechnology

2.1 History and Milestones

Traditionally, microfluidic LOC systems have been fabricated via complex etching processes and photolithography (a relatively old technology that was developed back in the 1950s) which require cleanrooms [23] (Fig. 3a). The first microchannels

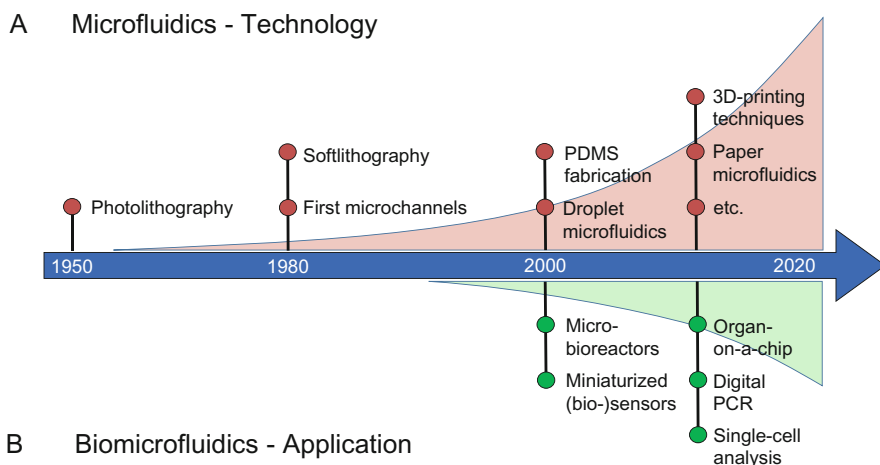


Fig. 3 Milestones in the development of microfluidic technologies for applications in biotechnology to date. (a) Important milestones and developments on the way to LOC systems, and (b) Overview of microfluidic milestones with applications in biotechnology

fabricated by soft lithography were described in the 1980s [24, 25]. Thereafter, a major breakthrough in manufacturing technology occurred in 1998, with the advent of PDMS (polydimethylsiloxane) fabrication and manufacturing [26, 27]. Over the last 25 years, a wide variety of microfluidic technologies have now emerged – including droplet microfluidics, microfluidic pneumatic valves and pumps. Today, most microfluidic systems are fabricated using PDMS in casting processes [28]. This allows for the production of very fine channels in the micrometer range, and, at the same time, for the use of transparent polymers, which permit microscopic observation of the system. Especially for certain biological applications, the oxygen permeability of this material can offer a critically important advantage. Of course, glass may also be used as a material for the fabrication of microfluidic systems where oxygen permeability is not required (and in addition to its transparency, it also offers the benefit of both mechanical and chemical stability). Thanks to an ongoing revolution in 3D printing technologies [29], even highly complex structures can now be designed on the computer and manufactured from plastic or metal using the appropriate additive printing processes. The steady development of novel materials and fabrication technologies continuously pushes novel technologies forward (e.g., paper-based microfluidics [30], liquid glass technology [31], etc.), and the curious reader is hereby referred to the available literature on that exciting topic for further information [32].

This progress in various microfluidic manufacturing technologies has spurred on the development of a plethora of microfluidic applications within the fields of biology and biotechnology – often collectively referred to as “biomicrofluidics” [33, 34] (Fig. 3b), although we note that that term is not used consistently throughout the literature [35]. The combination of both of these fields has sparked extraordinary research interest, and LOC systems for many biotechnological topics have been developed within the last two decades. The possible combinations of functional units seem endless: mechanical, electrochemical, optical, and even acoustic influences can all be integrated simultaneously into a single LOC system. The development of novel miniaturized bioreactor setups first saw a big push in the early 2000s [36], and microbioreactors are increasingly being used within industry to enable cost-effective and efficient process development or as screening platforms for the investigation of different production cell lines. Thanks to ever smaller cultivation and sample volumes, the demand for miniaturized (bio)sensors – which can be integrated directly into the process – has also increased during the past years.

Of course, by combining suitable miniaturized sensors and analytical systems with small-scale bioreactors, bioprocess monitoring, and optimization can still stand to be further improved in the future. The related field of the so-called organ-on-a-chip (OoC) first emerged in approximately 2010, and today it has become the single fastest growing type of microfluidic application within the field of biotechnology [37]. Through organ-on-a-chip technology, pharmacological studies can already be carried out in some cases without the use of animals as test subjects – and there is good reason to hope that animal experimentation will continue to be increasingly replaced by OoC systems in the future [38]. In the field of bioanalytics, a very well-known example is droplet digital PCR (ddPCR) technology – which generates small,

separate reaction units based on droplet microfluidics (water-oil emulsion technology), and thus facilitates the absolute quantification of target molecules [38]. At the same time, the field of single-cell analysis has emerged rapidly; examples include single-cell genomics, transcriptomics, proteomics, and metabolomics, which can be used to reveal cell-to-cell heterogeneity within relevant cells [36]. The development of single-cell technologies has also helped researchers to gain a more systematic understanding of cellular heterogeneity across a wide range of tissues and cell populations, and, in combination with emerging computational methods, there is reason to believe that this research will lead to a better and richer understanding of cellular behavior in the future [38].

2.2 Application Areas

Microfluidic systems have now found application across many different biotechnological fields – although it is fair to say that to date, most microfluidic systems and methods have been deployed in the fields of medical biotechnology [39] and industrial biotechnology [40] (Fig. 4a). The most prominent examples for applications of this technology within these fields are for novel analytical methods and systems – including the so-called point-of-use diagnostic systems, microfluidic systems used for the screening of cells and substances, and/or systems that allow for the defined cultivation, handling, manipulation, and processing of (living) cells (Fig. 4b). Microfluidics have also contributed to the emerging fields of single-cell analysis and single-cell “omics”, aiming to generate a more detailed understanding of cellular physiology in diverse biotechnological contexts. Within the subfields of the so-called yellow (food), blue (marine), gray (environmental), and green (plant) biotechnology, microfluidic methods remain a relative niche form of technology and have not yet been systematically adapted for research purposes [41]. However, proof-of-concept studies have already indicated that they may start to offer substantial utility in some or all of these areas in the near future.

3 Analytics and Screening

Microfluidic systems are of particular interest for their potential analytical purposes (Fig. 4b – top) [32], since many analytical steps can be automated and run in sequence – thereby improving the handling and performance of sensors. The advantages of system miniaturization noted above (in terms of both experimental reproducibility and automatability) also offer the tantalizing promise of improving existing analytical research methods while simultaneously helping to make point-of-care sensor systems more readily accessible to patients in real-world settings [42]. Representative examples include microfluidics that have been integrated with biosensors to facilitate specific protein detection in the field of medical

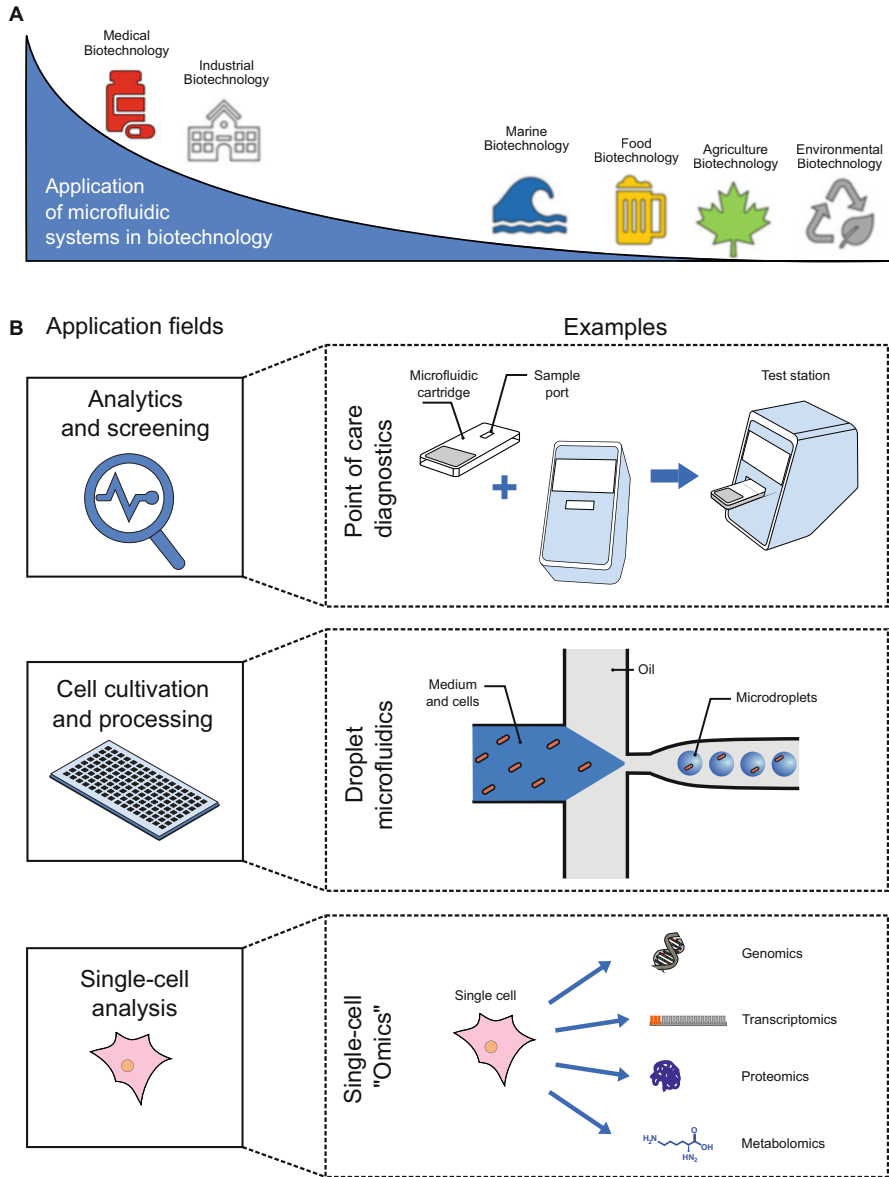


Fig. 4 Application of microfluidic systems within biotechnology. **(a)** To date, the widespread application of microfluidic systems has predominantly occurred in the fields of medical and industrial biotechnology. Application in other biotechnological fields is emerging, but still remains primarily restricted to research environments; **(b)** Overview of the most common application fields of microfluidic systems in biotechnology, which include analytics and screening, cultivation and processing of cells and metabolites (e.g., by droplet microfluidic systems), and the emerging field of single-cell analysis (e.g., single-cell “Omics”)

biotechnology [43], as well as the measurement of analytes within bioprocesses using miniaturized sensor systems [44, 45].

Much research is currently being focused on improving the use of microfluidics as online-analytical tools to measure bioreactor performance in real-time. A major challenge in this context is the challenge of effectively miniaturizing existing sensor technology so that it can be integrated into microfluidic systems while still delivering high performance.

Microdevices are also already being extensively used to collect environmental samples, as a means of facilitating the detection and quantification of targeted components even within miniscule sample sources [46]. In the area of environmental biotechnology, present microfluidic applications include the use of sensors as tools for water contaminant analysis (e.g., heavy metals and organic pollutants), as tools for microorganism detection (e.g., viruses and bacteria), and as platforms for the investigation of environment-related problems (e.g., bacteria electron transfer and biofilm formation) [46].

Food safety analysis is yet another important procedure used to prevent or detect food contamination. In that context, microfluidic technology exhibits several distinct advantages – including requiring small sample sizes, facilitating fast detection of contamination, presenting methods of simple operation, and offering multi-functional integration and multiplex detection capabilities in a highly-portable format [47, 48]. In the field of marine biotechnology, proof-of-concepts for water pollutant monitoring are also now being developed, as discussed in [49].

Cell screening is a process for the detection and isolation of microorganisms of interest. Accomplishments in microfluidics have significantly accelerated screening speed while decreasing attendant costs. Typically, only a few cells (out of thousands to millions) are selected from a batch, based on their properties. In medical biotechnology, these cells can be of interest for the production of specific pharmaceutical products (such as antibodies). In addition, microfluidic cell separators can also be used to isolate and separate target cells from complex mixtures (such as blood). Such systems are already being used in the field of cell therapy [50]. In white biotechnology, screening is used to obtain better performing industrial strains [51]. The most popular method for deploying microfluidic technology in this context is via droplet microfluidics [52]. In these devices, water-in-oil or oil-in-water droplets are generated at a controlled volume and speed. These droplets form separate compartments in which, for example, cells can be individually enclosed (this principle is also used in ddPCR). Thus, these small compartments provide the ability to screen cells or new enzymes in a high-throughput manner. Alternatively, microfluidic flow cytometry methods are emerging, combining advantages of conventional flow cytometry and microfluidics [53].

Proof-of-concept studies have also been reported in green biotechnology, especially for the screening of microalgae [54–56]. In environmental biotechnology, microfluidic-inspired approaches for the separation and treatment of contaminated water and air (such as the removal of heavy metals and waterborne pathogens from wastewater and carbon capture) are also being increasingly investigated [57].

4 Cell Cultivation and Processing

Another emerging application of microfluidic systems lies in the cultivation, handling, and processing of living cells. This ranges from cultivation to analysis and characterization of cells, all using miniaturized bioreactors and analytical systems (Fig. 4b – middle). In the field of medical and industrial biotechnology, for example, there is increasing interest in the utilization of microfluidic systems – which enable a continuous and automated processing of cell samples. At the interface of these two fields is the continuous transient transfection of mammalian cells by means of microfluidic systems, which can enable more flexible and cost-effective production of pharmaceutically relevant proteins on a smaller scale [29]. The development and use of miniaturized chromatographic devices in the field of cell culture technology also shows great potential to facilitate continuous automated product purification [58].

Microbioreactors or miniaturized cell culture platforms (featuring small volumes and space-saving formats) allow researchers to perform a large number of parallel experiments under different cultivation conditions (e.g., to observe the influence of different process parameters on cells at the same time within a single experimental format). Cell culture-on-chip and organ-on-a-chip are some of the most prominent examples of microfluidic technology applications that have been adopted to date in this field. Indeed, these systems are already being used across virtually all biotechnological domains to help improve our understanding of cellular processes and heterogeneity. Such systems are also being used for the targeted manipulation of cells or for drug screening experiments; in particular, the automation of miniaturized systems allows such experiments (from cell handling, defined addition of drugs, media or detergents to processing (such as separation of cells) and analysis) to be performed in a more reproducible manner and with comparatively higher throughput than is seen in traditional macro-level experimental methods [59, 60].

As small-scale bioreactors are increasingly used for process development in the context of biotechnological production, microfluidic systems are also being increasingly leveraged for the benefit of their comparatively greater process control. One example of this phenomenon is provided by microfluidic spiral separators, which enable continuous cell separation and cell recovery, allowing for perfusion cultivations to be run on a very small scale [61].

In the field of marine biotechnology, microfluidic proof-of-concept studies have been developed to study the motility response of marine bacteria in the wake of microscale nutrient changes [62]. So far, it should be noted that relatively few systems have actually been used to study marine cells; nevertheless, already well-established microfluidic technologies could (and, we believe, should) be transferred and used widely in this context within the near future.

In green biotechnology, the cultivation of root cells using microfluidic technology is already underway [63]. Relatedly, while it has long been understood that a thorough understanding of how organisms actually interact with a complex soil environment would pay substantial ecological dividends in the real world, current

laboratory-based methods depend on reductionist approaches that are inherently incapable of simulating or mimicking that level of natural diversity. The application of microfluidic technologies to organismal studies in order to help mimic “natural” environmental conditions, therefore, offers unique benefits and promising new opportunities for the cultivation experimentalist [64, 65].

4.1 Single-Cell Analysis and “Omics”

Progress in the development of microfluidic methods for the cultivation, handling, and isolation of cells inevitably facilitates progress in the related field of microfluidic single-cell analysis. The most prominent areas of study in this context are the genomics [66], transcriptomics [67], proteomics [68], metabolomics [68] of single cells, often collectively called single-cell “Omics” (Fig. 4b – bottom). In the field of medical and industrial biotechnology, there is increasing interest in single-cell data, to the extent that it can potentially help researchers gain a greater understanding of heterogeneity among individual cells. Application fields can range from the study of cancer cells [69] in a medical context to the study of industrially relevant microorganisms [70]. For a recent review regarding the state-of-the-art microchip platforms for multi-omics studies at single-cell resolution, the curious reader is referred to Deng et al. [71].

Most recently, the field of single-cell cultivation has allowed for the cultivation and analysis of single cells and cell clusters at precise environmental conditions [16, 65]. In combination with live-cell imaging, this technology is facilitating an improved understanding of the phenomenon of cell-to-cell heterogeneity as it occurs under various environmental conditions [72]. Examples range from the study of medical relevant cell lines [73] to strains that have many potentially useful applications within industrial biotechnology [73]. These systems also enable the detailed study of cell–cell interactions at the single-cell level [74].

4.2 Chances and Challenges

As the foregoing examples illustrate, microfluidic devices are already becoming ubiquitous within the realm of biotechnological research. Yet more work still remains to be done to help make this highly promising technology even more widely applicable across other fields. Ortseifen et al. [75] describe six distinct but interrelated gaps that might explain the relatively poor integration of microfluidics, to date, into certain fields of research. These include a communication gap; a knowledge gap; a motivation gap; a methodology gap; a technology gap; and a commercialization gap. These gaps must all be systematically studied and addressed in order to continue to push forward the application and adoption of microfluidic technologies within the research laboratory. This vital process will require (among other things) a closer

cooperation between engineers and biologists, which can be accelerated via the establishment of interdisciplinary conferences and study courses. Ortseifen et al. also identify several more technical issues – such as the need for greater standardization of devices and the development of ready-to-use devices – for which a solution would help to accelerate the integration of microfluidic systems into biotechnological workflows.

The race is not yet won, and we still remain far away from the ultimate goal of fully realizing the ideal of fully self-contained LOC systems in most cases – but integrating more and more “function-on-a-chip” elements is a very achievable and worthwhile next step that we should absolutely take along the path to further integrating microfluidic systems into biotechnology research. And although the development of new LOC systems remains cutting-edge work that is most commonly seen in prototype form within the confines of research facilities, the inevitable commercialization of LOC systems is now starting to pick up as well – as evidenced by the emergence of a booming crop of start-up companies that are squarely focused on this sector [31].

5 Conclusion

Many microfluidic applications across the field of biotechnology are now emerging in the course of regular lab work. Although the fields of food, marine, and environmental biotechnology have not yet embraced microfluidic applications on a wide scale, we strongly believe that these subfields can, should, and inevitably will take the adoption of microfluidic technologies seen in biotechnology as a blueprint for how microfluidic methods can be used efficiently to streamline and facilitate ever-increasing array of tasks. Through this short introduction and review, we hope to trigger further discussion about how microfluidic methods can best be applied moving forward.

Acknowledgments The authors would like to thank Steffen Winkler for the design and creation of Fig. 3, and Julian Schmitz for the design and creation of the icons for the different biotechnology fields (see Fig. 4). We furthermore would like to thank Christopher Heuer for proof-reading this manuscript.

Conflict of Interest No conflict of interest to declare.

References

1. Chmiel H, Takors R, Weuster-Botz D (2018) Bioprozesstechnik. Springer, Berlin
2. Antranikian G (2006) Angewandte mikrobiologie. Springe

3. Haaf A, Hofmann S. Measuring the economic footprint of the biotechnology industry in Europe. https://www.europabio.org/wp-content/uploads/2021/02/201208_WifOR_EuropaBIO_Economic_Impact_Biotech_FINAL.pdf
4. National Academies of Sciences Engineering and Medicine (2017) Preparing for future products of biotechnology. National Academies Press
5. Lokko Y et al (2018) Biotechnology and the bioeconomy – towards inclusive and sustainable industrial development. *New Biotechnol* 40:5–10
6. Sampson TR, Weiss DS (2014) Exploiting CRISPR/Cas systems for biotechnology. *BioEssays* 36:34–38
7. Donohoue PD, Barrangou R, May AP (2018) Advances in industrial biotechnology using CRISPR-Cas systems. *Trends Biotechnol* 36:134–146
8. Murphy SV, Atala A (2014) 3D bioprinting of tissues and organs. *Nat Biotechnol* 32:773–785
9. Kahl M, Gertig M, Hoyer P, Friedrich O, Gilbert DF (2019) Ultra-low-cost 3D bioprinting: modification and application of an off-the-shelf desktop 3D-printer for biofabrication. *Front Bioeng Biotechnol* 7:184
10. Conlisk AT (2007) Introduction to microfluidics. *J Fluid Mech* 570:503–507
11. Duncombe TA, Tentori AM, Herr AE (2015) Microfluidics: reframing biological enquiry. *Nat Rev Mol Cell Biol* 16:554–567
12. Marques MPC, Lorente-Arevalo A, Bolivar JM (2021) Biocatalysis in continuous-flow microfluidic reactors. Springer, Berlin, pp 1–36. https://doi.org/10.1007/10_2020_160
13. Hage-Hülsmann J et al (2018) Natural biocide cocktails: combinatorial antibiotic effects of prodigiosin and biosurfactants. *PLoS One* 13:e0200940
14. Du G, Fang Q, den Toonder JMJ (2016) Microfluidics for cell-based high throughput screening platforms – a review. *Anal Chim Acta* 903:36–50
15. Velve-Casquillas G, le Berre M, Piel M, Tran PT (2010) Microfluidic tools for cell biological research. *Nano Today* 5:28–47
16. Grünberger A, Wiechert W, Kohlheyer D (2014) Single-cell microfluidics: opportunity for bioprocess development. *Curr Opin Biotechnol* 29:15–23
17. Wang H et al (2017) A portable microfluidic platform for rapid molecular diagnostic testing of patients with myeloproliferative neoplasms. *Sci Rep* 7:1–11
18. Beebe DJ, Mensing GA, Walker GM (2003) Physics and applications of microfluidics in biology. *Annu Rev Biomed Eng* 4:261–286
19. Daw R, Finkelstein J (2006) Lab on a chip. *Nature* 442:367
20. Salieb-Beugelaar GB, Simone G, Arora A, Philippi A, Manz A (2010) Latest developments in microfluidic cell biology and analysis systems. *Anal Chem* 82:4848–4864
21. Jamshaid T et al (2016) Magnetic particles: from preparation to lab-on-a-chip, biosensors, microsystems and microfluidics applications. *TrAC Trends Anal Chem* 79:344–362
22. Bahnemann J, Stahl F, Scheper T (2020) Spezielle labortechnische Reaktoren: lab-on-a-chip. Springer Spektrum, Berlin, pp 1391–1418. https://doi.org/10.1007/978-3-662-56434-9_49
23. Levinson HJ (2001) Principles of lithography. SPIE Press
24. Weibel DB, DiLuzio WR, Whitesides GM (2007) Microfabrication meets microbiology. *Nat Rev Microbiol* 5:209–218
25. Xia Y, Whitesides GM (1998) Soft lithography. *Annu Rev Mater Sci* 28:153–184
26. Duffy DC, McDonald JC, Schueller OJA, Whitesides GM (1998) Rapid prototyping of microfluidic systems in poly(dimethylsiloxane). *Anal Chem* 70:4974–4984
27. Kiran Raj M, Chakraborty S (2020) PDMS microfluidics: a mini review. *J Appl Polym Sci* 137: 48958
28. Klein A-K, Dietzel A (2020) A primer on microfluidics: from basic principles to microfabrication. Springer, Berlin, pp 1–19. https://doi.org/10.1007/10_2020_156
29. Heuer C, Preuß JA, Habib T, Enders A, Bahnemann J (2021) 3D printing in biotechnology – an insight into miniaturized and microfluidic systems for applications from cell culture to bioanalytics. *Eng Life Sci*. <https://doi.org/10.1002/ELSC.202100081>

30. Cate DM, Adkins JA, Mettakoonpitak J, Henry CS (2014) Recent developments in paper-based microfluidic devices. *Anal Chem* 87:19–41
31. Winkler S, Grünberger A, Bahnemann J (2021) Microfluidics in biotechnology: quo vadis. Springer, Berlin, pp 1–26. https://doi.org/10.1007/10_2020_162
32. Berlanda SF, Breittfeld M, Dietsche CL, Dittrich PS (2020) Recent advances in microfluidic technology for bioanalysis and diagnostics. *Anal Chem* 93:311–331
33. Muñoz-Sánchez BN, Silva SF, Pinho D, Vega EJ, Lima R (2016) Generation of micro-sized PDMS particles by a flow focusing technique for biomicrofluidics applications. *Biomicrofluidics* 10:014122
34. Das T, Chakraborty S (2010) Bio-microfluidics: overview. *Microfluid Microfabr.* https://doi.org/10.1007/978-1-4419-1543-6_4
35. Domachuk P, Tsiotis K, Omenetto FG, Kaplan DL (2010) Bio-microfluidics: biomaterials and biomimetic designs. *Adv Mater* 22:249–260
36. Frey LJ, Krull R (2020) Microbioreactors for process development and cell-based screening studies. Springer, Berlin, pp 1–34. https://doi.org/10.1007/10_2020_130
37. Maschmeyer I, Kakava S (2020) Organ-on-a-chip. *Adv Biochem Eng Biotechnol.* https://doi.org/10.1007/10_2020_135
38. Yuan GC et al (2017) Challenges and emerging directions in single-cell analysis. *Genome Biol* 18:1–8
39. Tokeshi M (2019) Applications of microfluidic systems in biology and medicine, vol 7. Springer, Singapore
40. Marques MP, Szita N (2017) Bioprocess microfluidics: applying microfluidic devices for bioprocessing. *Curr Opin Chem Eng* 18:61–68
41. Hamon M, Dai J, Jambovane S, Hong JW (2015) Microfluidic systems for marine biotechnology. In: Springer handbook of marine biotechnology, pp 509–530. https://doi.org/10.1007/978-3-642-53971-8_20
42. Arshavsky-Graham S, Segal E (2020) Lab-on-a-chip devices for point-of-care medical diagnostics. Springer, Berlin, pp 1–19. https://doi.org/10.1007/10_2020_127
43. Arshavsky-Graham S, Enders A, Ackerman S, Bahnemann J, Segal E (2021) 3D-printed microfluidics integrated with optical nanostructured porous aptasensors for protein detection. *Microchim Acta* 188:1–12
44. Frey LJ et al (2021) 3D-printed micro bubble column reactor with integrated microsensors for biotechnological applications: from design to evaluation. *Sci Rep* 11:1–14
45. Wang B, Wang Z, Chen T, Zhao X (2020) Development of novel bioreactor control systems based on smart sensors and actuators. *Front Bioeng Biotechnol* 8:7
46. Wang T, Yu C, Xie X (2020) Microfluidics for environmental applications. Springer, Berlin, pp 1–24. https://doi.org/10.1007/10_2020_128
47. Gao H, Yan C, Wu W, Li J (2020) Application of microfluidic chip technology in food safety sensing. *Sensors* 20:1792
48. Kim G, Lim J, Mo C (2016) Applications of microfluidics in the agro-food sector: a review. *J Biosyst Eng* 41:116–125
49. Kim SK (2015) Springer handbook of marine biotechnology. Springer, pp 1–1512. <https://doi.org/10.1007/978-3-642-53971-8>
50. Aranda Hernandez J, Heuer C, Bahnemann J, Szita N (2021) Microfluidic devices as process development tools for cellular therapy manufacturing. Springer, Berlin, pp 1–27. https://doi.org/10.1007/10_2021_169
51. Zeng W, Guo L, Xu S, Chen J, Zhou J (2020) High-throughput screening technology in industrial biotechnology. *Trends Biotechnol* 38:888–906
52. Teh SY, Lin R, Hung LH, Lee AP (2008) Droplet microfluidics. *Lab Chip* 8:198–220
53. Gong Y, Fan N, Yang X, Peng B, Jiang H (2019) New advances in microfluidic flow cytometry. *Electrophoresis* 40:1212–1229
54. Ozdalgic B et al (2021) Microfluidics for microalgal biotechnology. *Biotechnol Bioeng* 118:1716–1734

55. Kim HS, Guzman AR, Thapa HR, Devarenne TP, Han A (2016) A droplet microfluidics platform for rapid microalgal growth and oil production analysis. *Biotechnol Bioeng* 113: 1691–1701
56. Girault M, Beneyton T, del Amo Y, Baret JC (2019) Microfluidic technology for plankton research. *Curr Opin Biotechnol* 55:134–150
57. Yew M, Ren Y, Koh KS, Sun C, Snape C (2019) A review of state-of-the-art microfluidic technologies for environmental applications: detection and remediation. *Global Chall* 3: 1800060
58. Habib T et al (2022) 3D-printed microfluidic device for protein purification in batch chromatography. *Lab Chip*. <https://doi.org/10.1039/D1LC01127H>
59. Bahnemann J, Enders A, Winkler S (2021) Microfluidic systems and organ (human) on a chip. Springer, pp 175–200. https://doi.org/10.1007/978-3-030-66749-8_8
60. Rothbauer M, Ertl P (2020) Emerging biosensor trends in organ-on-a-chip. Springer, Berlin, pp 1–12. https://doi.org/10.1007/10_2020_129
61. Enders A, Preuss JA, Bahnemann J (2021) 3D printed microfluidic spiral separation device for continuous, pulsation-free and controllable CHO cell retention. *Micromachines* 12:1060
62. Stocker R, Seymour JR, Samadani A, Hunt DE, Polz MF (2008) Rapid chemotactic response enables marine bacteria to exploit ephemeral microscale nutrient patches. *Proc Natl Acad Sci* 105:4209–4214
63. Moussus M, Meier M (2021) A 3D-printed *Arabidopsis thaliana* root imaging platform. *Lab Chip* 21:2557
64. Stanley CE, Grossmann G, Casadevall I, Solvas X, DeMello AJ (2016) Soil-on-a-Chip: microfluidic platforms for environmental organismal studies. *Lab Chip* 16:228–241
65. Täuber S et al (2020) Dynamic environmental control in microfluidic single-cell cultivations: from concepts to applications. *Small* 16:1906670
66. Zhou W et al (2021) Microfluidics applications for high-throughput single cell sequencing. *J Nanobiotechnol* 19:1–21
67. Lin S et al (2021) Microfluidic single-cell transcriptomics: moving towards multimodal and spatiotemporal omics. *Lab Chip* 21:3829–3849
68. Guo S, Zhang C, Le A (2021) The limitless applications of single-cell metabolomics. *Curr Opin Biotechnol* 71:115–122
69. Rossi E, Zamarchi R (2019) Single-cell analysis of circulating tumor cells: how far have we come in the-omics era? *Front Genet* 7:958
70. Freiherr von Boeselager R, Pfeifer E, Frunzke J (2018) Cytometry meets next-generation sequencing – RNA-Seq of sorted subpopulations reveals regional replication and iron-triggered prophage induction in *Corynebacterium glutamicum*. *Sci Rep* 8:1–13
71. Deng Y, Finck A, Fan R (2019) Single-cell omics analyses enabled by microchip technologies. *Annu Rev Biomed Eng* 21:365–393
72. Dusny C, Grünberger A (2020) Microfluidic single-cell analysis in biotechnology: from monitoring towards understanding. *Curr Opin Biotechnol* 63:26–33
73. Höving AL et al (2021) Human blood serum induces p38-MAPK- and Hsp27-dependent migration dynamics of adult human cardiac stem cells: single-cell analysis via a microfluidic-based cultivation platform. *Biology* 10:708
74. Wang D, Bodovitz S (2010) Single cell analysis: the new frontier in ‘omics’. *Trends Biotechnol* 28:281–290
75. Ortseifen V, Viehues M, Wobbe L, Grünberger A (2020) Microfluidics for biotechnology: bridging gaps to foster microfluidic applications. *Front Bioeng Biotechnol* 8:1324

A Primer on Microfluidics: From Basic Principles to Microfabrication



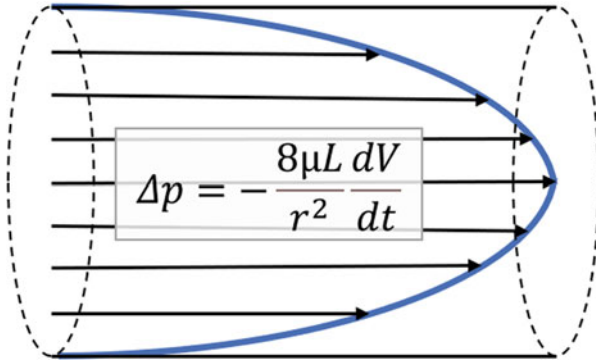
Ann-Kathrin Klein and Andreas Dietzel

Contents

1	Introduction	18
2	Microfluidic Fundamentals	19
2.1	Flow Behavior at Small Scales	19
2.2	Surface Effects	21
2.3	Diffusion and Mixing	22
2.4	Transport of Suspended Particles	23
3	Microfluidic Fabrication Techniques	24
3.1	Clean-Room Microfabrication	24
3.2	Photolithography	25
3.3	Deposition Techniques	25
3.4	Etching Techniques	26
3.5	Bonding Techniques	27
3.6	Soft Lithography	28
3.7	Maskless Micro- and Nanofabrication	29
4	Conclusion	31
	References	32

Abstract Microfluidic systems enable manipulating fluids in different functional units which are integrated on a microchip. This chapter describes the basics of microfluidics, where physical effects have a different impact compared to macroscopic systems. Furthermore, an overview is given on the microfabrication of these systems. The focus lies on clean-room fabrication methods based on photolithography and soft lithography. Finally, an outlook on advanced maskless micro- and nanofabrication methods is given. Special attention is paid to laser structuring processes.

Graphical Abstract



Keywords Advanced microfabrication, Diffusion length, Laminar flow, Laser structuring processes, Micromachining, Photolithography, Reynolds number, Soft lithography

1 Introduction

Microfluidics deals with the manipulation and control of fluids, particles, and drugs, as well as biological materials like cells and proteins in small fluid volumes. The amount of fluid typically processed ranges from micro- to picoliters (10^{-6} – 10^{-12} L) [1]. Microfluidic systems in the format of a microchip (the edge length is typically centimeters) consist of microchannel networks, cavities, and vias as inlets and outlets for fluids to process mixing, separating, sorting, and transporting. Furthermore, microfluidic systems enable continuous processing and analysis. In general, miniaturization allows:

- decreased sample/reagent consumption,
- strong parallelization of processes,
- possibility of compact and portable systems (Point-of-Care),
- shorter analysis time,
- reduced costs per analysis,
- reduction of contamination risk,
- sensor integration,
- increased sensitivity and specificity,
- and efficient analysis when only small sample amounts are available [2–4].

2 Microfluidic Fundamentals

2.1 Flow Behavior at Small Scales

Fluids comprise liquids and gases. A difference between fluids and solids is that fluids deform continuously under the influence of shear forces. Viscosity describes how much a fluid yields under shear stress. It can be defined by two parallel plates (one moving and one fixed) separated by a liquid film of thickness Δy (as shown in Fig. 1). The force required to move the moving plate depends on the velocity difference Δv and the viscosity μ [5]:

$$F = \mu A \frac{\Delta v}{\Delta y}$$

where F is the shear force and A is the overlapping area of the two plates. The viscosity is characteristic of a certain fluid. The shear force is proportional to the rate of deformation (Δv). For Newtonian fluids like water, the viscosity can be assumed independent of the velocity.

The behavior of microflows can be understood using the basic principles of fluid mechanics and taking into account that microfluidic environments are characterized by an increased ratio of surface over volume. For more details on the theory of microfluidics, see [4–7].

Small volumes of fluid in microchannels behave differently than fluids in the macroworld [8]. The physical forces in the system remain the same, but their balance changes depending on their size: the (viscous) friction forces lose importance relative to inertial forces. The dimensionless Reynolds number Re is the ratio of inertial forces to viscous forces [9] and allows determining whether the flow is dominated by viscous forces or inertial forces:

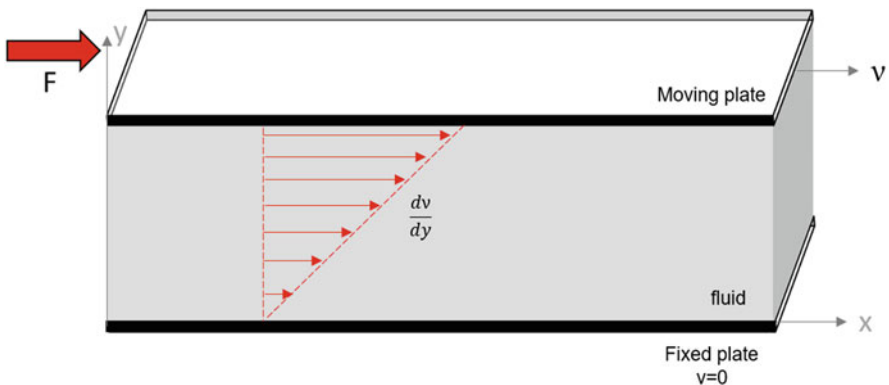


Fig. 1 Schematic illustration of the concept of viscosity using the example of two parallel plates (one moving and one fixed) separated by a liquid film

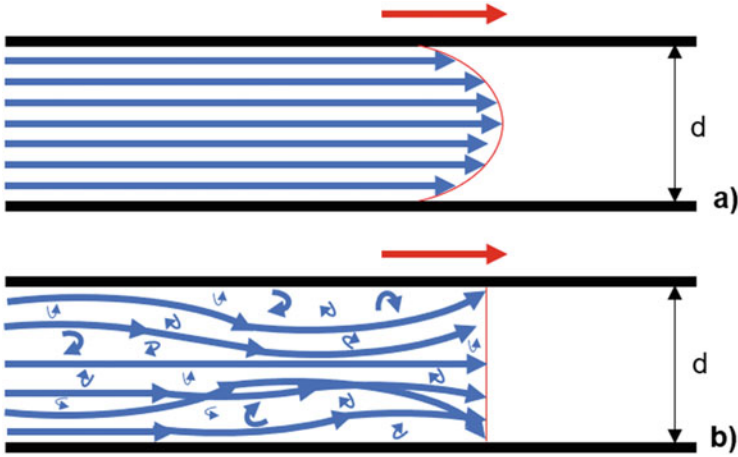


Fig. 2 Velocity profiles of laminar (a) and turbulent flow (b)

$$Re = \frac{\text{inertial forces}}{\text{viscous forces}} = \frac{\rho \cdot \nu \cdot L}{\mu}$$

ρ is the fluid density, ν is the characteristic fluid velocity, L is the characteristic length of the system, and μ is the viscosity. A system accommodates a laminar flow if the Reynolds number is less than $\sim 2,000$. For $Re > \sim 2,000$, the flow is turbulent [10]. In microfluidic systems, the Reynolds number is much smaller and often even below 1 [4]. For this reason, these systems are characterized by laminar flow in which the flow velocities in the entire fluid volume are constant in time. It is steady and smooth. The Hagen-Poiseuille equation applies to the pressure-driven laminar flow of a Newtonian fluid:

$$\Delta p = - \frac{8 \mu L}{r^2} \frac{dV}{dt}$$

where Δp is the pressure drop across a flow channel, L is the length of the channel, r the radius of the channel, and $\frac{dV}{dt}$ is the volume flow rate. The laminar flow develops a parabolic velocity profile where the fastest flow is located in the center of the channel farthest away from the frictional effects of the walls. The Hagen-Poiseuille equation is a solution under laminar conditions of the Navier-Stokes equations, which describe the behavior of the fluid flow in a general way [11]. Many books deal with the Navier-Stokes equations in more detail [5, 6, 12, 13].

In contrast to laminar flow, the regime of turbulent flow is characterized by inconsistent flow patterns and timely variations of velocity. This leads to a chaotic fluid mixture. Laminar and turbulent flow profiles (parabolic and constant) in a channel are illustrated in Fig. 2.

For Re below one, the behavior of a fluid depends mainly on its viscosity. This flow is called creeping flow or Stokes flow [6]. Laminar flows with Reynolds

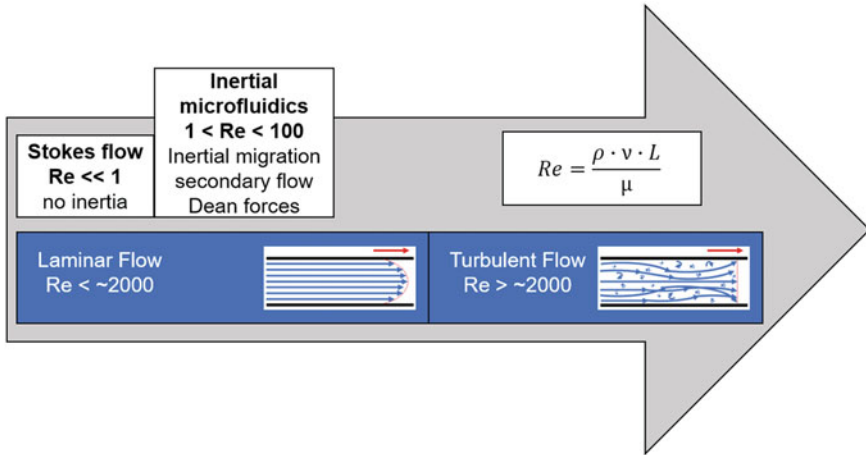


Fig. 3 The different regimes of flows in dependence of the Reynolds number

numbers between 1 and 100, where the momentum of the fluid cannot be neglected, also provide an interesting field of application, called inertial microfluidics [10, 14]. This regime offers schemes for the size-dependent separation of particles suspended in a fluid. The different regimes of flows are shown in Fig. 3 in dependence of the Reynolds number.

2.2 Surface Effects

With miniaturization, surface effects including surface tension and electrokinetic effects are becoming more and more important. Interface effects between phases (solid, gaseous or liquid) can be exploited as drive concepts for microfluidics.

The surface tension is created by cohesive forces between liquid molecules. Cohesion describes the tendency of similar molecules to adhere to each other. A molecule of a liquid feels attraction forces in all directions from other nearby molecules as long as it is located within the volume of the liquid. This is the lowest energy configuration for liquid molecules unless they are in contact with hydrophilic materials. A molecule that has moved to the surface has assumed a less energetically favorable state. It is now only attracted by the molecules below the surface. Therefore, creating and enlarging a surface or an interface consumes energy or sets energy free [15]. In microfluidic channels, surface tension and interface tension forces between fluid and wall lead to moving or holding fluids [16]. Interface generation (wetting) and interface reduction (dewetting) have also to be considered for two-phase flows and droplet formation [17].

Electrokinetic effects are based on surface charges at the interface between a solid and a liquid phase or between two liquid phases. The electrokinetic effects are

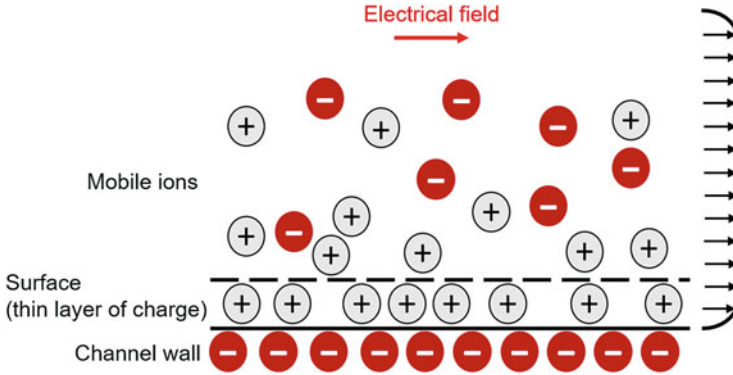


Fig. 4 Illustration of the electrokinetic effect: electric double layer and flat velocity profile of electroosmotic flow

produced by an electric double layer [18] created by the interaction between an electrolyte and a charged surface. The ions in a solution are attracted by the charged surface and form a thin layer of charge which adheres to the surface by the electrostatic force. An adjacent more diffuse layer with mobile ions can move under the influence of an electric field. In a microchannel, this motion draws the entire liquid with it and causes a flat velocity profile with a uniform flow velocity (see Fig. 4) [19]. There are four electrokinetic effects that are important in microfluidics:

- Electrophoretic particle motion (by double layer at the interface of suspended particles and liquid)
- Electroosmotic flow (by double layer at the interface of microchannel wall and liquid)
- Sedimentation potential (by an ionized liquid flowing against a charged particle surface)
- Streaming potential (by the movement of charge carriers along charged surfaces)

2.3 Diffusion and Mixing

By diffusion, molecules or very small particles are transported from an area of higher concentration to an area of lower concentration [20]. Diffusion is irreversible and random [6]. The diffusion-driven motion of a single molecule or particle cannot be accurately predicted. The flux of substance particles or molecules can be described by Fick's laws [21].

One-dimensional Fick's first law: the flux j , the mass of a substance through a unit area in a unit of time, in one direction, is proportional to the gradient of concentration in this direction [18]:

$$j = -D \frac{\partial c}{\partial x}$$

where D is the diffusion coefficient [m^2/s] which indicates how quickly a substance is dispersed in the medium [22] and c is the concentration of solute [mol/m^3]. With conserved mass, the Fick's first law results in Fick's second law [20]. It describes the change of the concentration gradient by diffusion overtime at any given point:

$$\frac{\partial c}{\partial t} = D \frac{\partial^2 c}{\partial x^2}$$

To solve this equation, boundary and initial conditions must be set which describe the shape of the time-dependent concentration profile [20]. The solution of the equation is dependent on the boundary conditions but the term $2\sqrt{Dt}$ can be found in many solutions [3]. This term indicates how far in the x -direction the initial concentration has diffused in the time t and is therefore referred to as diffusion length. The diffusion time is proportional to the square of the length [6, 21]. So that diffusion as mass transport is only suitable for short lengths.

Diffusion transport and wall effects (e.g., wall friction) are of greater importance in microfluidic systems than in macrosystems. In laminar flow, fluids flow in parallel layers that do not mix by convection. Transversal mass transport and mixing are therefore only driven by diffusion [23]. The mass transport is characterized by the dimensionless Péclet number Pe which reflects the ratio of the convection rate to the diffusion rate in a system [23]

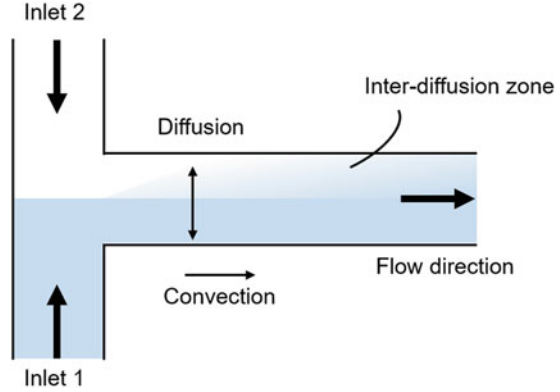
$$Pe = \frac{1}{2} \frac{t_{\text{diffusion}}}{t_{\text{convection}}} = \frac{\nu \cdot L}{D}$$

where $t_{\text{diffusion}}$ is the typical time for diffusive transport and $t_{\text{convection}}$ is the typical time for convective transport and D is the diffusion coefficient for the material to be transported or mixed in a certain fluid. For $Pe \ll 1$, diffusion dominates the transport as is typically the case with small channel diameters (tens to hundreds of micrometers [7]) in microfluidic systems. Therefore, mixing in microfluidic environments requires different concepts than in the macroworld. Figure 5 illustrates the mass transport in a microfluidic channel with two adjacent liquid phases.

2.4 Transport of Suspended Particles

Under laminar conditions with $Re > 1$ (the regime of inertial microfluidics), the parabolic velocity profile in Poiseuille flow produces a shear-induced inertial lift force that drives particles away from the center of the channel towards the channel walls [24]. At the same time, a wall-effect lift force resulting from a pressure increase

Fig. 5 Mass transport between two fluids within a microfluidic channel



between the particle and the wall pushes a particle away from the wall. As a result particles in a fluid are not evenly distributed but take up an equilibrium position. The positions of the particles depend on the size of the particles and the channel size and geometry. The two lift forces compose the inertial lift force F_L [25, 26]:

$$F_L = f_L \left(\text{Re}, \frac{x}{h} \right) \cdot \frac{\rho U_m^2 a^4}{D_h^2}$$

where ρ is the density, U_m is the maximum flow velocity, a is the particle diameter, D_h is the hydraulic diameter, and f_L is the nondimensional lift coefficient which depends on the Reynolds number of the channel and the lateral position of the particle.

On this basis of dimensionless numbers and physical laws, processes such as mixing, separating, sorting, splitting, and recombining, two-phase flows, droplets, and surface tension can be characterized [6, 20].

3 Microfluidic Fabrication Techniques

3.1 Clean-Room Microfabrication

Most microfluidic systems consist of different micro- or nanofabricated layers that are assembled to a three-dimensional system. The fabrication of such microfluidic systems is based on processes adapted from semiconductor or MEMS (micro electro mechanical system) fabrication technology that require a clean-room environment and are typically based on monocrystalline silicon and/or glass wafers as base materials. Typical fabrication routes consist of photolithography, etching techniques, thin film deposition, and other clean-room methods [3]. In recent years, these methods have been further developed leading to various deposition, wet and dry etching, as well as bonding techniques. When photolithography is used for the

fabrication of master molds, multiple replications of microsystems made of polymers are facilitated. This fabrication route is called soft lithography indicating that the key process still comes back to photolithography.

3.2 Photolithography

Photolithography is a mask-based technique using light-sensitive polymers (photoresists). Photoresists allow a transfer of microstructures onto a substrate by exposing and developing because they are reactive to UV-light typically in wavelengths between 193 and 436 nm. Commonly, masks made of UV-transparent material like glass with chromium microstructures are used for the pattern transfer. Exposure leads to a chemical modification of the photoresist. The exposed parts of the photoresist are rendered soluble (positive resist) or insoluble (negative resist) in a development solution, as shown in Fig. 6. The structured layer of photoresist is subsequently used for masking, e.g., in an etching process.

3.3 Deposition Techniques

In micro- and nanofabrication, different material layers or thin films are deposited to create, e.g., 3-dimensional structures, integrate electrical elements, or generate masking layers, insulating layers, or biochemically selective layers (like antibodies or enzymes) on a substrate. Usually, layers of metals, silicon-containing compounds, or plastics are used to create functional microsystems [27].

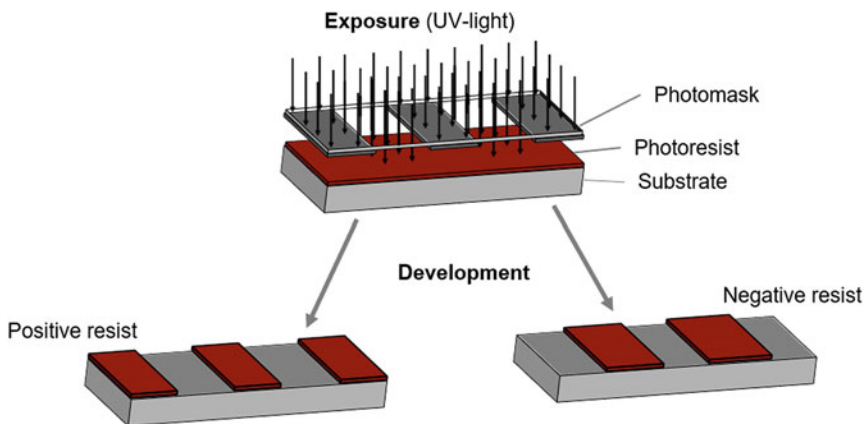


Fig. 6 Sketch illustrating photolithographic patterning with positive and negative resist

Thin film deposition techniques are categorized in physical vapor deposition (PVD), chemical vapor deposition (CVD), and chemical solution deposition. In PVD techniques, the deposition material is transferred by physical effects (evaporation or sputtering) into the vapor phase. The released atoms condense at the surface of the substrates. In CVD techniques, chemical reactions are used for deposition. The chemical reaction is triggered by thermal energy, by plasma or using a laser beam.

3.4 Etching Techniques

Etching techniques are exploited to remove solid materials during the microfabrication. In this way, 3-dimensional structures can be created from planar continuous layers. Etching techniques can be divided into isotropic and anisotropic as well as into wet and dry etching. The first distinction of etching techniques is based on the etching profile. In isotropic etching, the etch rate is identical in all directions [28]. In anisotropic etching, the etch rate is direction-dependent. The value A describing the anisotropy represents the relation between the lateral and the vertical etch rate [20]. A equals one for isotropic etching and zero for completely anisotropic etching. The schematic in Fig. 7 illustrates the difference between isotropic and anisotropic etching processes.

The distinction of wet and dry etching techniques results from the aggregated conditions under which the etching process takes place. For wet chemical etching, a chemical solution is used to etch thin films. The substrate is either placed in the etching solution or the solution is sprayed onto the substrate. Many wet etching techniques for monocrystalline silicon allow very selective etching, but wet metal etching techniques are isotropic [13]. For silicon and glass, solutions based on hydrofluoric acid (HF) are used to achieve large etching depths. In the case of single-crystalline materials such as silicon, anisotropic etching follows the crystal directions [28].

Etching in a gaseous atmosphere is called dry etching. Here, the material is removed by chemical or physical reactions or a combination of both. For chemical mechanisms, reactive radicals are used. This etching technique is very selective and isotropic. If etching is achieved by bombarding the material with reactive or non-reactive ions, the effects can be chemical or physical. Purely physical mechanisms result in anisotropic etching profiles. The material selectivity of physical etching techniques is low [29].

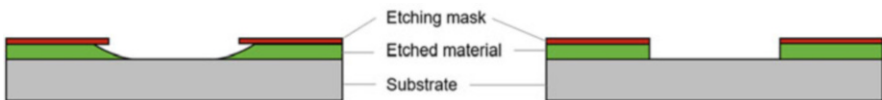


Fig. 7 Schematic illustration of isotropic etching (left) and anisotropic etching (right)

3.5 Bonding Techniques

Bonding techniques are required to assemble different layers to form 3-dimensional closed and sealed microfluidic systems. These techniques can be divided into direct or indirect bonding. Indirect techniques use an intermediate material layer. For glass and silicon bonding, anodic bonding is usually used, in which the layers to be combined are exposed to an electric field and an elevated temperature (shown in Fig. 8) [4]. This can be used to produce complex microfluidic chips [30–32]. An example is shown in Fig. 9.

For the bonding of two silicon layers, there is either the possibility of a thin glass layer as an intermediate material to enable anodic bonding or the possibility of direct silicon bonding. The direct bonding process of silicon is performed at 800°C [3]. In the case of two glass layers, the surfaces are first activated by O₂-plasma and then

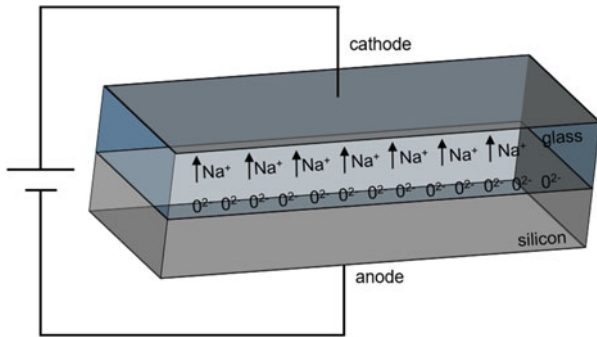


Fig. 8 The mechanism of silicon-glass anodic bonding

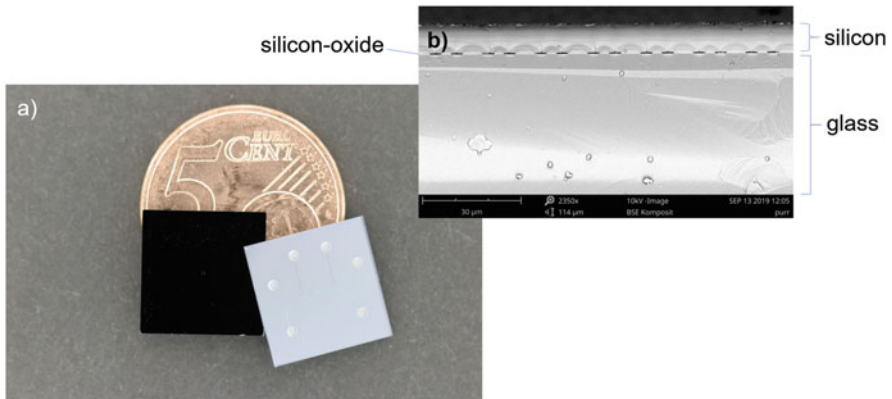
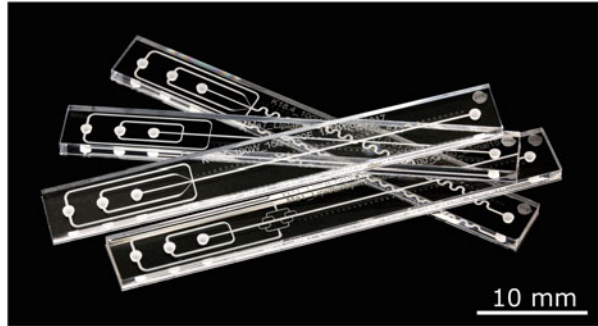


Fig. 9 Point-of-care diagnostic chip for the detection of specific biomolecules in small analytes with low concentrations using an optofluidic grating [32]. The optical grating consists of nanochannels in a thin silicon-oxide layer. By anodic bonding with unstructured glass, these channels are closed. (a) optofluidic chip front and back side; (b) SEM cross-sectional view of the optofluidic grating after anodic bonding of the top glass

Fig. 10 Transparent and chemically inert micromixers made entirely of glass for nanoparticle precipitation to improve the bioavailability of drugs. Two mirror-like structured glass wafers are cleaned with a high-pressure jet and Caro's acid and then thermally bonded together under pressure [33, 34]



combined by thermal bonding (in vacuum at 500–650°C for several hours) [3]. Another possibility to activate and clean the glass surface before thermal bonding under a pressure is the use of Caro's acid (sulfuric acid with hydrogen peroxide 1:1) [33, 34]. Systems made entirely of glass by thermal bonding are fully transparent and provide an inert environment as shown by the example of a Taylor Flow micromixers [33, 34] in Fig. 10. For other materials not mentioned, other bonding techniques (including adhesive interlayers) have to be used.

3.6 *Soft Lithography*

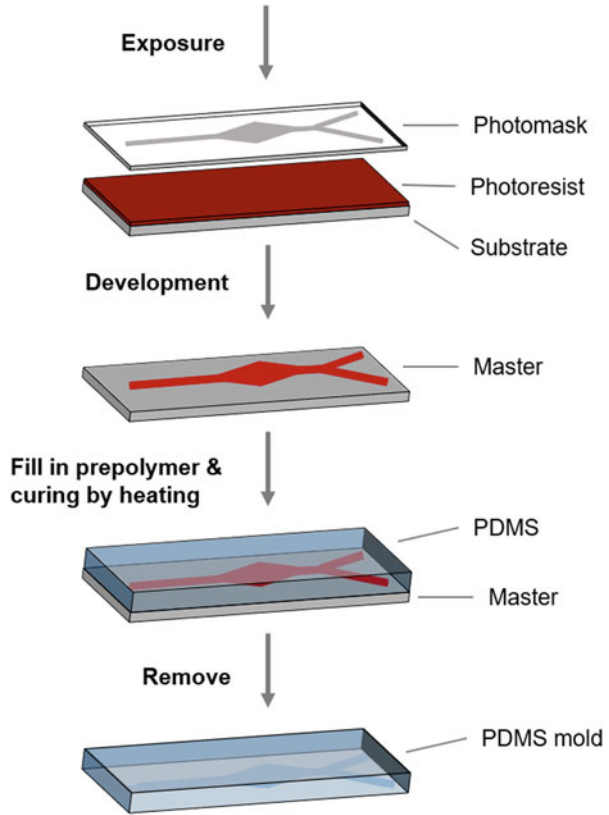
With soft lithography, the fabrication possibilities of photolithography could be extended by a replication method which requires only low cost equipment. Soft lithography comprises a group of techniques using a soft, elastomeric material to create structures with a high resolution between 30 nm and about 500 μm [35]. Soft lithography offers a low cost approach for creating microfluidic systems by replica molding [13].

Soft lithography consists of two steps: First, a master is traditionally created with the help of photolithography using hard materials like silicon or SU-8 photoresist. The master is used to structure stamps or molds. Polydimethylsiloxane (PDMS) is typically used for stamps and molds [36]. A prepolymer is filled into the master. By heating, the prepolymer crosslinks to a polymer and cures solid. After curing, the structured polymer can be removed from the mold as illustrated in Fig. 11. The master is not damaged by this process and can be used several times to fabricate many microsystem copies.

Soft lithography comprises several other techniques that may differ in resolution and procedure. An overview of the techniques and their resolutions is given in [37–41].

For the fabrication of a 3-dimensional closed and sealed microfluidic system, PMDS layers with microchannels can be bonded to another PDMS layer or a glass layer. The surfaces of both layers are pretreated by O₂-plasma. This first step cleans the surface and activates it (makes it hydrophilic) for the subsequent chemical bonding process. When two activated surfaces are brought into contact for a few

Fig. 11 Schematic illustration of fabricating a PDMS mold using a master



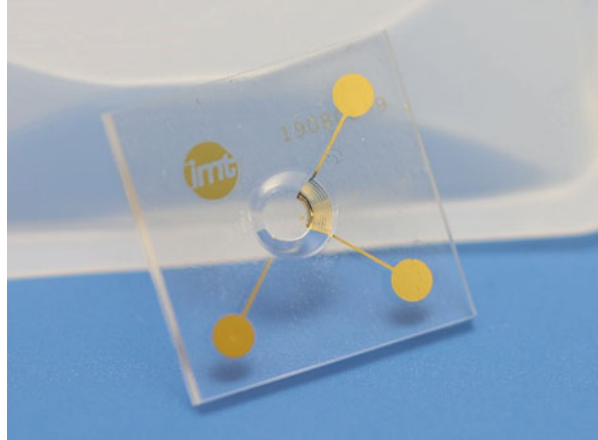
hours, they bond irreversibly. An increased temperature accelerates the bonding process [42, 43].

3.7 Maskless Micro- and Nanofabrication

Many mask- and moldless fabrication techniques have been invented. The benefit is to reduce the effort for design changes and to allow microfabrication with alternative materials and in some cases higher resolution. In the further development of photolithography, an electron beam is used as an exposure source. Here, an electron beam is used to expose an electron reactive resist. This technique is maskless as the electron beam can be moved over the sample and cures the resist locally. Due to the short wavelength of accelerated electrons, higher resolutions can be achieved compared to optical lithography. Structure sizes of less than 10 nm are possible [44].

Pulsed laser ablation is also a maskless process. Laser ablation is the removal of surface material by laser beam exposure [45]. Integrated CAD (computer-aided design) software enables different heights and widths of each structure. With

Fig. 12 Microbioreactor fabricated by femtosecond laser pulses in which any moving mixer component is eliminated by using capillary surface waves for homogenization [47]. Essential data during cell growth can be recorded using embedded sensors



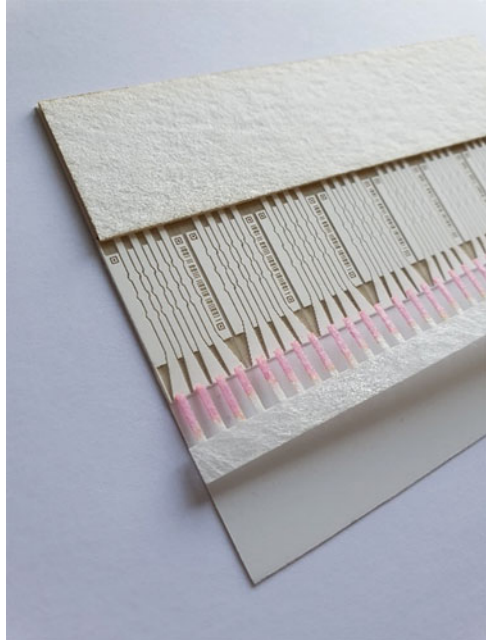
ultrashort laser pulses ($< 10^{-12}$ s), the ablation is almost non-thermal [46]. Since the expulsion of the ablated material is very fast, there is no thermal exchange with the environment. The working edges of this process are very sharp and smooth. Due to the non-linear absorption of the femtosecond (fs) laser pulses, this technology is particularly suitable for glass processing [46]. Since no heat is generated, even thermally sensitive materials can be structured. Figure 12 shows the example of a microbioreactor fabricated by pulsed laser ablation of glass for cell cultivation in pharmaceutical testing [47].

Because of their non-linear absorption, fs-lasers can also be used to modify small volumes inside an otherwise transparent material such as glass [48]. Subsequent etching of these modified areas allows direct 3-dimensional fabrication of a microfluidic glass device [49].

Additive fabrication techniques such as 3D-printing allow rapid prototyping of microfluidics made of polymers without a master, or the necessity for substrate bonding techniques. There are a number of rapid prototyping techniques such as stereolithography, fused deposition molding, and multi jet molding, which are discussed in [50]. However, the resolution of 3D-printing is in most cases not yet comparable to the resolution that can be obtained with lithographic approaches. For the fabrication of complex 3-dimensional structures with high resolution, two-photon polymerization (2PP) by femtosecond laser pulses can be used. This technique enables structures down to 100 nm [51]. By focusing ultrashort laser pulses into a UV-curable photoresist, only in a small volume around the focal point, sufficiently high intensity for curing by two-photon absorption is achieved. Using a material that is sufficiently transparent to the laser wavelength, it is possible to induce polymerization in small voxel elements in deeper layers of the material [52, 53]. Thus 3-dimensional structures can be created. After exposure, the photoresist is developed to remove all non-polymerized areas.

Through the further development of fabrication techniques, microfluidic systems with paper as base material could also be further developed. The basic principle for

Fig. 13 Biosensor on nitrocellulose paper structured by laser ablation with functionalized detection areas [56]



paper-based microfluidics consists of paper division into hydrophilic and hydrophobic areas [54]. This creates areas that transport the liquids by capillary forces and areas that repel them. Today there are many maskless production techniques besides photolithography [54]. Here, wax printing is often used [55]. Wax structures are printed directly onto the paper surface and solidify on contact to create selective hydrophobic areas. By subsequently heating the paper, the wax melts and penetrates the entire thickness of the paper. Hydrophobic barriers and thus hydrophilic channels are created. Other mask- and moldless techniques for fabrication of paper-based microfluidics use, e.g., laser treatment or inkjet printing [54]. Figure 13 shows an example of a paper-based biosensor. Hydrophilic nitrocellulose channels are defined by laser ablation [56]. The resolution of barriers and channels created with this technique is much better than with the methods described above, allowing the integration of complex fluidic networks for multiparametric detection and calibration.

4 Conclusion

This chapter has given an overview of the basic concepts and fabrication methods, which characterize the development of microfluidic systems.

The smaller the system, the greater the ratio of surface area to volume. In microchannels, laminar flow can be assumed, since the (viscous) frictional forces

Table 1 Differences between macro- and microfluid flows

	Microworld		Macroworld
	Stokes flow	Inertial microfluidics	
Main operating forces	Surface and viscous forces: e.g., surface tension, electrostatic and electrokinetic forces	Viscous as well as inertial forces: e.g., inertial migration, fluid (secondary flow), particle (centrifugal force)	Volume forces e.g., gravity and inertia: Surface tension and electrokinetic forces are neglectable
Flow	$Re \ll 1$ Laminar flow	$1 < Re < 100$ Laminar flow	Turbulent flow for $Re \gg 2,000$
Transverse mass transport and mixing	$Pe \ll 1$ Diffusion dominates	Diffusion and convection	$Pe \gg 1$ Convection dominates; diffusion neglectable

relative to the inertial forces lose importance. The laminar flow has a parabolic velocity profile and the fastest flow is in the center of the microchannel. Surface tension and interfacial tension forces between fluid and wall cause fluids to be moved or held in microchannels. Diffusional transport and wall effects are more important in microfluidic systems than in macrosystems. Transversal mass transport and mixing are driven only by diffusion. Fluids flow in different parallel layers that do not mix by convection. Table 1 is summing up the most important differences between macro- and microworld.

Typical microfabrication routes consist of photolithography, etching techniques, thin film deposition, and other clean-room methods based on monocrystalline silicon and/or glass wafers as base materials. Soft lithography techniques extend the fabrication possibilities of photolithography using a soft, elastomeric material. Today, for example, electron beam as exposure source, pulsed laser ablation, or rapid prototyping techniques additionally enable a mask- and moldless fabrication of microfluidic systems.

This chapter can serve as a condensed introduction to the field of microfluidics before examples of special systems and special procedures are discussed in the following chapters.

References

1. Zhang JXJ, Hoshino K (2019) Microfluidics and micro total analytical systems molecular sensors and nanodevices. Elsevier, Amsterdam, pp 113–179
2. Li D (2015) Encyclopedia of microfluidics and Nanofluidics. Springer, New York
3. Büttgenbach S, Constantinou I, Dietzel A, Leester-Schädel M (2020) Case studies in micromechatronics. Springer, Berlin
4. Song Y, Cheng D, Zhao L (eds) (2018) Microfluidics. Fundamentals, devices and applications. Wiley-VCH, Weinheim

5. Dietzel A (2016) A brief introduction to microfluidics. In: Dietzel A (ed) *Microsystems for pharmatechnology*, Bd 235. Springer, Cham, pp 1–21
6. Bruus H (2011) *Theoretical microfluidics*. Oxford master series in physics condensed matter physics, Bd 18. Oxford Univ. Press, Oxford
7. Nguyen N-T, Wereley ST, Shaegh SAM (2019) *Fundamentals and applications of microfluidics*. Integrated microsystems series. Artech House, Norwood
8. Sackmann EK, Fulton AL, Beebe DJ (2014) The present and future role of microfluidics in biomedical research. *Nature* 507(7491):181–189. <https://doi.org/10.1038/nature13118>
9. Whitesides GM (2006) The origins and the future of microfluidics. *Nature* 442(7101):368–373. <https://doi.org/10.1038/nature05058>
10. Zhang J, Li W, Alici G (2017) Inertial microfluidics: mechanisms and applications. In: Zhang D, Wei B (eds) *Advanced mechatronics and MEMS devices II*, Bd 189. Springer, Cham, pp 563–593
11. Ruffert C (2018) *Mikrofluidische Separationsverfahren und -systeme. Ihr Einsatz zur Rückgewinnung von Katalysatorwerkstoffen*. Lehrbuch. Springer, Berlin
12. Castillo-León J, Svendsen WE (eds) (2015) *Lab-on-a-chip devices and micro-total analysis systems. A practical guide*. Springer, Cham
13. Zhang JXJ, Hoshino K (2018) *Molecular sensors and nanodevices. Principles, designs and applications in biomedical engineering*. Micro & nano technologies. Elsevier, Amsterdam
14. Zhang J, Yan S, Yuan D, Alici G, Nguyen N-T, Ebrahimi Warkiani M, Li W (2016) Fundamentals and applications of inertial microfluidics: a review. *Lab Chip* 16(1):10–34. <https://doi.org/10.1039/c5lc01159k>
15. Convery N, Gadegaard N (2019) 30 years of microfluidics. *Micro Nano Eng* 2:76–91. <https://doi.org/10.1016/j.mne.2019.01.003>
16. Chen X, Wu H, Wu J (2018) Surface-tension-confined droplet microfluidics. *Chinese Phys B* 27(2):29202. <https://doi.org/10.1088/1674-1056/27/2/029202>
17. Bashir S, XCi S, Bashir M, Rees JM, Zimmerman WBJ (2014) Dynamic wetting in microfluidic droplet formation. *Biochip J* 8(2):122–128. <https://doi.org/10.1007/s13206-014-8207-y>
18. Nguyen N-T (2004) *Mikrofluidik*. Vieweg+Teubner Verlag, Wiesbaden
19. Holmes D, Gawad S (2010) The application of microfluidics in biology. *Methods Mol Biol* 583:55–80. https://doi.org/10.1007/978-1-60327-106-6_2
20. Dietzel A (ed) (2016) *Microsystems for pharmatechnology*. Springer, Cham
21. Yildiz-Ozturk E, Yesil-Celiktas O (2015) Diffusion phenomena of cells and biomolecules in microfluidic devices. *Biomicrofluidics* 9(5):52606. <https://doi.org/10.1063/1.4923263>
22. Chen J, Chen D, Xie Y, Yuan T, Chen X (2013) Progress of microfluidics for biology and medicine. *Nano-Micro Lett* 5(1):66–80. <https://doi.org/10.1007/BF03354852>
23. Squires TM, Quake SR (2005) Microfluidics: fluid physics at the nanoliter scale. *Rev Mod Phys* 77(3):977–1026. <https://doi.org/10.1103/RevModPhys.77.977>
24. Amini H, Lee W, Di Carlo D (2014) Inertial microfluidic physics. *Lab Chip* 14(15):2739–2761. <https://doi.org/10.1039/c4lc00128a>
25. Wang L, Dandy DS (2017) A microfluidic concentrator for cyanobacteria harvesting. *Algal Res* 26:481–489. <https://doi.org/10.1016/j.algal.2017.03.018>
26. Gou Y, Jia Y, Wang P, Sun C (2018) Progress of inertial microfluidics in principle and application. *Sensors (Basel)* 18(6). <https://doi.org/10.3390/s18061762>
27. Betancourt T, Brannon-Peppas L (2006) Micro- and nanofabrication methods in nanotechnological medical and pharmaceutical devices. *Int J Nanomedicine* 1(4):483–495. <https://doi.org/10.2147/nano.2006.1.4.483>
28. Katzen HH, Saile V, Leuthold J (2015) *Micro and nano fabrication*. Springer, Berlin
29. Madou MJ (2011) *Fundamentals of microfabrication and nanotechnology, three-volume set*. CRC Press, Boca Raton
30. Purr F, Bassu M, Lowe RD, Thürmann B, Dietzel A, Burg TP (2017) Asymmetric nanofluidic grating detector for differential refractive index measurement and biosensing. *Lab Chip* 17(24):4265–4272. <https://doi.org/10.1039/c7lc00929a>

31. Purr F, Eckardt M-F, Kieserling J, Gronwald P-L, Burg TP, Dietzel A (2019) Robust smartphone assisted biosensing based on asymmetric nanofluidic grating interferometry. *Sensors (Basel)* 19(9). <https://doi.org/10.3390/s19092065>
32. Purr F, Lowe RD, Stehr M, Singh M, Burg TP, Dietzel A (2020) Biosensing based on optimized asymmetric optofluidic nanochannel gratings. *Micro Nano Eng* 8:100056. <https://doi.org/10.1016/j.mne.2020.100056>
33. Erfle P, Riewe J, Bunjes H, Dietzel A (2019) Stabilized production of lipid nanoparticles of tunable size in Taylor flow glass devices with high-surface-quality 3D microchannels. *Micromachines (Basel)* 10(4). <https://doi.org/10.3390/mi10040220>
34. Erfle P, Riewe J, Bunjes H, Dietzel A (2017) Optically monitored segmented flow for controlled ultra-fast mixing and nanoparticle precipitation. *Microfluid Nanofluid* 21(12):1089. <https://doi.org/10.1007/s10404-017-2016-2>
35. Büttgenbach S (2016) *Mikrosystemtechnik*. Springer, Berlin
36. Fiorini GS, Chiu DT (2005) Disposable microfluidic devices: fabrication, function, and application. *Biotechniques* 38(3):429–446. <https://doi.org/10.2144/05383RV02>
37. Kim E, Xia Y, Whitesides GM (1996) Micromolding in capillaries: applications in materials science. *J Am Chem Soc* 118(24):5722–5731. <https://doi.org/10.1021/ja960151v>
38. King E, Xia Y, Zhao X-M, Whitesides GM (1997) Solvent-assisted microcontact molding: a convenient method for fabricating three-dimensional structures on surfaces of polymers. *Adv Mater* 9(8):651–654. <https://doi.org/10.1002/adma.19970090814>
39. Xia Y, Whitesides GM (1998) Soft lithography. *Annu Rev Mater Sci* 28(1):153–184. <https://doi.org/10.1146/annurev.matsci.28.1.153>
40. Kaufmann T, Ravoo BJ (2010) Stamps, inks and substrates: polymers in microcontact printing. *Polym Chem* 1(4):371. <https://doi.org/10.1039/b9py00281b>
41. Lipomi DJ, Martinez RV, Cademartiri L, Whitesides GM (2012) Soft lithographic approaches to nanofabrication polymer science: a comprehensive reference. Elsevier, Amsterdam, pp 211–231
42. Demming S (2011) Disposable lab-on-chip systems for biotechnological screening. *Shaker*
43. Eddings MA, Johnson MA, Gale BK (2008) Determining the optimal PDMS–PDMS bonding technique for microfluidic devices. *Prog Biomed Eng* 18(6):67001. <https://doi.org/10.1088/0960-1317/18/6/067001>
44. Gale B, Jafek A, Lambert C, Goenner B, Moghimifam H, Nze U, Kamarapu S (2018) A review of current methods in microfluidic device fabrication and future commercialization prospects. *Inventions* 3(3):60. <https://doi.org/10.3390/inventions3030060>
45. Sima F, Sugioka K, Vázquez RM, Osellame R, Kelemen L, Ormos P (2018) Three-dimensional femtosecond laser processing for lab-on-a-chip applications. *Nanophotonics* 7(3):613–634. <https://doi.org/10.1515/nanoph-2017-0097>
46. Guo B, Sun J, Hua Y, Zhan N, Jia J, Chu K (2020) Femtosecond laser micro/nano-manufacturing: theories, measurements, methods, and applications. *Nanomanuf Metrol* 3(1):26–67. <https://doi.org/10.1007/s41871-020-00056-5>
47. Meinen S, Frey LJ, Krull R, Dietzel A (2019) Resonant mixing in glass bowl microbio-reactor investigated by microparticle image velocimetry. *Micromachines (Basel)* 10(5). <https://doi.org/10.3390/mi10050284>
48. Sugioka K, Xu J, Wu D, Hanada Y, Wang Z, Cheng Y, Midorikawa K (2014) Femtosecond laser 3D micromachining: a powerful tool for the fabrication of microfluidic, optofluidic, and electrofluidic devices based on glass. *Lab Chip* 14(18):3447–3458. <https://doi.org/10.1039/c4lc00548a>
49. Włodarczyk KL, Carter RM, Jahanbakhsh A, Lopes AA, Mackenzie MD, Maier RRJ, Hand DP, Maroto-Valer MM (2018) Rapid laser manufacturing of microfluidic devices from glass substrates. *Micromachines (Basel)* 9(8). <https://doi.org/10.3390/mi9080409>
50. Kotz F, Helmer D, Rapp BE (2020) Emerging technologies and materials for high-resolution 3D printing of microfluidic chips. *Adv Biochem Eng Biotechnol*. https://doi.org/10.1007/10_2020_141

51. Burmeister F, Steenhusen S, Houbertz R, Asche TS, Nickel J, Nolte S, Tucher N, Josten P, Obel K, Wolter H, Fessel S, am Schneider, Gärtner K-H, Beck C, Behrens P, Tünnermann A, Walles H (2015) *Optically induced nanostructures: biomedical and technical applications. Two-photon polymerization of inorganic-organic polymers for biomedical and microoptical applications*, Berlin
52. Seniutinas G, Weber A, Padeste C, Sakellari I, Farsari M, David C (2018) Beyond 100 nm resolution in 3D laser lithography – post processing solutions. *Microelectron Eng* 191:25–31. <https://doi.org/10.1016/J.MEE.2018.01.018>
53. Nguyen AK, Narayan RJ (2017) Two-photon polymerization for biological applications. *Mater Today* 20(6):314–322. <https://doi.org/10.1016/j.mattod.2017.06.004>
54. Land KJ, McCabe LAND (2019) *Paper-based diagnostics*, 1. Aufl. Springer, Cham
55. Bhattacharya S, Kumar S, Agarwal AK (eds) (2019) *Paper microfluidics. Advanced functional materials and sensors*. Springer, Singapore
56. Hecht L, van Rossum D, Dietzel A (2016) Femtosecond-laser-structured nitrocellulose membranes for multi-parameter point-of-care tests. *Microelectron Eng* 158:52–58. <https://doi.org/10.1016/j.mee.2016.03.020>

Emerging Technologies and Materials for High-Resolution 3D Printing of Microfluidic Chips



Frederik Kotz, Dorothea Helmer, and Bastian E. Rapp

Contents

1	Introduction	38
2	Emerging Technologies	42
2.1	Stereolithography	42
2.2	Upcoming Trends in Optical 3D Printing	48
2.3	2-Photon Polymerization	50
2.4	Upcoming Trends in 2-Photon Polymerization	52
3	Emerging Materials	54
3.1	Noncytotoxic Polymers	54
3.2	Transparent Glass	56
3.3	Polydimethylsiloxane	59
3.4	Polymethylmethacrylate	62
4	Outlook	63
	References	63

F. Kotz (✉)

Laboratory of Process Technology, NeptunLab, Department of Microsystems Engineering (IMTEK), University Freiburg, Freiburg, Germany

Freiburg Materials Research Center (FMF), University Freiburg, Freiburg, Germany

e-mail: frederik.kotz@imtek.de

D. Helmer and B. E. Rapp

Laboratory of Process Technology, NeptunLab, Department of Microsystems Engineering (IMTEK), University Freiburg, Freiburg, Germany

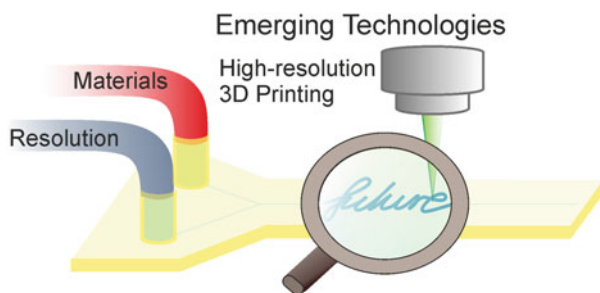
Freiburg Materials Research Center (FMF), University Freiburg, Freiburg, Germany

FIT Freiburg Centre for Interactive Materials and Bioinspired Technologies,
University Freiburg, Freiburg, Germany

e-mail: bastian.rapp@imtek.de

Abstract In recent years, 3D printing has had a huge impact on the field of biotechnology: from 3D-printed pharmaceuticals to tissue engineering and microfluidic chips. Microfluidic chips are of particular interest and importance for the field of biotechnology, since they allow for the analysis and screening of a wide range of biomolecules – including single cells, proteins, and DNA. The fabrication of microfluidic chips has historically been time-consuming, however, and is typically limited to 2.5 dimensional structures and a restricted palette of well-known materials. Due to the high surface-to-volume ratios in microfluidic chips, the nature of the chip material is of paramount importance to the final system behavior. With the emergence of 3D printing, however, a wide range of microfluidic systems are now being printed for the first time in a manner that facilitates flexibility while minimizing time and cost. Nevertheless, resolution and material choices still remain challenges and in the focus of current research, aiming for (1) 3D printing with high resolutions in the range of tens of micrometers and (2) a wider range of available materials for these high-resolution prints. The first part of this chapter highlights recent emerging technologies in the field of high-resolution printing via stereolithography (SL) and 2-photon polymerization (2PP) and seeks to identify particularly interesting emerging technologies which could have a major impact on the field in the near future. The second part of this chapter highlights current developments in the field of materials that are used for these high-resolution 3D printing technologies.

Graphical Abstract



Keywords 2-photonpolymerization, 3D printed microfluidics, Materials, Stereolithography

1 Introduction

The field of microfluidics deals with the control and transfer of small quantities of liquids and thus requires miniaturized channel structures with sizes in the range of a few tens to hundreds of micrometers [1]. In the last few decades, microfluidics has found widespread applications ranging from chemical synthesis to biochemistry and

biotechnology. The field of biotechnology has particularly become closely linked with microfluidics – which is not surprising, given that biological substances are commonly dissolved in aqueous liquid and/or buffer solutions [2]. Microfluidics has been widely used in the field for a wide range of so-called lab-on-a-chip (LoC) systems in, e.g., drug discovery, diagnostics, biohazard detection, and bioanalytical devices, to name just a few applications [1, 3, 4].

Traditionally, microfluidic chips have been fabricated using silicon or glass micromachining [5, 6]. In the so-called “classical” manufacturing process, a mask is applied to the substrate, and the channels are then etched either using a wet or dry etching processes. These processes are complex, however, and accordingly require a high standard of laboratory equipment. Especially when a number of designs must be tested for a certain application, the “time-to-chip” (i.e., the time required from design to a ready chip) is crucial, and classical micromachining is typically very slow in that respect. A major game changer for the field of microfluidics has been the emergence of polymer microfluidics, which were much easier to structure and assemble [7]. An important contribution was the concept of rapid prototyping of microfluidic chips in polydimethylsiloxane (PDMS) which made microfluidic devices accessible to any standard laboratory without the need for any specialized equipment [8]. Over the years, many rapid prototyping approaches for microfluidics have been developed – including structuring of dry-film photoresists, laser structuring or casting of prepolymers [9–11]. These polymer processing technologies are typically limited in terms of freedom of design, however, and do not allow the fabrication of truly three-dimensional structures. Furthermore, they also usually require at least a two-step process, with an additional subsequent bonding step to close the microfluidic channel.

It is therefore not surprising that 3D printing has created major interest within the microfluidic community – promising to facilitate easy chip manufacturing while simultaneously shortening the “time-to-chip” and abolishing the need for lid bonding, thus allowing assessment of a great variety of designs at an early stage. Thus, 3D printing has been quickly adapted for microfluidics, and many different 3D printing technologies have so far been used including fused deposition modeling (FDM), inkjet printing, multijet printing, and stereolithography (SL) [12–17]. However, until recently, most of the 3D-printed microfluidic systems demonstrated features in the range of millimeters down to a few hundreds of micrometers. The field has therefore often been named *millifluidics* [18]. Researchers have printed a great variety of chips which actively use the 3D manufacturing processes to develop millifluidic systems – including components such as 3D mixers and gradient or droplet generators but also active components like valves or pumps [19–22]. Figure 1 shows the comparison of a microfluidic structure fabricated by a dry-film rapid prototyping approach needing multilayer lamination and alignment (see Fig. 1a) and the equivalent mixer structure fabricated using SL printing (see Fig. 1b). The structures printed with a commercial SL printer are an order of magnitude larger than the conventional structures, with channel sizes of $1,000 \times 500 \mu\text{m}$ [19].

The primary focus of 3D printing of millifluidics on such commercial machines has been largely focussed on producing novel and complex structures that are

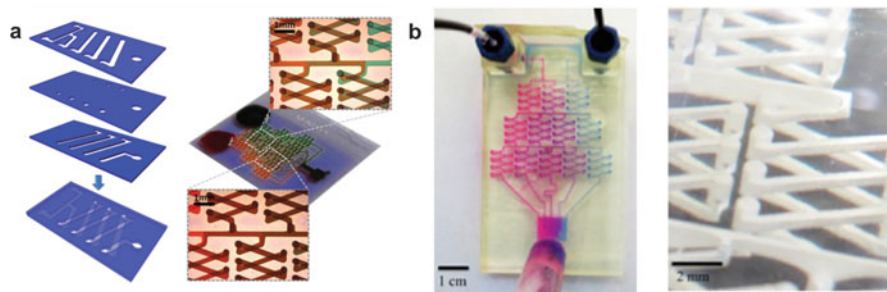


Fig. 1 Comparison of microfluidic rapid prototyping and millifluidic 3D printing: **(a)** Classical multistep fabrication process for the fabrication of a microfluidic gradient generator. Left: Scheme of the multilayer manual assembly process. Right: Assembled microfluidic chip. Reproduced with permission from Royal Society of Chemistry (RSC), 2009 [9]. **(b)** The same design directly fabricated using stereolithography printing. Reproduced with permission from RSC, 2014 [19]

impractical to manufacture through conventional fabrication techniques. For example, Grigoryan et al. have demonstrated the fabrication of vascular networks useful for exploring the oxygen transport and flow of human red blood cells (see Fig. 2a) [23]. They have further demonstrated that the photoresins developed in their work can be used for the fabrication of complex tissue engineering models by fabricating structural features inside printed hydrogels to design liver tissue (see Fig. 2b) [23]. Other effects of fluid dynamics have also been exploited in millifluidic structures, such as separation of magnetic particles and analytes by Dean forces, as reported, for instance, by Lee et al. (see Fig. 2c-e) [24].

Why is distinguishing between milli- and microfluidics important for biotechnology applications? First, the more general advantages of microfluidics, e.g., reduced sample and dead volume, reduced footprint of the devices as well as high sensitivity and high resolution cannot be fully exploited in millifluidics, and second, because the channel size of a system has a direct impact on the fluidic flow condition of the liquid which is transported within that system. Turbulence, for example, is an experimental parameter which is notoriously hard to control. Therefore the use of channel structures with laminar flow is often preferred. This is typically the case in microfluidics, but it cannot be guaranteed when the channel size is increased into the millimeter region, at least not with flow rates relevant to mimic natural environments. Cells however react very differently to changing flow conditions and profiles, as different shear stresses and forces are induced [25]. Third, to mimic the microenvironments of cells in nature, micrometer-sized channels need to be considered. In the human body, for instance, channel sizes range from $\sim 8 \mu\text{m}$ for capillaries to several millimeters for arteries, while cell sizes range between a few micron to around $100 \mu\text{m}$. Thus, especially for biotechnological applications (e.g., to facilitate effective control and recreation of complex microenvironments for cells), channel sizes must be reduced and brought to the third dimension.

Once the processes and machines for creating the right-sized microfluidic devices are available, another challenge lies within the available material palette accessible

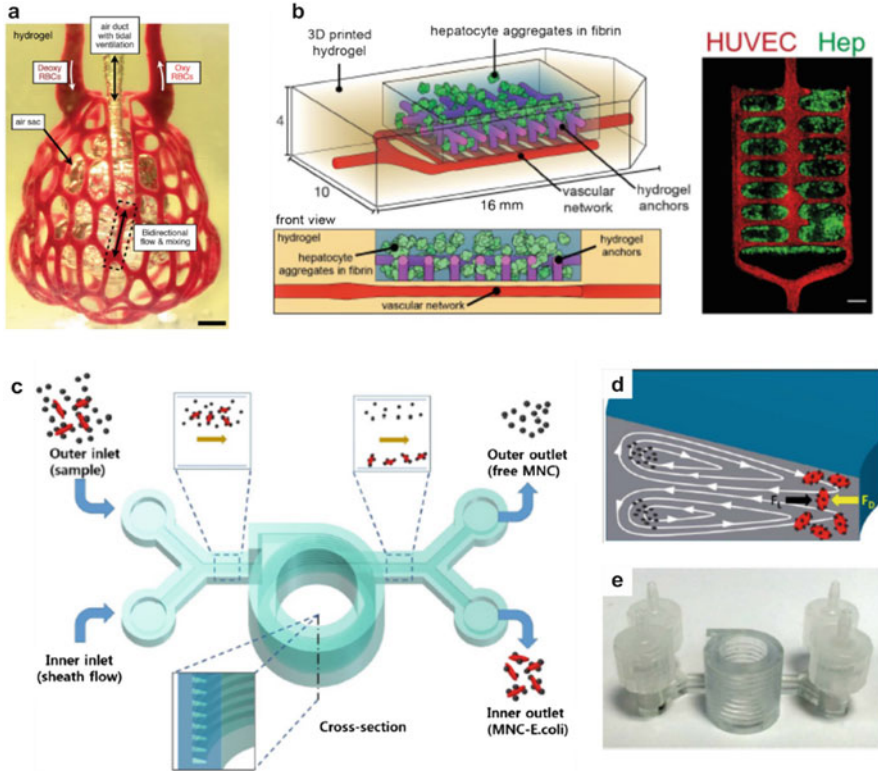


Fig. 2 Novel millifluidic concepts enabled by 3D printing on benchtop systems: **(a)** SL-printed channels in a photocurable hydrogel mimicking the distal lung subunit. **(b)** Vascular microchannel network printed in photocurable hydrogel below the tissue engineering construct consisting of a prevascularized hydrogel seeded with endothelial cells. **(a and b)** Reproduced with permission from Grigoryan et al., AAAS, 2019 [23]. **(c)** Principle of separation of captured bacteria by inertial focusing in a 3D-printed microfluidic channel. **(d)** Dean flow vortices in the channel. **(e)** 3D-printed device used for the detection of bacteria. **(c–e)** reproduced with permission from Lee et al., Springer Nature, 2015 [24]

via high-resolution 3D printing – especially for techniques such as SL. Most of the commercial resins used in the early stage were of unknown composition and barely biocompatible rendering these systems incompatible for the use in biotechnology. In this chapter, we will review some of the most recent trends in emerging technologies for the fabrication of truly microfluidic systems using high-resolution SL and 2-photon polymerization (2PP). We will further highlight upcoming trends which we believe have the potential to significantly impact this field in the near future. The second part of this chapter will provide an overview of emerging materials used for the fabrication of these truly microfluidic systems for biotechnology and gives an outlook on future work which may become possible by combining emerging technologies with promising new materials.

2 Emerging Technologies

2.1 Stereolithography

SL was the first 3D printing technology that was developed by Chuck Hull in 1986 [26]. Of all 3D printing technologies that are now available, SL remains one of the most established and most suitable technologies for the fabrication of microfluidic chips combining high resolution with affordable machinery. In SL, a photocurable material (so-called photoresin) is polymerized using structured light in a layer-by-layer fashion. The spatial shaping of light is achieved either using spatial light modulators (SLM) like a digital mirror device (DMD) or a liquid crystal display (LCD) or by using a laser in combination with a galvanometer scanner [27–30]. DMD-based systems are currently by far the most commonly used systems for printing microfluidic chips.

SL takes place in one of two forms: either a so-called bath configuration or a constrained surface configuration [31]. In the bath configuration, the photoresin is placed inside of a reservoir in which a movable stage is lowered layer by layer into the liquid photoresin. The polymerization of each single layer takes place at the air/photoresin interface. The *constrained surface configuration* is nowadays the mostly used configuration on the laboratory scale for fabricating microfluidic chips and will thus be discussed in more detail. Here, the photoresin is also placed inside a reservoir – however, the polymerization takes place through a transparent window on the bottom of the reservoir (see Fig. 3a). During the printing process, a build platform is immersed into the bath, and the first layer is polymerized in the constrained volume between the platform and the transparent window. Afterward, the stage is moved upward, allowing the photoresin to rewet the transparent window. Subsequently, the platform is lowered again such that a defined layer of liquid photoresin is formed between the last printed layer and the window.

The most common choices for photoresins are acrylate- or epoxy-based monomers in combination with a photoinitiator to trigger the photopolymerization process [32]. To further increase the resolution, admixtures can be added to the resin. Absorbers can be added to control the penetration of light into the resin and control the cure depth. Photoinhibitors can be added to optimize the lateral resolution and minimize effects like the so-called dark polymerization (i.e., the extension of the polymerization front into regions which have not been exposed) [32]. After the printing process has been completed, any non-polymerized photoresin is removed in a developing step using appropriate solvents.

SL has been widely used to fabricate microfluidic chips with channel dimensions in the range of millimeters down to a few hundreds of micrometers [18, 19, 33]. 3D printing of embedded channels with tens of micron resolution, however, is challenging and requires high-resolution printers combined with well-adapted resins. A sufficiently high lateral and horizontal resolution of the 3D printer can be achieved by using appropriate projection systems and actuators, and several groups have reported the development of these so-called microstereolithography systems

[28, 31, 34]. However, these systems alone do not directly allow 3D printing of embedded microfluidic channels, since several additional challenges have to be taken into account when compared to SL printing of open microstructures on the surface of a substrate. These challenges can be summarized as follows: (1) The resin inside the embedded channel may become polymerized by subsequent layer polymerization (*z-overcuring*); (2) during the printing process, uncured resin may become entrapped inside the channel, which cannot be removed during the developing step; and/or (3) systems with sufficiently high-resolution often lack the required lateral processing size as typical microfluidic chips require both high resolution and the ability to create structures of macroscopic feature sizes, e.g., for chip-to-world interfaces.

2.1.1 Challenge 1: Z-Overcuring – Polymerizing Resin in the Embedded Channel

Polymerization of uncured resin inside the embedded microfluidic channel (often called the “z-overcuring error”) has been one of the key challenges associated with fabrication of embedded microfluidic chips preventing a high control over the height of the channel. Looking at the model in Fig. 3a, the problem becomes obvious. Light

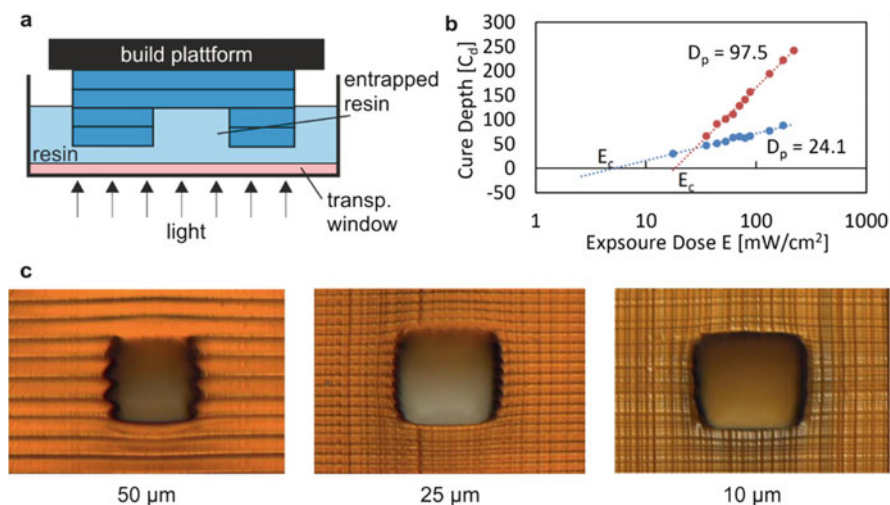


Fig. 3 3D printing of high-resolution microfluidic channels using SL: (a) SL printing in the so-called constrained surface technique. One challenge in printing embedded microfluidic channel lies in polymerizing the top layer of the channel without polymerizing entrapped resin inside the channel. (b) Working curve for SL printing showing two different curves with different critical exposure dose (E_c) and penetration depth (D_p). For high-resolution printing of embedded microfluidic systems, a slope with a D_p of 10–20 μm should be chosen. (c) Influence of the layer thickness on the printing process. (c) reproduced with permission from Gong et al., RSC Advances, 2015 [35]

needs to penetrate into the resin initiating the polymerization. The minimum cure depth hereby needs to be the thickness of the layer itself. However when polymerizing the first top layer which encloses the microfluidic channel, the light should not penetrate too deeply in order not to polymerize the resin entrapped inside the channel. Furthermore one needs to consider that all subsequent layers will furthermore deliver a small portion of exposure dose to the resin entrapped inside the channel [35]. If the sum of these exposure doses passes a critical polymerization threshold, the material in the channel will be polymerized. Therefore, it is important that the resin itself has a high absorbance at the specific wavelength spectrum of the printer. This is usually achieved by adding absorber molecules (e.g., isopropylthioxanthone (ITX) or 2-nitrophenyl phenyl sulfide (NPS)) with a high absorbance at the specific wavelength of 385 nm. The photoresin needs to be calibrated on the printer by measuring the cure depth in dependence of the exposure time resulting in a graph similar to the one in Fig. 3b. This working curve often follows the so-called Jacobs equation, named after Paul Francis Jacobs the Director of Research and Development in the early years of 3D systems [36].

$$C_p = D_p \ln \left(\frac{E}{E_c} \right)$$

C_p cure depth, D_p penetration depth, E exposure dose at the interface window resin, and E_c critical exposure dose.

These parameters can be easily derived by putting a droplet of resin on a slide and illuminating a test structure (like a rectangular or circular pattern) from the bottom through the slide while varying the exposure time at a fix intensity. Ideally, the slide should have the same thickness and be made out of the same materials as the transparent window. After development using appropriate solvents, the height of the created layer is measured. When plotting the measured height over exposure dose, D_p is the slope of the semi-logarithmic graph, and E_c is the intersection with the x-axis (see Fig. 3b). Since low cure depth values and the resulting small layer thicknesses are hard to measure, the curve is usually interpolated. To achieve a high control of the height dimension as required for 3D printing of microfluidic channels, a photoresin with a very low penetration depth D_p needs to be selected which can be achieved by increasing the amount of absorber. Gong et al. have shown that the minimum channel heights can be fabricated when the channel has the size of around 2–5 times D_p [28, 35]. Thus, when sub-100 μm channels are desired, the D_p should be around 10–20 μm .

Another important parameter for the fabrication of high-resolution microfluidic channels is the overall exposure dose required to print the part. This means that for creating a layer, one uses an exposure dose that is higher than the one needed for the polymerization of the desired layer thickness. Especially for macroscopic structures, this so-called offset is used to increase the mechanical stability of the print and prevent a delamination of the layers. The offset corresponds to an additional exposure dose compared to the corresponding value in the working curve. As an

example for a certain layer thickness, the exposure dose is often in the range of 1.2–2.0 times the dose estimated from the working curve. The offset is defined during *slicing* – the conversion of a 3D object into 2D projection patterns which are used for illuminating the single layers. This additional offset exposure dose is essential for attaching the layers to each other, but it also poses a problem for generating embedded channel structures – the additional exposure dose illuminates into the channel void and causes the channel to lose height. To prevent this problem, some slicers can correct for these offsets by making the channel structure higher than the set offset; this process is often called *z-compensation*. However, Gong et al. have demonstrated that for SL printing of sub-100 μm channels, this offset should be set to zero [28, 35]. Because this approach results in only a partial curing of the single layers, the parts are usually mechanically fragile after the print and require additional thermal or photocuring to allow for improved mechanical strength [28].

Another important parameter for printing high-resolution microfluidic channels is the layer thickness of the 3D-printed object. If a rather high layer thickness of, e.g., 50 μm is chosen instead of a smaller layer thickness (e.g., 10 μm), then the layer will experience a much more inhomogeneous exposure throughout the layer height. According to Lambert Beers law, in a full frontal polymerization, the front side of the layer receives a higher dose than the backside. This disparity not only generates significant internal stress, but it further results in less reactive groups at the front of the layer – thereby reducing the layer-to-layer adhesion [35]. For macroscopic parts, the illumination time can be increased to increase the layer-to-layer adhesion via the offset. Unfortunately, for fabricating microfluidic channels, this would once again lead to a polymerization of the entrapped resin. As a result, smaller layer thicknesses are usually preferred in that context in order to facilitate and ensure homogenous exposure and higher layer-to-layer adhesion. As can be seen from Fig. 3c, this results in much smoother side walls, since the inhomogeneous exposure profile results in serration effects. As a rule of thumb, 0.3–1 times D_p is usually a good start for the minimum layer thickness in high-resolution printing of microfluidic chips [35].

Using a benchtop SL printer with a lateral resolution of 27 μm and a layer height of 10 μm , microfluidic channels with a size of $60 \times 108 \mu\text{m}^2$ were printed using custom-made photoresins with appropriate absorption for the used wavelength of the printer [35]. Using a custom-built 3D printer with improved resolution in combination with an optimized resin which even shows a higher absorbance, the group has managed to 3D print microfluidic channels with a size of $18 \times 20 \mu\text{m}^2$ (see Fig. 4a). The developed process was further used to fabricate microfluidic pumps (see Fig. 4b, c); simple features like pillars, ridges, and traps which can be directly integrated into the embedded microfluidic channel (see Fig. 4d, e) and sub-100 μm microfluidic electrophoresis devices for the analysis of preterm birth biomarkers (see Fig. 4f) [28, 37, 38].

Männel et al. have studied several parameters in an effort to optimize the resolution of SL-printed microchannels using a commercial SL printer in combination with commercial photoresins. In particular, they focused on (1) printing orientation of the microfluidic chip; (2) movement of the build platform, and (3) voxel compensation. They found that by printing the channel along the z-axis and moving,

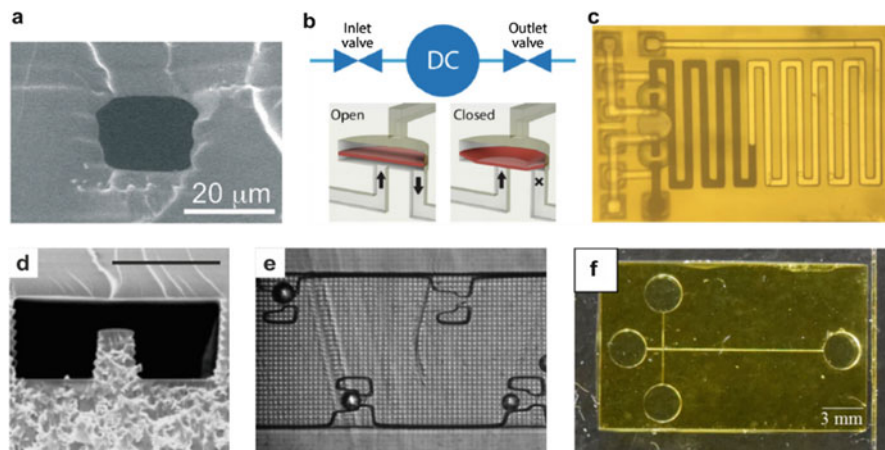


Fig. 4 Stereolithography printing of sub-100 μm channel microfluidic chips: (a) Scanning electron microgram (SEM) of channel cross section of a 3D-printed microfluidic channel with a size of $18 \times 20 \mu\text{m}^2$. Reproduced with permission from Gong et al., RSC, 2017 [28]. (b) Principle of 3D-printed microfluidic pump. (c) 3D-printed pump pumping liquid through the channel. (b and c) reproduced with permission from Gong et al., AIP, 2019 [39]. (d) SEM of an integrated ridge inside a microfluidic channel (scale bar: 100 μm). (e) Bead traps inside a microfluidic channel, which captured 25 μm particles. (d and e) Reproduced with permission from Beauchamp et al. MDPI, 2018 [37]. (f) Microfluidic electrophoresis device for the analysis of preterm birth biomarkers with a channel cross section of 50 μm . Reproduced with permission from Beauchamp, ACS, 2019 [38]

the build platform higher than the resin level after each printed layer, simple geometries like a straight channel can be printed with a channel diameter as small as 100 μm . A further improvement was realized by applying voxel compensation, whereby grayscale values are adjusted around the outer dimension of the channel structure. Using a combination of these approaches, the authors created channels with a cross section of 75 μm (see Fig. 5b) and demonstrated a successful approach in a 3D-printed flow cell for emulsion formation (see Fig. 5c–e) [40].

2.1.2 Challenge 2: Non-cured Resin Inside the Embedded Channel

The second challenge which limits high-resolution printing of microfluidic channels using SL is non-polymerized resin which blocks the channel. If the viscosity of the resin becomes too high, the fluidic resistance will become large enough to prevent the material from being fully washed out of the channel during development. This is why for high-resolution 3D printing of microfluidic channels, so far only low-viscosity photoresins with a viscosity in the range of around 50 mPas have been used. The concept of achieving a high control over the optical absorbance of the photoresin has thus far been limited to low molecular weight and low-viscosity monomers (mostly polyethylene glycol diacrylate 250 (PEGDA 250)) with a relatively small average molecular weight of 250 g/mol. Using higher viscous materials

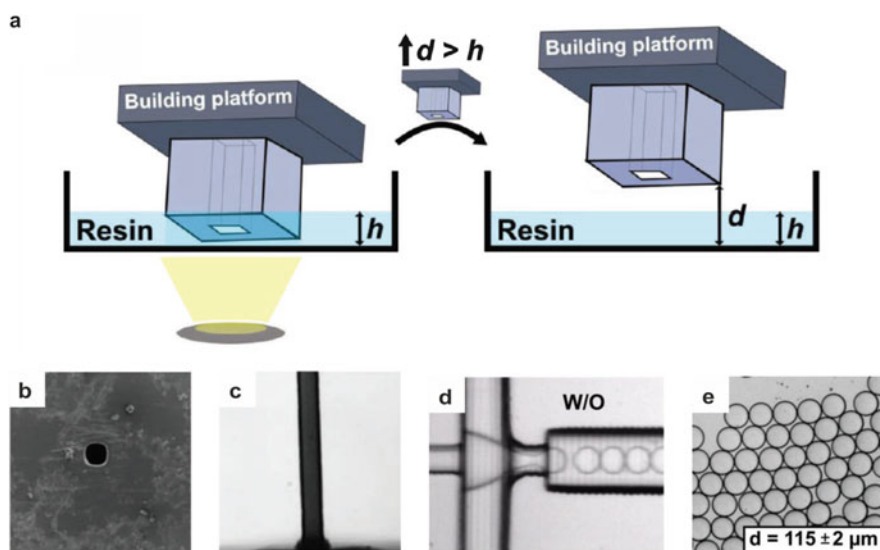


Fig. 5 High-resolution SL printing of microfluidic chips: (a) Higher-resolution printing of embedded microfluidic channels can be enabled by printing the channel in plane along the z-axis. The risk of blocked channels by non-cured resin can be reduced by moving the platform out of the resin vat before illuminating the next layer. (b) Microfluidic channel cross section with a cross section of $75 \times 75 \mu\text{m}^2$ achieved by using the outlined strategies (c) Top view of the microfluidic channel in (b). (d) Microfluidic flow cell printed using this methodology with a nozzle size of $75 \times 75 \mu\text{m}^2$ for water-in-oil and oil-in-water emulsion formation. (e) Droplets fabricated using the flow cell shown in (d). Reproduced with permission from Männel et al., Wiley, 2019 [40]

tends to result in clogged channels, since the entrapped non-polymerized resin is too viscous to be washed out of the channel. This has limited the usage of a wide range of photocurable materials with tailored material properties for the fabrication of embedded channels. One possible strategy could be 3D printing and post-processing at elevated temperatures, which would reduce the viscosity of the resin. The approach by Männel et al., (see Fig. 5), has also been shown to reduce the risk of entrapped material: printing the channel along the z-axis and lifting the build platform above the resin bath level after each printed layer allows the resin to flow out of the channel after each layer (see Fig. 5a). Using this method, commercial resins with a viscosity of around 500 mPas have been printed and successfully washed out of a channel [40]. Combinations of such strategies could allow the fabrication of more complex microfluidic chips in the future with a greater freedom in the choice of materials [23].

2.1.3 Challenge 3: High Resolution at High Lateral Sizes

Another issue of SL using SLMs like DMDs lies in the fact that increasing the resolution comes with a decrease in print area. To achieve non-clogged embedded

channels, the minimum feature size should be at least four times bigger than the projected pixel size [35]. To fabricate structures with high fidelity, the pixel size should ideally be at least ten times smaller than the minimum feature size. For example, for a structure in the range of 25 μm , the pixels of a DMD must be demagnified to 2.5 μm . However, using a state-of-the-art video resolution DMD with a pixel count of $1,920 \times 1,200$, this would result in a lateral print area of only around $5 \times 3 \text{ mm}^2$. This is a major issue – particularly since microfluidics usually requires tens of micron resolutions on a multiple centimeter-sized chip, especially if chip-to-world interfaces have to be included. Our group has therefore developed a (micro-)stereolithography system wherein a custom-made projection optics with a minimum pixel resolution of around 700 nm is assembled on a x/y linear stage [27, 41]. This setup allows stitching several high-resolution images beside each other – thus achieving the required high resolutions on a lateral printing area of $20 \times 15 \text{ cm}^2$. The Tesla mixer shown in Fig. 12b, for example, was structured using this system and was stitched together from 64 single images. This concept has so far only been shown for open microfluidic structures in a 2.5-dimensional lithography setup. The fabrication of 3D embedded microchannels remains to be shown.

2.2 Upcoming Trends in Optical 3D Printing

Recently, novel technologies have been introduced which specifically addressed the speed issues usually associated with SL. While all of these technologies have been labeled as new processes, they all essentially build on the single-photon polymerization 3D printing process which was first used in SL.

One of the first approaches in this context was introduced by Tumbleston et al. and is known as *continuous liquid interface printing* (CLIP), which is basically a high-speed SL process [42]. CLIP uses the controlled inhibition of the photopolymerization at the interface between the transparent window and the photoresin (see Fig. 6a). This process uses an oxygen-permeable window made of *Teflon AF* and creates a so-called dead zone by exposing the interface to oxygen. Above this dead zone, the photoresin stays liquid in a layer with a thickness of around 20–30 μm , and the build platform can be continuously moved out of the bath. Since the rewetting of the window and the reflow of photoresin are usually the most time-consuming process steps in SL printing, CLIP has been claimed to be $100\times$ faster than conventional SL printing. CLIP is further interesting for printing microstructures, since separation forces are naturally very small in this process. Figure 6b and c show exemplary micropaddles and microneedles with feature sizes in the range of tens of micron. Printing of embedded microchannels using CLIP has not yet been reported.

Similar approaches have followed the idea of CLIP in using a non-polymerized interface layer. De Beer et al. have created an inhibited dead zone by illuminating a custom-made photoresin with complementary photoinitiators and photoinhibitors [43]. The resin is illuminated with two different wavelengths – a flood exposure at

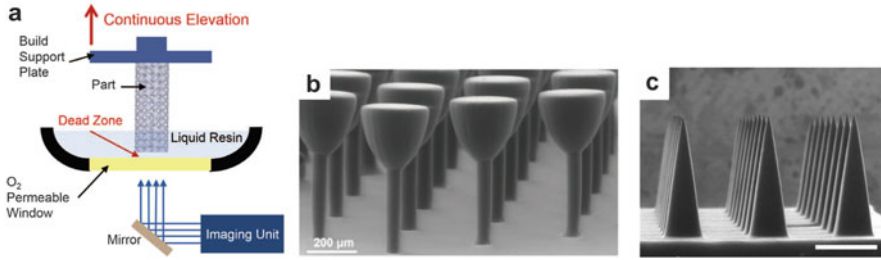


Fig. 6 *Continuous liquid interface printing (CLIP)* (a) Principle of CLIP. A dead zone is created between the oxygen-permeable window and the liquid resin. The part is fabricated on top of the dead zone by continuously moving the build platform and simultaneously changing the images from the projection optic. (b) High-resolution 3D printing using CLIP showing micropaddles with stems with a diameter of 50 μm . Figure a/b reproduced with permission from Tumbleston et al., AAAS, 2019 [42]. (c) Microneedles array fabricated using CLIP (scale bar: 500 μm). Reproduced with permission from Johnson et al., PLOS ONE, 2016 [45]

365 nm inhibits the polymerization, while illumination at 458 nm polymerizes the material. A combination of both wavelength creates an inhibited *dead zone* at the interface of the resin and the transparent window allowing for continuous printing. *Nexa3D* has commercialized a SL printer using a membrane infused with a liquid lubricant, which also allows for high-speed continuous SL printing. Alternatively, *NewPro3D* has used a wettable hydrogel membrane which allows to continuously print with high-speeds. Recently, Walker et al. presented a technology termed *high-area rapid printing* (HARP), which prints on top of a moving immiscible fluorinated oil [44]. By continuously moving the liquid oil layer with respect to the printed part, the adhesion forces are reduced, and polymerization debris can be removed from the interface while directly cooling the printed area. Although all of these concepts are promising candidates for high-speed manufacturing of microfluidic channels, to date none of them have actually been used to fabricate microfluidic structures.

A novel technology termed computed axial lithography (CAL) was also recently introduced by Kelly et al., which avoided the layer-by-layer manufacturing methodology entirely [46]. Instead of building an object up in a layer-by-layer fashion, in the CAL approach, light patterns are projected into the material volume as 2D images from different angles (see Fig. 7a). The superposition of the single exposures results in a 3D dose distribution that is high enough to locally polymerize the material. The process is capable of printing centimeter-scaled objects significantly faster than common layer-by-layer-based principles, with total processing times between 30 and 120 s. The authors have demonstrated that using this process, they can fabricate lattice structures with features as small as 300 μm (see Fig. 7b). Bernal et al. have used this optical tomography-inspired approach to generate cell-laden tissue constructs (see Fig. 7c) fabricated out of gelatin-based photoresponsive hydrogels, which showed a viability greater 85% [47]. Besides printing trabecular bone models and meniscal grafts, the authors also printed hydrogel-based ball and cage fluidic valves (see Fig. 7d).

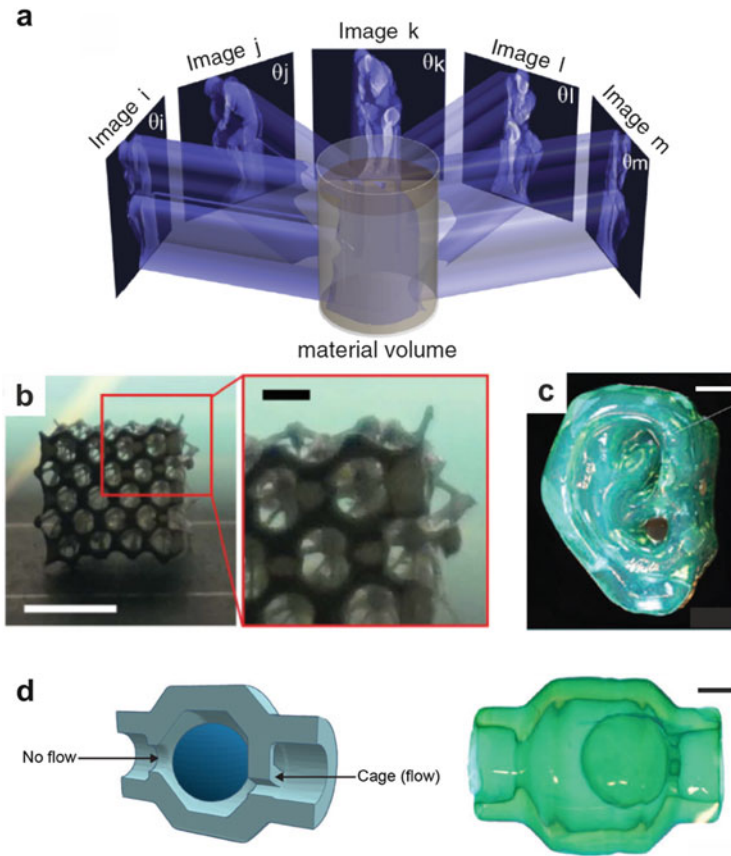


Fig. 7 Volumetric printing of photocurable resins using computed axial lithography (CAL). (a) Schematic of volumetric printing process. The pattern is illuminated from different directions resulting in a local exposure dose pattern inside the photocurable material. (b) Lattice structure fabricated using CAL (scale bar: 5 mm; inset: 1 mm). (c) 3D-printed hydrogel (scale bar: 2 mm). (d) Fluidic ball-cage valve (left: CAD model, right: actual 3D-printed valve structure, scale bar: 2 mm). Figure (a and b) reproduced with permission from Kelly et al., AAAS, 2019 [46]. Figure (c and d) reproduced with permission from Bernal et al., Wiley, 2019 [47]

2.3 2-Photon Polymerization

2-photon direct laser writing (DLW), commonly referred to simply as 2-photon polymerization (2PP), is a widely used technology for the fabrication of three-dimensional micron and submicron resolution structures. The feasibility of fabricating 3D microstructures using 2PP was first demonstrated by Maruo et al. in 1997 [48]. More than 20 years later, the basic principle remains the same: A photoresin is illuminated with an ultrashort pulse laser at wavelengths of around two times its absorption wavelength. The resin must be transparent for the emitted wavelength,

and only in the focal area of the laser, the intensity is high enough to allow for two- or multi-photon absorption (which will induce the photopolymerization). The absorption rate is proportional to the square root of the intensity; therefore the polymerization is located in an isolated volume element (voxel). By scanning the voxel through the photoresin, nearly arbitrary microstructures can be fabricated with high-resolution. Non-polymerized resin is subsequently removed in a developing step. Using 2PP, structures with tens of nanometer resolution have been successfully achieved. Larger areas can also be illuminated by moving the stage relative to the optics or by moving the voxel relative to the photoresist (see Sect. 2.4).

A major drawback of 2PP is its serial nature – which makes this process relatively slow and significantly limits the printing volume. This drawback has so far limited the use of 2PP for the fabrication of microfluidic devices, since they usually require high-resolution on a comparatively large lateral scale [12]. However, 2PP is already widely used to integrate high-resolution components directly into existing microfluidic channels – which would be difficult to fabricate using standard micromachining. For example, Perrucci et al. have fabricated microfluidic channels using SL and have integrated a 4 μm pore filter using 2PP into the existing channels [49]. In this way, a suspended microfilter with a size of 0.5 mm^2 was successfully fabricated in just 30 min. In the future, work concepts like these could be used, e.g., for sorting of blood cells. Furthermore, high-resolution components like 3D spring coiled diodes, microfluidic barriers, or complex 3D structures (like microfluidic transistors) have already been integrated into microfluidic channels (see Fig. 8a) [50, 51].

Further, 2PP is a promising technology for the fabrication of nanochannels for use in nanofluidics – an area of increasing interest in the fields of biotechnology and medicine, due to recent advances in biomolecule preparation and analysis, single-molecule interrogations, and molecular manipulation techniques [52]. For example, Vanderpoorten et al. have recently used 2PP to fabricate nanochannels with a size of around 400 nm into the microchannel of a replication structure, which were then subsequently molded into PDMS (see Fig. 8b, c) [53]. Other groups have also

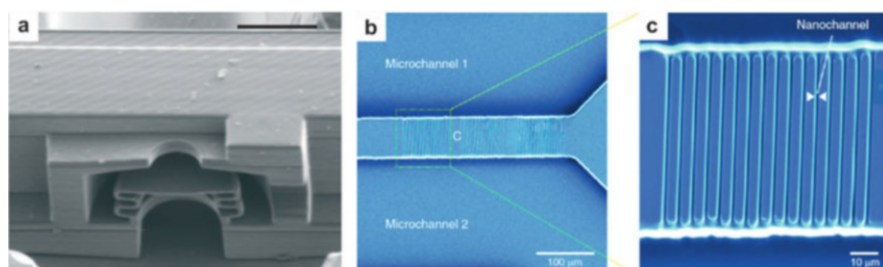


Fig. 8 Integration of high-resolution components into microfluidic chips. (a) SEM of a microfluidic transistor element fabricated using 2PP (scale bar: 15 μm). Reproduced from Alsharhan et al., RSC, 2019 [50]. (b) Nanofluidic channel inside a microfluidic channel template for soft lithography. (c) Close-up of the nanochannel inside the microchannel seen in (b). Figure (b and c) reproduced from Vanderpoorten et al., Springer Nature, 2019 [53]

reported on the fabrication of submicron scale features – like the fabrication of defined surface roughnesses [54] or nanomembranes with pore sizes of around 500 nm [55].

2.4 *Upcoming Trends in 2-Photon Polymerization*

As noted above, due to its serial nature, 2PP is an extremely slow method, which has so far limited the use of 2PP for the fabrication of microfluidic devices. However, in the last several years, numerous concepts have been developed with the aim of increasing the speed of 2PP. These concepts can be grouped into three categories: (1) increasing single-focus writing speed, (2) increasing the number of polymerizing spots, and (3) regulating the voxel size.

Increasing the writing speed for a single-focus system can be done by using appropriate scanning systems. While piezoelectric stages for moving the photoresist and using a fixed laser focus usually show slow scanning speeds of around 0.1–30 mm/s, galvoscaners which move the laser focus have been shown to increase the laser scan rate to tens and even hundreds of mm/s [56–59]. Recently, galvoscaners which are operated at their resonant frequency have been reported to allow for print speeds of up to 8000 mm/s while still achieving resolutions of around 1 μm [56]. These resolutions are sufficient for most applications in microfluidics, which usually require resolutions in the range of a few tens of micrometers. Another strategy which has been often employed for single-focus 2PP is the writing strategy itself like the core-shell polymerization where a shell wall is polymerized using 2PP which encloses the unpolymerized material, which is polymerized, e.g., using flood light exposure after the printing and developing step [60].

Increasing the number of polymerizing spots has been presented as another strategy to increase the throughput in 2PP and has been achieved already at quite an early stage, by integrating microlens arrays, diffractive beam splitters, or SLMs based on liquid crystals into the light path allowing parallel structure writing [61–63]. For this, 2D arrangements of foci are usually created which remained unchanged while the photoresist is moved in 3D. Using this technique, identical microstructures can be fabricated at each focus spot. Using SLMs, the next step in the development process was to rearrange the multiple focus spots in 3D without moving the stage – a technique often called holographic beam shaping [64]. In this way, microstructures can be fabricated by the coordinated movement of the holographic focus points. While early attempts used liquid crystals which had a limited refresh rate of around 60 Hz, more recent attempts using DMDs have demonstrated a much higher refresh rate of 22.7 kHz and a resolution of 500 nm [65, 66]. The authors have shown that they can simultaneously pattern with three different foci. An approach which successfully used multifocal 2PP to structure a millimeter-scaled metamaterial with micron resolution has recently been presented by Hahn et al. They used a multifocal approach using a DOE creating nine foci, in combination with an appropriate optical setup demonstrating a major increase in writing repetitive

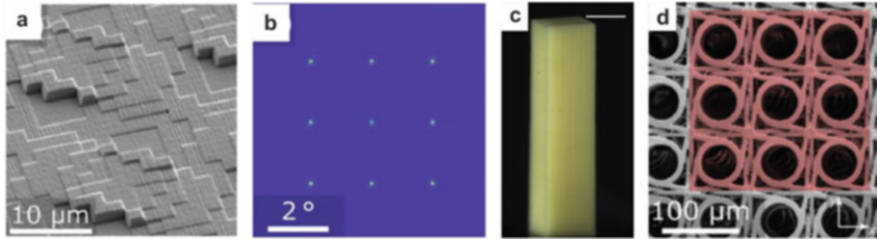


Fig. 9 Increasing the throughput of 2PP using multiple voxels: (a) Scanning electron micrograph of a diffractive optical element (DOE) used to split the laser beam. (b) Diffraction pattern created by the DOE. (c) Metamaterial structured using the DOE showing a chiral 3D metamaterial containing 108,000 3D unit cells (scale bar: 2 mm). (d) SEM of the metamaterial in (c). The simultaneously printed unit cells are highlighted in red. Reproduced with permission from Hahn et al., Wiley, 2020 [67]

structures like the metamaterial seen in Fig. 9 with an overall width of 2 mm printed within 2 days [67]. Figure 9d shows the nine unit cells which have been written simultaneously.

One limitation of the deployment of multiple foci currently lies in a reduction of the writing speed, since the laser power per foci is considerably lower which does not allow scanning as rapidly as with the single focus [67]. The development of highly sensitive photoresins with a low polymerization threshold is therefore a critical future step to unlock the full potential of multifocal 2PP [67].

A different approach for increasing throughput – especially for the fabrication of structures with single digit to some tens of micrometer in resolution – lies in the regulation of the voxel size. This has been achieved, for example, by using objectives with a low numerical aperture (see Fig. 10a) in combination with a compensation for the resulting spherical aberration [68, 69]. The usage of a high numerical aperture (NA) objective results in a small and more spherical voxel, while using a lower NA will result in an elliptical and larger voxel. Therefore, for microfluidic structures where many structures are relatively large, lower NA objectives can be used. Jonusauskas et al. have presented an approach by varying the numerical aperture of the beam focussing objectives [70]. In this way, low-resolution structures can be printed with high throughput without losing spatial resolution for the high-resolution regions. Figure 10b, c show a vertical microfluidic tube featuring an integrated filter with a filter period of 4 μm and a thread width of 400 nm. The bulk structure was written with a low NA, while the filter itself was written with a high NA. The time gain here is especially high if the part has relatively bulky components with integrated small structures – as it is often the case in microfluidic devices with integrated submicron structures. An alternative method has also been recently shown by using *simultaneous spatiotemporal focussing* (SSTF) to modulate the voxel size in dependence of the beam intensity [71]. Using this method, the authors have successfully adjusted the voxel size in a range of a few microns to 40 μm by varying the laser power allowing to print multi-scale microstructures. These novel concepts for increasing the fabrication throughput in 2PP are promising

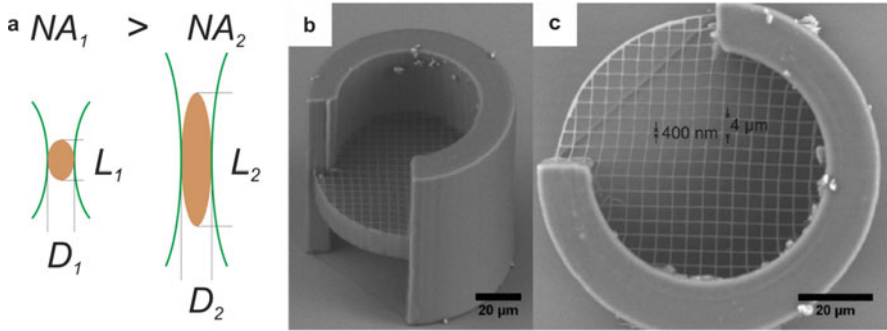


Fig. 10 Increasing the throughput of 2PP using voxel size regulation: (a) Comparison of the shape of the 2PP voxel for different numerical apertures. A decrease in NA will result in a larger and more elliptical voxel. (b) Tube containing an integrated filter fabricated using two objectives with different NA. (c) Top view of the object in (b) showing the filter element with a period of 4 μm and a thread width of 400 nm. Figure (a–c) reproduced with permission from Jonusauskas et al., SPIE, 2014 [70]

candidates which could facilitate the implementation of novel concepts and components into future microfluidic chip fabrication within a reasonable time.

3 Emerging Materials

The choice of materials compatible for use in rapid prototyping and 3D printing of high-resolution truly microfluidic chips has been fairly limited, to date. However, within the last 5 years, multiple novel material systems have been introduced which allow for high-resolution 3D structuring of microfluidic chips. The following section presents an overview of these recent developments, with a particular focus on materials of interest for their applications in microfluidics in biotechnology – including biocompatible polymers, transparent glass, PDMS, and polymethylmethacrylate (PMMA).

3.1 Noncytotoxic Polymers

Biocompatibility is of outmost importance for using 3D-printed microfluidic devices in the field of biotechnology, since there is an inherent contact between the materials used in such devices and biological samples. Unfortunately, most of the photoresins commonly used in SL are not biocompatible. While polymerized materials are usually noncytotoxic, toxicities can nevertheless arise from unreacted monomer as well as photoinitiator or absorber which leach out of the part and interact with the cells [72]. The amount of leachable products is highly affected by factors including

geometry, the resin formulation, and the polymerization turnover. Especially the latter parameter changes substantially across different prints, due to varying parameters like exposure dose and layer thickness [73]. Therefore, the current protocol is to undertake a detailed study of the biocompatibility of all materials involved, prior to and for each application. Many researchers have explored methods aimed at increasing the biocompatibility of photocurable materials by rendering them noncytotoxic. This topic has been already studied for a long time especially in the field of dentistry before it came up in the field of microfluidics [72]. Cytotoxicity can be studied, according to ISO 10993-5, using colorimetric cell viability assays like the MTT-test (MTT is the abbreviation for the compound 3-(4,5-Dimethylthiazol-2-yl)-2,5-diphenyltetrazoliumbromide). One method to evaluate the cell viability is to seed cells within a conventional polystyrene well plate and then place the printed part directly into contact with the cells. Alternatively, the substances can be extracted and be put into contact with the cells. A reduction of the viability of 30% of the cells is considered to evidence a cell-toxic effect, according to ISO 10993-5.

As described above in Sect. 2.1, resins for 3D printing of embedded microfluidic devices must be adapted to allow for high-resolution printing. Several strategies have been employed to reduce the cytotoxicity of the printed parts and thereby increase the cell viability. Since radical polymerization never reaches full conversion, especially for 3D printing of embedded channels, it is recommended to increase the monomer-to-polymer conversion using a subsequent UV or thermal posttreatment. For macroscopic parts, several strategies have been employed like coating the printed parts with biocompatible coatings like parylene C or wax, which prevent leaching of the cell-toxic components [74, 75]. Unfortunately, these approaches cannot be employed for high-resolution embedded microfluidic channels. Residual cell-toxic components are therefore usually removed via subsequently washing the 3D-printed parts using an appropriate solvent (often ethanol) in a bath or in a Soxhlet extractor [76]. Hereby it is recommended to use solvents which swell the polymer to a certain degree and thus enable the “washout” of non-polymerized material while avoiding extensive swelling which may cause a component to lose its structural integrity [77]. Furthermore, the admixtures to be removed should have a high solubility in the used solvent. For example, when using acrylate-based resins which swell in water, a washing procedure in phosphate-buffered saline (PBS) and *Tween 20* was demonstrated. PEGDA 258 resins, which were used successfully for high-resolution printing of embedded microfluidic chips, were washed for around 12 h in ethanol to remove residual cell-toxic components [78]. For the usage of the polydimethylsiloxane-based resins (see Sect. 3.3 above), protocols based on serial extraction in xylene isomers, xylene/2-propanol, and 2-propanol and water – followed by a heat treatment of 120°C for 12 h – were applied for making the printed components cytocompatible. Grigoryan et al. have used biocompatible food dyes like the azo dye *tartrazine* with a strong absorbance in the visible light spectrum, in combination with a photocurable hydrogel mixture composed of PEGDA and water to 3D print fluidic channel structures like vascular networks in hydrogels (see Fig. 2b) [23]. The hydrophilic tartrazine absorber and the

non-polymerized monomers were removed by washing the printed parts in water or saline solutions [23].

Besides cell viability, cell adhesion to the printed part can be an important aspect which may need to be considered, depending on the biotechnological application in question. It has been shown by several groups that cells do not adhere well to printed acrylate-based resin – even after washing procedures [77]. Optimizations have been demonstrated by activating high-resolution printed PEGDA parts with oxygen plasma increasing the cell adhesion relative to a non-treated reference [78].

Although work has just started on the development of protocols to reduce cell toxicity and increase the cell viability of the 3D-printed acrylates, current work is still somewhat preliminary and rather time-consuming with protocols for washing out residual toxic components which can span up to several days. Additionally, research is ongoing in an effort to optimize and adapt protocols for functionalization and coatings, in order to achieve the “gold standard” of biocompatibility on par with standard polystyrene [40].

3.2 *Transparent Glass*

Transparent silicate glasses are among the most important materials for the fabrication of microfluidic chips. Outstanding optical transparency, low autofluorescence, high biocompatibility, and a high chemical and thermal resistance make glasses very attractive for both biotechnology and bioanalytics applications – especially with respect to high-resolution analysis and synthesis. The importance of glasses for the field of pharmaceutical on-demand continuous-flow synthesis has been most recently highlighted by Kitson et al. showing that for the successful implementation of pharmaceutical synthesis in polymer-based reaction ware, a translation process would be necessary – but which would not be required if glass could be used in the first place [79].

Unfortunately, structuring glass on the microscale is particularly challenging and usually requires hazardous etching processes like wet chemical etching via hydrofluoric acid [80]. It took more than two decades after the invention of 3D printing until transparent glasses finally were established in this field. While direct printing technologies can be used to simply extrud melted glass through a nozzle or by melting glass fibers, these processes are not capable of fabricating structures with a micron resolution. Usually, the layers of these printed structures are in the range of a few millimeters, and the lateral resolution is significantly limited [81, 82].

The first high-resolution 3D printing process for structuring fused silica glass was presented in 2017 by Kotz et al., using an indirect printing approach. Instead of printing the glass itself, we developed a nanocomposite material (called *Glassomer*) which consists of nanoparticles in a photocurable binder matrix [27, 83–85]. This material can be printed using high-resolution SL with tens of microns in resolution. Alternative formulations of the material further allow to use the material for soft lithography replication, subtractive machining, thermal nanoimprinting or even

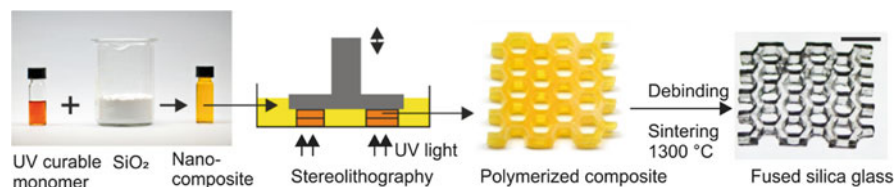


Fig. 11 Stereolithography printing of fused silica glass using the *Glassomer* process. *Glassomer* consists of silica nanoparticles in a photocurable binder matrix. It can be printed using stereolithography resulting in a polymeric nanocomposite. The polymeric nanocomposite is converted to transparent fused silica glass using thermal debinding and sintering (scale bar: 7 mm). Permission from Kotz et al., Springer Nature, 2017 [27]

roll-to-roll replication [83, 86]. After the shaping process is completed, the polymeric *Glassomer* part is converted to high-purity fused silica glass via thermal debinding at 600°C and sintering at a maximum temperature of 1,300°C (see Fig. 11).

The resulting glass is indistinguishable from commercial fused silica glass in its chemical and physical properties, showing the same high optical transparency of 92% in the visible wavelength range, a low autofluorescence, as well as a high thermal, chemical, and mechanical stability. This is a major advantage for applications in the field of biotechnology. In contrast to polymeric material, cell-toxic components like absorbers, photoinitiators, and residual monomers are all removed in the thermal debinding step. As described in Sect. 3.1 above, these components result in impaired biocompatibility as well as a reduced optical transparency, which is problematic for imaging inside these systems. The sintered *Glassomer* fused silica glass is standard fused silica glass which has been used for decades in the field of biotechnology.

Using micro(stereo-)lithography, components with tens of microns resolution can be printed like the castle gate or the Tesla mixer (see Fig. 12a, b). The Tesla mixer was printed as an open channel and was then bonded as a green part using partial curing. Using replication processes, single-micron resolution was achieved as

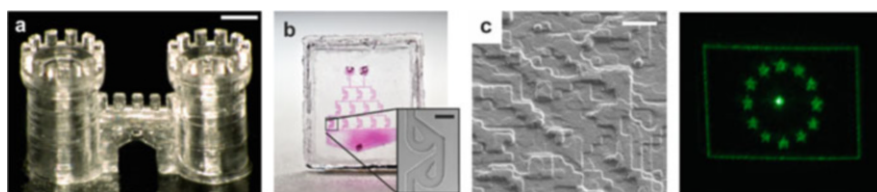


Fig. 12 Exemplary structures fabricated using the *Glassomer* process. (a) Sintered micro-sized castle gate fabricated using microstereolithography (scale bar: 270 μm). (b) Sintered microfluidic Tesla mixer structured using lithography. The chip was bonded in the green part state using partial curing (scale bar: 200 μm). Reproduced with permission from Kotz et al., Springer Nature, 2017 [27]. (c) Sintered DOE structured using hot embossing and the corresponding diffraction pattern when illuminated with a green laser (scale bar: 10 μm). Reproduced with permission from Kotz et al., Wiley, 2018 [86]

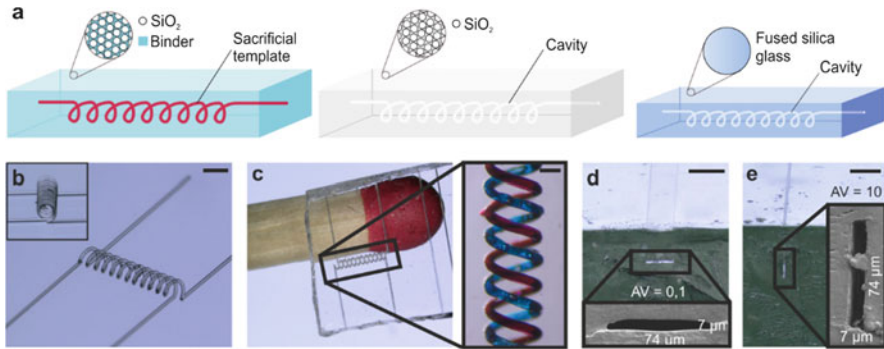


Fig. 13 Fabrication of fused silica microfluidic chips using sacrificial template replication (STR): (a) The STR process. A sacrificial template is embedded in the *Glassomer* resin. During the thermal debinding process, the binder matrix as well as the template is removed. Sintering results in a highly transparent fused silica glass with the inverse embedded microfluidic channel. (b) Intertwining spiral template fabricated using 2PP (scale bar: 900 μm). (c) Sintered channel structure with a channel width and height of 74 μm fused silica glass using the template from b (scale bar: 140 μm). (d and e) Cross section of a microchannel with aspect ratios of 0.1 and 10 (scale bar: 100 μm). Reproduced with permission from Kotz et al., Springer Nature, 2019 [87]

illustrated in Fig. 12c (which shows a diffractive optical element with its corresponding diffraction pattern).

As mentioned above in Sect. 2.1, high-resolution SL printing of microfluidic channels is limited to low-viscosity photoresins, and many of the printing strategies that exist are difficult to adapt to viscous materials like the *Glassomer* nanocomposites. We have therefore developed a novel process, which we termed *sacrificial template replication* (STR). For the very first time, the STR process permits the fabrication of nearly arbitrary 3D embedded microchannels inside fused silica glass [87]. Instead of 3D printing the whole microfluidic chip, only the channel-defining structure is printed – using a polymeric photoresin. This template structure is then embedded in the *Glassomer* material and removed during the thermal debinding process – resulting in the inverse channel structure in fused silica glass after the sintering process (see Fig. 13a). Since the template is removed in the gas phase, there is no risk of either material redeposition or channel blocking due to incomplete removal.

Using STR, a wide range of templates can be used from a simple nylon thread to photoresist structures using 2PP. STR is capable of fabricating nearly arbitrary microchannels in fused silica glass, with channel sizes in the range of a few micrometers on a length scale of several centimeters. Figure 13b, c show two intertwined microfluidic spirals with a channel size of 74 μm . This process is further capable of fabricating channels with a great variety of aspect ratios and channel geometries as can be seen in Fig. 13d, e.

In combination with 2PP, STR also offers the high-resolution advantages inherent to 2PP with the speed of a replication process. Since only the channel-defining

structures are printed in the STR method, the processing time is significantly reduced.

3.3 *Polydimethylsiloxane*

PDMS is one of the most commonly used materials for rapid prototyping of microfluidic devices on the laboratory scale. PDMS has shaped the field of microfluidics in biotechnology and in life sciences like no other material in the last years – combining high optical transparency, biocompatibility, gas permeability, and, perhaps most importantly of all, ease of handling and manufacturing. Its elasticity makes it an interesting material for the incorporation of membranes, valves, and actuators inside the microfluidic channel system for active fluid control. Disadvantages of PDMS include its swelling tendency in organic solvents and its tendency to absorb small hydrophobic molecules [88]. Traditionally, PDMS microfluidics have been fabricated using soft lithography replication, whereby the PDMS precursors are poured onto a mold and allowed to cross-link before bonding the open channels to form an embedded channel structure [8].

Photocurable PDMS precursors have also been widely studied for the fabrication of microfluidic chips or microstructures on substrates. Many shaping approaches have been presented – including soft lithography and direct structuring using lithography either as a negative or a positive resist [89–91]. However, these processes all result in open microstructures which require subsequent bonding for the fabrication of a microfluidic chip. Furthermore, although a great variety of elastomeric photoresins are now commercially available (including *Formlabs Flexible* and *TangoPlus*), these materials are usually not capable of fabricating components with the same high optical transparency, elasticity, and biocompatibility prized in PDMS and its most commonly used commercial variants, Sylgard-184 and Elastosil 601 [92].

Bhattacharjee et al. have recently reported a methacrylate-based PDMS photoresin which can be printed using SL [92]. They used commercially available methacrylate-terminated PDMS precursors, blended them with an appropriate photoinitiator and absorber, and then printed these photoresins using a benchtop SL printer. In doing so, they demonstrated that by using this process; transparent and mechanically stable embedded 2.5-dimensional microfluidic chips can be printed which show material properties similar to Sylgard-184 (see Fig. 14). In addition, they also demonstrated that the use of a multistep washing, UV treatment, and heat treatment procedure could render the printed PDMS cytocompatible (see Sect. 3.1 above). However, it should be noted that this printing process is significantly longer than the process used for standard acrylic resins. Several seconds were needed for each 50 μm thick layer, which can be attributed to the strong oxygen-binding affinity of PDMS which inhibits radical polymerization. The PDMS prepolymers also showed a relatively high viscosity of $\sim 1\text{--}9$ Pas (depending on the molecular weight of the precursor), which unfortunately renders printing of sub-100 μm channels

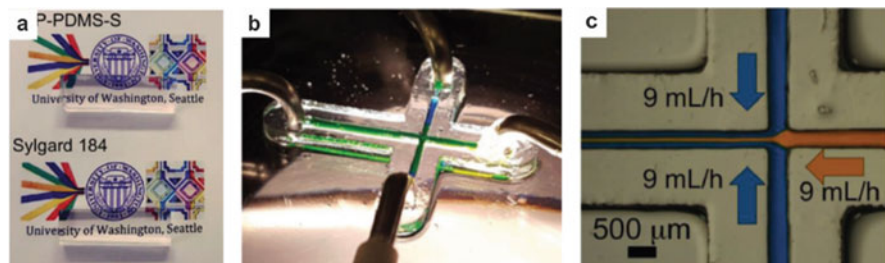


Fig. 14 SL printing of methacrylate-terminated PDMS: (a) A 4 mm thick block of printed PMDS compared to replicated PDMS, showing the high transparency in the visible wavelength region. (b) Microfluidic flow focussing device fabricated using SL of methacrylate-terminated PDMS photoresin. (c) Laminar flow focussing of an orange dye flanked by two sheath flows of blue dye in the printed device. Reproduced with permission from Bhattacharjee et al., Wiley, 2018 [92]

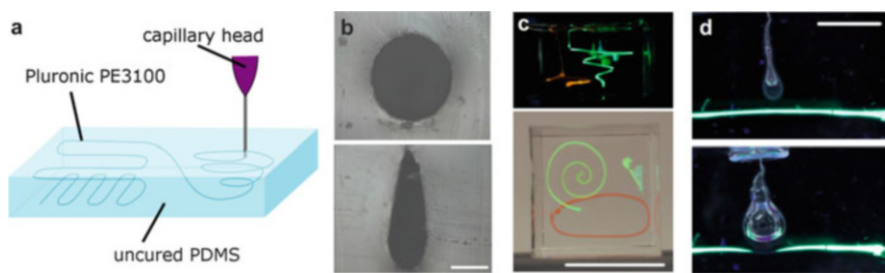


Fig. 15 Suspended liquid subtractive lithography (SLSL): (a) Schematic of the SLSL method for printing microfluidic channels into PDMS using the surfactant *Pluronic PE3100*. (b) SEM of a circular and a high-aspect ratio structure fabricated by SLSL (scale bar: 250 μm). (c) Three-dimensional printed spiral in PDMS (scale bar: 18 mm). (d) Quake-type membrane actuator with a green fluid channel on the bottom and an expandable control channel on the top. By pressurizing the upper channel, the membrane is expanded blocking the fluidic channel (scale bar: 5 mm). Reproduced with permission from Helmer et al. Springer Nature, 2017 [93]

impossible. Only embedded 2.5 dimensional channels with a size of 500 μm could be printed (see Fig. 14b, c). Another issue is the price of the PDMS precursor – which, at around 2,200€ per kg, is significantly more expensive than state-of-the-art PDMS prepolymers used for soft lithography (which only cost around 60€ per kg).

A faster and cheaper process which can achieve circular microchannels in PDMS with a size of around 200 μm could be achieved using a process called *Suspended Liquid Subtractive Lithography* (SLSL), which is an indirect 3D printing method that has been developed by Helmer et al. [93] Instead of 3D printing the bulk chip material, the channel-defining structure is printed into the curing PDMS matrix using a surfactant which generates freely definable three-dimensional channel structures (see Fig. 15a). After the polymerization process is completed, the surfactant is washed out of the material, leaving only the microfluidic channel structure. A great variety of microfluidic channels have already been fabricated using this process – including three-dimensional spirals and loops (see Fig. 15c) and

microfluidic valves (see Fig. 15d). For this process, the surfactant has to match the properties of the medium in which it is written. It should also have a density close to PDMS, in order to prevent sedimentation or floatation; a low surface energy to prevent droplet formation; a low viscosity to simplify extrusion; and a high biocompatibility. This method is ideal for printing circular channel structures (e.g., structures that mimic biological environments like blood vessels) [94]. As can be seen in Fig. 15b, the resulting channel cross section is perfectly circular, and does not show defects which are typically seen in layer-by-layer-based processes like SL. By wetting the needle at the first extrusion of the dispersant, an oval distortion can be created which further allows the manufacturer to write noncircular channel structures like the high-aspect ratio structure shown in Fig. 15b. Another significant advantage of this process compared to SL is that standard PDMS types like Elastosil 601 can be used without any modification. The resulting material is PDMS with the same material properties known from soft lithography processes. The process has been shown for the fabrication of, e.g., Quake-type membrane actuators – a commonly used pneumatic microfluidic valve (see Fig. 15d).

2PP of PDMS prepolymers has been demonstrated for the fabrication of high-resolution components. Radical polymerization, as well as photohydrosilylation of PDMS prepolymers using 2PP, has already been shown in 2004 by Coenjarts et al. [95]. They showed that by doping the PDMS prepolymer with a photoactive platinum catalyst or a photoinitiator, PDMS can be structured with submicron resolution using 2PP. Using this process, structures with a line width of around 300 nm could be achieved using photohydrosilylation (see Fig. 16a). By employing radical initiators, they further demonstrated that 3D microstructures with single-micron resolution like the microcapillaries or the intersections shown in Fig. 16b, c can be fabricated. However, this process is very slow – with a throughput of around $12 \mu\text{m}^3 \text{s}^{-1}$ [96]. To that end, Rekstyte et al. have demonstrated that the 2PP process can at least be accelerated to a throughput of $\sim 720 \mu\text{m}^3 \text{s}^{-1}$ while still achieving structure resolutions of around $5 \mu\text{m}$ [96], by using well-adjusted photoinitiators.

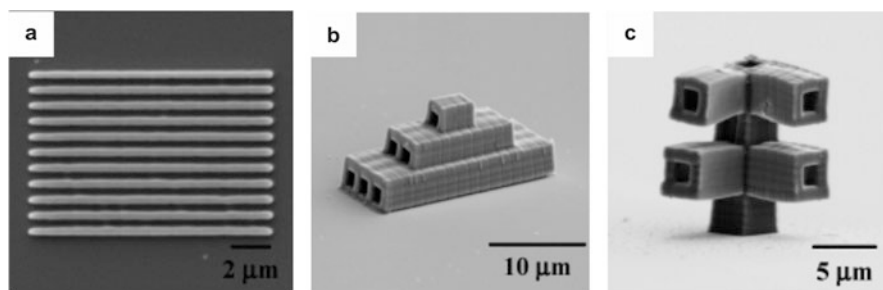


Fig. 16 Microstructuring of polydimethylsiloxane using 2PP: (a) Line pattern with a width of 300 nm fabricated in PDMS using photohydrosilylation. (b) 3D stack of microcapillaries in PDMS fabricated using radical polymerization 2PP. (c) Microcapillary intersections fabricated using radical polymerization 2PP. Reproduced with permission from Coenjarts et al., ACS, 2004 [95]

The combination of high-resolution 2PP of PDMS with the methods described above for the fabrication of embedded microchannels could open up new possibilities in the future, allowing researchers to manufacture far more complex and highly integrated systems using one of the most widely favored rapid prototyping materials used in the microfluidic community.

3.4 Polymethylmethacrylate

One drawback of SL printing is that the available materials are all cross-linked thermosets. While this is not a significant issue for the fabrication of chips on the laboratory scale, it becomes a drawback when technology moves from the lab to industrial mass manufacturing. Mass manufacturing is done using highly scalable technologies like injection molding or hot embossing, which usually require thermoplastic materials. This scale-up problem is a major impediment to industrializing microfluidic concepts, since changing the material and thereby the associated surface properties have a major effect on the final system behavior. This lack of transfer is a problem which has been criticized also for classical PDMS replication which has been the standard for rapid prototyping of microfluidic chips for decades [97].

We have therefore developed a novel method which makes one of the most used thermoplastic materials in mass productions, i.e., polymethylmethacrylate (PMMA), accessible for high-resolution direct printing. PMMA is an important material for microfluidics in the field of biotechnology and has been widely used for (among other applications) the analysis of proteins, DNA, amino acids, and peptides [11]. It is highly transparent and biocompatible and features a low autofluorescence. It is also a particularly interesting material for disposable microfluidics since it decomposes to its monomer at elevated temperatures. To achieve this a PMMA prepolymer called *Liquid PMMA* has been developed which is a fast curing viscous PMMA prepolymer which can be structured like a negative photoresist [98]. This material consists of the monomer methylmethacrylate (MMA) and up to 50 wt% of the polymer PMMA, with a defined molecular weight (see Fig. 17a). Due to the

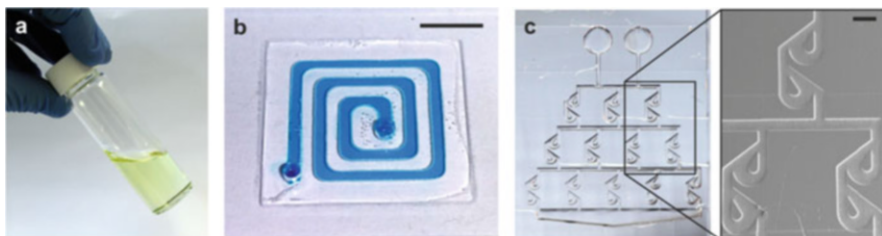


Fig. 17 High-resolution direct structuring of thermoplastic polymethylmethacrylate (PMMA): (a) *Liquid PMMA* after synthesis. (b) Microfluidic spiral filled with dyed water after successful bonding (scale bar: 7 mm). (c) Tesla mixer cascade fabricated by stitching 42 single images next to each other (scale bar: 400 μm). Reproduced from Kotz et al., Wiley, 2018 [98]

increased viscosity of *Liquid PMMA* compared to the pure monomer, the inset of the polymerization autoacceleration is shifted, and the material can be polymerized significantly faster. *Liquid PMMA* has already been structured using DMD-based lithography and was recently also used to fabricate open microfluidic channels with tens of micron resolution. Figure 17 shows exemplary microfluidic structures that have been fabricated using this method. The polymerized *Liquid PMMA* demonstrates high optical transparency, low autofluorescence, and surface properties like commercial PMMA [98].

4 Outlook

The emergence of novel high-resolution 3D printing technologies and processes will facilitate the evolution and development of the next generation of microfluidic systems. Using different manufacturing processes will allow for the fabrication of more complex and integrated microfluidic systems. As highlighted in this chapter, the usefulness of these hybrid concepts has already been demonstrated using classical polymeric materials and even transparent glass – but they remain to be shown for functional or even multimaterial prints. Furthermore, high-speed and high-resolution 3D printing on the micro- and nanoscale is just starting to evolve. Exploring these technologies for the fabrication of biocompatible microfluidic chips will pave the way for using 3D printing not only as a laboratory prototyping method, but rather as a manufacturing technology on an industrial scale.

Furthermore, material innovations have just started to revolutionize the field of 3D printing and will enable not only the fabrication of previously unseen components and designs but also novel processes for high-resolution structuring. One issue which has just started to be investigated is the biocompatibility of printed microfluidic systems developed using these emerging technologies. Current work on this front remains rather time-consuming, and standard protocols will require further adaption for the functionalization of coatings. One potential strategy to overcome these issues could be by using established materials like polystyrene or glass in high-resolution printing and processing.

Acknowledgments BER thanks the German Research Foundation (Deutsche Forschungsgemeinschaft, DFG) for funding through the Center for Excellence *livMatS* Exec 2193/1 – 390951807.

References

1. Whitesides GM (2006) *Nature* 442:368
2. Berthier J, Silberzan P (2010) *Microfluidics for biotechnology*. Artech House
3. Gervais L, de Rooij N, Delamarche E (2011) *Adv Mater* 23:H151

4. Holmes D, Gawad S (2010) Hughes MP, Hoettges KF (eds) *Microengineering in biotechnology*. Humana Press, Totowa, pp 55–80
5. Manz A, Fettinger JC, Verpoorte E, Lüdi H, Widmer HM, Harrison DJ (1991) *TrAC Trends Anal Chem* 10:144
6. Harrison DJ, Manz A, Fan Z, Luedi H, Widmer HM (1992) *Anal Chem* 64:1926
7. De Mello A (2002) *Lab Chip* 2:31N
8. Duffy DC, McDonald JC, Schueller OJ, Whitesides GM (1998) *Anal Chem* 70:4974
9. Zhao S, Cong H, Pan T (2009) *Lab Chip* 9:1128
10. Hong T-F, Ju W-J, Wu M-C, Tai C-H, Tsai C-H, Fu L-M (2010) *Microfluid Nanofluid* 9:1125
11. Chen Y, Zhang L, Chen G (2008) *Electrophoresis* 29:1801
12. Waldbaur A, Rapp H, Lange K, Rapp BE (2011) *Anal Methods* 3:2681
13. Kotz F, Risch P, Helmer D, Rapp BE (2018) *Micromachines* 9:115
14. Li F, Macdonald NP, Guijt RM, Breadmore MC (2017) *Anal Chem* 89:12805
15. Su W, Cook BS, Fang Y, Tentzeris MM (2016) *Sci Rep* 6:35111
16. Waheed S, Cabot JM, Macdonald NP, Lewis T, Guijt RM, Paull B, Breadmore MC (2016) *Lab Chip* 16:1993
17. Sochol RD, Sweet E, Glick CC, Venkatesh S, Avetisyan A, Ekman KF, Raulinaitis A, Tsai A, Wienkers A, Korner K, Hanson K, Long A, Hightower BJ, Slatton G, Burnett DC, Massey TL, Iwai K, Lee LP, Pister KSJ, Lin L (2016) *Lab Chip* 16:668
18. Nielsen AV, Beauchamp MJ, Nordin GP, Woolley AT (2020) *Ann Rev Anal Chem* 13
19. Shallan AI, Smejkal P, Corban M, Guijt RM, Breadmore MC (2014) *Anal Chem* 86:3124
20. Rogers CI, Qaderi K, Woolley AT, Nordin GP (2015) *Biomicrofluidics* 9:016501
21. Lee Y-S, Bhattacharjee N, Folch A (2018) *Lab Chip* 18:1207
22. Enders A, Siller IG, Urmann K, Hoffmann MR, Bahnemann J (2019) *Small* 15:1804326
23. Grigoryan B, Paulsen SJ, Corbett DC, Sazer DW, Fortin CL, Zaita AJ, Greenfield PT, Calafat NJ, Gounley JP, Ta AH, Johansson F, Randles A, Rosenkrantz JE, Louis-Rosenberg JD, Galie PA, Stevens KR, Miller JS (2019) *Science* 364:458
24. Lee W, Kwon D, Choi W, Jung GY, Jeon S (2015) *Sci Rep* 5:7717
25. Shemesh J, Jalilian I, Shi A, Yeoh GH, Tate MLK, Warkiani ME (2015) *Lab Chip* 15:4114
26. Hull CW (1986) Patent US4575330
27. Kotz F, Arnold K, Bauer W, Schild D, Keller N, Sachsenheimer K, Nargang TM, Richter C, Helmer D, Rapp BE (2017) *Nature* 544:337
28. Gong H, Bickham BP, Woolley AT, Nordin GP (2017) *Lab Chip* 17:2899
29. Lee MP, Cooper GJT, Hinkley T, Gibson GM, Padgett MJ, Cronin L (2015) *Sci Rep* 5:1
30. Xu G, Zhao W, Tang Y, Lu B (2006) *Rapid Prototyp J* 12:12
31. Behroodi E, Latifi H, Najafi F (2019) *Sci Rep* 9:1
32. Ligon SC, Liska R, Stampfl J, Gurr M, Mülhaupt R (2017) *Chem Rev* 117:10212
33. Au AK, Huynh W, Horowitz LF, Folch A (2016) *Angew Chem Int Ed* 55:3862
34. Bertsch A, Jiguet S, Bernhard P, Renaud P (2002) *MRS Online Proceedings Library*, p 759
35. Gong H, Beauchamp M, Perry S, Woolley AT, Nordin GP (2015) *RSC Adv* 5:106621
36. Jacobs PF (1992) *Rapid prototyping and manufacturing: fundamentals of stereolithography*. Society of Manufacturing Engineers
37. Beauchamp MJ, Gong H, Woolley AT, Nordin GP (2018) *Micromachines (Basel)* 9:9
38. Beauchamp MJ, Nielsen AV, Gong H, Nordin GP, Woolley AT (2019) *Anal Chem* 91:7418
39. Gong H, Woolley AT, Nordin GP (2019) *Biomicrofluidics* 13:014106
40. Männel MJ, Selzer L, Bernhardt R, Thiele J (2019) *Adv Mater Technol* 4:1800408
41. Waldbaur A, Carneiro B, Hettich P, Wilhelm E, Rapp BE (2013) *Microfluid Nanofluid* 15:625
42. Tumbleston JR, Shirvanyants D, Ermoshkin N, Januszewicz R, Johnson AR, Kelly D, Chen K, Pinschmidt R, Rolland JP, Ermoshkin A (2015) *Science* 347:1349
43. de Beer MP, van der Laan HL, Cole MA, Whelan RJ, Burns MA, Scott TF (2019) *Sci Adv* 5: eaau8723
44. Walker DA, Hedrick JL, Mirkin CA (2019) *Science* 366:360

45. Johnson AR, Caudill CL, Tumbleston JR, Bloomquist CJ, Moga KA, Ermoshkin A, Shirvanyants D, Mecham SJ, Luft JC, DeSimone JM (2016) *PLoS One* 11:e0162518
46. Kelly BE, Bhattacharya I, Heidari H, Shusteff M, Spadaccini CM, Taylor HK (2019) *Science* 363:1075
47. Bernal PN, Delrot P, Loterie D, Li Y, Malda J, Moser C, Levato R (2019) *Adv Mater* 31:1904209
48. Maruo S, Nakamura O, Kawata S (1997) vol 22. OSA Publishing, p 132
49. Perrucci F, Bertana V, Marasso SL, Scordo G, Ferrero S, Pirri CF, Cocuzza M, El-Tamer A, Hinze U, Chichkov BN, Canavese G, Scaltrito L (2018) *Microelectron Eng* 195:95
50. Alsharhan AT, Acevedo R, Warren R, Sochol RD (2019) *Lab Chip* 19:2799
51. Lamont AC, Alsharhan AT, Sochol RD (2019) *Sci Rep* 9:1
52. Schoch RB, Han J, Renaud P (2008) *Rev Mod Phys* 80:839
53. Vanderpoorten O, Peter Q, Challa PK, Keyser UF, Baumberg J, Kaminski CF, Knowles TPJ (2019) *Microsyst Nanoeng* 5:1
54. Hengsbach S, Lantada AD (2014) *Biomed Microdevices* 16:617
55. Amato L, Gu Y, Bellini N, Eaton SM, Cerullo G, Osellame R (2012) *Lab Chip* 12:1135
56. Pearre BW, Michas C, Tsang J-M, Gardner TJ, Otchy TM (2019) *Addit Manuf* 30:100887
57. Straub M, Gu M (2002) *Opt Lett* 27:1824
58. Ovsianikov A, Deiwick A, van Vlierberghe S, Dubruel P, Möller L, Dräger G, Chichkov B (2011) *Biomacromolecules* 12:851
59. Skylar-Scott MA, Liu M-C, Wu Y, Dixit A, Yanik MF (2016) *Adv Healthc Mater* 5:1233
60. Thiel M, Reiner RR, Niesler F, Tanguy Y (2016) Method for producing a three-dimensional structure, US20160114530A1
61. Kato J, Takeyasu N, Adachi Y, Sun H-B, Kawata S (2005) *Appl Phys Lett* 86:044102
62. Dong X-Z, Zhao Z-S, Duan X-M (2007) *Appl Phys Lett* 91:124103
63. Takahashi H, Hasegawa S, Takita A, Hayasaki Y (2008) *Opt Express* 16:16592
64. Jenness NJ, Wulff KD, Johannes MS, Padgett MJ, Cole DG, Clark RL (2008) *Opt Express* 16:15942
65. Geng Q, Wang D, Chen P, Chen S-C (2019) *Nat Commun* 10:1
66. Viznyiczai G, Kelemen L, Ormos P (2014) *Opt Express* 22:24217
67. Hahn V, Kiefer P, Frenzel T, Qu J, Blasco E, Barner-Kowollik C, Wegener M (2020) *Adv Funct Mater*:1907795
68. Stichel T, Hecht B, Houbertz R, Sextl G (2015) *Appl Phys A Mater Sci Process* 121:187
69. Stichel T, Hecht B, Steenhusen S, Houbertz R, Sextl G (2016) *Opt Lett* 41:4269
70. Jonušauskas L, Rekštytė S, Malinauskas M (2014) *OE* 53:125102
71. Tan Y, Chu W, Wang P, Li W, Qi J, Xu J, Wang Z, Cheng Y (2018) *Phys Scr* 94:015501
72. Carve M, Wlodkowic D (2018) *Micromachines* 9:91
73. Fouassier JP, Lalevée J (2014) *Polymers* 6:2588
74. Van den Driesche S, Lucklum F, Bunge F, Vellekoop MJ (2018) *Micromachines* 9:71
75. Macdonald NP, Zhu F, Hall CJ, Reboud J, Crosier PS, Patton EE, Wlodkowic D, Cooper JM (2016) *Lab Chip* 16:291
76. Leigh SJ, Gilbert HTJ, Barker IA, Becker JM, Richardson SM, Hoyland JA, Covington JA, Dove AP (2013) *Biomacromolecules* 14:186
77. Männel MJ, Fischer C, Thiele J (2020) *Micromachines* 11:246
78. Warr C, Valdoz JC, Bickham BP, Knight CJ, Franks NA, Chartrand N, Van Ry PM, Christensen KA, Nordin GP, Cook AD (2020) *ACS Appl Bio Mater* 3:2239
79. Kitson PJ, Marie G, Francoia J-P, Zalesskiy SS, Sigerson RC, Mathieson JS, Cronin L (2018) *Science* 359:314
80. Hülsenberg D, Harnisch A, Bismarck A (2005) *Microstructuring of glasses*. Springer, Berlin
81. Klein J, Stern M, Franchin G, Kayser M, Inamura C, Dave S, Weaver JC, Houk P, Colombo P, Yang M, Oxman N (2015) *3D printing and additive manufacturing*. 2:92
82. Kotz F, Risch P, Helmer D, Rapp BE (2019) *Adv Mater* 31:1805982

83. Kotz F, Plewa K, Bauer W, Schneider N, Keller N, Nargang T, Helmer D, Sachsenheimer K, Schäfer M, Worgull M, Greiner C, Richter C, Rapp BE (2016) *Adv Mater* 28:4646
84. Kotz F, Helmer D, Rapp BE (2018) *Int Soc Opt Photo*:104910A
85. Kotz F, Plewa K, Bauer W, Hanemann T, Waldbaur A, Wilhelm E, Neumann C, Rapp BE (2015) *Int Soc Opt Photo*:932003–932006
86. Kotz F, Schneider N, Striegel A, Wolfschläger A, Keller N, Worgull M, Bauer W, Schild D, Milich M, Greiner C, Helmer D, Rapp BE (2018) *Adv Mater* 30:1707100
87. Kotz F, Risch P, Arnold K, Sevim S, Puigmartí-Luis J, Quick A, Thiel M, Hrynevich A, Dalton PD, Helmer D, Rapp BE (2019) *Nat Commun* 10:1439
88. Toepke MW, Beebe DJ (2006) *Lab Chip* 6:1484
89. Bhagat AAS, Jothimuthu P, Papautsky I (2007) *Lab Chip* 7:1192
90. Choi KM, Rogers JA (2003) *J Am Chem Soc* 125:4060
91. Desai SP, Taff BM, Voldman J (2008) *Langmuir* 24:575
92. Bhattacharjee N, Parra-Cabrera C, Kim YT, Kuo AP, Folch A (2018) *Adv Mater* 30:1800001
93. Helmer D, Voigt A, Wagner S, Keller N, Sachsenheimer K, Kotz F, Nargang TM, Rapp BE (2017) *Sci Rep* 7:7387
94. Perry H, Greiner C, Georgakoudi I, Cronin-Golomb M, Omenetto FG (2007) *Rev Sci Instrum* 78:044302
95. Coenjarts CA, Ober CK (2004) *Chem Mater* 16:5556
96. Rekštytė S, Malinauskas M, Juodkazis S (2013) *Opt Exp* 21:17028
97. Becker H (2010) *Lab Chip* 10:271
98. Kotz F, Arnold K, Wagner S, Bauer W, Keller N, Nargang TM, Helmer D, Rapp BE (2018) *Adv Eng Mater* 20:1700699

Microbioreactors for Process Development and Cell-Based Screening Studies



Lasse Jannis Frey and Rainer Krull

Contents

1	Microbioreactors for Cell Cultivation	69
2	Homogenization of Microbioreactors	70
2.1	Mixing via Stirring	71
2.2	Pumping	71
2.3	Pneumatic Gassing	71
2.4	Orbital Shaking	72
2.5	Mixing of Droplet Microbioreactors	74
3	Application of Microbioreactors	75
3.1	Microbioreactors for Process Development and Scale-Up	76
3.2	Droplet Bioreactors as Analytical Screening Tool	86
4	Conclusions and Future Perspectives	89
	References	90

Abstract Microbioreactors (MBRs) have emerged as potent cultivation devices enabling automated small-scale experiments in parallel while enhancing their cost efficiency. The widespread use of MBRs has contributed to recent advances in industrial and pharmaceutical biotechnology, and they have proved to be indispensable tools in the development of many modern bioprocesses. Being predominantly applied in early stage process development, they open up new fields of research and enhance the efficacy of biotechnological product development. Their reduced reaction volume is associated with numerous inherent advantages – particularly the possibility for enabling parallel screening operations that facilitate high-throughput cultivations with reduced sample consumption (or the use of rare and expensive educts). As a result, multiple variables can be examined in a shorter time and with a

L. J. Frey and R. Krull (✉)

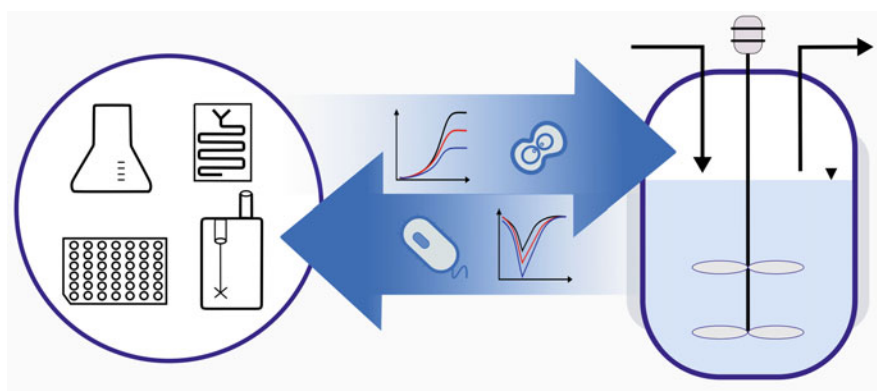
Institute of Biochemical Engineering (ibvt), Technische Universität Braunschweig,
Braunschweig, Germany

e-mail: l.frey@tu-braunschweig.de; r.krull@tu-braunschweig.de

lower expense. This leads to a simultaneous acceleration of research and process development along with decreased costs.

MBRs range from simple miniaturized cultivations vessels (i.e., in the milliliter scale with limited possibilities for process control) to highly complex and automated small-scale microreactors with integrated sensors that allow for comprehensive screenings in very short time or a precise reflection of large-scale cultivation conditions. Progressive developments and improvements in manufacturing and automation techniques are already helping researchers to make use of the advantages that MBRs offer. This overview of current MBR systems surveys the diverse application for microbial and mammalian cell cultivations that have been developed in recent years.

Graphical Abstract



Keywords High throughput, Microbioreactor, Process development, Scale-up, Screening, Sensor integration

Abbreviations

μBC	Microbubble column-bioreactor
μ_{max}	Specific growth rate
CHO	Chinese hamster ovary
cwMBR	Capillary wave MBR
D	Dilution rate
DMF	Digital microfluidics
DO	Dissolved oxygen
EWOD	Electrowetting on dielectric
hMBR	Horizontally arranged plug flow-based microbioreactor
$k_{\text{L}a}$	Volumetric liquid phase oxygen transfer coefficient
K_{S}	Monod constant

LHS	Liquid handling system
MBR	Microbioreactor
MTP	Microtiter plate
n_{crit}	Critical shaking frequency
OD	Optical density
OTR	Oxygen transfer rate
OUR	Oxygen uptake rate
P/V	Mean volumetric power input
PCR	Polymerase chain reaction
PDMS	Poly(dimethylsiloxane)
PMMA	Polymethylmethacrylate
q_P	Specific product formation rate
q_S	Specific substrate consumption rate
Re	Reynolds number
SAW	Surface acoustic waves
t_M	Mixing time
u_G	Superficial gas velocity
$Y_{X/S}$, $Y_{P/S}$, $Y_{P/X}$	Biomass- and product-related yield coefficients from substrate/ biomass, respectively

1 Microbioreactors for Cell Cultivation

To support and control a biologically active environment, any bioreactor must fulfill several elementary tasks – regardless of the reaction scale at issue [1]. In essence, it must create a mono-septic environment, where defined biological reactions can be performed within controlled ambient conditions. These basic requirements apply with equal force to microbioreactors (MBRs), which usually have a reaction volume of less than 1 mL. Other definitions describe a MBR as a small-scale cultivation system containing at least one microfluidic element. A MBR can generally be seen as a miniaturized device that sustains biology [2], combining high-throughput experimentation with profound bioprocess monitoring and control [3].

Working with MBR systems offers several advantages over more traditional systems. First, multiple simultaneous experiments can be conducted in parallel – allowing researchers to study more parameters affecting the cellular functions or process conditions at the same time. Due to this increase in high-throughput capability, biotechnological research and process development can be substantially accelerated. Additionally, lower amounts of samples, reagents, and consumables in general are required for each experiment – resulting in substantial increases in cost effectivity. The shorter distances and increased surface-to-volume ratio are also advantageous for more sensitive analytics and for improved heat and mass transfer. And finally, space requirements are reduced across the board.

These advantages are valuable for both industry and academia – a fact that is illustrated by the great variety seen in developed MBR systems as well as the rate at which they are being incorporated into modern biotechnological research.

Depending on the specific experimental needs, MBRs can be mixed via stirring, orbital and vertical shaking, or pumping or oscillating – with each mixing technique offering its own specific benefits. Besides high-throughput screenings and strain engineering, MBRs have extensively been applied for bioprocess development.

This chapter aims to provide a comprehensive overview of key available MBR technologies. First, different techniques for achieving MBR homogenization are described (Sect. 2). The mixing process in small-scale cultivation systems is a key requirement to ensure effective heat and mass transfer, to avoid creating unwanted gradients inside the reaction volume, and to keep cells in suspension. Various approaches have been developed in an attempt to tackle this challenge. The different fields of MBR applications are then reviewed (Sect. 3). For example, MBR systems have been developed for process development (aiming mainly at scale-up/down experiments) – contrasted with MBR systems that have been developed for analytical screening applications. Finally, future developments and fields of particular research interest are highlighted.

2 Homogenization of Microbioreactors

Ensuring rapid homogenization and sufficient mass transport is a key requirement of all bioreactors. Reproducible measurements generating conclusive and reliable data are only achievable if the creation of unwanted pH , temperature, and concentration gradients are effectively avoided, if cells are reliably supplied with sufficient amounts of nutrients, and if cell sedimentation is prevented [4, 5]. Inhomogeneity and heterogeneities are both major sources of measurement discrepancies and process variances [6–8]. Not only must the fluid phase itself be homogenized, but the mass transfer between liquid and gas phase must also be enhanced. In so doing, both the removal of metabolites and the oxygen transfer into the cultivation broth are intensified. Due to both the low solubility of oxygen in water and the high oxygen uptake of aerobic microorganisms with high specific growth rates, achieving adequate oxygen supply within the liquid phase is considered to be one of the greatest challenges in bioprocess development [9, 10]. Diffusive transport is generally considered to be insufficient for most purposes – necessitating the adoption of an adequate active mixing technique to avoid running into limitations that hinder biomass growth and/or product formation [11, 12]. Additionally, heat and mass transfer must be comparable across scales, if scalability during bioprocess development from micro- to lab- and pilot-scale is to be ensured [13].

Mixing small fluid volumes, however, comes with several inherent major challenges. As the specific systems dimension is reduced, capillary and viscous forces – caused by the enlarged surface-to-volume ratio – increasingly dominate over gravitational and inertial forces [14–16]. And due to the increased surface area, specific interactions between cells and the MBR walls must be carefully considered. Furthermore, the fluid flow in microsystems is by definition laminar, with low Reynolds numbers (mostly $<1,000$) [17]. As a result, the absence of turbulent flow or fluid

vortices can substantially impede proper mixing. To overcome these challenges and provide a wide operating window for particular bioprocess, various strategies have been reported that successfully assure suitable conditions for cell growth and/or product formation. Indeed, the sheer variety of published techniques aimed at solving these issues underscores the importance of ensuring rapid homogenization within biological applications.

Since fully turbulent conditions are very difficult to achieve within the confines of MBR systems, most mixing techniques instead aim to induce and increase chaotic advection and convection in order to enhance the mass transport [14, 17]. To ensure comparability across different mixing techniques, MBR setups, and reactor scales, researchers frequently designate the mixing time (t_M) – i.e., the duration of mixing necessary to achieve a certain homogeneity criteria [18–20]. In most cases, a 95% criterion is applied, meaning that t_M is the time until a homogeneity level of 95% is reached [21].

2.1 Mixing via Stirring

Following the common mixing technique of many lab-, pilot- and technical scale bioreactors, MBRs can be mixed via stirring. Under this method, using a centrally or eccentrically mounted stirrer shaft to blend the fluid and disperse gas into the liquid phase homogenization is achieved using rotating stirrers [22–26]. One advantage of stirred systems is the similarity to bioreactors of larger scale and the resulting analogies in the fluid motion and characteristics [27] – which can facilitate a subsequent scale-up. Additionally, systems with smaller fluid volumes have also been reported with integrated miniaturized stirrer bars or rod agitators [28–32].

2.2 Pumping

To avoid moving elements inside the reaction chamber, MBRs may instead be mixed via a pumping mechanism [33]. Using a digital hydraulic drive for pneumatic pumping, Tsai et al. [34] have developed a miniaturized and robust actuation system that can be connected to standard 96-well plates. The fluid is continuously mixed through up and down pumping, achieving a very gentle homogenization, which is why the main field of application is cell culture analysis.

2.3 Pneumatic Gassing

For increased gas exchange and oxygen transfer rates, MBRs can also be operated as bubble columns by inducing pressurized air at the reactor bottom [35–39]. Lladó Maldonado et al. [36, 37] have characterized the mixing performance of

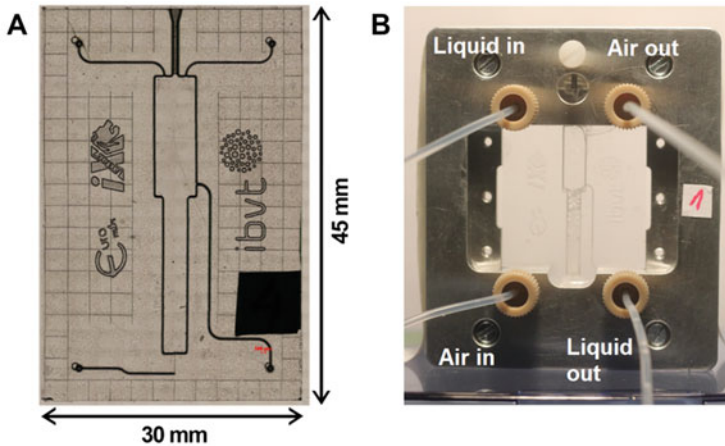


Fig. 1 (a) Borosilicate glass-based microbubble column-bioreactor (μ BC), (b) μ BC inside the supporting reactor holder [36] (© Copyright 2018 Elsevier B.V)

microbubble column-bioreactor (μ BC) for biotechnological research. The μ BC was manufactured with a reaction chamber (3 mm in width, 1 mm in depth, and 18 mm in height) and a funnel at the upper part (5 mm in width, 1 mm in depth, and 14 mm in height) for adequate phase separation (Fig. 1a). The μ BC was also equipped with two inlets and two outlets, one for each phase (gas and liquid) (Fig. 1b).

Mixing experiments were performed at different airflow rates. Figure 2a shows an example of the sequence of images produced immediately after the injection of the fluorescent tracer pulse with a frame rate of ~ 1 fps at an aeration of a superficial gas velocity u_G of $1.3 \times 10^{-3} \text{ m s}^{-1}$. In addition to mixing lab experiments, simulated tracer profiles were also calculated through transient simulations. As an example, time-lapse image series of the transient simulation with the same aeration of $u_G = 1.3 \times 10^{-3} \text{ m s}^{-1}$ are shown in Fig. 2b with a frame rate of ~ 1 fps. When the experimental and simulated tracer profiles are compared for the same aeration rate, this model properly predicted the tracer profile distribution [36].

2.4 Orbital Shaking

The reaction volume of MBRs can also be shaken orbitally, inducing a circular motion of the cultivation broth due to inertial forces. This process is frequently used in micro titer plates (MTP) and shake flasks [40–43]. To overcome the surface tension of a fluid and induce motion, the appropriate critical shaking frequency (n_{crit}) must be exceeded. Due to the increased centrifugal force seen at higher orbital shaking frequencies, the liquid height rises at the outer reactor wall, and the hydrodynamic flow is changed [41, 44]. Hermann et al. [44] have proposed the following equation to calculate n_{crit} :

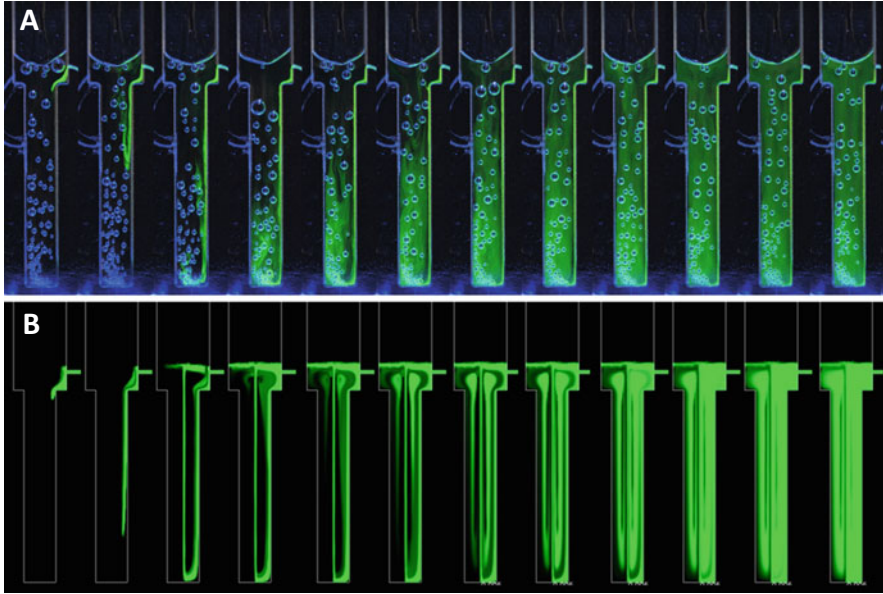


Fig. 2 Mixing time experiments and transient computational fluid dynamics (CFD) simulation in a microbubble column-bioreactor (μ BC) (working volume 60 μ L): (a) Time-lapse image series with a superficial gas velocity set at $1.3 \times 10^{-3} \text{ m s}^{-1}$ after the injection of a pulse of 2 μ L of the fluorescent tracer solution through a needle pump and (b) the transient CFD simulation. The images are shown with a frame rate of $\sim 1 \text{ fps}$ [36] (© Copyright 2018 Elsevier B.V.)

$$n_{\text{crit}} = \sqrt{\frac{\sigma \cdot D_{\text{W}}}{4 \cdot \pi \cdot V_{\text{L}} \cdot \rho_{\text{L}} \cdot d_0}} \quad (1)$$

Here, σ is the surface tension, D_{W} is the well diameter, V_{L} is the liquid volume, ρ_{L} is the density of the fluid, and d_0 is the shaking diameter. For given fluid properties, n_{crit} is inversely proportional to V_{L} and d_0 . Smaller fluid volumes of less than 50 μ L are more difficult to mix – an observation which can be explained by reference to the larger surface forces seen in smaller volumes. As a result, more power must be expended to overcome these forces. It is important to note that orbital shaking only have limited practicability within MBR systems. For increasingly smaller systems, n_{crit} rises quickly – ultimately resulting in impracticable process conditions. However, increasingly smaller systems explicitly benefit from the advantages of MBRs, especially the saving of expensive substrates and facilitated opportunities for parallelization. Since diffusive species mixing is usually too slow to prevent mass transfer limitations in aerobic processes and inadequate for μ L-scale volumes, suitable techniques for small scale mixing are required.

2.5 *Mixing of Droplet Microbioreactors*

To allow for manipulation of smaller fluid volumes below 10 μL , various strategies have been reported that effectively introduce advective transport. MBRs in the low μL range have been reported to be mixed using the application of an electrical potential by implementing a pair of electrodes, which can be configured either in a planar configuration or with a wire hanging from the top into the fluid. This technique is commonly referred to in the literature as *electrowetting on dielectric* (EWOD) [45–48]. By bringing electrostatic charges on the fluid, the latter can be manipulated, spread, moved, and ultimately mixed. EWOD is performed on a pair of insulator-coated electrodes which are covered by an insulating film working as the substrate for a conducting fluid [47]. The technique is characterized by an increased flexibility and possibility to manipulate the fluid volume, and as a result it has achieved wide application within droplet-based analysis systems [46, 49]. The fluid can alternatively be excited in resonance using piezoelectric transducers [50]. Creating frequencies above 10 kHz, the fluid is thereby effectively mixed via vibration. *Surface acoustic waves* (SAW) excited by acoustic streaming propagate through the liquid and set the liquid into motion, achieving extremely fast mixing within small volumes [14]. The technique and its advantages for the application in microfluidics are described in depth by Yeo and Friend [51]. In the latter techniques, mixing energy is being transmitted via oscillations that excite the phase boundary to resonate. Through the high-frequency oscillations and the resulting increased power input, however, the fluid temperature in small fluid volumes tends to rise, and cells are potentially disrupted [50]. Additionally, manufacturing these devices requires extensive efforts for shielding the electronics.

Another mixing technique for small fluid volumes that requires even less operational effort is the induction of capillary waves on the liquid surface via vertical oscillation [52]. If excited in resonance, a stationary wave is formed on the phase boundary of the liquid and the gas, due to competing inertia and surface tension forces [53–55]. This wave subsequently leads to rapid bulk mixing – which has been successfully used for mixing a 20 μL MBR [56] as well as a 7 μL system [57, 58] and achieving fast homogenization in less than 3 s using oscillations below 400 Hz. The capillary wave MBR (cwMBR) is shown in Fig. 3.

In the cwMBR setup, a Foturan® glass chip is used to form a defined fluid droplet with a reproducible interphase, which can be excited in resonance by vertical oscillation. Using four electromagnets, an oscillation table – where the reactor chip is mounted – is excited with specific oscillation conditions [58]. Here, oscillation in resonance leads to unique modes, which is defined by the number and position of the nodes [53, 55, 59].

In Fig. 4, different oscillation modes of a cwMBR filled with dyed water excited at resonance frequencies are illustrated. The resulting mode patterns are characteristic for each frequency.

Aside from the vertical displacement, excitation frequency is the decisive factor for resonance and the resulting power input. In Fig. 5, the inverse mixing time $1/t_M$ is

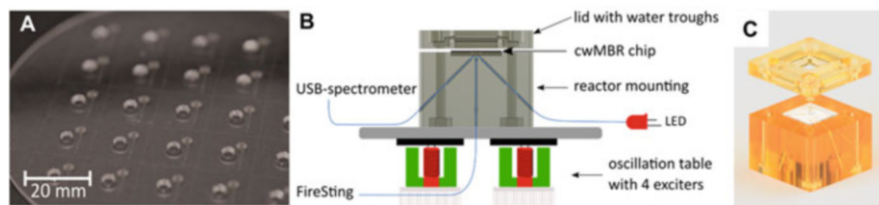


Fig. 3 Capillary wave MBR (cwMBR) setup: (a) 5×5 array manufactured on a 4 in. Foturan® wafer [57] (© Copyright 2019 MDPI AG). (b) Side view of reactor mounting with optical fiber side-in module and sensor assembly of optical measurements. (c) Perspective view on rendered cwMBR mounting with base element, cwMBR and lid, having four water troughs in the walls. All parts are clamped together using four screws [58] (© Copyright 2020 Elsevier B.V)

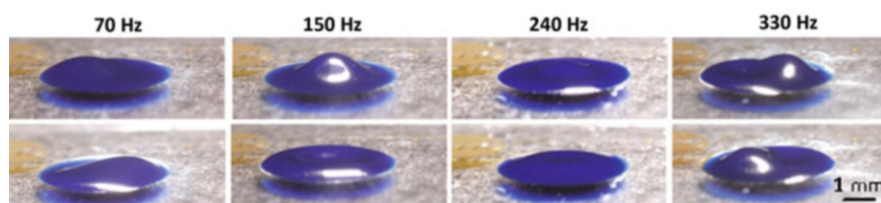


Fig. 4 Perspective view on the cwMBR filled with dyed water excited at its resonance frequencies. Different oscillation patterns are formed on the liquid surface, whereby the wavenumber increases for higher excitation frequency. Two characteristic time points are shown, where the amplitude of the oscillating liquid interface is the highest. Images were taken with a single-lens reflex camera (EOS 60d, Canon, Tokyo, Japan) connected to a micro-Nikkor objective (Nikon, Tokyo, Japan) with a focal length of 55 mm and a triggered ultrashort time flash with an exposure time of 1×10^{-5} s [58] (© Copyright 2020 Elsevier B.V)

shown for frequencies up to 400 Hz. The maxima of $1/t_M$, which corresponds to fast mixing, correlate well with the calculated resonance frequencies shown on top in red [58].

Finally, it is worth noting that mixing MBRs with continuous flow in enclosed micro-channels – which open up possibilities for massive high throughput – have also been described in detailed reviews [17, 59].

3 Application of Microbioreactors

There is a tremendous and growing demand for potent MBR systems that can be used to cultivate cells in the micro-scale and simultaneously permit automatized highly parallelized operations in which various process parameters can be independently modified. These systems are increasingly being applied in the field of bioprocess development, where they aim to mimic larger-scale (from lab- to pilot- and process-scale) cultivation systems. The knowledge acquired in these smaller-

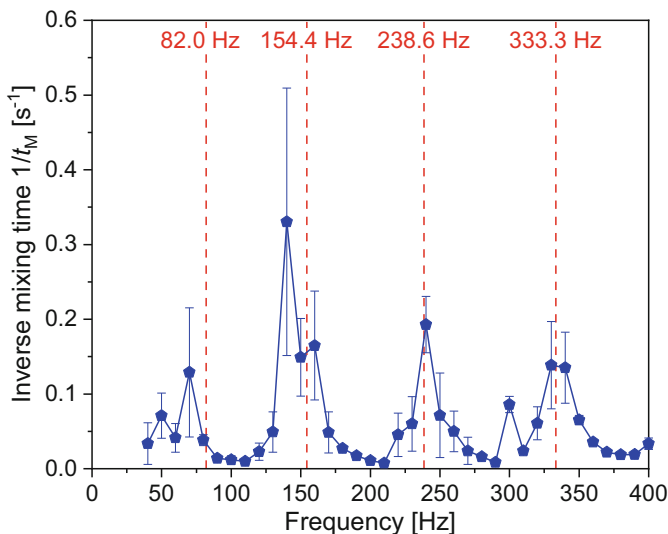


Fig. 5 Inverse mixing time $1/t_M$ for frequencies up to 400 Hz at excitation strength of 20%. Calculated resonance frequencies are shown on top in red. All data are given as mean and standard deviation ($n = 3$) [58] (© Copyright 2020 Elsevier B.V)

scale systems can then be transferred to the sequential process steps used to perform a process scale-up. But even aside from process development and the related scale-up, the advantages of MBRs are also increasingly being leveraged for screening applications – where these systems are used mainly for analytical purposes. In this context, the more pressing concern is the performance of cellular experiments in an automated high-throughput fashion for rapid generation of experimental data. It is therefore more important to sustain the cell population under carefully defined conditions and perform ongoing measurements, rather than to precisely mimic large-scale process conditions.

By applying MBR systems, lower sample consumption is achieved – which translates lastly into cost savings [60]. Additionally, the process development can also be substantially accelerated, since the number of samples processed in parallel is increased [61].

3.1 Microbioreactors for Process Development and Scale-Up

Bioprocesses are influenced by numerous factors that can significantly affect the performance efficiency of bioconversion. Profound knowledge of biological reaction kinetics is of crucial importance for high yield bioproduction to achieve optimal process conditions. For example, growth behavior, product formation, and yields are all heavily dependent on physicochemical parameters such as pH , temperature, and

nutrient availability, as well as overall media composition [62]. Additionally, ambient cultivation conditions in the bioreactor have a direct bearing on the entire process. Power input and the associated mixing performance are key parameters affecting nutrient availability and fluid homogeneity, as well as the operating shear stress appearing on the biocatalyst [10, 63, 64].

Accordingly, in order to effectively develop and improve a bioprocess, a holistic knowledge and insight into the entire bioprocess is a prerequisite. Acquiring this knowledge requires multiple experiments to thoroughly investigate all decisive factors in detail. In order to effectively reduce the applied substrates and volumes used per experiment, miniaturized cultivation systems are increasingly being applied to bioprocess development [3, 9, 65–68]. By reducing the reaction volumes required and applying small-scale cultivation systems instead, expenses can frequently be slashed – and, even more importantly, the degree of parallelization (i.e., simultaneous experiments) can be substantially increased [69].

In standard lab-scale bioreactors with a volume of 1 to 30 L, bioreactions and growth kinetics, product titer, and ultimate quality are also adequately representative to a pilot-scale reactor. But the achievable throughput is limited, and experimental operation is frequently elaborate. Especially in early stage process development, the number of variables that need to be examined often exceeds the capabilities of these lab-scale cultivation systems. As a result, it typically requires at least 50 experiments for characterization of a cultivation process – which can take up to 8 months to complete [69, 70]. Not surprisingly against the backdrop, systems that enable higher experimental throughput are in great demand.

A typical development of a biotechnological process is a sequence of consecutive steps. Starting from small reaction volumes with lower information content (but with a high number of variables to be examined), the reaction throughput decreases, and the information content gradually rises throughout the development process. The number of biological variables that need to be investigated is continuously being reduced in the course of the process development [3]. Initial screenings for an optimal production strain are often conducted in microtiter plates (MTPs) to enable the performance of up to 96 simultaneous reactions in parallel. Aside from the selection of the requested production strain, media development and adjustment can also be performed in this stage. The gathered information then informs the next larger-scale stage, which is mostly conducted in shaking flasks with a fluid volume of 10 to 100 mL. The number of parallel cultivation experiments that may be conducted in shaking flasks is already significantly limited, however, due to the labor-intensive nature of this phase of operations. Only the most promising cultivation conditions for the depicted production strain or host are then brought to the lab-scale bioreactor, where a level of process control comparable to that seen in the pilot scale is once again possible. In this pilot-scale stage, challenges related to the final large reaction volumes and scale-up must be addressed; these can include a higher hydrodynamic pressure, higher Reynolds numbers, higher mixing times, as well as more pronounced bioreactor inhomogeneities for increasing reaction volumes [65].

MBR systems aim to enhance and optimize this traditional process development workflow. The bioprocess itself is aimed to only minimally be affected by the scale-down and related changes in the cultivation scale. At the same time, the experimental throughput is ought to be enlarged maintaining the operational control of miniaturized cultivation systems. By mimicking a large-scale reactor, a quantitative characterization as well as a comparison across scales is supposed to be enabled.

For this purpose, a great variety of MBR designs and setups have been reported and applied, and several systems are currently commercially available. These systems differ significantly in the reaction volume required, the form of the cultivation vessel, the applied mixing techniques, and the gas supply – but shaking and stirred methods still constitute the majority of reported MBR systems.

3.1.1 Microtiter Plate-Based Microbioreactors

Addressing the lack of monitoring physiological parameters that characterize the early stages of process development, MTP-based cultivation systems with integrated online sensors (biomass, DO, *pH*, fluorescence) are prevalently applied [71]. These systems are mixed via orbital shaking, and the aeration is solely performed via the head space – resulting in volumetric liquid phase oxygen transfer coefficients ($k_L a$) up to 250 h^{-1} which enable even oxygen-demanding *Escherichia coli* cultivations, depending on the respective oxygen uptake rate (OUR) and the biomass concentration. To enlarge the oxygen transfer rate (OTR) and improve the mixing performance inside the micro-wells, a baffled MTP was also developed and applied for bioprocess development. With $k_L a$ values up to 600 h^{-1} , oxygen limitations can be avoided, and the OTR of large-scale cultivations can be modeled [42, 43, 72, 73]. The so-called *Biolector* system (m2p-labs, Baesweiler, Germany) was applied for the quantitative evaluation of media and nutrients, in order to detect differences in biomass and product yields [74, 75].

Due to their inherent enhanced degree of parallelization, MTP-based cultivation systems are well suited for screenings, determining optimal media compositions [76], growth conditions [77], and identifying optimal clones from strain libraries [78–82]. These working groups have therefore shown that they have developed versatile and major systems in high-throughput cultivation devices.

Besides microbial cultivations, MTP-based systems have also been applied as cultivation and process development tool for mammalian cells. The 24 deep square well plate (standard SBS (Society for Biomolecular Screening) format) system *micro-Matrix* (Applikon, Delft, Netherlands) was used for cell culture process development [83–85]. The system consists of 24 individual reaction elements, where each well can be individually controlled for *pH*, temperature, and dissolved oxygen (DO). Applying an additional feeding module, automated addition of substrates is enabled – which facilitates process development in the fed-batch mode. It can therefore be applied to optimize both feed and growth parameters [3]. Additional commercial systems are available from Pall (*micro-24*, New York, USA) featuring continuous aeration [86–89] and from Oy Growth Curves Ab (*Bioscreen C*,

Helsinki, Finland) with up to 200 reaction vessels in parallel [90–92]. Other systems have been reported by Harms et al. [93], Lamping et al. [85], and Zhang et al. [94].

Cultivation in MTP-based systems enables parallel examination of various reactions, although cultivation conditions (i.e., shaking frequency, temperature, etc.) can only be adapted for all wells in parallel. To individually manipulate separate culture wells, the shaking movement must be stopped – which can negatively affect the growth performance, due to oxygen transfer and decline of mass transfer [78, 87]. If more global parameters on the process performance are to be investigated, separate MTP cultivation runs must be performed, which also negatively effects the throughput [3].

Shaken MBR systems are advantageous due to the absence of movable parts inside the reaction chamber, which are prone to error and challenging in microfabrication. The fluid movement can also be compared to shake flasks with ease, which is often the next larger scale in process development workflow.

3.1.2 Microbioreactors with Rotating Mixers

In addition to the orbitally shaken systems, several stirred cultivation systems have been reported in the literature – and some are even coming onto the commercial market. These stirred systems can mimic the predominant conditions of lab-scale reactors even more precisely. For example, a single-use miniaturized stirred cultivation system with 24 or 48 parallel MBR, having a reaction volume of 10–15 mL, has been developed for cell culture applications, cell line development, and feed and growth parameter optimization [23, 24, 27, 95–97] – although it is also being applied for microbial process development [98]. The cultivation broth in the *ambr*[®] 15 (Sartorius, Göttingen, Germany) is mixed via stirring by an eccentrically positioned stirrer. For monitoring the cultivation process, *pH* and DO can be measured quasi-continuously online via optodes, and the elevated reaction volume also enables some degree of sampling. The high-throughput capabilities of the system are fully amplified if the *ambr*[®] 15 is operated by a liquid handling system (which enables automated cultivations). Besides batch and fed-batch processes, the *ambr*[®] 15 can also be operated in a quasi-continuous perfusion mode. Using sedimentation for cell retention, a scale-down perfusion cell culture reactor was applied to predict viable cell concentrations of human cell lines [95]. When compared to 1 and 1,000 L approaches, this miniaturized system showed accurate prediction of product quality attributes – especially glycosylation profiles. Yet the cell culture media requirements were reduced 80-fold, and the daily operator time was halved – resulting in a massive cost saving and facilitation of much more resource-efficient process development. Extensively applied in process optimization and scale-up, the *ambr*[®] 15 has proven to be an excellent scale-down model for large-scale bioreactors [27, 99].

A miniaturized cultivation system ($V_L = 10$ mL) with a magnetically driven one-sided paddle impeller is reported by Hortsch et al. [25, 100]. This system is specifically designed to promote the growth of mycelium forming microorganisms. The rotating stirrer forms a liquid lamella to effectively prevent wall growth or

foaming. The system was characterized in terms of k_1a coefficients and volumetric power input, to compare its performance to a 2 L lab-scale bioreactor. For a given mean volumetric power input, the maximum local energy dissipation in the stirred MBR was reduced (compared to the lab-scale bioreactor) and showed a more uniform power distribution into the reaction medium for the smaller scale. Despite these discrepancies, similar power consumption characteristics were found on both systems – proving a reliable scale-up possibility with the miniaturized bioreactor. To enhance the applicability for enzymatic processes, the stirrer setup was further optimized and applied to the hydrolysis of suspended plant cells [101]. Additionally, when the stirred miniaturized reactor systems were applied for the microbial expression of recombinant proteins in a reactor cascade setup, they outperformed a continuous process [102, 103].

Downsizing the reaction volume of cultivation systems primarily restricts their ability to monitor and control the cultivation process – which is why MBR systems for process development are generally limited to the upper μL or lower mL range, where the information content and its validity are somewhat higher [104–106]. But smaller systems are still being developed in an effort to continue to refine and optimize the potential benefits of miniaturization.

The use of miniaturized stirrers to achieve an active mixing technique in liquids at the μL range certainly still poses challenges. It was successfully reported by Szita et al. [28] in a system made of fused layers of polymethylmethacrylate (PMMA) and poly(dimethylsiloxane) (PDMS) housing a liquid volume of 150 μL . Monitoring DO and pH , this system can log elementary procedures in the small reaction chamber which is fed by microfluidic channels connected to fluidic ports. With agitation frequencies up to 700 min^{-1} , batch cultivations of *E. coli* were performed which corresponded well with similar cultivations performed in 500 mL lab-scale reactors (SixFors®, Infors, Bottmingen, Switzerland), as well as in shake flasks [32]. Using the microfluidic inlets for reagent feeding, chemostat cultivations were also performed [107]. After modifying the system setup slightly (by increasing the vessel height and reinforcing a membrane barrier), this system was also applied for gene expression studies of *Saccharomyces cerevisiae* and *E. coli* in glucose and galactose media [29, 30].

A considerably smaller system for batch or continuous cultivations of suspension cells with a cylindrical reaction volume of 100 μL was reported by Schäpper et al. [31]. It aims to combine the advantages of MTPs (small working volume) with more versatile bench-top reactors. In this system, homogenization is ensured and cell sedimentation prevented by use of a stirrer bar that is left to freely float within the reaction chamber. Similar to many previously reported systems, DO and pH can be monitored online in the presented MBR. Additionally, via absorbance measurements, the cell density and cell growth can be determined.

3.1.3 Microbioreactors Without Movable Mixing Elements

Taking a similar approach, and in an effort to accommodate biological reaction kinetics from stationary process data of a chemostat cultivation, Edlich et al. [108] have developed a horizontally arranged plug flow-based microbioreactor (hMBR) where the main flow direction is perpendicular to the lift force. The hMBR foregoes movable parts inside the reaction chamber and operated with a reaction volume of 8 μL . The hMBR was made of glass and PDMS manufactured by soft lithography technology and had integrated sensors for optical density (OD) and DO. The oxygen was diffused into the cultivation broth through the PDMS membrane. Here, the concentration gradients of the limiting substrate, metabolites, and products occur not only over the length of the reactor but also along the hMBR height in terms of cell distribution and the oxygen supply. However, this system came with one significant disadvantage: bubbles that arose in the mixture could remain in the system, thereby displacing the liquid and/or influencing or even completely blocking the liquid flow and disturbing optical measurements.

An alternative and improved operation was developed by Peterat et al. [35], in a vertical configuration featuring active pneumatic gassing and material surface hydrophilization to ensure planktonic cultivation of microorganisms and to prevent wall growth [109]. By inducing a continuous fine bubble stream at the reactor bottom, Peterat et al. [35] created a μBC made of borosilicate glass with a reaction volume of 70 μL [35, 38], which was further developed by Lladó Maldonado et al. [36] (compare Figs. 1 and 2). By harnessing pneumatic aeration with pressurized air, several key challenges in MBR development were addressed: namely, inadequate homogenization and related mass transfer limitations. This MBR setup with the particular mixing technique has proven to support an environment favorable for growth of yeast cells, which was monitored via absorbance and optical DO measurement.

In this μBC , Krull and Peterat [38] carried out cultivations with the Crabtree-positive yeast *S. cerevisiae* CCOS 538 in chemostat cultivation by varying the dilution rate D between 0.12 and 0.42 h^{-1} . The values for the parameters of the reaction kinetic model were determined analytically, using experimental data for the stationary concentrations of biomass, substrate, and ethanol as primary product on the micro-scale. The maximal specific growth rate (μ_{\max}) and the Monod constant (K_S) were calculated using linearization methods (Lineweaver-Burk, Eadie-Hofstee, and Hanes-Woolf). Considering the empirical model of Luedeking and Piret for product kinetics, the yield coefficients $Y_{X/S}$, $Y_{P/S}$, and $Y_{P/X}$ were determined from plots of the specific substrate consumption rate $q_S = f(\text{dilution rate}, D)$ and the specific product formation rate $q_P = f(D)$, respectively. The kinetic reaction model was in agreement with the experimental data – and hence it provided a solid mathematical description of the biotechnological process (Fig. 6).

Considering the Crabtree effect on yeast metabolism, the two following validity ranges of the kinetic model were discussed in detail: (a) $\mu = D < D_{\text{crab}}$, applied to purely oxidative metabolism, in which glucose was completely converted into

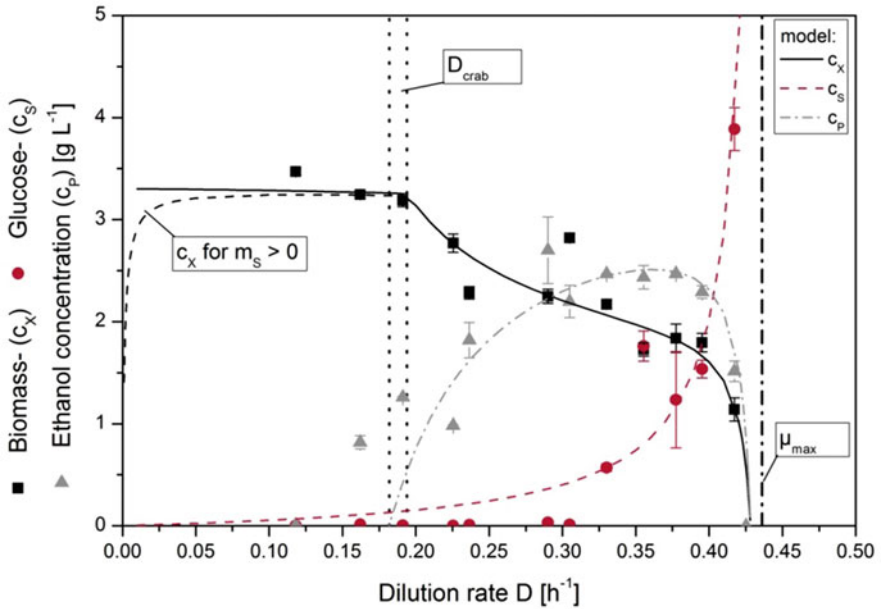
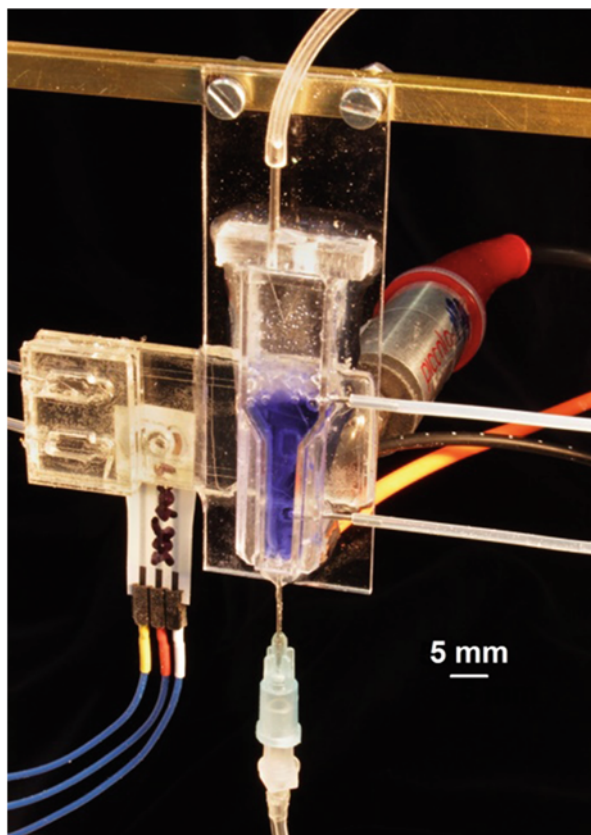


Fig. 6 Comparison of the values obtained using the reaction kinetic model, using estimations of the steady-state glucose (c_S , - - -), biomass (c_X , —), and ethanol concentrations (c_P , - · -) and the experimental data (c_S , ●), (c_X , ■), and (c_P , ▲) for the continuous cultivation of *S. cerevisiae* in the μ BC as a function of the dilution rate D . The parameters used in the reaction kinetic model were as follows: $c_{S,in} = 10 \text{ g}_S \text{ L}^{-1}$, $0.182 \leq D_{crab} \leq 0.194 \text{ h}^{-1}$, (a) $\mu = D < D_{crab}$ (purely oxidative metabolism) $\mu_{max} = 0.436 \text{ h}^{-1}$, $K_S = 0.182 \text{ g}_S \text{ L}^{-1}$, $Y_{X/S} = 0.335 \text{ g}_{CDW} \text{ g}_S^{-1}$, $m_S = 0$ and c_X , - with m_S (maintenance coefficient) $= 0.004 \text{ g}_P \text{ g}_{CDW}^{-1} \text{ h}^{-1}$, and $Y_{P/X} = 0$; and (b) $\mu = D > D_{crab}$ (oxido-reductive metabolism with an active Crabtree effect), the same values as above for μ_{max} , K_S and $Y_{X/S}$, $Y_{P/S} = 0.715 \text{ g}_P \text{ g}_S^{-1}$, $Y_{P/X} = 2.637 \text{ g}_P \text{ g}_{CDW}^{-1}$, and $m_S = 0$ [38] (© Copyright 2016 Elsevier B.V)

biomass or was used for endogenous maintenance metabolism and no ethanol was generated, and (b) $\mu = D > D_{crab}$, applied during oxido-reductive metabolism occurring under the Crabtree effect, in which ethanol was formed at the expense of biomass generation under aerobic conditions. This production of ethanol was strictly coupled to the metabolic activity occurring and was growth-associated. The data obtained using the μ BC was then compared with the results obtained in chemostat experiments conducted on a macro-scale in stirred tank reactors (2.5 and 2.85 L) by Rieger et al. [110] and von Meyenburg [111, 112], respectively. Despite the fact that the volumes in question differed by a factor of $\sim 50,000$, the values determined using the microsystem were of the same order as the values for the kinetic constants of the published experimental data from laboratory scale and thus validate the applicability of the μ BC as a suitable screening tool for aerobic submerged cultivations [38].

To facilitate the integration of miniaturized sensors, another prototype was also developed. Based on similar reaction geometries combined with the active pneumatic bubble aeration, a reaction setup with 550 μL made of polystyrene was equipped with additional online sensors [37] (Fig. 7).

Fig. 7 Picture of the μ BC with the microfluidic flow chip and glucose biosensor; the inlets and outlets of the liquid and gas phases; and the integrated sensors for pH , dissolved oxygen, and optical density with their associated glass fibers [113] (© Copyright 2019 Wiley)



To avoid sampling, glucose as the limiting carbon source was measured with a microfluidic chip housing an electrochemical biosensor. The addition of online OD , pH , and DO sensors facilitated a holistic evaluation of the biological process. The system was then applied for multiphase chemostat cultivations in the μ BC to determine reaction kinetics of *Staphylococcus carnosus* proving its applicability for submerged cell cultivations by achieving steady-state biomass and substrate concentration in chemostat mode for various dilution rates [113]. Additional microbubble column bioreactors were also reported by Doig et al. [114, 115], Betts et al. [89], and Weuster-Botz [116].

3.1.4 Challenges in Upscaling of Processes Evaluated in Microbioreactors

The aforementioned MBR systems aim to scale-down bioprocesses and thereby provide effective platforms to execute efficient process development. However, due to differences in fluid dynamic properties, mass gradient profiles, and

inhomogeneities, a large-scale bioprocess can only ever be mimicked partially and insufficiently by miniaturized cultivation systems. As a result, any MBR system will always remain (at best) an approximation of the corresponding large-scale bioprocess it is supposed to mimic. The further research must therefore be especially attuned to the potential for process confounding variabilities, making a surround understanding of the entire process of crucial importance [117, 118]. This leads to a diverging physiology and productivity of the production organism when it is evaluated in the scale-down experiment. Miniaturizing the reaction volume is always also accompanied by an increase in surface area-to-volume ratio, which results in disproportional effects of capillary and viscous forces compared to gravitational and inertial forces [14–16]. Consequently, greater efforts must be made to ensure homogenization and to prevent mass transfer gradients requiring higher agitation speeds for mixing. The risk of wall growth is also comparatively greater, due to the altered fluid dynamics and the higher tendency of microsystems to form eddies. Another phenomenon with enhanced effect in small-scale systems is liquid evaporation – and the resulting dilution and concentration effects [69, 119, 120]. By contrast, large-scale bioreactors exhibit higher hydrostatic pressures by nature, which cannot be imaged insufficiently in small-scale systems. Fluid dynamics in microfluidics cannot by definition exceed transitional regimes – whereas turbulent flow is mostly aimed to achieve for homogeneous process control [121]. Furthermore, mixing times in large scales also tend to be larger, which frequently results in the formation of concentration and temperature gradients. Microorganisms or cells therefore often experience oscillating environmental conditions, which can substantially impact growth kinetics, product formation, and quality [27, 122].

3.1.5 Scaling Parameters

To obtain similar environments across scales, several scaling parameters are reported in the relevant literature which must be kept constant for increasing the reaction scope [123]. Relevant scaling parameters can refer to either mean volumetric power input (P/V) or power consumption [63, 64]. Notably, however, the power input also influences multiple other parameters – affecting mass transfer and mixing, as well as shear stress and (resultingly) cell morphology and viability [25, 89, 124]. Because oxygen transfer into the liquid phase is for aerobic bioprocesses one of the most important transport processes [9, 10], a common scaling parameter is the volumetric liquid phase oxygen transfer coefficient k_{La} [11, 125–127]. Oxygen is poorly soluble in aqueous solutions and therefore constitutes a limiting factor for cell growth. The k_{La} value represents the capacity of a system to transport oxygen from the gas to the liquid phase, which is kept constant across scales to ensure similar oxygen supply. If the oxygen driving force, being the concentration gradient between gas and liquid phase, is also considered, then the oxygen transfer rate (OTR) can be used as an additional scaling parameter [11].

$$\text{OTR} = k_L a \cdot (c_{\text{O}_2, \text{L}}^* - c_{\text{O}_2, \text{L}}) \quad (2)$$

Here, $c_{\text{O}_2, \text{L}}^*$ is the DO saturation constant and $c_{\text{O}_2, \text{L}}$ is the apparent DO concentration in the liquid phase. If the driving force across the scales is not equal (due to the hydrostatic pressure or other effects increasing the oxygen saturation concentration), then scaling down of a bioprocess to the MBR scale by keeping the $k_L a$ constant will result in an altered OTR [65]. Hence, the oxygen availability and supply for cells in the reaction volume are affected – which may result in differences in cell growth and bioprocess kinetics.

To avoid creating unwanted concentration and/or temperature gradients inside the reaction volume, mixing and mass transfer must be ensured at all scales. The mixing time t_M can therefore be used to compare process scales, keeping homogenization constant. t_M tends to increase for large-scale bioreactors, however [126, 128]. Another vulnerable scaling parameter is the Reynolds number (Re), being the relation of inertial to viscous forces. It appears that turbulences of geometrical similar bodies are identical at the same Reynolds numbers – meaning that flow conditions can be compared via Re . But as a result of enhanced viscosity and surface forces dominating inertia and gravity at small scales, velocity and flow conditions cannot be accurately mimicked by keeping Re constant across scales [14–16]. Since Re refers to the characteristic system dimension, it tends to be small and under-predicted, resulting in a laminar flow for microfluidics by definition [14]. These missing turbulent flows can impede proper mixing as the system dimension is reduced, thereby hampering the scale-up process. Aside from $k_L a$, OTR, t_M , or Re , stirrer tip speed for stirred systems [129, 130] or the superficial gas velocity u_G [131] for actively aerated systems can also be used as scaling parameters.

A great variety of studies are now being reported in which bioprocesses are scaled up based on a single process parameter, while other parameters are not taken into account. To truly develop a holistic image of a large-scale process using miniaturized cultivation systems, however, a much more complex characterization of the process parameters is critical. This requires the consideration of multiple scale-up parameters – all of which exert a strong influence on the process performance. Tajsleiman et al. [65] report one such illustrative case study about the influence of different scaling parameters on the success of the process transfer. Here, different scaling parameters overlap in a pilot-scale bioprocess mimicking a 100 m³ bioreactor, but lie far away from each other in a MBR system.

For an additional and more comprehensive view on small-scale cultivation systems for process development, in-depth reviews from Breslauer et al. [132], El-Ali et al. [133], Schäpper et al. [66], Bareither and Pollard [69], Hegab et al. [67], Kirk and Szita [9], Lattermann and Büchs [68], Krull et al. [4], Hemmerich et al. [3], as well as Junne and Neubauer [134] are all recommended.

3.2 *Droplet Bioreactors as Analytical Screening Tool*

The application of MBR systems to accelerate the optimization of bioprocesses has become an increasingly common practice in industrial and academic research fields – which has led to a substantial rise in the number of commercially available miniaturized cultivation devices. But aside from process development and scale-up, MBRs are also potent analytical tools for obtaining deeper insight into cellular processes and microbial physiology [135]. Compared to the application in bioprocess development (where the main focus lies on mimicking a larger-scale cultivation system), MBR systems can help to analyze the internal cellular physiological and to perform specific monitoring tasks. These advantages are particularly potent in facilitating early screening procedures or strain selections with extensive probes and variables requiring a high degree of parallelization [65].

Screenings with enhanced throughput are routinely performed in MTP formats. Offering between 6 and 1,536 reaction cavities, simultaneous experimentation can potentially accelerate the rate of biotechnological research and development with minimal manual intervention [136]. Having said that, sensor integration, monitoring, and control are more difficult and limited in comparison with larger cultivation systems – in which can in turn negatively affect the quality and validity of the generated data. The evaluation and analysis of experimental data consequently becomes a highly important consideration.

MTPs have been used to screen for specific microbial strains with a desired capacity concerning the metabolism, displaying a novel enzyme activity, or having certain adaptive capacities to environmental conditions [136]. Here, in-house or external cell libraries can be routinely tested for biocatalytic activity [78]. Additionally, cell lines can be improved using directed evolution and a variety of genetic techniques to enhance enzymatic specificity. After cell line development has been completed, the apparent process conditions, as well as media compositions, bioprocess kinetics, cell growth, yields, and oxygen requirements, can all be optimized [136]. Genome engineering of *E. coli* for enhanced growth rate and a reduced lag time was conducted in a MTP-based system [82, 137]. An improvement of product yields and formation rates in *Bacillus subtilis* was also performed by Motta dos Santos et al. [138]. Furthermore, for synthetic biology approaches, *Corynebacterium glutamicum* was modified, and irrelevant gene clusters were deleted [139]. Using a complementary *respiration activity monitoring system (RAMOS)*, comprehensive data about growth behavior and product formation was achieved [74]. MTP systems have also been applied for clone screening and optimization of feeding strategies [81].

The application of MTPs has greatly improved the capabilities to perform multiple experimental preparations – whether in a metabolic assay or a cultivation process – in parallel. Compared to classical laboratory shaking flask experiments, generation of valuable experimental data can be massively accelerated – but MTP-based systems can also involve a certain lack of flexibility and versatility and also pose challenges in fluid manipulation and operation.

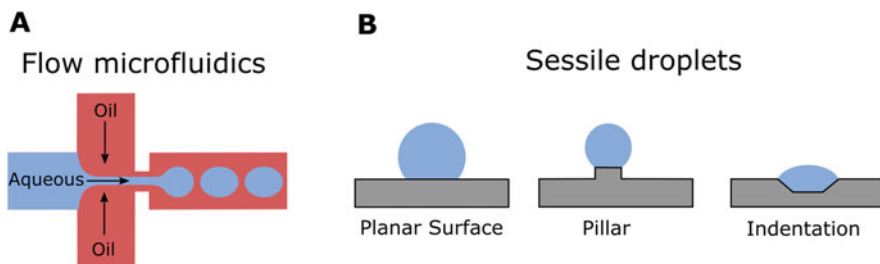


Fig. 8 Operation modes in droplet microfluidics in cross-sectional view. (a) Generation of droplets in an enclosed microchannel/capillary with a continuous fluid flow for droplet convection. Here, the droplets are generated via flow focusing. Additional method to generate droplets in flow is via a T-junction or a co-flow in a capillary (adapted from [141]). (b) Sessile droplets either pinned to a planar surface, placed on a pillar (adapted from [60, 142]), or positioned into an indentation of a flat surface ([57], adapted from [58])

Droplet-based cultivations systems are striving to fill this gap and meet the increasing demand for experimental data in biopharmaceutical research with a particular focus on versatility and high throughput. Each droplet is a separate fluid element and can therefore be seen as an individual reactor vessel [60]. For droplet-based microfluidics, two distinct operation modes have been developed: the droplets are either (a) generated in an enclosed microchannel or capillary and conveyed via a continuous fluid flow (see Fig. 8a) or (b) formed on an open and planar surface where they are shaped due to the surface tension of the fluid and interactions at the liquid-solid interphase (see Fig. 8b) [46, 60, 140].

A holistic outline on droplet microfluidics is given in the chapter *Droplet Microfluidics for Biotechnology* (M. Agler-Rosenbaum) within this book. Here, the primary focus lies on an operation mode, which is also referred to as “sessile droplets.” The form of these sessile droplets can range from rather flat puddles and spherical shapes – mostly depending on the hydrophobicity of the solid surface and the resulting contact angle of the droplet forming fluid [143]. The droplets can be positioned on a flat surface, on a pillar, or in an indentation to edge it and define the location. While these droplets are generally non-mobile and fixed to a defined position, different techniques have also been employed to control and move droplets on the solid surface. This droplet manipulation can be performed using acoustic or electric actuation. If droplets are manipulated via electrowetting on an array of electrodes, it is referred to as *digital microfluidics* (DMF) [45, 46, 60]. Sessile droplets are mostly in the nL to μL range – larger than droplets in flow microfluidics, where mostly pL to nL droplets are handled. This facilitates the generation of sessile droplets, what can be performed using regular pipettes or piezoelectric transducers [144]. In contrast to flow-based microfluidics, each droplet in DMF can be controlled individually, without the need for microfluidic channels, pumps, or valves [46]. Due to the small fluid volumes in DMF and sessile droplet systems, the capacity for parallelization and automation is increased, sample consumption is decreased, and integration of straightforward analytical techniques is facilitated [145]. These

advantages all render sessile droplets a particularly versatile platform that can serve as a potential alternative to microplates [60].

Sessile droplet systems were applied for cell-based testing of active pharmaceutical ingredients [146, 147]. This system has been utilized (among others) for droplet manipulation by transferring, splitting, fusion, deposition, and mixing; cell culturing and drug testing can be performed on a droplet array. Using a PDMS droplet operation array, drug screening assays on lung cancer cells were reported by Du et al. [148]. Over a period of 11 days, cell culture experiments were performed in 500 nL droplets. Another cell-based assay device has been reported by Fang et al. [149]. This device is able to perform 3D cell culture, cell co-culture, and cell migration assays. Sessile droplet systems have also been applied for chemical and enzymatic synthesis, to study reaction kinetics or discover new compounds [49, 150, 151]. Since the droplet bioreactor systems require less consumables and have a lower sample or reagent consumption, these systems are particularly advantageous in situations where only small amounts of samples are available. This holds true for analytical applications including immunoassays [152–155]; nucleic acid amplifications or other DNA-based assays such as polymerase chain reaction (PCR), sequencing, hybridization, and extraction [156–161]; and clinical diagnostics [153, 162].

In addition to the operation mode of sessile droplet bioreactors, there is also another operation mode which is closely related to sessile droplets on planar surfaces – only with a flipped arrangement. In such systems, the droplet is pinned to a solid surface (via surface forces which exceed gravitational force). This has been applied for cell spheroid cultivation, creation of organoids, and cell migration assays [60, 149]. Both operation modes can also be combined, as showed by Ma et al. [149], in systems where upper sessile droplet is separated via a horizontal membrane from a lower hanging droplet. In-depth description of further applications of sessile droplets and DMF has also been reported by Choi et al. [46], Ng et al. [45], and Garcia-Cordero and Fan [60].

One inherent challenge of sessile droplet systems is fluid evaporation – which leads to proportionally high losses of fluid in relation to the droplet volume. Evaporation, and the related drying out of the droplet, can begin immediately after the droplet generation and exposure to a gaseous atmosphere [163]. Through this fluid loss, concentrations in the droplet are raised, leading to sample enrichment – which subsequently affects data accuracy and reduces the duration for potential experiments. The rate of evaporation kinetics is influenced by many factors, including fluid properties (i.e., volatility, surface tension, viscosity), the properties of the solid surface in question (wettability, roughness, thermal conductivity), and the properties of the surroundings (temperature, relative humidity, and pressure) [60, 164]. Without adequate countermeasures, a typical droplet with an almost spherical shape dries in between 200 s and 3 h [165, 166]. If the cultivation media (i.e., the fluid properties) cannot be modified, then the experimental surroundings and droplet environment must be adjusted. Since the evaporation rate is higher at the edges of the droplet – where the fluid height is smaller – the aim should be to induce a spherical droplet shape. The humidity of the droplet atmosphere can also be increased to achieve a vapor-saturated environment. Evaporation can also be

reduced through additional installations, including restricting the headspace above the droplet [56] or covering the droplet with (mineral) oil. Finally, the liquid level of the droplet can simply be closely monitored, and evaporative losses can be compensated using microfluidic feeding channels or *liquid handling systems* (LHS). In some circumstances, evaporation can also be used as an advantage – i.e., by implementing it into the experimental procedure itself. For example, in diagnostics with very low analyte concentrations, for example, evaporation can be applied to perform a sample enrichment, enhance sensitivity, and/or accelerate measurements due to lower traveling distances of an analyte to the sensor area [60, 167, 168].

Sessile droplets can be analyzed using image acquisition and appropriate analysis software to monitor cell concentrations or conditions. MBR-related research can gain a deeper insight into metabolic processes using fluorescent microscopy or spectroscopy. A great variety of biosensors or plasmonic nano-sensors to perform Raman spectroscopy have reported [168–173]. Droplet-based arrays can also be connected to matrix-assisted laser desorption/ionization (MALDI) mass spectrometry, to perform analysis of droplets without the need for analyte labeling [174]. In sessile droplet approaches, comprehensive experiments and cell-based assays can be performed in very low fluid volumes and in a highly parallel fashion – although the level of monitoring and control in droplet-based MBR systems remains restricted.

Even though droplet-based systems provide very small reaction elements, usually a vast number of cells are cultivated per droplet resulting in the analysis of a profile of a cell population. The overall growth kinetics of a cell cultivation is highly affected by the variability of physiology and the phenotypic behavior [175, 176]. Specific devices, however, are increasingly being developed to cultivate single cells and analyze their phenotypic heterogeneity and its impact on growth behavior [177, 178]. Using single-cell MBRs, cellular interactions can be monitored, and the history of cells can be tracked over time – which is not possible using other techniques, such as flow cytometry [135].

4 Conclusions and Future Perspectives

The great variety of reported MBR applications illustrates both the growing importance and the immense potential benefits that this technology holds for biotechnological research. Studies have been conducted in an attempt to improve bioprocess development, scale-up processes, cultivation optimization, and survey many different cellular assays as well as analyze reaction kinetics, metabolic fluxes, and toxicity screenings.

This article has aimed to provide an overview of the MBR setups reported in the relevant literature and to give the reader a sense of the breadth and versatility of their practical deployment. On the one hand, there are rather simple reaction elements which come with limited monitoring and control but offer increased possibilities for parallelization and high-throughput experimentation. On the other hand, there are extensively equipped cultivation devices which can effectively mimic larger-scale

bioreactor systems, providing in-depth and valid experimental data especially for process development. Current research is increasingly aimed at bridging these two fields, facilitate even greater parallel experimentation while simultaneously, progressively decreasing reaction volumes of MBR systems.

However, there remains a great (and currently unmet) demand for effective MBR systems in which process parameters can be varied individually, to allow for highly parallelized experimentation with precise analytics. Consistent standards among reaction platforms would further encourage and promote the implementation of MBR technology for general biotechnological research. With improving analytics, the fields of application and the achieved outcomes will only continue to increase.

For future applications, achieving increased throughput is a point of special interest – because it facilitates even faster research progression. Extensive sensor integration for more informative and significant data, even in smallest scale, will also be required to facilitate this goal. The next steps must be to generate significant cross-scaling criteria, in order to be able to map large-scale processes on a small-scale, and vice versa. Adequately mimicking large-scale process conditions using MBRs still poses tremendous challenges, and improving this key metric demands a more thorough understanding in order to securely perform process scale-up operations. Since certain particular process conditions of the large-scale process cannot be realized in the MBR, holistic models imaging these conditions are urgently required. In order to achieve more efficient implementation and more widespread use of MBR technology in process development, the challenge of bringing multiple scaling parameters together must be even more actively addressed moving forward. But if these demands are met, then it is almost certain that MBR technologies will become indispensable tools for daily laboratory operations across a wide range of applications.

Acknowledgments The authors gratefully acknowledge financial support from the German Research Foundation (DFG) within the project *Development of micro-reactors for biopharmaceutical applications* (KR 1897/5-1, 310619924).

References

1. McNaught AD, Wilkinson A, Scientific B (2014) IUPAC. Compendium of chemical terminology, 2nd edn. (the “Gold Book”). <https://doi.org/10.1351/goldbook.I03352>
2. Gernaey KV, Baganz F, Franco-Lara E et al (2012) Monitoring and control of microbioreactors: an expert opinion on development needs. *Biotechnol J* 7:1308–1314. <https://doi.org/10.1002/biot.201200157>
3. Hemmerich J, Noack S, Wiechert W, Oldiges M (2018) Microbioreactor systems for accelerated bioprocess development. *Biotechnol J* 13:1700141. <https://doi.org/10.1002/biot.201700141>
4. Krull R, Lladó-Maldonado S, Lorenz T et al (2016) Microbioreactors. In: Dietzel A (ed) *Microsystems for pharmatechnology*. Springer, Cham, pp 99–152
5. Comley J (2003) Assay interference – a limiting factor in HTS? *Drug Discov World* 4:91–98

6. Rosseburg A, Fitschen J, Wutz J et al (2018) Hydrodynamic inhomogeneities in large scale stirred tanks – influence on mixing time. *Chem Eng Sci* 188:208–220. <https://doi.org/10.1016/j.ces.2018.05.008>
7. Lara AR, Galindo E, Ramírez OT, Palomares LA (2006) Living with heterogeneities in bioreactors: understanding the effects of environmental gradients on cells. *Mol Biotechnol* 34:355–382. <https://doi.org/10.1385/MB:34:3:355>
8. Grünberger A, Wiechert W, Kohlheyer D (2014) Single-cell microfluidics: opportunity for bioprocess development. *Curr Opin Biotechnol* 29:15–23. <https://doi.org/10.1016/j.copbio.2014.02.008>
9. Kirk TV, Szita N (2013) Oxygen transfer characteristics of miniaturized bioreactor systems. *Biotechnol Bioeng* 110:1005–1019. <https://doi.org/10.1002/bit.24824>
10. Lübbert A, Bay Jørgensen S (2001) Bioreactor performance: a more scientific approach for practice. *J Biotechnol* 85:187–212. [https://doi.org/10.1016/S0168-1656\(00\)00366-7](https://doi.org/10.1016/S0168-1656(00)00366-7)
11. Garcia-Ochoa F, Gomez E, Santos VE, Merchuk JC (2010) Oxygen uptake rate in microbial processes: an overview. *Biochem Eng J* 49:289–307. <https://doi.org/10.1016/j.bej.2010.01.011>
12. Hessel V, Löwe H, Schönfeld F (2005) Micromixers – a review on passive and active mixing principles. In: *Chemical engineering science*. Pergamon, Oxford, pp 2479–2501
13. Marques MPC, Cabral JMS, Fernandes P (2010) Bioprocess scale-up: quest for the parameters to be used as criterion to move from microreactors to lab-scale. *J Chem Technol Biotechnol* 85:1184–1198. <https://doi.org/10.1002/jctb.2387>
14. Shilton RJ, Yeo LY, Friend JR (2011) Quantification of surface acoustic wave induced chaotic mixing-flows in microfluidic wells. *Sensors Actuators B Chem* 160:1565–1572. <https://doi.org/10.1016/j.snb.2011.09.007>
15. Yeo LY, Chang H-C, Chan PP, Friend JR (2011) Microfluidic devices for bioapplications. *Small* 7:12–48. <https://doi.org/10.1002/sml.201000946>
16. Squires TM, Quake SR (2005) Microfluidics: fluid physics at the nanoliter scale. *Rev Mod Phys* 77:977–1026. <https://doi.org/10.1103/RevModPhys.77.977>
17. Nguyen N-T, Wu Z (2005) Micromixers – a review. *J Micromech Microeng* 15:R1–R16. <https://doi.org/10.1088/0960-1317/15/2/R01>
18. Werner S, Eibl R, Lettenbauer C et al (2010) Innovative, non-stirred bioreactors in scales from milliliters up to 1000 liters for suspension cultures of cells using disposable bags and containers – a Swiss contribution. *Chim Int J Chem* 64:819–823. <https://doi.org/10.2533/chimia.2010.819>
19. Kraume M (2012) Mischen und Rühren. In: *Transportvorgänge in der Verfahrenstechnik*. Springer, Berlin, pp 555–601
20. Merchuk JC, Contreras A, García F, Molina E (1998) Studies of mixing in a concentric tube airlift bioreactor with different spargers. *Chem Eng Sci* 53:709–719. [https://doi.org/10.1016/S0009-2509\(97\)00340-0](https://doi.org/10.1016/S0009-2509(97)00340-0)
21. Bai G, Armenante PM, Plank RV (2007) Experimental and computational determination of blend time in USP dissolution testing apparatus II. *J Pharm Sci* 96:3072–3086. <https://doi.org/10.1002/jps.20994>
22. Bareither R, Bargh N, Oakeshott R et al (2013) Automated disposable small scale reactor for high throughput bioprocess development: a proof of concept study. *Biotechnol Bioeng* 110:3126–3138. <https://doi.org/10.1002/bit.24978>
23. Hsu W-T, Aulakh RPS, Traul DL, Yuk IH (2012) Advanced microscale bioreactor system: a representative scale-down model for bench-top bioreactors. *Cytotechnology* 64:667–678. <https://doi.org/10.1007/s10616-012-9446-1>
24. Moses S, Manahan M, Ambrogelly A, Ling WLW (2012) Assessment of AMBR as a model for high-throughput cell culture process development strategy. *Adv Biosci Biotechnol* 03:918–927. <https://doi.org/10.4236/abb.2012.37113>
25. Hortsch R, Weuster-Botz D (2010) Power consumption and maximum energy dissipation in a milliliter-scale bioreactor. *Biotechnol Prog* 26:595–599. <https://doi.org/10.1002/btpr.338>

26. Puskeiler R, Kaufmann K, Weuster-Botz D (2005) Development, parallelization, and automation of a gas-inducing milliliter-scale bioreactor for high-throughput bioprocess design (HTBD). *Biotechnol Bioeng* 89:512–523. <https://doi.org/10.1002/bit.20352>
27. Nienow AW, Rielly CD, Brosnan K et al (2013) The physical characterisation of a microscale parallel bioreactor platform with an industrial CHO cell line expressing an IgG4. *Biochem Eng J* 76:25–36. <https://doi.org/10.1016/j.bej.2013.04.011>
28. Szita N, Boccazzi P, Zhang Z et al (2005) Development of a multiplexed microbioreactor system for high-throughput bioprocessing. *Lab Chip* 5:819. <https://doi.org/10.1039/b504243g>
29. Boccazzi P, Zanzotto A, Szita N et al (2005) Gene expression analysis of *Escherichia coli* grown in miniaturized bioreactor platforms for high-throughput analysis of growth and genomic data. *Appl Microbiol Biotechnol* 68:518–532. <https://doi.org/10.1007/s00253-005-1966-6>
30. Boccazzi P, Zhang Z, Kurosawa K et al (2006) Differential gene expression profiles and real-time measurements of growth parameters in *Saccharomyces cerevisiae* grown in microliter-scale bioreactors equipped with internal stirring. *Biotechnol Prog* 22:710–717. <https://doi.org/10.1021/bp0504288>
31. Schapper D, Stocks SM, Szita N et al (2010) Development of a single-use microbioreactor for cultivation of microorganisms. *Chem Eng J* 160:891–898. <https://doi.org/10.1016/j.cej.2010.02.038>
32. Zhang Z, Szita N, Boccazzi P et al (2006) A well-mixed, polymer-based microbioreactor with integrated optical measurements. *Biotechnol Bioeng* 93:286–296. <https://doi.org/10.1002/bit.20678>
33. Li X, van der Steen G, van Dedem GWK et al (2008) Improving mixing in microbioreactors. *Chem Eng Sci* 63:3036–3046. <https://doi.org/10.1016/j.ces.2008.02.036>
34. Tsai C-H, Wu X, Kuan D-H et al (2018) Digital hydraulic drive for microfluidics and miniaturized cell culture devices based on shape memory alloy actuators. *J Micromech Microeng* 28:084001. <https://doi.org/10.1088/1361-6439/aabd1e>
35. Peterat G, Schmolke H, Lorenz T et al (2014) Characterization of oxygen transfer in vertical microbubble columns for aerobic biotechnological processes. *Biotechnol Bioeng* 111:1809–1819. <https://doi.org/10.1002/bit.25243>
36. Lladó Maldonado S, Rasch D, Kasjanow A et al (2018) Multiphase microreactors with intensification of oxygen mass transfer rate and mixing performance for bioprocess development. *Biochem Eng J* 139:57–67. <https://doi.org/10.1016/j.bej.2018.07.023>
37. Lladó Maldonado S, Panjan P, Sun S et al (2019) A fully online sensor-equipped, disposable multiphase microbioreactor as a screening platform for biotechnological applications. *Biotechnol Bioeng* 116:65–75. <https://doi.org/10.1002/bit.26831>
38. Krull R, Peterat G (2016) Analysis of reaction kinetics during chemostat cultivation of *Saccharomyces cerevisiae* using a multiphase microreactor. *Biochem Eng J* 105:220–229. <https://doi.org/10.1016/j.bej.2015.08.013>
39. Demming S, Peterat G, Llobera A et al (2012) Vertical microbubble column—A photonic lab-on-chip for cultivation and online analysis of yeast cell cultures. *Biomicrofluidics* 6:034106. <https://doi.org/10.1063/1.4738587>
40. Büchs J (2001) Introduction to advantages and problems of shaken cultures. *Biochem Eng J* 7:91–98. [https://doi.org/10.1016/S1369-703X\(00\)00106-6](https://doi.org/10.1016/S1369-703X(00)00106-6)
41. Klöckner W, Büchs J (2012) Advances in shaking technologies. *Trends Biotechnol* 30:307–314. <https://doi.org/10.1016/j.tibtech.2012.03.001>
42. Funke M, Diederichs S, Kensy F et al (2009) The baffled microtiter plate: increased oxygen transfer and improved online monitoring in small scale fermentations. *Biotechnol Bioeng* 103:1118–1128. <https://doi.org/10.1002/bit.22341>
43. Buchenauer A, Funke M, Büchs J et al (2009) Microbioreactors with microfluidic control and a user-friendly connection to the actuator hardware. *J Micromech Microeng* 19:074012. <https://doi.org/10.1088/0960-1317/19/7/074012>

44. Hermann R, Lehmann M, Büchs J (2003) Characterization of gas-liquid mass transfer phenomena in microtiter plates. *Biotechnol Bioeng* 81:178–186. <https://doi.org/10.1002/bit.10456>
45. Ng AHC, Li BB, Chamberlain MD, Wheeler AR (2015) Digital microfluidic cell culture. *Annu Rev Biomed Eng* 17:91–112. <https://doi.org/10.1146/annurev-bioeng-071114-040808>
46. Choi K, Ng AHC, Fobel R, Wheeler AR (2012) Digital microfluidics. *Annu Rev Anal Chem* 5:413–440. <https://doi.org/10.1146/annurev-anchem-062011-143028>
47. Quilliet C, Berge B (2001) Electrowetting: a recent outbreak. *Curr Opin Colloid Interface Sci* 6:34–39. [https://doi.org/10.1016/S1359-0294\(00\)00085-6](https://doi.org/10.1016/S1359-0294(00)00085-6)
48. Bansal S, Sen P (2016) Mixing enhancement by degenerate modes in electrically actuated sessile droplets. *Sensors Actuators B Chem* 232:318–326. <https://doi.org/10.1016/j.snb.2016.03.109>
49. Fair RB, Khlystov A, Taylor TD et al (2007) Chemical and biological applications of digital-microfluidic devices. *IEEE Des Test Comput* 24:10–24. <https://doi.org/10.1109/MDT.2007.8>
50. Kardous F, Yahiaoui R, Aoubiza B, Manceau J-F (2014) Acoustic mixer using low frequency vibration for biological and chemical applications. *Sensors Actuators A Phys* 211:19–26. <https://doi.org/10.1016/j.sna.2014.03.003>
51. Yeo LY, Friend JR (2009) Ultrafast microfluidics using surface acoustic waves. *Biomicrofluidics* 3:012002. <https://doi.org/10.1063/1.3056040>
52. Landau LD, Lifshitz EM (1987) Fluid mechanics. In: *Course of theoretical physics*, vol 6. 2nd edn
53. Chang C-T, Bostwick JB, Daniel S, Steen PH (2015) Dynamics of sessile drops. Part 2. Experiment. *J Fluid Mech* 768:442–467. <https://doi.org/10.1017/jfm.2015.99>
54. Milne AJB, Defez B, Cabrerizo-Vílchez M, Amirfazli A (2014) Understanding (sessile/constrained) bubble and drop oscillations. *Adv Colloid Interf Sci* 203:22–36. <https://doi.org/10.1016/j.cis.2013.11.006>
55. Noblin X, Buguin A, Brochard-Wyart F (2004) Vibrated sessile drops: transition between pinned and mobile contact line oscillations. *Eur Phys J E* 14:395–404. <https://doi.org/10.1140/epje/i2004-10021-5>
56. Frey LJ, Vorländer D, Rasch D et al (2019) Novel electrodynamic oscillation technique enables enhanced mass transfer and mixing for cultivation in micro-bioreactor. *Biotechnol Prog* 35:e2827. <https://doi.org/10.1002/btpr.2827>
57. Meinen S, Frey LJ, Krull R, Dietzel A (2019) Resonant mixing in glass bowl microbioreactor investigated by microparticle image velocimetry. *Micromachines* 10:284. <https://doi.org/10.3390/mi10050284>
58. Frey LJ, Vorländer D, Rasch D et al (2020) Defining mass transfer in a capillary wave micro-bioreactor for dose-response and other cell-based assays. *Biochem Eng J*:107667. <https://doi.org/10.1016/j.bej.2020.107667>
59. Enders A, Siller IG, Urmann K et al (2018) 3D printed microfluidic mixers – a comparative study on mixing unit performances. *Small* 15:1804326. <https://doi.org/10.1002/smll.201804326>
60. Garcia-Cordero JL, Fan ZH (2017) Sessile droplets for chemical and biological assays. *Lab Chip* 17:2150–2166. <https://doi.org/10.1039/C7LC00366H>
61. Burbaum JJ (1998) Miniaturization technologies in HTS: how fast, how small, how soon? *Drug Discov Today* 3:313–322. [https://doi.org/10.1016/S1359-6446\(98\)01203-3](https://doi.org/10.1016/S1359-6446(98)01203-3)
62. Krull R, Haarstrick A, Hempel DC (2014) Bioverfahrenstechnik. In: Grote K-H, Feldhusen J (eds) *Dubbel*. Springer, Berlin, pp 972–992
63. Büchs J, Maier U, Milbradt C, Zoels B (2000) Power consumption in shaking flasks on rotary shaking machines: II. Nondimensional description of specific power consumption and flow regimes in unbaffled flasks at elevated liquid viscosity. *Biotechnol Bioeng* 68:594–601. [https://doi.org/10.1002/\(SICI\)1097-0290\(20000620\)68:6<594::AID-BIT2>3.0.CO;2-U](https://doi.org/10.1002/(SICI)1097-0290(20000620)68:6<594::AID-BIT2>3.0.CO;2-U)
64. Büchs J, Maier U, Milbradt C, Zoels B (2000) Power consumption in shaking flasks on rotary shaking machines: I. power consumption measurement in unbaffled flasks at low liquid

- viscosity. *Biotechnol Bioeng* 68:589–593. [https://doi.org/10.1002/\(SICI\)1097-0290\(20000620\)68:6<589::AID-BIT1>3.0.CO;2-J](https://doi.org/10.1002/(SICI)1097-0290(20000620)68:6<589::AID-BIT1>3.0.CO;2-J)
65. Tajssoleiman T, Mears L, Krühne U et al (2019) An industrial perspective on scale-down challenges using miniaturized bioreactors. *Trends Biotechnol* 37:697–706. <https://doi.org/10.1016/j.tibtech.2019.01.002>
 66. Schäpper D, Alam MNHZ, Szita N et al (2009) Application of microbioreactors in fermentation process development: a review. *Anal Bioanal Chem* 395:679–695. <https://doi.org/10.1007/s00216-009-2955-x>
 67. Hegab HM, ElMekawy A, Stakenborg T (2013) Review of microfluidic microbioreactor technology for high-throughput submerged microbiological cultivation. *Biomicrofluidics* 7:021502. <https://doi.org/10.1063/1.4799966>
 68. Lattermann C, Büchs J (2015) Microscale and miniscale fermentation and screening. *Curr Opin Biotechnol* 35:1–6. <https://doi.org/10.1016/j.copbio.2014.12.005>
 69. Bareither R, Pollard D (2011) A review of advanced small-scale parallel bioreactor technology for accelerated process development: current state and future need. *Biotechnol Prog* 27:2–14. <https://doi.org/10.1002/btpr.522>
 70. Rathore AS, Winkle H (2009) Quality by design for biopharmaceuticals. *Nat Biotechnol* 27:26–34. <https://doi.org/10.1038/nbt0109-26>
 71. Kesy F, John GT, Hofmann B, Büchs J (2005) Characterisation of operation conditions and online monitoring of physiological culture parameters in shaken 24-well microtiter plates. *Bioprocess Biosyst Eng* 28:75–81. <https://doi.org/10.1007/s00449-005-0010-7>
 72. Lattermann C, Funke M, Hansen S et al (2014) Cross-section perimeter is a suitable parameter to describe the effects of different baffle geometries in shaken microtiter plates. *J Biol Eng* 8:1–10. <https://doi.org/10.1186/1754-1611-8-18>
 73. Kesy F, Zang E, Faulhammer C et al (2009) Validation of a high-throughput fermentation system based on online monitoring of biomass and fluorescence in continuously shaken microtiter plates. *Microb Cell Factories* 8:31. <https://doi.org/10.1186/1475-2859-8-31>
 74. Wewetzer SJ, Kunze M, Ladner T et al (2015) Parallel use of shake flask and microtiter plate online measuring devices (RAMOS and BioLector) reduces the number of experiments in laboratory-scale stirred tank bioreactors. *J Biol Eng* 9:9. <https://doi.org/10.1186/s13036-015-0005-0>
 75. Ladner T, Mühlmann M, Schulte A et al (2017) Prediction of *Escherichia coli* expression performance in microtiter plates by analyzing only the temporal development of scattered light during culture. *J Biol Eng* 11:1–15. <https://doi.org/10.1186/s13036-017-0064-5>
 76. Back A, Rossignol T, Krier F et al (2016) High-throughput fermentation screening for the yeast *Yarrowia lipolytica* with real-time monitoring of biomass and lipid production. *Microb Cell Factories* 15:147. <https://doi.org/10.1186/s12934-016-0546-z>
 77. Käb F, Prasad A, Tillack J et al (2014) Rapid assessment of oxygen transfer impact for *Corynebacterium glutamicum*. *Bioprocess Biosyst Eng* 37:2567–2577. <https://doi.org/10.1007/s00449-014-1234-1>
 78. Mühlmann M, Kunze M, Ribeiro J et al (2017) Cellulolytic RoboLector – towards an automated high-throughput screening platform for recombinant cellulase expression. *J Biol Eng* 11:1. <https://doi.org/10.1186/s13036-016-0043-2>
 79. Böhm E, Voglauer R, Steinfellner W et al (2004) Screening for improved cell performance: selection of subclones with altered production kinetics or improved stability by cell sorting. *Biotechnol Bioeng* 88:699–706. <https://doi.org/10.1002/bit.20271>
 80. Huber R, Ritter D, Hering T et al (2009) Robo-lector – a novel platform for automated high-throughput cultivations in microtiter plates with high information content. *Microb Cell Factories* 8:42. <https://doi.org/10.1186/1475-2859-8-42>
 81. Hemmerich J, Adelantado N, Barrigón JM et al (2014) Comprehensive clone screening and evaluation of fed-batch strategies in a microbioreactor and lab scale stirred tank bioreactor system: application on *Pichia pastoris* producing *Rhizopus oryzae* lipase. *Microb Cell Factories*. <https://doi.org/10.1186/1475-2859-13-36>

82. Jensen SI, Lennen RM, Herrgård MJ, Nielsen AT (2016) Seven gene deletions in seven days: fast generation of *Escherichia coli* strains tolerant to acetate and osmotic stress. *Sci Rep* 5:17874. <https://doi.org/10.1038/srep17874>
83. Wiegmann V, Martinez CB, Baganz F (2020) Using a parallel micro-cultivation system (micro-matrix) as a process development tool for cell culture applications. In: Pörtner R (ed) *Animal cell biotechnology. Methods in molecular biology*, vol 2095. Humana, New York, pp 69–81
84. Micheletti M, Barrett T, Doig SD et al (2006) Fluid mixing in shaken bioreactors: implications for scale-up predictions from microlitre-scale microbial and mammalian cell cultures. *Chem Eng Sci* 61:2939–2949. <https://doi.org/10.1016/j.ces.2005.11.028>
85. Lamping S, Zhang H, Allen B, Ayazi Shamlou P (2003) Design of a prototype miniature bioreactor for high throughput automated bioprocessing. *Chem Eng Sci* 58:747–758. [https://doi.org/10.1016/S0009-2509\(02\)00604-8](https://doi.org/10.1016/S0009-2509(02)00604-8)
86. Betts JPI, Warr SRC, Finka GB et al (2014) Impact of aeration strategies on fed-batch cell culture kinetics in a single-use 24-well miniature bioreactor. *Biochem Eng J* 82:105–116. <https://doi.org/10.1016/j.bej.2013.11.010>
87. Isett K, George H, Herber W, Amanullah A (2007) Twenty-four-well plate miniature bioreactor high-throughput system: assessment for microbial cultivations. *Biotechnol Bioeng* 98:1017–1028. <https://doi.org/10.1002/bit.21484>
88. Chen A, Chitta R, Chang D, Amanullah A (2009) Twenty-four well plate miniature bioreactor system as a scale-down model for cell culture process development. *Biotechnol Bioeng* 102:148–160. <https://doi.org/10.1002/bit.22031>
89. Betts JI, Doig SD, Baganz F (2006) Characterization and application of a miniature 10 mL stirred-tank bioreactor, showing scale-down equivalence with a conventional 7 L reactor. *Biotechnol Prog* 22:681–688. <https://doi.org/10.1021/bp050369y>
90. Reed JL, Patel TR, Chen KH et al (2006) Systems approach to refining genome annotation. *Proc Natl Acad Sci U S A*. <https://doi.org/10.1073/pnas.0603364103>
91. Friedman AJ, Blecher K, Schairer D et al (2011) Improved antimicrobial efficacy with nitric oxide releasing nanoparticle generated S-nitrosoglutathione. *Nitric Oxide* 25:381–386. <https://doi.org/10.1016/j.niox.2011.09.001>
92. Medina A, Lambert RJW, Magan N (2012) Rapid throughput analysis of filamentous fungal growth using turbidimetric measurements with the bioscreen C: a tool for screening antifungal compounds. *Fungal Biol*. <https://doi.org/10.1016/j.funbio.2011.11.001>
93. Harms P, Kostov Y, French JA et al (2006) Design and performance of a 24-station high throughput microbioreactor. *Biotechnol Bioeng* 93:6–13. <https://doi.org/10.1002/bit.20742>
94. Zhang H, Lamping SR, Pickering SCR et al (2008) Engineering characterisation of a single well from 24-well and 96-well microtitre plates. *Biochem Eng J* 40:138–149. <https://doi.org/10.1016/j.bej.2007.12.005>
95. Kreye S, Stahn R, Nawrath K et al (2019) A novel scale-down mimic of perfusion cell culture using sedimentation in an automated microbioreactor (SAM). *Biotechnol Prog* 35:1–11. <https://doi.org/10.1002/btpr.2832>
96. Ratcliffe E, Glen KE, Workman VL et al (2012) A novel automated bioreactor for scalable process optimisation of haematopoietic stem cell culture. *J Biotechnol* 161:387–390. <https://doi.org/10.1016/j.jbiotec.2012.06.025>
97. Rameez S, Mostafa SS, Miller C, Shukla AA (2014) High-throughput miniaturized bioreactors for cell culture process development: reproducibility, scalability, and control. *Biotechnol Prog* 30:718–727. <https://doi.org/10.1002/btpr.1874>
98. Velez-Suberbie ML, Betts JPI, Walker KL et al (2018) High throughput automated microbial bioreactor system used for clone selection and rapid scale-down process optimization. *Biotechnol Prog* 34:58–68. <https://doi.org/10.1002/btpr.2534>
99. Wales R, Lewis G (2010) Novel automated micro-scale bioreactor technology: a qualitative and quantitative mimic for early process development. *Bioprocess J* 9:22–25. <https://doi.org/10.12665/J91.Wales>

100. Hortsch R, Weuster-Botz D (2009) Power consumption and maximum energy dissipation in a milliliter-scale bioreactor. *Biotechnol Prog* 26. <https://doi.org/10.1002/btpr.338>
101. Riedlberger P, Brüning S, Weuster-Botz D (2013) Characterization of stirrers for screening studies of enzymatic biomass hydrolyses on a milliliter scale. *Bioprocess Biosyst Eng* 36:927–935. <https://doi.org/10.1007/s00449-012-0826-x>
102. Schmideder A, Weuster-Botz D (2017) High-performance recombinant protein production with *Escherichia coli* in continuously operated cascades of stirred-tank reactors. *J Ind Microbiol Biotechnol*. <https://doi.org/10.1007/s10295-017-1927-y>
103. Schmideder A, Severin TS, Cremer JH, Weuster-Botz D (2015) A novel milliliter-scale chemostat system for parallel cultivation of microorganisms in stirred-tank bioreactors. *J Biotechnol* 210:19–24. <https://doi.org/10.1016/j.jbiotec.2015.06.402>
104. Long Q, Liu X, Yang Y et al (2014) The development and application of high throughput cultivation technology in bioprocess development. *J Biotechnol* 192:323–338. <https://doi.org/10.1016/j.jbiotec.2014.03.028>
105. Betts JI, Baganz F (2006) Miniature bioreactors: current practices and future opportunities. *Microb Cell Factories* 5:21. <https://doi.org/10.1186/1475-2859-5-21>
106. Funke M, Buchenauer A, Schnakenberg U et al (2010) Microfluidic biolector-microfluidic bioprocess control in microtiter plates. *Biotechnol Bioeng* 107:497–505. <https://doi.org/10.1002/bit.22825>
107. Zhang Z, Boccazzi P, Choi H-G et al (2006) Microchemostat – microbial continuous culture in a polymer-based, instrumented microbioreactor. *Lab Chip* 6:906–913. <https://doi.org/10.1039/B518396K>
108. Edlich A, Magdanz V, Rasch D et al (2010) Microfluidic reactor for continuous cultivation of *Saccharomyces cerevisiae*. *Biotechnol Prog* 26:1259–1270. <https://doi.org/10.1002/btpr.449>
109. Schmolke H, Demming S, Edlich A et al (2010) Polyelectrolyte multilayer surface functionalization of poly(dimethylsiloxane) (PDMS) for reduction of yeast cell adhesion in microfluidic devices. *Biomicrofluidics* 4:044113. <https://doi.org/10.1063/1.3523059>
110. Rieger M, Kappeli O, Fiechter A (1983) The role of limited respiration in the incomplete oxidation of glucose by *Saccharomyces cerevisiae*. *Microbiology* 129:653–661. <https://doi.org/10.1099/00221287-129-3-653>
111. von Meyenburg K (1969) Energetics of the budding cycle of *Saccharomyces cerevisiae* during glucose limited aerobic growth. *Arch Mikrobiol* 66:289–303. <https://doi.org/10.1007/BF00414585>
112. von Meyenburg K (1969) Katabolitrepression und der Sprossungszyklus von *Saccharomyces cerevisiae*. ETH Zürich
113. Lladó Maldonado S, Krull J, Rasch D et al (2019) Application of a multiphase microreactor chemostat for the determination of reaction kinetics of *Staphylococcus carnosus*. *Bioprocess Biosyst Eng* 42:953–961. <https://doi.org/10.1007/s00449-019-02095-9>
114. Doig SD, Diep A, Baganz F (2005) Characterisation of a novel miniaturised bubble column bioreactor for high throughput cell cultivation. *Biochem Eng J* 23:97–105. <https://doi.org/10.1016/j.bej.2004.10.014>
115. Doig SD, Ortiz-Ochoa K, Ward JM, Baganz F (2008) Characterization of oxygen transfer in miniature and lab-scale bubble column bioreactors and comparison of microbial growth performance based on constant kLa. *Biotechnol Prog* 21:1175–1182. <https://doi.org/10.1021/bp050064j>
116. Weuster-Botz D, Altenbach-Rehm J, Hawrylenko A (2001) Process-engineering characterization of small-scale bubble columns for microbial process development. *Bioprocess Biosyst Eng* 24:3–11. <https://doi.org/10.1007/s004490100222>
117. Stocks SM (2013) Industrial enzyme production for the food and beverage industries: process scale up and scale down. In: *Microbial production of food ingredients, enzymes and nutraceuticals*. Elsevier, pp 144–172

118. Crater JS, Lievens JC (2018) Scale-up of industrial microbial processes. *FEMS Microbiol Lett* 365. <https://doi.org/10.1093/femsle/fny138>
119. Wiegmann V, Martinez CB, Baganz F (2018) A simple method to determine evaporation and compensate for liquid losses in small-scale cell culture systems. *Biotechnol Lett* 40:1029–1036. <https://doi.org/10.1007/s10529-018-2556-x>
120. Silk NJ, Denby S, Lewis G et al (2010) Fed-batch operation of an industrial cell culture process in shaken microwells. *Biotechnol Lett* 32:73–78. <https://doi.org/10.1007/s10529-009-0124-0>
121. Dietzel A (2016) *Microsystems for pharmaceutical technology*. Springer, Cham. <https://doi.org/10.1007/978-3-319-26920-7>
122. Ying Lin H, Neubauer P (2000) Influence of controlled glucose oscillations on a fed-batch process of recombinant *Escherichia coli*. *J Biotechnol* 79:27–37. [https://doi.org/10.1016/S0168-1656\(00\)00217-0](https://doi.org/10.1016/S0168-1656(00)00217-0)
123. Tescione L, Lambropoulos J, Paranandi MR et al (2015) Application of bioreactor design principles and multivariate analysis for development of cell culture scale down models. *Biotechnol Bioeng* 112:84–97. <https://doi.org/10.1002/bit.25330>
124. Xu P, Clark C, Ryder T et al (2017) Characterization of TAP Ambr 250 disposable bioreactors, as a reliable scale-down model for biologics process development. *Biotechnol Prog* 33:478–489. <https://doi.org/10.1002/btpr.2417>
125. Islam RS, Tisi D, Levy MS, Lye GJ (2008) Scale-up of *Escherichia coli* growth and recombinant protein expression conditions from microwell to laboratory and pilot scale based on matched $k_L a$. *Biotechnol Bioeng* 99:1128–1139. <https://doi.org/10.1002/bit.21697>
126. Nienow AW (2015) Mass transfer and mixing across the scales in animal cell culture. In: Al-Rubeai M (ed) *Animal cell culture*. Springer, Cham, pp 137–167. https://doi.org/10.1007/978-3-319-10320-4_5
127. Gill NK, Appleton M, Baganz F, Lye GJ (2008) Design and characterisation of a miniature stirred bioreactor system for parallel microbial fermentations. *Biochem Eng J* 39:164–176. <https://doi.org/10.1016/j.bej.2007.09.001>
128. Haringa C, Tang W, Wang G et al (2018) Computational fluid dynamics simulation of an industrial *P. chrysogenum* fermentation with a coupled 9-pool metabolic model: towards rational scale-down and design optimization. *Chem Eng Sci* 175:12–24. <https://doi.org/10.1016/j.ces.2017.09.020>
129. Margaritis A, Zajic JE (1978) Mixing, mass transfer, and scale-up of polysaccharide fermentations. *Biotechnol Bioeng* 20:939–1001. <https://doi.org/10.1002/bit.260200702>
130. Schmidt FR (2005) Optimization and scale up of industrial fermentation processes. *Appl Microbiol Biotechnol* 68:425–435. <https://doi.org/10.1007/s00253-005-0003-0>
131. Xu S, Hoshan L, Jiang R et al (2017) A practical approach in bioreactor scale-up and process transfer using a combination of constant P/V and vvm as the criterion. *Biotechnol Prog* 33:1146–1159. <https://doi.org/10.1002/btpr.2489>
132. Breslauer DN, Lee PJ, Lee LP (2006) Microfluidics-based systems biology. *Mol BioSyst* 2:97. <https://doi.org/10.1039/b515632g>
133. El-Ali J, Sorger PK, Jensen KF (2006) Cells on chips. *Nature* 442:403–411. <https://doi.org/10.1038/nature05063>
134. Junne S, Neubauer P (2018) How scalable and suitable are single-use bioreactors? *Curr Opin Biotechnol* 53:240–247. <https://doi.org/10.1016/j.copbio.2018.04.003>
135. Ladner T, Grünberger A, Probst C et al (2017) Application of mini- and micro-bioreactors for microbial bioprocesses. In: *Current developments in biotechnology and bioengineering*. Elsevier, Amsterdam, pp 433–461
136. Doig SD, Baganz F, Lye GJ (2006) High-throughput screening and process optimisation. In: Ratledge C, Kristiansen B (eds) *Basic biotechnology*. Cambridge University Press, Cambridge, pp 289–306
137. Lennen RM, Nilsson Wallin AI, Pedersen M et al (2016) Transient overexpression of DNA adenine methylase enables efficient and mobile genome engineering with reduced off-target effects. *Nucleic Acids Res* 44:e36–e36. <https://doi.org/10.1093/nar/gkv1090>

138. Motta Dos Santos LF, Coutte F, Ravallec R et al (2016) An improvement of surfactin production by *B. subtilis* BBG131 using design of experiments in microbioreactors and continuous process in bubbleless membrane bioreactor. *Bioresour Technol* 218:944–952. <https://doi.org/10.1016/j.biortech.2016.07.053>
139. Unthan S, Baumgart M, Radek A et al (2015) Chassis organism from *Corynebacterium glutamicum* – a top-down approach to identify and delete irrelevant gene clusters. *Biotechnol J* 10:290–301. <https://doi.org/10.1002/biot.201400041>
140. Kaminski TS, Scheler O, Garstecki P (2016) Droplet microfluidics for microbiology: techniques, applications and challenges. *Lab Chip* 16:2168–2187. <https://doi.org/10.1039/C6LC00367B>
141. Casadevall I, Solvas X, Demello A (2011) Droplet microfluidics: recent developments and future applications. *Chem Commun* 47:1936–1942. <https://doi.org/10.1039/c0cc02474k>
142. Hernandez-Perez R, Fan ZH, Garcia-Cordero JL (2016) Evaporation-driven bioassays in suspended droplets. *Anal Chem* 88:7312–7317. <https://doi.org/10.1021/acs.analchem.6b01657>
143. Gao L, McCarthy TJ (2006) Contact angle hysteresis explained. *Langmuir* 22:6234–6237. <https://doi.org/10.1021/la060254j>
144. Huebner A, Sharma S, Srisa-Art M et al (2008) Microdroplets: a sea of applications? *Lab Chip* 8:1244. <https://doi.org/10.1039/b806405a>
145. Malic L, Brassard D, Veres T, Tabrizian M (2010) Integration and detection of biochemical assays in digital microfluidic LOC devices. *Lab Chip* 10:418–431. <https://doi.org/10.1039/b917668c>
146. Zhu Y, Zhang Y-X, Cai L-F, Fang Q (2013) Sequential operation droplet array: an automated microfluidic platform for Picoliter-scale liquid handling, analysis, and screening. *Anal Chem* 85:6723–6731. <https://doi.org/10.1021/ac4006414>
147. Dong Z, Fang Q (2020) Automated, flexible and versatile manipulation of nanoliter-to-picoliter droplets based on sequential operation droplet array technique. *TrAC Trends Anal Chem* 124:115812. <https://doi.org/10.1016/j.trac.2020.115812>
148. Du G-S, Pan J-Z, Zhao S-P et al (2013) Cell-based drug combination screening with a microfluidic droplet array system. *Anal Chem* 85:6740–6747. <https://doi.org/10.1021/ac400688f>
149. Ma Y, Pan J-Z, Zhao S-P et al (2016) Microdroplet chain array for cell migration assays. *Lab Chip* 16:4658–4665. <https://doi.org/10.1039/C6LC00823B>
150. Taniguchi T, Torii T, Higuchi T (2002) Chemical reactions in microdroplets by electrostatic manipulation of droplets in liquid media. *Lab Chip* 2(1):19–23
151. Keng PY, Chen S, Ding H et al (2012) Micro-chemical synthesis of molecular probes on an electronic microfluidic device. *Proc Natl Acad Sci U S A* 109:690–695. <https://doi.org/10.1073/pnas.1117566109>
152. Rastogi V, Velev OD (2007) Development and evaluation of realistic microbioassays in freely suspended droplets on a chip. *Biomicrofluidics* 1:014107. <https://doi.org/10.1063/1.2714185>
153. Sista RS, Eckhardt AE, Wang T et al (2011) Digital microfluidic platform for multiplexing enzyme assays: implications for lysosomal storage disease screening in newborns. *Clin Chem* 57:1444–1451. <https://doi.org/10.1373/clinchem.2011.163139>
154. Sista RS, Eckhardt AE, Srinivasan V et al (2008) Heterogeneous immunoassays using magnetic beads on a digital microfluidic platform. *Lab Chip* 8:2188. <https://doi.org/10.1039/b807855f>
155. Vergauwe N, Witters D, Ceyskens F et al (2011) A versatile electrowetting-based digital microfluidic platform for quantitative homogeneous and heterogeneous bio-assays. *J Micromech Microeng* 21:054026. <https://doi.org/10.1088/0960-1317/21/5/054026>
156. Wulff-Burchfield E, Schell WA, Eckhardt AE et al (2010) Microfluidic platform versus conventional real-time polymerase chain reaction for the detection of mycoplasma pneumoniae in respiratory specimens. *Diagn Microbiol Infect Dis* 67:22–29. <https://doi.org/10.1016/j.diagmicrobio.2009.12.020>

157. Liu Y-J, Yao D-J, Lin H-C et al (2008) DNA ligation of ultramicro volume using an EWOD microfluidic system with coplanar electrodes. *J Micromech Microeng* 18:045017. <https://doi.org/10.1088/0960-1317/18/4/045017>
158. Malic L, Veres T, Tabrizian M (2009) Biochip functionalization using electrowetting-on-dielectric digital microfluidics for surface plasmon resonance imaging detection of DNA hybridization. *Biosens Bioelectron* 24:2218–2224. <https://doi.org/10.1016/j.bios.2008.11.031>
159. Malic L, Veres T, Tabrizian M (2011) Nanostructured digital microfluidics for enhanced surface plasmon resonance imaging. *Biosens Bioelectron* 26:2053–2059. <https://doi.org/10.1016/j.bios.2010.09.001>
160. Chang Y-H, Lee G-B, Huang F-C et al (2006) Integrated polymerase chain reaction chips utilizing digital microfluidics. *Biomed Microdevices* 8:215–225. <https://doi.org/10.1007/s10544-006-8171-y>
161. Welch ERF, Lin YY, Madison A, Fair RB (2011) Picoliter DNA sequencing chemistry on an electrowetting-based digital microfluidic platform. *Biotechnol J* 6:165–176. <https://doi.org/10.1002/biot.201000324>
162. Jebrail MJ, Yang H, Mudrik JM et al (2011) A digital microfluidic method for dried blood spot analysis. *Lab Chip* 11:3218–3224. <https://doi.org/10.1039/c1lc20524b>
163. Erbil HY, McHale G, Newton MI (2002) Drop evaporation on solid surfaces: constant contact angle mode. *Langmuir* 18:2636–2641. <https://doi.org/10.1021/la011470p>
164. Lee CY, In WK (2014) Prediction of water droplet evaporation on zircaloy surface. *J Nucl Sci Technol* 51:448–456. <https://doi.org/10.1080/00223131.2014.873359>
165. Larson RG (2014) Transport and deposition patterns in drying sessile droplets. *AICHE J* 60:1538–1571. <https://doi.org/10.1002/aic.14338>
166. Hu H, Larson RG (2005) Analysis of the microfluid flow in an evaporating sessile droplet. *Langmuir* 21:3963–3971. <https://doi.org/10.1021/la047528s>
167. De Angelis F, Gentile F, Mecarini F et al (2011) Breaking the diffusion limit with super-hydrophobic delivery of molecules to plasmonic nanofocusing SERS structures. *Nat Photonics*. <https://doi.org/10.1038/nphoton.2011.222>
168. Yang S, Dai X, Stogin BB, Wong T-S (2016) Ultrasensitive surface-enhanced Raman scattering detection in common fluids. *Proc Natl Acad Sci* 113:268–273. <https://doi.org/10.1073/pnas.1518980113>
169. Ebrahimi A, Dak P, Salm E et al (2013) Nanotextured superhydrophobic electrodes enable detection of attomolar-scale DNA concentration within a droplet by non-faradaic impedance spectroscopy. *Lab Chip* 13:4248. <https://doi.org/10.1039/c3lc50517k>
170. Coluccio ML, Gentile F, Das G et al (2015) Detection of single amino acid mutation in human breast cancer by disordered plasmonic self-similar chain. *Sci Adv* 1:e1500487. <https://doi.org/10.1126/sciadv.1500487>
171. Wong T-S, Kang SH, Tang SKY et al (2011) Bioinspired self-repairing slippery surfaces with pressure-stable omniphobicity. *Nature* 477:443–447. <https://doi.org/10.1038/nature10447>
172. Dak P, Ebrahimi A, Alam MA (2014) Non-faradaic impedance characterization of an evaporating droplet for microfluidic and biosensing applications. *Lab Chip* 14:2469–2479. <https://doi.org/10.1039/C4LC00193A>
173. Yanagimachi I, Nashida N, Iwasa K, Suzuki H (2005) Enhancement of the sensitivity of electrochemical stripping analysis by evaporative concentration using a super-hydrophobic surface. *Sci Technol Adv Mater* 6:671–677. <https://doi.org/10.1016/j.stam.2005.06.017>
174. Küster SK, Fagerer SR, Verboket PE et al (2013) Interfacing droplet microfluidics with matrix-assisted laser desorption/ionization mass spectrometry: label-free content analysis of single droplets. *Anal Chem* 85:1285–1289. <https://doi.org/10.1021/ac3033189>
175. Delvigne F, Zune Q, Lara AR et al (2014) Metabolic variability in bioprocessing: implications of microbial phenotypic heterogeneity. *Trends Biotechnol* 32:608–616. <https://doi.org/10.1016/j.tibtech.2014.10.002>
176. Avery SV (2006) Microbial cell individuality and the underlying sources of heterogeneity. *Nat Rev Microbiol* 4:577–587. <https://doi.org/10.1038/nrmicro1460>

177. Love KR, Bagh S, Choi J, Love JC (2013) Microtools for single-cell analysis in biopharmaceutical development and manufacturing. *Trends Biotechnol* 31:280–286. <https://doi.org/10.1016/j.tibtech.2013.03.001>
178. Dusny C, Schmid A (2015) Microfluidic single-cell analysis links boundary environments and individual microbial phenotypes. *Environ Microbiol* 17:1839–1856. <https://doi.org/10.1111/1462-2920.12667>

Microfluidic Devices as Process Development Tools for Cellular Therapy Manufacturing



Jorge Aranda Hernandez, Christopher Heuer, Janina Bahnemann, and
Nicolas Szita

Contents

1	Challenges of Cellular Therapy Manufacturing and Advantages of Microfluidics	103
2	Microfluidic Devices for Cell Processing Unit Operations	107
2.1	Cell Isolation and Separation	107
2.2	T Cell Activation	109
2.3	Gene Delivery	110
2.4	Cell Expansion	112
2.5	Stem Cell Differentiation	115
3	Summary and Perspective	118
	References	121

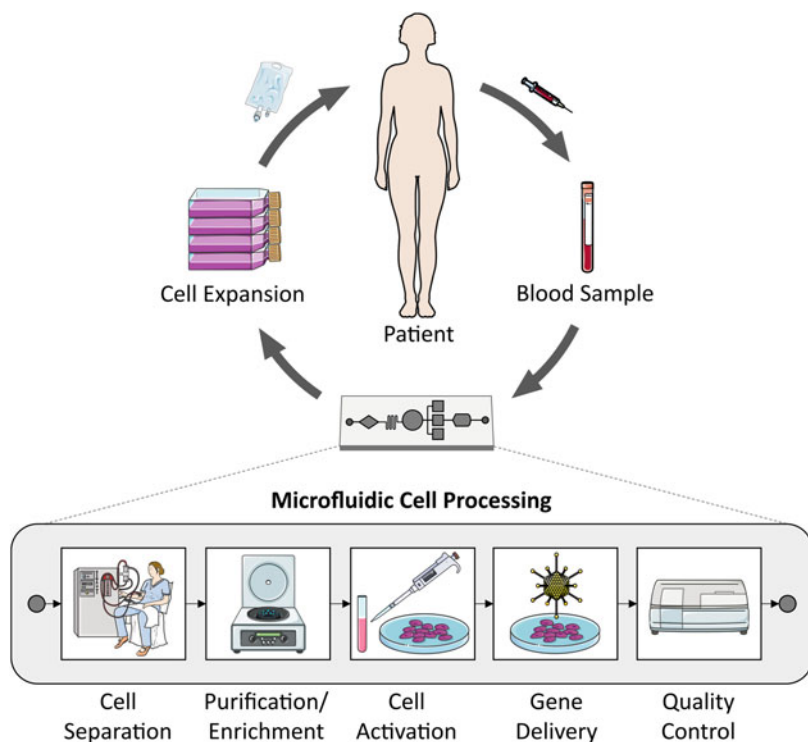
Abstract Cellular therapies are creating a paradigm shift in the biomanufacturing industry. Particularly for autologous therapies, small-scale processing methods are better suited than the large-scale approaches that are traditionally employed in the industry. Current small-scale methods for manufacturing personalized cell therapies, however, are labour-intensive and involve a number of ‘open events’. To overcome these challenges, new cell manufacturing platforms following a GMP-in-a-box concept have recently come on the market (GMP: Good Manufacturing Practice). These are closed automated systems with built-in pumps for fluid handling and sensors for in-process monitoring. At a much smaller scale, microfluidic devices exhibit many of the same features as current GMP-in-a-box systems. They are closed systems, fluids can be processed and manipulated, and sensors integrated for

J. Aranda Hernandez and N. Szita (✉)
Biochemical Engineering Department, University College London (UCL), London, UK
e-mail: n.szita@ucl.ac.uk

C. Heuer and J. Bahnemann
Institute of Technical Chemistry, Leibniz University Hannover, Hannover, Germany

real-time detection of process variables. Fabricated from polymers, they can be made disposable, i.e. single-use. Furthermore, microfluidics offers exquisite spatiotemporal control over the cellular microenvironment, promising both reproducibility and control of outcomes. In this chapter, we consider the challenges in cell manufacturing, highlight recent advances of microfluidic devices for each of the main process steps, and summarize our findings on the current state of the art. As microfluidic cell culture devices have been reported for both adherent and suspension cell cultures, we report on devices for the key process steps, or unit operations, of both stem cell therapies and cell-based immunotherapies.

Graphical Abstract



Keywords Biomanufacturing, CAR-T, Cell and gene therapy, Cell culture, Cell manufacturing, GMP-in-a-box, Immunotherapy, Medical biotechnology, Microfluidics, Scale-down, Scale-up, Stem cells, Translation

1 Challenges of Cellular Therapy Manufacturing and Advantages of Microfluidics

Cellular therapies, and cell and gene therapies (CGT), have become an attractive approach for treating some of humanity's most life-threatening and burdensome diseases when current therapies fail, or can only palliate. Cell-based therapies aim to treat disease through cell-mediated repair or, potentially, by replacing whole tissues or even organs. Much work has been reported over the last years on the application of stem cells for the treatment of a wide range of conditions, including neurodegenerative and musculoskeletal diseases, diabetes and macular degeneration [1–4]. In the field of haematological diseases, immunotherapies such as the novel chimeric antigen receptor (CAR) modified T cells have also shown promising results in treating leukaemia, including non-Hodgkin and Hodgkin lymphoma. There are already two approved and commercially available CAR T cell therapies: Novartis' *Kimryah* and Kite Pharma's *Yescarta* [5–7].

The manufacturing processes of cell-based immunotherapies, such as CAR T cells, and of stem cell therapies differ from each other, but certain process steps, also known as unit operations, are required in both types of processes. A simplified representation of the two processes is shown in Fig. 1. With CAR T cells (Fig. 1a), the process typically commences by isolating the non-adherent white blood cells (WBCs) from the patient's blood. After T cell enrichment, the T cells are activated (via stimulation of proliferation and differentiation), and the CAR transgene is inserted by gene delivery. Subsequently, CAR T cell expansion increases the cell count to sufficient numbers, before the cells are re injected into the patient for therapy [8]. Similarly, stem cell manufacturing processes (Fig. 1b) include an expansion step, before the cells are differentiated to the desired cell type for the therapy. Following differentiation the cells are injected back into the patient for regeneration of damaged or diseased tissues [9]. The starting point of the process varies depending on the type of stem cell therapy. For example, for therapies using induced pluripotent stem cells (iPSC), somatic cells are transfected with reprogramming factors [10]. These reprogramming factors induce pluripotency to the cells (hence iPSC), before the cells are processed further (Fig. 1b).

Cellular therapy manufacturing does not follow the one-size-fits-all approach known from pharmaceuticals and biopharmaceuticals. The approach is more stratified or even personalized. Particularly autologous therapies, where cells are obtained from a patient, then processed, and finally re injected into the patient, are patient-scale therapies: comparatively small amounts of cells are carried through each of the process steps (Fig. 1) as individual batches; as opposed to the one-size-fits-all approach, where a large number of cells (or large volumes of chemicals) are processed, and a large number of doses are created 'in one go'. The large plants used in traditional biotechnology are therefore not suitable for the small-scale manufacturing of these therapies, and new manufacturing methods and approaches are under development.

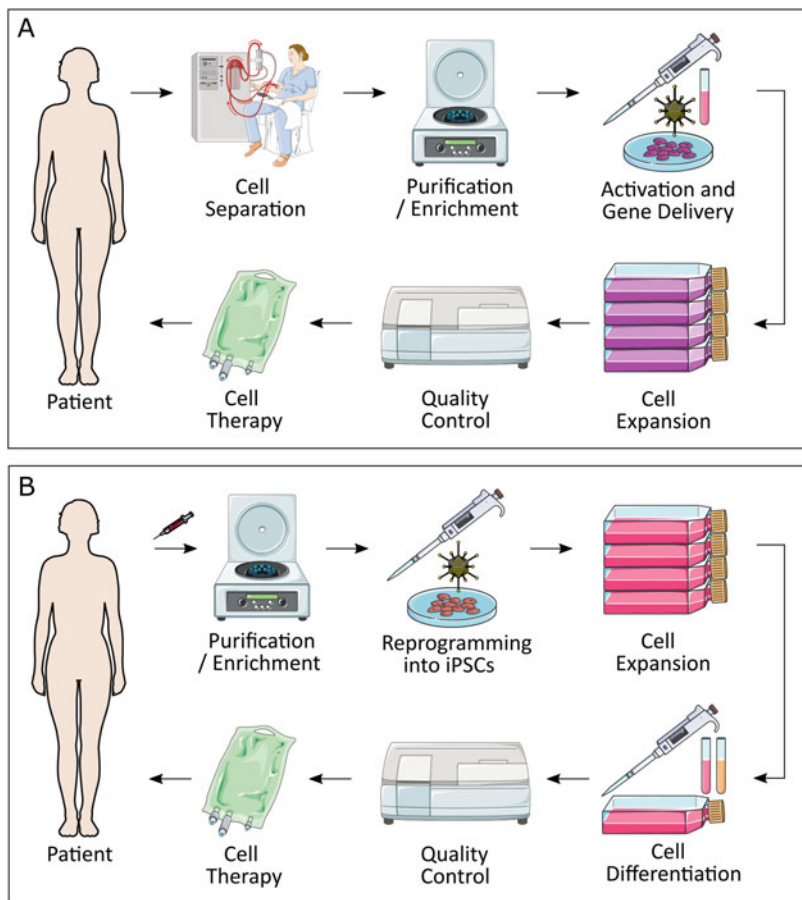


Fig. 1 Simplified manufacturing process sequences for (a) CAR T cell and (b) induced pluripotent stem cell (iPSCs) autologous therapies. Autologous manufacturing begins with the withdrawal of a cell sample from the patient, which is then modified ex vivo to introduce therapeutical properties and expanded before reintroduction to the patient. Cells must be first separated from the sample, which may require several steps for blood or tissue samples. Once the target cells have been isolated from other cells present in the sample, they are modified and expanded. Quality control testing is carried out either between steps or at the end of the process, and it generally includes phenotypical and functional testing of the cells. The cartoons are adapted with permission from Servier Medical Art

The culture of cells is conventionally being done in static vessels, such as flasks. These vessels provide a simple in vitro system to expand cells. They have however significant limitations for the controlled and reproducible manufacture of cells. Culture media volumes in these vessels are limited and only allow culture for a few days. This duration is typically not enough to expand the cells to the large numbers of cells necessary to ultimately attain therapeutic doses. Also, processes

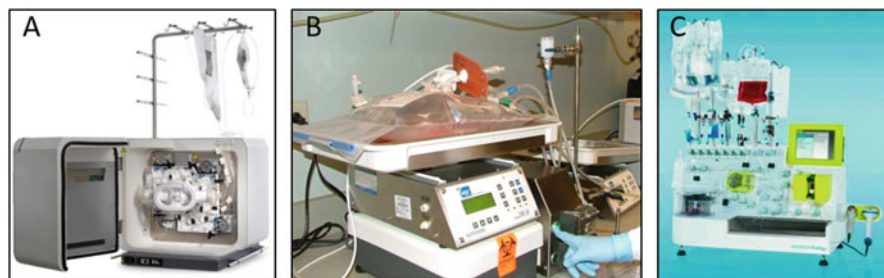


Fig. 2 Examples of automated cell processing platforms currently available for manufacturing of clinically relevant cell lines such as stem cells and CAR T cells. (a) Quantum Cell Processing System (Terumo). Adapted with permission from [12]. (b) Xuri Rocking Bag Bioreactor (Cytiva Lifesciences). Adapted with permission from [13]. (c) CliniMACS Prodigy (Miltenyi Biotec). Adapted with permission from [14]

based on static vessels are typically not automated, therefore requiring manual handling procedures. These procedures then create ‘open events’, which increase the risk of contamination of the cells. As an additional complication, variations inherent in manual handling procedures often introduce inconsistencies in process outcomes [11].

To address these limitations, closed and automated manufacturing systems have been developed. These GMP-in-a-box platforms have been applied to both stem cell and CAR T cell processing. For instance, human embryonic stem cells were cultured in the Quantum Cell Expansion System (Terumo BCT), a hollow fibre bioreactor system with automated liquid handling capabilities (Fig. 2a). This cell processing platform achieved a nearly 12-fold rate of expansion while maintaining 97.7% expression of pluripotency markers in the cells [15]. The same platform was also used for the expansion of bone-marrow-derived mesenchymal stem cells (MSCs). After an average of 20.5 days, 6.6×10^8 cells were harvested, outperforming flask cultures by 9.3 days with twice the yield, while retaining the potency markers [16]. The Quantum Cell Expansion System expanded T cells to clinically relevant numbers using automated media feeding strategies. These strategies resulted in up to 450-fold expansions, while cell viability and cell quality marker expression levels were maintained above 90% [17]. Key steps in CAR T cell manufacturing, such as gene delivery and activation, were performed in an automated fashion in the Xuri rocking-bed bioreactor by Cytiva [18] and in the CliniMACS Prodigy by Miltenyi Biotec [5, 19, 20], see Fig. 2b, c, respectively. Other GMP-in-a-box systems include the Facer system by Aglaris Ltd. [21] or Lonza’s Cocoon [22], highlighting the increasing interest for automated cell manufacturing platforms. Automation results in reduced labour, reduced variations and inconsistencies in process outcomes, and if paired with sensors, feed-back control loops become feasible which further increase yield and reproducibility [8, 19, 23].

Microfluidic devices share many characteristics with GMP-in-a-box systems. They are closed systems, and fluids can be processed and manipulated, for example

to continuously supply nutrients to the cells and remove waste product. Sensors can be integrated allowing real-time monitoring of process variables. Fabricated from polymers, they can be made disposable, i.e. single-use (similar to the disposable bags or cassettes of GMP-in-a-box systems). Additionally, microfluidic devices offer advantages specific only to them, such as an exquisite spatiotemporal control over the cellular microenvironment. Evidently, the more precisely environmental conditions can be controlled, the more accurate the information we gain on the impact of process conditions on cellular behaviour becomes. Microfluidic devices might therefore be suitable test-beds to analyse and potentially to resolve challenges in cell manufacture. Furthermore, microfluidics is powerful for analytics; microfluidic devices work with very small quantities of samples and reagents, provide short times for analysis and high sensitivity of detection (for example of fluorescence signals), and can be parallelized for high-throughput screening. These characteristics and advantages make them an attractive proposition to underpin and accelerate the development of cell-based therapies. Whilst they might find their obvious home in the rapid screening of process conditions, they may also take on other roles as the cell manufacturing field develops. The scale mis-match (in both culture volume and area) between microfluidic devices and process vessels is (currently) significantly smaller for cell therapy manufacturing than for the production of pharmaceuticals and biopharmaceuticals; this may therefore open up new opportunities for microfluidics in (early) process development and in quality control of cellular attributes (Fig. 3).

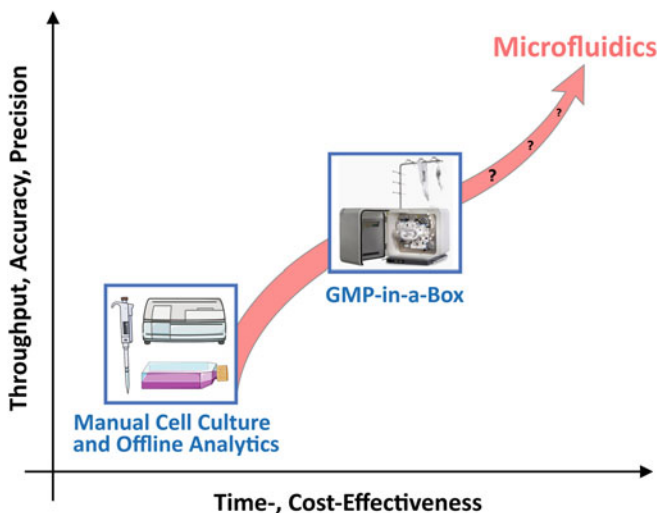


Fig. 3 Graphical representation comparing the performance of traditional cell culture methods and offline analytical systems with automated cell processing systems, or GMP-in-a-box systems, with integrated sensors and fluid handling. Automated systems result in increased performance, reproducibility (i.e. precision) and cost-effectiveness. Microfluidic systems have the potential to further increase cost-effectiveness and process control (i.e. accuracy) significantly while increasing or maintaining throughput. The cartoons are adapted with permission from Servier Medical Art. The GMP-in-a-box system is adapted with permission from [12]

In this chapter, to highlight the potential of microfluidics in this field, we present recent advances (mainly over the last 5 years) in microfluidic devices from the perspective of stem cell and CAR T cell therapy manufacturing. To achieve this perspective, we report on the advances by grouping them according to the unit operations typical of cell manufacturing processes (Fig. 1). Whilst some unit operations have been treated in greater detail than others, we hope the reader will find the reviews provided suitable to learn more about a particular topic in this exciting field.

2 Microfluidic Devices for Cell Processing Unit Operations

2.1 Cell Isolation and Separation

The first step for CAR T cell manufacturing is the isolation of white blood cells (WBC), including the T cells, from a patient's blood. For this, gradient density centrifugation is used to remove the red blood cells (RBCs), and platelets and antibody-coated paramagnetic beads are then employed to achieve either enrichment or depletion of specific cell subsets [8]. These traditional approaches require time-consuming pipetting and centrifugation steps, and the use of antibodies is expensive [1].

In the area of purification and sorting of cells, a large number of devices were realized over the last decades. To underline this, a review article on the subject even posed the thought-provoking question whether microfluidic cell separation is actually a solved problem [24]. As stated in this review article, 'inertial microfluidics' and 'deterministic lateral displacement' are the two methods with the highest throughput for discriminating cell sizes and shape (and thus cell type) in a label-free manner. Using deterministic lateral displacement, Kim et al., for example, developed a polydimethylsiloxane (PDMS)-based device for one-step WBC separation from whole blood by rejecting 99.9% of red blood cells (RBCs) and blood plasma (Fig. 4a). The first separation mechanism, in the format of ridges organized as a discontinuous slant array (DSA), provided a 'high-throughput yet low-purity' enrichment of the WBCs. It removed the bulk of the RBCs and transferred them into a waste outlet, while directing the flow of the WBCs towards the second separation step. The second separation mechanism delivered a 'low-throughput but high-purity' enrichment: A slant, asymmetric microfluidic lattice-based washing unit separated the cells via steric effects, while residual RBCs migrated through side channels, the WBCs passed through the main channels and were thereby washed. Finally, they were flowed into their designated outlet. Both steps were performed on-chip and in a continuous sequence, yielding ultimately a high-throughput and high-purity separation of WBCs [25].

Chiu et al. employed inertial microfluidics to separate WBCs from blood, specifically the T and B lymphocytes (Fig. 4b) [26]. A spiral-shaped microfluidic PDMS-based device isolated the cells label-free with high throughput (approximately 1.3×10^5 cells min^{-1}) and high viability (>95%) using inertial microfluidics [26,

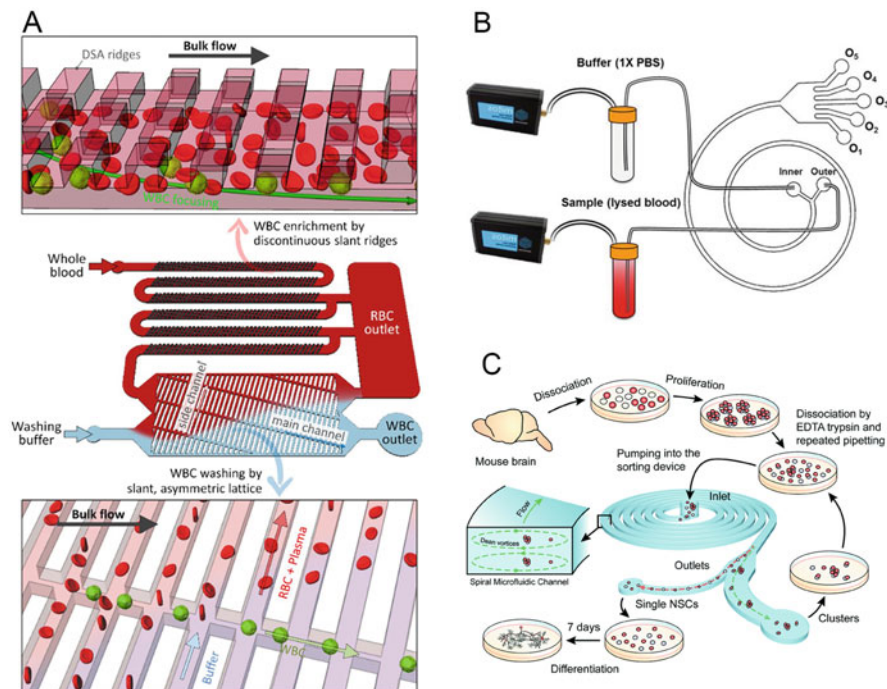


Fig. 4 Examples of microfluidic cell isolation and separation devices. (a) White blood cell (WBC) purification from whole blood by combining microfluidic enrichment and washing units. Reprinted with permission from [25]. Copyright (2019) American Chemical Society. (b) A spiral-shaped inertial microfluidic device enabled T and B cell isolation from prelysed blood. Adapted with permission from [26]. (c) Inertial focusing separated single stem cells from stem cell clusters to improve polyclonal analysis and differentiation studies. Reproduced with permission from [27] with permission from The Royal Society of Chemistry

28]. This principle does not depend on antibodies or cell labelling, but instead achieves cell separation due to the blood cells' different physical properties. Compared to the traditional gradient density method, a similar purity of isolated T cells was achieved, while substantial reductions in both assay time (15 min vs. 70 min) were realized. Spiral inertial microfluidic devices can also enable stem cell sorting, as depicted in Fig. 4c. Inertial focusing allowed isolating single neuronal stem cells (NSCs) from a mixed population of single and clustered cells with high viability (>90%). This separation is crucial to improve polyclonal analysis and differentiation studies, since both these techniques rely on single-cell suspensions [27]. While single NSCs are focused near the inner wall of the microfluidic device, cell clusters are frequently found in the centre of the channel due to their larger size [27]. A comprehensive overview of other spiral microfluidic devices for cell separation and sorting applications and their principles was presented in a review article by Herrmann et al. [29], and the review article by Acevedo et al. provides more

examples on stem cell isolation [30]. Examples of microfluidic separation devices which were applied to enhance current expansion protocols are mentioned in the corresponding Cell Expansion section below.

Recently, Ringwelski et al. applied dielectrophoretic (DEP) cell purification to separate T cells from cancer cells [31]. They removed chronic myelogenous and acute lymphoblastic leukaemia cells from a pre-purified mixture obtained from conventional T-cell isolation from whole blood. Under conditions of low flow rates and elevated electric potential, the DEP device attained 100% purity with minimal loss (10%) of cell viability. Highlighting the applicability of microfluidic devices for quality control in CAR T cell manufacturing, Wang et al. applied an immuno-magnetic separation method to deplete leukaemic B cells from a cell solution [32]. The magnetic separation was based on the detection of surface markers which are expressed by these rare B leukaemic cells (but not by T cells). To attain separation, magnetic nanoparticles (MNP) were conjugated with antibodies which bound to these surface markers of the rare cell. The drag force from the liquid flow then flushed the T cells through the device, whilst the magnetic force, experienced only by the MNP-tagged cells, withheld the leukaemic B cells.

2.2 T Cell Activation

The activation of T cells stimulates their proliferation and differentiation, and is triggered *in vivo* by antigen-presenting cells (APC), for example dendritic cells. In cell therapy manufacturing, the activation precedes gene delivery and T cell expansion, and is performed by adding monoclonal antibodies, antibody-coated magnetic beads, or artificial antigen-presenting cells to the cell culture medium [8].

Single-cell platforms such as droplets, cell-trapping microfluidic devices and micro- and nanowell arrays enable the study of cell–cell interaction [33, 34]. They offer high-throughput analysis of the heterogeneities of single cell responses and are as such well suited to investigate T-cell activation. Furthermore, T cell activation occurs within seconds, and the transparent nature of polymer microfluidic devices enables real-time recording of the interactions.

Sarkar et al. fabricated a microfluidic droplet microarray device to study the dynamic activation state of single T cells following stimulation with the calcium ionophore ionomycin or with antigen-loaded dendritic cells (Fig. 5) [35]. The PDMS-based microfluidic device consisted of three inlets for the separate introduction of T cells, dendritic cells or ionomycin, and oil. At a T-junction, the three fluid streams converged to form droplets of about half a nanoliter, where both the T cells and the respective stimulating agent were encapsulated. The droplets were then flowed to a droplet trapping array where the activation state was studied. Monitoring calcium levels using time-lapse fluorescence microscopy and Fluo-4 (a fluorescent calcium indicator preloaded to the cells off-chip) revealed significant heterogeneities in the dynamic activation profiles in both cell populations. Droplet technology was also employed to monitor T-cell activation kinetics in real-time following interaction

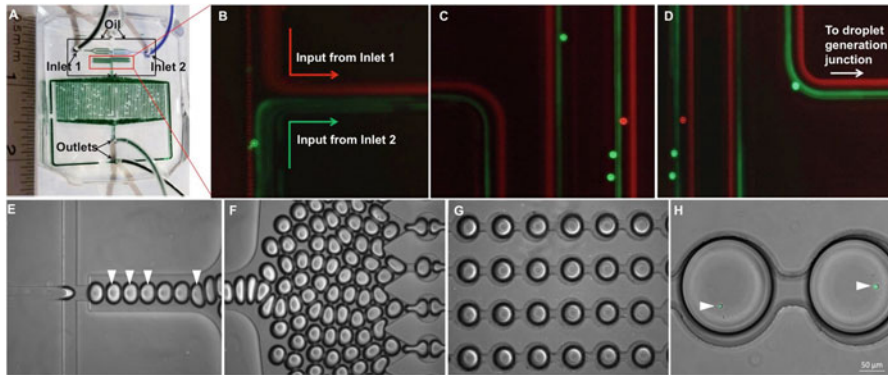


Fig. 5 Example of a microfluidic droplet generation platform to evaluate the activation state of T cells. **(a)** The PDMS-based device with inlets for oil, T cells (inlet 1), and ionomycin or dendritic cells (inlet 2). **(b–d)** Visualization of two input streams in the area indicated by the red rectangle using fluorescent polystyrene beads with a diameter of 7 μm . **(e–g)** Droplets generated at the T-shaped junction encapsulate T cells and the respective stimulating agent. Subsequently, the droplets were driven to the docking microarray. **(h)** Fluorescently labelled T cells within the droplets. Figure reproduced with permission from [35]

with a cancer cell for TCR (T cell receptor) T cell therapy, i.e. for a different adoptive T cell therapy than CAR T cells [36]. A microwell array-based approach paired T cell hybridoma cells with soluble reagents, such as ionomycin and anti-CD3 antibodies, or with APCs and offered time-resolved monitoring of activation profiles using fluorescence microscopy [37].

Recently, Ide et al. reported on an open-type microfluidic PDMS device with cell traps mimicking a lymph node environment [38]. T-cells were flowed into an array of traps containing APCs which were preloaded using the open structure of the device. The traps were designed to capture the APCs and enable serial encounter of the APCs for the T-cells; Ca^{2+} signal measurement returned the information on activation dynamics.

2.3 Gene Delivery

The transfection of T cells is an essential step in the manufacturing of CAR-T cells, since the CAR transgene is delivered into the cells via either viral transduction or electroporation techniques [8]. The transfection of human somatic cells with reprogramming factor encoding mRNAs results in human induced pluripotent stem cells (hiPSCs) that can potentially be used as source material for stem cell-based therapies [10].

Microfluidic devices demonstrated improved gene delivery into stem and T cells compared to conventional methods. Lissandrello et al. achieved high-throughput electrotransfection of mRNA into human T cells using a microfluidic device with

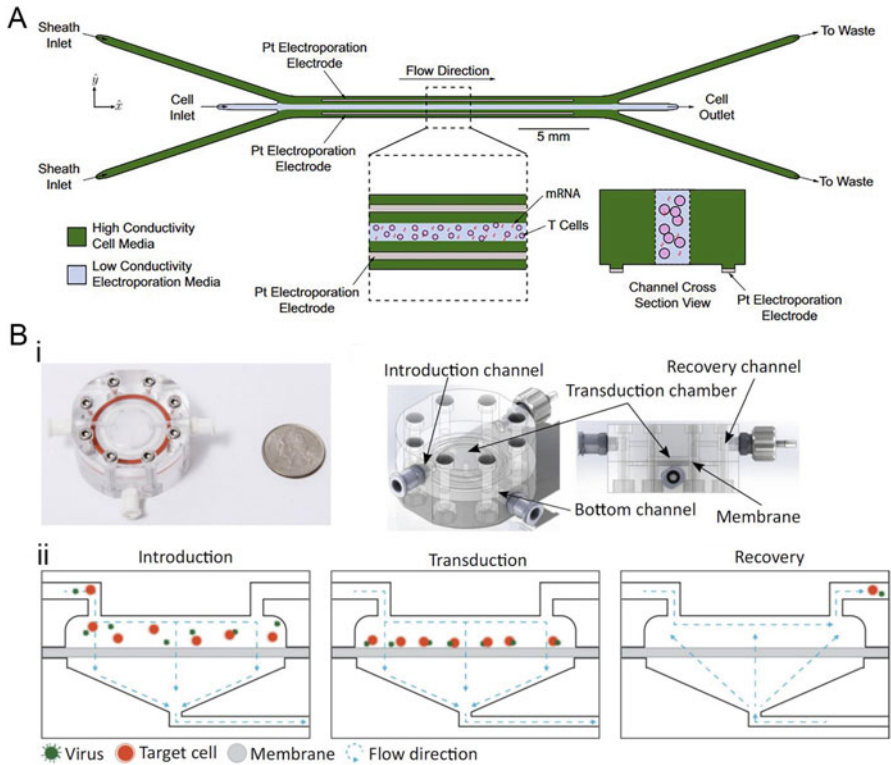


Fig. 6 Examples of microfluidic devices for gene delivery. **(a)** A trifurcated microfluidic device for high-throughput electroporation of mRNA into human T cells consisting of one cell inlet and two surrounding sheath inlets. Two platinum electrodes in contact with the microchannel enabled electroporation. Figure adapted with permission from [39]. **(b)** A microfluidic device for lentiviral transduction of T cells and stem cells. **(i)** Two acrylic plates separated by a semipermeable membrane created a microfluidic transduction chamber exhibiting introduction-, bottom- and recovery channel. **(ii)** Cells were introduced into the chamber and effectively colocalized during the transduction procedure. Cell recovery was achieved by reversing the fluidic flow. Figure adapted with permission from [40]

three inlets and outlets [39] (Fig. 6a). The device was made out of polyetherimide (PEI) sheets and the central stream contained the cells and mRNA in a low conductivity electroporation media, whereas the surrounding side sheath streams were filled with high conductivity cell culture media and were in contact with platinum electrodes. The electrodes deliver a pulsed electric field to the microchannel, electroporating and transfecting the cells. This set-up enabled to concentrate the electric field across the width of the low-conductivity medium. Furthermore, high cell recovery and viability was ensured due to the cells being kept away from both the electrodes and the microchannel’s sidewalls. While traditional cuvette-based electroporation approaches transfect cells batch by batch with limited numbers per batch (~10–50 million cells), this device demonstrated continuous transfection of 500 million cells

at a rate of 20 million cells min^{-1} and with an efficiency of up to 95% [39]. Further separation of viable cells from necrotic or apoptotic cells after electroporation can be achieved using dielectrophoretic means [31].

Luni et al. developed a PDMS-based microfluidic device for reprogramming human somatic cells to induced pluripotent stem cells (hiPSC) by delivering synthetic mRNA into the cells which encodes the transcription factor [41]. By using culture chamber volumes of a few microlitres, the reprogramming efficiency was increased up to 50-fold compared to conventional techniques performed in well plates. This is due to the reduced ratio of media volume to cell growth surface area in a microlitre volume chamber. Moreover, this system showed the potential of microfluidics to parallelize unit operations in cell therapy manufacturing: 32 independent experiments were conducted in parallel in one device, while multiple devices could be used simultaneously.

Moore et al. presented improved lentiviral transduction efficiency for T-cells and haematopoietic stem cells (HSC) [40]. The perfused microfluidic flow chamber consisted of a semipermeable polyethersulfone (PES) membrane compressed between FDA-approved class VI acrylic plates, which were structured with wells and channels (Fig. 6b). The transmembrane fluid flow led to an increased virus concentration at or near the membrane, and therefore effectively colocalizing viral vectors with the target cells. Additionally, cells are kept under continuous nutrient supply and waste removal. Compared to conventional techniques – where the viral vector is introduced to the cells in culture media under static culture conditions – an up to fourfold improvement of transduction efficiency was realized using this device. Microfluidic devices have also been leveraged to secure automatic chemical transfection during long-term cell culture. Raimés et al. achieved transfection of a green fluorescent protein (GFP) plasmid into mouse embryonic stem cells with higher efficiency than with standard procedures [42]. In addition to improving transfection efficiency, this study also showed successful combination of chemical transfection with long-term culturing, i.e. the integration of two unit operations in one single microfluidic device. Long-term culture and transfection were also integrated on-chip in a much smaller culture chamber [43]. Here the differentiation of neural stem cells was followed by localized electroporation of the cells with a GFP plasmid, demonstrating high viability of combined on-chip culture and electroporation of adherent cells.

2.4 Cell Expansion

Microfluidic cell culture devices are recognized as more suitable to create *in vivo*-like conditions than their conventional counterparts, such as flasks, Petri dishes, microtiter plates which operate under static conditions. The ‘soluble’ microenvironment over the cells, temperature, forces and physico-chemical factors are easier to control in microfluidic devices. A huge amount of microfluidic devices for cellular biology, including for cell culture, exploited these advantages [44–49], often with a

focus on quantitative biology and systems biology [50–52], and also as 3D culture models for drug discovery and development [53–56]. Advances in microfluidic culture devices for stem and for immune cells have also been extensively reviewed [30, 57–60]. Additionally, Varma & Voldman analysed the impact of microsystem design on cells and made recommendations on assessing cell-safe device design and operation [61]. Coluccio et al. discussed specific design aspects of microfluidic devices for both adherent and non-adherent cell cultures [62].

Cell expansion aims to stimulate cell proliferation and increase cell numbers by culturing the cells. This process is particularly crucial for T cell and stem cell manufacturing purposes, since cell therapies require very high cell numbers. The exact number of cells, and therefore the scale of production, is defined by the therapy, yet for all therapies a significant expansion is necessary. For example, applications that are based on the transplantation of fully differentiated stem cells may require more than 10^{10} cells [63]. Therefore, cell culture is a key step in cell manufacturing, it is one of the most labour-intensive steps, and ways to accelerate expansion and thereby reduce the duration of this step are of high relevance for process development and optimization.

In microfluidic devices, cells can be continuously perfused with fresh culture media, i.e. a constant supply of nutrients and oxygen is provided, while metabolic waste is continuously removed from the cells. Additionally, shear stress from fluid flow which affects pluripotent stem cells can be modulated in these devices. These devices are therefore well suited to determine the window of fluid regimes, for which the proliferation of stem cells is optimal, and by extension, cell expansion could be accelerated [58].

To evaluate such window of operations for self-renewal of hiPSCs, Yoshimitsu et al. developed a microchamber array chip of 64 chambers [64]. The device was made out of PDMS and the chambers with a volume of 6.4 μL each were coated with fibronectin. Fibronectin was chosen following a screening of extra-cellular matrices (ECM) to determine which ECMs work well for cells cultured on PDMS. Analysing different culture media replenishment regimes, the cells in the PDMS device exhibited a higher growth rate under culture media perfusion than under static culture, i.e. 1 or 3 media exchanges per day. There was however no difference in growth between the two perfusion flow rates tested, and the growth rates under perfusion matched the one found in the 24-well control cultures. Earlier work by Korin et al. [65] and Titmarsh et al. [66] demonstrated that there is a relatively narrow range of optimal flow rates for human embryonic stem cells (hESC) for optimal expansion in microfluidic devices. Below this range, cells grow poorly possibly due to nutrient limitation, and above it the cells also expanded poorly. The latter may be due to elevated shear rates, cell detachment or removal of signalling factors. Similar to Yoshimitsu et al., they found that expansion rates within the optimal range corresponded well with rates in static culture controls [66].

The transparent nature of these microfluidic devices enables real-time monitoring of cellular behaviour with high-resolution imaging modalities. This enables real-time monitoring of culture growth kinetics which is necessary to develop robust processes for cell therapies. In our laboratory, Reichen et al. successfully

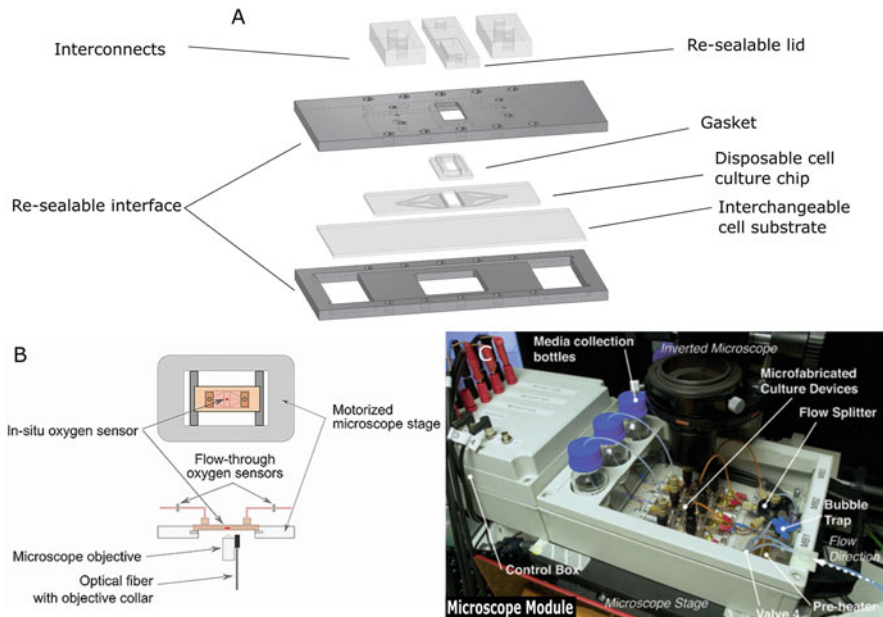


Fig. 7 Example of a multiplexed microfluidic system and of monitoring of dissolved oxygen and degree of cellular confluency. (a) Exploded view of a microfluidic cell culture device. (b) Dissolved oxygen monitoring schematic with optical sensors (inline and in situ). Reprinted with permission from [67]. (c) Photograph of the microscope module attached to the stage of an inverted fluorescence microscope. Reprinted with permission from [68]

demonstrated the maintenance and real-time growth monitoring of hESCs colonies co-cultured on feeder cells (Fig. 7) [69]. In this device, the hES cells grew on gelatin-coated tissue culture polystyrene, replicating the cell growth substrate used in conventional static plates. Super et al. enhanced the monitoring capabilities of the same device and achieved real-time monitoring of specific oxygen uptake rates of ESCs [67]. Non-invasive and label-free monitoring of cell growth was attained from phase contrast microscopy images using bespoke image segmentation algorithms [71], and cell respiration was detected using integrated optical sensors for dissolved oxygen [72, 73].

Another way to underpin the expansion step using microfluidics was shown by Yin et al. [74]. They combined a spiral microchannel device with conventional flask culture methods. The spiral microchannel isolated subpopulations of mesenchymal stem cells, using the principle of inertial microfluidics as described earlier in this section. Between each passaging step, cells whose size lay outside the optimal range were excluded, which increased the chondrogenic potential and proliferation rate of the culture. Similarly, for T-cells, Strachan et al. developed a filtration device consisting of a centre channel separated from two adjacent side channels by pillars [75]. The pillar geometry and the widening side channels were designed such that

larger particles accumulated in the centre channel. Using this device, they improved lymphocyte recovery, enhanced growth rates and thus shortened expansion time for the T-cells.

Finally, surface modification has been shown to enhance cell growth. PDMS nano-modified scaffolds containing biocompatible nanomaterials (such as gold nanowires), for example, improved cell proliferation within a microfluidic device when compared to pristine PDMS [76].

2.5 Stem Cell Differentiation

Differentiation of stem cells requires a well-controlled environment to present the necessary biological, chemical and physical cues to the cells. The superior control over the cellular microenvironment afforded by microfluidics enables this and also allows the careful study of the influence of individual factors on stem cell differentiation. Therefore, a vast amount of microfluidic devices have been designed to investigate stem cell fate and cell differentiation, using both 2D and 3D cultures [30, 55–58, 76]. Zhang et al. provide a tabular overview over microfluidic devices recent as of 2017 by stem cell and differentiation types [59]. The advances that microfluidic devices made are also highlighted by the type of review articles where they are nowadays found. They are, for example, reported in reviews describing the state of the art of iPSCs-derived endothelial cells [77] and of MSC-derived cells [78] for disease modelling and drug development. An FDA-sponsored study evaluated the application of microfluidics tools for iPSC-derived cardiac and hepatic cells, and how they can improve in vitro models in drug development programs [79]. They are reviewed from a user perspective alongside different platforms, for example to underpin multi-lineage hiPSC-based models for disease modelling and drug discovery [80]. Finally, a recent overview of currently developed microfluidic devices for osteogenic, neural and endothelial stem cell differentiation, has been presented by Ye et al. [76]

Differentiation protocols often take several weeks to complete, requiring the long-term maintenance of cells in microfluidic culture devices. Examples of long-term differentiation protocols executed in microfluidic devices show that the devices routinely sustain 3-week-long protocols: Human neuroepithelial stem cells were differentiated within 30 days into dopaminergic neurons transferring an established protocol to the microfluidic scale [81]. Later, an automated system was built for the microfluidic 3D cell culture plate and combined with liquid handling robots [82]. A calcium imaging assay after 24 days showed the neurons to be electrophysiologically active and immunostaining confirmed the expression of relevant neuronal markers. Long-term differentiation of human iPSCs was successfully demonstrated with the device of Fig. 7a [83]. Compared to traditionally employed culture devices like T-flask or well-plates, this microfluidic device provided a stable microenvironment due to controlled and continuous culture media perfusion. Different flow rates were investigated over 3 weeks of retinal differentiation and the perfusion flow rate

was found to have an impact on the expression of key retinal progenitor markers. Kim et al. fabricated a microfluidic device consisting of an equilateral triangular microchannel (Fig. 8a), which generated shear stress gradients (Fig. 8b) to demonstrate their impact on endothelial differentiation of human mesenchymal stem cells (hMSC) over the duration of 3 weeks [84]. The device was fabricated by bonding a triangular PDMS channel created by replica moulding onto polystyrene (PS) substrate. Exposure to very low shear stress over 3 weeks on the other hand aided to understand the mechanism of osteogenic differentiation of hMSC under interstitial flow [86]. And also the impact of culture media replacement rates on neural cell differentiation of mouse neural SC was shown using a 3-week-long microfluidic culture [87]. Adipogenic differentiation over 2 weeks of hMSC was achieved in a PDMS device in chambers of 6.1 μL , with the cells stimulated both chemically and mechanically [88]. Both adipogenesis and osteogenesis of hMSCs was shown over 3-week-long culture in a device with a modified polystyrene substrate; cell-supportive in the culture chamber and cell-repellent outside of it, thus preventing migration of the cells into the feeding channels [89]. A unique monitoring approach was applied by Pully et al [90]. They obtained differentiation of human bone marrow stromal cells (hBMSCs) in a PDMS/ CaF_2 device, again over 3 weeks. The cells were monitored using Raman spectroscopy and mineralization was detected after 2 weeks. To avoid interfering Raman scattering from the PDMS material, the PDMS was peeled off from the CaF_2 substrate during monitoring. Human liver progenitor cells were grown over 1 week in a microfluidic device containing a micropillar array, and then differentiated for 2 weeks into hepatocyte-like cells in the same device [91]. The micropillar array spatially confined a cell culture compartment wherein the cells were immobilized three-dimensionally. Finally, Kilic et al. used microfluidics to create a microenvironment mimicking the central nervous system and pluripotent human NTera2 cells differentiated into mature neuronal and astroglial cells over a 4-week period [92].

An elegant way to monitor differentiation progress is the encapsulation of cells in hydrogel beads; however, it is typically not possible to keep the cells in the droplets for several weeks. The response of monoclonal mouse embryonic cells to two different growth media was, for example, analysed in droplet beads [93], and the effect of retinoic acid on the neuronal differentiation of mouse embryonic carcinoma cells was observed over 10 days in such beads [94].

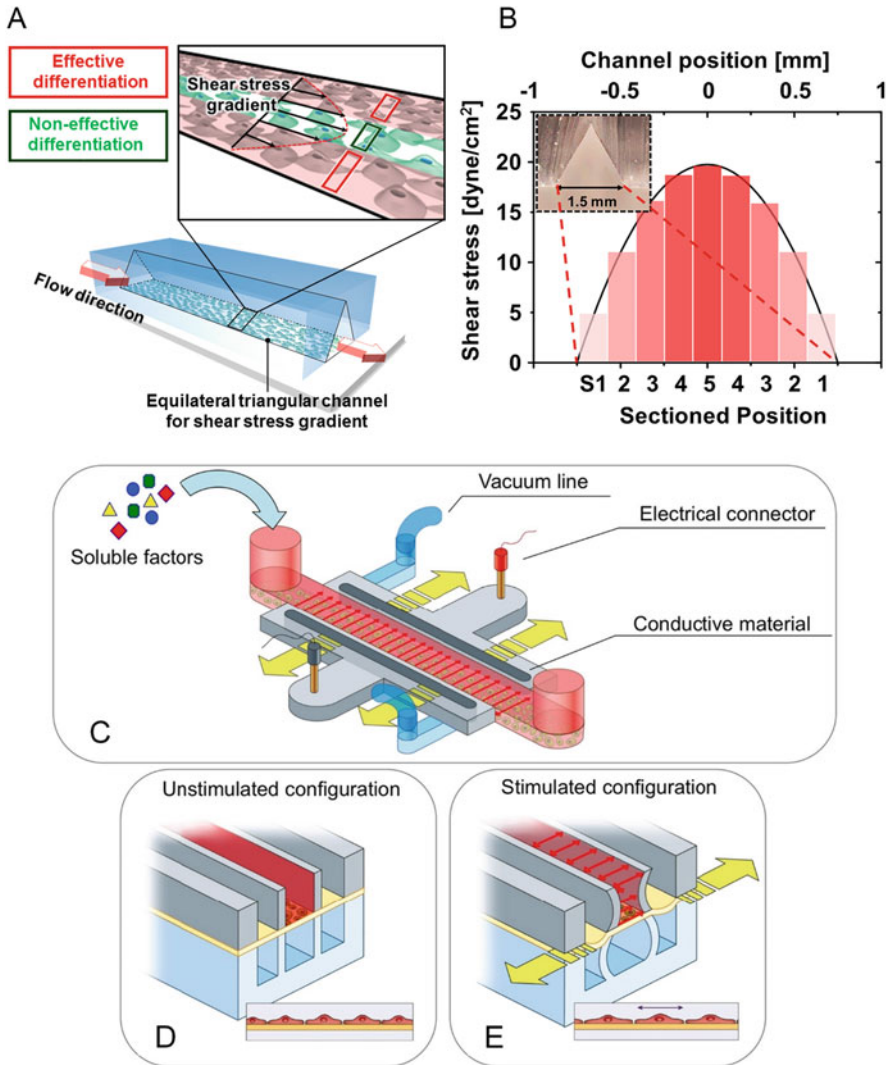


Fig. 8 Examples of microfluidic devices to investigate stem cell differentiation. (a, b) Microfluidic device to study the effect of shear stress on endothelial differentiation of MSCs (a) Schematic of the equilateral triangular channel with stem cells cultured on the PS substrate. (b) Calculated shear stress distribution on the microfluidic channel's bottom. Figure adapted with permission from [84]. Copyright © 2019 Elsevier B.V. (c–e) Microfluidic device developed to apply electrical, mechanical and chemical stimuli for mesenchymal stem cell (MSC) differentiation. (c) Schematic view of the device. The central channel (red) contained media to provide nutrients and soluble factors to cells. Pneumatic channels (blue) allowed mechanical stimulation by stretching the PDMS membrane (yellow arrows) where the cells adhered. The electrical layer contained conductive regions composed of a mixture of carbon nanotubes (CNTs) and PDMS (light grey), which were connected to the stimulator through two external connectors (red and black). The electric field across the cell culture region was represented by the red arrows. Cross section of the device in the unstimulated (d) and electromechanically stimulated (e) configurations. Figure reprinted with permission from [85]

3 Summary and Perspective

Cell-based therapies are expected to play an increasingly prominent role in medicine. With *Yescarta* and *Kymriah*, two cell-based immunotherapies for cancer have recently come on the market, and more therapies are under development. To meet the regulatory demands on process control, product quality and reproducibility for these therapies, closed and automated cell therapy manufacturing systems have been developed. These GMP-in-a-box systems achieve higher control through dynamic monitoring and automatic fluid handling, while reducing the risk of contamination.

Microfluidic devices are closed systems with exquisite control over the cellular microenvironment, making them ideally suited for revealing the interplay between the cell's environment and cellular behaviour. In the preceding section, we highlighted opportunities that microfluidics offers and grouped these according to typical process unit operations for cell-based therapies. In regard to CAR T cell-based therapies, we found microfluidic devices for isolation of white blood cells (WBCs) from the blood [25], T lymphocyte enrichment [26, 74], as well as for delivery of the CAR gene [39, 40] and T cell activation [35]. This encompasses most of the unit operations for a CAR T cell therapy manufacturing process. We are not aware of a demonstration of CAR-T cell culture or expansion on chip, though certainly T cell or Jurkat cells culture has been shown [95]. Furthermore, microfluidics have enabled organ-on-a-chip approaches for disease modelling and drug development [16]. Additionally, *in vitro* functional testing of immunotherapies [96], including the testing of CAR-T cells on solid 3D tumour models was shown [97, 98].

Microfluidic approaches have also been realized for stem cell processing, and the devices discussed in the previous section included the sorting of cells to enrich subpopulations such as the stem cells themselves, the culture of stem cells, their differentiation and their transfection. Some of the reports investigated aspects directly relevant to process development. For stem cell expansion, a few studies, for example, were concerned with finding the optimal culture media exchange rates or with monitoring culture conditions in combination with cell growth kinetics. Similarly, for differentiation, the impact of culture media exchange rates or perfusion rates was investigated for differentiation protocols that stretch over several weeks. As for transfection, typically higher yields are reported, likely due to the improved mass transfer conditions at the microfluidic scale.

There has been exciting, though yet limited progress towards using microfluidic devices as part of a process train. Microfluidic sorting was demonstrated to enhance the yield of conventional expansion MSC protocols when subpopulations with defined cell sizes were isolated during each passaging step [74]. Similarly, microfluidic filtration shortened the expansion times for T-cells [75]. Self-renewal and differentiation protocols of stem cells were executed using the same device [64]. Similarly, adherent cell culture and transfection were coupled and performed in one device [43]. In our lab, we also developed a microfluidic culture device which allowed long-term culture and transfection with the same device [42]. Additionally,

we successfully executed a long-term differentiation protocol [83]. The device was equipped with optical sensors for real-time monitoring of oxygen growth kinetics, and the cell seeding and harvesting procedures mimicked those typically employed for routine stem cell maintenance in cell culture laboratories [67].

Most reported devices were fabricated using poly(methylsiloxane) (PDMS), mainly due to its amenability to rapid prototyping techniques [49]. The following concerns are frequently raised when it comes to using PDMS for cell culture applications [47, 49, 99]: the porous network of PDMS may sequester small, hydrophobic molecules from the culture media [100]; its uncured oligomers may leach into the culture media [100, 101]; and its hydrophobicity requires surface treatment to attain cell adhesion and to promote cell proliferation [102]. Furthermore, tissue culture polystyrene (TC-PS) is predominant in conventional cell culture, which presents a certain schism between microfluidic and conventional cell culture [49]. Gelatin, for example, which is frequently used in combination with TC-PS, does not appear to promote cell adhesion when used with PDMS. In our lab (unpublished results), we found that mouse ESC did not adhere on PDMS and on PDMS coated with gelatin. Both Yoshimitsu et al. and Kamei et al. screened for the extra-cellular matrix which best promotes cell proliferation on PDMS before conducting cell culture experiments in their PDMS devices, and both reported that gelatin on PDMS does not produce satisfactory results [64, 103]. Yoshimitsu et al. found that both fibronectin and laminin promoted cell attachment and proliferation and retained pluripotency marker expression for hiPSCs for 4 days. Kamei et al. applied a combination of fibronectin and gelatin, and equally the expression of pluripotency markers for hESCs was retained for 6 days.

To attain long-term cell adhesion on PDMS, a large number of strategies have been proposed [104]; for example, silanization of PDMS supported long-term cell adhesion and osteogenic differentiation of MSCs [105], and coating of PDMS with a polydopamine enabled osteogenic and adipogenic differentiation of MSCs [106]. Recently, a PDMS modification using functionalized pluronic was proposed and exhibited superior cellular effects compared to the standard coating of polystyrene for neuronal cell culture [107]. Such advances would indicate that PDMS can be used for long-term cell culture.

Despite the challenges in microfabrication with polystyrene [49], stem cell culture devices with polystyrene as part of the cell growth substrate have been realized. PDMS microfluidic structures were bonded to a gelatin-coated tissue culture dish for hESC culture [108], and to a modified polystyrene substrate for adipogenic and osteogenic differentiation of MSCs [89]. PDMS microfluidic structures were also clamped between rigid thermoplastic materials or aluminium for mouse [109], for human embryonic stem cell culture [69], and for 3-week-long retinal differentiation protocol [83]. Yet the combination of different materials poses bonding challenges, which can lead to reduced yield.

Using thermoplastic polymers also addresses the issues of molecule absorption and monomer leaching with PDMS. Devices made from these materials can also be manufactured robustly, as single-use devices, and mass fabricated for low cost. Furthermore, novel microfabrication technologies are emerging. One of the most

recent additions to this arsenal of microfabrication technologies is the use of 3D printers. This additive manufacturing technology significantly enhances both the speed and flexibility and has the potential to close the gap between rapid prototyping and mass fabrication, though long-term stem cell culture has not yet been demonstrated [110–113]. The jury might therefore still be out, which material and which material/ECM combination produces the best results and which of these removes any concerns that results from the microfluidic scale can easily be translated to larger systems, such as the novel automated GMP-in-a-box systems.

Impressive levels of parallelization of microfluidic culture chambers have been achieved and applied to cell analysis and combinatorial screening [68, 114, 115]. For instance, Titmarsh et al. developed a microfluidic device with 8,100 culture chambers in parallel for combinatorial screening of iPSC-derived cardiomyocyte cultures [114]. Similarly, Occhetta et al. studied the development of MSC 3D cultures in 60 cubic microchambers [116] using a gradient generator approach. This approach enables massive parallelization as demonstrated by Bhattacharjee et al. who created a large-scale gradient array of 1,024 chambers to study axon growth from neuronal cells [117]. Cambier et al. investigated differentiation in HSCs in a device containing 800 culture chambers with a combined footprint of just 1 cm square [115]. Skafted-Pedersen et al. presented a self-contained and automated system with 24 culture chambers and reported on all aspects of microfluidic system integration to achieve a stand-alone cell culture device which can be shuttled between a microscope stage and an incubator chamber [118]. The total culture chamber area is typically very small despite the massive parallelization, as the aim was to make these devices suitable for high-throughput screening of small amounts of cells (and minimal use of reagents). To produce a smaller batch of cells which is representative of batches that are obtained from larger scales, it will likely be necessary to parallelize comparatively large microfluidic culture chambers. And they will ideally contain sensors with which the process conditions and their impact of cell proliferation and differentiation can be monitored. First steps in this direction have been demonstrated with real-time and automated monitoring of cells in culture area of $\sim 0.5 \text{ cm}^2$ per chamber [67, 119] and with limited amount of parallelization [68, 120]. More is required, but it is likely that only a moderate degree of parallelization will be necessary to create a scale-down tool for cell-based therapies.

Current microfluidic devices for cell culture already present most, if not all, of the attributes that are sought in modern cell processing systems: they are closed, automated and amenable for single use. Due to these characteristics and the demands for more accurate technology for CGT manufacturing, it is likely that there will be a continued push for novel tools to support ‘GMP-in-a-box’ systems in the near future, and microfluidics will be a well-suited platform to create such tools. It can also be expected that microfluidic devices will become much more prevalent in both CGT research and manufacturing facilities, due to the demand for more cost-effective and accurate technologies, in much the same way as some microfluidic analytical devices have already found their way into commercial products. As more robust microfluidic devices are developed, they may also become suitable for use as quality control systems in both centralized or de-centralized manufacturing or in some instances

even become key components of cell therapy manufacturing systems. However, while the potential for microfluidic devices to enable efficient and cost-effective process development and characterization is obvious, it still remains to be seen whether robust, cost-effective and sufficiently parallelized systems will ultimately emerge to fulfil the requirements of cell therapy manufacturing, particularly in terms of scale.

Acknowledgements We would like to acknowledge the excellent service of the Servier Medical Art (SMART) website <https://smart.servier.com/> providing icons and cartoons free-of-charge that we used for our illustrations, including the graphical abstract. UCL Biochemical Engineering hosts the Future Targeted Healthcare Manufacturing Hub in collaboration with UK universities and with funding from the UK Engineering & Physical Sciences Research Council (EPSRC, EP/P006485/1) and a consortium of industrial users and sector organisations. The authors also gratefully acknowledge the Engineering and Physical Sciences Research Council (EPSRC, EP/I005471/1, EP/L01520X/1, EP/S01778X/1, EP/S021868/1) and the Biotechnology and Biological Sciences Research Council (BBSRC, BB/L000997/1) for further funding.

References

1. Hirsch T, Rothoef T, Teig N et al (2017) Regeneration of the entire human epidermis using transgenic stem cells. *Nature* 551(7680):327–332. <https://doi.org/10.1038/nature24487>
2. Shortt AJ, Tuft SJ, Daniels JT (2011) Corneal stem cells in the eye clinic. *Br Med Bull* 100 (1):209–225. <https://doi.org/10.1093/bmb/ldr041>
3. Limb GA, Daniels JT (2008) Ocular regeneration by stem cells: present status and future prospects. *Br Med Bull* 85(1):47–61. <https://doi.org/10.1093/bmb/ldn008>
4. Chari S, Nguyen A, Saxe J (2018) Stem cells in the clinic. *Cell Stem Cell* 22(6):781–782. <https://doi.org/10.1016/j.stem.2018.05.017>
5. Mock U, Nickolay L, Weng P et al (2019) Automated manufacturing of CAR-T cells for adoptive immunotherapy using CliniMACS prodigy. *J Chem Inf Model* 53(9):1689–1699
6. Wang X, Rivière I (2016) Clinical manufacturing of CAR T cells: foundation of a promising therapy. *Mol Ther Oncolytics* 3:16015. <https://doi.org/10.1038/mto.2016.15>
7. Levine BL, Miskin J, Wonnacott K, Keir C (2017) Global manufacturing of CAR T cell therapy. *Mol Ther Methods Clin Dev* 4:92–101. <https://doi.org/10.1016/j.omtm.2016.12.006>
8. Vormittag P, Gunn R, Ghorashian S, Veraitch FS (2018) A guide to manufacturing CAR T cell therapies. *Curr Opin Biotechnol* 53:164–181. <https://doi.org/10.1016/j.copbio.2018.01.025>
9. Hirschi KK, Li S, Roy K (2014) Induced pluripotent stem cells for regenerative medicine. *Annu Rev Biomed Eng* 16:277–294. <https://doi.org/10.1146/annurev-bioeng-071813-105108>
10. Yamanaka S (2020) Pluripotent stem cell-based cell therapy – promise and challenges. *Cell Stem Cell* 27(4):523–531. <https://doi.org/10.1016/j.stem.2020.09.014>
11. Veraitch FS, Scott R, Wong JW, Lye GJ, Mason C (2008) The impact of manual processing on the expansion and directed differentiation of embryonic stem cells. *Biotechnol Bioeng* 99 (5):1216–1229. <https://doi.org/10.1002/bit.21673>
12. Frank ND, Jones ME, Vang B, Coeshott C (2019) Evaluation of reagents used to coat the hollow-fiber bioreactor membrane of the quantum® cell expansion system for the culture of human mesenchymal stem cells. *Mater Sci Eng C* 96:77–85. <https://doi.org/10.1016/j.msec.2018.10.081>
13. O’Hanlon CF, Fedczyna T, Eaker S, Shingleton WD, Helfer BM (2017) Integrating a 19F MRI tracer agent into the clinical scale manufacturing of a T-cell immunotherapy. *Contrast Media Mol Imaging* 2017. <https://doi.org/10.1155/2017/9548478>

14. Radek C, Bernadin O, Drechsel K et al (2019) Vectofusin-1 improves transduction of primary human cells with diverse retroviral and lentiviral pseudotypes, enabling robust, automated closed-system manufacturing. *Hum Gene Ther* 30(12):1477–1493. <https://doi.org/10.1089/hum.2019.157>
15. Roberts I, Baila S, Rice RB et al (2012) Scale-up of human embryonic stem cell culture using a hollow fibre bioreactor. *Biotechnol Lett* 34(12):2307–2315. <https://doi.org/10.1007/s10529-012-1033-1>
16. Hanley PJ, Mei Z, Durett AG et al (2014) Efficient manufacturing of therapeutic mesenchymal stromal cells with the use of the quantum cell expansion system. *Cytotherapy* 16 (8):1048–1058. <https://doi.org/10.1016/j.jcyt.2014.01.417>
17. Nankervis B, Jones M, Vang B, Brent Rice R, Coeshott C, Beltzer J (2018) Optimizing T cell expansion in a hollow-fiber bioreactor. *Curr Stem Cell Rep* 4(1):46–51. <https://doi.org/10.1007/s40778-018-0116-x>
18. Xuri Cell Expansion System W25. Cytiva, formerly GE healthcare life sciences. <https://www.cytivalifesciences.com/en/us/shop/cell-therapy/systems/xuri-cell-expansion-system-w25-p-06192>. Accessed 29 Mar 2021
19. Smith TA (2020) CAR-T cell expansion in a Xuri cell expansion system W25. In: Swiech K, Malmegrim KCR, Picanço-Castro V (eds) *Chimeric antigen receptor T cells: development and production*. Springer, New York, pp 151–163. https://doi.org/10.1007/978-1-0716-0146-4_11
20. CliniMACS Prodigy | Cell manufacturing platform | Products | Miltenyi Biotec | USA. <https://www.miltenyibiotec.com/US-en/products/cell-manufacturing-platform/clinimacs-prodigy.html>. Accessed 29 Mar 2021
21. Aglaris Facer 1.0 Cell culture platform – Aglaris. <http://aglaris.co.uk/aglaris-facer-1-0-bioreactor/>. Accessed 29 Mar 2021
22. Cocoon[®] Platform | Lonza. <https://pharma.lonza.com/technologies-products/cocoon-platform>. Accessed 29 Mar 2021
23. Leong W, Nankervis B, Beltzer J (2018) Automation: what will the cell therapy laboratory of the future look like? *Cell Gene Ther Insights* 4(9):679–694. <https://doi.org/10.18609/cgti.2018.067>
24. Murthy SK (2014) Perspective on microfluidic cell separation: a solved problem? *Anal Chem* 86(23):11481–11488
25. Kim B, Kim KH, Chang Y, Shin S, Shin EC, Choi S (2019) One-step microfluidic purification of white blood cells from whole blood for immunophenotyping. *Anal Chem* 91 (20):13230–13236. <https://doi.org/10.1021/acs.analchem.9b03673>
26. Chiu PL, Chang CH, Lin YL, Tsou PH, Li BR (2019) Rapid and safe isolation of human peripheral blood B and T lymphocytes through spiral microfluidic channels. *Sci Rep* 9 (1):1–10. <https://doi.org/10.1038/s41598-019-44677-3>
27. Nathamgari SSP, Dong B, Zhou F et al (2015) Isolating single cells in a neurosphere assay using inertial microfluidics. *Lab Chip* 15(24):4591–4597. <https://doi.org/10.1039/c5lc00805k>
28. Di Carlo D (2009) Inertial microfluidics. *Lab Chip* 9(21):3038–3046. <https://doi.org/10.1039/b912547g>
29. Herrmann N, Neubauer P, Birkholz M (2019) Spiral microfluidic devices for cell separation and sorting in bioprocesses. *Biomicrofluidics* 13(6):061501. <https://doi.org/10.1063/1.5125264>
30. Acevedo JP, Angelopoulos I, van Noort D, Khoury M (2018) Microtechnology applied to stem cells research and development. *Regen Med* 13(2):233–248. <https://doi.org/10.2217/rme-2017-0123>
31. Ringwelski B, Jayasooriya V, Nawarathna D (2020) Dielectrophoretic high-purity isolation of primary T-cells in samples contaminated with leukemia cells, for biomufacturing of therapeutic CAR T-cells. *J Phys D Appl Phys* 54(6). <https://doi.org/10.1088/1361-6463/abc2f3>
32. Wang Z, Sargent EH, Kelley SO (2021) Ultrasensitive detection and depletion of rare leukemic B cells in T cell populations via Immunomagnetic cell ranking. *Anal Chem* 93 (4):2327–2335. <https://doi.org/10.1021/acs.analchem.0c04202>

33. Seah YFS, Hu H, Merten CA (2018) Microfluidic single-cell technology in immunology and antibody screening. *Mol Aspects Med* 59:47–61. <https://doi.org/10.1016/j.mam.2017.09.004>
34. Choi JR (2020) Advances in single cell technologies in immunology. *Biotechniques* 69(3):227–236. <https://doi.org/10.2144/btn-2020-0047>
35. Sarkar S (2015) T cell dynamic activation and functional analysis in nanoliter droplet microarray. *J Clin Cell Immunol* 6(3):334. <https://doi.org/10.4172/2155-9899.1000334>
36. Segaliny AI, Li G, Kong L et al (2018) Functional TCR T cell screening using single-cell droplet microfluidics. *Lab Chip* 18(24):3733–3749. <https://doi.org/10.1039/c8lc00818c>
37. Desalvo A, Bateman F, James E, Morgan H, Elliott T (2020) Time-resolved microwell cell-pairing array reveals multiple T cell activation profiles. *Lab Chip* 20(20):3772–3783. <https://doi.org/10.1039/d0lc00628a>
38. Ide H, Espulgar WV, Saito M et al (2021) Profiling T cell interaction and activation through microfluidics-assisted serial encounter with APCs. *Sens Actuators B* 330:129306. <https://doi.org/10.1016/j.snb.2020.129306>
39. Lissandrello CA, Santos JA, Hsi P et al (2020) High-throughput continuous-flow microfluidic electroporation of mRNA into primary human T cells for applications in cellular therapy manufacturing. *Sci Rep* 10(1):1–16. <https://doi.org/10.1038/s41598-020-73755-0>
40. Moore N, Chevillet JR, Healey LJ et al (2019) A microfluidic device to enhance viral transduction efficiency during manufacture of engineered cellular therapies. *Sci Rep* 9(1):1–11. <https://doi.org/10.1038/s41598-019-50981-9>
41. Luni C, Giullitti S, Serena E et al (2016) High-efficiency cellular reprogramming with microfluidics. *Nat Methods* 13(5):446–452. <https://doi.org/10.1038/nmeth.3832>
42. Raimes W, Rubi M, Super A, Marques MPC, Veraitch F, Szita N (2017) Transfection in perfused microfluidic cell culture devices: a case study. *Process Biochem* 59:297–302. <https://doi.org/10.1016/j.procbio.2016.09.006>
43. Kang W, Giraldo-Vela JP, Nathamgari SSP et al (2014) Microfluidic device for stem cell differentiation and localized electroporation of postmitotic neurons. *Lab Chip* 14(23):4486–4495. <https://doi.org/10.1039/c4lc00721b>
44. El-Ali J, Sorger PK, Jensen KF (2006) Cells on chips. *Nature* 442(7101):403–411. <https://doi.org/10.1038/nature05063>
45. Kim L, Toh YC, Voldman J, Yu H (2007) A practical guide to microfluidic perfusion culture of adherent mammalian cells. *Lab Chip* 7(6):681–694. <https://doi.org/10.1039/b704602b>
46. Young EWK, Beebe DJ (2010) Fundamentals of microfluidic cell culture in controlled microenvironments. *Chem Soc Rev* 39(3):1036–1048. <https://doi.org/10.1039/b909900j>
47. Halldorsson S, Lucumi E, Gómez-Sjöberg R, Fleming RMT (2015) Advantages and challenges of microfluidic cell culture in polydimethylsiloxane devices. *Biosens Bioelectron* 63:218–231. <https://doi.org/10.1016/j.bios.2014.07.029>
48. Sackmann EK, Fulton AL, Beebe DJ (2014) The present and future role of microfluidics in biomedical research. *Nature* 507(7491):181–189. <https://doi.org/10.1038/nature13118>
49. Berthier E, Young EWK, Beebe D (2012) Engineers are from PDMS-land, biologists are from polystyrenia. *Lab Chip* 12(7):1224–1237. <https://doi.org/10.1039/c2lc20982a>
50. Mehling M, Tay S (2014) Microfluidic cell culture. *Curr Opin Biotechnol* 25:95–102. <https://doi.org/10.1016/j.copbio.2013.10.005>
51. Sibbitts J, Sellens KA, Jia S, Klasner SA, Culbertson CT (2017) Cellular analysis using microfluidics. *Anal Chem* 89:711–719. <https://doi.org/10.1021/acs.analchem.7b04519>
52. García Alonso D, Yu M, Qu H, Ma L, Shen F (2019) Advances in microfluidics-based technologies for single cell culture. *Adv Biosyst* 3(11):1900003. <https://doi.org/10.1002/adbi.201900003>
53. Gupta N, Liu JR, Patel B, Solomon DE, Vaidya B, Gupta V (2016) Microfluidics-based 3D cell culture models: utility in novel drug discovery and delivery research. *Bioeng Transl Med* 1(1):63–81. <https://doi.org/10.1002/btm2.10013>

54. Cochrane A, Albers HJ, Passier R et al (2019) Advanced in vitro models of vascular biology: human induced pluripotent stem cells and organ-on-chip technology. *Adv Drug Deliv Rev* 140:68–77. <https://doi.org/10.1016/j.addr.2018.06.007>
55. Grün C, Altmann B, Gottwald E (2020) Advanced 3D cell culture techniques in micro-bioreactors, part I: a systematic analysis of the literature published between 2000 and 2020. *Processes* 8(12):1656. <https://doi.org/10.3390/pr8121656>
56. Altmann B, Grün C, Nies C, Gottwald E (2020) Advanced 3D cell culture techniques in micro-bioreactors, part II: systems and applications. <https://doi.org/10.3390/pr9010021>
57. Leshner-Perez SC, Frampton JP, Takayama S (2013) Microfluidic systems: a new toolbox for pluripotent stem cells. *Biotechnol J* 8(2):180–191. <https://doi.org/10.1002/biot.201200206>
58. Titmarsh DM, Chen H, Glass NR, Cooper-White JJ (2014) Concise review: microfluidic technology platforms: poised to accelerate development and translation of stem cell-derived therapies. *Stem Cells Transl Med* 3(1):81–90. <https://doi.org/10.5966/sctm.2013-0118>
59. Zhang J, Wei X, Zeng R, Xu F, Li XJ (2017) Stem cell culture and differentiation in microfluidic devices toward organ-on-a-chip. *Future Sci OA* 3:FSO187. <https://doi.org/10.4155/foa-2016-0091>
60. Morsink M, Willemen N, Leijten J, Bansal R, Shin S (2020) Immune organs and immune cells on a chip: an overview of biomedical applications. *Micromachines* 11(9):849. <https://doi.org/10.3390/mi11090849>
61. Varma S, Voldman J (2018) Caring for cells in microsystems: principles and practices of cell-safe device design and operation. *Lab Chip* 18(22):3333–3352. <https://doi.org/10.1039/C8LC00746B>
62. Coluccio ML, Perozziello G, Malara N et al (2019) Microfluidic platforms for cell cultures and investigations. *Microelectron Eng* 208:14–28. <https://doi.org/10.1016/j.mee.2019.01.004>
63. Kirouac DC, Zandstra PW (2008) The systematic production of cells for cell therapies. *Cell Stem Cell* 3(4):369–381. <https://doi.org/10.1016/j.stem.2008.09.001>
64. Yoshimitsu R, Hattori K, Sugiura S et al (2014) Microfluidic perfusion culture of human induced pluripotent stem cells under fully defined culture conditions. *Biotechnol Bioeng* 111(5):937–947. <https://doi.org/10.1002/bit.25150>
65. Korin N, Bransky A, Dinnar U, Levenberg S (2009) Periodic “flow-stop” perfusion microchannel bioreactors for mammalian and human embryonic stem cell long-term culture. *Biomed Microdevices* 11:87–94. <https://doi.org/10.1007/s10544-008-9212-5>
66. Titmarsh D, Hidalgo A, Turner J, Wolvetang E, Cooper-White J (2011) Optimization of flowrate for expansion of human embryonic stem cells in perfusion microbioreactors. *Biotechnol Bioeng* 108(12):2894–2904. <https://doi.org/10.1002/bit.23260>
67. Super A, Jaccard N, Marques MPC et al (2016) Real-time monitoring of specific oxygen uptake rates of embryonic stem cells in a microfluidic cell culture device. *Biotechnol J* 11(9):1179–1189. <https://doi.org/10.1002/biot.201500479>
68. Reichen M, Veraitch FS, Szita N (2013) Development of a multiplexed microfluidic platform for the automated cultivation of embryonic stem cells. *J Lab Autom* 18(6):519–529. <https://doi.org/10.1177/2211068213499917>
69. Reichen M, Macowne RJ, Jaccard N et al (2012) Microfabricated modular scale-down device for regenerative medicine process development. *PLoS One* 7(12):e52246. <https://doi.org/10.1371/journal.pone.0052246>
70. Jaccard N, Szita N, Griffin LD (2017) Segmentation of phase contrast microscopy images based on multi-scale local basic image features histograms. *Comput Methods Biomed Eng Imaging Vis* 5(5):359–367. <https://doi.org/10.1080/21681163.2015.1016243>
71. Gruber P, Marques MPC, Szita N, Mayr T (2017) Integration and application of optical chemical sensors in microbioreactors. *Lab Chip* 17(16):2693–2712. <https://doi.org/10.1039/c7lc00538e>
72. Zirath H, Rothbauer M, Spitz S et al (2018) Every breath you take: non-invasive real-time oxygen biosensing in two- and three-dimensional microfluidic cell models. *Front Physiol* 9:815. <https://doi.org/10.3389/fphys.2018.00815>

73. Yin L, Wu Y, Yang Z et al (2018) Lab on a chip microfluidic label-free selection of mesenchymal stem cell subpopulation during culture expansion extends the chondrogenic potential in vitro. *Lab Chip* 18:878. <https://doi.org/10.1039/c7lc01005b>
74. Strachan BC, Xia HUI, Vörös E, Gifford SC, Shevkoplyas SS (2019) Improved expansion of T cells in culture when isolated with an equipment-free, high-throughput, flow-through microfluidic module versus traditional density gradient centrifugation. *Cytotherapy* 21 (2):234–245. <https://doi.org/10.1016/j.jcyt.2018.12.004>
75. Hashemzadeh H, Allahverdi A, Sedghi M et al (2020) PDMS Nano-modified scaffolds for improvement of stem cells proliferation and differentiation in microfluidic platform. *Nanomaterials (Basel)* 10(4):668. <https://doi.org/10.3390/nano10040668>
76. Ye F, Yan Z, Zhang H, Chang H, Neuzil P (2020) Microfabricated stem cell targeted differentiation systems. *Trends Anal Chem* 126:115858. <https://doi.org/10.1016/j.trac.2020.115858>
77. Jang S, Collin de l'Hortet A, Soto-Gutierrez A (2019) Induced pluripotent stem cell-derived endothelial cells: overview, current advances, applications, and future directions. *Am J Pathol* 189(3):502–512. <https://doi.org/10.1016/j.ajpath.2018.12.004>
78. Afflerbach AK, Kiri MD, Detinis T, Maoz BM (2020) Mesenchymal stem cells as a promising cell source for integration in novel in vitro models. *Biomol Ther* 10(9):1–30. <https://doi.org/10.3390/biom10091306>
79. Dame K, Ribeiro AJS (2021) Microengineered systems with iPSC-derived cardiac and hepatic cells to evaluate drug adverse effects. *Exp Biol Med* 246(3):317–331. <https://doi.org/10.1177/1535370220959598>
80. Jang J, Yoo J-E, Lee J-A et al (2012) Disease-specific induced pluripotent stem cells: a platform for human disease modeling and drug discovery. *Exp Mol Med* 44(3):202–213. <https://doi.org/10.3858/emm.2012.44.3.015>
81. Moreno EL, Hachi S, Hemmer K et al (2015) Differentiation of neuroepithelial stem cells into functional dopaminergic neurons in 3D microfluidic cell culture. *Lab Chip* 15(11):2419–2428. <https://doi.org/10.1039/c5lc00180c>
82. Kane KIW, Moreno EL, Hachi S et al (2019) Automated microfluidic cell culture of stem cell derived dopaminergic neurons. *Sci Rep* 9(1):1–12. <https://doi.org/10.1038/s41598-018-34828-3>
83. Abdolvand N, Tostoes R, Raimes W, Kumar V, Szita N, Veraitch F (2019) Long-term retinal differentiation of human induced pluripotent stem cells in a continuously perfused microfluidic culture device. *Biotechnol J* 14(3):1800323. <https://doi.org/10.1002/biot.201800323>
84. Kim HW, Lim J, Rhie JW, Kim DS (2017) Investigation of effective shear stress on endothelial differentiation of human adipose-derived stem cells with microfluidic screening device. *Microelectron Eng* 174:24–27. <https://doi.org/10.1016/j.mee.2016.12.022>
85. Pavesi A, Adriani G, Rasponi M, Zervantonakis IK, Fiore GB, Kamm RD (2015) Controlled electromechanical cell stimulation on-a-chip. *Sci Rep* 5:11800. <https://doi.org/10.1038/srep11800>
86. Kim KM, Choi YJ, Hwang J-HJH et al (2014) Shear stress induced by an interstitial level of slow flow increases the osteogenic differentiation of mesenchymal stem cells through TAZ activation. *PLoS One* 9(3):92427. <https://doi.org/10.1371/journal.pone.0092427>
87. Wang B, Jedlicka S, Cheng X (2014) Maintenance and neuronal cell differentiation of neural stem cells C17.2 correlated to medium availability sets design criteria in microfluidic systems. *PLoS One* 9(10):1–15. <https://doi.org/10.1371/journal.pone.0109815>
88. Wu HW, Lin CC, Hwang SM, Chang YJ, Bin LG (2011) A microfluidic device for chemical and mechanical stimulation of mesenchymal stem cells. *Microfluid Nanofluid* 11(5):545–556. <https://doi.org/10.1007/s10404-011-0820-7>
89. Tenstad E, Tourouvskaia A, Folch A, Myklebost O, Rian E (2010) Extensive adipogenic and osteogenic differentiation of patterned human mesenchymal stem cells in a microfluidic device. *Lab Chip* 10(11):1401–1409. <https://doi.org/10.1039/b926738g>

90. Vishnu VP, Lenferink A, Van Manen HJ, Subramaniam V, Van Blitterswijk CA, Otto C (2010) Microbioreactors for raman microscopy of stromal cell differentiation. *Anal Chem* 82 (5):1844–1850. <https://doi.org/10.1021/ac902515c>
91. Ong LJY, Chong LH, Jin L et al (2017) A pump-free microfluidic 3D perfusion platform for the efficient differentiation of human hepatocyte-like cells. *Biotechnol Bioeng* 114 (10):2360–2370. <https://doi.org/10.1002/bit.26341>
92. Kilic O, Pamies D, Lavell E et al (2016) Brain-on-a-chip model enables analysis of human neuronal differentiation and chemotaxis. *Lab Chip* 16(21):4152–4162. <https://doi.org/10.1039/c6lc00946h>
93. Kleine-Brüggeney H, van Vliet LD, Mulas C et al (2019) Long-term perfusion culture of monoclonal embryonic stem cells in 3D hydrogel beads for continuous optical analysis of differentiation. *Small* 15(5):1–11. <https://doi.org/10.1002/sml.201804576>
94. Kim C, Bang JH, Kim YE, Lee JH, Kang JY (2012) Stable hydrodynamic trapping of hydrogel beads for on-chip differentiation analysis of encapsulated stem cells. *Sens Actuators B* 166–167:859–869. <https://doi.org/10.1016/j.snb.2012.02.008>
95. Guzzi F, Candeloro P, Coluccio ML et al (2020) A disposable passive microfluidic device for cell culturing. *Biosensors* 10(3):1–14. <https://doi.org/10.3390/bios10030018>
96. Adriani G, Pavesi A, Tan AT, Bertoletti A, Thiery JP, Kamm RD (2016) Microfluidic models for adoptive cell-mediated cancer immunotherapies. *Drug Discov Today* 21(9):1472–1478. <https://doi.org/10.1016/j.drudis.2016.05.006>
97. Ando Y, Siegler EL, Ta HP et al (2019) Evaluating CAR-T cell therapy in a hypoxic 3D tumor model. *Adv Healthc Mater* 8(5):1–15. <https://doi.org/10.1002/adhm.201900001>
98. Xu R, Zhou X, Wang S, Trinkle C (2021) Tumor organoid models in precision medicine and investigating cancer-stromal interactions. *Pharmacol Ther* 218:107668. <https://doi.org/10.1016/j.pharmthera.2020.107668>
99. Tanyeri M, Tay S (2018) Viable cell culture in PDMS-based microfluidic devices. *Methods Cell Biol* 148:3–33. <https://doi.org/10.1016/bs.mcb.2018.09.007>
100. Regehr K, Domenech M, Koepsel J et al (2009) Biological implications of polydimethylsiloxane-based microfluidic cell culture. *Lab Chip* 9(15):2132–2139. <https://doi.org/10.1039/b903043c>. *Biological*
101. Renckens TJA, Janeliunas D, van Vliet H, van Esch JH, Mul G, Kreutzer MT (2011) Micromolding of solvent resistant microfluidic devices. *Lab Chip* 11(12):2035–2038. <https://doi.org/10.1039/c0lc00550a>
102. Zhou J, Ellis AV, Voelcker NH (2010) Recent developments in PDMS surface modification for microfluidic devices. *Electrophoresis* 31(1):2–16. <https://doi.org/10.1002/elps.200900475>
103. Kamei KI, Guo S, Yu ZTF et al (2009) An integrated microfluidic culture device for quantitative analysis of human embryonic stem cells. *Lab Chip* 9(4):555–563. <https://doi.org/10.1039/b809105f>
104. Wolf MP, Salieb-Beugelaar GB, Hunziker P (2018) PDMS with designer functionalities – properties, modifications strategies, and applications. *Prog Polym Sci* 83:97–134. <https://doi.org/10.1016/j.progpolymsci.2018.06.001>
105. Chuah YJ, Koh YT, Lim K, Menon NV, Wu Y, Kang Y (2015) Simple surface engineering of polydimethylsiloxane with polydopamine for stabilized mesenchymal stem cell adhesion and multipotency. *Sci Rep* 5:1–12. <https://doi.org/10.1038/srep18162>
106. Chuah YJ, Kuddannaya S, Lee MHA, Zhang Y, Kang Y (2015) The effects of poly (dimethylsiloxane) surface silanization on the mesenchymal stem cell fate. *Biomater Sci* 3 (2):383–390. <https://doi.org/10.1039/c4bm00268g>
107. Liu W, Sun M, Han K, Hu R, Liu D, Wang J (2020) Comprehensive evaluation of stable neuronal cell adhesion and culture on one-step modified polydimethylsiloxane using functionalized Pluronic. *ACS Omega* 5(50):32753–32760. <https://doi.org/10.1021/acsomega.0c05190>
108. Villa-Diaz LG, Torisawa YS, Uchida T et al (2009) Microfluidic culture of single human embryonic stem cell colonies. *Lab Chip* 9(12):1749–1755. <https://doi.org/10.1039/b820380f>

109. Blagovic K, Kim LY, Voldman J (2011) Microfluidic perfusion for regulating diffusible signaling in stem cells. *PLoS One* 6(8). <https://doi.org/10.1371/journal.pone.0022892>
110. Siller IG, Enders A, Steinwedel T et al (2019) Real-time live-cell imaging technology enables high-throughput screening to verify in vitro biocompatibility of 3D printed materials. *Materials (Basel)* 12(13):1–17. <https://doi.org/10.3390/ma12132125>
111. Siller IG, Epping NM, Lavrentieva A, Scheper T, Bahnemann J (2020) Customizable 3D-printed (Co-)cultivation systems for in vitro study of angiogenesis. *Materials (Basel)* 13(19):1–17. <https://doi.org/10.3390/ma13194290>
112. Ong LJY, Islam A, Dasgupta R, Iyer NG, Leo HL, Toh YC (2017) A 3D printed microfluidic perfusion device for multicellular spheroid cultures. *Biofabrication* 9(4). <https://doi.org/10.1088/1758-5090/aa8858>
113. Beckwith AL, Borenstein JT, Velasquez-Garcia LF (2018) Monolithic, 3D-printed microfluidic platform for recapitulation of dynamic tumor microenvironments. *J Microelectromech Syst* 27(6):1009–1022. <https://doi.org/10.1109/JMEMS.2018.2869327>
114. Titmarsh DM, Glass NR, Mills RJ et al (2016) Induction of human iPSC-derived cardiomyocyte proliferation revealed by combinatorial screening in high density microbio reactor arrays. *Sci Rep* 6:1–15. <https://doi.org/10.1038/srep24637>
115. Cambier T, Honegger T, Vanneaux V et al (2015) Design of a 2D no-flow chamber to monitor hematopoietic stem cells. *Lab Chip* 15(1):77–85. <https://doi.org/10.1039/c4lc00807c>
116. Occhetta P, Centola M, Tonnarelli B, Redaelli A, Martin I, Rasponi M (2015) High-throughput microfluidic platform for 3D cultures of mesenchymal stem cells, towards engineering developmental processes. *Sci Rep* 5:1–12. <https://doi.org/10.1038/srep10288>
117. Bhattacharjee N, Folch A (2017) Large-scale microfluidic gradient arrays reveal axon guidance behaviors in hippocampal neurons. *Microsyst Nanoeng* 3(1). <https://doi.org/10.1038/micronano.2017.3>
118. Skafte-Pedersen P, Hemmingsen M, Sabourin D, Blaga FS, Bruus H, Dufva M (2012) A self-contained, programmable microfluidic cell culture system with real-time microscopy access. *Biomed Microdevices* 14(2):385–399. <https://doi.org/10.1007/s10544-011-9615-6>
119. Jaccard N, Macown RJ, Super A, Griffin LD, Veraitch FS, Szita N (2014) Automated and online characterization of adherent cell culture growth in a microfabricated bioreactor. *J Lab Autom* 19(5):437–443. <https://doi.org/10.1177/2211068214529288>
120. Macown RJ, Veraitch FS, Szita N (2014) Robust, microfabricated culture devices with improved control over the soluble microenvironment for the culture of embryonic stem cells. *Biotechnol J* 9(6):805–813. <https://doi.org/10.1002/biot.201300245>

Droplet Microfluidics for Microbial Biotechnology



Sundar Hengoju, Miguel Tovar, DeDe Kwun Wai Man, Stefanie Buchheim, and Miriam A. Rosenbaum

Contents

1	Introduction	130
2	Droplet Microfluidics for Microbial Cultivation	132
3	Detecting Microbial Activity in Droplet Microfluidics	134
4	Droplet Cultivations of Rare Microbes and to Search for New Antimicrobials	142
5	Ultrahigh-Throughput Enzyme Activity Screening and Selection	147
6	Conclusions	150
	References	151

Abstract Droplet microfluidics has recently evolved as a prominent platform for high-throughput experimentation for various research fields including microbiology. Key features of droplet microfluidics, like compartmentalization, miniaturization, and parallelization, have enabled many possibilities for microbiology including cultivation of microorganisms at a single-cell level, study of microbial interactions in a community, detection and analysis of microbial products, and screening of extensive microbial libraries with ultrahigh-throughput and minimal reagent consumptions. In this book chapter, we present several aspects and applications of droplet microfluidics for its implementation in various fields of microbial biotechnology. Recent advances in the cultivation of microorganisms in droplets including methods for isolation and domestication of rare microbes are reviewed. Similarly, a

S. Hengoju, S. Buchheim, and M. A. Rosenbaum (✉)

Bio Pilot Plant, Leibniz Institute for Natural Product Research and Infection Biology – Hans-Knöll-Institute (HKI), Jena, Germany

Faculty of Biological Sciences, Friedrich Schiller University (FSU), Jena, Germany

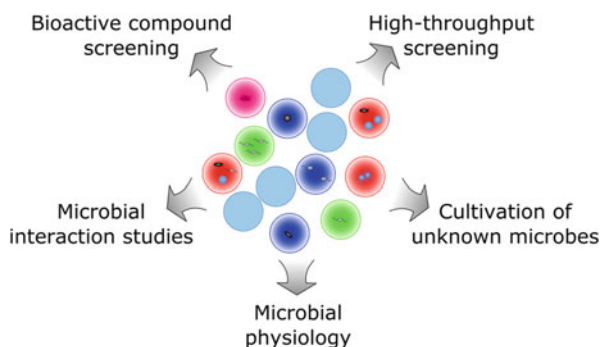
e-mail: miriam.rosenbaum@leibniz-hki.de

M. Tovar and D. K. W. Man

Bio Pilot Plant, Leibniz Institute for Natural Product Research and Infection Biology – Hans-Knöll-Institute (HKI), Jena, Germany

comparison of different detection and analysis techniques for microbial activities is summarized. Finally, several microbial applications are discussed with a focus on exploring new antimicrobials and high-throughput enzyme activity screening. We aim to highlight the advantages, limitations, and current developments in droplet microfluidics for microbial biotechnology while envisioning its enormous potential applications in the future.

Graphical Abstract



Keywords Antibiotic screening, Cultivation of rare microbes, Droplet microfluidics, Enzyme screening, Fluorescence-activated cell sorting, Ultrahigh-throughput microbial cultivation

1 Introduction

Within the rapidly growing field of microfluidics, droplet-based microfluidics refers to systems based on the combination of immiscible phases, which results in the formation of drops of one phase embedded in the other. This simple approach has revolutionized various experimentation platforms as it combines microfluidic miniaturization and ultrahigh-throughput with compartmentalization, one of nature's (life's) oldest key strategies. When generating aqueous droplets surrounded by an inert carrier phase, it is possible to reduce the working volume by more than six orders of magnitude, specifically from μL to pL or even fL . Furthermore, the stringent and controllable conditions during droplet formation allow the production of thousands of compartments per second with a minimal volume variance. Thereby, not only costs but also time can be spared in comparison with traditional liquid-handling methods while maintaining excellent experimental quality. These conditions have led to thousands of technological developments and applications based on droplets in the fields of chemistry and biology, some representing particularly high-impact breakthroughs enabling omics techniques at single-cell resolution with very

high throughput [1–8], or harnessed to screen for improved antibodies [9–11], or enzymes [12–15].

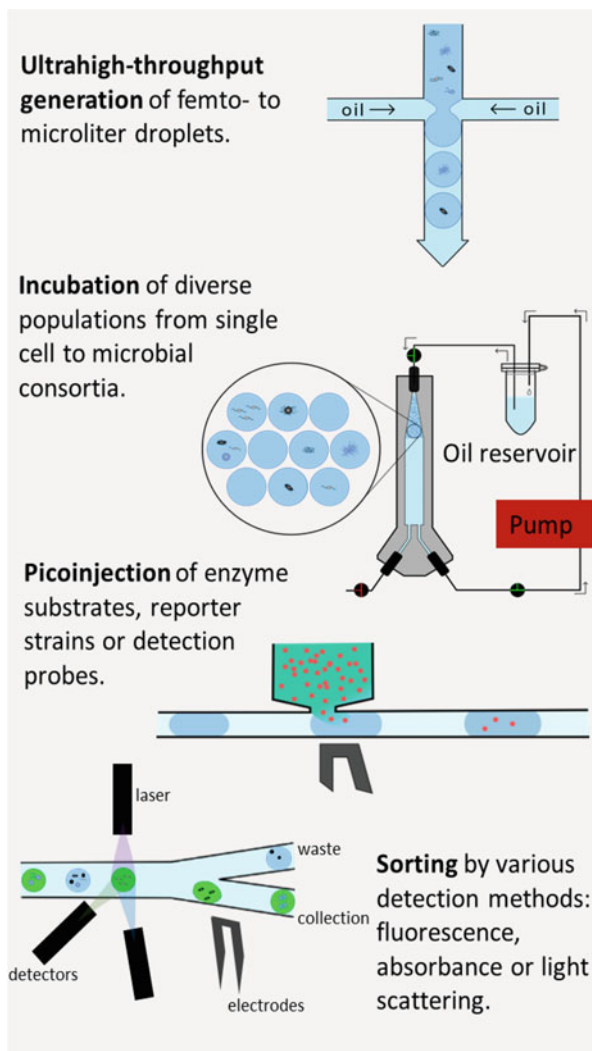
From the microbiologist perspective, droplets provide a paradigm-changing experimental approach. Ironically, except from microscopy, the science of studying microorganisms has been the science of growing them to scales fitting our hands and volumes, given that further experimentation at the micrometer scale was impossible until recently. This inadvertently biased microbiological research towards the development of techniques, strategies, and equipment that restrict the window of diversity that can be analyzed. Microfluidic approaches enable experimentation controlling and monitoring physical scales much closer to those of the microbial world, albeit with some challenges that must be addressed for broad-range applicability.

In droplet microfluidics, even single cells will be compartmentalized in a volume between 1 and 100 pL, i.e., droplets of approx. 10 to 100 μm in diameter. In terms of concentrations, this is similar to 10^7 – 10^9 cells/mL, which is the standard working range at which large-scaled methods work. Therefore, droplets provide a platform in which the biochemical and physiological parameters of a single cell can be studied in a similar fashion as normally done for millions of cells. This, in combination with the extremely fast production of droplets, results in an experimental platform with the capability to explore the enormous diversity of microbiological samples (Fig. 1).

The specific features of microfluidic droplets should render these a promising starting point to isolate, culture, and identify a significant fraction of the until now unculturable and undiscovered microbial biodiversity along with its vast metabolic potential (Fig. 2a). Due to the ultrahigh-throughput, complex heuristic experimental design can be performed to identify ideal nutrient conditions (Fig. 1). Additionally, the minimal volume requirements inherent to microfluidic techniques enable the preparation and analysis of rare and limited – therefore mostly unexplored – samples in their natural conditions, such as microbiota from small animals and plants. Moreover, discretization of microbial cells in compartments with a similar order of magnitude is accompanied by crucial physiological advantages. First, isolation eliminates competition for nutrients, providing the possibility to culture strains commonly hidden under faster-growing communities [16, 17] (Fig. 2b). Alternatively, the droplets can also be exploited to foster microbial interactions, which in many cases have been shown to be critical for growth and metabolite production [18, 19]. Second, higher cell and metabolite effective concentrations are easily detectable and activate concentration-based processes such as quorum sensing [20]. Finally, micro-compartmentalization enables the separation and distinction of otherwise identical cells that present different expression profiles, e.g., scout cells [21] or silent vs. activated gene clusters.

Similarly, droplets can also be exploited to screen human-made microbiological diversity, such as mutant [22] and metagenomic [23] libraries (Fig. 2). For the goal to detect and isolate microbial variants that expand the boundaries of industrial microbiology, droplets provide a platform for the implementation of ultrahigh-throughput assays for improved enzymes and producer strains. The diversity in mutant or metagenomic libraries can easily reach more than 10 million different variants that are impossible to analyze in detail with traditional methods. Yet, in a field where

Fig. 1 Droplet microfluidics workflow overview. A microfluidic device encapsulates single cell or microbial consortia into monodispersed droplets containing growth medium. Microbes are grown in microdroplets inside the incubator which maintains the continuous flow of oxic oil. Electric field-activated picoinjection modifies droplet contents by allowing the delivery of an external solution in a regulated fashion. At designated time points, droplets of interest are recovered by on-chip active sorting. Integration of different detection methods generates trigger, leading to deflection of desired droplets into the collection channel through dielectrophoresis



improvements of a fraction of a percentage may define the viability of an application [24], it is essential to explore the full extent of the created diversity to find the most promising variants and understand the corresponding performance improvements.

2 Droplet Microfluidics for Microbial Cultivation

During the development of droplet microfluidic techniques, microorganisms have been used as effective models for proof-of-concept studies [25]. This is especially the case for the isolation of individual cells in ultra-small volumes. Confinement in

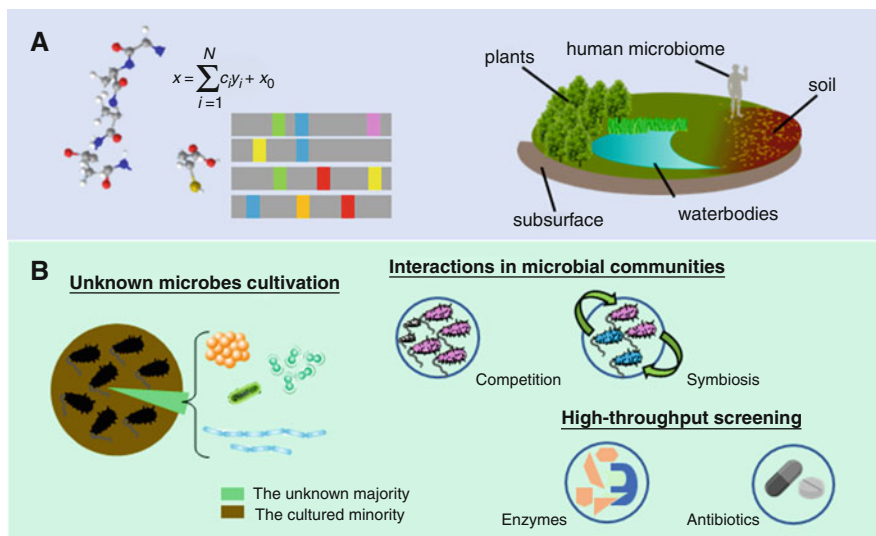


Fig. 2 From biological diversity to applications. **(a)** Microbial resources for droplet cultivations: droplet microfluidics enables ultrahigh-throughput screening of mutant libraries generated from random mutagenesis, statistical modelling and computational design (left), as well as tremendous reservoir of microbial communities in diverse environments (right). **(b)** Applications for droplet microfluidics: droplet microfluidics have been demonstrated as a capable platform for detection and identification of microbes. Compartmentalization allows isolation of unknown and slow-growing species and the study of interactions between microbes from complex environments. Finally, droplets can be employed as microreactors for high-throughput enzyme and antibiotic screening within a controlled chemical environment

such reduced volumes decreases detectable growth time and eventually increases the effective concentration of secreted molecules [26]. Moreover, the ability to create and analyze millions of droplets per day enables the examination of large and diverse samples, find rare cells, and analyze whole populations in terms of genetic and phenotypic varieties.

Most of the initial applications have focused on single-cell campaigns, mostly because droplets are the first high-throughput experimental platform that enables this high impact approach [1, 3, 8, 10, 34–36]. Yet, a number of studies have also used the singularization of cells in droplets with subsequent incubation that results in growth as growth is a powerful yet easy strategy that can be used as a response variable or signal amplifier [22, 37–44]. This is particularly relevant when microorganisms for biotechnological applications are being evaluated or screened. Often initial incubations were performed in tubing loops or arrays on chip [28, 29, 45]. Simple off-chip cultivation in contrast was performed in syringes or reaction tubes [30]. Measuring growth is essential when searching for microorganisms or variants under different nutrient sources or stress conditions or simply when the desired product is biomass or strongly correlated to biomass production. In addition, a number of studies aiming to explore global microbial phenotypes [46–48],

antibiotic resistance [49–51], or community culture and composition [52–60] have relied on growth inside of droplets.

However, as more complex and comprehensive protocols are envisioned, a higher degree of microbiological craftsmanship [61] should be implemented for droplet-based experimentation. Such is the case for studies involving more complex microorganisms with distinct metabolic profiles. Therefore, incubation conditions must be appropriately controlled in order to provide ideal conditions for the microorganisms and the different experiments being performed. Maximizing homogeneity for the millions of droplets per experiment can result in either maximized growth or production of the molecules of interest. In this context, oxygen and pH control in millions of droplets [32, 33] provide the tools to effectively link droplet microfluidics and classic microbiological standards (Fig. 3). The possibility to measure and control oxygen availability and pH provides natural or artificial incubation conditions in droplets that could be adjusted to imitate the original bacterial habitat (soil pores, static or agitated water, animal intestines, etc.) or bioreactor conditions. In fact, it is of great advantage for biotechnological screening applications to provide bioreactor-like conditions and control, as the selected variants must be scaled up for their implementation in industrial production processes. Further applications of optimized incubation setups include the exploration of hypoxic conditions, the usage of gases as growth or enzymatic substrates, and the screening for molecules and microbes active under adverse pH conditions.

3 Detecting Microbial Activity in Droplet Microfluidics

The development and integration of effective detection techniques to a microfluidic system is a critical step for any biotechnological and microbiological analysis. Implementation of traditional laboratory techniques, which provide high sensitivity and accuracy, requires proper integration strategies, since they typically require expensive and bulky instruments, skilled personnel, and extensive analysis time [62, 63]. In addition, miniaturization of sample volume and fast-flowing droplets in a microfluidic system poses significant challenges for rapid and sensitive detection. Therefore, an ideal detection technique for droplet microfluidics includes features like simple, rapid response, high sensitivity, compact, flexible, and low cost.

For analysis and quantification of microbiological samples in droplet microfluidics, different detection methods have been developed and implemented including optical-, electrical-, and mass spectrometry-based detection (for an overview see Table 1) [64]. Among others, optical methods have become very popular with the advancement of detection instruments, miniaturization of optical components, and development of dyes and biomarkers. Optical methods have been demonstrated for diverse chemical and biological applications along with research focusing on improving detection sensitivity and dynamic range [65, 66]. Various spectroscopic methods used for analysis include fluorescence, absorbance, light scattering, and Raman signals.

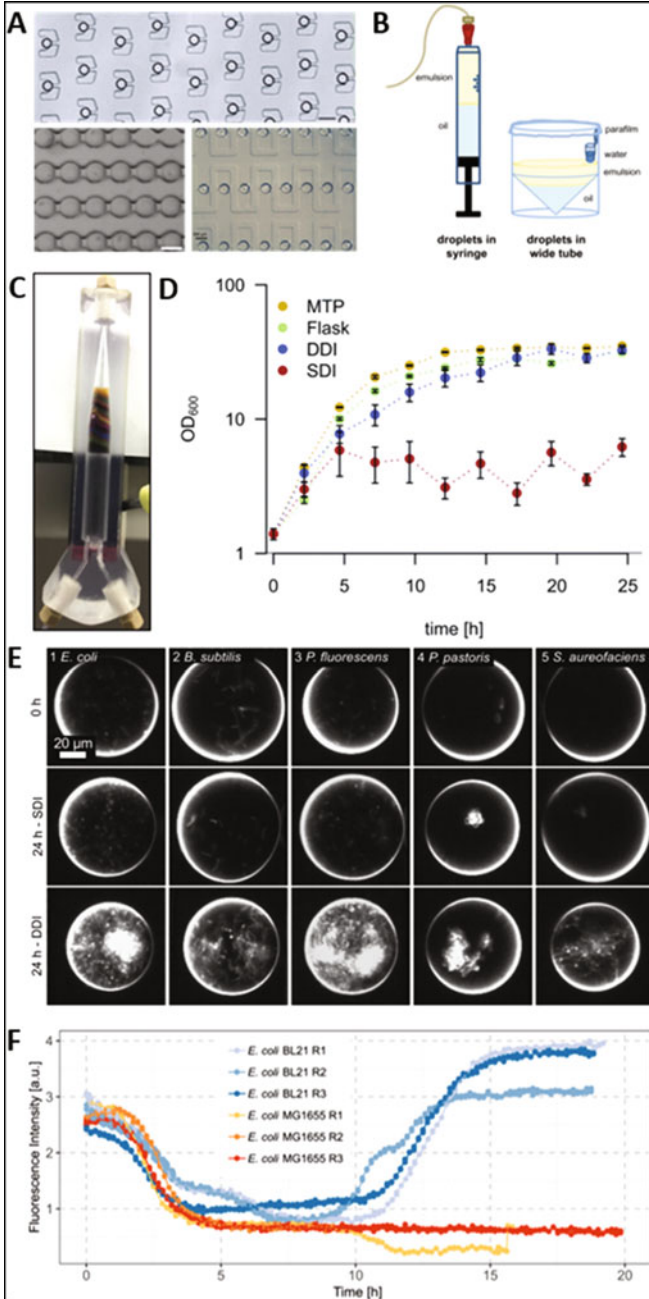


Fig. 3 Examples for droplet incubation strategies and microbial growth characterization. (a) Droplets incubated inside microfluidic structures in traps or delay lines (with reprints from [27–29]). (b) Off-chip droplet incubation is usually done in reaction tubes or inside syringes [30]. (c) Dynamic droplet incubator to enhance oxygenation and homogeneity of droplet populations [31]. (d) Picoliter cultures of microorganisms grow similar to larger-scaled methods when dynamically incubated [32]. (e) Colonies formed inside of dynamically incubated droplets reach much

Fluorescence is the most widely used detection technique for chemical and biological analysis considering various factors like high-signal intensity, highly sensitive dyes, selective fluorescent labelling biomarkers, well-established protocols, high-end instruments, etc. Using fluorescence detection method, microbial activity can be detected by various approaches like direct measurement of fluorescence from cellular metabolites, labelling cellular metabolites with fluorescent dyes, using fluorogenic substrates for enzyme assays, using reporter strains expressing fluorescent proteins, or using fluorescent-based probes. Availability of several fluorogenic substrates with higher quantum yield has enabled development of sensitive fluorescence detection and efficient sorting mechanism for high-throughput enzyme screening. Details regarding these applications are discussed in the respective subchapter below.

On the other hand, microbial viability markers based on fluorescent dyes have been used in droplets for growth and survival analysis. Assays based on highly fluorescent resorufin, which is formed through metabolic activity from resazurin [67] and dodecylresorufin [68], have been implemented for bacterial and antibiotic inhibition analysis. Resorufin-based substrates have also been used for detection of ethanol-producing cyanobacteria [69] and screening for high xylose-consuming yeast strains [39]. However, leakage of resorufin from droplets [68] has restricted its application to microbial growth assays requiring long time incubation. Recently, a FRET-based RNA probe has been demonstrated for the detection of growth, sorting, and analysis of a microbial community from environmental samples [57]. Similarly bacterial cells stained with SYTO 9, propidium iodide [70], and SyTox Orange [71] dyes have been used for drug susceptibility testing and screening metagenomics library for antibiotic producers.

Bacterial strains expressing fluorescent proteins have been popular as a sensor or reporter for various microbial assays including antibiotic screening and microbial interaction studies. Fluorescent proteins are expressed continuously with fluorescence intensity depicting the concentration of cells. Such reporter strains were used to demonstrate growth and long-term cultivation of microorganisms in droplets [30, 72, 73], analyzing bacterial dynamics [74], and performing MIC (minimum inhibitory concentration) assays [75]. *Escherichia coli* and *Bacillus subtilis* strains expressing fluorescent proteins like GFP, mKate, and mCherry have been extensively utilized. For high-throughput screening of antibiotic producers from complex environmental samples, reporter strain expressing mCherry proteins was picoinjected to pre-cultivated droplets containing environmental microorganisms, and fluorescence signals were measured to determine the inhibition activity [38, 76]. Similarly, multiple fluorogenic strains with auxotrophic variants have been used to investigate microbial interactions between *E. coli* and *Pseudomonas putida* in a microfluidic system [77].

Fig. 3 (continued) higher biomass levels [32]. (f) Using dynamic incubation, it is also possible to monitor and control the pH of the entire droplet population [33]. Images are reprints of the indicated publications with permission of the original publisher

Table 1 Analytical methods for detecting microbial activity in droplets

Detection method	Screening technique	Application	Microorganism	Remarks	Refs.	
Fluorescence	Direct detection of cellular metabolites	Monitoring microbial production of riboflavin	<i>E. coli</i>	Continuous monitoring for long-term incubation	[73]	
		Screening for enhanced riboflavin producers	<i>Y. lipolytica</i>	FACS analysis using double emulsion	[41]	
		Detection of chlorophyll production	<i>E. gracilis</i> and <i>C. reinhardtii</i>	Gel droplets with FACS analysis	[37]	
	Labelling with fluorescent dyes	Live/dead assay		<i>E. coli</i>	Cell viability assay and drug susceptibility testing by staining cells with SYTO 9 and propidium iodide	[70]
			Screening for bacteria inhibiting <i>S. aureus</i>	<i>S. aureus</i>	Double emulsion droplets with FACS analysis	[38]
		Screening for high lipid-producing microalgae	<i>E. gracilis</i> and <i>C. reinhardtii</i>	Gel droplets with FACS analysis	[37]	
		Screening for antibiotic producers	<i>S. aureus</i>	Screening metagenomic library by co-encapsulating <i>E. coli</i> and <i>S. aureus</i> and staining dead cells with SyTox Orange	[71]	
		Fluorescent-based substrates for enzyme screening	Alkaline phosphatase		<i>Tetraselmis</i> sp.	Measurement of enzymatic activity at single-cell level
				<i>E. coli</i>	Enzyme kinetics study	[103]
	Cellulase		Bacterial community from soil sample		High-throughput screening	[42]
			<i>T. reesei</i>	Screening of filamentous fungi in droplets	[104]	
Lipase	Environmental water and soil sample			Compact optical system for fluorescence measurement	[66]	

(continued)

Table 1 (continued)

Detection method	Screening technique	Application	Microorganism	Remarks	Refs.
		Amylase	<i>A. niger</i>	Growth and analysis of fungi in droplets	[105]
		Xylanase	<i>Y. lipolytica</i>	High-throughput screening technique for improved enzyme activity	[106]
		Esterases	<i>E. coli</i>	Screening of metagenomic library from environmental sample	[23]
		Cot A laccase	<i>E. coli</i>	Flexible screening platform and picoinjection of substrate	[107]
	Reporter strains expressing fluorescent proteins	Growth and cultivation of microorganisms	<i>E. coli</i>	Easy detection of microbial growth in droplets	[72]
		Growth analysis	<i>B. subtilis</i>		[30]
		Analysis of bacterial dynamics	<i>E. coli</i>		[74]
		Screening antibiotic producers from environmental sample	Environmental soil sample		[76]
		Demonstration of microbial co-cultivation	<i>E. coli</i> and <i>B. subtilis</i>	Simultaneous detection of multiple colors using a single sensor	[78]
		Bacterial growth monitoring	<i>E. coli</i>	Continuous monitoring for long-term incubation	[73]
		Cultivation of microorganisms	<i>E. coli</i> and <i>P. aeruginosa</i>	Cultivation in plates by streaking droplets	[53]
		Growth kinetics and MIC assays	<i>E. coli</i>	Automated fluid handling	[75]
		Microbial interaction study	<i>E. coli</i> and <i>P. putida</i>	Cultivation of microbes in adjacent chambers separated by nanochannels, demonstration for	[77]

(continued)

Table 1 (continued)

Detection method	Screening technique	Application	Microorganism	Remarks	Refs.
				metabolic cross-feeding and microbial gene transfer	
	Reporter strains based on product specific expression of fluorescent proteins	Screening for vitamin B2 producers	<i>B. subtilis</i>	<i>E. coli</i> sensor cells with a riboswitch specific for vitamin B2	[108]
	Fluorescence-based dyes/probes	Growth analysis	Environmental sample	FRET-based RNA probes cleaved by RNase produced by growing microorganisms, sorting droplets with high growth	[57]
		Microbial viability assay	<i>E. coli</i> and <i>E. aerogenes</i>	Use of dodecylresorufin-based dyes	[68]
		Antimicrobial susceptibility assessment	<i>E. coli</i>	Use of resorufin for detection of cell growth	[67]
Absorbance	Absorbance-based substrate	Directed enzyme evolution	<i>E. coli</i>	Absorbance-based screening for high producers of phenylalanine dehydrogenase	[79]
		Study fermentation process	<i>Z. mobilis</i>	Determination of ethanol concentration using colorimetric assay	[80]
	Direct monitoring of droplet content	Measurement of viscosity and optical density	<i>E. coli</i>	Lower throughput	[109]
Sorting colonies of similar cell density		<i>S. cerevisiae</i>	Multi-parametric analysis and sorting	[81]	
Light scattering	Detection of scattered light from droplet content	High-throughput screening of antibiotic-resistant bacteria	<i>E. coli</i>	Label-free screening	[51]
	Imaging of scattered light pattern	Detection of <i>E. coli</i>	<i>E. coli</i>	Label-free detection with high sensitivity	[86]

(continued)

Table 1 (continued)

Detection method	Screening technique	Application	Microorganism	Remarks	Refs.
Raman signal	Surface-enhanced Raman spectroscopy	Bacterial strain identification	<i>E. coli</i>	Fast recording of SERS spectra from droplets	[110]
Image-based	Image analysis of droplet content	Enrichment of droplets with growth	<i>S. puniceus</i>	Triggered imaging and sorting of droplets, label-free method	[87]
		Identification and recognition of cells in droplets	<i>D. tertiolecta</i> and <i>P. tricorutum</i>	Discrimination of cells based on morphologies and sorting	[88]
	Colored beads for encoding droplets	MIC assay	<i>E. coli</i>	Encoding various experimental conditions using colored beads	[31]
	Immunoassay with fluorescent-labelled antibodies	Detection and identification of bacteria	<i>E. coli</i>	Use of magnetic beads to capture <i>E. coli</i> and labelling with fluorescently labelled anti- <i>E. coli</i> antibodies	[89]
Electrical conductance	Measurement of conductivity signals with integrated electrodes	Quantification of <i>E. coli</i>	<i>E. coli</i>	3D-printed chip with integrated electrodes allowing contactless measurement	[97]
	Impedance measurement	Monitoring cell differentiation		Label-free and noninvasive detection of cells	[96]
Mass spectrometry	Electrospray ionization	Mass-activated droplet sorting		Splitting droplets and sorting based on mass	[101]
		Detection of microbial secondary metabolites	<i>S. griseus</i>	Intensity analysis at known mass-charge ratio	[76]
			<i>S. griseus</i>	Combined fluorescence and MS detection	[100]

Recent developments also demonstrated the simultaneous detection of multiple fluorescence signals for antibiotic screening and microbial co-cultivation assays [78]. With such setups, multiple parameters can be analyzed from individual droplets, which open the door to multiplexing biochemical and microbiological assays.

Though fluorescence-based detection setups are popular in droplet microfluidics, one should take into account the degradation of fluorogenic substrates over time, stability, and inter-droplet transfer of fluorophore molecules. A general prerequisite for all droplet-specific fluorescence assays is a containment of the fluorophore to the respective droplet. If fluorophores can move out of the droplet into the oil phase, the specificity of the signal to a droplet gets lost and the signal intensity decreases. However, the mobility of specific fluorophores can also be exploited for monitoring bulk droplet properties. Measurements of several parameters critical for microbial growth and metabolite productions, like change in pH and oxygen level, have been assessed by using fluorescence detection methods [32, 33].

Absorbance is a label-free technique and can be measured in droplets by monitoring change in optical properties of droplet content. Absorbance-based techniques have been demonstrated for monitoring cell density and screening of microbial libraries. A chromogenic substrate, WST-1 resulting in the absorbing dye WST-1 formazan, was used for screening of an *E. coli* mutant library producing phenylalanine dehydrogenase [79]. A similar colorimetric assay was implemented for monitoring ethanol production by *Zymomonas mobilis* during fermentation [80]. Furthermore, absorbance signals were utilized for monitoring droplet content and sorting colonies of similar cell densities to minimize assay variability arising from growth phenotypes [81]. However due to miniaturization in microfluidic system, the active optical path length for absorbance measurement is highly decreased in comparison with traditional optical readers, thus resulting in lower detection sensitivity. Recently, several optimizations and modifications, including elongated channel designs [82, 83], lock-in-based detection [84], and optofluidic approaches [85], have been demonstrated in realizing absorbance measurement in microfluidic platform.

Light-scattering-based analysis of microorganisms has also been demonstrated in droplets. A high-throughput label-free detection setup was developed to analyze bacterial growth in droplets and screen antibiotic-resistant mutants [51]. In the presence of the antibiotic fusidic acid, growth of a normal *E. coli* strain is inhibited, while antibiotic-resistant mutant bacteria could grow resulting in higher scattered light signals. Furthermore, a recent microfluidic droplets study monitored microbial growth and quantified microorganisms by imaging 2D light-scattering patterns [86].

Image-based analyses of droplets have also been utilized for microbial analysis. Bright-field images were analyzed for sorting and enriching droplets with grown microorganisms from empty droplets [87]. Similarly, different morphologies of cells [88] or fluorescent microscopy images based on immunoassays [89] have also been utilized for the identification and detection of microbial samples in droplets. With advanced image analysis algorithms based on machine learning and deep neural networks, microbial samples have been analyzed in 3D culture system [90] and in multiplexed assays [31]. Within the latter work, different experimental conditions were coded using colored beads, which were decoded by droplet image analysis.

Another approach is to modify droplets either to gel droplets [37, 71] or to double emulsions [38] for analysis with conventional FACS (fluorescence-based cell sorting) instruments. This allows simultaneous analysis of multiple fluorescent

signals and scattered light parameters, enabling multi-parametric analysis and sorting of droplets. This approach significantly increased the throughput of the screening process. However, generating double emulsions and gel emulsions is not straightforward and limits the fluid handling operations like merging and splitting.

Most of the current optical detection setups are based on bulky microscopes along with complex and often expensive optical configurations. Recent developments in the combination of optical and fluidic systems have resulted in the emergence of optofluidic devices, synergistic integration of optical components with a microfluidic device [91, 92]. The integration of optics into microfluidic chips allows alignment-free setups with higher sensitivity and multiplexing capability of chemical and biological assays [62], which also greatly benefit microbial experimentations [93].

In addition to optical methods, other detection methods including electrical signals and mass spectrometry (MS) have also been utilized for the detection of microbial activity. Electrical conductance and impedance measurement have been demonstrated for measuring droplet dimensions including velocity [94, 95] and characterizing cell growth in droplets [96]. Label-free detection and counting of *E. coli* cells were demonstrated in droplets by contactless conductivity measurements [97]. Mass spectrometry (MS) is a label-free method and provides information about analytes depending on mass-to-charge ratio. Several studies have combined a droplet microfluidic system with MS [98, 99]. Microfluidic droplets are sprayed into a MS head either by using a capillary connector or by modifying chip designs with cone-shaped outlets. A droplet MS platform was developed for detecting secondary metabolites produced by *Actinobacteria* [76, 100]. However, MS is a destructive method, resulting in a loss of possible hits. Recently, new microfluidic handling techniques have been introduced with the capability of splitting droplets, analyzing one daughter droplet by MS, and sorting other daughter droplets based on MS results [101]. Such setup possesses broad prospects for microbial screening using droplet microfluidics.

In addition to the above mentioned online analysis tools, several offline detection techniques have been demonstrated for droplet microfluidics. In most cases, droplets are broken and analyzed for droplet content. These include DNA sequencing, liquid and gas chromatography, and mass spectrometry among others.

4 Droplet Cultivations of Rare Microbes and to Search for New Antimicrobials

Cultivation of microorganisms in very small droplets has several critical advantages for some of the most pressing challenges in environmental microbiology: the cultivation of microorganisms considered unculturable and the search for new anti-infective natural products. This advantage particularly is generated by (1) the ultrahigh-throughput of droplets experiments, which allows very deep sampling of the environmental microbial consortia; (2) the very small size of the cultivation

vessel between 50 and 200 pL, which allows to conduct high numbers of experiments with a minimum input of resources and preparative work; and (3) an increasing portfolio of high-speed functional assays to evaluate microbial growth and activity.

It has long been acknowledged that the majority of today's anti-infective compounds have first been isolated from microbial producers or are derivatives of microbial natural products. However, after the golden age of antibiotics discovery in the 1940–1960s, no novel antibiotic structures and functionalities have been discovered. Intensive efforts to rationally and statistically generate new lead compounds through chemical synthesis proved not very fruitful. Today, with the urgent need for discovery of functionally new lead structures because of emerging antibiotic resistances, scientists increasingly go back to the initial source of anti-infective compounds: the unlimited pool of microbial natural products. The central challenge for this approach is to reduce the level of rediscovery of already known molecules. Thereby, three strategies are followed: (1) genome-based mining for new biosynthetic gene clusters possibly with different structural properties, which might point to new chemical functionalities [111–113]; (2) the search for natural products in so far under explored environmental habitats like marine resources or host-associated microbial communities [114, 115]; and (3) a deeper and more strategic microbial cultivation effort to access natural products from slow-growing, previously uncultured, or synergistically growing microorganisms. Often even a combination of these three strategies is applied.

Especially for the last two strategies, droplet microfluidics has shown great potential. A statistical distribution for inoculating either a single microbial cell or a small consortium into one droplet as an individual growth vessel enables the parallel cultivation of millions of microbial cultures in a bulk volume of one milliliter or less (Fig. 3). Controlled cultivation conditions at defined temperature, oxygenation level, pH, and time provide a large operational window for successful cultivations. Such strategy has been used, for example, to characterize the diversity and ability to grow on different carbon sources for the microbiota from human fecal samples [116]. Functional screening of these individual droplets can be achieved at around 100–1,000 droplets per second, resulting in a capacity to evaluate almost 10 million cultivations per day. Since the individual droplet size is very small, specific chemical analysis for natural products is challenging, but not impossible. For example, it has been successfully shown that individual droplets can directly be injected into a mass spectrometer to quantify the production of a microbial natural product in a droplet [76, 100]. Droplets of *Streptomyces griseus* producing streptomycin were analyzed and validated for efficient detection from single droplets. However, so far the valuable microbial droplet content is sacrificed during such an invasive chemical analysis. Alternatively, functional reporter assays can predict the presence of a bioactive natural product and can be applied to preselect high potential microbial droplets from either empty droplets without growth or droplets without bioactivity. In this case, a reporter agent is added to the pre-cultivated microbial droplet. In the search for antimicrobials, this is typically a microbial strain or defined strain mixture sensitive against inhibition by antimicrobials in the droplet (Fig. 4) [38, 76, 117]. A

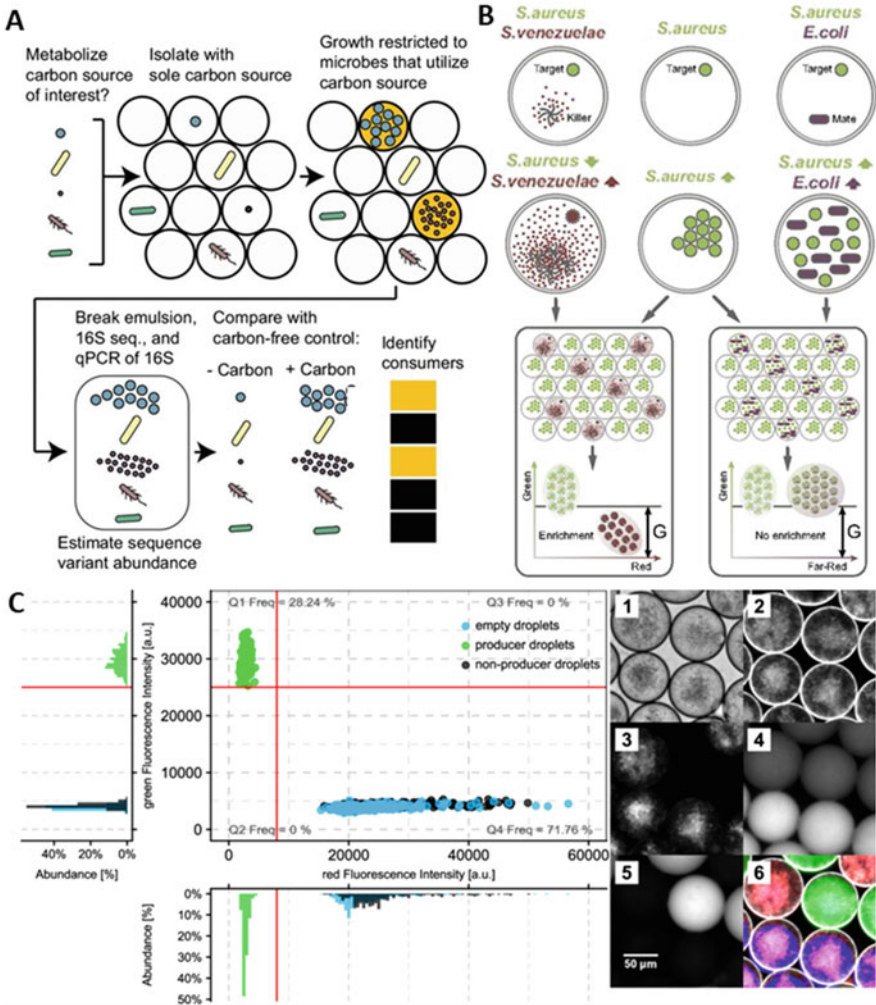


Fig. 4 Applications of ultrahigh-throughput microbial cultivations in picoliter droplets. (a) Characterization of carbon source (prebiotic) consumption within human gut bacteria [116]. (b, c) Negative interaction assays (i.e., antibiotic production) using co-encapsulation of possible producers and fluorescently labelled reporter strains [38, 76]. Images are reprints of the indicated publications with permission of the original publisher

growth-based fluorescence signal of the reporter strain indicates uninhibited growth (clear increase in fluorescence signal) or inhibition (no signal). With this approach a much more specific and targeted initial isolation of microorganisms with antimicrobial potential is possible. Even more, through the combination of reporter strains of different target groups (e.g., Gram positive and Gram negative), a differential selection of antimicrobial strains against a specific target group (e.g., active against only gram negatives) would become possible. Beyond this, for different screening

assays, reporter strains, which can report even on the mode of action of antimicrobial compounds, are already available [118].

An even simpler application of droplet microfluidic cultivation is the high-throughput determination of microbial antibiotic resistances by detecting growth or growth inhibition of a target strain in presence of antibiotics [31, 51, 67, 119]. In case the target compound does not have antimicrobial activity, biosensor strains can be employed, which induce antimicrobial activity or sensitivity to the reporter strain in presence of the target compound. This has, for example, been realized for the detection of muconic acid producing strains of *P. putida*, where muconic acid induces sensitivity of a normally resistant *E. coli* reporter strain against streptomycin [120]. If the target natural product is an enzyme, a selection assay based on an enzyme activity screen with a fluorogenic substrate can be employed to select the most active microbial droplet subpopulation [42].

Increasing resolution of culture-independent sequencing-based techniques has enriched us with better understanding of the identity and role of rare microbes. Nevertheless, culture-dependent methods are still essential for the surveying of microbial functional biodiversity. With the vast majority of microbial community members in diverse environments ranging from human guts to plant rhizosphere yet unknown or considered unculturable, new strategies are needed for the isolation of uncultured species and the study of the interaction within natural microbial consortia. In addition to the high-throughput and minimal input of resources, droplet microfluidics offers exceptional advantages over conventional methods in the cultivation and analysis of unknown microbes through single-cell technology, compartmentalization, and parallelization.

Rare microbes in large sample volume are difficult to detect and isolate since they are usually present in low numbers in their natural environment and coexist with other microorganisms, which are often much faster-growing species [26]. To overcome the outcompetition by fast-growing populations, microfluidics enables the stochastic confinement of single cells in discrete droplets. Stochastic confinement refers to the separation of a sample into small volume such that the number of small volumes is greater than the total number of cells in the sample [121]. This blocks the effect of outgrowth and influence of inhibitory signals by competitors and predators therefore allowing a more accurate representation of rare taxa. Accumulation of products of metabolism and quorum sensing molecules by bacterial cells confined in small droplet volumes attain the critical threshold faster than in bulk culture so that their growth can be promoted [20]. Enhanced detection of cellular activities can also be achieved as the dilution of secreted molecules would be limited [26]. Isolation of single cells in droplets has been demonstrated to improve recovery of slow-growing environmental species [57, 122, 123]. Liu et al. employed microfluidic single-cell isolation to separate slow-growing *Paenibacillus curdlanolyticus* from the competition of fast growing *E. coli*, which would otherwise dominate in mixed bulk culture [124]. Isolation and characterization of rare populations from soil, mouse, and human gut microbiomes have been achieved by single-cell encapsulation using a microfluidic platform [56, 117]. Compared to conventional culture methods, a larger representation of rare taxa was achieved, attaining up to four-fold increase in

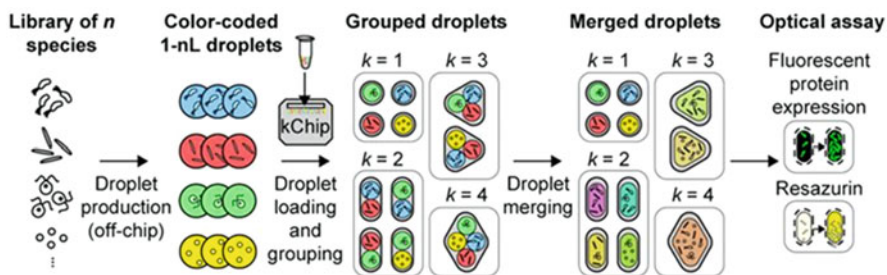


Fig. 5 Testing synthetic microbial communities in randomized combinations of different microorganisms [59]. Images are reprints of the indicated publications with permission of the original publisher

richness of microbial growth. Automated sorting based on colony density further enhanced the relative abundance of slow-growing species. A previously unknown *Blastococcus* species with high polycyclic aromatic hydrocarbons degradation efficiency was discovered in a soil community using a microfluidic streak plate method of single-cell droplets [53].

Natural microbiota or microbiomes are governed by the interactions between microbes and those with the environment. Deciphering these interactive networks can help to unravel the composition, functions, and dynamics of these complex microbial ecosystems. While most cell-cell communication and interactions are mediated by the secretion or consumption of small diffusible molecules [125], conventional laboratory bulk cultivation techniques largely overlook and severely limit the study of these interactions. Alternatively, microfluidic approaches allow miniaturized compartmentalization, which creates well-controlled environments in massively parallelized fashion to investigate interaction between microbes (Fig. 5) [55, 59, 126]. Dilution of microbial communities to multiple cells per droplet permits the co-cultivation of symbiotic microbial communities and therefore the study of partner-dependent relationships. For instance, Park et al. demonstrated a proof of concept study using a synthetic model system constructed with cross-feeding *E. coli* mutants to mimic various compositions of natural consortia [126]. Microbial Interaction Network Inference in microdroplets (MINI-Drop) was developed by Hsu et al. [55] to analyze the microbial interactions mediated by distinct molecular mechanisms in droplets containing one- to three-member consortia. Complex interplay between the presence of antibiotics and change in temperature on species interactions was also revealed in a three-member consortium. Cross-kingdom communication was shown by Jarosz et al. through co-encapsulating yeast and bacteria [127]. Carbon metabolism of yeast was transformed in the presence of bacteria which produce [GAR(+)], a protein-based epigenetic element, resulting in the mutual benefit of both organisms. KChip, a droplet-based platform that permits rapid and highly parallel screening of microbial communities, was recently introduced by Kehe et al. [59]. This platform enabled the identification of soil isolates that promoted the growth of a model plant symbiont *Herbaspirillum frisingense* and

therefore can potentially be adopted for the characterization of microbial consortia possessing functions in environmental remediation.

In a slightly different approach, micro- and nano-fabricated growth chambers provide a spatial separation of microbial cells in droplets while allowing the diffusion of growth compounds and secreted metabolites through porous chamber walls [128]. In situ and in vitro culture of unknown microbes from river water, soil, and human gut has been demonstrated with micro-compartmentalization devices, but technologies that allow the elucidation of microbial interactive networks are still lacking. The recently reported nanoporous microscale microbial incubator platform enables size-dependent control and transport of chemical factors and signaling molecules, facilitating the monitoring of growth dynamics of microbes by various stimuli [129]. Thus, the incubator is foreseeable to be useful to investigate the community interactions of uncultivated biosphere members. Challenges remain in the development of high-throughput microchamber devices for spatial isolation and cultivation of uncultured microbial species. However, overall the advancement of droplet microfluidic technologies provides a completely new and highly promising toolbox to access the metabolic potential of so far uncultured microorganisms.

5 Ultrahigh-Throughput Enzyme Activity Screening and Selection

Microbes provide a rich source for many novel enzymes, which are inherently eco-friendly, nontoxic, and adaptable for large-scale production through fermentation [130]. Hence, such enzymes are sought for various biotechnological applications. For instance, they can replace harsh chemicals in cleaning products mitigating their negative effects on the environment and increase sustainability [131]. They might even help in pressing problems, such as degradation or recycling of plastics [132, 133]. Therefore, the discovery and improvement of biological catalysts are of paramount importance. The environmental enzyme pool is fairly unlimited, and the synthetic creation of enzyme variants, e.g., through mutagenesis approaches, results in enzyme libraries of indefinite numbers of variants. However, finding the desired variants is comparable with searching for the needle in the haystack due to the huge diversity of microbes or enzyme versions in either natural or experimental samples.

State-of-the-art high-throughput screening techniques for biocatalysts are based on conventional microtiter plates (MTP) with automated liquid handling robotic platforms and approaches based on fluorescence-activated cell sorting (FACS) [40, 134]. In general, a MTP screening approach covers maximal 10^5 individual samples, with a maximum theoretical throughput of one assay event per second. Such campaigns require extensive equipment investments and exaggerated consumable consumption (mostly plastic tips and plates). On the other hand, FACS enables ultrahigh-throughput, allowing the analysis of more than 10^3 events per second, easily reaching millions per experiment or day. MTPs are not feasible to be operated

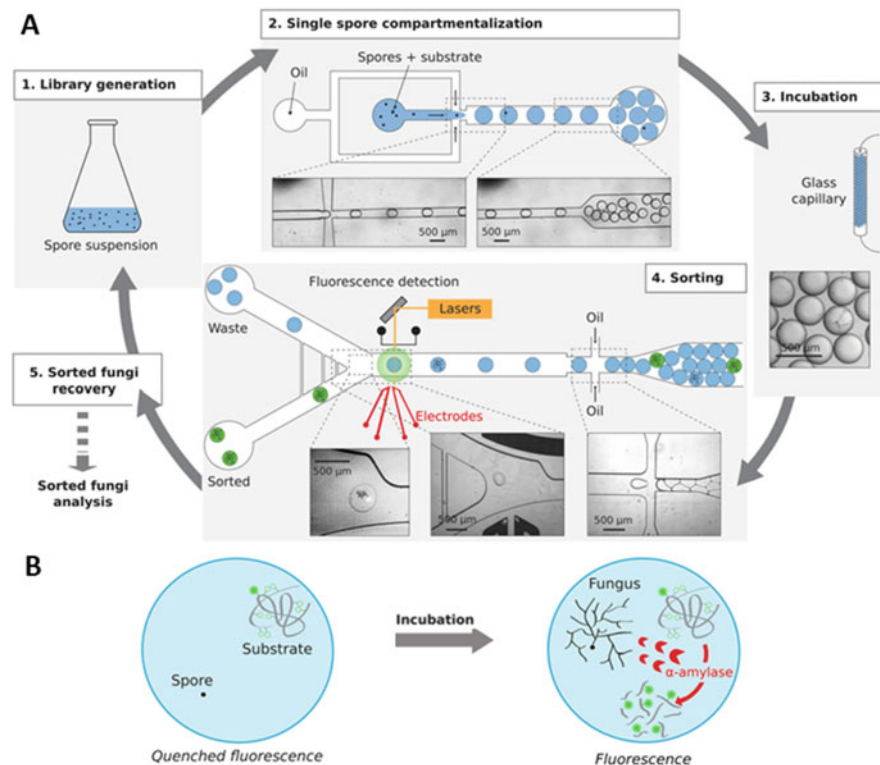


Fig. 6 Droplet-based microfluidic platform for enzyme screening. (a) Schematic showing different steps of enzyme screening. (b) Example concept for indication of enzyme activity through fluorogenic assay [105]

for single-cell analysis preventing the ability to unveil cell-to-cell heterogeneity. In contrast, with FACS, single cells can be measured and sorted, but this approach lacks compatibility with screening of secreted compounds and is therefore mostly limited to intracellular or cellular membrane-associated enzyme activity [135], which are not so relevant for industrial biotechnology. Droplet microfluidic approaches take advantage of the best properties of both technologies (Fig. 6a). They can be operated at a throughput similar to FACS, with fluorescence-activated droplet sorting (FADS) working in the range of 100–30,000 Hz [136]. Yet, encapsulation of single cells in droplets provides the genotype-phenotype linkage even for secreted molecules. The study by Obexer et al. clearly demonstrated the throughput benefit of droplets isolating a high potential variant of a combinatorial designed retroaldolase in only one round of directed evolution and FADS [137]. The catalytic efficiency of the isolate is comparable to a variant obtained from five rounds of conventional directed evolution using MTP screening. Wagner et al. compared FACS to droplet sorting by screening for better producers of riboflavin, concluding that the droplet approach is able to isolate higher titer producers [41].

Droplets do not have to contain liquid content. They can also be gelled by either agarose or alginate [37, 138]. For these gel microdroplets or for double emulsions (drop within a drop), even established FACS devices can be used. Multiple studies have used this approach [37, 138, 139]. It was successfully shown that gel microdroplets, which were embedded in a biomimetic polyelectrolyte shell, yielded an eightfold improved *Pseudomonas diminuta* producer of a phosphotriesterase after FACS screening [13]. In a similar fashion, a *Pichia pastoris* mutant library was encapsulated in gel microdroplets and screened via FACS [140]. The best performing clone showed 1.3-fold higher xylanase expression compared to the parent strain. In any case, more optimization of microfluidic processes for generating gel microdroplets is required, since currently the stability of the operation is generally more error prone. Furthermore various manipulation techniques, like picoinjection, splitting, and coalescence of droplets, which have been extensively developed for water-oil droplets, are not compatible with gel microdroplets [25, 141, 142].

Commonly, fluorescence assays are implemented for the indication of enzyme activity in droplets. This is mainly due to the available approaches for detecting and quantifying droplet contents (see previous sections). Fluorogenic substrates, with quenched fluorophore molecules, are either co-encapsulated or picoinjected into droplets. The fluorophore molecule is released in the presence of an enzyme, resulting in higher fluorescence intensity and demonstrating higher enzyme activity (Fig. 6b). For every screening task, reliable assay development is of critical importance, and fundamental differences must be taken into account. Unlike in MTP-based assays, the usage of expensive reagents does not hinder the screening campaigns because the total required amounts are in the microliter scale. It is important to understand the mechanisms of the microbial host for enzyme expression, in particular if it is either intracellularly located or secreted out of the cells. The former often requires the addition of cell lysis agents upon droplet generation or after a first round of incubation. Such additives can be either co-encapsulated or picoinjected into the droplet. Once the enzyme is released from the cell, its activity results in the release of the fluorophore molecule. Typically, the subsequent increase of fluorescence intensity is correlated to a higher enzyme activity. For example, miniaturized cell lysate assays have led to sixfold higher sulfatase activity and expression after three rounds of screening [143]. However, the addition of lysis agents holds several risks, such as affecting the enzymatic reaction, releasing interfering cell components, preventing subsequent cell growth after selection, reducing droplet stability, and increasing deviation due to inhomogeneous lysis across the droplets [144]. In contrast, the screening of secreted compounds can be performed under milder conditions. Since the cells are not getting damaged, sorted isolates can be recovered easily on agar plates or in liquid media. However, cell cultures in droplets can affect the assay both positively and negatively. On one hand, incubated cells have probably increased in numbers, and thus the effective concentration of enzyme is higher, increasing the signal intensity. However, microorganisms also produce by-products that can interfere with the assay signal or stability. Therefore, it is a common practice in MTP-based assays to include centrifugation or

washing steps. This is not possible in the microdroplet format. Nevertheless, mutant and metagenomics libraries of microorganisms have been successfully screened to find strains with higher enzyme activity. Several microbial producers including *E. coli*, *Trichoderma reesei*, and *Yarrowia lipolytica* have been screened for several enzymes like cellulases, amylases, xylanases, alkaline phosphatases, esterases, etc. [23, 42, 66, 102–106]. However, it should be noted that due to the usage of substrate analogues with fluorescence properties, the selected variants are often less active with the native substrate. To circumvent the necessity for fluorogenic model substrates, coupled enzyme assays are also applicable in droplets. Here the product of a realistic enzyme reaction functions as the substrate for another easily detectable reaction. With this concept, an oxidase mutant library has been screened in droplets by activating a horseradish peroxidase cascade resulting in a red fluorescence signal directly proportional to the target enzyme activity [145].

Overall, the strategies for the discovery and improvement of enzymatic activity and production can be divided into three fundamental steps. The first is bioprospecting for novel activities. Here, the potential of droplets is unprecedented. Ultrahigh-throughput is essential to consequently screen natural samples of extracted microbes or metagenomes, which contain millions of variants [23, 38, 42, 60]. Subsequently, enzymes are subject to a directed evolution approach in order to understand key residues in their structures [146] but also to increase the activity under general and particular operational conditions [12, 79, 143, 147, 148]. Finally, production hosts can be analyzed and optimized to achieve the highest possible production activities and yields [22, 105, 106, 108, 149, 150]. This relatively simple pipeline, when combined with a targeted industrial interest, has the potential to dramatically reduce costs and development time while achieving superior results compared to traditional screening campaigns.

6 Conclusions

Droplet microfluidic has emerged as a high potential tool for ultrahigh-throughput microbial cultivation with applications in single-cell analysis, cultivation of rare microbes, discovery of new natural products, and biocatalyst evolution. Despite the major advantages such as speed of throughput, reduction of costs, and resolution to single cells, the penetration rate of the technique into microbiology labs is still slow. This is probably based on two reasons. First, adopting microfluidic techniques is not yet straightforward. As a very multidisciplinary approach, a variety of skills and equipments is required to establish the necessary competences to handle these platforms. As for now, there is no commercially available device that offers a plug and play solution despite various ongoing efforts. Second, microfluidics provides an experimental perspective, which in many cases is counterintuitive to the well-established and validated methods in microbiology. This implies that some parameters monitored and controlled for quality under classic approaches might be sometimes irrelevant or not yet possible to monitor or control. For example, optical

density in a picoliter droplet cannot be measured, and therefore cell proliferation must be controlled with other methods. Another major difference/challenge is associated to the nature of droplet production and handling. While thousands or even millions of droplets will be produced per experiment, it is extremely cumbersome to distinguish one from the other, in contrast to what is done with labelled reaction tubes or wells. That means, predefined conditions and variables might be difficult to track on a droplet-by-droplet basis. A similar difficulty arises with single-droplet handling. While sorting operations have been developed, isolating a particular single droplet for further processing remains elusive.

Yet, most of the works reviewed here highlight both the rapid technical advancements taking place in the field and applications which clearly showcase the potential for groundbreaking research. Importantly, as more research groups and companies adopt microfluidic approaches, more creative solutions and applications arise.

References

1. Brouzes E, Medkova M, Savenelli N et al (2009) Droplet microfluidic technology for single-cell high-throughput screening. *Proc Nat Acad Sci U S A* 106(34):14195–14200
2. Macosko EZ, Basu A, Satija R et al (2015) Highly parallel genome-wide expression profiling of individual cells using nanoliter droplets. *Cell* 161(5):1202–1214
3. Klein AM, Mazutis L, Akartuna I et al (2015) Droplet barcoding for single-cell transcriptomics applied to embryonic stem cells. *Cell* 161(5):1187–1201
4. Zilionis R, Nainys J, Veres A et al (2017) Single-cell barcoding and sequencing using droplet microfluidics. *Nat Protoc* 12(1):44–73
5. Rotem A, Ram O, Shores N et al (2015) Single-cell ChIP-seq reveals cell subpopulations defined by chromatin state. *Nat Biotechnol* 33(11):1165–1172
6. Zheng GXY, Lau BT, Schnall-Levin M et al (2016) Haplotyping germline and cancer genomes with high-throughput linked-read sequencing. *Nat Biotechnol* 34(3):303–311
7. Borgstrom E, Redin D, Lundin S et al (2015) Phasing of single DNA molecules by massively parallel barcoding. *Nat Commun* 6:7173
8. Lan F, Demaree B, Ahmed N et al (2017) Single-cell genome sequencing at ultra-high-throughput with microfluidic droplet barcoding. *Nat Biotechnol* 35(7):640–646
9. El Debs B, Utharala R, Balyasnikova IV et al (2012) Functional single-cell hybridoma screening using droplet-based microfluidics. *Proc Nat Acad Sci U S A* 109(29):11570–11575
10. Mazutis L, Gilbert J, Ung WL et al (2013) Single-cell analysis and sorting using droplet-based microfluidics. *Nat Protoc* 8(5):870–891
11. Eyer K, Doineau RCL, Castrillon CE et al (2017) Single-cell deep phenotyping of IgG-secreting cells for high-resolution immune monitoring. *Nat Biotechnol* 35(10):977–982
12. Agresti JJ, Antipov E, Abate AR et al (2010) Ultrahigh-throughput screening in drop-based microfluidics for directed evolution. *Proc Nat Acad Sci U S A* 107(9):4004–4009
13. Fischlechner M, Schaeerli Y, Mohamed MF et al (2014) Evolution of enzyme catalysts caged in biomimetic gel-shell beads. *Nat Chem* 6(9):791–796
14. Obexer R, Godina A, Garrabou X et al (2017) Emergence of a catalytic tetrad during evolution of a highly active artificial aldolase. *Nat Chem* 9(1):50–56
15. Larsen AC, Dunn MR, Hatch A et al (2016) A general strategy for expanding polymerase function by droplet microfluidics. *Nat Commun* 7:11235
16. Bachmann H, Fischlechner M, Rabbers I et al (2013) Availability of public goods shapes the evolution of competing metabolic strategies. *Proc Nat Acad Sci U S A* 110(35):14302–14307

17. Ma L, Kim J, Hatzenpichler R et al (2014) Gene-targeted microfluidic cultivation validated by isolation of a gut bacterium listed in human microbiome project's most wanted taxa. *Proc Nat Acad Sci U S A* 111(27):9768–9773
18. Stewart EJ (2012) Growing unculturable bacteria. *J Bacteriol* 194(16):4151–4160
19. Traxler MF, Kolter R (2015) Natural products in soil microbe interactions and evolution. *Nat Prod Rep* 32(7):956–970
20. Boedicker JQ, Vincent ME, Ismagilov RF (2009) Microfluidic confinement of single cells of bacteria in small volumes initiates high-density behavior of quorum sensing and growth and reveals its variability. *Angew Chem Int Ed Engl* 48(32):5908–5911
21. Epstein SS (2013) The phenomenon of microbial uncultivability. *Curr Opin Microbiol* 16(5):636–642
22. Huang MT, Bai YP, Sjoström SL et al (2015) Microfluidic screening and whole-genome sequencing identifies mutations associated with improved protein secretion by yeast. *Proc Nat Acad Sci U S A* 112(34):E4689–E4696
23. Colin PY, Kintses B, Gielen F et al (2015) Ultrahigh-throughput discovery of promiscuous enzymes by picodroplet functional metagenomics. *Nat Commun* 6:10008
24. Lee SY, Kim HU (2015) Systems strategies for developing industrial microbial strains. *Nat Biotechnol* 33(10):1061–1072
25. Kaminski TS, Scheler O, Garstecki P (2016) Droplet microfluidics for microbiology: techniques, applications and challenges. *Lab Chip* 16(12):2168–2187
26. Vincent ME, Liu W, Haney EB et al (2010) Microfluidic stochastic confinement enhances analysis of rare cells by isolating cells and creating high density environments for control of diffusible signals. *Chem Soc Rev* 39(3):974–984
27. Shi W, Qin J, Ye N et al (2008) Droplet-based microfluidic system for individual *Caenorhabditis elegans* assay. *Lab Chip* 8(9):1432–1435
28. Schmitz CH, Rowat AC, Köster S et al (2009) Drops: a picoliter array in a microfluidic device. *Lab Chip* 9(1):44–49
29. Huebner A, Bratton D, Whyte G et al (2009) Static microdroplet arrays: a microfluidic device for droplet trapping, incubation and release for enzymatic and cell-based assays. *Lab Chip* 9(5):692–698
30. Bjork SM, Sjoström SL, Andersson-Svahn H et al (2015) Metabolite profiling of microfluidic cell culture conditions for droplet based screening. *Biomicrofluidics* 9(4):044128
31. Svensson CM, Shvydkiv O, Dietrich S et al (2019) Coding of experimental conditions in microfluidic droplet assays using colored beads and machine learning supported image analysis. *Small* 15(4):1–14
32. Mahler L, Tovar M, Weber T et al (2015) Enhanced and homogeneous oxygen availability during incubation of microfluidic droplets. *RSC Adv* 5(123):101871–101878
33. Tovar M, Mahler L, Buchheim S et al (2020) Monitoring and external control of pH in microfluidic droplets during microbial culturing. *Microb Cell Fact* 19(1):16
34. Joansson HN, Andersson Svahn H (2012) Droplet microfluidics – a tool for single-cell analysis. *Angew Chem Int Ed* 51(49):12176–12192
35. Rakszewska A, Tel J, Chokkalingam V et al (2014) One drop at a time: toward droplet microfluidics as a versatile tool for single-cell analysis. *NPG Asia Mater* 6(10):e133–e133
36. Lareau CA, Duarte FM, Chew JG et al (2019) Droplet-based combinatorial indexing for massive-scale single-cell chromatin accessibility. *Nat Biotechnol* 37(8):916–924
37. Li M, van Zee M, Riche CT et al (2018) A gelatin microdroplet platform for high-throughput sorting of hyperproducing single-cell-derived microalgal clones. *Small* 14(44):1–9
38. Terekhov SS, Smirnov IV, Stepanova AV et al (2017) Microfluidic droplet platform for ultrahigh-throughput single-cell screening of biodiversity. *Proc Nat Acad Sci U S A* 114(10):2550–2555
39. Wang BL, Ghaderi A, Zhou H et al (2014) Microfluidic high-throughput culturing of single cells for selection based on extracellular metabolite production or consumption. *Nat Biotechnol* 32(5):473–478

40. Bowman EK, Alper HS (2019) Microdroplet-assisted screening of biomolecule production for metabolic engineering applications. *Trends Biotechnol* 38(7):701–714
41. Wagner JM, Liu L, Yuan SF et al (2018) A comparative analysis of single cell and droplet-based FACS for improving production phenotypes: riboflavin overproduction in *Yarrowia lipolytica*. *Metab Eng* 47:346–356
42. Najah M, Calbrix R, Mahendra-Wijaya IP et al (2014) Droplet-based microfluidics platform for ultra-high-throughput bioprospecting of cellulolytic microorganisms. *Chem Biol* 21(12):1722–1732
43. Kim HS, Hsu S-C, Han S-I et al (2017) High-throughput droplet microfluidics screening platform for selecting fast-growing and high lipid-producing microalgae from a mutant library. *Plant Direct* 1(3):e00011
44. Hammar P, Angermayr SA, Sjoström SL et al (2015) Single-cell screening of photosynthetic growth and lactate production by cyanobacteria. *Biotechnol Biofuels* 8(1):193
45. Godina A (2013) In vivo and in vitro direct evolution of enzymes using droplet-based microfluidics. In: *Chemical sciences*. University of Strasbourg, Strasbourg
46. Thibault D, Jensen PA, Wood S et al (2019) Droplet Tn-Seq combines microfluidics with Tn-Seq for identifying complex single-cell phenotypes. *Nat Commun* 10(1):5729
47. Cottinet D, Condamine F, Bremond N et al (2016) Lineage tracking for probing heritable phenotypes at single-cell resolution. *PLoS One* 11(4):e0152395
48. Boitard L, Cottinet D, Kleinschmitt C et al (2012) Monitoring single-cell bioenergetics via the coarsening of emulsion droplets. *Proc Nat Acad Sci U S A* 109(19):7181–7186
49. Scheler O, Makuch K, Debski PR et al (2020) Droplet-based digital antibiotic susceptibility screen reveals single-cell clonal heteroresistance in an isogenic bacterial population. *Sci Rep* 10:3282
50. Postek W, Gargulinski P, Scheler O et al (2018) Microfluidic screening of antibiotic susceptibility at a single-cell level shows the inoculum effect of cefotaxime on *E. coli*. *Lab Chip* 18(23):3668–3677
51. Liu X, Painter RE, Enesa K et al (2016) High-throughput screening of antibiotic-resistant bacteria in picodroplets. *Lab Chip* 16(9):1636–1643
52. Dong L, Chen D-W, Liu S-J et al (2016) Automated chemotactic sorting and single-cell cultivation of microbes using droplet microfluidics. *Sci Rep* 6(1):24192
53. Jiang C-Y, Dong L, Zhao J-K et al (2016) High-throughput single-cell cultivation on microfluidic streak plates. *Appl Environ Microbiol* 82(7):2210–2218
54. Zhang Q, Wang T, Zhou Q et al (2017) Development of a facile droplet-based single-cell isolation platform for cultivation and genomic analysis in microorganisms. *Sci Rep* 7(1):41192
55. Hsu RH, Clark RL, Tan JW et al (2019) Microbial interaction network inference in microfluidic droplets. *Cell Systems* 9(3):229–242.e4
56. Watterson WJ, Tanyeri M, Watson AR et al (2019) High-throughput isolation and sorting of gut microbes reduce biases of traditional cultivation strategies. [bioRxiv:759969](https://doi.org/10.1101/759969)
57. Ota Y, Saito K, Takagi T et al (2019) Fluorescent nucleic acid probe in droplets for bacterial sorting (FNAP-sort) as a high-throughput screening method for environmental bacteria with various growth rates. *PLoS One* 14(4):e0214533
58. Ohan J, Pelle B, Nath P et al (2019) High-throughput phenotyping of cell-to-cell interactions in gel microdroplet pico-cultures. *Biotechniques* 66(5):218–224
59. Kehe J, Kulesa A, Ortiz A et al (2019) Massively parallel screening of synthetic microbial communities. *Proc Nat Acad Sci U S A* 116(26):12804–12809
60. Terekhov SS, Smirnov IV, Malakhova MV et al (2018) Ultrahigh-throughput functional profiling of microbiota communities. *Proc Nat Acad Sci U S A* 115(38):9551–9556
61. Egli T (2015) Microbial growth and physiology: a call for better craftsmanship. *Front Microbiol*:6(287)
62. Yang H, Gijss MAM (2018) Micro-optics for microfluidic analytical applications. *Chem Soc Rev* 47(4):1391–1458

63. Tung Y-C, Huang N-T, Oh B-R et al (2012) Optofluidic detection for cellular phenotyping. *Lab Chip* 12(19):3552–3565
64. Zhu Y, Fang Q (2013) Analytical detection techniques for droplet microfluidics—a review. *Anal Chim Acta* 787:24–35
65. J-R C, Song H, Sung JH et al (2016) Microfluidic assay-based optical measurement techniques for cell analysis: a review of recent progress. *Biosens Bioelectron* 77:227–236
66. Qiao Y, Zhao X, Zhu J et al (2018) Fluorescence-activated droplet sorting of lipolytic microorganisms using a compact optical system. *Lab Chip* 18(1):190–196
67. Kaushik AM, Hsieh K, Chen L et al (2017) Accelerating bacterial growth detection and antimicrobial susceptibility assessment in integrated picoliter droplet platform. *Biosens Bioelectron* 97:260–266
68. Scheler O, Kaminski TS, Ruszczak A et al (2016) Dodecylresorufin (C12R) outperforms resorufin in microdroplet bacterial assays. *ACS Appl Mater Interfaces* 8(18):11318–11325
69. Abalde-Cela S, Gould A, Liu X et al (2015) High-throughput detection of ethanol-producing cyanobacteria in a microdroplet platform. *J R Soc Interface* 12(106):20150216
70. Kang DK, Gong X, Cho S et al (2015) 3D droplet microfluidic systems for high-throughput biological experimentation. *Anal Chem* 87(21):10770–10778
71. Scanlon TC, Dostal SM, Griswold KE (2014) A high-throughput screen for antibiotic drug discovery. *Biotechnol Bioeng* 111(2):232–243
72. Martin K, Henkel T, Baier V et al (2003) Generation of larger numbers of separated microbial populations by cultivation in segmented-flow microdevices. *Lab Chip* 3(3):202–207
73. Jusková P, Schmid YRF, Stucki A et al (2019) “Basicles”: microbial growth and production monitoring in giant lipid vesicles. *ACS Appl Mater Interfaces* 11(38):34698–34706
74. Huang S, Srimani JK, Lee AJ et al (2015) Dynamic control and quantification of bacterial population dynamics in droplets. *Biomaterials* 61:239–245
75. Baraban L, Bertholle F, Salverda MLM et al (2011) Millifluidic droplet analyser for microbiology. *Lab Chip* 11(23):4057–4057
76. Mahler L, Wink K, Beulig RJ et al (2018) Detection of antibiotics synthesized in microfluidic picolitre-droplets by various actinobacteria. *Sci Rep* 8(1):1–11
77. Burmeister A, Hilgers F, Langner A et al (2019) A microfluidic co-cultivation platform to investigate microbial interactions at defined microenvironments. *Lab Chip* 19(1):98–110
78. Tovar M, Hengoju S, Weber T et al (2019) One sensor for multiple colors: fluorescence analysis of microdroplets in microbiological screenings by frequency-division multiplexing. *Anal Chem* 91(4):3055–3061
79. Gielen F, Hours R, Emond S et al (2016) Ultrahigh-throughput—directed enzyme evolution by absorbance-activated droplet sorting (AADS). *Proc Nat Acad Sci U S A* 113(47):E7383–E7389
80. Churski K, Ruszczak A, Jakiela S et al (2015) Droplet microfluidic technique for the study of fermentation. *Micromachines (Basel)* 6(10):1514–1525
81. Siltanen CA, Cole RH, Poust S et al (2018) An oil-free picodrop bioassay platform for synthetic biology. *Sci Rep* 8(1):7913–7913
82. Oscar S-V, Fernando O-CL, del Pilar C-MM (2017) Total polyphenols content in white wines on a microfluidic flow injection analyzer with embedded optical fibers. *Food Chem* 221:1062–1068
83. Ottevaere H, Van Overmeire S, Albero J et al (2015) Plastic light coupler for absorbance detection in silicon microfluidic channels. *Microfluid Nanofluidics* 18(4):559–568
84. Deal KS, Easley CJ (2012) Self-regulated, droplet-based sample chopper for microfluidic absorbance detection. *Anal Chem* 84(3):1510–1516
85. Yang T, Stavrakis S, de Mello A (2017) A high-sensitivity, integrated absorbance and fluorescence detection scheme for probing picoliter-volume droplets in segmented flows. *Anal Chem* 89(23):12880–12887
86. Yu JQ, Huang W, Chin LK et al (2014) Droplet optofluidic imaging for λ -bacteriophage detection via co-culture with host cell *Escherichia coli*. *Lab Chip* 14:3519–3524

87. Zang E, Brandes S, Tovar M et al (2013) Real-time image processing for label-free enrichment of actinobacteria cultivated in picolitre droplets. *Lab Chip* 13(18):3707–3713
88. Girault M, Kim H, Arakawa H et al (2017) An on-chip imaging droplet-sorting system: a real-time shape recognition method to screen target cells in droplets with single cell resolution. *Sci Rep* 7:40072–40072
89. Golberg A, Linshiz G, Kravets I et al (2014) Cloud-enabled microscopy and droplet microfluidic platform for specific detection of *Escherichia coli* in water. *PLoS One* 9(1):4–12
90. Anagnostidis V, Sherlock B, Metz J et al (2020) Deep learning guided image-based droplet sorting for on-demand selection and analysis of single cells and 3D cell cultures. *Lab Chip* 20(5):889–900
91. Psaltis D, Quake SR, Yang C (2006) Developing optofluidic technology through the fusion of microfluidics and optics. *Nature* 442(7101):381–386
92. Song C, Nguyen N-T, Tan SH (2017) Toward the commercialization of optofluidics. *Microfluidics Nanofluidics* 21(8):139
93. Hengoju S, Wohlfeil S, Munser AS et al (2020) Optofluidic detection setup for multi-parametric analysis of microbiological samples in droplets. *Biomicrofluidics* 14(2):024109
94. Cahill BP, Land R, Nacke T et al (2011) Contactless sensing of the conductivity of aqueous droplets in segmented flow. *Sens Actuators B* 159(1):286–293
95. Moiseeva EV, Fletcher AA, Harnett CK (2011) Thin-film electrode based droplet detection for microfluidic systems. *Sens Actuators B* 155(1):408–414
96. Fan W, Chen X, Ge Y et al (2019) Single-cell impedance analysis of osteogenic differentiation by droplet-based microfluidics. *Biosens Bioelectron* 145:111730–111730
97. Duarte LC, Figueredo F, Ribeiro LEB et al (2019) Label-free counting of *Escherichia coli* cells in nanoliter droplets using 3D printed microfluidic devices with integrated contactless conductivity detection. *Anal Chim Acta* 1071:36–43
98. Küster SK, Fagerer SR, Verboket PE et al (2013) Interfacing droplet microfluidics with matrix-assisted laser desorption/ionization mass spectrometry: label-free content analysis of single droplets. *Anal Chem* 85(3):1285–1289
99. Gasilova N, Yu QL, Qiao L et al (2014) On-chip spyhole mass spectrometry for droplet-based microfluidics. *Angew Chem Int Ed Engl* 53(17):4408–4412
100. Wink K, Mahler L, Beulig JR et al (2018) An integrated chip-mass spectrometry and epifluorescence approach for online monitoring of bioactive metabolites from incubated Actinobacteria in picoliter droplets. *Anal Bioanal Chem* 410(29):7679–7687
101. Holland-Moritz DA, Wismer M, Mann B et al (2020) Mass activated droplet sorting (MADS) enables high throughput screening of enzymatic reactions at nanoliter scale. *Angew Chem Int Ed* 59(11):4470–4477
102. Girault M, Beneyton T, Pekin D et al (2018) High-content screening of plankton alkaline phosphatase activity in microfluidics. *Anal Chem* 90(6):4174–4181
103. Huebner A, Olguin LF, Bratton D et al (2008) Development of quantitative cell-based enzyme assays in microdroplets. *Anal Chem* 80(10):3890–3896
104. He R, Ding R, Heyman JA et al (2019) Ultra-high-throughput picoliter-droplet microfluidics screening of the industrial cellulase-producing filamentous fungus *Trichoderma reesei*. *J Ind Microbiol Biotechnol* 46(11):1603–1610
105. Beneyton T, Wijaya IPM, Postros P et al (2016) High-throughput screening of filamentous fungi using nanoliter-range droplet-based microfluidics. *Sci Rep* 6(1):27223–27223
106. Beneyton T, Thomas S, Griffiths AD et al (2017) Droplet-based microfluidic high-throughput screening of heterologous enzymes secreted by the yeast *Yarrowia lipolytica*. *Microb Cell Fact* 16(1):18
107. Beneyton T, Coldren F, Baret J-C et al (2014) CotA laccase: high-throughput manipulation and analysis of recombinant enzyme libraries expressed in *E. coli* using droplet-based microfluidics. *Analyst* 139:3314–3323

108. Meyer A, Pellaux R, Potot S et al (2015) Optimization of a whole-cell biocatalyst by employing genetically encoded product sensors inside nanolitre reactors. *Nat Chem* 7 (8):673–678
109. Sklodowska K, Debski PR, Michalski JA et al (2018) Simultaneous measurement of viscosity and optical density of bacterial growth and death in a microdroplet. *Micromachines (Basel)* 9 (5):251
110. Walter A, März A, Schumacher W et al (2011) Towards a fast, high specific and reliable discrimination of bacteria on strain level by means of SERS in a microfluidic device. *Lab Chip* 11(6):1013–1021
111. Ziemert N, Alanjary M, Weber T (2016) The evolution of genome mining in microbes – a review. *Nat Prod Rep* 33(8):988–1005
112. Bergmann S, Schümann J, Scherlach K et al (2007) Genomics-driven discovery of PKS-NRPS hybrid metabolites from *Aspergillus nidulans*. *Nat Chem Biol* 3(4):213–217
113. Hertweck C (2009) Hidden biosynthetic treasures brought to light. *Nat Chem Biol* 5 (7):450–452
114. Petersen L-E, Kellermann MY, Schupp PJ (2020) Secondary metabolites of marine microbes: from natural products chemistry to chemical ecology. In: Jungblut S, Liebich V, Bode-Dalby M (eds) *YOUMARES 9 – the oceans: our research, our future: proceedings of the 2018 conference for YOUnG MARine RESEARCHer in Oldenburg, Germany*. Springer, Cham, pp 159–180
115. Milshteyn A, Colosimo DA, Brady SF (2018) Accessing bioactive natural products from the human microbiome. *Cell Host Microbe* 23(6):725–736
116. Villa MM, Bloom RJ, Silverman JD et al (2019) High-throughput isolation and culture of human gut bacteria with droplet microfluidics. *bioRxiv*:630822
117. Mahler L, Niehs S, Martin K et al (2019) Highly parallelized microfluidic droplet cultivation and prioritization on antibiotic producers from complex natural microbial communities. *bioRxiv*. <https://doi.org/10.1101/2019.12.18.877530>
118. Hutter B, Fischer C, Jacobi A et al (2004) Panel of *Bacillus subtilis* reporter strains indicative of various modes of action. *Antimicrob Agents Chemother* 48(7):2588–2594
119. Kang W, Sarkar S, Lin ZS et al (2019) Ultrafast parallelized microfluidic platform for antimicrobial susceptibility testing of gram positive and negative bacteria. *Anal Chem* 91 (9):6242–6249
120. Millet LJ, Velez JM, Michener JK (2018) Genetic selection for small molecule production in competitive microfluidic droplets. *bioRxiv*:469007
121. Boedicker JQ, Li L, Kline TR et al (2008) Detecting bacteria and determining their susceptibility to antibiotics by stochastic confinement in nanoliter droplets using plug-based microfluidics. *Lab Chip* 8(8):1265–1272
122. Ma L, Datta SS, Karymov MA et al (2014) Individually addressable arrays of replica microbial cultures enabled by splitting SlipChips. *Integr Biol (Camb)* 6(8):796–805
123. Hu B, Xu B, Yun J et al (2020) High-throughput single-cell cultivation reveals the underexplored rare biosphere in deep-sea sediments along the Southwest Indian Ridge. *Lab Chip* 20(2):363–372
124. Liu W, Kim HJ, Lucchetta EM et al (2009) Isolation, incubation, and parallel functional testing and identification by FISH of rare microbial single-copy cells from multi-species mixtures using the combination of chemistat and stochastic confinement. *Lab Chip* 9(15):2153–2162
125. Lauffenburger D, Linderman J (1993) *Receptors: models for binding, trafficking, and signaling*. Oxford University Press, Oxford
126. Park J, Kerner A, Burns MA et al (2011) Microdroplet-enabled highly parallel co-cultivation of microbial communities. *PLoS One* 6(2):e17019
127. Jarosz DF, Brown JCS, Walker GA et al (2014) Cross-kingdom chemical communication drives a heritable, mutually beneficial prion-based transformation of metabolism. *Cell* 158 (5):1083–1093

128. Huys GR, Raes J (2018) Go with the flow or solitary confinement: a look inside the single-cell toolbox for isolation of rare and uncultured microbes. *Curr Opin Microbiol* 44:1–8
129. Ge Z, Girguis PR, Buie CR (2016) Nanoporous microscale microbial incubators. *Lab Chip* 16(3):480–488
130. Devi R, Madhavan Nampoothiri K, Sukumaran RK et al (2020) Lipase of *Pseudomonas guariconesis* as an additive in laundry detergents and transesterification biocatalysts. *J Basic Microbiol* 60(2):112–125
131. Porter JL, Rusli RA, Ollis DL (2016) Directed evolution of enzymes for industrial biocatalysis. *ChemBioChem* 17(3):197–203
132. Austin HP, Allen MD, Donohoe BS et al (2018) Characterization and engineering of a plastic-degrading aromatic polyesterase. *Proc Nat Acad Sci U S A* 115(19):E4350
133. Yang Y, Yang J, Wu W-M et al (2015) Biodegradation and mineralization of polystyrene by plastic-eating mealworms: part 1. Chemical and physical characterization and isotopic tests. *Environ Sci Technol* 49(20):12080–12086
134. Autour A, Ryckelynck M (2017) Ultrahigh-throughput improvement and discovery of enzymes using droplet-based microfluidic screening. *Micromachines (Basel)* 8(4):128
135. Guo MT, Rotem A, Heyman JA et al (2012) Droplet microfluidics for high-throughput biological assays. *Lab Chip* 12(12):2146–2155
136. Schutz SS, Beneyton T, Baret JC et al (2019) Rational design of a high-throughput droplet sorter. *Lab Chip* 19(13):2220–2232
137. Obexer R, Pott M, Zeymer C et al (2016) Efficient laboratory evolution of computationally designed enzymes with low starting activities using fluorescence-activated droplet sorting. *Protein Eng Des Sel* 29(9):355–366
138. Hâti AG, Bassett DC, Ribe JM et al (2016) Versatile, cell and chip friendly method to gel alginate in microfluidic devices. *Lab Chip* 16(19):3718–3727
139. Schærli Y (2018) Bacterial microcolonies in gel beads for high-throughput screening. *Bio Protoc* 8(13):e2911
140. Ma C, Tan ZL, Lin Y et al (2019) Gel microdroplet-based high-throughput screening for directed evolution of xylanase-producing *Pichia pastoris*. *J Biosci Bioeng* 128(6):662–668
141. Shang L, Cheng Y, Zhao Y (2017) Emerging droplet microfluidics. *Chem Rev* 117(12):7964–8040
142. Theberge AB, Courtois F, Schærli Y et al (2010) Microdroplets in microfluidics: an evolving platform for discoveries in chemistry and biology. *Angew Chem Int Ed* 49(34):5846–5868
143. Kintses B, Hein C, Mohamed MF et al (2012) Picoliter cell lysate assays in microfluidic droplet compartments for directed enzyme evolution. *Chem Biol* 19(8):1001–1009
144. Karamitros CS, Morvan M, Vigne A et al (2020) Bacterial expression systems for enzymatic activity in droplet-based microfluidics. *Anal Chem* 92(7):4908–4916
145. Debon A, Pott M, Obexer R et al (2019) Ultrahigh-throughput screening enables efficient single-round oxidase remodelling. *Nat Cat* 2(9):740–747
146. Romero PA, Tran TM, Abate AR (2015) Dissecting enzyme function with microfluidic-based deep mutational scanning. *Proc Nat Acad Sci U S A* 112(23):7159–7164
147. Gielen F, Colin P-Y, Mair P et al (2018) Ultrahigh-throughput screening of single-cell lysates for directed evolution and functional metagenomics. In: Bornscheuer U, Höhne M (eds) *Protein engineering – methods and protocols*. Humana Press, Totowa
148. Ma F, Chung MT, Yao Y et al (2018) Efficient molecular evolution to generate enantioselective enzymes using a dual-channel microfluidic droplet screening platform. *Nat Commun* 9(1):1030
149. Fujitani H, Tsuda S, Ishii T et al (2019) High-throughput screening of high protein producer budding yeast using gel microdrop technology. *bioRxiv*:830596
150. Wang G, Björk SM, Huang M et al (2019) RNAi expression tuning, microfluidic screening, and genome recombineering for improved protein production in *Saccharomyces cerevisiae*. *Proc Nat Acad Sci U S A* 116(19):9324–9332

Microfluidic Single-Cell Analytics



Christian Dusny

Contents

1	Introduction	160
2	Growth Analysis of Single Cells	162
2.1	Cell Counting, Morphometrics, and Segmentation	163
2.2	Mass Imaging	167
2.3	Picobalances	168
3	Substrate Uptake	168
3.1	Fluorescence Analysis	170
3.2	Mass Spectrometry	171
3.3	Inferring Kinetic Constants of Substrate Uptake	172
4	Product Formation	172
4.1	Fluorescence Analysis	172
4.2	Mass Spectrometry	175
5	Gene Expression, Protein Synthesis, and Regulation	176
6	Analytical Pitfalls in Microfluidic Single-Cell Analysis	179
7	Conclusion	180
	References	180

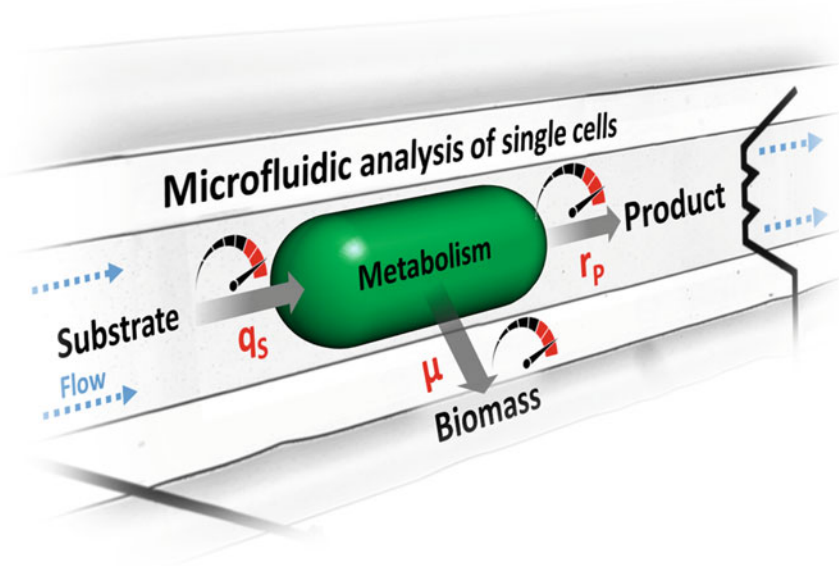
Abstract What is the impact of cellular heterogeneity on process performance? How do individual cells contribute to averaged process productivity? Single-cell analysis is a key technology for answering such key questions of biotechnology, beyond bulky measurements with populations. The analysis of cellular individuality, its origins, and the dependency of process performance on cellular heterogeneity has tremendous potential for optimizing biotechnological processes in terms of metabolic, reaction, and process engineering. Microfluidics offer unmatched environmental control of the cellular environment and allow massively parallelized cultivation of single cells. However, the analytical accessibility to a cell's physiology is of crucial importance for obtaining the desired information on the single-cell

C. Dusny (✉)

Department of Solar Materials, Microbial Single Cell Analysis, Helmholtz-Centre for Environmental Research – UFZ Leipzig, Leipzig, Germany
e-mail: christian.dusny@ufz.de

production phenotype. Highly sensitive analytics are required to detect and quantify the minute amounts of target analytes and small physiological changes in a single cell. For their application to biotechnological questions, single-cell analytics must evolve toward the measurement of kinetics and specific rates of the smallest catalytic unit, the single cell. In this chapter, we focus on an introduction to the latest single-cell analytics and their application for obtaining physiological parameters in a biotechnological context from single cells. We present and discuss recent advancements in single-cell analytics that enable the analysis of cell-specific growth, uptake, and production kinetics, as well as the gene expression and regulatory mechanisms at a single-cell level.

Graphical Abstract

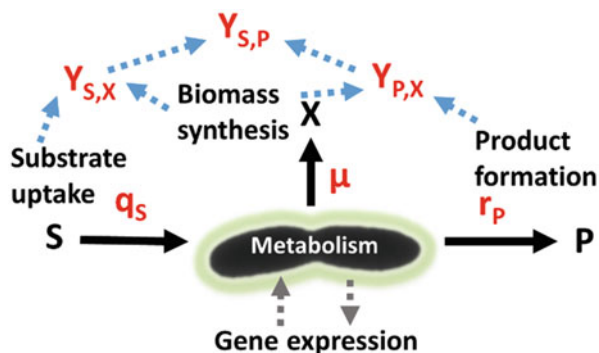


Keywords Analytics, Biochemical engineering, Microfluidics, Single-cell analysis, Whole-cell biocatalysis

1 Introduction

Cells are used as living catalysts for the efficient production of chemicals and energy carriers [1, 2]. In whole-cell biocatalysis, the efficiency of the catalytic conversion of a substrate to the desired product is a result of cell physiology [3, 4]. At the population level, the performance of microbial biocatalysts is typically determined by analyzing kinetic parameters in physiological key experiments, where substrate

Fig. 1 Quantitative physiology and performance characterization of whole-cell biocatalysts in biotechnology based on cell kinetics and yield coefficients



uptake and production rates are used to quantify cell physiology in terms of growth rate, production, gene expression, and regulation (see Fig. 1) [5, 6].

With advanced analytical concepts, such as transcriptome and proteome profiling, as well as metabolic flux analysis, these links can be further refined to obtain a global picture of biocatalyst physiology and to establish a systems-level understanding of the functioning of living cells that serve as catalytic units [7–9]. This holistic approach for the analytical dissection of producer cell physiology is often termed systems biotechnology. This systems-level approach relies, however, on averaged data from populations and does not consider the individual cell dynamics and heterogeneities due to the lack of true quantitative data on the physiology of single cells [10]. It is therefore of utmost interest to make use of the latest analytical concepts to bring single-cell analysis to the next level for realizing single-cell-based system biotechnology.

The current situation underlines the increasing discrepancy between the rapid evolution of microfluidic cultivation and the lack of analytical concepts for microfluidics and single cells [11]. However, this is not without reason – single-cell analysis poses tremendous analytical challenges in terms of dimension, analyte amounts, and resulting concentrations. These challenges can be exemplified with the corresponding numbers in terms of cell size, volume, and single-cell specific uptake rates and productivities, as well as product and biomass yield coefficients of microbial biocatalysts (see Fig. 2).

As can be deduced from these key figures, the analytical and conceptual challenges for quantitatively analyzing these biotechnologically relevant parameters at a single-cell level are tremendous [10, 13, 19]. This is why microscopic technologies, such as time-lapse microscopy in combination fluorescent markers or biosensors, are still the analytical tool of choice for obtaining quantitative and time-resolved data of single cells. Optical analytics and imaging technologies are relatively simple to use and can be sensitive down to the single-molecule level with technologies such as super-resolution microscopy [20, 21]. Even with standard microscopy equipment, smaller cell types, such as coccoid bacteria, can be easily visualized. Cell dynamics and heterogeneities in terms of growth, morphology, gene expression, or regulation can be assessed via fluorescence time-lapse microscopy imaging [22–25]. However,




Cell	Diameter	Volume	Wet weight	Dry weight	μ_{\max}	q_s	r_p
 <i>Escherichia coli</i>	2.5 x 0.8 μm	1-2 fl	0.6-1 pg	0.2-0.3 pg	0.1-0.77 h^{-1}	1-10 $\text{fmol cell}^{-1} \text{h}^{-1}$	0.1-5 $\text{fmol cell}^{-1} \text{h}^{-1}$
 <i>Synechocystis</i> sp. PCC6803	2-3 μm	5-15 fl	12-15 pg	4-5 pg	0.01-0.13 h^{-1}	150 $\text{fmol CO}_2 \text{ cell}^{-1} \text{h}^{-1}$	0.01-0.3 $\text{fmol cell}^{-1} \text{h}^{-1}$
 <i>Saccharomyces cerevisiae</i>	3-6 μm	20-100 fl	80-100 pg	25-35 pg	0.05-0.45 h^{-1}	1-10 $\text{fmol cell}^{-1} \text{h}^{-1}$	0.01-0.3 $\text{fmol cell}^{-1} \text{h}^{-1}$

Fig. 2 Key numbers for analyzing the physiology of whole-cell biocatalysts at the single-cell level. The numbers are given for cell diameter, cell volume, cell wet weight, cell dry weight, specific growth rates μ , specific substrate uptake rate q_s , and product formation rates r_p of *Escherichia coli*, *Synechocystis* sp. PCC6803, and *Saccharomyces cerevisiae* [12–18]

obtaining truly quantitative data with absolute numbers is still difficult via imaging. Even simple global physiological parameters, such as specific growth rates and biomass, cannot be easily deduced from microscopy, although growth is one the key parameters when it comes to the characterization of cells in technical processes [26–29]. Yet, data on growth kinetics and biomass formation provide the basis for the holistic description of whole-cell biocatalysts at a single-cell level. This lack of analytical concepts for assessing producer cells at the microscale is the reason why microfluidic single-cell analysis is given little consideration in biotechnology [11]. Rendering microfluidic analysis more meaningful for biotechnology hence starts with making growth kinetics available at the single-cell level. In the following section, we describe fundamental technologies beyond visualization that enable us to quantitatively assess growth and biomass with high accuracy of single microbes in microfluidic bioreactors.

2 Growth Analysis of Single Cells

Cell growth is a pivotal descriptor for global cell physiology. The kinetics of biomass formation, the specific growth rate μ , provides information about cellular fitness and the functional state of the cell. Many cellular parameters, such as plasmid copy number, mRNA and ribosome abundance, protein synthesis, and hence cell productivity, are tightly linked to the specific growth rate of a cell [30–32]. In steady-state growth, the environmental influences are directly manifested in the growth rate itself and directly reflect the impact of extracellular conditions on the cellular machinery and its efficiency for performing catalytic conversions [33]. The power of single-cell growth analysis for answering questions of biotechnological relevance has been demonstrated in countless studies. These studies investigated fundamental characteristics of microbial growth that are indispensable for optimizing cell performance and efficiency in a technical context. The topics investigated encompass compensation auxotrophy in mixed-species microcultures [34], cell aging in yeast

[35] and bacteria [36], linking growth rate and extracellular environment [37], linking growth kinetics and gene expression [38] growth dynamics upon nutrient shifts [39], and the impact of spatial confinement in cell growth [40]. In nature, heterogeneity in growth across an isogenic population is a simple but most effective measure to cope with environmental changes or threatening conditions such as the presence of antibiotics [41–46]. Determining specific growth rates of single cells, its dynamics, and heterogeneities is hence of utmost interest for understanding the physiological structure of a productive population under distinct growth or process conditions (see Fig. 3).

For determining growth at the level of populations, the experimenter can rely on numerous standardized methods, such as optical density measurements, weighing of wet and dry biomass, manual or automated cell counting with a microscope, a flow cytometer, or Coulter counter devices [29, 48, 49]. With knowledge on cell or biomass concentration, important performance descriptors such as uptake and synthesis rates can be specified and normalized to the respective concentration measure, allowing for an absolute and laboratory-independent evaluation of the catalytic efficiency of populations [28]. As can be inferred from this information, proper analytics for growth and mass profiling are a basal prerequisite for characterizing single cells in a biotechnology context. In the following, we will discuss current state-of-the-art analytics for single-cell growth and biomass analysis and review cutting-edge methods that hold the potential for becoming standard methods for the precise determination of cell wet and dry weights in future.

2.1 Cell Counting, Morphometrics, and Segmentation

Microscopy is the simplest but also one of the most powerful methods for analyzing single cells and their physiology. Quantitative morphometric analyses of single microbes have been established more than a century ago but almost vanished during the last decades [50–53]. It was only with the introduction of automated time-lapse microscopy and powerful image processing routines that made microscopy the measure of choice for single-cell analysis. Enabled by narrow microfluidic structures that force the cells to grow in monolayers or even as separated single cells, a large number of cells can optically be analyzed without artifacts arising from cell overlapping [36, 54, 55]. Arguably, the simplest measure to determine cellular growth kinetics at the microscale is cell counting [56–58]. Recording cell-division kinetics enables the experimenter to normalize physiological parameters, such as induction or adaption kinetics, to obtain cell-specific values [24]. Tracking cell divisions in bacteria can be performed with the bare eye and represents an excellent measure to compare division kinetics at the microscale with the increase in cell numbers of a population [59, 60]. Only such comparative studies reveal environmental effects on growth that remain hidden at a population scale. In a significant exemplary study, Unthan et al. used manual cell counting in micropopulations of *Corynebacterium glutamicum* cells and revealed that the cells divided much faster in

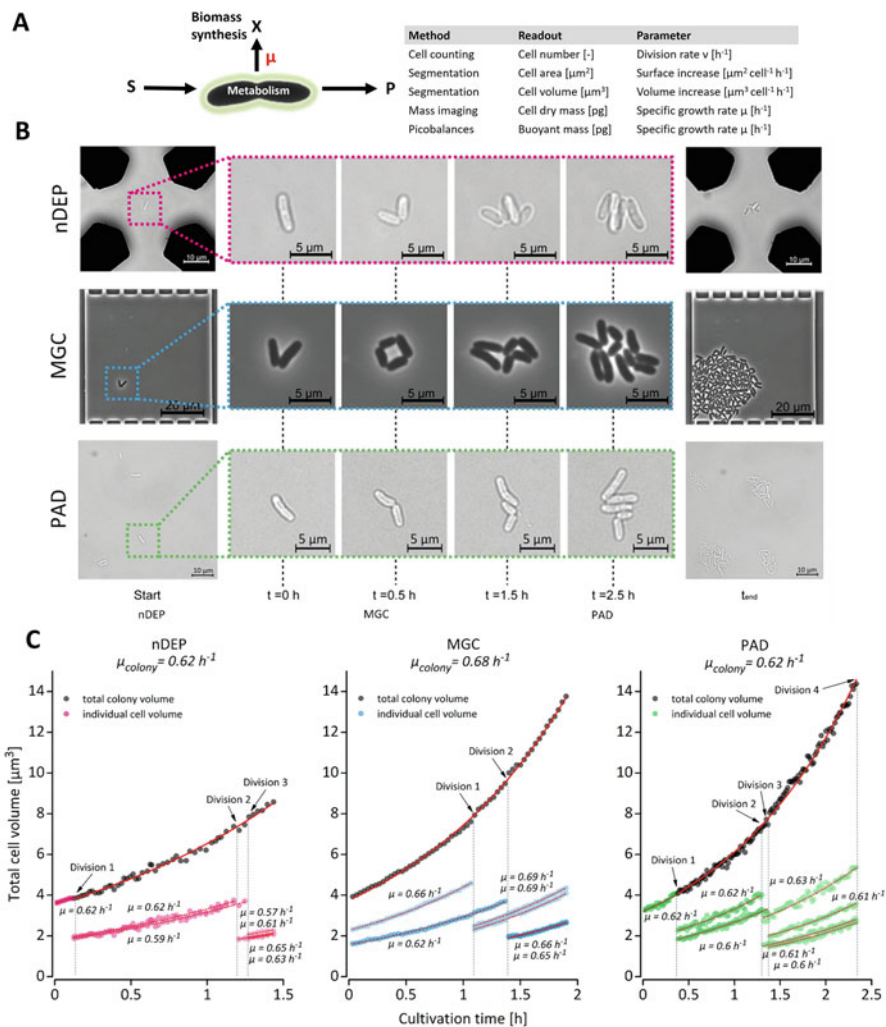


Fig. 3 (a) Analytical methods, readouts, and deducible kinetic parameters for growth rate analysis at a single-cell level. (b) Time-lapse imaging of single *C. glutamicum* cells grown in different microfluidic cultivation systems. (c) Image-based analysis of single cell-specific volumetric growth rates in the different microfluidic cultivation systems [47] – published by the Royal Society of Chemistry

the microfluidic perfusion environment as compared to division kinetics of populations, although the same defined growth medium was used [26]. This observation was the kickoff for a systems-level study that disclosed the reasons for the observed elevated growth rates at the microscale. Based on single-cell cultivations, bioreactor experiments at extremely low cell densities, as well as transcriptomics,

metabolomics, and integrative in silico analysis, it was disclosed that protocatechuic acid was utilized as a hidden co-substrate that drove *C. glutamicum* cells to higher specific growth rates than ever observed before in minimal CGXII medium [26]. Cell counting can also be used to assess single-cell growth of more uncommon cell types. Helingwerf et al. applied cell counting of phototrophic *Synechocystis* sp. PCC6803 for determining growth in massively parallelized droplet cultivations. In conjunction with an enzyme-based assay for the quantification of lactate in the individual droplets, an enrichment of high-producing lactate-forming strains could be realized [61].

Determining growth kinetics via cell counting assumes that all observed cells are similar in length and volume [29]. While this is often true for balanced growth under steady-state conditions, environmental fluctuations and stress in production setups often entail a diversification in cell size, which has to be considered when calculating growth kinetics from cell counts [62, 63]. For many investigations, such as in silico models of growth in populations based on single-cell data or analyses that focus on growth kinetics in between two cell divisions, the need for data on growth kinetics of individual cells arises. Here, morphometric analysis is the measure of choice. Quantitative measurements of cell dimensions, such as cell area and length volumes, are more precise than cell counting and can be better compared to optical density measurements or cell dry matter determination performed at the population scale. Following the dynamics of individual cell geometry, such as the cell projection area or cell volumes calculated from cell dimension, enables us to quantify the growth of individual cells, even between two cell divisions or budding events [64]. Moreover, this type of image-based growth analysis can also account for cell proliferation mechanisms other than binary fission, such as budding in yeast or asymmetric cell division [29]. The most straightforward approach to determine the growth of individual cells between division or budding events is to measure the area and volume of cells via manual segmentation from microscopic images. Several studies demonstrated the applicability and use of this method for determining specific growth rates and their heterogeneities of single microbes and comparing the obtained values to populations [27, 37, 65]. With the assumption that the density of the cells remains constant at balanced growth, the cell volume is a suitable proxy for cell mass and can be directly compared to cell dry matter concentrations in lab-scale cultivations. Manual cell volume approximation has been shown to deliver solid results with several distinct microfluidic bioreactor concepts such as microfluidic monolayer growth chambers and cell traps based on negative dielectrophoresis [27, 37, 65]. A striking insight of microfluidic growth analyses was that the volumetric growth rates of single cells consistently exceeded population growth rates by up to 50% and demonstrated the biological potential in terms of maximal possible growth rates [37]. Realizing such high growth rates at the bulk scale might improve biocatalyst formation and averaged volumetric productivities in bioprocesses. Morphometric analyses revealed that division rates, division angles, and division symmetry of cells were influenced by the specific microfluidic habitat. These results suggest a careful choice of the microfluidic cultivation format to avoid artifacts stemming from the

respective microenvironments. One of the most striking studies of the past years on single-cell growth revealed the basic laws of bacterial size control in *Escherichia coli* [66]. Taheri-Araghi et al. monitored the cell length during the cell cycle of individual *E. coli* cells upon the shift of growth media. Based on the imaged cell length, the authors calculated cell volumes and found that the average cell volume scales exponentially with DNA replication and growth rate. However, in such high-throughput growth experiments, manual determination of cell dimension is virtually impossible and demands automated cell segmentation algorithms.

Manual image processing is tedious and time-consuming. When the number of observed cells is high or cell reproduction has to be tracked in colonies of hundreds of single cells, manual cell counting is not a viable option anymore. With advanced image processing algorithms, automated cell segmentation can be conveniently performed at high-throughput [62, 63]. However, due to the huge variety of microbial morphology within isogenic populations and across different microbial strains, error rates of segmentation algorithms can be high and require extensive adaption of the segmentation codes to the strain of interest [67, 68]. Next to morphological challenges, segmentation algorithms have to be robust against poor image quality, out-of-focus images, overlapping of neighboring, and noise [67].

Available image segmentation algorithms such as Schnitzcells, Oufiti, or MicrobeTracker are optimized for tracking certain types of microbes [22, 69, 70]. It is not of surprise that the detection of cell boundaries and the corresponding morphological traits has been adapted to rod-shaped bacteria such as *E. coli*, *C. glutamicum*, *Bacillus subtilis*, *Pseudomonas* sp., and other commonly used model strains [22, 69]. As the natural variety of cell morphology is overwhelming, the growth of many uncommon microorganisms cannot be quantified out of the box with available software packages. However, recent image analysis algorithms such as Oufiti are tackling this problem and offer extensive customization options to segment cells with uncommon or even irregular shapes [71, 72]. Oufiti allows the quantification of various cell morphologies, irregular shapes, and even the identification of individual cells that form confluent monolayers by using powerful and flexible segmentation algorithms for high-content imaging. The algorithm includes, for example, mathematical routines for the identification of differential growth behavior among single cells such as significantly slower or faster growth of cells. MicrobeJ is another recent image-processing framework for extracting gray-value, cell dimension, and morphological routines, as well as subcellular analysis of fluorescence localization from microscopy images [73]. A powerful code for data integrity validation has been integrated as well. Among the wealth of image analysis algorithms, highly customized solutions exist as well. An important example constitutes the tool Molyso, which has been specifically developed to extract growth data from mother machine time lapse [74].

In general, this is only a small excerpt from the many image analysis tools available. It is recommended to cross-check the available tools for specific scientific strains, scientific questions, and experimental setups. The above-described algorithms pose universally applicable tools that enable automated high-throughput analyses of single-cell traits from images and are invaluable for processing the

massive data amounts from time-lapse experiments. However, automated image analysis algorithms are error-prone, and supervision of segmentation results is still indispensable. As a possible remedy, deep-learning and AI-based algorithms might allow higher accuracy and handling of challenging image sets for determining growth kinetics at the single-cell level.

2.2 *Mass Imaging*

Mass imaging has the potential to become the next evolutionary stage in single-cell growth analysis [11]. In contrast to the extraction of spatial data from images for growth analysis, novel phase imaging concepts promise the fast, accurate, and noninvasive optical profiling of single-cell dry weights with sub-pg resolution [75–78]. Tracking growth at such resolution is the only measure to accurately analyze specific growth rates, as the growth rate is defined as the mass increase in a given biological system over time. Time-resolved data on cell mass enables us to directly normalize physiological parameters to single-cell dry matter and render them comparable to population data by that [29]. Mass imaging is based on interferometry and quantitative phase microscopy. By measuring the phase shift of light that passes a cell, the refractive index of the cell can be determined and related to cell mass. While mass imaging has been extensively applied to profile growth and density of mammalian cells, corresponding examples for bacteria or yeast are rare [79–81]. Nevertheless, mass imaging enabled profiling mass and calculating specific growth rates of individual *E. coli* cells [82]. In this study, significant heterogeneity in terms of cell mass increase was observed and demonstrated for the first time the contribution of individual bacteria growth to the macroscopic growth of populations. Two studies performed density mapping of individual *E. coli* cells with a lateral resolution of 90 nm by integrating super-resolution microscopy and phase microscopy for [83] or visualized subcellular structure via tomography [84]. As can be seen, mass imaging is not widespread in microfluidic single-cell analysis for biotechnology, despite its huge potential for unraveling process-relevant growth mechanisms and heterogeneities at the smallest possible scale. Nonetheless, we are convinced that this will change in the future, as mass imaging technologies are universally applicable, compatible with other modalities such as fluorescence microscopy, and require merely the upgrade of a time-lapse microscope with a simple camera. By now, many companies offer commercialized calibration-free mass imaging solutions that are sufficiently sensitive and accurate to profile mass and growth kinetics at the single microbe level.

2.3 Picobalances

Microfluidic resonators based on dynamic cantilevers can be used as picobalances for weighing single cells and enable us to measure the buoyant mass of a cell with extreme precision [85, 86]. Sophisticated resonator designs exist that swing in a vacuum and can be perfused with cell suspension [87, 88]. The passing cells influence the cantilever resonance frequency and allow to measure cell mass with a resolution in the low fg range, which makes the analytical concepts applicable to even the smallest known types of microbial cells [89]. Microfluidic resonators have been applied for the detection of single *E. coli* already two centuries ago [90]. As the cells are suspended, this microfluidic resonator enables the investigation of physicochemical perturbations on cell mass and growth [91, 92]. Due to the high precision, correlations between growth rate and cell mass could be revealed [87]. A comparison between mass and volume growth kinetics in single yeast cells was achieved by combining a Coulter counter with a microfluidic resonator [93]. Mass and density profiles of viable, stressed, and dead *E. coli* cells could be investigated with resonator structures at high throughput for the first time and demonstrated that dead cells have a larger density but a lower cell mass [94]. Suspended microfluidic resonators were used to determine the weight of single marine bacteria, and these results from the microscale were used to estimate the total amount of marine biomass on earth for calculating global oceanic carbon fluxes [91]. The examples demonstrate the usefulness of picobalances for fundamental research. However, questions of biotechnological interest have not been approached with picobalances yet. This is mostly due to the complicated and extensive microfabrication that is needed. Moreover, combining resonators with other imaging techniques might be difficult. It can be stated that microfluidic resonators are well suited for high-precision measurements of single-cell mass but always involve a trade-off between the time-period of tracking and the number of cells that can be tracked.

3 Substrate Uptake

Next to growth, the kinetics of substrate utilization, namely, the specific substrate uptake rate q_S , is of utmost interest when analyzing the performance of whole-cell biocatalysts. Bioprocesses are often controlled by limited substrate feeding to prevent the formation of bioproducts or limit growth [95–98]. Moreover, specific yield coefficients of biomass on the substrate can be calculated with q_S , and the specific growth rate μ . Measuring specific substrate uptake is therefore mandatory to identify the efficiencies of substrate to biomass and product conversions and its heterogeneities at a single-cell level (see Fig. 4).

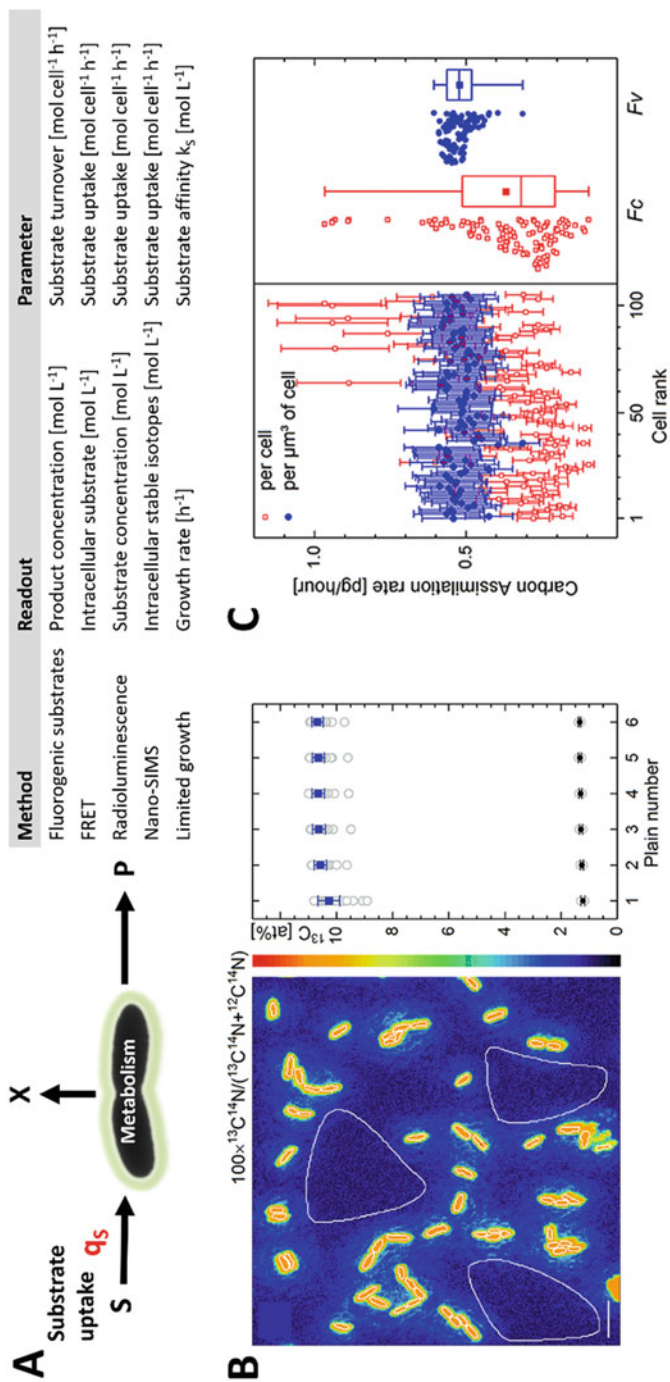


Fig. 4 (a) Analytical methods, readouts, and deducible kinetic parameters for substrate uptake rates at a single-cell level. (b) NanoSIMS-based chemical microscopy of carbon and nitrogen stable isotope ratios in single cells. (c) Cell-volume- and cell-specific carbon uptake rates of single *P. putida* cells calculated from isotope ratios [99]

3.1 Fluorescence Analysis

To date, quantitative studies of substrate uptake in single cells mostly rely on specific labels, such as fluorescence, stable isotopes, or radiolabels [100–103]. Label-free analytical concepts for measuring uptake in single cells comprise genetically encoded fluorescence biosensors, mostly basing on intracellular and extracellular substrate-sensitive Förster resonance electron transfer (FRET) probes; transcriptional reporters or specific binding motifs of fluorescent proteins have been utilized to study substrate uptake [104–107]. However, most of the published studies on substrate uptake in single microbes can be found in the field of environmental microbiology for characterizing carbon, phosphorous, and nitrogen assimilation processes in natural environments [99, 108, 109]. Studies focusing specifically on single-cell substrate uptake for tackling biotechnological questions are still rare. Nevertheless, promising analytical concepts have been developed and will be discussed in the following.

One of the simplest concepts for following substrate uptake in live single cells is to use fluorescently labeled substrate conjugates. Hehemann et al. used fluorescent glycan conjugates to image and quantify its uptake in intestinal bacteria [101]. Another study by Straeuber et al. used N-(7-nitrobenz-2-oxa-1,3-diazol-4-yl)amino (NBD)-labelled toluene to visualize its incorporation into different live *Pseudomonas* strains and *E. coli* [110]. However, the uptake data obtained with such modified substrates have to be carefully evaluated, as the chemical changes might lead to significant differences in transmembrane transport kinetics V_{\max} and K_S in comparison with the unmodified compounds. Natarajan et al. demonstrated a noteworthy concept for quantifying glucose uptake in single *E. coli* cells [111, 112]. By exploiting the competitive inhibition of the fluorescent glucose analog 2-(N-(7-nitrobenz-2-oxa-1,3-diazol-4-yl)amino)-2-deoxyglucose (2-NBDG) on glucose uptake, the authors used flow cytometry measure-specific uptake rates in single cells from populations grown in chemostat cultures. This elegant concept for quantifying cell-specific substrate uptake rates shows that it is not compulsory to label the substrate of interest but exploit the competition of a fluorescent analog at the transport porin. However, following the temporal dynamics of glucose incorporation in specific single cells is not possible with this method due to the snapshot character of flow cytometer analyses. It rather exploits the characteristics of the uptake mechanism and its kinetics for indirectly determining glucose uptake. Due to the need for fast medium exchange and recording of fluorescence increase, this concept has never been transferred to microfluidic cultivations.

Next to fluorescence labeling, quantifying the intracellular accumulation of radiolabeled ^{18}F -fluorodeoxyglucose is a common method to approximate glucose uptake in single cells [100, 102, 113]. Using radioluminescence microscopy, which can be integrated into common light microscopes, multimodal analysis of single-cell substrate incorporation and other physiological parameters such as growth is possible.

FRET-based sensors, exploiting conformational changes or energetic interactions of two fluorescent proteins by binding of a substrate molecule, are useful for monitoring intracellular substrate concentrations in individual cells [114–116]. The uptake of several different hydrocarbons by living microbes could be realized with genetically encoded FRET probes. A highly responsive CFP/YFP-based FRET sensor was demonstrated to facilitate the visualization of intracellular glucose accumulation in *Saccharomyces cerevisiae* uptake mutants [117]. Based on a similar FRET design, maltose uptake in single *S. cerevisiae* cells could be quantified [106]. Visualization of arabinose and maltose influx was also demonstrated for single *E. coli* cells [118]. Purified FRET probes can be also used *ex vivo*. Purified FRET-based glucose biosensors could be applied to measure extracellular glucose concentrations in an *E. coli* culture [105]. Although this concept has not been implemented in microfluidic cultivation devices, it has the potential to enable substrate measurements in microbioreactors in the future.

Other genetic elements, such as transcriptional regulators, can be exploited as indirect reporters for the capacity of single cells to process and take up nutrients. Such transcriptional reporters were applied to control GFP expression in *E. coli* cultures [107]. The obtained results indicated the heterogeneous expression of genes involved in glucose uptake.

3.2 Mass Spectrometry

Label-free mass spectrometry-based methods such as nanoSIMS can be used to study the assimilation of isotope-labeled substrates into microbial cells. Nikolic et al. applied ^{13}C - and ^2H -labelled glucose to characterize glucose uptake in a clonal *E. coli* population via nanoSIMS analysis [119]. This method enabled to identify the magnitude of metabolic heterogeneity in terms of glucose uptake in the cultures. Glucose uptake rates did not correlate with gene expression profiles. Furthermore, the experimental results suggest a metabolic specialization of subpopulations in terms of sugar metabolism. The applications of nanoSIMS are manifold in single-cell analysis and allow assessing phenomena that are not analytically accessible otherwise. In mixed-species systems, nanoSIMS could be used to the nutrient transfer between fungi and bacteria [120]. Despite its sensitivity and spatial resolution, it is difficult to obtain quantitative data on cell-specific uptake kinetics [121]. Nevertheless, Stryhanyuk et al. succeeded in determining cell-specific glucose uptake rates of *Pseudomonas* cells based on a comprehensive mathematical framework [99]. Unfortunately, SIMS analysis destroys the cell during analysis and does not enable to follow individual cell dynamics in glucose uptake.

3.3 *Inferring Kinetic Constants of Substrate Uptake*

Kinetic parameters such as the affinity of transporter enzymes toward the substrate govern the cellular uptake. To date, there is only a little knowledge about whole-cell kinetics and its heterogeneity. A notable example that demonstrates how substrate affinities of microbial cells could be determined in microfluidics was recently presented by Lindemann et al. [122]. The authors applied carbon-limiting conditions in perfusion microfluidics and quantified growth of *C. glutamicum* cells and its heterogeneity in response to the extracellular substrate availability. At extremely limiting carbon conditions, it was found that the variability in cell-specific division times increased significantly. These results suggest a strong individuality among isogenic microbes in terms of glucose uptake and metabolism. Moreover, the authors could approximate K_S values from single-cell cultivations for the first time.

The presented studies impressively demonstrate the significant advancements of analytical technologies for quantifying substrate uptake at a single-cell level. It must be stated, however, that there is no universally applicable analytical concept available for quantifying substrate utilization in single cells. Rather, it has to be decided depending on the biological questions which the analytical method can be applied to for obtaining meaningful data. For the future, advances in single-cell mass spectrometry might deliver remedies for the current situation and enable us to determine substrate concentrations in microfluidic bioreactors and cell-specific uptake rates with high accuracy.

4 Product Formation

The efficiency and kinetics of product formation are the most important performance parameters in bioprocesses. Maximizing the specific product formation rate r_P of the whole-cell biocatalyst is the central goal of strain and process engineering endeavors (see Fig. 5). But what is the effect of physiological heterogeneity and cell dynamics with regard to individual product formation on the performance of a process? To date, many indications exist that suggest a significant influence of phenotypic heterogeneity on the productivity of a process. Understanding the activity structure of population-based on single-cell-specific performance analyses is important and might lead to novel engineering targets for process improvement in the future [123].

4.1 *Fluorescence Analysis*

Analytical concepts have been developed to analyze productivity in microfluidic cultivation experiments. As extreme sensitivity is required to accomplish quantitative product analysis at a single-cell level, optical methods are dominating and often

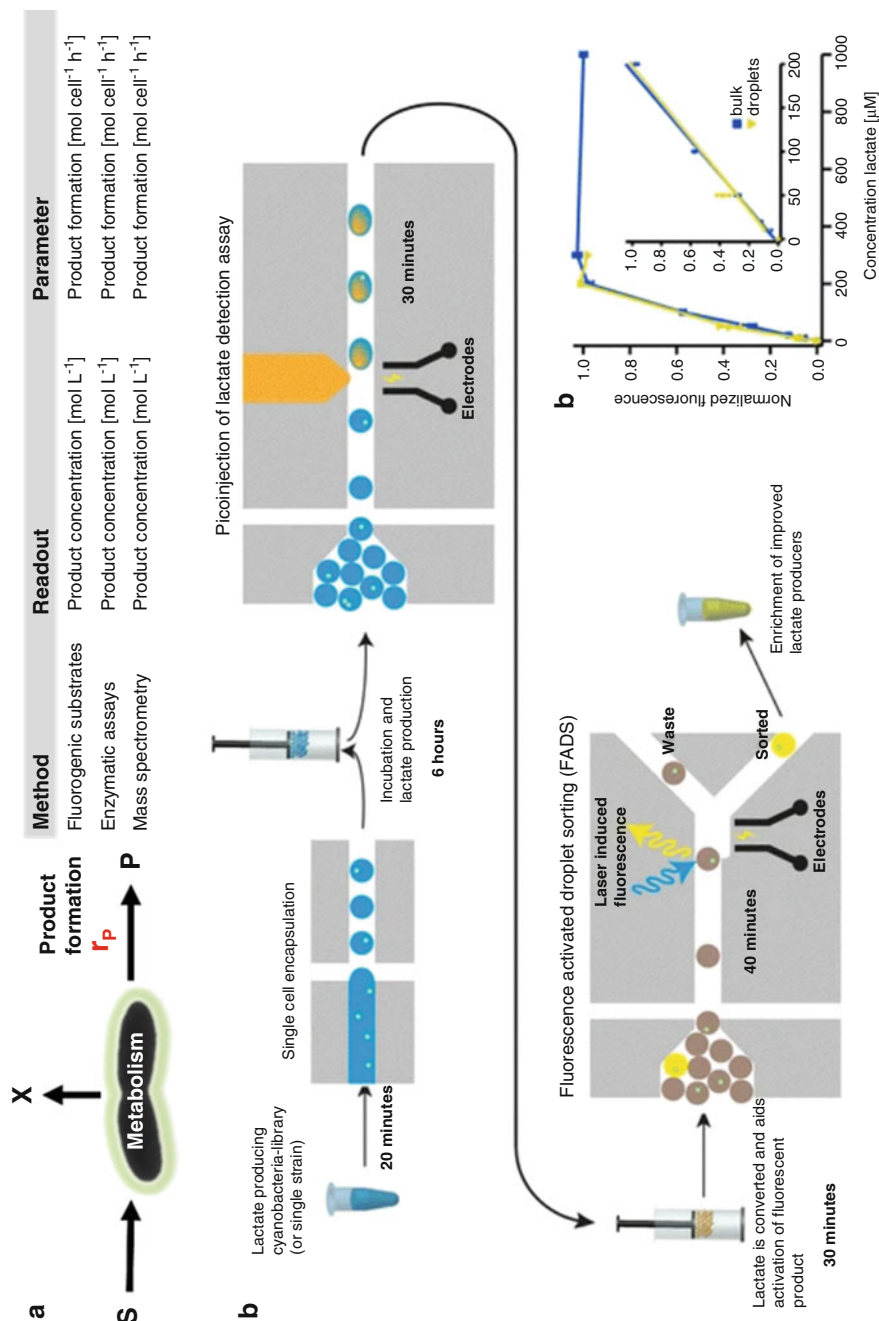


Fig. 5 (a) Analytical methods, readouts, and deducible kinetic parameters for product formation rates at a single-cell level. (b) Quantifying lactate production by phototropic cyanobacteria cultivated in microfluidic droplets via a pico-injected enzymatic assay [61]

the measure of choice [12]. A recently published key study impressively demonstrated the massive effect of phenotypic heterogeneity on the output of a productive process [124]. Xiao et al. applied fluorescence staining to visualize and quantify free fatty acid and tyrosine production in isogenic *E. coli* mutants. Their investigations confirmed the existence of high and low producer cell variants and showed that only 15% of the cell population was responsible for more than 50% of product formation. Based on this knowledge, a molecular population control strategy was developed and implemented, which led to a significantly enhanced productivity of the controlled populations. However, simple fluorescence staining methods cannot be used to cover the wealth of microbial products.

Another prevalent method to determine productivities at a single-cell level is the application of fluorogenic substrates [125]. A wealth of nonfluorescent substrate compounds exist that turn fluorescent upon microbial conversion. The class of fluorogenic substrates is restricted to the detection of hydrolytic activity, by amylases, cellulases, xylanases, lysozyme, and phosphatases. One of the most widely applied and most sensitive substances of this class are fluorogenic β -galactosidase substrates such as fluorescein di- β -D-galactopyranoside (FDG).

Next to the application of fluorogenic substrates, relative intracellular product levels can also be visualized by exploiting titratable regulatory circuits that control the expression of a fluorescent indicator gene in response to metabolite abundance. A prominent example was demonstrated by Binder et al. who coupled the concentration-dependent expression of fluorescent genes to transcription factors in *E. coli* and *C. glutamicum* [126]. Based on this concept, transcription factor-based product sensors for several different amino acids were established and validated. In a follow-up study, the l-lysine, l-arginine, and l-histidine sensors were applied for rerouting metabolic fluxes toward the desired products in *C. glutamicum* [127]. Although this approach does not allow determining absolute cytosolic product concentrations or even production at a single-cell level, it is a valuable tool for strain improvement and mutant screening using microfluidics. In the future, such intracellular sensors might be calibrated to determine absolute cytosolic product concentrations or even product formation kinetics.

Some examples also demonstrate the direct visualization of cell products via antibody assays in microfluidic cultivations. In pioneering studies, Love and coworkers implemented microarray technology to microfluidics to quantify secreted protein of single or few *Pichia pastoris* cells cultivated in nanowells [128, 129]. For protein quantification, a glass slide was functionalized with an antibody specific to a human FC fragment and was bonded to the nanowell array. After a specific incubation time, the glass slide was removed, and bound protein was quantified via fluorescence microscopy. With this concept, the authors were able to determine volumetric protein secretion rates in the nanowells. Based on this technology, the authors could disclose a stochastic protein secretion in single yeast cells [128]. A comprehensive follow-up study revealed that the secretory capacity of single yeast cells is the productivity-determining bottleneck in the production of heterologous protein in *P. pastoris* [129].

It was also demonstrated that enzymatic assays can be used in microfluidic cultivation devices for product quantification. Hammar et al. performed the on-chip analysis of lactate production by phototrophic *Synechocystis* sp. PCC6803 cells cultivated in microdroplets [61]. The produced lactate served as a substrate for a subsequent enzymatic reaction that yielded a fluorescent product. The enzyme assay solution was pico-injected into the microdroplets after cell incubation. Based on the intensity of the fluorescent signal, the droplets were sorted and subcultivated to yield a population with improved lactate-production characteristics. Next to this prominent study, other concepts have been developed to quantify products such as antibodies in microfluidics, but these mostly focus on the analysis of yeast, mammalian cells, or enzyme mutants [130–134].

4.2 Mass Spectrometry

Modern mass spectrometry is sensitive enough to detect and quantify products from single whole-cell biocatalysts. The power of single-cell mass spectrometry for analyzing mammalian cell systems was demonstrated already, but for the analysis of microbes and their catalytic products, mass spectrometry is still in its infancy [135–137]. However, several key studies recently illustrated the power of mass spectrometry analysis for productivity analyses at the single-cell level and will be reviewed and discussed in the following.

Electrospray ionization-Fourier transform ion cyclotron (ESI-FTICR) mass spectrometry coupled to microfluidic cell cultivation enabled for the first time to detect and quantify the productivity of microbial cell factories at a single-cell level without the need for labeling [138]. In this key study, a few living L-lysine-producing *C. glutamicum* were trapped via negative dielectrophoresis with the Envirostat microfluidic single-cell bioreactor [65, 139, 140]. The cell supernatant was continuously sampled in chip-coupled fused-silica capillaries and analyzed via nanospray-ESI-FTICR mass spectrometry. The produced lysine was accurately quantified by spiking the cell medium with a stable isotope-labeled internal standard. Cell-specific L-lysine production rates r_p ranged from 2 to 20 $\text{fmol}^{-1} \text{ cell h}^{-1}$. Despite the analytical power of mass spectrometry, this study is the first example of how specific product formation rates in microbes can be obtained from microfluidic single-cell experiments. Ion suppression caused by the high salt cargo of standard growth and production media for microbes were recently identified as the key reason for this lack of successful studies. The development of a volatile, ammonium salt-based reaction medium, that was causing low ion suppression but enabled high cellular activity, was the key to success for realizing single-cell product analysis via mass spectrometry [138]. Microfluidics interfaced with ultrasensitive label-free mass spectrometry might become one of the key concepts for unraveling strain productivity and its heterogeneity based on single-cell data.

Next to FTICR-MS, a chip-MS interface based in droplet microarrays and subsequent ionization via matrix-assisted laser desorption Ionization (MALDI)

was demonstrated in the multimodal analysis of protein secretion and enzymatic activity with only 50–100 living *Komagataella phaffii* cells [141, 142]. Via MALDI-MS and the application of a fluorogenic substrate, the multistep conversion of phytic acid by secreted phytase could be monitored with several modalities [141]. The approach was further refined and even allowed the separation of yeast cells and droplet supernatant for subcultivation of the analyzed micropopulations based on the results obtained from the multimodal analysis of the secreted enzyme [142]. Noteworthy, these studies were also enabled by the application of volatile salt buffers as reaction media [138]. The developed analytical concept has a broad range of applications and can be adapted to on-chip microfluidic droplet cultivations but also interfaced with any other microbioreactor concepts, such as perfusion reactors.

The above described high-density droplet arrays for interfacing microfluidics and mass spectrometry were designed to aliquot droplets of solutions or cell suspensions. With this concept, high-throughput analyses of intracellular metabolites in single *S. cerevisiae* cells were realized with a detection limit down to 10 fmol total analyte amount [143, 144]. Intrinsic heterogeneity in terms of relative intracellular metabolite concentration could be revealed, which correlated with cell size, cell age, or cell cycle stage. Based on these intracellular levels of the glycolytic metabolite fructose-1,6-bisphosphate, two distinct metabolic phenotypes could be identified [143]. Another study intensified the application of the high-density droplet arrays and disclosed that yeast cells exhibited a more active pentose phosphate pathway upon perturbation of glycolysis [144]. The authors used ^{13}C -labelled glucose to infer the pathway activity of single cells via MALDI-MS. The pioneering studies demonstrate how the analysis of metabolic fluxes can be accomplished with single cells and mark the first steps toward systems biotechnology with single microbial cells.

Product analysis and quantification for determining synthesis kinetics of single cells are close. Optical methods, basing on fluorescence readouts, cover a broad range of important microbial products, and concepts like novel FRET sensors for product measurements in microfluidic cultivations are likely to emerge. With the latest developments in mass spectrometry, a universal and label-free analytical concept for detecting tiniest product amounts comes into reach. However, this requires future research in terms of microfluidic interfacing and media design [11]. With the discussed technologies, cellular heterogeneities and its manifestation in the catalytic efficiencies are now accessible and will lead to the development of novel strategies for strain development and process engineering. Indeed, this might enable us to perform systems-level studies with the cell as the minimal unit of biotechnological processes.

5 Gene Expression, Protein Synthesis, and Regulation

Fluorescence analysis of individual microbes reawakened the field of microfluidic single-cell analysis a decade ago. Cell-to-cell differences in gene expression were revealed by the application of fluorescent proteins and microscopy and the results

pointed to significant functional heterogeneity in isogenic populations (see Fig. 6) [145]. Many comprehensive studies followed that elucidated the fundamental concepts of stochasticity and noise in gene expression [146–150]. The excellent control of extracellular conditions in microfluidics enabled to link observations of gene expression with environmental cues and fluctuations [149, 151, 152]. With the ever-increasing sensitivity of analytical technologies, it became even possible to track gene expression at the level of single molecules [153]. In biotechnological processes, the content of catalytically active enzyme comprises important parameters for the activity of whole-cell biocatalysts. On a population level, it is therefore a common procedure to characterize the expression of key enzymes for a target catalytic conversion.

Analyses of gene expression can be performed at a single-cell level, mostly by molecular fusion of reporter genes, coding for fluorescent proteins, to the gene of interest [154, 155]. With microfluidic cultivation, novel insight into the general mechanisms of gene expression could be obtained by the application of such fusion constructs. However, a fluorescent reporter can also be just simply put under the control of a certain regulatory element such as a promoter to study its functioning. Gefen et al. analyzed gene expression kinetics and magnitudes in single starving *E. coli* cells [156]. The microfluidic chip was connected to a shake flask batch culture to establish identical growth conditions in the flask and in on-chip cultures. Upon reaching the stationary growth phase, the majority of cells stopped growing due to the lack of carbon source, while approximately 7% of the cells lysed. Inducing the expression of genes coding for fluorescent proteins, it was found that the starving cells still maintained their capability to synthesize protein de novo for several days. It could be hence proven that the synthesis activity of *E. coli* in the stationary growth phase is maintained for longer periods of starvation. The obtained results also suggest that cells can be metabolically active, despite the absence of growth. However, this is only one prominent example of how gene expression analysis with fluorescent reporters can be accomplished. The use of fluorescent proteins and microscopy for probing cellular behavior, promoter activity, protein localization, gene expression dynamics, and many other cellular parameters is certainly the most widespread method for analyzing single cells in microfluidics [157–162]. As an extensive discussion of these applications would exceed the scope of this chapter, we refer to key review papers on this topic [22, 163, 164].

Gene expression analysis via fluorescent reporter enzyme gives access to relative protein amounts inside the cell. Absolute enzyme levels are usually determined via mass spectrometry-based proteomics, but proteomics with single microbes are difficult to perform due to the low number of enzyme copies inside a cell [12]. The amount of a target enzyme in *E. coli* cells could be quantified via a microscale enzyme-linked immunosorbent assay (ELISA) and the corresponding fluorescence readout [165]. For this, individual cells were trapped hydrodynamically in sealable fluidic microchambers. Upon cell trapping, the chambers were closed, and the target enzyme β -galactosidase was liberated via on-chip cell lysis. The free enzyme was bound to immobilized antibodies. The enzyme quantity was then determined by the addition of the fluorogenic substrate fluorescein di- β -D-

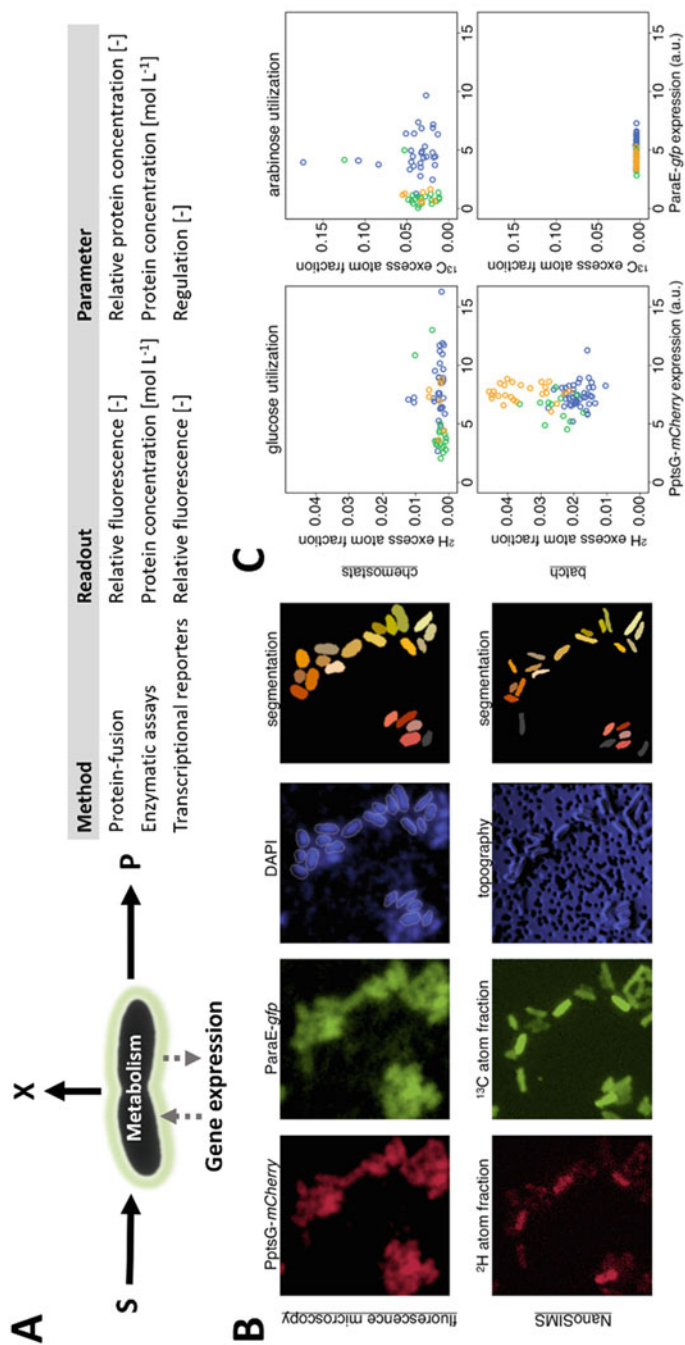


Fig. 6 (a) Analytical methods, readouts, and parameters for gene expression and regulation at a single-cell level. (b) Measuring heterogeneity in gene expressions of the sugar metabolism in single *E. coli* cells via the expression of dual fluorescent reporter genes. Next to the synthesis of reporter proteins, carbon uptake of the cells were analyzed via nanoSIMS. (c) Correlation between stable isotope incorporation and expression of two genes involved in sugar metabolism [119]

galactopyranoside (FDG), which was hydrolyzed to fluorescein and galactose. With this method, enzyme copy numbers as low as 200 copies per cell could be detected. The authors found that the abundance of β -galactosidase was variable among individual *E. coli* cells and depended on the extracellular cultivation conditions, proving proteome heterogeneity in isogenic populations.

Microfluidic single-cell analysis can also be used to unravel regulatory mechanisms that are hidden behind averaged values of populations. The analysis of carbon-catabolite repression in the yeast *Ogataea polymorpha* (formerly known as *Hansenula polymorpha*) at a single cell-level disclosed that threshold glucose concentrations for promoter repression differed up to four orders of magnitude at the microscale compared to population experiments [166]. The authors simply put the gene expression of a GFP under the control of the *MOX* promoter to unravel these intriguing insights into promoter repression. Optimized carbon-limited fed-batch strategies for increasing the productivity of the *MOX* promoter system could be derived from the microfluidic single-cell experiments.

As can be seen, the analysis of gene expression and its regulation at a single-cell level can contribute significantly to the improvement of bioprocesses and microbial cell factories via rational genetic or process modifications.

6 Analytical Pitfalls in Microfluidic Single-Cell Analysis

Many analytical pitfalls have to be considered when analyzing cellular behavior at a microscale. Bias arising from the analytical method can result in biological artifacts that lead to misinterpretation of the obtained results. The microfluidic cultivation habitat, including the physical laws at the microscale and the high surface-to-volume ratios, constitute the most important sources of technical bias in microfluidic single-cell analysis [47, 66, 167, 168]. It is therefore important to perform suitable control experiments to ensure that the physiological state of the cells to be analyzed is not a result of the cultivation environment.

As discussed before, optical methods are the most widespread analytical technologies for investigating the behavior of single microbes. Optical analyses are generally seen as noninvasive but can have tremendous impact on cellular physiology. Although optical analysis technologies are mechanically noninvasive, illumination transfers energy to the cells. Light-induced phototoxic effects can severely affect the physiology of the cells, mostly by the formation of reactive oxygen species (ROS) or radicals [169, 170]. Such photochemical-induced toxicity can be even caused by standard white illumination for brightfield imaging [171, 172]. Photo-induced physiological effects inversely scale with the UV light contents of the white-light source. By using filters or LED illumination with defined spectra, UV-induced effects on physiology can be minimized or even circumvented.

While phototoxicity can be critical during white-light illumination, it is mandatory to study the effects of phototoxicity during fluorescence imaging. As the excitation light for fluorescence analysis is typical of high intensity, the physiology

of microbes can be strongly influenced by fluorescence excitation [173]. A negative correlation was found between the dose of excitation light at 488 nm (typical wavelength for GFP excitation) and doubling times in single *E. coli* cells [174]. Minimizing of phototoxicity during fluorescence imaging involves a reduction of exposure times and excitation. Comprehensive guidelines for optimal experimental design for fluorescence imaging have been published [175, 176]. The basic principles for avoiding the technical bias of fluorescence imaging can be also applied for microbes, although most work bases on cell cultures.

Protein synthesis and degradation dynamics have to be considered when using genetically fluorescent probes for the visualization of dynamic processes in single cells [177]. This included maturation times of the fluorescent proteins, as well as their extended cytosolic half-life of often more than 24 h [178]. It is advisable to apply fast maturing mutants of fluorescent proteins and, if necessary, to add a proteasome degradation tag for decreasing the protein's half-life [179].

When using chemical dyes for fluorescence imaging, the experimenter has to consider that these compounds can intercalate DNA or alter the properties of the stained molecules [180]. These aspects have to be considered, and its effects should be properly characterized via control experiments to ensure the analysis of undisturbed single-cell physiology.

7 Conclusion

The analytical concepts for microfluidic single-cell analysis now enable measuring and quantifying the physiology and the underlying cellular parameters of whole-cell biocatalysts at the level of individual cells. Advanced analytics, such as optical imaging technologies and mass spectrometry, matured and give access to the kinetics of biomass and product formation, as well as substrate uptake. With knowledge on cell-specific μ , q_s , and r_p , mass and energy balances of single cells can be established to uncover the catalytic landscape of cellular performance and efficiency. Based on such kinetic single-cell data, we will learn about the role of individual phenotypes and their contribution to the output of the bioprocesses. In combination with powerful microfluidic cultivation concepts, single-cell analytics will uncover hidden links between environmental conditions and individual cell performance that are blurred by averaged values from populations. Novel engineering targets for metabolic, reaction, and process engineering will be derived from data on single-cell physiology.

References

1. Schmid A, Dordick JS, Hauer B, Kiener A, Wubbolts M, Witholt B (2001) Industrial biocatalysis today and tomorrow. *Nature* 409(6817):258–268

2. Schrewe M, Julsing MK, Buhler B, Schmid A (2013) Whole-cell biocatalysis for selective and productive C-O functional group introduction and modification. *Chem Soc Rev* 42 (15):6346–6377
3. Blank LM, Ebert BE, Buhler B, Schmid A (2008) Metabolic capacity estimation of *Escherichia coli* as a platform for redox biocatalysis: constraint-based modeling and experimental verification. *Biotechnol Bioeng* 100(6):1050–1065
4. Olaofe OA, Fenner CJ, Gudimich R, Smit MS, Harrison ST (2013) The influence of microbial physiology on biocatalyst activity and efficiency in the terminal hydroxylation of n-octane using *Escherichia coli* expressing the alkane hydroxylase, CYP153A6. *Microb Cell Factories* 12:8
5. Litsios A, Ortega AD, Wit EC, Heinemann M (2018) Metabolic-flux dependent regulation of microbial physiology. *Curr Opin Microbiol* 42:71–78
6. Davies J (2002) Re-birth of microbial physiology. *Environ Microbiol* 4(1):6
7. Royle K, Kontoravdi C (2013) A systems biology approach to optimising hosts for industrial protein production. *Biotechnol Lett* 35(12):1961–1969
8. Schuetz R, Zamboni N, Zampieri M, Heinemann M, Sauer U (2012) Multidimensional optimality of microbial metabolism. *Science* 336(6081):601–604
9. Lee SY, Lee DY, Kim TY (2005) Systems biotechnology for strain improvement. *Trends Biotechnol* 23(7):349–358
10. Fritzsche FS, Dusny C, Frick O, Schmid A (2012) Single-cell analysis in biotechnology, systems biology, and biocatalysis. *Ann Rev Chem Biomol Eng* 3(1):129–155
11. Dusny C, Grunberger A (2019) Microfluidic single-cell analysis in biotechnology: from monitoring towards understanding. *Curr Opin Biotechnol* 63:26–33
12. Kortmann H, Blank LM, Schmid A (2011) Single cell analytics: an overview. *Adv Biochem Eng Biotechnol* 124:99–122
13. Schmid A, Kortmann H, Dittrich PS, Blank LM (2010) Chemical and biological single cell analysis. *Curr Opin Biotechnol* 21(1):12–20
14. Reshes G, Vanounou S, Fishov I, Feingold M (2008) Cell shape dynamics in *Escherichia coli*. *Biophys J* 94(1):251–264
15. Boyd ES, Leavitt WD, Geesey GG (2009) CO₂ uptake and fixation by a thermoacidophilic microbial community attached to precipitated sulfur in a geothermal spring. *Appl Environ Microbiol* 75(13):4289–4296
16. Zakhartsev M, Reuss M (2018) Cell size and morphological properties of yeast *Saccharomyces cerevisiae* in relation to growth temperature. *FEMS Yeast Res* 18(6)
17. Zavrel T, Ocnasova P, Cerveny J (2017) Phenotypic characterization of *Synechocystis* sp. PCC 6803 substrains reveals differences in sensitivity to abiotic stress. *PLoS One* 12 (12):e0189130
18. Milo R, Jorgensen P, Moran U, Weber G, Springer M (2010) BioNumbers—the database of key numbers in molecular and cell biology. *Nucleic Acids Res* 38:D750–D753
19. Dittrich P, Jakubowski N (2014) Current trends in single cell analysis. *Anal Bioanal Chem* 406 (27):6957–6961
20. Lubeck E, Cai L (2012) Single-cell systems biology by super-resolution imaging and combinatorial labeling. *Nat Methods* 9(7):743–748
21. Altinoglu I, Merrifield CJ, Yamaichi Y (2019) Single molecule super-resolution imaging of bacterial cell pole proteins with high-throughput quantitative analysis pipeline. *Sci Rep* 9 (1):6680
22. Young JW, Locke JCW, Altinok A, Rosenfeld N, Bacarian T, Swain PS, Mjolsness E, Elowitz MB (2012) Measuring single-cell gene expression dynamics in bacteria using fluorescence time-lapse microscopy. *Nat Protoc* 7(1):80–88
23. Locke JC, Elowitz MB (2009) Using movies to analyse gene circuit dynamics in single cells. *Nat Rev Microbiol* 7(5):383–392
24. Young JW, Locke JC, Elowitz MB (2013) Rate of environmental change determines stress response specificity. *Proc Natl Acad Sci U S A* 110(10):4140–4145

25. Locke JCW, Young JW, Fontes M, Jimenez MJH, Elowitz MB (2011) Stochastic pulse regulation in bacterial stress response. *Science* 334(6054):366–369
26. Unthan S, Gruenberger A, van Ooyen J, Gaetgens J, Heinrich J, Paczia N, Wiechert W, Kohlheyer D, Noack S (2014) Beyond growth rate 0.6: what drives *Corynebacterium glutamicum* to higher growth rates in defined medium. *Biotechnol Bioeng* 111(2):359–371
27. Dusny C, Gruenberger A, Probst C, Wiechert W, Kohlheyer D, Schmid A (2015) Technical bias of microcultivation environments on single-cell physiology. *Lab Chip* 15(8):1822–1834
28. Dusny C, Schmid A (2015) Challenging biological limits with microfluidic single cell analysis. *Microb Biotechnol* 8(1):23–25
29. Dusny C, Schmid A (2015) Microfluidic single-cell analysis links boundary environments and individual microbial phenotypes. *Environ Microbiol* 17(6):1839–1856
30. Klumpp S, Hwa T (2014) Bacterial growth: global effects on gene expression, growth feedback and proteome partition. *Curr Opin Biotechnol* 28:96–102
31. Klumpp S (2011) Growth-rate dependence reveals design principles of plasmid copy number control. *PLoS One* 6(5):e20403
32. Ullman G, Wallden M, Marklund EG, Mahmutovic A, Razinkov I, Elf J (2013) High-throughput gene expression analysis at the level of single proteins using a microfluidic turbidostat and automated cell tracking. *Philos Trans R Soc B* 368(1611):20120025
33. Klumpp S, Zhang ZG, Hwa T (2009) Growth rate-dependent global effects on gene expression in bacteria. *Cell* 139(7):1366–1375
34. Moffitt JR, Lee JB, Cluzel P (2012) The single-cell chemostat: an agarose-based, microfluidic device for high-throughput, single-cell studies of bacteria and bacterial communities. *Lab Chip* 12(8):1487–1494
35. Lee SS, Avalos Vizcarra I, Huberts DH, Lee LP, Heinemann M (2012) Whole lifespan microscopic observation of budding yeast aging through a microfluidic dissection platform. *Proc Natl Acad Sci U S A* 109(13):4916–4920
36. Wang P, Robert L, Pelletier J, Dang WL, Taddei F, Wright A, Jun S (2010) Robust growth of *Escherichia coli*. *Curr Biol* 20(12):1099–1103
37. Dusny C, Fritsch FS, Frick O, Schmid A (2012) Isolated microbial single cells and resulting micropopulations grow faster in controlled environments. *Appl Environ Microbiol* 78(19):7132–7136
38. Sweedler JV, Arriaga EA (2007) Single cell analysis. *Anal Bioanal Chem* 387(1):1–2
39. Boulineau S, Tostevin F, Kiviet DJ, ten Wolde PR, Nghe P, Tans SJ (2013) Single-cell dynamics reveals sustained growth during diauxic shifts. *PLoS One* 8(4):1–9
40. Mannik J, Wu F, Hol FJ, Bisicchia P, Sherratt DJ, Keymer JE, Dekker C (2012) Robustness and accuracy of cell division in *Escherichia coli* in diverse cell shapes. *Proc Natl Acad Sci U S A* 109(18):6957–6962
41. Balaban NQ, Merrin J, Chait R, Kowalik L, Leibler S (2004) Bacterial persistence as a phenotypic switch. *Science* 305(5690):1622–1625
42. Evans SN, Ralph PL, Schreiber SJ, Sen A (2013) Stochastic population growth in spatially heterogeneous environments. *J Math Biol* 66(3):423–476
43. Gefen O, Balaban NQ (2009) The importance of being persistent: heterogeneity of bacterial populations under antibiotic stress. *FEMS Microbiol Rev* 33(4):704–717
44. Gefen O, Gabay C, Mumcuoglu M, Engel G, Balaban NQ (2008) Single-cell protein induction dynamics reveals a period of vulnerability to antibiotics in persister bacteria. *Proc Natl Acad Sci U S A* 105(16):6145–6149
45. Li B, Qiu Y, Glidle A, Cooper J, Shi H, Yin H (2014) Single cell growth rate and morphological dynamics revealing an "opportunistic" persistence. *Analyst* 139(13):3305–3313
46. Lidstrom ME, Konopka MC (2010) The role of physiological heterogeneity in microbial population behavior. *Nat Chem Biol* 6(10):705–712
47. Dusny C, Gruenberger A, Probst C, Wiechert W, Kohlheyer D, Schmid A (2015) Technical bias of microcultivation environments on single-cell physiology. *Lab Chip* 15(8):1822–1834

48. Bryan AK, Hecht VC, Shen WJ, Payer K, Grover WH, Manalis SR (2014) Measuring single cell mass, volume, and density with dual suspended microchannel resonators. *Lab Chip* 14 (3):569–576
49. Bryan AK, Engler A, Gulati A, Manalis SR (2012) Continuous and long-term volume measurements with a commercial coulter counter. *PLoS One* 7(1):e29866
50. Schaechter M (2015) A brief history of bacterial growth physiology. *Front Microbiol* 6:289
51. Schaechter M, Williamson JP, Hood Jr JR, Koch AL (1962) Growth, cell and nuclear divisions in some bacteria. *J Gen Microbiol* 29:421–434
52. Schaechter M, Maaloe O, Kjeldgaard NO (1958) Dependency on medium and temperature of cell size and chemical composition during balanced growth of *Salmonella typhimurium*. *J Gen Microbiol* 19(3):592–606
53. Kjeldgaard NO, Maaloe O, Schaechter M (1958) The transition between different physiological states during balanced growth of *Salmonella typhimurium*. *J Gen Microbiol* 19 (3):607–616
54. Dal Co A, van Vliet S, Ackermann M (2019) Emergent microscale gradients give rise to metabolic cross-feeding and antibiotic tolerance in clonal bacterial populations. *Philos Trans R Soc Lond Ser B Biol Sci* 374(1786):20190080
55. Gruenberger A, Probst C, Heyer A, Wiechert W, Frunzke J, Kohlheyer D (2013) Microfluidic picoliter bioreactor for microbial single-cell analysis: fabrication, system setup, and operation. *J Vis Exp JoVE* 82:50560
56. Saeki T, Hosokawa M, Lim TK, Harada M, Matsunaga T, Tanaka T (2014) Digital cell counting device integrated with a single-cell array. *PLoS One* 9(2):e89011
57. Lu H, Caen O, Vrignon J, Zonta E, El Harrak Z, Nizard P, Baret JC, Taly V (2017) High throughput single cell counting in droplet-based microfluidics. *Sci Rep* 7(1):1366
58. Peitz I, van Leeuwen R (2010) Single-cell bacteria growth monitoring by automated DEP-facilitated image analysis. *Lab Chip* 10(21):2944–2951
59. Grunberger A, Paczia N, Probst C, Schendzielorz G, Eggeling L, Noack S, Wiechert W, Kohlheyer D (2012) A disposable picolitre bioreactor for cultivation and investigation of industrially relevant bacteria on the single cell level. *Lab Chip* 12(11):2060–2068
60. Grunberger A, van Ooyen J, Paczia N, Rohe P, Schendzielorz G, Eggeling L, Wiechert W, Kohlheyer D, Noack S (2013) Beyond growth rate 0.6: *Corynebacterium glutamicum* cultivated in highly diluted environments. *Biotechnol Bioeng* 110(1):220–228
61. Hammar P, Angermayr SA, Sjostrom SL, van der Meer J, Hellingwerf KJ, Hudson EP, Joensson HN (2015) Single-cell screening of photosynthetic growth and lactate production by cyanobacteria. *Biotechnol Biofuels* 8:193
62. Probst C, Grunberger A, Wiechert W, Kohlheyer D (2013) Microfluidic growth chambers with optical tweezers for full spatial single-cell control and analysis of evolving microbes. *J Microbiol Method* 95(3):470–476
63. Probst C, Grunberger A, Wiechert W, Kohlheyer D (2013) Polydimethylsiloxane (PDMS) sub-micron traps for single-cell analysis of bacteria. *Micromachines-Basel* 4(4):357–369
64. Harris LK, Theriot JA (2018) Surface area to volume ratio: a natural variable for bacterial morphogenesis. *Trends Microbiol* 26(10):815–832
65. Rosenthal K, Falke F, Frick O, Dusny C, Schmid A (2015) An inert continuous microreactor for the isolation and analysis of a single microbial cell. *Micromachines-Basel* 6 (12):1836–1855
66. Taheri-Araghi S, Bradde S, Sauls JT, Hill NS, Levin PA, Paulsson J, Vergassola M, Jun S (2015) Cell-size control and homeostasis in bacteria. *Curr Biol* 25(3):385–391
67. Wang Z (2019) Cell segmentation for image cytometry: advances, insufficiencies, and challenges. *Cytometry A* 95(7):708–711
68. Leygeber M, Lindemann D, Sachs CC, Kaganovitch E, Wiechert W, Noh K, Kohlheyer D (2019) Analyzing microbial population heterogeneity-expanding the toolbox of microfluidic single-cell cultivations. *J Mol Biol* 431(23):4569–4588

69. Sliusarenko O, Heinritz J, Emonet T, Jacobs-Wagner C (2011) High-throughput, subpixel precision analysis of bacterial morphogenesis and intracellular spatio-temporal dynamics. *Mol Microbiol* 80(3):612–627
70. Garner EC (2011) MicrobeTracker: quantitative image analysis designed for the smallest organisms. *Mol Microbiol* 80(3):577–579
71. Campos M, Surovtsev IV, Kato S, Paintdakhi A, Beltran B, Ebmeier SE, Jacobs-Wagner C (2014) A constant size extension drives bacterial cell size homeostasis. *Cell* 159(6):1433–1446
72. Paintdakhi A, Parry B, Campos M, Irnov I, Elf J, Surovtsev I, Jacobs-Wagner C (2016) Outfit: an integrated software package for high-accuracy, high-throughput quantitative microscopy analysis. *Mol Microbiol* 99(4):767–777
73. Ducret A, Quardokus EM, Brun YV (2016) MicrobeJ, a tool for high throughput bacterial cell detection and quantitative analysis. *Nat Microbiol* 1(7):16077
74. Sachs CC, Grunberger A, Helfrich S, Probst C, Wiechert W, Kohlheyer D, Noh K (2016) Image-based single cell profiling: high-throughput processing of mother machine experiments. *PLoS One* 11(9):e0163453
75. Popescu G, Park K, Mir M, Bashir R (2014) New technologies for measuring single cell mass. *Lab Chip* 14(4):646–652
76. Popescu G (2008) Quantitative phase imaging of nanoscale cell structure and dynamics. *Methods Cell Biol* 90:87–115
77. Popescu G, Park Y, Lue N, Best-Popescu C, Deflores L, Dasari RR, Feld MS, Badizadegan K (2008) Optical imaging of cell mass and growth dynamics. *Am J Physiol Cell Physiol* 295(2):C538–C544
78. Phillips KG, Jacques SL, McCarty OJ (2012) Measurement of single cell refractive index, dry mass, volume, and density using a transillumination microscope. *Phys Rev Lett* 109(11):118105
79. Zangle TA, Chun J, Zhang J, Reed J, Teitell MA (2013) Quantification of biomass and cell motion in human pluripotent stem cell colonies. *Biophys J* 105(3):593–601
80. Chun J, Zangle TA, Kolarova T, Finn RS, Teitell MA, Reed J (2012) Rapidly quantifying drug sensitivity of dispersed and clumped breast cancer cells by mass profiling. *Analyst* 137(23):5495–5498
81. Reed J, Troke JJ, Schmit J, Han S, Teitell MA, Gimzewski JK (2008) Live cell interferometry reveals cellular dynamics during force propagation. *ACS Nano* 2(5):841–846
82. Mir M, Wang Z, Shen Z, Bednarz M, Bashir R, Golding I, Prasanth SG, Popescu G (2011) Optical measurement of cycle-dependent cell growth. *Proc Natl Acad Sci U S A* 108(32):13124–13129
83. Cotte Y, Toy F, Jourdain P, Pavillon N, Boss D, Magistretti P, Marquet P, Depeursinge C (2013) Marker-free phase nanoscopy. *Nat Photonics* 7(2):113–117
84. Mir M, Babacan SD, Bednarz M, Do MN, Golding I, Popescu G (2012) Visualizing *Escherichia coli* sub-cellular structure using sparse deconvolution spatial light interference tomography. *PLoS One* 7(6):e39816
85. Johnson BN, Mutharasan R (2012) Biosensing using dynamic-mode cantilever sensors: a review. *Biosens Bioelectron* 32(1):1–18
86. Martinez-Martin D, Flaschner G, Gaub B, Martin S, Newton R, Beerli C, Mercer J, Gerber C, Muller DJ (2017) Inertial picobalance reveals fast mass fluctuations in mammalian cells. *Nature* 550(7677):500
87. Godin M, Delgado FF, Son SM, Grover WH, Bryan AK, Tzur A, Jorgensen P, Payer K, Grossman AD, Kirschner MW, Manalis SR (2010) Using buoyant mass to measure the growth of single cells. *Nat Methods* 7(5):387–390
88. Godin M, Bryan AK, Burg TP, Babcock K, Manalis SR (2007) Measuring the mass, density, and size of particles and cells using a suspended microchannel resonator. *Appl Phys Lett* 91(12):123121
89. Son S, Tzur A, Weng Y, Jorgensen P, Kim J, Kirschner MW, Manalis SR (2012) Direct observation of mammalian cell growth and size regulation. *Nat Methods* 9(9):910–912

90. Ilic B, Czaplowski D, Zalalutdinov M, Craighead HG, Neuzil P, Campagnolo C, Batt C (2001) Single cell detection with micromechanical oscillators. *J Vac Sci Technol B* 19(6):2825–2828
91. Weng Y, Delgado FF, Son S, Burg TP, Wasserman SC, Manalis SR (2011) Mass sensors with mechanical traps for weighing single cells in different fluids. *Lab Chip* 11(24):4174–4180
92. Zangle TA, Teitell MA (2014) Live-cell mass profiling: an emerging approach in quantitative biophysics. *Nat Methods* 11(12):1221–1228
93. Bryan AK, Goranov A, Amon A, Manalis SR (2010) Measurement of mass, density, and volume during the cell cycle of yeast. *Proc Natl Acad Sci U S A* 107(3):999–1004
94. Lewis CL, Craig CC, Senecal AG (2014) Mass and density measurements of live and dead gram-negative and gram-positive bacterial populations. *Appl Environ Microbiol* 80(12):3622–3631
95. Ackermann M (2015) A functional perspective on phenotypic heterogeneity in microorganisms. *Nat Rev Microbiol* 13(8):497–508
96. Baumann K, Maurer M, Dragosits M, Cos O, Ferrer P, Mattanovich D (2008) Hypoxic fed-batch cultivation of *Pichia pastoris* increases specific and volumetric productivity of recombinant proteins. *Biotechnol Bioeng* 100(1):177–183
97. Chen BY, You JW, Hsieh YT, Chang JS (2008) Feasibility study of exponential feeding strategy in fed-batch cultures for phenol degradation using *Cupriavidus taiwanensis*. *Biochem Eng J* 41(2):175–180
98. d'Anjou MC, Daugulis AJ (2000) Mixed-feed exponential feeding for fed-batch culture of recombinant methylotrophic yeast. *Biotechnol Lett* 22(5):341–346
99. Stryhanyuk H, Calabrese F, Kummel S, Musat F, Richnow HH, Musat N (2018) Calculation of single cell assimilation rates from SIP-NanoSIMS-derived isotope ratios: a comprehensive approach. *Front Microbiol* 9:2342
100. Sengupta D, Mongersun A, Kim TJ, Mongersun K, von Eyben R, Abbyad P, Pratz G (2019) Multiplexed single-cell measurements of FDG uptake and lactate release using droplet microfluidics. *Technol Cancer Res Trans* 18
101. Hehemann JH, Reintjes G, Klassen L, Smith AD, Ndeh D, Arnosti C, Amann R, Abbott DW (2019) Single cell fluorescence imaging of glycan uptake by intestinal bacteria. *ISME J* 13(7):1883–1889
102. Sung Y, Tetrault MA, Takahashi K, Ouyang J, Pratz G, Fakhri GE, Normandin MD (2020) Dependence of fluorodeoxyglucose (FDG) uptake on cell cycle and dry mass: a single-cell study using a multi-modal radiography platform. *Sci Rep* 10(1):4280
103. Achilles J, Muller S, Bley T, Babel W (2004) Affinity of single *S. cerevisiae* cells to 2-NBDglucose under changing substrate concentrations. *Cytom Part A* 61A(1):88–98
104. VanEngelenburg SB, Palmer AE (2008) Fluorescent biosensors of protein function. *Curr Opin Chem Biol* 12(1):60–65
105. Otten J, Tenhaef N, Jansen RP, Dobber J, Jungbluth L, Noack S, Oldiges M, Wiechert W, Pohl M (2019) A FRET-based biosensor for the quantification of glucose in culture supernatants of mL scale microbial cultivations. *Microb Cell Factories* 18(1)
106. Fehr M, Frommer WB, Lalonde S (2002) Visualization of maltose uptake in living yeast cells by fluorescent nanosensors. *Proc Natl Acad Sci U S A* 99(15):9846–9851
107. Nikolic N, Barner T, Ackermann M (2013) Analysis of fluorescent reporters indicates heterogeneity in glucose uptake and utilization in clonal bacterial populations. *BMC Microbiol* 13:258
108. Musat N, Foster R, Vagner T, Adam B, Kuypers MM (2012) Detecting metabolic activities in single cells, with emphasis on nanoSIMS. *FEMS Microbiol Rev* 36(2):486–511
109. Schoffelen NJ, Mohr W, Ferdelman TG, Littmann S, Duerschlag J, Zubkov MV, Ploug H, Kuypers MM (2018) Single-cell imaging of phosphorus uptake shows that key harmful algae rely on different phosphorus sources for growth. *Sci Rep* 8
110. Straeuber H, Huebschmann T, Jehmlich N, Schmidt F, von Bergen M, Harms H, Mueller S (2010) NBDT (3-(N-(7-nitrobenz-2-oxa-1,3-diazol-4-yl)amino)-3-toluene) – a novel

- fluorescent dye for studying mechanisms of toluene uptake into vital bacteria. *Cytometry A* 77 (2):113–120
111. Natarajan A, Srien F (2000) Glucose uptake rates of single *E. coli* cells grown in glucose-limited chemostat cultures. *J Microbiol Methods* 42(1):87–96
 112. Natarajan A, Srien F (1999) Dynamics of glucose uptake by single *Escherichia coli* cells. *Metab Eng* 1(4):320–333
 113. Heuker M, Sijbesma JWA, Suarez RA, de Jong JR, Boersma HH, Luurtsema G, Elsinga PH, Glaudemans AWJM, van Dam GM, van Dijk JM, Slart RHJA, van Oosten M (2017) In vitro imaging of bacteria using F-18-fluorodeoxyglucose micro positron emission tomography. *Sci Rep* 7:1–9
 114. Berg J, Hung YP, Yellen G (2009) A genetically encoded fluorescent reporter of ATP:ADP ratio. *Nat Methods* 6(2):161–166
 115. Yaginuma H, Kawai S, Tabata KV, Tomiyama K, Kakizuka A, Komatsuzaki T, Noji H, Imamura H (2014) Diversity in ATP concentrations in a single bacterial cell population revealed by quantitative single-cell imaging. *Sci Rep* 4:6522
 116. Boersma AJ, Zuhorn IS, Poolman B (2015) A sensor for quantification of macromolecular crowding in living cells. *Nat Methods* 12(3):227–229
 117. Ha JS, Song JJ, Lee YM, Kim SJ, Sohn JH, Shin CS, Lee SG (2007) Design and application of highly responsive fluorescence resonance energy transfer biosensors for detection of sugar in living *Saccharomyces cerevisiae* cells. *Appl Environ Microbiol* 73(22):7408–7414
 118. Kaper T, Lager I, Looger LL, Chermak D, Frommer WB (2008) Fluorescence resonance energy transfer sensors for quantitative monitoring of pentose and disaccharide accumulation in bacteria. *Biotechnol Biofuels* 1(1):11
 119. Nikolic N, Schreiber F, Dal Co A, Kiviet DJ, Bergmiller T, Littmann S, Kuypers MMM, Ackermann M (2017) Cell-to-cell variation and specialization in sugar metabolism in clonal bacterial populations. *PLoS Genet* 13(12):e1007122
 120. Worrich A, Stryhanyuk H, Musat N, Konig S, Banitz T, Centler F, Frank K, Thullner M, Harms H, Richnow HH, Miltner A, Kastner M, Wick LY (2017) Mycelium-mediated transfer of water and nutrients stimulates bacterial activity in dry and oligotrophic environments. *Nat Commun* 8:1–9
 121. Kopf SH, McGlynn SE, Green-Saxena A, Guan YB, Newman DK, Orphan VJ (2015) Heavy water and N-15 labelling with NanoSIMS analysis reveals growth rate-dependent metabolic heterogeneity in chemostats. *Environ Microbiol* 17(7):2542–2556
 122. Lindemann D, Westerwalbesloh C, Kohlheyer D, Grunberger A, von Lieres E (2019) Microbial single-cell growth response at defined carbon limiting conditions. *RSC Adv* 9 (25):14040–14050
 123. Binder D, Drepper T, Jaeger KE, Delvigne F, Wiechert W, Kohlheyer D, Grunberger A (2017) Homogenizing bacterial cell factories: analysis and engineering of phenotypic heterogeneity. *Metab Eng* 42:145–156
 124. Xiao Y, Bowen CH, Liu D, Zhang F (2016) Exploiting nongenetic cell-to-cell variation for enhanced biosynthesis. *Nat Chem Biol* 12(5):339–344
 125. Manafi M, Kneifel W, Bascomb S (1991) Fluorogenic and chromogenic substrates used in bacterial diagnostics. *Microbiol Rev* 55(3):335–348
 126. Binder S, Schendzielorz G, Stabler N, Krumbach K, Hoffmann K, Bott M, Eggeling L (2012) A high-throughput approach to identify genomic variants of bacterial metabolite producers at the single-cell level. *Genome Biol* 13(5):R40
 127. Schendzielorz G, Dippong M, Grunberger A, Kohlheyer D, Yoshida A, Binder S, Nishiyama C, Nishiyama M, Bott M, Eggeling L (2013) Taking control over control: use of product sensing in single cells to remove flux control at key enzymes in biosynthesis pathways. *ACS Synth Biol* 3:21–29
 128. Love KR, Panagiotou V, Jiang B, Stadheim TA, Love JC (2010) Integrated single-cell analysis shows *Pichia pastoris* secretes protein stochastically. *Biotechnol Bioeng* 106(2):319–325

129. Love KR, Politano TJ, Panagiotou V, Jiang B, Stadheim TA, Love JC (2012) Systematic single-cell analysis of *Pichia pastoris* reveals secretory capacity limits productivity. *PLoS One* 7(6):e37915
130. Mazutis L, Gilbert J, Ung WL, Weitz DA, Griffiths AD, Heyman JA (2013) Single-cell analysis and sorting using droplet-based microfluidics. *Nat Protoc* 8(5):870–891
131. Wang BL, Ghaderi A, Zhou H, Agresti J, Weitz DA, Fink GR, Stephanopoulos G (2014) Microfluidic high-throughput culturing of single cells for selection based on extracellular metabolite production or consumption. *Nat Biotechnol* 32(5):473–478
132. El Debs B, Utharala R, Balyasnikova IV, Griffiths AD, Merten CA (2012) Functional single-cell hybridoma screening using droplet-based microfluidics. *Proc Natl Acad Sci U S A* 109(29):11570–11575
133. Sjoström SL, Bai Y, Huang M, Liu Z, Nielsen J, Joensson HN, Andersson Svahn H (2014) High-throughput screening for industrial enzyme production hosts by droplet microfluidics. *Lab Chip* 14(4):806–813
134. Prodanovic R, Ung WL, Durdic KI, Fischer R, Weitz DA, Ostafe R (2020) A high-throughput screening system based on droplet microfluidics for glucose oxidase gene libraries. *Molecules* 25(10):2418
135. Amantonico A, Urban PL, Zenobi R (2010) Analytical techniques for single-cell metabolomics: state of the art and trends. *Anal Bioanal Chem* 398:2493–2504
136. Heinemann M, Zenobi R (2011) Single cell metabolomics. *Curr Opin Biotechnol* 22(1):26–31
137. Zenobi R (2013) Single-cell metabolomics: analytical and biological perspectives. *Science* 342(6163):1201–1211
138. Dusny C, Lohse M, Reemtsma T, Schmid A, Lechtenfeld OJ (2019) Quantifying a biocatalytic product from a few living microbial cells using microfluidic cultivation coupled to FT-ICR-MS. *Anal Chem* 91(11):7012–7018
139. Fritzsche FS, Rosenthal K, Kampert A, Howitz S, Dusny C, Blank LM, Schmid A (2013) Picoliter nDEP traps enable time-resolved contactless single bacterial cell analysis in controlled microenvironments. *Lab Chip* 13(3):397–408
140. Kortmann H, Chasanis P, Blank LM, Franzke J, Kenig E, Schmid A (2009) The envirostat – a new bioreactor concept. *Lab Chip* 9(4):576–585
141. Haidas D, Bachler S, Kohler M, Blank LM, Zenobi R, Dittrich PS (2019) Microfluidic platform for multimodal analysis of enzyme secretion in nanoliter droplet arrays. *Anal Chem* 91(3):2066–2073
142. Haidas D, Napiorkowska M, Schmitt S, Dittrich PS (2020) Parallel sampling of nanoliter droplet arrays for noninvasive protein analysis in discrete yeast cultivations by MALDI-MS. *Anal Chem* 92(5):3810–3818
143. Ibanez AJ, Fagerer SR, Schmidt AM, Urban PL, Jefimovs K, Geiger P, Dechant R, Heinemann M, Zenobi R (2013) Mass spectrometry-based metabolomics of single yeast cells. *Proc Natl Acad Sci U S A* 110(22):8790–8794
144. Urban PL, Schmidt AM, Fagerer SR, Amantonico A, Ibanez A, Jefimovs K, Heinemann M, Zenobi R (2011) Carbon¹³ labelling strategy for studying the ATP metabolism in individual yeast cells by micro-arrays for mass spectrometry. *Mol BioSyst* 7(10):2837–2840
145. Elowitz MB, Levine AJ, Siggia ED, Swain PS (2002) Stochastic gene expression in a single cell. *Science* 297(5584):1183–1186
146. Ozbudak EM, Thattai M, Kurtser I, Grossman AD, van Oudenaarden A (2002) Regulation of noise in the expression of a single gene. *Nat Genet* 31(1):69–73
147. Swain PS, Elowitz MB, Siggia ED (2002) Intrinsic and extrinsic contributions to stochasticity in gene expression. *Proc Natl Acad Sci U S A* 99(20):12795–12800
148. Meng TC, Somani S, Dhar P (2004) Modeling and simulation of biological systems with stochasticity. *In Silico Biol* 4(3):293–309
149. Thattai M, van Oudenaarden A (2004) Stochastic gene expression in fluctuating environments. *Genetics* 167(1):523–530

150. Kaern M, Elston TC, Blake WJ, Collins JJ (2005) Stochasticity in gene expression: from theories to phenotypes. *Nat Rev Genet* 6(6):451–464
151. Kussell E, Leibler S (2005) Phenotypic diversity, population growth, and information in fluctuating environments. *Science* 309(5743):2075–2078
152. Raser JM, O'Shea EK (2005) Noise in gene expression: origins, consequences, and control. *Science* 309(5743):2010–2013
153. Yu J, Xiao J, Ren XJ, Lao KQ, Xie XS (2006) Probing gene expression in live cells, one protein molecule at a time. *Science (New York, NY)* 311(5767):1600–1603
154. Lindmeyer M, Jahn M, Vorpahl C, Muller S, Schmid A, Buhler B (2015) Variability in subpopulation formation propagates into biocatalytic variability of engineered *Pseudomonas putida* strains. *Front Microbiol* 6:1042
155. Nikel PI, Silva-Rocha R, Benedetti I, de Lorenzo V (2014) The private life of environmental bacteria: pollutant biodegradation at the single cell level. *Environ Microbiol* 16(3):628–642
156. Gefen O, Fridman O, Ronin I, Balaban NQ (2014) Direct observation of single stationary-phase bacteria reveals a surprisingly long period of constant protein production activity. *Proc Natl Acad Sci U S A* 111(1):556–561
157. Stricker J, Maddox P, Salmon ED, Erickson HP (2002) Rapid assembly dynamics of the *Escherichia coli* FtsZ-ring demonstrated by fluorescence recovery after photobleaching. *Proc Natl Acad Sci U S A* 99(5):3171–3175
158. Dai J, Yoon SH, Sim HY, Yang YS, Oh TK, Kim JF, Hong JW (2013) Charting microbial phenotypes in multiplex nanoliter batch bioreactors. *Anal Chem* 85(12):5892–5899
159. Sun YQ, Casella S, Fang Y, Huang F, Faulkner M, Barrett S, Liu LN (2016) Light modulates the biosynthesis and organization of cyanobacterial carbon fixation machinery through photosynthetic electron flow. *Plant Physiol* 171(1):530–541
160. Long ZC, Olliver A, Brambilla E, Sclavi B, Lagomarsino MC, Dorfman KD (2014) Measuring bacterial adaptation dynamics at the single-cell level using a microfluidic chemostat and time-lapse fluorescence microscopy. *Analyst* 139(20):5254–5262
161. Kimmerling RJ, Prakadan SM, Gupta AJ, Calistri NL, Stevens MM, Olcum S, Cermak N, Drake RS, Pelton K, De Smet F, Ligon KL, Shalek AK, Manalis SR (2018) Linking single-cell measurements of mass, growth rate, and gene expression. *Genome Biol* 19(1):207
162. Friedman N, Vardi S, Ronen M, Alon U, Stavans J (2005) Precise temporal modulation in the response of the SOS DNA repair network in individual bacteria. *PLoS Biol* 3(7):e238
163. Bennett MR, Hasty J (2009) Microfluidic devices for measuring gene network dynamics in single cells. *Nat Rev Genet* 10(9):628–638
164. Ma Z, Chu PM, Su Y, Yu Y, Wen H, Fu X, Huang S (2019) Applications of single-cell technology on bacterial analysis. *Quant Biol* 7(3):171–181
165. Stratz S, Eyer K, Kurth F, Dittrich PS (2014) On-chip enzyme quantification of single *Escherichia coli* bacteria by immunoassay-based analysis. *Anal Chem* 86(24):12375–12381
166. Dusny C, Schmid A (2016) The *MOX* promoter in *Hansenula polymorpha* is ultrasensitive to glucose-mediated carbon catabolite repression. *FEMS Yeast Res* 16(6):fow067
167. Taheri-Araghi S, Brown SD, Sauls JT, McIntosh DB, Jun S (2015) Single-cell physiology. *Annu Rev Biophys* 44:123–142
168. Langdahl BR, Ingvorsen K (1997) Temperature characteristics of bacterial iron solubilisation and C-14 assimilation in naturally exposed sulfide ore material at Citronen fjord, North Greenland (83 degrees N). *FEMS Microbiol Ecol* 23(4):275–283
169. Zipfel WR, Williams RM, Webb WW (2003) Nonlinear magic: multiphoton microscopy in the biosciences. *Nat Biotechnol* 21(11):1369–1377
170. Davies MJ (2004) Reactive species formed on proteins exposed to singlet oxygen. *Photochem Photobiol Sci* 3(1):17–25
171. Merbt SN, Stahl DA, Casamayor EO, Marti E, Nicol GW, Prosser JI (2012) Differential photoinhibition of bacterial and archaeal ammonia oxidation. *FEMS Microbiol Lett* 327(1):41–46

172. Woodward JR, Cirillo VP, Edmunds LN (1978) Light effects in yeast – inhibition by visible light of growth and transport in *Saccharomyces cerevisiae* grown at low temperatures. *J Bacteriol* 133(2):692–698
173. Tinevez JY, Dragavon J, Baba-Aissa L, Roux P, Perret E, Canivet A, Galy V, Shorte S (2012) A quantitative method for measuring phototoxicity of a live cell imaging microscope. *Method Enzymol* 506:291–309
174. Jun S, Taheri-Araghi S (2015) Cell-size maintenance: universal strategy revealed. *Trends Microbiol* 23(1):4–6
175. Frigault MM, Lacoste J, Swift JL, Brown CM (2009) Live-cell microscopy – tips and tools. *J Cell Sci* 122(Pt 6):753–767
176. Dixit R, Cyr R (2003) Cell damage and reactive oxygen species production induced by fluorescence microscopy: effect on mitosis and guidelines for non-invasive fluorescence microscopy. *Plant J* 36(2):280–290
177. Hebisch E, Knebel J, Landsberg J, Frey E, Leisner M (2013) High variation of fluorescence protein maturation times in closely related *Escherichia coli* strains. *PLoS One* 8(10):e75991
178. Andersen JB, Sternberg C, Poulsen LK, Bjorn SP, Givskov M, Molin S (1998) New unstable variants of green fluorescent protein for studies of transient gene expression in bacteria. *Appl Environ Microbiol* 64(6):2240–2246
179. McGinness KE, Baker TA, Sauer RT (2006) Engineering controllable protein degradation. *Mol Cell* 22(5):701–707
180. Terai T, Nagano T (2013) Small-molecule fluorophores and fluorescent probes for bioimaging. *Pflugers Arch* 465(3):347–359

Analytics in Microfluidic Systems



Martina Viefhues

Contents

1	Introduction	192
2	Theory of Analytical Methods	195
2.1	Electrophoresis	195
2.2	Dielectrophoresis	196
2.3	Electric Impedance Analysis	198
3	Applications of Analytical Methods	199
3.1	Electrophoretic Analysis	199
3.2	Dielectrophoretic Analysis	200
3.3	Electric Impedance Analysis	202
4	Conclusion	204
	References	204

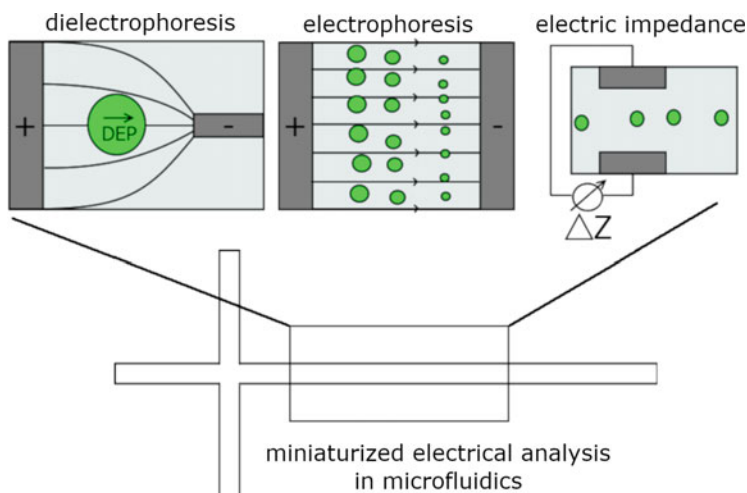
Abstract Microfluidic analysis proved to be very sufficient in supporting biotechnological studies. This is due to the wide range of new analysis methods that provide further insight into biotechnological questions but also to intrinsic advantages of the systems themselves. To name two of them, only very small sample amounts are needed, and the analytics are very fast. In this overview paper, microfluidic analysis methods are introduced with a special focus on electric analysis methods. The aim of this work is to shed light on the special advantages of miniaturized electrical analysis in microfluidics; the main theoretical aspects of the methods are given together with the potential scientific insight that can be gained by the respective methods.

M. Viefhues (✉)

Experimental Biophysics and Applied Nanosciences, Faculty of Physics, Bielefeld University,
Bielefeld, Germany

e-mail: viefhues@physik.uni-bielefeld.de

Graphical Abstract



Keywords Analysis, Dielectrophoresis, Electric impedance, Electrophoresis, Microfluidics

1 Introduction

Microfluidic analysis is an emerging field in biotechnology research since the devices with typical dimension in the range of $10\ \mu\text{m}$ to few $100\ \mu\text{m}$ provide several advantages like a small amount of sample and reagents (nl-pl), fast analysis and short reaction times, especially compared to standard bench-top apparatus, access to high automatization, high portability, and last but not least the huge possibility to high-throughput applications [1, 2]. Microfluidics offer manifold opportunities for new insights into biotechnological objectives like optimization of whole cell or biocatalytic production processes. The methods include inter alia studies of environment impact on (single) cells or characterization of new biocatalysts [3–8], separation and purification of samples [9–14], and determination of numerous, specific parameters, e.g., dielectric properties, enzymatic productivity, or cell viability [11, 15].

Some of the used methods are miniaturizations of well-established methods, like electrophoresis, which offer new advantages after miniaturization in microfluidics. Other methods used for analysis in microfluidics rely on the small dimensions that lead to new effects, e.g., dielectrophoresis or acoustophoresis [16–21]. In 2013, Dorfman et al. reviewed microfluidic analysis methods that go beyond electrophoresis and discussed their respective advantages [22]. Various analysis methods have been developed in the past years for microfluidic applications like electric analysis with, inter alia, electrophoresis, Fig. 1b, dielectrophoresis, Fig. 1a, or electric

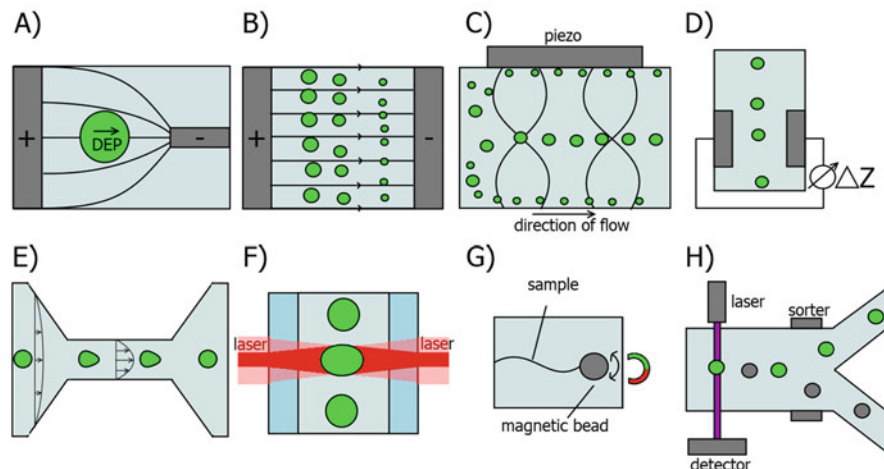


Fig. 1 Overview of selected microfluidic analysis methods, the samples are indicated in green, respectively. **(a)** Dielectrophoresis in inhomogeneous electric fields; **(b)** electrophoresis in homogeneous electric fields; **(c)** acoustophoresis exploiting standing waves generated by piezo elements; **(d)** electric impedance analysis measuring the changed impedance; **(e)** hydrodynamic deformation, exploiting fast changes in velocity; **(f)** optical stretching in counter-propagating lasers; **(g)** magnetic tweezers with magnetic bead applying rotational forces to the sample; **(h)** fluorescence activated cell sorting

impedance, Fig. 1d analysis; fluorescence analysis with, e.g., the well-established fluorescence activated cell sorting [23] or specific fluorescence staining to investigate protein expression along cell cycles [24]; and mechanical analysis or separation due to mechanical cell properties, e.g., elasticity, by various approaches like hydrodynamic cell deformation or separation, optical tweezers stretching, or compression [25–29]. In Fig. 1 the microfluidic analysis methods are illustrated.

Acoustophoresis is a technique which uses the density and compressibility properties of elastic samples, e.g., cells, to distinguish different samples both for analysis and separation purposes. The basic principle of acoustophoresis is that high-intensity sound-waves interact with the microfluidic device, i.e., the waves are reflected at the channel walls and establish a standing wave. A strong pressure gradient is generated along the standing wave, which pushes the sample toward specific positions in the channel; see Fig. 1c. The force of the acoustic pressure depends on the sample volume and density, compressibility of the sample and the surrounding medium, and the amplitude of the acoustic wave [30, 31]. The samples remain in the respective fluid stream once positioned by acoustophoresis. Therefore, this method is a very versatile method for cell separation, like separation of red blood cells from whole blood [20].

The analysis method of hydrodynamic deformation exploits changes in shear forces. The changed shear forces can be generated either by the device geometry, i.e., the cross-section changes drastically at certain regions [25], Fig. 1e, or by application of counter flows at channel crossings, e.g., used by Gossett et al.

[28]. In both cases, the cells are affected by fluid forces that stretch the cells over a short period of time. Analysis of the elongation and reshaping provide information about the cells' elasticity [25, 28, 32].

The basic principle of an optical stretcher is the same as for optical tweezers. There, optically transparent objects are manipulated by light due to light diffraction and reflection. If light is refracted or reflected at an interface, its direction of propagation is changed. Therefore, its momentum changes as well. Due to conservation of momentum, some momentum is transferred from the light to the object at which the light is reflected or refracted. Therefore, a force is exerted on the respective object. This can be exploited to move, trap, or stretch an object [29, 33, 34]. The setup of an optical stretcher consists of two counter-propagating laser beams, which each apply a force on the object, Fig. 1f. Cell stretcher can be used, for example, to gain information about cell elasticity as one parameter in medical diagnostics [26, 29, 35].

Magnetic tweezers rely on well-defined external magnetic fields in which magnetic objects are controlled. Paramagnetic beads are bound, often via specific interactions, to samples, which then can be manipulated by the external magnetic fields, Fig. 1g. The samples then can be rotated around axes to apply forces. In 2012 De Vlaminck and Dekker reviewed the advances in magnetic tweezers [36]. Recently, Kreft et al. used magnetic tweezers to investigate the binding mechanism of an anti-cancer chemotherapeutic drug to DNA [37].

Fluorescence-activated cell sorters are a well-established method, which exploits (specific) fluorescence staining of cells to select cells. After a fluorescent signal, over certain threshold, is detected, the respective cells are sorted into different outlets [23, 38–40], Fig. 1h. The cells can be directed into the different outlets either electrically, especially if droplets are used, by dielectrophoresis, or short pressure pulses. Commercially available FACS systems provide very high throughputs of >100,000 cells/s.

Mechanical properties of cells are one parameter to characterize cells regarding their health status. For instance, the cell stiffness of cardiac cells changes if the patient suffers from arrhythmogenic right ventricular cardiomyopathy (ARVC). But also in early terms or preclinical states, the cell stiffness is different from patients without the ARVC disease and thus is one criterion for early diagnostics [41]. The cell stiffness also is a relevant criterion in cancer diagnostics; it is different for healthy cells compared with cancer cells [42, 43]. Thus, novel fast methods to analyze the cell stiffness are a wide field of research in micro-analysis methods. In Table 1 we list analysis methods and the respective analyzed properties. Some of the methods provide access to high throughput analysis.

In this overview paper, the focus is on electric analysis methods in microfluidic systems. The aim of this work is to shed light on the special advantages of miniaturized electrical analysis in microfluidics; the main theoretical aspects of the methods are given together with the potential scientific insight that can be gained by the respective methods.

Table 1 Overview of analysis methods, the analyzed properties of the samples and comments

Method	Analyzed properties	Comments
Electrophoresis	Electrophoretic mobility (size, charges, isoelectric point, etc.)	Often matrices are used to gain a size selectivity; can be used for sample separation; commercial systems available
Dielectrophoresis	Electric polarisability (size, charges, conductivity, species, dead-alive)	Label-free method that can be combined with specific binding to enhance detection sensitivity; can be used for sample separation
Electric impedance analysis	Changes in capacitance and conductivity (e.g., in membranes or cytoplasm)	Label-free method, capable to detect fast changes; commercial systems available
Acoustophoresis	Mechanical properties (stiffness, elasticity, size, density, etc.)	Label-free method allows high throughput analysis; can be used for sample separation
Optical tweezers/stretchers	Mechanical properties (stiffness, elasticity), controlled movement	Can be used with specific binding; high force resolution; high throughput possible with limited force resolution
Magnetic tweezers/stretchers	Mechanical properties (stiffness, elasticity), controlled movement	Often with specific binding to sample; high force resolution; so far no high throughput
Hydrodynamic deformation	Mechanical properties (stiffness, elasticity, size, etc.)	Label-free method; allows high throughput analysis; can be used for sample separation
Fluorescence activated cell sorting	Specific selectivity parameter (differentiation due to fluorescence or diffraction, labeling of proteins, organelles, etc.)	Sample is separated due to set parameter; high throughput achieved >100,000 cells/s; commercial systems available

2 Theory of Analytical Methods

2.1 Electrophoresis

Electrophoresis is a well-established method in biotechnology and can be found in most biotechnological laboratories nowadays. It is a very versatile method to separate samples due to their electrophoretic mobility, i.e., the ability of an object with a net-charge to migrate in a homogeneous electric field. The electrophoretic velocity, \vec{v}_{ep} , can be described by [44].

$$\vec{v}_{ep} = \mu_{ep} \vec{E}$$

with μ_{ep} electrophoretic mobility and \vec{E} electric field.

Some biological molecules, e.g., DNA, exhibit an electrophoretic mobility that is independent of the molecules size in free solution, e.g., in water. Therefore, a size

selective matrix, like a gel or microstructured geometry is necessary for successful electrophoretic separation or analysis of those samples [45]. Here, microfluidics provides the advantage that artificial structures with well-defined geometries can be fabricated and optimized according to the respective sample.

A specific case of electrophoretic separation is the so-called pulsed-field electrophoresis. The orientation of a homogeneous electric field is periodically switched by a specific angle for that electrophoretic approach [46]. This separation concept is used to separate long DNA molecules by size. The size selectivity of the separation is due to the length-dependent reorientation time of the samples in the electric field. For instance, a linear molecule in a fluid is affected by entropic and repulsive forces that lead to a random coil formation [47, 48]. If an electric field is applied to the charged molecule, it will orient, respectively, and migrate in the electric field and, *vice versa*, form a random coil if the electric field is switched off again. The time for processes, orientation, and “recoiling” is length dependent. Therefore, size dependent migration velocity and trajectory angle appear [46].

Besides the application of electrophoresis for sample separation, it is often used in microfluidics to move the samples through the device. Many biological samples have a net charge and thus can be moved by homogeneous electric fields. The electrophoretic migration can be easily combined with other analysis methods, e.g., dielectrophoresis [49], or other migration approaches, e.g., pressure driven flow.

2.2 Dielectrophoresis

Dielectrophoresis is the migration on an electrically polarizable object in an inhomogeneous electric field. The dielectrophoretic force of a homogeneous, spherical particle can be described by [50]:

$$\vec{F}_{\text{DEP}} = \alpha \nabla E^2$$

and the electric polarizability α as

$$\alpha = 4 \pi \epsilon R^3 \Re \left(\frac{\epsilon_p^* - \epsilon_m^*}{\epsilon_p^* + 2\epsilon_m^*} \right)$$

$$\epsilon^* = \epsilon + i \frac{\sigma}{\omega}$$

with $R, \epsilon_{p,m}^*$ the particle radius and complex valued dielectric permittivity of medium and particle, respectively [51]. Thus, it is obvious that the DEP force strongly depends on a particle’s size and on the (di)electric properties. Therefore, analysis of the DEP migration can reveal insight into those parameters, e.g., in study cells [52].

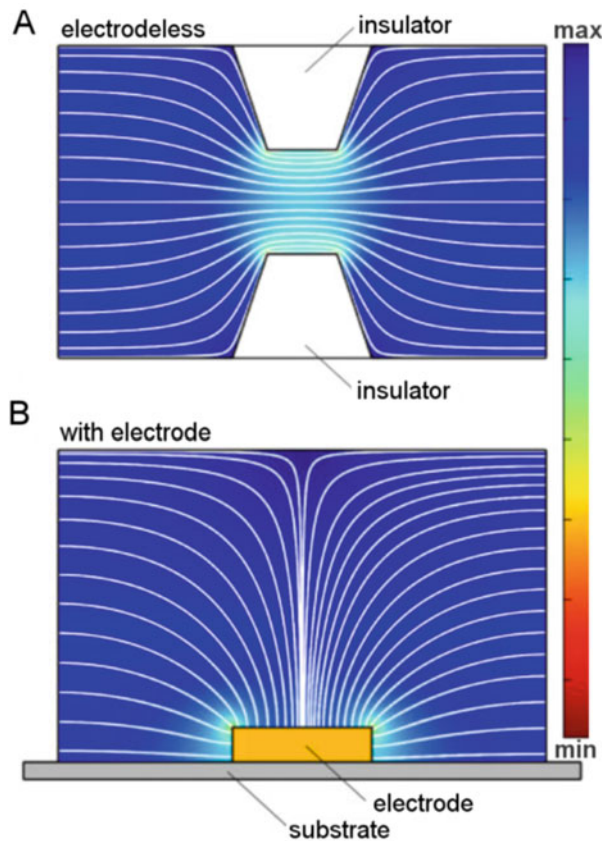
The square proportionality of the DEP force on the electric field provides the advantage that the migration governed by linear electric fields, i.e., electrophoresis and electroosmotic flow, and DEP migration can be decoupled and controlled individually for $U_{AC} \gg U_{DC}$. Therefore, the mean electrokinetic migration can be described by the following equation [51].

$$\vec{u} = (\mu_{eo} + \mu_{ep}) \vec{E}_{DC} + \mu_{DEP} \nabla E_{AC}^2$$

with $\mu_{eo, ep, DEP}$ electroosmotic, electrophoretic, and dielectrophoretic mobility and $E_{DC, AC}$ the DC and AC electric field.

The inhomogeneous electric fields necessary for DEP applications can be generated by different methods; see Fig. 2. Here, the two main approaches are described. The first approach, which is used for a longer period of time, is based on integrated microelectrodes. For instance, a microfluidic channel consists of well-defined microelectrodes, which shape is designed in accordance to the respective application. For the second approach, insulating features are structured in the microfluidic device,

Fig. 2 Illustration of the concepts of electrodeless (a) and microelectrode-based (b) dielectrophoresis. The white lines indicate the electric field lines, and the color code represents E^2 (increasing from blue to yellow). (a) The voltage is applied to the system at electrodes far away from the DEP active region, i.e., usually in the device reservoirs. Adapted from [53] with permission from WILEY-VCH Verlag, Weinheim, copyright 2011



which reduce the channel cross-sectional area. Therefore, the electric field is increased in those regions [53]. The shape of the insulating features is designed according to the respective application, as for the microelectrode approach.

2.3 Electric Impedance Analysis

Electrophoresis and dielectrophoresis are electrical analysis methods that mainly rely on the migration of samples in electric fields, either homogeneous or inhomogeneous. Another analysis method that gives insight into the electric properties of a sample is the electric impedance measurement. Though in that analysis, it is not the migration in an electric field but the complex valued electric resistance that is determined to characterize the dielectric properties of biological samples like cells.

The electric impedance is calculated by dividing a voltage that is applied to a system by the respective current that is measured. The electric impedance Z can be described by [54].

$$Z = Z_0 e^{i\phi} = \frac{U_0}{I_0} e^{i\phi}$$

$$Z_R = R, Z_L = i\omega L, Z_C = \frac{1}{i\omega C}$$

with Z_0 absolute value of impedance, ϕ the phase angle between voltage, U_0 , and current, I_0 , $Z_{R,L,C}$ impedance of an ideal ohmic resistance, conductivity, and capacity, and ω frequency of AC voltage. The impedance value is strongly dependent on the frequency of the AC measurement voltage and thus another criterion for sample characterization. When calculating the theoretical impedance of a measurement system, the same rules apply for calculations of serial or parallel impedances as for calculations of electric resistances. Impedance measurements can be used to gain deeper insight into, e.g., cell cycles or membrane physiologies [55].

An electric impedance measurement setup can be described electrically by the equivalent circuit model in Fig. 3.

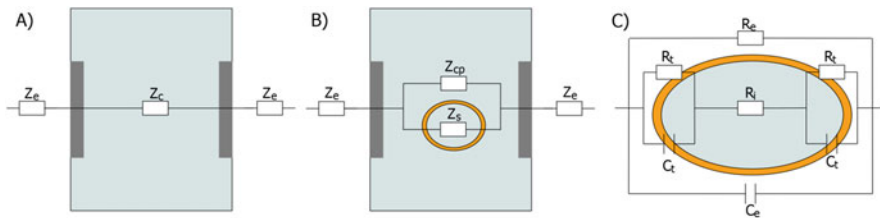


Fig. 3 Scheme of the equivalent circuit model of the measurement setup. (a, b) $Z_{e,c,cp,s}$ are the electric impedances of the electrodes, channel connecting the electrodes, channel parallel to sample, and sample, respectively. (c) Simplified scheme of electric impedance of a cell (orange). $R_{t,e,i}$ are the electric resistances of the cell membrane, inside the cell and outside the cell, respectively. $C_{t,e}$ are the capacitances of the cell membrane and outside of the cell, respectively

3 Applications of Analytical Methods

3.1 Electrophoretic Analysis

Ou et al. just recently reviewed microfluidic applications with electrophoresis for biochemical analysis [9]. The advantages of microfluidic electrophoresis beyond the classical gel plate-based electrophoresis are low sample consumption, fast analysis, sufficient approach for high-throughput analysis, and the capability to couple the method with other analysis methods like, e.g., mass spectrometry [9, 56, 57]. Lechner et al. reviewed capillary electrophoretic applications for analysis of monoclonal antibodies. They described various applications of capillary electrophoresis like zone electrophoresis, isoelectric focusing, or gel capillary electrophoresis; that are techniques well-established in larger gel-plate apparatus, which could be improved along miniaturization [58].

Electrophoretic separation approaches like pulsed-field electrophoresis, in which the orientation of the electric field is changing, provided access to separation of long DNA molecules. But those techniques were very time-consuming in macroscopic gel-based apparatus [59]. In microfluidics, separation matrices, as necessary for DNA electrophoresis, can be well-designed, e.g., by integration of post arrays with distinct radii, distances, and post pattern; see, e.g., Fig. 4a. This provides the ability to optimize the device to the respective separation needs. In 2002, Huang et al. presented a device that sorts large DNA fragments (61–209 kbp) in 15 s [60]. Nazemifard developed a model to describe the motion of DNA molecules through a small, ordered confinement. This enabled further optimization of devices for pulsed-field electrophoresis [61].

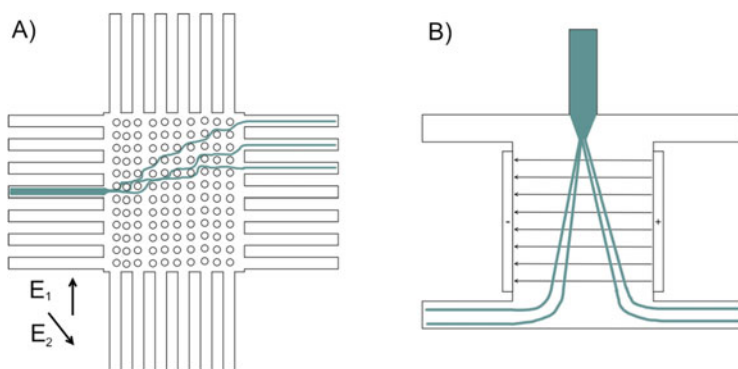


Fig. 4 Schemes of pulsed-field electrophoretic separation (a) and free flow electrophoresis (b). (a) A periodically switching electric field (E_1 and E_2) is applied to drive the sample through an array of posts. The trajectory is due to the respective relaxation and orientation time scale of the molecules and length dependent. The separated samples are harvested in separate collection channels. (b) Samples are continuously separated in a homogeneous electric field perpendicular to the flow direction. The samples migrate according to their respective electrophoretic mobility and are harvested in separate channels

Free flow electrophoresis, i.e., the continuous deflection of charged samples perpendicular to the direction of flow in an electric field, see Fig. 4b, is a sufficient approach to high-throughput separation applications [62]. In 2017, Novo and Janasek critically reviewed the advantages and challenges of free flow electrophoresis. Especially the transferability of the method toward industrial, mass fabrication methods was identified as important parameter of success [63].

Microfluidic electrophoresis is well-established nowadays. This is due to commercial devices that allow usage of microfluidic electrophoresis, mainly zone electrophoresis, by biotechnologists without the need of in-depth training and knowledge of microfluidics. Fully integrated apparatus, e.g., consisting of pumps, driving electrodes and detection system, into which microfluidic chips, loaded with the respective samples, can be placed are commercially available, e.g., from Agilent [64], Trivitron [65], or Illumina [66].

3.2 Dielectrophoretic Analysis

Dielectrophoresis (DEP) is exploited in cell studies, either to separate cells or to gain knowledge about the cell (electro)physiology. Just recently Epping et al. used a DEP approach to study the impact of isopropyl alcohol on *Escherichia coli* (*E. coli*) [67]. Their study revealed different DEP responses after incubation in isopropyl alcohol of 5%, 10%, and 15%, indicating two biophysical effects that take part during the incubation. So, a decreased polarizability of the *E. coli* was observed after incubation in 5% isopropyl alcohol; this behavior was explained with a slow, diffusion driven leaking of charged molecules out of the cells. Whereas an increased polarizability was observed after incubation in 10% and 15% isopropyl alcohol. The increase was explained by Epping et al. with an integration of the organic solvent molecules into the cell membrane and consecutive increased membrane fluidity [67].

Lapizco-Encinas and co-workers performed several studies on cells exploiting insulator-based dielectrophoresis. They successfully demonstrated a label-free separation of dead and live cells in a DEP device, Fig. 5a [68], and different cell species, e.g., Gram-negative or positive [69–71]. Investigation of cell viability after DEP treatment revealed no significant impact on the cells [72]. Therefore, dielectrophoresis is a potential method for screening and separation of cells. A microelectrode-based continuous-flow purification of a cell micro-bead mixture is shown in Fig. 5c. In 2014, Jones et al. could identify different serotypes of *E. coli* by their respective dielectric response [73]. Thus, already small changes in the cellular (bio)chemical composition have significant impact on the electric properties. Thus, the dielectric properties of the cells are suitable criteria to characterize cells.

Beyond exploiting DEP for analysis of intrinsic (bio)physical parameter, this method also can be exploited for trapping cells in a confinement without the need of mechanical contact. Fritzsche et al. used microelectrodes to dielectrophoretically trap various types of cells and observed those over a period of time while applying a constant flow rate. They could successfully demonstrate that the trapped cells were

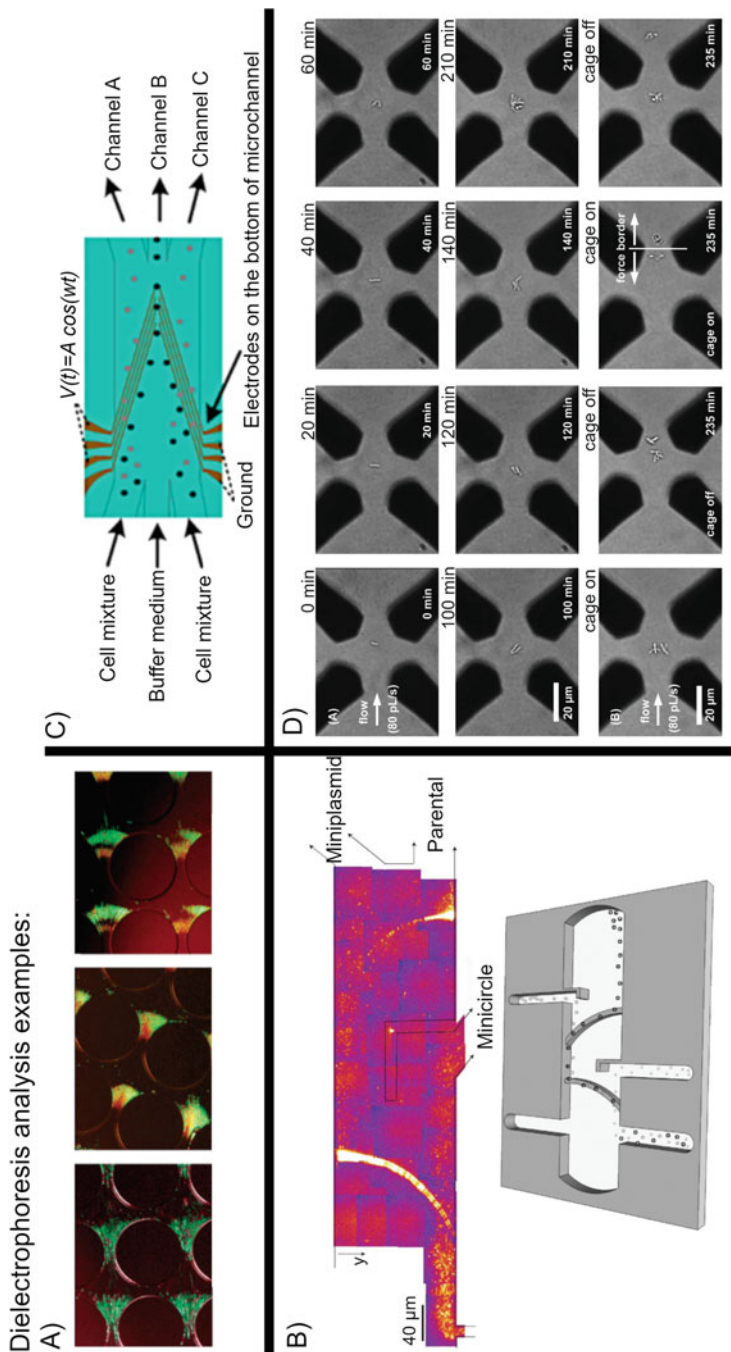


Fig. 5 Examples of insulator-based (a, b) and microelectrode dielectrophoresis (c, d). (a) Separation of live and dead *E. coli* in an array of posts. The electric field was increased (16 V/mm, 40 V/mm, 60 V/mm), which resulted in trapping of live cells (green) only, trapping of live and dead (red) cells, and a clear spatial separation of live and dead cells, respectively. Adapted with permission from [68]. Copyright (2004) American Chemical Society. (b) Continuous flow separation of three DNA species of different size. The smallest specie (minicircle) was not dielectrophoretically deflected at all. The middle-sized specie (miniplasmid) was deflected at the first ridge exhibiting stronger DEP force but not at the second ridge. The largest specie (parental) was deflected at both ridges, i.e., even at the second with weaker DEP force. Adapted from [77] with permission from The Royal Society of Chemistry, copyright 2013. (c) Sketch of continuous

alive and proliferated, Fig. 5d [74]. Their approach was based on negative dielectrophoresis, i.e., the cells were trapped in the region of minimal electric field strength and thus the impact of the electric field was minimized.

Besides analysis and separation of cells, dielectrophoresis applications are very versatile tools in microfluidics to analyze or purify DNA samples [17]. Dielectrophoresis has been exploited in numerous studies to separate DNA samples with respect to the molecules size [49, 75–80]. We successfully, demonstrated a continuous-flow separation of three DNA species appearing during gene vaccine production. The separation was conducted at an insulating ridge reducing the channel height down to about 500 nm. DNA was then selectively, dielectrophoretically trapped in the nanoslit and deflected from the sample stream; see Fig. 5b [77]. Additionally, dielectrophoresis also provides a separation of DNA samples with regard to the DNA configuration [80–82], i.e., linear, open circle (oc), or covalently closed circle (ccc). The latter is of very high importance for gene vaccines, while the purity of gene vaccines has to be very high; this concerns DNA impurities, such as bacterial plasmids from production, as well as the DNA conformation [83–85]. In 2017, it was demonstrated that by specific adaptation of the electric field parameters, i.e., electric field strength and frequency of AC voltage, the DNA conformation that is dielectrophoretically manipulated and selected can be chosen [49]. For instance, the parameter can be chosen such that only the ccc conformation is separated out of a sample mixture by means of dielectrophoresis.

DNA separation and analysis by means of dielectrophoresis has been conducted in both process modes, batch [80, 87, 88], and continuous-flow [49, 75, 77, 89]. The best suited method always relies on the intended application. Though dielectrophoretic separation is a method that does not rely on specific labels, several studies used the specific binding of DNA to microbeads, e.g., to separate specific genes and to amplify the detection [76, 90–93].

3.3 Electric Impedance Analysis

Electric impedance analysis can be used for detection of samples and characterization thereof, e.g., cell cycles or the impact of chemicals. Impedance detection of sample positions is assumed to be a versatile method to get rid of sample staining, as used in microfluidic applications with DNA. DNA is frequently stained with the

Fig. 5 (continued) flow separation of a cell-bead mixture at microelectrodes. The cells pass the electrodes without being dielectrophoretically deflected, while the microbeads are deflected toward the middle outlet channel. Reprinted with permission from [86]. Copyright (2018) American Chemical Society. **(d)** Study of cell proliferation in DEP trapping potential and controlled release of daughter cells. A flow of 80 pL/s was applied from the left to the device. Top and middle row show time-lapse photographs of contactless DEP trapping of *C. glutamicum*. Bottom row shows controlled separation of four daughter cells by deactivation and activation of DEP potential. The force border, separating cells, is indicated with a white line. Adapted from [74] with permission from The Royal Society of Chemistry, copyright 2013

fluorophore YOYO-1 [22, 49, 75]; it is known that bound molecules affect the DEP response [89, 94]. Thus, staining free detection methods like impedance analysis are new promising techniques.

Sabounchi et al. used electric impedance measurements to detect *B. subtilis* spores. They did not evaluate the detection resolution on single cell level but in concentrations of $10^3 - 10^8$ spores/ml [95]. Wang et al. used electric impedance measurements to determine the position at which 11 μm and 6 μm beads passed through the microfluidic channel. Their device consisted of microelectrodes that were placed in the channel such that the distance between them varied and so did the impedance signal depend on the position in the channel, Fig. 6b [96].

Electric impedance analysis examples:

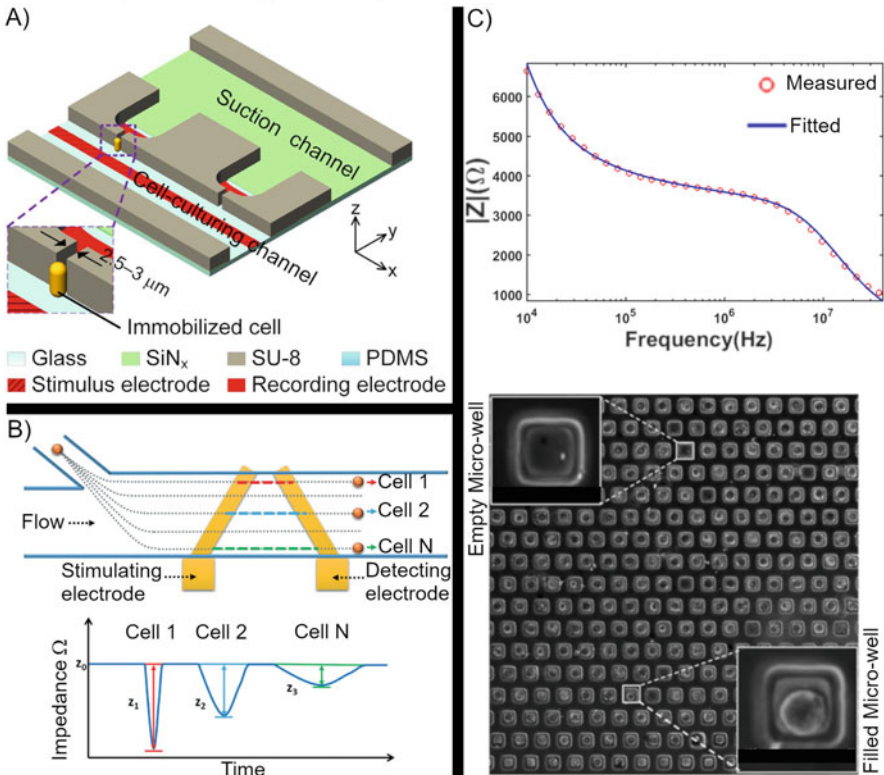


Fig. 6 Example electric impedance analysis applications. (a) Time-lapse cell cycle analysis. *S. pombe* cells are sucked into the small channel connecting the stimulus and recording electrode. Thus the impedance is monitored through the trapped cell to determine the cell size. Reprinted with permission from [97]. Copyright (2015) Springer Nature. (b) Electric impedance detection of position of cells in microfluidic channel. The impedance changed according to the position of the cells. Reprinted with permission from [96]. Copyright (2017) Royal Society of Chemistry. (c) PC-3 cells were dielectrophoretically trapped in micro-wells and analyzed via electro impedance analysis. Top, experimental and fitted values of impedance value vs frequency. Parameter of the cell membrane and cytoplasm were gained from fits to the experimentally determined impedance value and phase angle. Adapted with permission from [54]. Copyright (2018) American Chemical Society

Time-lapse cell cycle analysis was conducted with *S. pombe* cells that were sucked into a small channel connecting the stimulus and recording electrode, Fig. 6a. Afterward, the impedance was monitored through the trapped cell to determine the cell size along the cell cycle [97]. Shah et al. trapped cells in microwells and studied cells with and without nanoparticles over time by means of impedance resistance [98]. Syed et al. used DEP to trap *E. coli* and gained Bode plots, i.e., the electric impedance resistance was plotted against the logarithm of the AC frequency [99]. Mansoorifar et al. also used DEP to trap cells in microwells. They consecutively performed electric impedance analysis measurements to gain biophysical parameters of the cells like the conductivity and capacitance of the cell membrane or cytosol, Fig. 6c. Starting from those parameters, they analyzed the impact of changing pH-values [54]. Wang et al. also used DEP trapping of *E. coli* and consecutive EIS detection. The concentration of cells was high (about 4×10^6) in that experiment [100].

A commercial microfluidic device for conducting electric impedance analysis is available, for example, from Micronit Microtechnologies. Their microfluidic chip consists of integrated electrode pairs for electric impedance measurements [101].

4 Conclusion

Microfluidic analysis tools are versatile for many biotechnological applications. Here, we focused on electric analysis methods and showed new methods that came along with microfluidic devices, like dielectrophoresis analysis and separation and (single) cell analysis by means of electric impedance analysis. The miniaturization of standard methods like electrophoresis provides advantages like smaller sample volumes and fast analysis results. New electrical analysis methods provide additional parameters for further characterization of biological systems. Thus, analytics in microfluidic systems provide access to new insights in biotechnological studies.

References

1. Oliveira AF, Pessoa ACSN, Bastos RG, de la Torre LG (2016) Microfluidic tools toward industrial biotechnology. *Biotechnol Prog* 32(6):1372–1389
2. Cetin B, Özer MB, Solmaz ME (2014) Microfluidic bio-particle manipulation for biotechnology. *Biochem Eng J* 92:63–82
3. Bolivar JM, Eisl I, Nidetzky B (2016) Advanced characterization of immobilized enzymes as heterogeneous biocatalysts. *Catalysis Today* 259:66–80
4. Bolivar JM, Nidetzky B (2012) Positively charged mini-protein zbasic2 as a highly efficient silica binding module: Opportunities for enzyme immobilization on unmodified silica supports. *Langmuir* 28(26):10040–10049
5. Bolivar JM, Wiesbauer J, Nidetzky B (2011) Biotransformations in microstructured reactors: more than flowing with the stream? *Trends Biotechnol* 29(7):333–342

6. Valikhani D, Bolivar JM, Viefhues M, Mcilroy DN, Vrouwe EX, Nidetzky B (2017) A spring in performance: silica nanosprings boost enzyme immobilization in microfluidic channels. *ACS Appl Mater Interf* 9(40):34641–34649
7. Engel CEA, Vorländer D, Biedendieck R, Krull R, Dohnt K (2020) Quantification of microaerobic growth of geobacter sulfurreducens. *PLoS One* 15:e0215341
8. Maldonado SL, Panjan P, Sun S, Rasch D, Sesay AM, Mayr T, Krull R (2019) A fully online sensor-equipped, disposable multiphase microbioreactor as a screening platform for biotechnological applications. *Biotechnol Bioeng* 116:65–75
9. Xiaowen O, Chen P, Huang X, Li S, Liu B-F (2020) Microfluidic chip electrophoresis for biochemical analysis. *J Sep Sci* 43(1, SI):258–270
10. Tang W, Jiang D, Li Z, Zhu L, Shi J, Yang J, Xiang N (2019) Recent advances in microfluidic cell sorting techniques based on both physical and biochemical principles. *Electrophoresis* 40:930–954
11. Dalili A, Samiei E, Hoorfar M (2018) A review of sorting, separation and isolation of cells and microbeads for biomedical applications: microfluidic approaches. *Analyst* 144:87–113
12. Alam MK, Koomson E, Zou H, Yi C, Li C-W, Xu T, Yang M (2018) Recent advances in microfluidic technology for manipulation and analysis of biological cells (2007-2017). *Anal Chim Acta* 1044:29–65
13. Kecskemeti A, Gaspar A (2018) Particle-based liquid chromatographic separations in microfluidic devices - a review. *Anal Chim Acta* 1021:1–19
14. Rodriguez-Ruiz I, Babenko V, Martinez-Rodriguez S, Gavira JA (2018) Protein separation under a microfluidic regime. *Analyst* 143:606–619
15. Shields CW, Reyes CD, López GP (2015) Microfluidic cell sorting: a review of the advances in the separation of cells from debulking to rare cell isolation. *Lab Chip* 15:1230–1249
16. Xuan X (2019) Recent advances in direct current electrokinetic manipulation of particles for microfluidic applications. *Electrophoresis* 40(18-19):2484–2513
17. Viefhues M, Eichhorn R (2017) DNA dielectrophoresis: theory and applications a review. *Electrophoresis* 38:1483–1506
18. Páez-Avilés C, Juanola-Feliu E, Punter-Villagrasa J, del Moral Zamora B, Homs-Corbera A, Colomer-Farrarons J, Miribel-Català PL, Samitier J (2016) Combined dielectrophoresis and impedance systems for bacteria analysis in microfluidic on-chip platforms. *Sensors* 16(9):1514
19. Barani A, Paktinat H, Janmaleki M, Mohammadi A, Mosaddegh P, Fadaei-Tehrani A, Sanati-Nezhad A (2016) Microfluidic integrated acoustic waving for manipulation of cells and molecules. *Biosens Bioelectron* 85:714–725
20. Karthick S, Sen AK (2018) Improved understanding of acoustophoresis and development of an acoustofluidic device for blood plasma separation. *Phys Rev Appl* 10:034037
21. Yousuff CM, Ho ETW, Hussain K, Hamid NHB et al (2017) Microfluidic platform for cell isolation and manipulation based on cell properties. *Micromachines* 8(1):15
22. Dorfman KD, King SB, Olson DW, Thomas JDP, Tree DR (2013) Beyond gel electrophoresis: microfluidic separations, fluorescence burst analysis, and DNA stretching. *Chem Rev* 113(4):2584–2667
23. Ngara TR, Zhang H (2018) Recent advances in function-based metagenomic screening. *Genom Proteomics Bioinform* 16:405–415
24. Greif D, Pobigaylo N, Frage B, Becker A, Regtmeier J, Anselmetti D (2010) Space- and time-resolved protein dynamics in single bacterial cells observed on a chip. *J Biotechnol* 149:280–288
25. Fregin B, Czerwinski F, Biedenweg D, Girardo S, Gross S, Aurich K, Otto O (2019) High-throughput single-cell rheology in complex samples by dynamic real-time deformability cytometry. *Nat Commun* 10:415
26. Roth KB, Neeves KB, Squier J, Marr DWM (2016) High-throughput linear optical stretcher for mechanical characterization of blood cells. *Cytometry Part A* 89:391–397

27. Mietke A, Otto O, Girardo S, Rosendahl P, Taubenberger A, Golfier S, Ulbricht E, Aland S, Guck J, Fischer-Friedrich E (2015) Extracting cell stiffness from real-time deformability cytometry: theory and experiment. *Biophys J* 109:2023–2036
28. Gossett DR, Tse HTK, Lee SA, Ying Y, Lindgren AG, Yang OO, Rao J, Clark AT, Di Carlo D (2012) Hydrodynamic stretching of single cells for large population mechanical phenotyping. *Proc Natl Acad Sci U S A* 109:7630–7635
29. Guck J, Ananthakrishnan R, Mahmood H, Moon TJ, Cunningham CC, Käs J (2001) The optical stretcher: a novel laser tool to micromanipulate cells. *Biophys J* 81:767–784
30. Glynne-Jones P, Boltryk RJ, Hill M (2012) Acoustofluidics 9: modelling and applications of planar resonant devices for acoustic particle manipulation. *Lab Chip* 12:1417–1426
31. Bruus H (2009) Acoustofluidics: Theory and simulation of streaming and radiation forces at ultrasound resonances in microfluidic devices. *Acoust Soc Am J* 125(4):2592
32. Dudani JS, Gossett DR, Tse HTK, Di Carlo D (2013) Pinched-flow hydrodynamic stretching of single-cells. *Lab Chip* 13:3728–3734
33. Ashkin A (1997) Optical trapping and manipulation of neutral particles using lasers. *Proc Natl Acad Sci* 94(10):4853–4860
34. Yang T, Bragheri F, Minzioni P (2016) A comprehensive review of optical stretcher for cell mechanical characterization at single-cell level. *Micromachines* 7(30404265):90
35. Knust S, Sischka A, Milting H, Venzac B, Le Gac S, Vrouwe EX, Viefhues M, Anselmetti D, Gall K (2018) Elasto-tweezers: a novel platform for high-precision cell elasticity measurements. *Micro TAS* 2018, Kaohsiun, Taiwan
36. De Vlaminck I, Dekker C (2012) Recent advances in magnetic tweezers. *Annu Rev Biophys* 41(1):453–472
37. Kreft D, Wang Y, Rattay M, Toensing K, Anselmetti D (2018) Binding mechanism of anti-cancer chemotherapeutic drug mitoxantrone to dna characterized by magnetic tweezers. *J Nanobiotechnol* 16:56
38. Johnson KW, Dooner M, Quesenberry PJ (2007) Fluorescence activated cell sorting: a window on the stem cell. *Curr Pharm Biotechnol* 8:133–139
39. Farinas ET (2006) Fluorescence activated cell sorting for enzymatic activity. *Comb Chem High Throughput Screen* 9:321–328
40. Carter AD, Bonyadi R, Gifford ML (2013) The use of fluorescence-activated cell sorting in studying plant development and environmental responses. *Int J Dev Biol* 57:545–552
41. Dieding M, Debus JD, Kerkhoff R, Gaertner-Rommel A, Walhorn V, Milting H, Anselmetti D (2017) Arrhythmogenic cardiomyopathy related *dsg2* mutations affect desmosomal cadherin binding kinetics. *Sci Rep* 7(1):1–9
42. Yousafzai MS, Coceano G, Bonin S, Niemela J, Scoles G, Cojoc D (2017) Investigating the effect of cell substrate on cancer cell stiffness by optical tweezers. *J Biomech* 60:266–269
43. Wullkopf L, West A-KV, Leijnse N, Cox TR, Madsen CD, Oddershede LB, Erler JT (2018) Cancer cells' ability to mechanically adjust to extracellular matrix stiffness correlates with their invasive potential. *Mol Biol Cell* 29(30091653):2378–2385
44. Viovy J-L (2000) Electrophoresis of DNA and other polyelectrolytes: physical mechanisms. *Rev Mod Phys* 72(3):813–872
45. Stellwagen NC, Gelfi C, Righetti PG (1997) The free solution mobility of DNA. *Biopolymers* 42:687–703
46. Schwartz DC, Cantor CR (1984) Separation of yeast chromosome-sized dnas by pulsed field gradient gel electrophoresis. *Cell* 37(1):67–75
47. Kloczkowski A, Kolinski A (2007) Theoretical models and simulations of polymer chains. In: *Physical properties of polymers handbook*. Springer, Berlin, pp 67–81
48. Helfer CA, Mattice WL (2007) The rotational isomeric state model. In: *Physical properties of polymers handbook*. Springer, Berlin, pp 43–57
49. Täuber S, Kunze L, Grauberger O, Grundmann A, Viefhues M (2017) Reaching for the limits in continuous-flow dielectrophoretic DNA analysis. *Analyst* 142:4670–4677

50. Pethig R (2017) *Dielectrophoresis: theory, methodology, and biological applications*. Wiley, Hoboken
51. Viefhues M, Eichhorn R, Fredrich E, Regtmeier J, Anselmetti D (2012) Continuous and reversible mixing or demixing of nanoparticles by dielectrophoresis. *Lab Chip* 12(3):485–494
52. Hyun KA, Jung H-I (2013) Microfluidic devices for the isolation of circulating rare cells: a focus on affinity-based, dielectrophoresis, and hydrophoresis. *Electrophoresis* 34(7):1028–1041
53. Regtmeier J, Eichhorn R, Viefhues M, Bogunovic L, Anselmetti D (2011) Electrodeless dielectrophoresis for bioanalysis: theory, devices and applications. *Electrophoresis* 32(17):2253–2273
54. Mansoorifar A, Koklu A, Ma S, Raj GV, Beskok A (2018) Electrical impedance measurements of biological cells in response to external stimuli. *Anal Chem* 90(7):4320–4327
55. Chang B-Y, Park S-M (2010) Electrochemical impedance spectroscopy. *Annu Rev Anal Chem* 3:207–229
56. Miggiels P, Wouters B, van Westen GJP, Dubbelman A-C, Hankemeier T (2019) Novel technologies for metabolomics: more for less. *TrAC Trends in Analytical Chemistry* 120:115323
57. Voldman J (2006) Electrical forces for microscale cell manipulation. *Annu Rev Biomed Eng* 8(1):425–454
58. Lechner A, Giorgetti J, Gahoual R, Beck A, Leize-Wagner E, Francois Y-N (2019) Insights from capillary electrophoresis approaches for characterization of monoclonal antibodies and antibody drug conjugates in the period 2016–2018. *J Chromatogr B* 1122–1123:1–17
59. Zeng Y, He M, Harrison DJ (2008) Microfluidic self-patterning of large-scale crystalline nanoarrays for high-throughput continuous dna fractionation. *Angew Chem Int Ed* 47(34):6388–6391
60. Huang LR, Tegenfeldt JO, Kraeft JJ, Sturm JC, Austin RH, Cox EC (2002) A DNA prism for high-speed continuous fractionation of large DNA molecules. *Nat Biotechnol* 20(10):1048–1051
61. Nazemifard N, Bhattacharjee S, Masliyah JH, Harrison DJ (2010) Dna dynamics in nanoscale confinement under asymmetric pulsed field electrophoresis. *Angew Chem Int Ed* 49(19):3326–3329
62. Zhou W, Xia L, Xiao X, Li G, Qiaosheng P (2019) A microchip device to enhance free flow electrophoresis using controllable pinched sample injections. *Electrophoresis* 40(16–17):2165–2171
63. Novo P, Janasek D (2017) Current advances and challenges in microfluidic free-flow electrophoresis—a critical review. *Anal Chim Acta* 991:9–29
64. Agilent. <https://www.agilent.com/en/product/automated-electrophoresis/bioanalyzer-systems#0>. Accessed 11 Feb 2020
65. Trivitron. <https://www.trivitron.com/products/electrophoresis>. Accessed 11 Feb 2020
66. Illumina. <https://www.illumina.com/systems/sequencing-platforms.html>. Accessed 11 Feb 2020
67. Epping MS, Wedde S, Grundmann A, Radukic M, Gröger H, Hummel A, Viefhues M (2020) Dielectrophoretic analysis of the impact of isopropyl alcohol on the electric polarisability of *Escherichia coli* whole-cells. *Anal Bioanal Chem* 412(16):3925–3933
68. Lapizco-Encinas BH, Simmons BA, Cummings EB, Fintschenko Y (2004) Dielectrophoretic concentration and separation of live and dead bacteria in an array of insulators. *Anal Chem* 76(6):1571–1579
69. Khoshmanesh K, Baratchi S, Tovar-Lopez FJ, Nahavandi S, Wlodkowic D, Mitchell A, Kalantar-zadeh K (2012) On-chip separation of lactobacillus bacteria from yeasts using dielectrophoresis. *Microfluid Nanofluid* 12(1):597–606
70. Saucedo-Espinosa MA, LaLonde A, Gencoglu A, Romero-Creel MF, Dolas JR, Lapizco-Encinas BH (2016) Dielectrophoretic manipulation of particle mixtures employing asymmetric insulating posts. *Electrophoresis* 37(2):282–290

71. Lapizco-Encinas BH, Simmons BA, Cummings EB, Fintschenko Y (2004) Insulator-based dielectrophoresis for the selective concentration and separation of live bacteria in water. *Electrophoresis* 25(10–11):1695–1704
72. LaLonde A, Romero-Creel MF, Lapizco-Encinas BH (2015) Assessment of cell viability after manipulation with insulator-based dielectrophoresis. *Electrophoresis* 36(13):1479–1484
73. Jones PV, DeMichele AF, Kemp LK, Hayes MA (2014) Differentiation of *Escherichia coli* serotypes using DC gradient insulator dielectrophoresis. *Anal Bioanal Chem* 406:183–192
74. Fritzsche FSO, Rosenthal K, Kampert A, Howitz S, Dusny C, Blank LM, Schmid A (2013) Picoliter nDEP traps enable time-resolved contactless single bacterial cell analysis in controlled microenvironments. *Lab Chip* 13:397–408
75. Jones PV, Salmon GL, Ros A (2017) Continuous separation of DNA molecules by size using insulator-based dielectrophoresis. *Anal Chem* 89(3):1531–1539
76. Nakano M, Ding Z, Kasahara H, Suehiro J (2015) Rapid size determination of pcr amplified dna by beads-based dielectrophoretic impedance spectroscopy. In: 2015 transducers - 2015 18th international conference on solid-state sensors, actuators and microsystems (TRANSDUCERS), pp 1530–1532
77. Viefhues M, Wegener S, Rischmüller A, Schleef M, Anselmetti D (2013) Dielectrophoresis based continuous-flow nano sorter: fast quality control of gene vaccines. *Lab Chip* 13(15):3111–3118
78. Lao AIK, Hsing I-M (2005) Flow-based and sieving matrix-free DNA differentiation by a miniaturized field flow fractionation device. *Lab Chip* 5:687–690
79. Parikesit GOF, Markesteijn AP, Piciu OM, Bossche A, Westerweel J, Young IT, Garini Y (2008) Size-dependent trajectories of DNA macromolecules due to insulative dielectrophoresis in submicrometer-deep fluidic channels. *Biomicrofluidics* 2(2):24103
80. Regtmeier J, Duong TT, Eichhorn R, Anselmetti D, Ros A (2007) Dielectrophoretic manipulation of DNA: separation and polarizability. *Anal Chem* 79(10):3925–3932
81. Li S, Yuan Q, Morshed BI, Ke C, Wu J, Jiang H (2013) Dielectrophoretic responses of DNA and fluorophore in physiological solution by impedimetric characterization. *Biosens Bioelectron* 41:649–655
82. Regtmeier J, Eichhorn R, Bogunovic L, Ros A, Anselmetti D (2010) Dielectrophoretic trapping and polarizability of DNA: the role of spatial conformation. *Anal Chem* 82(17):7141–7149
83. Schleef M, Schirmbeck R, Reiser M, Michel M-L, Schmeer M (2015) Minicircle: next generation DNA vectors for vaccination. *Methods Mol Biol* 1317:327–339
84. Schmeer M, Schleef M (2015) Production of plasmid DNA as pharmaceutical. *Methods Mol Biol* 1317:315–326
85. Schmeer M, Schleef M (2014) Pharmaceutical grade large-scale plasmid DNA manufacturing process. *Methods Mol Biol* 1143:219–240
86. Wu Y, Ren Y, Tao Y, Hou L, Jiang H (2018) High-throughput separation, trapping, and manipulation of single cells and particles by combined dielectrophoresis at a bipolar electrode array. *Anal Chem* 90(19):11461–11469
87. Lin G, Camacho-Alanis F, Ros A (2015) Polarizability of six-helix bundle and triangle DNA origami and their escape characteristics from a dielectrophoretic trap. *Anal Chem* 87(24):12059–12064
88. Sonnenberg A, Marciniak JY, Rassenti L, Ghia EM, Skowronski EA, Manouchehri S, McCanna J, Widhopf 2nd GF, Kipps TJ, Heller MJ (2014) Rapid electrokinetic isolation of cancer-related circulating cell-free DNA directly from blood. *Clin Chem* 60(3):500–509
89. Viefhues M, Regtmeier J, Anselmetti D (2013) Fast and continuous-flow separation of DNA-complexes and topological DNA variants in microfluidic chip format. *Analyst* 138:186–196
90. Cheng I-F, Senapati S, Cheng X, Basuray S, Chang H-C, Chang H-C (2010) A rapid field-use assay for mismatch number and location of hybridized DNAs. *Lab Chip* 10(7):828–831

91. Ramón-Azcón J, Yasukawa T, Mizutani F (2011) Sensitive and spatially multiplexed detection system based on dielectrophoretic manipulation of DNA-encoded particles used as immunoreactions platform. *Anal Chem* 83(3):1053–1060
92. Nakano M, Ding Z, Kasahara H, Suehiro J (2014) Rapid microbead-based dna detection using dielectrophoresis and impedance measurement. *EPL (Europhys Lett)* 108(2):28003
93. Kawabata T, Washizu M (2001) *IEEE transactions on industry applications: dielectrophoretic detection of molecular bindings*, vol 37.
94. Viefhues M, Regtmeier J, Anselmetti D (2012) Nanofluidic devices for dielectrophoretic mobility shift assays by soft lithography. *J Micromech Microeng* 22(11):115024
95. Sabounchi P, Morales AM, Ponce P, Lee LP, Simmons BA, Davalos RV (2008) Sample concentration and impedance detection on a microfluidic polymer chip. *Biomed Microdevices* 10(5):661
96. Wang H, Sobahi N, Han A (2017) Impedance spectroscopy-based cell/particle position detection in microfluidic systems. *Lab Chip* 17:1264–1269
97. Zhu Z, Frey O, Haandbaek N, Franke F, Rudolf F, Hierlemann A (2015) Time-lapse electrical impedance spectroscopy for monitoring the cell cycle of single immobilized *s pombe* cells. *Sci Rep* 5:17180
98. Shah P, Zhu X, Zhang X, He J, Li C-z (2016) Microelectromechanical system-based sensing arrays for comparative in vitro nanotoxicity assessment at single cell and small cell-population using electrochemical impedance spectroscopy. *ACS Appl Mater Interfaces* 8:5804–5812
99. Syed LU, Liu J, Price AK, Li Y-f, Culbertson CT, Li J (2011) Dielectrophoretic capture of *E. coli* cells at micropatterned nanoelectrode arrays. *Electrophoresis* 32(17):2358–2365
100. Wang R, Xu Y, Liu H, Peng J, Irudayaraj J, Cui F (2017) An integrated microsystem with dielectrophoresis enrichment and impedance detection for detection of *escherichia coli*. *Biomed Microdevices* 19:34
101. Micronit Microtechnologies. <https://www.micronit.com/products/electrical-impedance-spectroscopy.html>. Accessed 11 Feb 2020

Biocatalysis in Continuous-Flow Microfluidic Reactors



Marco P. Cardoso Marques, Alvaro Lorente-Arevalo, and Juan M. Bolivar

Contents

1	Biocatalysis and Continuous-Flow Microreactors	212
1.1	Biocatalysis Goes with the Flow	212
1.2	New Demands of Biocatalysis for Reactor Engineering	214
1.3	Scope of this Book Chapter	217
2	Biocatalytic Microfluidic Reactors with Free Enzymes	217
2.1	Modern Biocatalysis with Free Enzymes and Emerging Demands: The Context of Microfluidic Technology	217
2.2	Biocatalysis in Monophasic Aqueous Medium	218
2.3	Biocatalysis in Multiphasic Medium	220
3	Biocatalytic Microfluidic Reactors with Immobilized Enzymes	222
3.1	Enzyme Immobilization and Conventional Continuous Reactors: The Need for New Technologies	222
3.2	Modern Heterogeneous Biocatalysis and Emerging Demands: The Context of Microfluidic Technology	225
3.3	Immobilized Enzymes in Microfluidic Reactors: Challenges and Practical Implementation	225
4	Exploitation of Microfluidic Enzyme-Immobilized Reactors	229
4.1	Promises and Advantages of Microfluidics in Enzyme-Immobilized Reactors	229
4.2	Intensification of Solid–Liquid Reactions in Microfluidic Reactors	230
4.3	Intensification of Solid–Fluid–Fluid Reactions in Microfluidic Reactors	232
4.4	Assembly of Enzyme-Immobilized Cascades	234
4.5	Generation of Novel Process Windows	235
4.6	Scale-Up and Scale-Down Impact on Productivity and Space-Time Yield	235
5	Conclusions	236
	References	237

M. P. Cardoso Marques (✉)

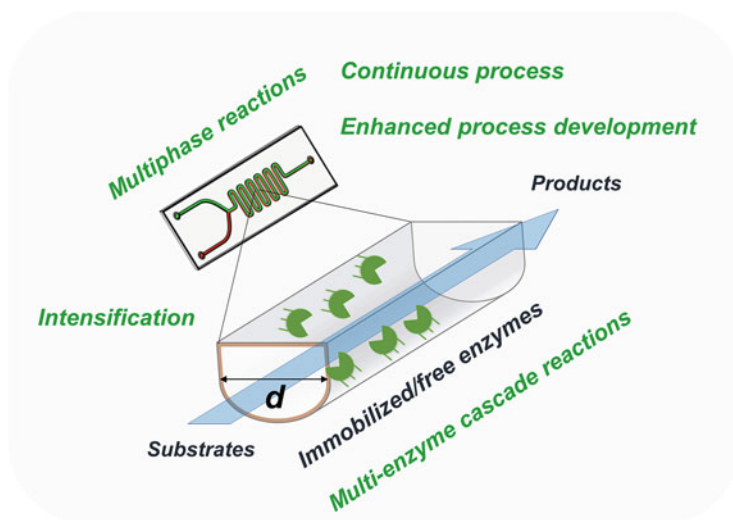
Department of Biochemical Engineering, University College London, London, UK
e-mail: marco.marques@ucl.ac.uk

A. Lorente-Arevalo and J. M. Bolivar (✉)

Chemical and Materials Engineering Department, Faculty of Chemical Sciences, Complutense
University of Madrid, Madrid, Spain
e-mail: Juanmbol@ucm.es

Abstract The implementation of continuous-flow transformations in biocatalysis has received remarkable attention in the last few years. Flow microfluidic reactors represent a crucial technological tool that has catalyzed this trend by promising tremendous improvement in biocatalytic processes across a host of different levels, including bioprocess development, intensification of reactions, implementation of new methods of reaction screening, and enhanced reaction scale-up. However, the full realization of this promise requires a synergy between these biocatalytic reaction features and the design and operation of microfluidic reactors. Here an overview on the different applications of flow biocatalysis is provided according to the format of the enzyme used: free vs immobilized form. Until now, flow biocatalysis has been implemented on a case-by-case approach but challenges and limitations are discussed in order to be overcome, and making continuous-flow microfluidic reactors as universal tool a reality.

Graphical Abstract



Keywords Continuous production, Enzyme immobilization, Flow biocatalysis, Microfluidic reactors, Miniaturization, Reaction intensification

1 Biocatalysis and Continuous-Flow Microreactors

1.1 Biocatalysis Goes with the Flow

Recent years have seen the emergence of a plenitude of new biocatalytic applications, mainly due to advances in protein engineering. These developments have, in

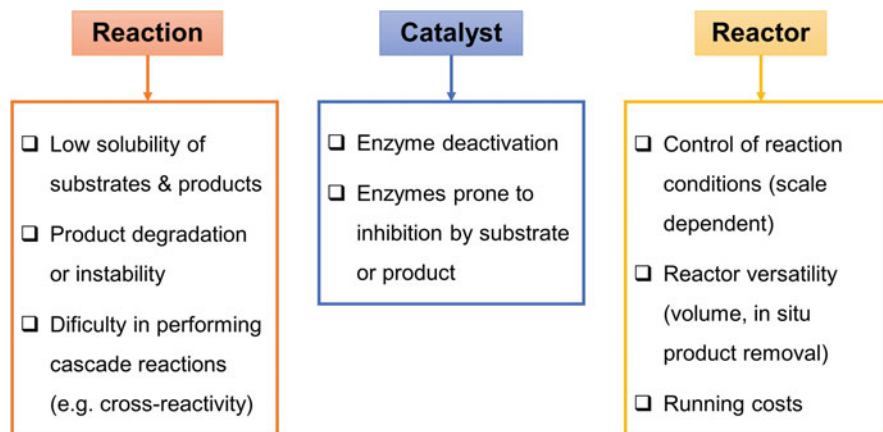


Fig. 1 Commonly encountered challenges to implement biocatalytic reactions in traditional reactors

turn, facilitated the improvement of catalytic properties of enzymes to better match the needs of industry (e.g., by facilitating the synthesis of chiral alcohols and amines). Furthermore, since enzymes are highly selective, renewable, and operate under mild conditions in aqueous media, these processes are also generally regarded as environmentally sustainable since they present a good atom economy, a reduced E-factor ($\text{kg}_{\text{waste}} \cdot \text{kg}_{\text{product}}^{-1}$), and reduced downstream costs associated [1]. Nonetheless, in order to realize all the benefits of the industrial use of enzymes, new routes to target molecules and feedstocks must be found by using biocatalytic retrosynthesis [2] and biocatalytic reactions must be operated close to industrial conditions (e.g., by matching sustainable process metrics, such as $g_{\text{product}} \cdot L_{\text{reactor}}^{-1} \cdot \text{h}^{-1}$, $g_{\text{product}} \cdot g_{\text{biocatalyst}}^{-1}$, and $g_{\text{product}} \cdot g_{\text{substrate}}^{-1}$). As a result, there is a subtle but important interplay between biocatalysts and process properties for process optimization [3], whereby enzyme activity and stability can be fine-tuned. While traditionally biocatalytic applications are carried out in classic stainless-steel batch reactors, novel reactor designs are increasingly being sought out by researchers interested in intensifying processes and overcoming common issues that have historically plagued these applications (Fig. 1). Continuous processing presents itself as a suitable alternative to these reactors, allowing researchers to obtain a constant product output quality while reducing the overall footprint of the process. Perhaps not surprisingly recent years have seen a strong trend towards continuous operation models [4–12].

Continuous-flow reactors offer an improved control over reaction conditions, with benefits in yield and productivity levels. This increase in efficiency and the concomitant minimization of waste result not only in cleaner processes, but also in lower overall production costs. Furthermore, continuous processes enable a reduction in process lines and facility footprints, which in turn results in less up-front capital cost. To exploit the full benefits of continuous processing, however, rigorous

kinetic analyses are necessary – as well as the characterization of reactor performance at all scales. Implementation of sensor technology to control the quality profile of the products and a product stability assessment are also requirements for a successful continuous process – and, of course, both process scalability and cost-effectiveness must be established [6, 7, 9, 13, 14].

Miniaturized continuous-flow reactors (with volumes ranging from μL to mL) are systems used to evaluate the suitability of biocatalytic reactions or, in particular cases, for production [7, 9, 13, 14]. The small dimensions of these reactors allow experiments to be performed with much smaller volumes compared to traditional batch systems, thereby offering significant cost reduction when using expensive substrates or enzymes. But the benefits do not stop there: these reactors also offer the ability to closely manage the parameters of an experiment; in-line purification with recovery of products can be more easily performed [6, 13]; and no mechanical mixing is typically required. In addition, reactions can be potentially accelerated due to enhanced mass transfer with a decrease in reaction time and significantly improved space-time yield.

1.2 New Demands of Biocatalysis for Reactor Engineering

Increasing demand for enzyme-catalyzed reactions by industry presents new opportunities for reaction engineering [15–23]. These fall into the framework of process intensification, whereby reaction intensification is manifested in terms of decrease in reaction time, reactor volumes, energy demands, and overall costs (Fig. 2).

In response to this demand, there has been a general shift away from batch production towards continuous production for biocatalytic reactions – and microfluidic approaches have become increasingly important as a result [4, 5, 7, 8,

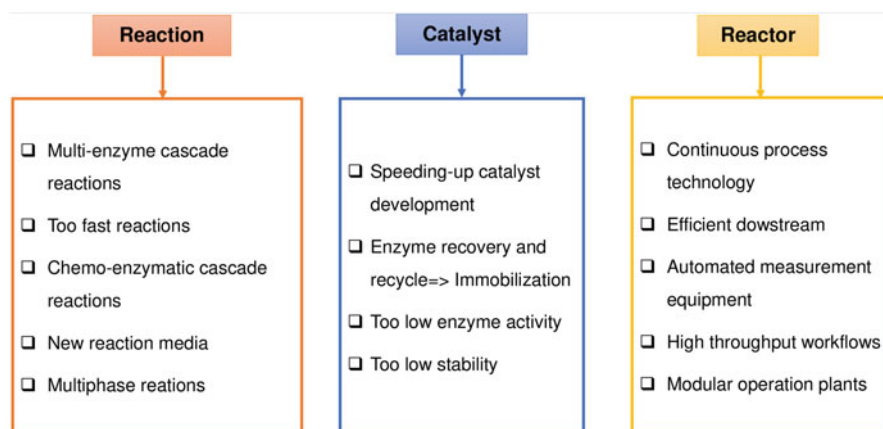


Fig. 2 Demands for reactor engineering in the context of new biocatalytic trends

24, 25]. The microfluidic approaches rely on the miniaturization of continuous-flow reactors, usually in the form of tubular reactors. This is a deviation from the common assumption that continuous reactors for biochemical engineering applications are stirred tank bioreactors, in which the reaction medium is kept at a maximum internal homogeneity by the means of mixing, or packed/fluidized bed macroreactors are used. To clarify this approach, important definitions are here introduced which are based on similar explanations previously applied in microprocess engineering and chemical flow microreactors [5, 6, 26, 27].

- The characteristic channel dimensions of the miniaturized continuous-flow reactors (with volumes ranging from μL to mL) range from the micrometer to the millimeter scale. Nonetheless, the dimension of the reactor channel is relative since the key aspect is whether at the selected channel dimension there is a specific enhancement of, for example, transport intensification with the absence of mass transfer limitations.
- Miniaturized continuous-flow reactors operate under continuous-flow conditions and flow regime is laminar.
- Integrated approaches are necessary where catalyst characteristics, kinetic data, transport phenomena, and reactor engineering are combined to develop flow system. The use of dimensionless numbers is particularly important to identify rate limiting steps and offer opportunities to enhance the overall reaction performance, in particular in solid–liquid biocatalytic reactions [28, 29].
- Transport phenomena that are beneficial for chemical synthesis (e.g., enhanced mass and heat transfer) usually take place below a certain channel diameter where regular laminar flow or surface-tension dominated droplet/bubble flow regimes are encountered [28, 29].

In this chapter, the analysis is limited to microfluidic reactors in continuous-flow tubular configuration and on applications where the miniaturized dimensions have a well-defined influence or advantage.

Miniaturized continuous-flow reactors can be manufactured using a variety of fabrication methods, depending on the reactor materials and feature sizes [5, 6, 14, 30–33]. Direct writing methods – such as CO_2 laser writing – offer rapid fabrication, but are limited to polymeric devices and only permit sizing down to approximately $100\ \mu\text{m}$. Devices with low aspect ratio features can also be produced using soft lithography techniques; but this requires access to a clean room, and this process is both time consuming and comparatively costly. CNC (computer numerical control) micromachining can be used to fabricate molds (i.e., cast and mold techniques to fabricate poly(dimethylsiloxane), PDMS, devices) or devices themselves in any microfluidic geometry. More recently, additive manufacturing (3D-printing) has been used to create whole devices [14, 32, 34] – although the resolution of printing must be such that fluid leakage is avoided. Flow reactors can also be realized using tubing (e.g., coil microreactors made of polytetrafluoroethylene, PTFE). In all cases, however, the hydraulic diameter and the length of the reactors will dictate the residence time of the fluid within the system.

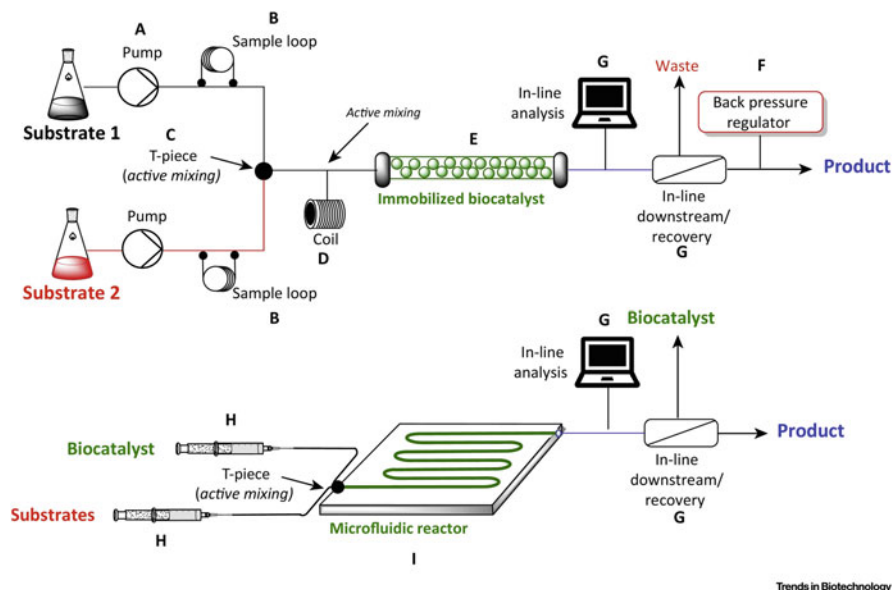


Fig. 3 Main type of miniaturized continuous-flow reactors: fixed-bed reactor (top panel) and tubular reactor (bottom panel). The reactors are complemented with several peripheral equipment comprising of pumps (delivery of substrates or enzyme in the case of tubular reactors), in-line purification or recovery units (e.g., modular microfluidic reactor and inline filtration system for the biocatalytic synthesis of chiral metabolites [30]) and *at-line* reaction analytics. The figure was reproduced with permission from [4]

These devices all require several pieces of peripheral equipment, such as pumps and actuators, to be operated. With recent advances in analytical methods, there now exist several ways to monitor reaction conditions (e.g., pH, temperature, and oxygen), reaction parameters (e.g., substrate and products concentrations), and operational conditions (e.g., flow rates and pressure). The reactors must therefore be fabricated using materials and configurations that permit interrogation with sensors and other analytical methods for the online monitoring of chemical and physical variables (pH, temperature, oxygen, and CO₂) [35], and for *at-line* reaction analytics (GC- and LC-MS). Online monitoring is crucial to ensure robust process control strategies and, ultimately, guarantee a stable process with precise synthesis of products (APIs and value-added chemicals). This robust analytical data will allow building high-quality models for process design and optimization and will ultimately enable feedback control strategies (e.g., controlled addition in multi-inlet reactors of acid and base [36] or oxygen rich fluid in case of oxygen-dependent reactions) [36–38].

There are two main categories of miniaturized continuous-flow reactors: tubular reactors (Fig. 3 bottom panel) and fixed-bed reactors Fig. 3 top panel). Combined with the form of enzymes used (i.e., free or in immobilized form), this fundamental delineation allows us to categorize these applications (Fig. 3).

1.3 Scope of this Book Chapter

Continuous-flow microreactors are promising tools to expand the applicability of biocatalysis in industry. This reactor type not only addresses some of the current limitations of conventional enzymatic, but also helps researchers to meet increasing industry demand for modern enzyme catalyzed transformations [3, 15–23]. They will ultimately facilitate the establishment of complex multi- or chemo-enzymatic reaction cascades, due to the modular nature of the microreactors system [39] and intensifying reactions and processes while generating new operating windows. Advances in continuous-flow microreactors will also help effectively further the development of continuous bioprocesses, and, ultimately, contribute to the establishment of modular, small efficient production plants. In this chapter, recent advances of biocatalysis in continuous-flow microreactors will be discussed based on the form of biocatalyst used (i.e., free or immobilized enzymes).

2 Biocatalytic Microfluidic Reactors with Free Enzymes

2.1 Modern Biocatalysis with Free Enzymes and Emerging Demands: The Context of Microfluidic Technology

Although continuous processing is frequently associated with the retention of enzymes inside the reactor by immobilization, there are also cases where the enzyme is used in a soluble form in the reaction medium. Since the dimension of the characteristic magnitude is volumetric (amount/activity of enzyme suspended per unit of volume), in principle there is no specific advantageous feature of reaction intensification due to reactor miniaturization (e.g., due to the increase of the specific surface area) [9, 28, 29]. The interest of using free enzymes in microfluidic reactors must be found, therefore, either in practical reasons or due to the presence of several fluid phases in contact. Practical reasons include the use of microfluidics as an enabling technology – for example, due to their ability to allow for the precise manipulation of small amounts of fluids, and control of reaction times. Additionally, these systems would allow the implementation of advanced scale-up strategies (including numbering up and scaling out) and the incorporation of advanced reactor instrumentation which enables the establishment of Process Analytical Technologies (PAT) and Quality by Design (QbD) approaches. Plug and play configurations of miniaturized continuous-flow reactors and miniaturized downstream unit operation allow the assembly of complex synthetic cascades, and ultimately the creation of automatized systems for reaction screening and the study of whole bioprocess sequences [36, 40]. Different system configurations can be operated as miniaturized continuous-flow reactors depending on device architecture and biocatalytic reaction conditions (Fig. 4). To maximize productivities and yields it may be necessary to implement in situ substrate supply (ISSS) [41] and in situ product removal (ISPR)

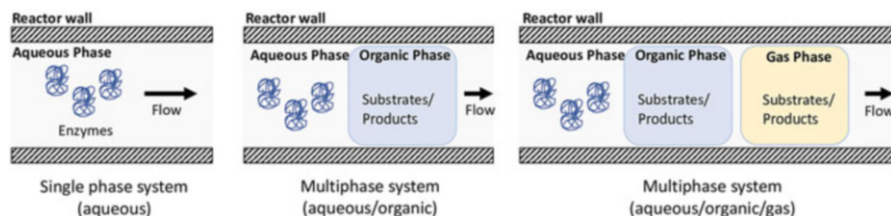


Fig. 4 Example of reactor configurations for free enzyme systems. The multiphase systems can have different flow characteristics rather than a droplet system (train of droplets of different phases) depending on the microfluidic device architecture. The enzymes are contained in the aqueous phase while substrates and products can be present in the organic and gas phase depending on their characteristics

strategies [42]. These strategies are commonplace in batch reactors and at larger scales, and different methodologies have been established according to the different physicochemical properties of both reactants and products. ISSS and ISPR can be applied in miniaturized continuous-flow reactors by the use of organic solvents and/or gases, in multiphase systems (e.g., aqueous-organic, aqueous-gas, or aqueous-organic-gas system). However, one challenge associated with multiphase systems is the inactivation of enzyme at the phases interface which can be circumvented by enzyme optimization via enzyme engineering or reduce solvent polarity difference.

2.2 Biocatalysis in Monophasic Aqueous Medium

2.2.1 Compartmentalization of Complex Reactions in Microfluidic Devices

The continuous production of high value, or difficult to synthesize, products is of increasing interest to the pharmaceutical industry. These reactions typically rely on the implementation of complex, multistep reaction sequences that resemble biological processes seen in living systems. Cascading reaction systems have already been employed for chemical synthesis with great success, allowing a quick change in reaction conditions and the easy addition of new reactants, as well as the expedient removal of unwanted side products. A cascading system can remove the need for isolating unstable intermediates, increasing the yield of a synthetic pathway. Based on the success for chemical synthesis, the question arises how cascading systems could be beneficial to chemoenzymatic or biocatalytic synthesis. Microreactors are promising tools for the development of such processes [40].

Multistep or cascading continuous-flow reactors are essentially several different reactors connected into a single flow sequence to carry out complex cascade reactions (Fig. 5). In this reactor cascade several biotransformations can be carried out at different conditions. For example, the fluid can be rapidly heated or cooled in

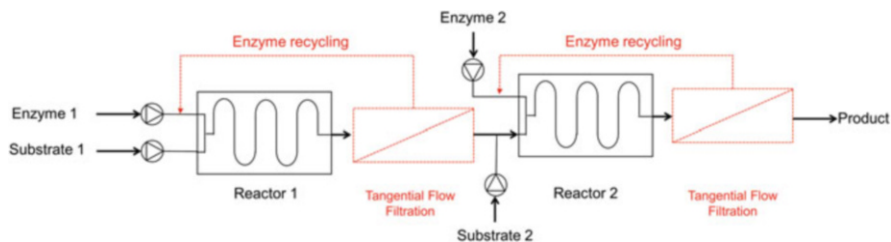


Fig. 5 Conceptual setup of a cascading reaction system using free enzymes. The two enzymes are compartmentalized and the enzymes are recovered through tangential flow filtration units [30]

different reactors to mediate an effective (bio)transformation. The reactor dimensions, e.g., hydraulic diameter and length, dictates the residence time inside the reactor and particular features, e.g., heat transfer [40]. Nonetheless, there can be issues when coupling these reactions in terms of incompatibility of reaction conditions, the balancing of suitable catalyst amounts, and the need to overcome inhibition issues. Guidelines and considerations how to overcome these key issues have been provided to set a framework to couple cascade reactions [40].

An application of this cascading approach is the synthesis of chiral amino-alcohols [39]. Chiral amino-alcohols are of particular practical interest, since they represent key industrial synthons for the production of complex molecules and optically pure pharmaceuticals. They can be synthesized from simple, non-chiral starting materials, by coupling a transketolase and a transaminase-catalyzed reaction. Low enzyme activities and inhibitory effects have limited their implementation. Usually, the systems are far from full conversion – and long reaction times are also commonly reported, making process modifications and improvement challenging. By implementing microreactor technology, however, full conversion can be achieved. Using the compartmentalization of the reactions afforded by the microreactor cascade, researchers have also successfully overcome inhibitory effects, increased the activity per unit volume, and optimized individual reaction conditions. The transketolase-catalyzed reaction was completed in under 10 min, following optimization of the transaminase-catalyzed reaction, and a volumetric activity was attained which led to full conversion of the coupled reaction in 2 h. This example represents a paradigmatic case of how continuous-flow microreactors can be applied for the design and optimization of biocatalytic processes.

2.2.2 Advanced Monitoring in Continuous Reactors

Controlling and monitoring intensive variables along reactors is more difficult within continuous-flow reactors, which creates difficulties in both understanding and optimizing reactions [43]. Controlling and monitoring pH, in particular, is essential to stabilize reaction conditions and reaction progress for many biocatalytic processes. The suitable design of microfluidic devices integrated with pH sensors can enable

the real-time pH monitoring of the progression of an enzymatic reaction in a microfluidic reactor and is a first step towards achieving pH control [35, 44]. To achieve this, fluidic inputs along the reaction channel can be implemented to adjust the pH of the reaction [37]. This concept was tested with reactions catalyzed by a transketolase and a penicillin G acylase with time-course profiles of pH were recorded within a microfluidic device. Without pH adjustment, the former showed a pH increase of one pH unit, and the latter a pH decrease of about 2.5 pH units. However, with pH adjustment the pH drop of the penicillin G acylase-catalyzed reaction was significantly attenuated and the product yield increased significantly, up to 29%.

2.3 Biocatalysis in Multiphasic Medium

Multiphase microreaction systems are emerging as powerful tools for the development of enzyme-catalyzed transformations involving two or more partly immiscible fluids in continuous flow [28, 29]. Mass transfer intensification due to miniaturization of the reactor dimensions, and the associated enlargement of the interfacial area, presents a powerful approach of effective reaction rate enhancement. Coupling microreactors and biocatalytic reactions in these systems is a highly complex process that requires an integrated approach addressing biocatalyst features, reaction kinetics, mass transfer, and reactor engineering [28, 29]. Multiphase flows are generated when two or more partially immiscible fluids are brought into contact. Such flows can be classified as either gas–liquid or liquid–liquid. Heterogeneous catalytic reactions are often encountered in process biocatalysis, where immobilized enzymes typically constitute the preferred form of catalyst (viz. Sect. 3). In liquid–liquid reactions, biocatalytic reactions take place in the water phase or directly at the fluids’ interface. On the other hand, in gas–liquid reactions the gaseous substrate usually requires transport into the aqueous liquid phase, where it reacts upon contact with the soluble form of the enzyme [28, 29].

2.3.1 Biocatalysis with Free Enzymes in Liquid–Liquid Flow

Multiphase conditions can facilitate substrate supply, product removal, or both through in situ extraction between the aqueous and organic phase [28, 29, 45]. The potential benefits to researchers are several but outstanding is the potential to substantially increase productivity, enhance the space-time yield, and intensify transport [28, 29]. The application of free lipases in a biphasic medium (aqueous/organic phase) has received considerable attention for the development of intensified reactions. The interest in the use of this organic system lies in the solubility enhancement of hydrophobic substrates, elimination of side reactions caused by water, and improvement of product recovery. Lipases have been used for the synthesis of isoamylacetate [28, 46, 47]. A two-phase system was used composed

of water and *n*-hexane, either in segmented or parallel flow, where the enzyme dissolved in the aqueous phase or hydrophilic ionic liquid and *n*-heptane containing enzyme adsorbed to the liquid–liquid interface. The microchannel microreactor showed superior performance to the well-mixed conventional batch reactor, in terms of both reaction rate and maximum conversions reached in relation to residence time needed, specifically 2.8 times faster than the batch reactor for the same conversion and 286% more productive. Product removal into the organic phase and continuous phase separation were also successfully accomplished.

Similar system is used in the oxidation of cholesterol performed by cholesterol oxidase. Reactions were carried out in stirred batch reactors and miniaturized microreactors in a two-phase parallel flow composed of water and *n*-heptane. In this particular case, both the substrate and the product of the reaction (cholestenone) are poorly soluble in water. Furthermore, the heptane was used to increase the concentration of oxygen (co-substrate) in the reaction mixture. The residence time required to reach target conversion was decreased almost 20-fold in the microchannel reactor when compared with the conventional batch reactor. A normalized residence time concept was used to account for differences in enzyme concentration applied in the different reactor configurations [28, 48, 49].

Most recently, the transfer of the enzyme synthesis of cephalixin from a batch reactor configuration to a continuous-flow microfluidic system was studied. The reactor system also comprised of integrated reaction product separation and enzyme recovery. Production of cephalixin is a paradigmatic example of synthesis in a kinetic regime, which is characterized by the appearance of a concentration maximum during the enzyme reaction. The control of the reaction time and reaction features is critical in order to achieve maximum conversion. The systems consisted of a biphasic reaction medium, with optimum composition of phosphate buffer, polyethylene glycol and water, forming a two-phase slug flow within a microfluidic capillary as the reaction-separation environment. Such a flow arrangement enabled a uniform residence time of the reaction mixture as well as providing in situ extraction of cephalixin and enzyme recycle [50].

Reaction optimization in biphasic systems is accomplished not just by miniaturization itself, but also by the fine-tuning of the microreactor geometry. The performance of the Corning AFR™ Low Flow (LF) fluidic module was shown for the *Candida Antarctica* lipase B (CALB) catalyzed isoamyl acetate synthesis in an *n*-heptane–buffer two-liquid phase system. The flow regime consisted in dispersed *n*-heptane droplets in a continuous buffer phase, which enables in situ extraction of the produced isoamyl acetate to the *n*-heptane phase. Additionally, it provides a very large interfacial area for the esterification reaction performed by an amphiphilic lipase B, which positions itself on the *n*-heptane–buffer interface. Productivities obtained (six-fold more per volume and 2.4-fold more in catalyst mass) were the highest reported so far for this reaction and indicate that Corning Advanced-Flow Reactor™ (AFR™) modules are also very efficient for carrying out biotransformations in two-phase systems [51].

2.3.2 Biocatalysis with Free Enzymes in Gas–Liquid Flow

Oxygen-dependent reactions are of great importance in biocatalytic applications [52]. O₂ is usually supplied to the liquid reaction medium containing the free enzyme via contact with a gas phase. The reaction rate is typically limited by the low O₂ transfer rate and low solubility of O₂ in aqueous reaction medium [53–55]. Different approaches based on increasing the oxygen transfer rate by reactor and reaction engineering have been studied [54, 56, 57]. Using continuous-flow microreactors the interfacial surface-to-volume ratio can be maximized while the overall reaction time is minimized [54, 56]. As an example, a continuous falling-film microreactor can be applied for the oxidation of glucose catalyzed by free glucose oxidase [58]. An agitated cell reactor (ACR) has also been applied to enhance the rate of biocatalytic oxidation reactions for the same transformation [59, 60]. Another interesting reactor setup is the tube-*in*-tube configuration where the aqueous and gas phase are physically separated physically by a membrane [29, 61–64]. This allows a continuous supply of gas while avoiding direct interfacial contact between enzyme and gas phase. Oxygen can also be produced in the reaction media itself for a bubble free supply of gas based on the controlled decomposition of hydrogen peroxide [65]. Under the confinement of a porous particle or a flow reactor [66, 67], this feature was exploited to enable the concentration of aqueous O₂ to be increased beyond equilibrium solubility under safe and practical conditions [67, 68].

3 Biocatalytic Microfluidic Reactors with Immobilized Enzymes

3.1 *Enzyme Immobilization and Conventional Continuous Reactors: The Need for New Technologies*

3.1.1 Enzyme Immobilization and Continuous Reactors

Enzyme immobilization is an approach that enables the confinement of an enzyme within a defined region of the space. The confinement can be carried out at reactor scale either by using membranes that allow retainment of the enzyme or by utilizing the insolubilization of an enzyme via incorporation into a solid matrix [69, 70]. The immobilization of the enzyme into a solid matrix implies a heterogenization of the reaction, since the reaction takes place at the solid–liquid interface and phenomena of mass transfer towards the solid catalytic phase take place. The use of enzyme immobilization in biocatalytic reactors is driven by both technical and functional considerations [71–73]. The technical considerations stem from the idea that the reuse or continuous use of the enzyme catalyst requires the application of a suitable method of enzyme retention or confinement within the reactor. This explains the strong historical link between the development of continuous-flow reactors and

immobilization methodologies [8, 24, 72, 74]. Additionally, fuelled by the advances of the protein immobilization science, the design of immobilized enzymes has integrated the immobilization as a fundamental tool to modulate the final properties of the heterogeneous biocatalysts [71, 73, 75, 76]. Reactor design and enzyme-immobilized design are therefore inextricably interdependent, and their integration must be adequate for both the application of enzymes and the specific reaction characteristics in question.

3.1.2 Format of Conventional Continuous Reactors with Immobilized Enzymes

There are several options for continuous operation using immobilized enzymes (Fig. 6). The primary option is a tubular format consisting of packed-bed reactors (Fig. 6e), where the immobilized enzyme is contained and fixed within the reactor while the substrate stream passes through and the stirred tank (Fig. 6a) where the enzyme is retained in the reactor by an appropriate screen or recovered by ex-situ filtration or centrifugation and recycled back into the reactor (Panels b-d in Fig. 6). An alternative is the expanded or fluidized bed reactor (Fig. 6f), where the enzyme

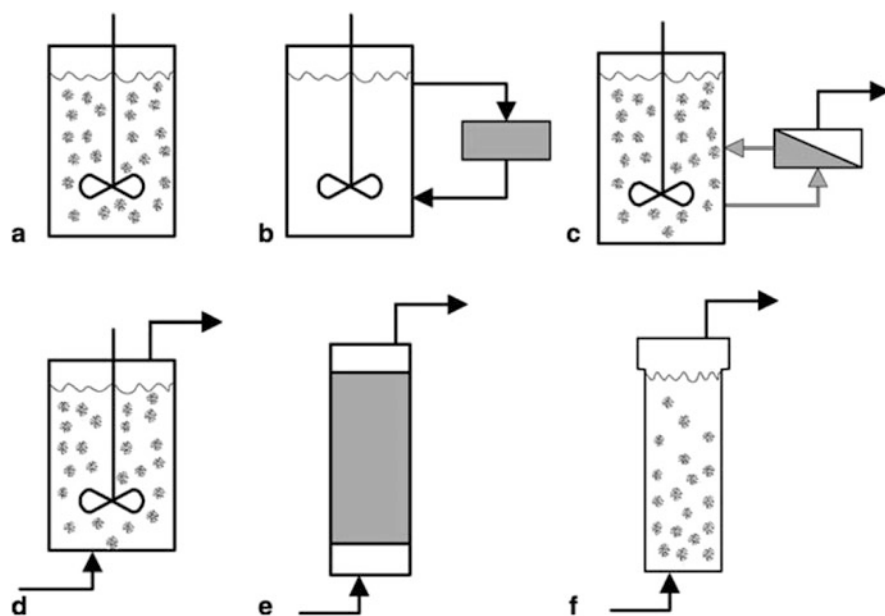


Fig. 6 Different configurations of enzyme-immobilized reactors. Panels (A-C) show reactor operated in batch mode or semicontinuously. Panels (D-F) show continuous-flow reactors. (a) Batch stirred-tank. (b) Recirculation batch stirred-tank. (c) Ultrafiltration stirred tank. (d): Continuous stirred tank. (e): Fixed-bed reactor. (f) Fluidized bed reactor. Figure was reproduced with permission from [69]

particles are retained by a hydrodynamic balance between gravity and drag forces promoted by the upflow substrate stream. Both tank and tubular configurations are operated under steady state. Multiple examples at lab-scale and industrial implementation can be found showing successful integration of immobilized enzymes in continuous flow [69, 70, 72, 74].

3.1.3 Conventional Continuous Reactors: Limitations and Need for New Technologies

Given the long tradition of continuous operation in the field of biocatalysis, researchers have accumulated significant knowledge about continuous enzyme reactors involving both soluble and immobilized enzymes over the last several decades [70–72, 74]. In recent years, however, the number of enzymes and transformations explored at lab-scale has expanded significantly, and a strong trend towards continuous operation rather than traditional batchwise (bio)chemical transformation has been widely recognized within the literature [4, 5, 8, 24, 25]. Many of these new transformations can be transferred to continuous operation using immobilized enzyme flow reactors [8, 24, 25]. However, there has also been a renewed wave of development and application of new continuous-flow reactors, which is being fuelled by three factors:

- Remaining unsolved problems of traditional immobilized-enzyme reactors, as described below.
- Increasing demands of biocatalysts and enzyme-catalyzed reactions (see Sect. 3.2).
- New technological possibilities offered by development in analytics and microfluidic technology.

Conventional enzyme-immobilized reactors share the limitations and casuistics of free enzyme reactions. Nonetheless, there are specific problems encountered in this type of reactors:

- Reactor designs relying on immobilized enzymes must commonly deal with the mass transfer limitations. Even when only a liquid phase reaction medium is used, there is still an external mass transport from the liquid phase to the solid phase component, as well as the additional internal diffusion step when the solid catalyst is porous [69, 77, 78].
- Continuous stirred tank reactors (CSTR) display poor kinetic performance at high conversions under most kinetic regimes since these reactors operate at the final conversion condition at steady state. The type of carrier material that can be integrated is also limited by considerations of mechanical stability, considering stirring physics and particle size realities. In addition, scalability can become problematic when the controlling phenomena change across scales [69, 77, 78].
- The fixed-bed reactor is restricted to certain types of carrier materials that provide suitable low back pressure. Furthermore, control of operational condition is

difficult along the entire length of the reactor as well as the integration of online monitoring. There is a defined operation window where suitable radial dispersion and absence of axial dispersion take place. Additionally, the residence time is related with the mass flow through the reactor and fluid flow which will influence suitable dispersion, mass, and heat transfer.

3.2 Modern Heterogeneous Biocatalysis and Emerging Demands: The Context of Microfluidic Technology

Modern biocatalysis processes have placed new demands on reactor engineering [3, 15–23] and include

- The format and stability of the immobilized catalyst must be adapted to continuous operation.
- Enzyme immobilization into the reactor must incorporate enough activity in cases of biocatalytic reactions with extremely low specific activity.
- Where biocatalytic reactions occur quickly, the reactor must guarantee an extremely efficient contact between the fluid reaction mixture and the solid catalyst.
- New systems require the contact of two fluid phases containing the substrates/products. The reactor design should be focused not only on the reaction kinetic but also on the phenomenology of the mass transfer between fluid–fluid–solid (catalyst) phases.
- Co-immobilization of multi-enzyme catalysts and chemo-enzyme catalysts frequently poses challenges.
- While modern industrial chemistry aims at the implementation of efficient processes, the intensification, characterization, and optimization of immobilized enzymes under operation conditions is extremely complex.

When current technology is confronted with new demands, enormous windows of opportunity arise. Microfluidic technology has arisen as an essential opportunity for implementation of heterogeneous biocatalytic reactions in shifting biocatalytic reactions from batch to continuous mode of operation, and concomitantly, towards intensified bioprocesses.

3.3 Immobilized Enzymes in Microfluidic Reactors: Challenges and Practical Implementation

3.3.1 Enzyme Immobilization into Microfluidic Reactors

The fundamental aspect of the design of immobilized-enzyme reactors is the enzyme for retention during continuous operation. The configuration of these reactors can

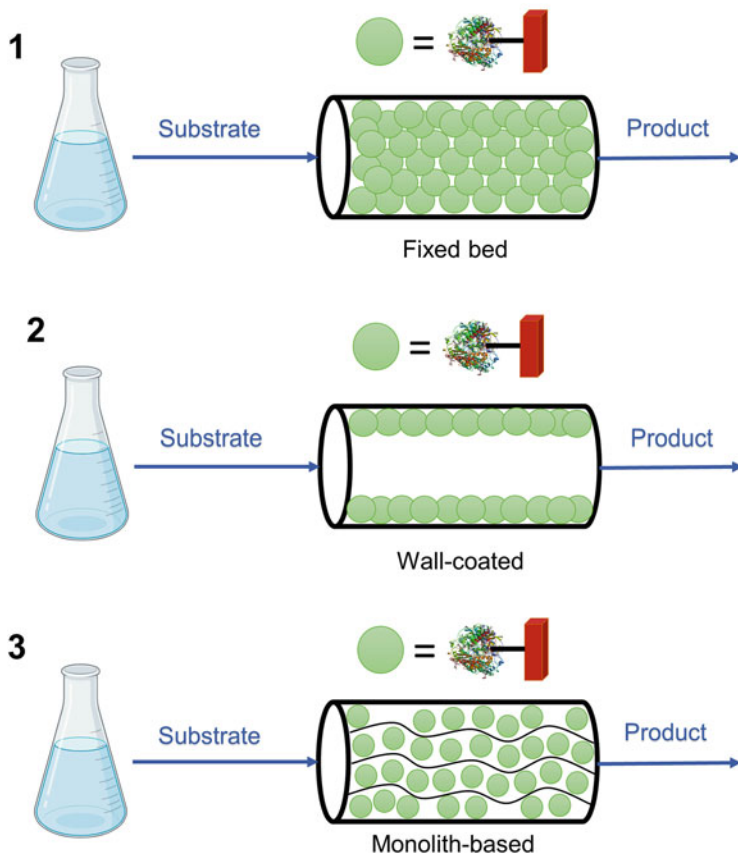


Fig. 7 Examples of enzyme-immobilized microreactors. (1) Wall-coated enzyme-immobilized microreactor where enzyme is directly integrated on the inner wall of the microchannels or supported on (nano)materials coating the inner walls. (2) Fixed-bed enzyme microreactor, where the enzyme is pre-immobilized into pre-existing carrier material that is packed. (3) Monolith enzyme microreactor, where the enzyme is immobilized onto the surface of the pores/channels constituting the monolithic structure

vary depending on the combination of reactor format and the enzyme immobilization method (Fig. 7).

The different reactor configurations can be encountered depending on how the enzymes are immobilized within the reactor space: packed microbead, wall-coated, and monolithic reactor, Fig. 7. The packed microbead reactor resembles traditional packed-bed reactors (PBRs). The enzymes are pre-immobilized into solid carriers, which are then further integrated in the form of a fixed-bed. The wall-coated configuration represents a reactor where the enzyme is surface-immobilized on the inner wall of microfluidic tubes creating a catalytic layer (with the reaction medium circulating through the tube). Lastly, in the monolithic reactor the microchannels are formed into a material network of meso- and macro-porosity. The monoliths material

can be either inorganic, organic, or biobased and natural hydrogels or made out of enzyme-based hydrogels. Enzymes can be immobilized onto these solid supports in several ways [71, 73, 75, 76, 79] and in flow reactors, specifically [8, 24, 25]. Nonetheless, the immobilization of enzymes within microfluidic reactors does pose some of the challenges commonly encountered in macroscale-based reactors [8, 9, 13, 24]. However, some specific considerations must be taken into account, such as:

- Immobilization must either be implemented off-site on previously synthesized materials, or directly onto the internal surface of the reactor.
- Materials used for microreactor fabrication must be compatible with the methodologies of enzyme immobilization or else they can create an unfavorable micro-environment that is not adverse for proper enzymatic function.
- For complex multistep reactions spatial compartmentalization and spatial orientation is essential to optimize the kinetic of the multistep reaction.
- For high-throughput screening and reactor characterization, reversible immobilization is preferable.
- At the microscale, phenomena as aggregation or channel clogging must be taken into account and are commonly encountered.

In addition to these technical requirements, enzyme immobilization must also address one critical question: how much biocatalytic activity per unit reactor volume is required for optimal performance? This is determined via consideration of two fundamental factors: the quantity and the quality of the immobilized enzyme. The quantity depends on the surface area and the volume available for the incorporation of the enzyme into the microreactor; the quality depends on the protein structure following immobilization, which is in turn dependent on the chemistry of the immobilization process that is utilized [71, 73, 75].

3.3.2 High Quality Enzyme Immobilization in Microfluidic Reactors

Among the different strategies to modulate protein-material chemical binding, covalent immobilization by aldehyde chemistry (glutaraldehyde) was initially implemented due to its relative simplicity [7, 8, 24, 25]. Unfortunately, this process lacks granular control of the protein-surface interaction by the glutaraldehyde chemistry. The science of enzyme immobilization has progressed significantly over the years, and researchers now have a rich toolbox of material activation and immobilization chemistries at their disposal to achieve high activity and stability.

Covalent immobilization on aldehyde- or epoxy activated carriers has been implemented in flow reactors [8, 24, 69]. Unfortunately, this immobilization process creates an irreversible binding between the micro-structured element and the protein, disabling reuse of the microreactor system. The functionalization chemistry can also be difficult to be implemented in microreactors. To overcome this problem, reversible binding resting on ionic interactions has been explored [8, 38, 80, 81]. To strengthen the binding and direct the immobilization, however, enzymes may need to be genetically fused to both binding modules and peptide tags. Different strategies

of directed immobilization by peptide modules have been implemented; through this strategy, both purification and immobilization are accomplished in just one-step [82–84]. Reversible immobilization based on protein-based cationic modules or His-tags have also been implemented in both wall-coated reactors and PBRs [8, 82, 83, 85–87]. Contrarily, directed irreversible immobilization can guarantee stable binding without enzyme leaching, although recyclability of the reactor and material might be problematic. Orthogonal or self-immobilizing techniques using Spy, Halo, and streptavidin protein motifs and formylglycine-generating enzymes have been used in microfluidic bed reactors or in wall-coated reactors [8, 88–91].

3.3.3 Enzyme Immobilization in High Quantity in Microfluidic Reactors

Increases in the amount of protein in question may necessitate an efficient use of the surface available for protein binding. The total surface available depends on the reactor format, and the relevant surface area is calculated by reference to the internal surface of the packed material in PBRs, the surface area generated during the monoliths manufacturing, and the inner area of microfluidic tubular reactors [8, 9, 92–102]. Recent examples of the continuous-flow reactors rest in the translation from batch reactors to PBRs using medium mesoporous or macroporous particles of a diverse nature – such as cross-linked agarose, cross-linked polyacrylic polymers, and silica [8, 24]. The combination of medium-high protein loadings (10–100 mg g⁻¹) and dense packing into PBRs typically leads to a high catalyst concentration [8, 24]. In the monolithic reactors, the enzyme is immobilized into an inner porous surface which is created during the synthesis process, which aims to obtain a uniform monolayer via controlled immobilization, or by the controlled formation of thin films [8]. Enhancing the practical use of intensified enzymatic reactors is also now being assisted by advancements in reactor engineering, which include new reactor concepts and fabrication technologies. 3D printed reactors [32, 34] and groove-typed channel microreactors have been tailored to increase the loading capacity [14].

Across all three reactor formats, the amount of catalyst and the format of the material need to be adequate within the interplay with fluid dynamics of the reactor and the suitable residence time [77, 103, 104]. The design of an immobilized enzyme must therefore always consider:

- Incorporating enough enzymes to reach a high space-time yield.
- The format of the immobilized enzyme and reactor dimensions, which must enable the operation of suitable mass flow to achieve a high conversion under suitable fluid flow conditions.
- Unfavorable fluid dynamics which can provoke presence of mass transfer resistances or the creation of preferential channels through the fixed-bed, thereby decreasing the expected conversion and the efficiency of the immobilized enzyme.

- Low back pressure, since the use of small particles packed in microreactors can cause high pressure to drop along the fixed-bed.
- The reactor dimensions (length and diameter), which must be designed according to the superficial velocity along the reactor to operate under suitable regime of excellent radial dispersion and absence of axial dispersion. Otherwise, the reactor operation can deviate from the ideal plug-flow configuration, leading to a corresponding decline in conversion.

In short, enzyme immobilization, reactor design, and operational parameters must all be well integrated into a holistic design [9, 105].

4 Exploitation of Microfluidic Enzyme-Immobilized Reactors

4.1 Promises and Advantages of Microfluidics in Enzyme-Immobilized Reactors

The possibilities and promises that microfluidic reactors offer can be briefly summarized as follows:

- *Improvement of the development of continuous bioprocesses.* The contribution of miniaturization during the development phase stems from both the velocity of the generation of information at low consumption of resources and enhanced controlled evaluation of process conditions [9, 36, 105–107].
- *Reaction intensification by exploitation of microfluidic features.* Microscale effects on transport arise due to short diffusional distances and high surface-to-volume ratio in the channels. These can contribute to the acceleration of the reaction, when compared to a reactor format that is more tightly limited by the mass-transfer across boundaries [9, 28, 29, 36, 105].
- *Generation of new operation windows.* The confinement of reactants under flow in microchannels under submillimeter scale can offer more precise process controls (i.e., regular flow pattern, fast response, and uniform temperature distribution) as well as reliable operations under novel process windows [108–112].
- *Contribution to the development of modular, small efficient production plants.* Recent trends in both pharma and fine chemicals production towards continuous manufacturing with full integration of unit operations are associated with the modularity of micro- and meso-reaction platforms [7, 9, 13, 113–117].

In the following section, we are offering some examples that illustrate how these benefits have at least to some extent already been realized – while also highlighting the considerable challenges that still remain relating to the implementation of immobilized enzymes in microfluidic systems.

4.2 Intensification of Solid–Liquid Reactions in Microfluidic Reactors

In solid–liquid reactions, the enzyme is considered the solid phase (i.e., the solid phase is the inner wall of wall-coated reactors, the surface of pores of monoliths or the internal surface of porous particles) while the reaction medium is the liquid phase. The liquid phase is directed by laminar flow through the channels, and the transport is affected via molecular diffusion. In this context, the first question that must be addressed is whether the internal area is sufficiently large to provide enough overall reaction rate?

4.2.1 Miniaturization in Flow Wall-Coated Reactors and Fast Reactions

In principle – given the relatively small dimension of the diameter channel – it might be expected that high enzyme concentration and high volumetric activities can be reached with high surface-to-volume ratio at the microfluidic scale, thereby enabling the operation under a kinetic control regime in the absence of diffusion limitations [118]. To analyze this effect, timescale analysis has been performed in wall-coated reactors. Timescale analysis is based on the comparison of the characteristic times of the respective phenomena being examined [118]. With this aim, the magnitude of the reaction time, diffusion time, and residence time are all calculated and then compared with draw different windows (Fig. 8). Such timescale analysis enables the identification of key variables in design (i.e., diameter tube) and immobilization (i.e., enzyme loading and specific activity) as they impact the operation itself (i.e., flow rate). The maximum space-time-yield scales directly with the enzyme activity immobilized on the available wall surface, which itself is reciprocally related to the diameter channel. Consequently, a reduction of the channel dimension below

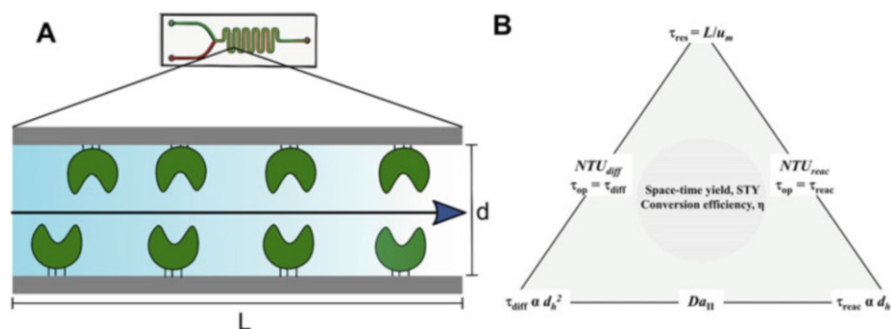


Fig. 8 Schematic representation of an enzyme-immobilized microfluidic reactor (a). Panel (b) shows reaction engineering analysis of the wall-coated immobilized enzyme microreactor. The operational window for space-time yield (STY) and conversion efficiency is determined by the interplay of the characteristic times of reaction (τ_{react}), diffusion (τ_{diff}) and reactor operation (mean residence time, τ_{res}). For details see [86, 118]. Figure was adapted with permission from [86, 118]

100 μm boosts reaction rate above 50 mM min^{-1} for enzymes with high catalytic turnover ($>50 \text{ s}^{-1}$). As the transport time decreases reciprocally to the diameter of the channel, the miniaturization not only boosts the reaction rate, but also enhances the transport enabling the reactor in an operation regime of kinetic control. The subsequent interplay between reaction characteristics, microchannel geometry, and reactor operation allows the identification of further operation windows (i.e., residence time) to achieve high conversion. This has been proved for both phosphorylation and glycosylation reactions [80, 118].

These features can be widely exploited to determine the intrinsic kinetic parameters of immobilized enzymes within a reactor [119], or to optimize both conversion and space-time yield aided by timescale analysis and mathematical modelling [85, 118]. The way an operation in microfluidic wall-coated reactor performs under a regime of a perfect radial mixture with low axial dispersion has been both experimentally and mathematically studied in some detail [85, 120]. Moreover, in this example, the model successfully predicted the performance of two consecutively connected microreactors coated enzyme – and could potentially be used to design and optimize efficient and sustainable processes of chiral amine synthesis catalyzed with surface-immobilized enzymes [121]. Capillary reactors have been also very effective to make effective use of their high surface to volume ratio [122].

4.2.2 Miniaturization in Flow and Reaction Intensification

For slow reactions (i.e., with a catalytic constant below 5 s^{-1}), the high inner area combined with a short characteristic dimension at the microscale could be insufficient, since the enzyme activity confined into the reactor is not enough to provide a high enough reaction rate. In such cases, surface coating with nanomaterials (i.e., nanoparticles, nanosprings, nanotubes, etc.) [123–126] and polymers [127] increases the enzyme loadings, thereby enhancing the reactor performance. The use of porous particles to coat the inner wall of microchannels also increases enzyme loading working in conditions of short diffusional paths. This has also been shown for phosphorylation and glycosylation reactions. In those examples, reaction rate is reduced from several days to several hours, with a space-time yield of $500 \text{ mmol L}^{-1} \text{ h}^{-1}$ at product titers of $\sim 200 \text{ mM}$ [123, 124]. Procedures based on the integration of material sciences, advanced reactor printing, protein chemistry, and protein engineering represent a wonderful opportunity. The enhancement of the catalytic phase and catalyst concentration has been also achieved by using enzyme immobilized onto nanoparticles that are flown through microchannels [128, 129].

Many recent examples of the called flow biocatalysis are built on the packing of porous particles into fixed-bed reactors. Increases in reaction rates when compared with batch processing are related to the high catalyst concentration compatible with a suitable mass transfer. This feature is exploited both to shorten the reaction time of slow reactions and also to ensure an extremely efficient contact between the fluid reaction mixture and the solid catalyst for fast reaction. In many cases this is accompanied by unstable product or unstable reaction intermediates. Intensification

in flow reactors at different dimensions has been recently reviewed in the literature [4, 8, 25]. In general, more extensive studies into reactor backpressure, dispersion, distribution of residence times, and external mass transfer still need to be carefully performed, both from an experimental and a modelling point of view, in order to gain a more fulsome assessment of the reactors and window of operation. These are based on the fact that in a fixed-bed reactor, internal diffusional limitations of the catalyst particle are not alleviated. On the contrary, it can actually aggravate external transport limitations when low superficial velocities are used [69, 78]. Additionally, the design and operation must ensure low backpressure and adequate distribution of the liquid through the fixed-bed. Nevertheless, opportunities also potentially arise from the window of operation at laminar flow at short diameter, characterized by a perfect mixing in the radial dimension but the absence of mixing along the axial dimension [62, 103, 104], an achievement of high volumetric activities, and more precise control of short residence times [130, 131].

Monoliths represent a combination of the large internal area of packed porous particles and the ordered laminar flow directed by the monolith channels. Silica monoliths enable high loading activity and are suitable to work under high flow at low backpressure at high reaction rate [8, 132, 133]. For instance, macrocellular silica monoliths prepared by a sol-gel method based on emulsion templating [134, 135] have been used for the adsorption and covalent grafting of transaminases. Aside from silica, monoliths can be also formed with biopolymers [136] like agarose [137, 138]. Through this approach, several thermostable enzymes have been successfully entrapped, recovering 80–90% activity upon the immobilization process. Alternatively, carrier-free immobilization has been proven to be very effective in achieving high enzyme loadings. The procedure can be based on the chemical cross-linking of proteins [139], or the aggregation can be genetically programmed via protein domains fused to the enzymes, in order to trigger the self-assembly of a 3D gel network within microreactors [88–90]. Studies on the influence of the mass transport (external and internal), residence time distribution, and the efficient use of enzymes are currently under current development [140–142].

4.3 Intensification of Solid–Fluid–Fluid Reactions in Microfluidic Reactors

In solid–fluid–fluid reactions, the enzyme is on solid phase (packed beads, inner surface) and the reaction medium is composed by at least two fluid phases [28, 143–146]. Multiphase flow with free enzymes has been previously discussed above, in Sect. 2 of this chapter. In this section, we focus more narrowly on enzyme-catalyzed reactions where two fluids are present, and the reaction takes place into the solid phase where the enzyme is immobilized involving gas–liquid–solid or liquid–liquid–solid systems.

4.3.1 Liquid–Liquid Reactions with Immobilized Enzymes in Flow

In liquid–liquid–solid reactions, the phenomena limiting the reaction rate and, thereby, the reactor performance is usually the mass transfer across phase boundaries. The main limitation can be focused on the transport between the two fluid phases or between the fluid phases towards the solid catalytic phase. Liquid–liquid–solid reactions are becoming increasingly common in continuous-flow reactions [28, 29]. The increase of the interfacial area in microfluidic reactors enhances these rates of transport reciprocally to the diameter of the flow channels. In fixed-bed reactors, to overcome mass transport limitation the dimension of the particles used and superficial velocity must be accordingly balanced [147, 148].

4.3.2 Gas–Liquid Reactions with Immobilized Enzyme in Microfluidic Reactions

In gas–liquid reactions, gaseous substrate usually requires transport into the aqueous liquid phase, where it reacts upon contact with surface-immobilized enzyme [9, 28, 144]. Gas–liquid–liquid reactions are of critical importance in bioprocessing. Oxidative O₂-dependent biotransformations are of interest for implementation in chemical synthesis, but their application is limited by the supply of oxygen to the active catalytic phase. As noted before, this limitation can be focused on the transport from gas to the liquid phase, or on the transport to the solid catalytic phase. These limitations are further aggravated by the relatively low oxygen solubility in the aqueous liquid phase. There are many examples of the intensification of O₂-dependent enzymatic reactions in continuous flow, but there are very few examples of the application with immobilized enzymes [9, 28, 81, 149–151]. The two main limitation steps of oxygen-dependent reactions can be studied comprehensively in microfluidic reactors.

First, the analysis can be focused on the transport from the dissolved oxygen from the liquid phase to the solid phase. For that purpose, immobilization of D-amino acid oxidase on borosilicate microchannel plates was performed. The immobilized enzyme activity was in the range expected for monolayer coverage of the plain surface with oxidase. Performance of the reactor was studied by employing in-line measurement of dissolved O₂, and off-line determination of the keto-acid product. Reaction-diffusion timescale analysis for different flow conditions showed that the heterogeneously catalyzed reaction was always slower than diffusion of O₂ to the solid surface, even though the immobilized enzyme confined in the microchannel reached a high volumetric activity of 10 mM min⁻¹. That demonstrates how the application of immobilized enzymes in microchannel wall-coated reactors not only boosts the volumetric activity but also enhances the transport rate of a scarce soluble compound to the catalytic phase [86]. In another study, a detailed analysis was performed on oxidation of cholesterol in microchannel reactor and compared reaction performance at microscale to reaction performances in stirred batch reactor and

continuously operated packed bed reactor [48, 49]. The results revealed a ~100-fold decrease in residence time at microscale process operation.

Second, the application of the oxygen-dependent reactions also increases the transport rate from the gas to liquid phase. Intensification of the transport across phases has been broadly demonstrated in process engineering [28]. To demonstrate the application of biocatalytic reactions a fully integrated falling film microreactor that provides controllable counter current gas–liquid phase contacting in a multi-channel micro-structured reaction plate was implemented. Advanced non-invasive optical sensing is applied to measure liquid phase oxygen concentrations in both in- and out-flow as well as directly in the microchannels to show how the reactor can supply up to 100 mM min^{-1} of oxygen to the liquid phase [152].

4.4 Assembly of Enzyme-Immobilized Cascades

The implementation of multistep enzyme catalyzed reactions in microfluidic systems was previously discussed. Enzyme cascades with the compartmentalization of the reactions by enzyme immobilization have been now addressed [14, 153]. Sequential and parallel cascades have already been assembled in enzyme-immobilized microreactors [154] but recently, the synthesis of the antiviral Islatravir was implemented by the immobilization of several engineered enzymes (galactose oxidase and kinases) and implemented in a continuous flow [153]. In another notable example, a wall-coated microfluidic reactor containing a three-enzyme cascade compartmentalized in three microreactor modules was implemented by using directed immobilization [155, 156], displaying precise control of the spatial organization and reaction control. An enzymatic reactor consisting of a packed tube was used to facilitate the *in vitro* study of this dual enzyme pathway consisting of a transketolase and transaminase. That allowed a quantitative evaluation of the conversion kinetics [87]. Another compartmentalization method arises from the use of magnetic microbeads loaded in microfluidic flow cells. Recently, a microfluidic system was used to optimize the enzymatic production of both levodopa (L-DOPA) and dopamine in both single-step and multistep reaction sequences, which led to a yield of approximately 30% for LDOPA production and 70% for dopamine production [157]. Incompatibility between different reaction steps in cascades in series has also been solved via compartmentalization in connected reactors [158]. Orthogonal cascades have been implemented to overcome some critical problems of the implementation of continuous processes. Continuous-flow applications for biocatalysis face substantial technical obstacles, particularly for enzymes that require cofactors [159–161].

4.5 *Generation of Novel Process Windows*

It has been proposed that the application of micro-structured reactors could expand the window of operation of the chemical processes [111, 112]. The confinement of reactants under flow in microchannels under submillimeter scale promises not only transport intensification, but also more precise process control (i.e., regular flow pattern, fast response, and uniform temperature distribution) and more reliable operation under novel process windows (i.e., elevated temperatures, high pressure, explosive, toxic conditions). In addition, some physical transport phenomena beneficial for chemical synthesis take place below a certain channel diameter (e.g., regular laminar flow, surface-tension dominated droplet/bubble flow, inhibition of explosion propagation for enhanced safety). Exploiting these effects, microreactors allow the achievement of operation conditions, and reactor performance not achievable in other configurations [26, 27].

One interesting case is the commented oxidative O₂-dependent biotransformations. It has been shown how continuous-flow microreactor technology can expand the process window by increasing the medium pressure range (≤ 34 bar), enabling biotransformations to be conducted within a single liquid phase at boosted concentrations of the dissolved O₂ (up to 43 mM). Using soluble enzymes in liquid flow, a rate enhancement (up to six-fold) stemming from the effect of elevated O₂ concentrations was observed on the oxidase kinetics. When additional catalase was used to recycle dissolved O₂ from the H₂O₂ released in the oxidase reaction, product formation was doubled compared to the O₂ supplied, in the absence of transfer from a gas phase. A packed-bed reactor containing oxidase and catalase co-immobilized on porous beads was implemented to demonstrate catalyst recyclability and operational stability during continuous high-pressure conversion. Product concentrations of up to 80 mM were obtained at low residence times (1–4 min) [81].

4.6 *Scale-Up and Scale-Down Impact on Productivity and Space-Time Yield*

Microfluidic reactors enable the achievement of a high space-time yield ($\text{g L}^{-1} \text{h}^{-1}$) at efficient use of the enzyme catalyst. One major question in the applications of microfluidic flow reactors is the scalability in terms of increasing (or suiting) the required total productivity (g h^{-1}). Studies performed in wall-coated enzyme-immobilized reactors have shown that a decrease in the characteristic reactor dimension can allow the reduction of the volume while still preserving conversion and total productivity [89]. Although it is widely acknowledged that microreactors can also be used for the actual production in addition to enhanced bioprocess development, studies actually comparing the effect of reactor format on space-time yield and productivity remain relatively scarce [8]. Most reports in the literature mention the usefulness of the microfluidic systems for process screening in enzymatic reactors,

but very few actually proceed to increase the scale in order to benchmark the results obtained [162]. In one recent example, a microfluidic enzymatic reactor for L-DOPA production was up-scaled (780-fold increase) to a milliliter scale system by maintaining similar mass transport properties resulting in the same yield, space-time yield, and biocatalyst yield as its microscale counterpart. The results obtained for yield and biocatalyst yield were like what is reported in the literature for similar systems, however the space-time yield was higher [157]. Calculations on productivity were made available for enzymatic microreactors and cost analysis shows the potential for high-value pharmaceutical synthesis [163, 164]. In another illustrative example, comparison between different laccase/reactor formats revealed that the catechol oxidation was more efficient when the enzyme was immobilized on the surface of microchannels [165]. Scale-out and numbering up are approaches to increase the total production while keeping constant characteristic distance [162, 166].

5 Conclusions

Microfluidic enzyme reactors play an important role in the current trend of transit to continuous bioprocesses and process intensification. Progress is strongly anchored on an interdisciplinary approach where material sciences, protein engineering, enzyme immobilization, process engineering, mathematical modelling and analytical chemistry are combined. However, despite all the progress in this field in recent years, not all promises of these systems have been fulfilled as their chemical synthesis counterparts (Table 1).

There are still challenges to be addressed for an effective use of continuous-flow microreactors, namely: the overall gain in process intensification and economic

Table 1 Demonstrated benefits of flow biocatalysis using continuous-flow microreactors (adapted from [13])

	Promised benefit of flow biocatalysis
Demonstrated	Continuous processing at smaller scales
	Better spatial and temporal control
	High surface-to-volume ratio
	Improved transport in multiphase systems
	Product removal/product isolation
Partially demonstrated	Faster process development
	Plug-and-play construction of process configuration
	Expanded biocatalytic process windows
Not demonstrated	Safety, health, and environmental advantages
	Mobile process plants
	Energy efficiency
	Cost-effectiveness (e.g., capital expenditures and cost of goods)

feasibility; the long-term robustness and stability of the enzymatic process; recycling of streams, including enzymes and recycling/regeneration of cofactor; enzyme preparation, in particular for immobilized form, and associated costs; and matching reaction and recovery times in cascade reactions. Additionally, general limitations for further uptake in industry include the lack of a more comprehensive monitoring of all process variables and automation, insufficient sample volume for quality control, and integration of downstream processing. The standardization of device and components, as well as, the development of sensor technology would allow the implementation of Process Analytical Technology (PAT), reducing dependency of end-users on specific manufactures, reducing operator-induced variability whilst improving product quality [36]. Until all these are addressed, flow biocatalysis will be implemented on a case-by-case approach and not truly universal.

References

1. Woodley JM (2020) New frontiers in biocatalysis for sustainable synthesis. *Curr Opin Green Sustain Chem* 21:22–26. <https://doi.org/10.1016/j.cogsc.2019.08.006>
2. Woodley JM, Turner NJ (2019) New Frontiers in biocatalysis. In: *Handbook of green chemistry*. Wiley, Weinheim, pp 73–86
3. Woodley JM (2019) Accelerating the implementation of biocatalysis in industry. *Appl Microbiol Biotechnol* 103:4733–4739. <https://doi.org/10.1007/s00253-019-09796-x>
4. Tamborini L, Fernandes P, Paradisi F, Molinari F (2018) Flow bioreactors as complementary tools for biocatalytic process intensification. *Trends Biotechnol* 36:73–88. <https://doi.org/10.1016/j.tibtech.2017.09.005>
5. Britton J, Majumdar S, Weiss GA (2018) Continuous flow biocatalysis. *Chem Soc Rev* 47:5891–5918. <https://doi.org/10.1039/C7CS00906B>
6. Hartman RL (2020) Flow chemistry remains an opportunity for chemists and chemical engineers. *Curr Opin Chem Eng* 29:42–50. <https://doi.org/10.1016/j.coche.2020.05.002>
7. Žnidaršič-Plazl P (2019) The promises and the challenges of biotransformations in microflow. *Biotechnol J* 14:1800580. <https://doi.org/10.1002/biot.201800580>
8. Bolivar JM, López-Gallego F (2020) Characterization and evaluation of immobilized enzymes for applications in flow reactors. *Curr Opin Green Sustain Chem* 25:100349. <https://doi.org/10.1016/j.cogsc.2020.04.010>
9. Bolivar JM, Wiesbauer J, Nidetzky B (2011) Biotransformations in microstructured reactors: more than flowing with the stream? *Trends Biotechnol* 29:333–342. <https://doi.org/10.1016/j.tibtech.2011.03.005>
10. Leemans Martin L, Peschke T, Venturoni F, Mostarda S (2020) Pharmaceutical industry perspectives on flow chemocatalysis and biocatalysis. *Curr Opin Green Sustain Chem* 25:100350. <https://doi.org/10.1016/j.cogsc.2020.04.011>
11. Guajardo N, Domínguez de María P (2019) Continuous biocatalysis in environmentally-friendly media: a triple synergy for future sustainable processes. *ChemCatChem* 11:3128–3137. <https://doi.org/10.1002/cctc.201900773>
12. De Santis P, Meyer L-E, Kara S (2020) The rise of continuous flow biocatalysis – fundamentals, very recent developments and future perspectives. *React Chem Eng*. <https://doi.org/10.1039/D0RE00335B>
13. Wohlgenuth R, Plazl I, Žnidaršič-Plazl P, Gernaey KV, Woodley JM (2015) Microscale technology and biocatalytic processes: opportunities and challenges for synthesis. *Trends Biotechnol* 33:302–314. <https://doi.org/10.1016/j.tibtech.2015.02.010>

14. Zhu Y, Chen Q, Shao L, Jia Y, Zhang X (2020) Microfluidic immobilized enzyme reactors for continuous biocatalysis. *React Chem Eng* 5:9–32. <https://doi.org/10.1039/C9RE00217K>
15. Sheldon RA, Pereira PC (2017) Biocatalysis engineering: the big picture. *Chem Soc Rev* 46:2678–2691. <https://doi.org/10.1039/C6CS00854B>
16. Bornscheuer UT (2018) The fourth wave of biocatalysis is approaching. *Philos Trans R Soc Math Phys Eng Sci* 376:20170063. <https://doi.org/10.1098/rsta.2017.0063>
17. Chen K, Arnold FH (2020) Engineering new catalytic activities in enzymes. *Nat Catal* 3:203–213. <https://doi.org/10.1038/s41929-019-0385-5>
18. Alcántara AR (2019) Biocatalysis and pharmaceuticals: a smart tool for sustainable development. *Catalysts* 9:792. <https://doi.org/10.3390/catal9100792>
19. Bernal C, Rodríguez K, Martínez R (2018) Integrating enzyme immobilization and protein engineering: an alternative path for the development of novel and improved industrial biocatalysts. *Biotechnol Adv* 36:1470–1480. <https://doi.org/10.1016/j.biotechadv.2018.06.002>
20. Sheldon RA, Woodley JM (2018) Role of biocatalysis in sustainable chemistry. *Chem Rev* 118:801–838. <https://doi.org/10.1021/acs.chemrev.7b00203>
21. Woodley JM (2019) Reaction engineering for the industrial implementation of biocatalysis. *Top Catal* 62:1202–1207. <https://doi.org/10.1007/s11244-019-01154-5>
22. Sheldon RA, Brady D, Bode ML (2020) The Hitchhiker’s guide to biocatalysis: recent advances in the use of enzymes in organic synthesis. *Chem Sci* 11:2587–2605. <https://doi.org/10.1039/C9SC05746C>
23. Clayton AD, Labes R, Blacker AJ (2020) Combination of chemo- and bio-catalysis in flow. *Curr Opin Green Sustain Chem*:100378. <https://doi.org/10.1016/j.cogsc.2020.100378>
24. Romero-Fernández M, Paradisi F (2020) Protein immobilization technology for flow biocatalysis. *Curr Opin Chem Biol* 55:1–8. <https://doi.org/10.1016/j.cbpa.2019.11.008>
25. Thompson MP, Peñafiel I, Cosgrove SC, Turner NJ (2019) Biocatalysis using immobilized enzymes in continuous flow for the synthesis of fine chemicals. *Org Process Res Dev* 23:9–18. <https://doi.org/10.1021/acs.oprd.8b00305>
26. Yue J (2018) Multiphase flow processing in microreactors combined with heterogeneous catalysis for efficient and sustainable chemical synthesis. *Catal Today* 308:3–19. <https://doi.org/10.1016/j.cattod.2017.09.041>
27. Rossetti I (2018) Continuous flow (micro-)reactors for heterogeneously catalyzed reactions: Main design and modelling issues. *Catal Today* 308:20–31. <https://doi.org/10.1016/j.cattod.2017.09.040>
28. Bolivar JM, Nidetzky B (2013) Multiphase biotransformations in microstructured reactors: opportunities for biocatalytic process intensification and smart flow processing. *Green Process Synth* 2. <https://doi.org/10.1515/gps-2013-0091>
29. Karande R, Schmid A, Buehler K (2016) Applications of multiphase microreactors for biocatalytic reactions. *Org Process Res Dev* 20:361–370. <https://doi.org/10.1021/acs.oprd.5b00352>
30. O’Sullivan B, Al-Bahrani H, Lawrence J, Campos M, Cázares A, Baganz F, Wohlgemuth R, Hailes HC, Szita N (2012) Modular microfluidic reactor and inline filtration system for the biocatalytic synthesis of chiral metabolites. *J Mol Catal B Enzym* 77:1–8. <https://doi.org/10.1016/j.molcatb.2011.12.010>
31. Maier MC, Valotta A, Hiebler K, Soritz S, Gavric K, Grabner B, Gruber-Woelfler H (2020) 3D printed reactors for synthesis of active pharmaceutical ingredients in continuous flow. *Org Process Res Dev*. <https://doi.org/10.1021/acs.oprd.0c00228>
32. Sans V (2020) Emerging trends in flow chemistry enabled by 3D printing: robust reactors, biocatalysis and electrochemistry. *Curr Opin Green Sustain Chem*:100367. <https://doi.org/10.1016/j.cogsc.2020.100367>
33. Bojang AA, Wu H-S (2020) Design, fundamental principles of fabrication and applications of microreactors. *PRO* 8:891. <https://doi.org/10.3390/pr8080891>

34. Peris E, Okafor O, Kulcinskaja E, Goodridge R, Luis SV, Garcia-Verdugo E, O'Reilly E, Sans V (2017) Tuneable 3D printed bioreactors for transaminations under continuous-flow. *Green Chem* 19:5345–5349. <https://doi.org/10.1039/C7GC02421E>
35. Gruber P, Marques MPC, Szita N, Mayr T (2017) Integration and application of optical chemical sensors in microbioreactors. *Lab Chip* 17:2693–2712. <https://doi.org/10.1039/C7LC00538E>
36. Marques MP, Szita N (2017) Bioprocess microfluidics: applying microfluidic devices for bioprocessing. *Curr Opin Chem Eng* 18:61–68. <https://doi.org/10.1016/j.coche.2017.09.004>
37. Gruber P, Marques MPC, Sulzer P, Wohlgemuth R, Mayr T, Baganz F, Szita N (2017) Real-time pH monitoring of industrially relevant enzymatic reactions in a microfluidic side-entry reactor (μ SER) shows potential for pH control. *Biotechnol J* 12:1600475. <https://doi.org/10.1002/biot.201600475>
38. Viefhues M, Sun S, Valikhani D, Nidetzky B, Vrouwe EX, Mayr T, Bolivar JM (2017) Tailor-made resealable micro(bio)reactors providing easy integration of in situ sensors. *J Micromech Microeng* 27:065012. <https://doi.org/10.1088/1361-6439/aa6eb9>
39. Gruber P, Carvalho F, Marques MPC, O'Sullivan B, Subrizi F, Dobrijevic D, Ward J, Hailes HC, Fernandes P, Wohlgemuth R, Baganz F, Szita N (2018) Enzymatic synthesis of chiral amino-alcohols by coupling transketolase and transaminase-catalyzed reactions in a cascading continuous-flow microreactor system. *Biotechnol Bioeng* 115:586–596. <https://doi.org/10.1002/bit.26470>
40. Gruber P, Marques MPC, O'Sullivan B, Baganz F, Wohlgemuth R, Szita N (2017) Conscious coupling: the challenges and opportunities of cascading enzymatic microreactors. *Biotechnol J* 12:1700030. <https://doi.org/10.1002/biot.201700030>
41. Kim PY, Pollard DJ, Woodley JM (2007) Substrate supply for effective biocatalysis. *Biotechnol Prog* 23(1):74–82. <https://doi.org/10.1021/bp060314b>
42. Freeman A, Woodley JM, Lilly MD (1993) In situ product removal as a tool for bioprocessing. *Bio/technology* 11(9):1007–1012. <https://doi.org/10.1038/nbt0993-1007>
43. Semenova D, Fernandes AC, Bolivar JM, Rosinha Grundtvig IP, Vadot B, Galvanin S, Mayr T, Nidetzky B, Zubov A, Gernaey KV (2020) Model-based analysis of biocatalytic processes and performance of microbioreactors with integrated optical sensors. *New Biotechnol* 56:27–37. <https://doi.org/10.1016/j.nbt.2019.11.001>
44. Bolivar JM, Consolati T, Mayr T, Nidetzky B (2013) Shine a light on immobilized enzymes: real-time sensing in solid supported biocatalysts. *Trends Biotechnol* 31:194–203. <https://doi.org/10.1016/j.tibtech.2013.01.004>
45. Adebar N, Choi JE, Schober L, Miyake R, Iura T, Kawabata H, Gröger H (2019) Overcoming work-up limitations of biphasic biocatalytic reaction mixtures through liquid-liquid segmented flow processes. *ChemCatChem* 11:5788–5793. <https://doi.org/10.1002/cctc.201901107>
46. Žnidaršič-Plazl P, Plazl I (2009) Modelling and experimental studies on lipase-catalyzed isoamyl acetate synthesis in a microreactor. *Process Biochem* 44:1115–1121. <https://doi.org/10.1016/j.procbio.2009.06.003>
47. Pohar A, Plazl I, Žnidaršič-Plazl P (2009) Lipase-catalyzed synthesis of isoamyl acetate in an ionic liquid/n-heptane two-phase system at the microreactor scale. *Lab Chip* 9:3385. <https://doi.org/10.1039/b915151f>
48. Marques MPC, Fernandes P, Cabral JMS, Žnidaršič-Plazl P, Plazl I (2012) Continuous steroid biotransformations in microchannel reactors. *New Biotechnol* 29:227–234. <https://doi.org/10.1016/j.nbt.2011.10.001>
49. Marques MPC, Fernandes P, Cabral JMS, Žnidaršič-Plazl P, Plazl I (2010) On the feasibility of in situ steroid biotransformation and product recovery in microchannels. *Chem Eng J* 160:708–714. <https://doi.org/10.1016/j.cej.2010.03.056>
50. Vobecká L, Tichá L, Atanasova A, Slouka Z, Hasal P, Příbyl M (2020) Enzyme synthesis of cephalixin in continuous-flow microfluidic device in ATPS environment. *Chem Eng J* 396:125236. <https://doi.org/10.1016/j.cej.2020.125236>

51. Novak U, Lavric D, Žnidaršič-Plazl P (2016) Continuous lipase B-catalyzed isoamyl acetate synthesis in a two-liquid phase system using corning® AFRTM module coupled with a membrane separator enabling biocatalyst recycle. *J Flow Chem* 6:33–38. <https://doi.org/10.1556/1846.2015.00038>
52. Dong J, Fernández-Fueyo E, Hollmann F, Paul CE, Pesic M, Schmidt S, Wang Y, Younes S, Zhang W (2018) Biocatalytic oxidation reactions: a Chemist's perspective. *Angew Chem Int Ed* 57:9238–9261. <https://doi.org/10.1002/anie.201800343>
53. Hone CA, Roberge DM, Kappe CO (2017) The use of molecular oxygen in pharmaceutical manufacturing: is flow the way to go? *ChemSusChem* 10:32–41. <https://doi.org/10.1002/cssc.201601321>
54. Gemoets HPL, Su Y, Shang M, Hessel V, Luque R, Noël T (2016) Liquid phase oxidation chemistry in continuous-flow microreactors. *Chem Soc Rev* 45:83–117. <https://doi.org/10.1039/C5CS00447K>
55. Garcia-Ochoa F, Gomez E (2009) Bioreactor scale-up and oxygen transfer rate in microbial processes: an overview. *Biotechnol Adv* 27:153–176. <https://doi.org/10.1016/j.biotechadv.2008.10.006>
56. Gemoets HPL, Hessel V, Noël T (2016) Reactor concepts for aerobic liquid phase oxidation: microreactors and tube reactors. In: Stahl SS, Alsters PL (eds) *Liquid phase aerobic oxidation catalysis: industrial applications and academic perspectives*. Wiley, Weinheim, pp 397–419
57. van Schie MMCH, Pedroso de Almeida T, Laudadio G, Tieves F, Fernández-Fueyo E, Noël T, Arends IWCE, Hollmann F (2018) Biocatalytic synthesis of the green note trans -2-hexenal in a continuous-flow microreactor. *Beilstein J Org Chem* 14:697–703. <https://doi.org/10.3762/bjoc.14.58>
58. Illner S, Hofmann C, Löb P, Kragl U (2014) A falling-film microreactor for enzymatic oxidation of glucose. *ChemCatChem* 6:1748–1754. <https://doi.org/10.1002/cctc.201400028>
59. Toftgaard Pedersen A, de Carvalho TM, Sutherland E, Rehn G, Ashe R, Woodley JM (2017) Characterization of a continuous agitated cell reactor for oxygen dependent biocatalysis: biocatalytic oxidation in a continuous agitated cell reactor. *Biotechnol Bioeng* 114:1222–1230. <https://doi.org/10.1002/bit.26267>
60. Jones E, McClean K, Housden S, Gasparini G, Archer I (2012) Biocatalytic oxidase: batch to continuous. *Chem Eng Res Des* 90:726–731. <https://doi.org/10.1016/j.cherd.2012.01.018>
61. Brzozowski M, O'Brien M, Ley SV, Polyzos A (2015) Flow chemistry: intelligent processing of gas-liquid transformations using a tube-in-tube reactor. *Acc Chem Res* 48:349–362. <https://doi.org/10.1021/ar500359m>
62. Ringborg RH, Toftgaard Pedersen A, Woodley JM (2017) Automated determination of oxygen-dependent enzyme kinetics in a tube-in-tube flow reactor. *ChemCatChem* 9:3285–3288. <https://doi.org/10.1002/cctc.201700811>
63. Tomaszewski B, Schmid A, Buehler K (2014) Biocatalytic production of catechols using a high pressure tube-in-tube segmented flow microreactor. *Org Process Res Dev* 18:1516–1526. <https://doi.org/10.1021/op5002116>
64. Tomaszewski B, Lloyd RC, Warr AJ, Buehler K, Schmid A (2014) Regioselective biocatalytic aromatic hydroxylation in a gas-liquid multiphase tube-in-tube reactor. *ChemCatChem* 6:2567–2576. <https://doi.org/10.1002/cctc.201402354>
65. Van Hecke W, Ludwig R, Dewulf J, Auly M, Messiaen T, Haltrich D, Van Langenhove H (2009) Bubble-free oxygenation of a bi-enzymatic system: effect on biocatalyst stability. *Biotechnol Bioeng* 102:122–131. <https://doi.org/10.1002/bit.22042>
66. Bolivar JM, Schelch S, Pfeiffer M, Nidetzky B (2016) Intensifying the O₂-dependent heterogeneous biocatalysis: superoxygenation of solid support from H₂O₂ by a catalase tailor-made for effective immobilization. *J Mol Catal B Enzym* 134:302–309. <https://doi.org/10.1016/j.molcatb.2016.10.017>
67. Chapman MR, Cosgrove SC, Turner NJ, Kapur N, Blacker AJ (2018) Highly productive oxidative biocatalysis in continuous flow by enhancing the aqueous equilibrium solubility of oxygen. *Angew Chem Int Ed* 57:10535–10539. <https://doi.org/10.1002/anie.201803675>

68. Cosgrove SC, Matthey AP, Riese M, Chapman MR, Birmingham WR, Blacker AJ, Kapur N, Turner NJ, Flitsch SL (2019) Biocatalytic oxidation in continuous flow for the generation of carbohydrate dialdehydes. *ACS Catal* 9:11658–11662. <https://doi.org/10.1021/acscatal.9b04819>
69. Illanes A (2008) *Enzyme biocatalysis: principles and applications*. Springer, Dordrecht
70. Buchholz K, Kasche V, Bornscheuer UT (2012) *Biocatalysts and enzyme technology*, 2nd edn. Completely rev., and enlarged ed. Wiley-Blackwell, Weinheim
71. Guisan JM, López-Gallego F, Bolivar JM, Rocha-Martín J, Fernandez-Lorente G (2020) The science of enzyme immobilization. In: Guisan JM, Bolivar JM, López-Gallego F, Rocha-Martín J (eds) *Immobilization of enzymes and cells*. Springer, New York, pp 1–26
72. Basso A, Serban S (2019) Industrial applications of immobilized enzymes – a review. *Mol Catal* 479:110607. <https://doi.org/10.1016/j.mcat.2019.110607>
73. Rodrigues RC, Ortiz C, Berenguer-Murcia Á, Torres R, Fernández-Lafuente R (2013) Modifying enzyme activity and selectivity by immobilization. *Chem Soc Rev* 42:6290–6307. <https://doi.org/10.1039/C2CS35231A>
74. DiCosimo R, McAuliffe J, Poulouse AJ, Bohlmann G (2013) Industrial use of immobilized enzymes. *Chem Soc Rev* 42:6437. <https://doi.org/10.1039/c3cs35506c>
75. Garcia-Galan C, Berenguer-Murcia Á, Fernandez-Lafuente R, Rodrigues RC (2011) Potential of different enzyme immobilization strategies to improve enzyme performance. *Adv Synth Catal* 353:2885–2904. <https://doi.org/10.1002/adsc.201100534>
76. Mateo C, Palomo JM, Fernandez-Lorente G, Guisan JM, Fernandez-Lafuente R (2007) Improvement of enzyme activity, stability and selectivity via immobilization techniques. *Enzym Microb Technol* 40:1451–1463. <https://doi.org/10.1016/j.enzmictec.2007.01.018>
77. Levenspiel O (1999) *Chemical reaction engineering*, 3rd edn. Wiley, New York
78. Doran PM (2013) Heterogeneous reactions. In: *Bioprocess engineering principles*. Elsevier, pp 705–759
79. Cantone S, Ferrario V, Corici L, Ebert C, Fattor D, Spizzo P, Gardossi L (2013) Efficient immobilisation of industrial biocatalysts: criteria and constraints for the selection of organic polymeric carriers and immobilisation methods. *Chem Soc Rev* 42:6262. <https://doi.org/10.1039/c3cs35464d>
80. Adebar N, Gröger H (2019) Flow process for ketone reduction using a superabsorber-immobilized alcohol dehydrogenase from *Lactobacillus brevis* in a packed-bed reactor. *Bioengineering* 6:99. <https://doi.org/10.3390/bioengineering6040099>
81. Bolivar JM, Mannsberger A, Thomsen MS, Tekautz G, Nidetzky B (2019) Process intensification for O₂-dependent enzymatic transformations in continuous single-phase pressurized flow. *Biotechnol Bioeng* 116:503–514. <https://doi.org/10.1002/bit.26886>
82. Valikhani D, Bolivar JM, Pfeiffer M, Nidetzky B (2017) Multivalency effects on the immobilization of sucrose phosphorylase in flow microchannels and their use in the development of a high-performance biocatalytic microreactor. *ChemCatChem* 9:161–166. <https://doi.org/10.1002/cctc.201601019>
83. Kulsharova G, Dimov N, Marques MPC, Szita N, Baganz F (2018) Simplified immobilisation method for histidine-tagged enzymes in poly(methyl methacrylate) microfluidic devices. *New Biotechnol* 47:31–38. <https://doi.org/10.1016/j.nbt.2017.12.004>
84. Döbber J, Gerlach T, Offermann H, Rother D, Pohl M (2018) Closing the gap for efficient immobilization of biocatalysts in continuous processes: HaloTagTM fusion enzymes for a continuous enzymatic cascade towards a vicinal chiral diol. *Green Chem* 20:544–552. <https://doi.org/10.1039/C7GC03225K>
85. Miložič N, Lubej M, Lakner M, Žnidaršič-Plazl P, Plazl I (2017) Theoretical and experimental study of enzyme kinetics in a microreactor system with surface-immobilized biocatalyst. *Chem Eng J* 313:374–381. <https://doi.org/10.1016/j.cej.2016.12.030>
86. Bolivar JM, Tribulato MA, Petrasek Z, Nidetzky B (2016) Let the substrate flow, not the enzyme: practical immobilization of D-amino acid oxidase in a glass microreactor for

- effective biocatalytic conversions: immobilization of D -amino acid oxidase in a glass microreactor. *Biotechnol Bioeng* 113:2342–2349. <https://doi.org/10.1002/bit.26011>
87. Abdul Halim A, Szita N, Baganz F (2013) Characterization and multi-step transketolase- ω -transaminase bioconversions in an immobilized enzyme microreactor (IEMR) with packed tube. *J Biotechnol* 168:567–575. <https://doi.org/10.1016/j.jbiotec.2013.09.001>
88. Peschke T, Bitterwolf P, Hansen S, Gasmi J, Rabe K, Niemeyer C (2019) Self-immobilizing biocatalysts maximize space–time yields in flow reactors. *Catalysts* 9:164. <https://doi.org/10.3390/catal9020164>
89. Peschke T, Skoupi M, Burgahn T, Gallus S, Ahmed I, Rabe KS, Niemeyer CM (2017) Self-immobilizing fusion enzymes for compartmentalized biocatalysis. *ACS Catal* 7:7866–7872. <https://doi.org/10.1021/acscatal.7b02230>
90. Peschke T, Bitterwolf P, Gallus S, Hu Y, Oelschlaeger C, Willenbacher N, Rabe KS, Niemeyer CM (2018) Self-assembling all-enzyme hydrogels for flow biocatalysis. *Angew Chem Int Ed* 57:17028–17032. <https://doi.org/10.1002/anie.201810331>
91. Jian H, Wang Y, Bai Y, Li R, Gao R (2016) Site-specific, covalent immobilization of dehalogenase ST2570 catalyzed by Formylglycine-generating enzymes and its application in batch and semi-continuous flow reactors. *Molecules* 21:895. <https://doi.org/10.3390/molecules21070895>
92. Matosevic S, Szita N, Baganz F (2011) Fundamentals and applications of immobilized microfluidic enzymatic reactors. *J Chem Technol Biotechnol* 86:325–334. <https://doi.org/10.1002/jctb.2564>
93. Hailes HC, Dalby PA, Lye GJ, Baganz F, Micheletti M, Szita N, Ward JM (2010) α , α' -dihydroxy ketones and 2-amino-1,3-diols: synthetic and process strategies using biocatalysts. *Curr Org Chem* 14:1883–1893. <https://doi.org/10.2174/138527210792927555>
94. He P, Davies J, Greenway G, Haswell SJ (2010) Measurement of acetylcholinesterase inhibition using bienzymes immobilized monolith micro-reactor with integrated electrochemical detection. *Anal Chim Acta* 659:9–14. <https://doi.org/10.1016/j.aca.2009.11.052>
95. He P, Greenway G, Haswell SJ (2010) Development of enzyme immobilized monolith micro-reactors integrated with microfluidic electrochemical cell for the evaluation of enzyme kinetics. *Microfluid Nanofluidics* 8:565–573. <https://doi.org/10.1007/s10404-009-0476-8>
96. Schwarz A, Thomsen MS, Nidetzky B (2009) Enzymatic synthesis of β -glucosylglycerol using a continuous-flow microreactor containing thermostable β -glycoside hydrolase CelB immobilized on coated microchannel walls. *Biotechnol Bioeng* 103:865–872. <https://doi.org/10.1002/bit.22317>
97. Thomsen MS, Nidetzky B (2008) Microfluidic reactor for continuous flow biotransformations with immobilized enzymes: the example of lactose hydrolysis by a Hyperthermophilic β -cont;-glycoside hydrolase. *Eng Life Sci* 8:40–48. <https://doi.org/10.1002/elsc.200720223>
98. Kawakami K, Abe D, Urakawa T, Kawashima A, Oda Y, Takahashi R, Sakai S (2007) Development of a silica monolith microreactor entrapping highly activated lipase and an experiment toward integration with chromatographic separation of chiral esters. *J Sep Sci* 30:3077–3084. <https://doi.org/10.1002/jssc.200700309>
99. Wiles C, Hammond MJ, Watts P (2009) The development and evaluation of a continuous flow process for the lipase-mediated oxidation of alkenes. *Beilstein J Org Chem* 5. <https://doi.org/10.3762/bjoc.5.27>
100. Ngamsom B, Hickey AM, Greenway GM, Littlechild JA, Watts P, Wiles C (2010) Development of a high throughput screening tool for biotransformations utilising a thermophilic l-aminoacylase enzyme. *J Mol Catal B Enzym* 63:81–86. <https://doi.org/10.1016/j.molcatb.2009.12.013>
101. Kataoka S, Endo A, Oyama M, Ohmori T (2009) Enzymatic reactions inside a microreactor with a mesoporous silica catalyst support layer. *Appl Catal A Gen* 359:108–112. <https://doi.org/10.1016/j.apcata.2009.02.035>

102. Ristenpart WD, Wan J, Stone HA (2008) Enzymatic reactions in microfluidic devices: Michaelis–Menten kinetics. *Anal Chem* 80:3270–3276. <https://doi.org/10.1021/ac702469u>
103. Aroh KC, Jensen KF (2018) Efficient kinetic experiments in continuous flow microreactors. *React Chem Eng* 3:94–101. <https://doi.org/10.1039/C7RE00163K>
104. Nagy KD, Shen B, Jamison TF, Jensen KF (2012) Mixing and dispersion in small-scale flow systems. *Org Process Res Dev* 16:976–981. <https://doi.org/10.1021/op200349f>
105. Marques MPC, Fernandes P (2011) Microfluidic devices: useful tools for bioprocess intensification. *Molecules* 16:8368–8401. <https://doi.org/10.3390/molecules16108368>
106. Micheletti M, Lye GJ (2006) Microscale bioprocess optimisation. *Curr Opin Biotechnol* 17:611–618. <https://doi.org/10.1016/j.copbio.2006.10.006>
107. Lye GJ, Ayazi-Shamlou P, Baganz F, Dalby PA, Woodley JM (2003) Accelerated design of bioconversion processes using automated microscale processing techniques. *Trends Biotechnol* 21:29–37. [https://doi.org/10.1016/S0167-7799\(02\)00011-2](https://doi.org/10.1016/S0167-7799(02)00011-2)
108. Gutmann B, Cantillo D, Kappe CO (2015) Continuous-flow technology—a tool for the safe manufacturing of active pharmaceutical ingredients. *Angew Chem Int Ed* 54:6688–6728. <https://doi.org/10.1002/anie.201409318>
109. Hessel V, Tibhe J, Noël T, Wang Q (2014) Biotechnical micro-flow processing at the EDGE – lessons to be learnt for a young discipline. *Chem Biochem Eng Q J* 28:167–188. <https://doi.org/10.15255/CABEQ.2014.1939>
110. Hessel V (2009) Novel process windows - gate to maximizing process intensification via flow chemistry. *Chem Eng Technol* 32:1655–1681. <https://doi.org/10.1002/ceat.200900474>
111. Hessel V, Vural Gürsel I, Wang Q, Noël T, Lang J (2012) Potential analysis of smart flow processing and micro process Technology for Fastening Process Development: use of chemistry and process design as intensification fields. *Chem Eng Technol* 35:1184–1204. <https://doi.org/10.1002/ceat.201200038>
112. Hessel V, Kralisch D, Kockmann N, Noël T, Wang Q (2013) Novel process windows for enabling, accelerating, and uplifting flow chemistry. *ChemSusChem* 6:746–789. <https://doi.org/10.1002/cssc.201200766>
113. Kockmann N, Gottsponer M, Zimmermann B, Roberge DM (2008) Enabling continuous-flow chemistry in microstructured devices for pharmaceutical and fine-chemical production. *Chem Eur J* 14:7470–7477. <https://doi.org/10.1002/chem.200800707>
114. Roberge DM, Zimmermann B, Rainone F, Gottsponer M, Eyholzer M, Kockmann N (2008) Microreactor technology and continuous processes in the fine chemical and pharmaceutical industry: is the revolution underway? *Org Process Res Dev* 12:905–910. <https://doi.org/10.1021/op8001273>
115. Clomburg JM, Crumbley AM, Gonzalez R (2017) Industrial biomanufacturing: the future of chemical production. *Science* 355:aag0804. <https://doi.org/10.1126/science.aag0804>
116. Adamo A, Beingessner RL, Behnam M, Chen J, Jamison TF, Jensen KF, Monbaliu J-CM, Myerson AS, Revalor EM, Snead DR, Stelzer T, Weeranoppanant N, Wong SY, Zhang P (2016) On-demand continuous-flow production of pharmaceuticals in a compact, reconfigurable system. *Science* 352:61–67. <https://doi.org/10.1126/science.aaf1337>
117. Žnidaršič-Plazl P (2017) Biotransformations in microflow systems: bridging the gap between academia and industry. *J Flow Chem* 7:111–117. <https://doi.org/10.1556/1846.2017.00021>
118. Bolivar JM, Valikhani D, Nidetzky B (2019) Demystifying the flow: biocatalytic reaction intensification in microstructured enzyme reactors. *Biotechnol J* 14:1800244. <https://doi.org/10.1002/biot.201800244>
119. Matosevic S, Lye GJ, Baganz F (2009) Design and characterization of a prototype enzyme microreactor: quantification of immobilized transketolase kinetics. *Biotechnol Prog*. <https://doi.org/10.1002/btpr.319>
120. Van Daele T, Fernandes del Pozo D, Van Hauwermeiren D, Gernaey KV, Wohlgemuth R, Nopens I (2016) A generic model-based methodology for quantification of mass transfer limitations in microreactors. *Chem Eng J* 300:193–208. <https://doi.org/10.1016/j.cej.2016.04.117>

121. Miložič N, Stojkovič G, Vogel A, Bouwes D, Žnidaršič-Plazl P (2018) Development of microreactors with surface-immobilized biocatalysts for continuous transamination. *New Biotechnol* 47:18–24. <https://doi.org/10.1016/j.nbt.2018.05.004>
122. Carvalho F, Marques M, Fernandes P (2017) Sucrose hydrolysis in a bespoke capillary Wall-coated microreactor. *Catalysts* 7:42. <https://doi.org/10.3390/catal7020042>
123. Valikhani D, Bolivar JM, Viefhues M, McIlroy DN, Vrouwe EX, Nidetzky B (2017) A spring in performance: silica Nanosprings boost enzyme immobilization in microfluidic channels. *ACS Appl Mater Interfaces* 9:34641–34649. <https://doi.org/10.1021/acsami.7b09875>
124. Bolivar JM, Luley-Goedl C, Leitner E, Sawangwan T, Nidetzky B (2017) Production of glucosyl glycerol by immobilized sucrose phosphorylase: options for enzyme fixation on a solid support and application in microscale flow format. *J Biotechnol* 257:131–138. <https://doi.org/10.1016/j.jbiotec.2017.01.019>
125. de León AS, Vargas-Alfredo N, Gallardo A, Fernández-Mayoralas A, Bastida A, Muñoz-Bonilla A, Rodríguez-Hernández J (2017) Microfluidic reactors based on rechargeable catalytic porous supports: heterogeneous enzymatic catalysis via reversible host–guest interactions. *ACS Appl Mater Interfaces* 9:4184–4191. <https://doi.org/10.1021/acsami.6b13554>
126. Szelwicka A, Zawadzki P, Sitko M, Boncel S, Czardybon W, Chrobok A (2019) Continuous flow chemo-enzymatic Baeyer–Villiger oxidation with Superactive and extra-stable enzyme/carbon nanotube catalyst: an efficient upgrade from batch to flow. *Org Process Res Dev* 23:1386–1395. <https://doi.org/10.1021/acs.oprd.9b00132>
127. Bi Y, Zhou H, Jia H, Wei P (2017) A flow-through enzymatic microreactor immobilizing lipase based on layer-by-layer method for biosynthetic process: catalyzing the transesterification of soybean oil for fatty acid methyl ester production. *Process Biochem* 54:73–80. <https://doi.org/10.1016/j.procbio.2016.12.008>
128. Bartha-Vári JH, Toşa MI, Irimie F-D, Weiser D, Boros Z, Vértessy BG, Paizs C, Poppe L (2015) Immobilization of phenylalanine ammonia-Lyase on single-walled carbon nanotubes for Stereoselective biotransformations in batch and continuous-flow modes. *ChemCatChem* 7:1122–1128. <https://doi.org/10.1002/cctc.201402894>
129. Weiser D, Bencze LC, Bánóczy G, Ender F, Kiss R, Kókai E, Szilágyi A, Vértessy BG, Farkas Ö, Paizs C, Poppe L (2015) Phenylalanine ammonia-Lyase-catalyzed deamination of an acyclic amino acid: enzyme mechanistic studies aided by a novel microreactor filled with magnetic nanoparticles. *Chembiochem* 16:2283–2288. <https://doi.org/10.1002/cbic.201500444>
130. Ruzic L, Bolivar JM, Nidetzky B (2020) Glycosynthase reaction meets the flow: continuous synthesis of lacto- N -triose II by engineered β -hexosaminidase immobilized on solid support. *Biotechnol Bioeng* 117:1597–1602. <https://doi.org/10.1002/bit.27293>
131. Romero-Fernández M, Moreno-Perez S, Orrego AH, Martins de Oliveira S, Santamaría RI, Díaz M, Guisan JM, Rocha-Martin J (2018) Designing continuous flow reaction of xylan hydrolysis for xylooligosaccharides production in packed-bed reactors using xylanase immobilized on methacrylic polymer-based supports. *Bioresour Technol* 266:249–258. <https://doi.org/10.1016/j.biortech.2018.06.070>
132. van der Helm MP, Bracco P, Busch H, Szymańska K, Jarzębski AB, Hanefeld U (2019) Hydroxynitrile lyases covalently immobilized in continuous flow microreactors. *Cat Sci Technol* 9:1189–1200. <https://doi.org/10.1039/C8CY02192A>
133. Strub DJ, Szymańska K, Hrydziuszko Z, Bryjak J, Jarzębski AB (2019) Continuous flow kinetic resolution of a non-equimolar mixture of diastereoisomeric alcohol using a structured monolithic enzymatic microreactor. *React Chem Eng* 4:587–594. <https://doi.org/10.1039/C8RE00177D>
134. van den Biggelaar L, Soumillion P, Debecker DP (2017) Enantioselective transamination in continuous flow mode with transaminase immobilized in a macrocellular silica monolith. *Catalysts* 7:54. <https://doi.org/10.3390/catal7020054>

135. van den Biggelaar L, Soumillion P, Debecker DP (2019) Biocatalytic transamination in a monolithic flow reactor: improving enzyme grafting for enhanced performance. *RSC Adv* 9:18538–18546. <https://doi.org/10.1039/C9RA02433F>
136. Weiser D, Nagy F, Bánóczy G, Oláh M, Farkas A, Szilágyi A, László K, Gellért Á, Marosi G, Kemény S, Poppe L (2017) Immobilization engineering – how to design advanced sol–gel systems for biocatalysis? *Green Chem* 19:3927–3937. <https://doi.org/10.1039/C7GC00896A>
137. Maier M, Radtke CP, Hubbuch J, Niemeyer CM, Rabe KS (2018) On-demand production of flow-reactor cartridges by 3D printing of thermostable enzymes. *Angew Chem Int Ed* 57:5539–5543. <https://doi.org/10.1002/anie.201711072>
138. Peng M, Mittmann E, Wenger L, Hubbuch J, Engqvist MKM, Niemeyer CM, Rabe KS (2019) 3D-printed phenacrylate decarboxylase flow reactors for the chemoenzymatic synthesis of 4-hydroxystilbene. *Chem Eur J* 25:15998–16001. <https://doi.org/10.1002/chem.201904206>
139. Yamaguchi H, Honda T, Miyazaki M (2016) Application of enzyme-immobilization technique for microflow reactor. *J Flow Chem* 6:13–17. <https://doi.org/10.1556/1846.2015.00039>
140. Bitterwolf P, Ott F, Rabe KS, Niemeyer CM (2019) Imine reductase based all-enzyme hydrogel with intrinsic cofactor regeneration for flow biocatalysis. *Micromachines* 10:783. <https://doi.org/10.3390/mi10110783>
141. Mittmann E, Gallus S, Bitterwolf P, Oelschlaeger C, Willenbacher N, Niemeyer CM, Rabe KS (2019) A phenolic acid decarboxylase-based all-enzyme hydrogel for flow reactor technology. *Micromachines* 10:795. <https://doi.org/10.3390/mi10120795>
142. Burgahn T, Pietrek P, Dittmeyer R, Rabe KS, Niemeyer CM (2020) Evaluation of a microreactor for flow biocatalysis by combined theory and experiment. *ChemCatChem* 12:2452–2460. <https://doi.org/10.1002/cctc.202000145>
143. Günther A, Jensen KF (2006) Multiphase microfluidics: from flow characteristics to chemical and materials synthesis. *Lab Chip* 6:1487–1503. <https://doi.org/10.1039/B609851G>
144. Kashid MN, Kiwi-Minsker L (2009) Microstructured reactors for multiphase reactions: state of the art. *Ind Eng Chem Res* 48:6465–6485. <https://doi.org/10.1021/ie8017912>
145. Liu Y, Chen G, Yue J (2020) Manipulation of gas-liquid-liquid systems in continuous flow microreactors for efficient reaction processes. *J Flow Chem* 10:103–121. <https://doi.org/10.1007/s41981-019-00062-9>
146. Utikar RP, Ranade VV (2017) Intensifying multiphase reactions and reactors: strategies and examples. *ACS Sustain Chem Eng* 5:3607–3622. <https://doi.org/10.1021/acssuschemeng.6b03017>
147. Fraile J, García J, Herrerías C, Pires E (2017) Synthetic transformations for the valorization of fatty acid derivatives. *Synthesis* 49:1444–1460. <https://doi.org/10.1055/s-0036-1588699>
148. Contente ML, Tamborini L, Molinari F, Paradisi F (2020) Aromas flow: eco-friendly, continuous, and scalable preparation of flavour esters. *J Flow Chem* 10:235–240. <https://doi.org/10.1007/s41981-019-00063-8>
149. Mi L, Yu J, He F, Jiang L, Wu Y, Yang L, Han X, Li Y, Liu A, Wei W, Zhang Y, Tian Y, Liu S, Jiang L (2017) Boosting gas involved reactions at nanochannel reactor with joint gas–solid–liquid interfaces and controlled wettability. *J Am Chem Soc* 139:10441–10446. <https://doi.org/10.1021/jacs.7b05249>
150. Dencic I, Meuldijk J, de Croon M, Hessel V (2012) From a review of Noble metal versus enzyme catalysts for glucose oxidation under conventional conditions towards a process design analysis for continuous-flow operation. *J Flow Chem* 1:13–23. <https://doi.org/10.1556/jfchem.2011.00005>
151. Dencic I, Hessel V, de Croon MHJM, Meuldijk J, van der Doelen CWJ, Koch K (2012) Recent changes in patenting behavior in microprocess technology and its possible use for gas-liquid reactions and the oxidation of glucose. *ChemSusChem* 5:232–245. <https://doi.org/10.1002/cssc.201100389>
152. Bolivar JM, Krämer CEM, Ungerböck B, Mayr T, Nidetzky B (2016) Development of a fully integrated falling film microreactor for gas-liquid-solid biotransformation with surface

- immobilized O₂-dependent enzyme: biocatalytic falling film microreactor. *Biotechnol Bioeng* 113:1862–1872. <https://doi.org/10.1002/bit.25969>
153. Huffman MA, Fryszkowska A, Alvizo O, Borra-Garske M, Campos KR, Canada KA, Devine PN, Duan D, Forstater JH, Grosser ST, Halsey HM, Hughes GJ, Jo J, Joyce LA, Kolev JN, Liang J, Maloney KM, Mann BF, Marshall NM, McLaughlin M, Moore JC, Murphy GS, Nawrat CC, Nazor J, Novick S, Patel NR, Rodriguez-Granillo A, Robaire SA, Sherer EC, Truppo MD, Whittaker AM, Verma D, Xiao L, Xu Y, Yang H (2019) Design of an in vitro biocatalytic cascade for the manufacture of islatravir. *Science* 366:1255–1259. <https://doi.org/10.1126/science.aay8484>
 154. Ghéczy N, Sasaki K, Yoshimoto M, Pour-Esmaeil S, Kröger M, Stano P, Walde P (2020) A two-enzyme cascade reaction consisting of two reaction pathways. Studies in bulk solution for understanding the performance of a flow-through device with immobilised enzymes. *RSC Adv* 10:18655–18676. <https://doi.org/10.1039/D0RA01204A>
 155. Fornera S, Kuhn P, Lombardi D, Schlüter AD, Dittrich PS, Walde P (2012) Sequential immobilization of enzymes in microfluidic channels for cascade reactions. *ChemPlusChem* 77:98–101. <https://doi.org/10.1002/cplu.201100068>
 156. Küchler A, Bleich JN, Sebastian B, Dittrich PS, Walde P (2015) Stable and simple immobilization of proteinase K inside glass tubes and microfluidic channels. *ACS Appl Mater Interfaces* 7:25970–25980. <https://doi.org/10.1021/acsami.5b09301>
 157. Brás EJS, Domingues C, Chu V, Fernandes P, Conde JP (2020) Microfluidic bioreactors for enzymatic synthesis in packed-bed reactors – multi-step reactions and upscaling. *J Biotechnol* 323:24–32. <https://doi.org/10.1016/j.jbiotec.2020.07.016>
 158. Grabner B, Schweiger AK, Gavric K, Kourist R, Gruber-Woelfler H (2020) A chemo-enzymatic tandem reaction in a mixture of deep eutectic solvent and water in continuous flow. *React Chem Eng* 5:263–269. <https://doi.org/10.1039/C9RE00467J>
 159. Hartley CJ, Williams CC, Scoble JA, Churches QI, North A, French NG, Nebl T, Coia G, Warden AC, Simpson G, Frazer AR, Jensen CN, Turner NJ, Scott C (2019) Engineered enzymes that retain and regenerate their cofactors enable continuous-flow biocatalysis. *Nat Catal* 2:1006–1015. <https://doi.org/10.1038/s41929-019-0353-0>
 160. Benítez-Mateos AI, Contente ML, Velasco-Lozano S, Paradisi F, López-Gallego F (2018) Self-sufficient flow-biocatalysis by coimmobilization of pyridoxal 5'-phosphate and ω -transaminases onto porous carriers. *ACS Sustain Chem Eng* 6:13151–13159. <https://doi.org/10.1021/acssuschemeng.8b02672>
 161. Velasco-Lozano S, Benítez-Mateos AI, López-Gallego F (2017) Co-immobilized phosphorylated cofactors and enzymes as self-sufficient heterogeneous biocatalysts for chemical processes. *Angew Chem Int Ed* 56:771–775. <https://doi.org/10.1002/anie.201609758>
 162. Bajic D, Craig MM, Mongerson CRL, Borsook D, Becerra L (2017) Identifying rodent resting-state brain networks with independent component analysis. *Front Neurosci* 11:685. <https://doi.org/10.3389/fnins.2017.00685>
 163. Fu H, Dencic I, Tibhe J, Sanchez Pedraza CA, Wang Q, Noel T, Meuldijk J, de Croon M, Hessel V, Weizenmann N, Oeser T, Kinkeade T, Hyatt D, Van Roy S, Dejonghe W, Diels L (2012) Threonine aldolase immobilization on different supports for engineering of productive, cost-efficient enzymatic microreactors. *Chem Eng J* 207–208:564–576. <https://doi.org/10.1016/j.cej.2012.07.017>
 164. Tibhe JD, Fu H, Noël T, Wang Q, Meuldijk J, Hessel V (2013) Flow synthesis of phenylserine using threonine aldolase immobilized on Eupergit support. *Beilstein J Org Chem* 9:2168–2179. <https://doi.org/10.3762/bjoc.9.254>
 165. Tušek AJ, Šalić A, Zelić B (2017) Catechol removal from aqueous media using laccase immobilized in different macro- and microreactor systems. *Appl Biochem Biotechnol* 182:1575–1590. <https://doi.org/10.1007/s12010-017-2419-2>
 166. Bajić M, Plazl I, Stloukal R, Žnidaršič-Plazl P (2017) Development of a miniaturized packed bed reactor with ω -transaminase immobilized in LentiKats®. *Process Biochem* 52:63–72. <https://doi.org/10.1016/j.procbio.2016.09.021>

Lab-on-a-Chip Devices for Point-of-Care Medical Diagnostics



Sofia Arshavsky-Graham and Ester Segal

Contents

1	Introduction	248
2	From Paper-Based Assays to Microfluidic Chips	249
3	Magnetic-Assisted Platforms	252
4	Centrifugal Microfluidic Platforms	255
5	Smartphone-Based Detection	258
6	Conclusions and Outlook	260
	References	261

Abstract The recent coronavirus (COVID-19) pandemic has underscored the need to move from traditional lab-centralized diagnostics to point-of-care (PoC) settings. Lab-on-a-chip (LoC) platforms facilitate the translation to PoC settings via the miniaturization, portability, integration, and automation of multiple assay functions onto a single chip. For this purpose, paper-based assays and microfluidic platforms are currently being extensively studied, and much focus is being directed towards simplifying their design while simultaneously improving multiplexing and automation capabilities. Signal amplification strategies are being applied to improve the performance of assays with respect to both sensitivity and selectivity, while smartphones are being integrated to expand the analytical power of the technology

S. Arshavsky-Graham

Department of Biotechnology and Food Engineering, Technion – Israel Institute of Technology, Haifa, Israel

Institute of Technical Chemistry, Leibniz University Hannover, Hanover, Germany

E. Segal (✉)

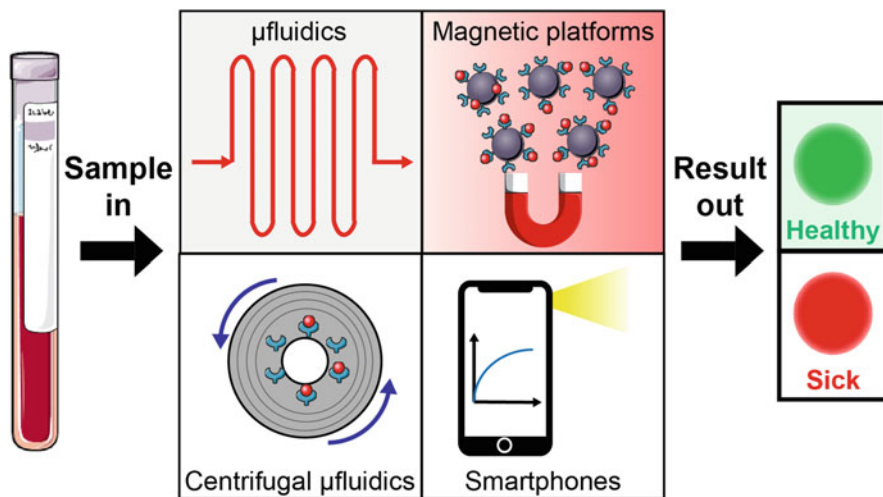
Department of Biotechnology and Food Engineering, Technion – Israel Institute of Technology, Haifa, Israel

The Russell Berrie Nanotechnology Institute, Technion – Israel Institute of Technology, Haifa, Israel

e-mail: esegal@technion.ac.il

and promote its accessibility. In this chapter, we review the main technologies in the field of LoC platforms for PoC medical diagnostics and survey recent approaches for improving these assays.

Graphical Abstract



Keywords Centrifugal microfluidics, Diagnostics, Lab-on-a-chip, Microfluidics, Paper, Point-of-care, Smartphone

1 Introduction

Over the years, medical diagnostics has been shifting away from imaging and invasive tissue sampling, towards far less invasive tests that detect disease biomarkers in extracted body fluids. Such biomarkers may include small metabolites, nucleic acids, proteins, and cells [1, 2]. Today, most assays for biomarker detection are mainly performed at centralized labs – requiring trained personnel for operation of complex benchtop analyzers, with a correspondingly long time-to-result period. The latter consideration is critical with respect to many medical conditions, for which time is frequently of the essence [3]. In addition, at low resource environments, such analyzers are necessarily limited due to their high costs and the need for skilled operators. As a result, significant efforts are now being directed towards development of point-of-care (PoC) tests, which can be operated at the patient site by non-trained personnel [1, 4–7]. Such tests should provide accurate, sensitive, and specific results in a rapid manner (with an optimal time-to-result in the range of few seconds to few hours) at relatively low-cost. The ideal vision for such a test would be

an independent and self-sustainable operation that allows a non-trained operator to load a sample of extracted body fluid (e.g., blood, urine, saliva, sweat, etc.) into the instrument and obtain informative results with minimal user intervention (i.e., sample in, result out). Fully integrated lab-on-a-chip (LoC) technologies, which incorporate all related analysis steps (including sample loading and preparation) in a single device, stand to significantly advance PoC medical diagnostics [1, 5, 8–13].

In this chapter, we provide an overview of the primary technologies in the field of PoC medical diagnostics. These include paper-based assays and microfluidics, magnetic-assisted detection, centrifugal microfluidics, and smartphone-based detection. We will highlight the main concepts and directions in each technology, provide several relevant examples from the past 3 years, discuss the main challenges in the field, and conclude by offering a future-oriented perspective.

2 From Paper-Based Assays to Microfluidic Chips

Lateral flow assays are widely used for PoC diagnostics. In these assays, a liquid sample containing the target analyte moves (via capillary forces) through various zones of polymeric strips, on which capture probes that can interact with the analyte are immobilized (see Fig. 1) [14, 15]. One of the most common lateral flow assays is the commercial pregnancy test for detecting human chorionic gonadotropin in urine – in which a sandwich-based immunoassay is performed, and detection of the target protein is realized via a color change, which can be observed with the naked eye [16–19]. The main advantages of lateral flow assays are their simplicity, ease of use, extended shelf life, and low-cost. However, lateral flow assays require numerous reagents and relatively large volumes of sample, and both multiplexing and the control of the flow rate pose challenges [16–19].

Microfluidic technology has been applied to address these limitations by enabling precise control of the flow by different microchannel geometries [19, 20]. Capillary-driven microfluidic chips have been used for PoC diagnostics of various analytes

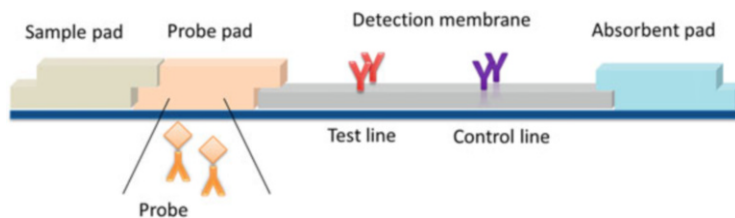


Fig. 1 Schematic illustration of a typical lateral flow assay strip. Few microliters of the sample are loaded to the sample pad and drawn to the probe pad, via capillary forces. The target is bound by labeled detection probes and transferred to the detection membrane and captured on a line of immobilized capture probes. Reprinted from Ref. [15] (Anfossi L. et al. Multiplex Lateral Flow Immunoassay: An Overview of Strategies towards High-throughput Point-of-Need Testing. *Bio-sensors*. 2018;9(1):2)

[17, 21–24]. For example, the commercially available Triage system – which is comprised of a portable analyzing instrument and a disposable protein chip – aims to diagnose a wide variety of health conditions [25, 26]. Like the lateral flow immunoassay, a biological sample is loaded onto this chip, and the target antigen is first bound to labeled antibodies. The bound conjugates then pass through the detection zone, where they are captured by pre-immobilized antibodies. The cartridge is fabricated from polymer microfluidic channels, which result in lower batch-to-batch variability when compared to traditional lateral flow immunoassays. The capillary flow is passively controlled by the microstructure and surface characteristics, which increase the incubation time of the target with the detection zone in a controllable manner without the need for active pumps and valves. Thus, for a relatively low-cost, a simple and rapid (~15 min) detection platform is realized. Multiplexed biomarker detection from whole blood was achieved by the Lateral Flow Integrated Blood Barcode Chip [27]. This microfluidic chip, fabricated from a hydrophilic polymer bonded to a glass slide, includes an array of immobilized antibodies that are specific for a variety of protein biomarkers. A few microliters of whole blood with an anticoagulant are loaded onto the chip, and a filter paper is then used to draw the sample and other loaded reagents through the chip via action of capillary forces. Separation of blood cells from the plasma is achieved by inertial force. A wash buffer is used to reduce background noise by removing an unbound label. Each step in the assay is automatically and sequentially executed, and the whole assay is performed within the span of just 40 min. To further automate the system, a self-coalescence module can also be integrated in a microfluidic chip, for the controlled reconstitution and delivery of inkjet-spotted and dried reagents. Well-defined reagent concentration profiles are established based on their initial spotting pattern [28]. This was applied in a silicon-based microfluidic chip for detection of a cardiac biomarker (troponin I) in human serum via a sandwich fluorescence immunoassay [16]. Figure 2a illustrates the platform, where a loading pad receives a sample, which is drawn by capillary forces to a self-coalescence module. The latter contains dried detection antibodies, which are reconstituted by a defined volume of the sample. That mixture then passes to a bead lane with capture antibodies, which selectively bind with the target-detection antibody complexes from the sample. The flow of the sample in the chip is controlled by a capillary pump. The design and image of the silicon microfluidic chip itself are presented in Fig. 2b, c, respectively. The assay requires 1 μL of sample, performed within 25 min, and a limit of detection of 4 ng mL^{-1} is realized.

An additional strategy for achieving reagent storage in paper-based microfluidic assays is seen in the use of a three-dimensional (3D) folding of a paper substrate with an origami-based technique. Different layers and dried reagents can be stacked vertically, and the addition of a buffer solution results in reconstitution via a controlled, multistep process. Parallel tests can be performed using a multilayer fluidic network in a compact device [18, 29]. Recently, 3D-origami-based paper device was used for detection of a biomarker for *Staphylococcus aureus* infection within human synovial fluid by an ELISA-based immunoassay [30]. That platform consists of a sliding strip and antibody storage functions on a single sheet of paper, as

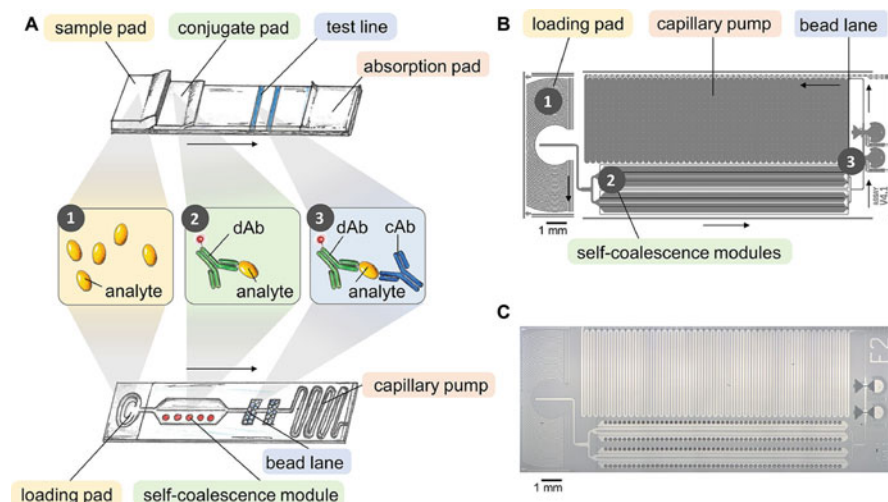


Fig. 2 (a) General concept of a lateral flow assay-based microfluidic chip, which integrates a self-coalescence module, containing dried inkjet-spotted detection antibodies. The flow of the sample is driven by a capillary pump. (b) The design of the corresponding microfluidic chip and (c) an optical microscopy image of the fabricated Si microfluidic chip. Reprinted with permission from Ref. [16] (Hemmig E. et al. Transposing Lateral Flow Immunoassays to Capillary-Driven Microfluidics Using Self-Coalescence Modules and Capillary-Assembled Receptor Carriers. *Analytical Chemistry*. 2020;92(1):940–6). Copyright (2020) American Chemical Society

shown in Fig. 3a. The sliding strip acts as a valve to control the serial steps of sample addition, interaction, washing, and detection. The sequential flow is carried out by sliding the tab to different positions (see Fig. 3b). Only 3 μL of sample are required, and this procedure can be completed within 7 min. Nevertheless, the manual addition of buffers is still required during this procedure.

Sensitivity enhancement of lateral flow assays has frequently been achieved by incorporating various nanomaterials – such as gold or silver nanoparticles, magnetic nanoparticles, and quantum dots – into the system [19, 31, 32]. An alternate strategy is the use of external fields (i.e., acoustic, thermal, electric, etc.). Electrophoretic methods, such as ion concentration polarization or isotachopheresis, have also been applied to facilitate separation and concentration within microfluidic devices. In isotachopheresis, ionic species can be focused, based on their electrophoretic mobility, using a discontinuous buffer system. The method enables the simultaneous extraction, separation, and concentration of the target species [33]. This method was recently applied for multiplexed detection of two cardiac biomarkers in human serum [34]. The platform is comprised of a lateral flow paper assembled on a 3D-printed cartridge for buffer reservoirs and electrode connection. The two protein targets are fluorescently labeled and detected by immobilized antibodies on the paper strip. The assay time is 6 min and results in $\sim 1,300$ -fold enrichment of the proteins. Label-free detection with isotachopheresis in a microfluidic assay was demonstrated

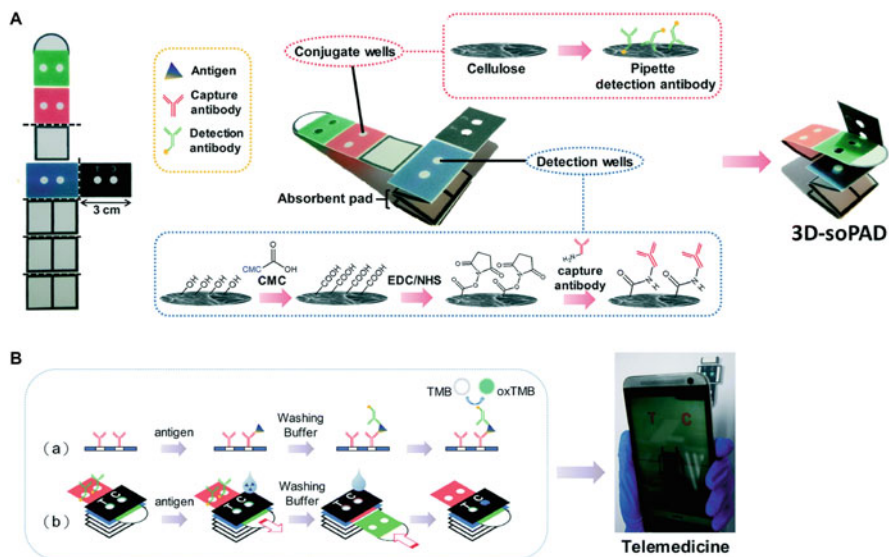


Fig. 3 3D-origami-based paper device used for detection of a protein A in human synovial fluid: (a) Illustration of the preparation of the platform, by an origami folding. The detection antibodies are impregnated in cellulose, while capture antibodies are covalently immobilized in the detection pad. (b) The testing procedure, where the sliding tab is used to control the flow and the serial step execution of the assay. Reproduced from Ref. [30] (Chen C. A et al. Three-dimensional origami paper-based device for portable immunoassay applications. *Lab on a Chip*. 2019;19(4):598–607) with permission from The Royal Society of Chemistry

with porous silicon-based optical biosensors, where the reflectivity changes of the latter upon target binding are monitored in real time, with no need for target labeling. This was shown for DNA and protein targets with up to 1,000-fold enhancement in sensitivity [35, 36]. Nevertheless, application of an external field does require peripheral equipment, which both increases the cost and complicates the setup of the system.

3 Magnetic-Assisted Platforms

Magnetic nano- and microparticles are used in LoC devices for fluid manipulation. In many cases, the particles in the fluid are actuated by applying a magnetic field to induce the mixing (which is often limited in microfluidic devices due to laminar flow) [37–41]. Moreover, the particles can be also used as carriers and labels to facilitate both transfer and separation of biomolecules [37–41]. Magnetic particles are commonly controlled by electromagnets, coils, or permanent magnets – all of which induce an external magnetic field – and often form supramolecular structures

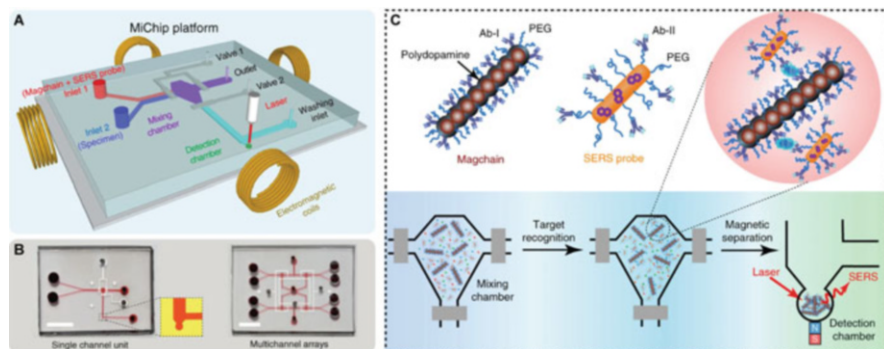


Fig. 4 Bio-conjugated magnetic nanochains on a microchip as rapid active liquid mixers and capture agents for bio-separation: (a) schematic illustration of the assay platform; (b) photographs of the platforms in a single- or multichannel format (scale bar: 0.5 cm); and (c) the detection assay: the sample, antibody-conjugated magnetic nanochains and surface-enhanced Raman spectroscopy (SERS)-encoded probes are mixed in the reaction chamber. Immune complexes are formed and isolated to the detection chambers, which are then subjected to Raman spectroscopic detection. Reprinted from Ref. [44] (Xiong Q. et al. Magnetic nanochain integrated microfluidic biochips. Nature Communications. 2018;9(1):1743). Copyright © 2018, Springer Nature

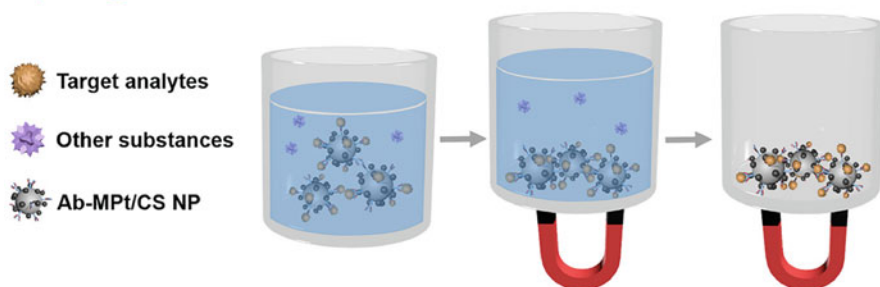
in the form of microcolumns due to dipole-dipole interactions [42, 43]. For example, bio-conjugated magnetic nanochains have been used on a microchip as stir bars to promote liquid mixing and as capture agents for bio-separation (see Fig. 4) [44]. A simple planar design of a microchip is realized based on flat channels on polydimethylsiloxane (PDMS)-on-glass, free of built-in components. The magnetic nanochains are biofunctionalized with target-specific antibodies, and surface-enhanced Raman spectroscopy (SERS)-encoded nanoprobe are used as signaling probes for multiplexed Raman spectroscopic detection. A small amount ($\sim 1 \mu\text{L}$) of sample fluid is mixed with both components, and the fluid flow and mixing are thereafter controlled via an external spinning magnetic field. Multiplexed detection of three cancer biomarkers in clinical serum and two bacterial species in saliva samples have been demonstrated in just 8 min [44].

Magnetic particles have been also used to automate processes in sandwich immunoassays, including the reaction and washing steps [45]. A sample is mixed with gold-coated iron oxide nanoparticles that have been functionalized with detection antibodies. The antibody-antigen reaction then forms immunocomplexes, which are electrochemically detected. The reaction and subsequent removal of unbound probes are controlled and accelerated by an external magnetic field. Thus, a simplified platform is obtained, without the need for fluid manipulation components and prestored washing buffer. Detection of a prostate-specific antigen in $10 \mu\text{L}$ of human serum is demonstrated with a limit of detection of 0.085 ng mL^{-1} within 5 min [45]. A similar concept was used for developing a PoC multiplexed diagnostic test for differential detection of Ebola, Lassa, and malaria biomarkers in whole blood samples within 30 min [46]. Detection antibodies for the target antigens are conjugated to specific SERS nanotags and magnetic nanoparticles, which are stored dried

in a test tube – providing a single-use and temperature stable platform that is ideal for field application. A whole blood sample (45 μL) and a lysis buffer are added to rehydrate the dried reagents. After a mixing step, the magnetic microparticles-antigen-SERS nanotag complexes are separated with an external magnet, and an external laser is used for SERS signal monitoring [46]. Magnetic particles have been also used for signal amplification in lateral flow immunoassay strips for human chorionic gonadotropin detection [47, 48]. For example, Pt-decorated magnetic core-shell nanoparticles, functionalized with detection antibodies, have been successfully deployed for this function [47]. These particles have both magnetic and enzyme-like properties, enabling target analyte magnetic enrichment and signal amplification by a peroxidase-like reaction mediated by the particles (see Fig. 5). The sensitivity is increased by two orders of magnitude when compared to a conventional lateral flow immunoassay [47].

In terms of nucleic acid analysis, magnetic particles are utilized for extraction, purification, amplification, and detection [49–51]. For nucleic acid amplification, isothermal methods are preferable for PoC testing, since they avoid the required

Step 1: Magnetic enrichment



Step 2: Detection using LFIA

Step 3: Nanozyme-mediated signal amplification

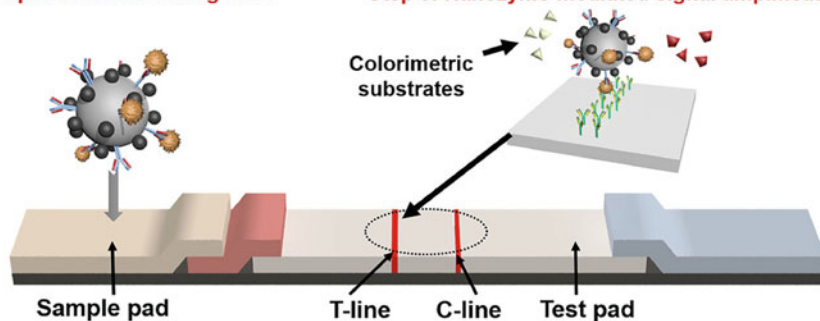


Fig. 5 Magnetic particles for signal amplification in lateral flow immunoassay (LFIA) for human chorionic gonadotropin detection. The particles have both magnetic and enzyme-like properties, enabling target analyte magnetic enrichment and signal amplification. Reprinted with permission from Ref. [47] (Kim M. S. et al. Pt-Decorated Magnetic Nanozymes for Facile and Sensitive Point-of-Care Bioassay. *ACS Applied Materials & Interfaces*. 2017;9(40):35133–40). Copyright (2020) American Chemical Society

thermal cycling in polymerase chain reaction [52–54]. One such method is so-called rolling circle amplification [55]: DNA or RNA target is annealed and ligated to a padlock probe, forming a circular template. The probe is highly sensitive to single base mutations, which results in high specificity [56]. Amplification reaction then proceeds via a phi29 polymerase, which creates a long single-stranded DNA concatemer containing repeated copies of the sequence complementary to the padlock probe [55]. Although this is a highly efficient isothermal method, the multiple steps in the assay and the different required reagents make the integration of this method onto a single-chip platform a challenging project. Magnetic particles can in turn facilitate the automation of the multistep assay [42, 57, 58]. For instance, a magnetic fluidized bed was recently integrated in a simple microfluidic chamber, generating a constant hydrodynamic recirculation in a continuous flow and thereby enabling efficient liquid perfusion and mixing [42]. The magnetic particles are functionalized with an oligonucleotide for the capture of the target DNA. A complete rolling circle amplification assay is performed on chip, with detection carried out in a low-cost polymer-based microarray module by fluorescence microscopy. The platform enables processing of large sample volumes, and a limit of detection of 1 pM is obtained [42]. A similar concept is presented in a multichamber polymer-based microfluidic chip, which integrates DNA target capture, transport, and a rolling circle amplification assay, using magnetic microbeads [57]. The platform requires the manual loading of reagents, after which the assay runs automatically in a sequential chamber filling by capillary stop valves and phase guide structures. Opto-magnetic detection of a synthetic DNA target for type-B influenza virus is realized in 45 min, with a limit of detection of 20 pM [57].

4 Centrifugal Microfluidic Platforms

Multiplexed LoC detection can also be achieved by centrifugal microfluidics, which have been applied for detection of a wide range of analytes and have been thoroughly reviewed in the past [59–62]. The technology is based on a “Lab-on-a-CD” concept, wherein the complete fluidic network and the analysis steps are all embedded onto a single disc. The fluidic processing steps – including separation and reagent mixing – are then automated by implementing different spinning profiles. Integration of multiple assays in a single platform can thereby be achieved. The main advantage of these systems is their simple method of fluid manipulation, which is achieved by a rotary motor without the need for external pumps or a high-voltage power supply. The disc can also be synthesized from low-cost polymers, which facilitate both mass production and economical disposal. The Lab-on-a-CD technology has been successfully utilized for PoC diagnostics by several commercial companies. For example, Piccolo Xpress by Abaxis Inc., USA, [63] offers a variety of CD-based blood chemistry analyzers with up to 14 tests on a single disc. The platform requires only 0.1 mL of a blood sample, and results are obtained within 12 min. Recently, the centrifugal microfluidic technology was also applied for a low

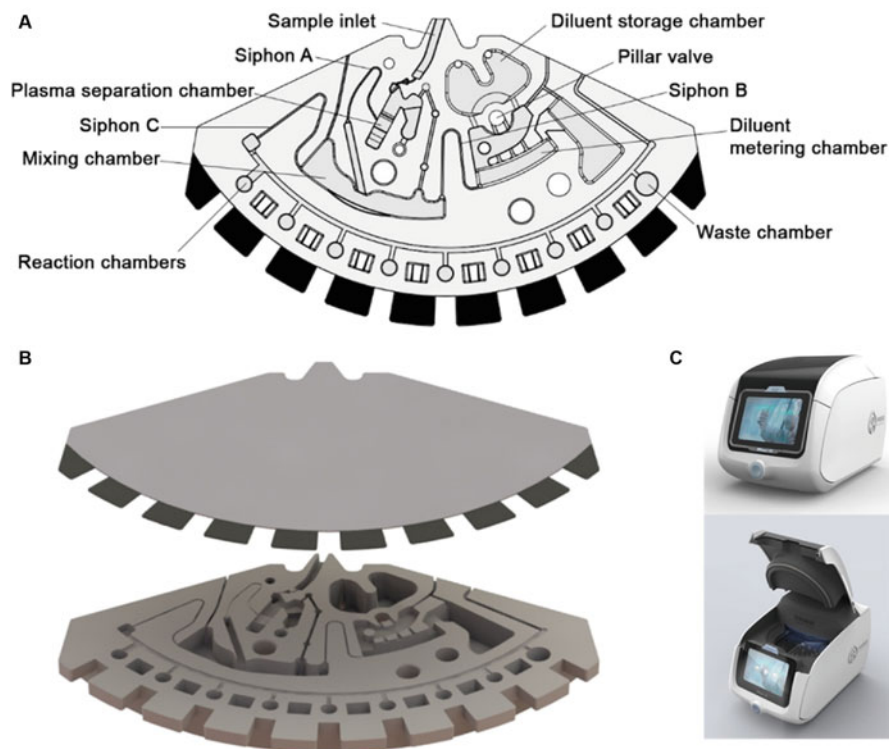


Fig. 6 (a) The design of the centrifugal microfluidic finger-prick blood biochemical analyzer; (b) exploded view of the chip, presenting an upper adhesive tape and bottom polycarbonate layer; (c) the portable biochemical analyzer. Reprinted with permission from Ref. [64] (Zhu Y. et al. Self-served and fully automated biochemical detection of finger-prick blood at home using a portable microfluidic analyzer. *Sensors and Actuators B: Chemical*. 2020;303:127235). Copyright © 2019 Elsevier B.V

volume blood analysis, using only 12 μL of blood from a finger prick, for automatic monitoring of blood glucose, total cholesterol, and triglycerides within ~ 15 min (see Fig. 6a, b). Plasma separation, mixing, reaction, and detection are fully automated with a portable analyzer (Fig. 6c), which shows great potential for blood monitoring at home [64].

Centrifugal microfluidics is especially advantageous for nucleic acid detection, which requires lengthy and laborious sample preprocessing steps such as cell lysis, DNA purification, and amplification [65, 66]. Using this approach, all these steps can be integrated into a single disc and performed automatically and sequentially. For example, a centrifugal microfluidic device was integrated with a 3D-printed solution-loading cartridge for multiplex foodborne pathogen detection, as illustrated in Fig. 7a. The solution-loading cartridge prestores all required solutions for molecular diagnostics and connects with the reservoirs on the centrifugal device – minimizing

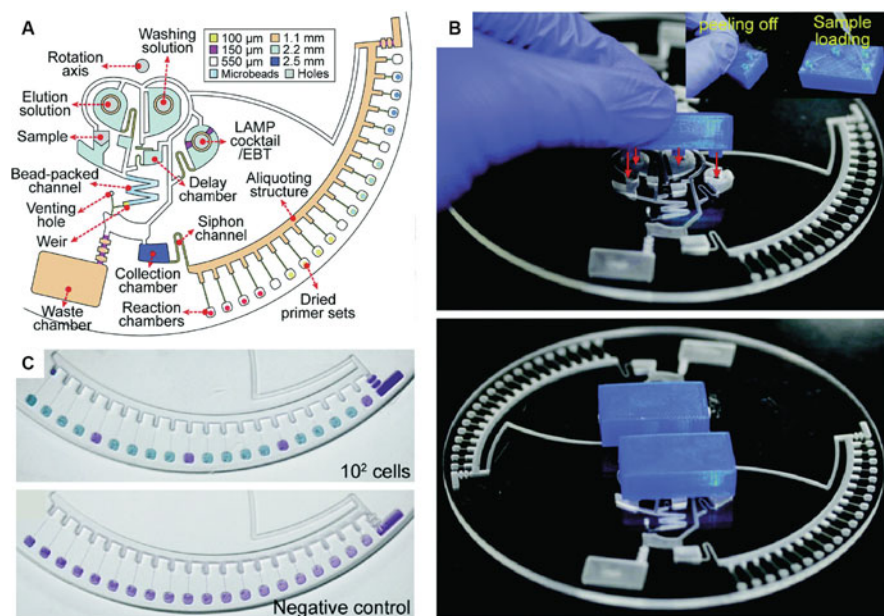


Fig. 7 (a) Design of the centrifugal microfluidics device for multiplex foodborne pathogen detection; (b) a real photograph of the microdevice with the solution loading and reagent storage cartridge; (c) multiplexed colorimetric detection of four different pathogens in milk sample in comparison to a negative control of pure milk. Reproduced from Ref. [67] (Oh S.J. and Seo T.S. Combination of a centrifugal microfluidic device with a solution-loading cartridge for fully automatic molecular diagnostics. *Analyst*. 2019;144(19):5766–74) with permission from The Royal Society of Chemistry

manual processing (see Fig. 7b). Sequential loading of the solutions to the device is achieved by controlling the rotational speed, and silica bead-assisted DNA extraction, isothermal DNA amplification, and colorimetric detection by Eriochrome Black T are then carried out. The platform enables detection of four kinds of foodborne pathogens in a real milk sample within 65 min and with a limit of detection of 10^3 cells per mL (see Fig. 7c) [67]. Another technology which enables integration of DNA processing is double rotation axes centrifugal microfluidics, in which the disc can rotate around two rotation shafts – thus not limiting the fluid flow only radially outwards [68, 69]. This technology has allowed for a completely automated sample-to-result analysis of hepatitis B virus in whole blood [70]. The disc comprises all process chains for the virus DNA detection, including plasma separation from whole blood, lysis, DNA purification, and amplification. The double rotation axes centrifugal microfluidics allow for unconstrained and reversible fluid pumping, as well as an efficient spatial utilization of the disc. All reagents are prestored on the disc, and their introduction is controlled by melting ferrowax plugs in the channels with laser irradiation. The only manual step in the assay is

the supply of 0.5 mL of a whole blood sample, while the time-to-result is 48 min, with a limit of detection of 10^2 copies per mL [70].

5 Smartphone-Based Detection

The high availability of smartphones worldwide and their sophisticated technological features (such as high quality cameras, connectivity, and computational power) have increasingly led to their integration into a wide range of analytical sensing systems [71–78]. Detection via smartphone is commonly based on various forms of optical measurements – including bright-field, colorimetric, luminescence, and/or fluorescence [71, 72]. The high resolution of the embedded complementary metal oxide semiconductor image sensor cameras enables high pixel density for optical monitoring, while the high computational power facilitates real-time image analysis [76]. Because smartphone-based PoC platforms have been extensively reviewed in the past few years [71–79], in this section we only briefly survey the main aspects of smartphone-based detection with a few examples from recent years.

Bright-field-based detection is the simplest method, where a sample is illuminated from below with white light and then the transmitted light is measured [72]. Imaging of living cells or large biomolecules can be achieved in this way [80, 81]. Colorimetric-based detection is also relatively simple, requiring only illumination and image processing. This has been commonly used in connection with paper-based assays to achieve quantitative results. For example, a custom-built smartphone application was used to quantitate a PoC lateral flow assay for detection of Ebola virus-specific antibodies in clinical human serum samples. This low-cost platform requires only the test strip and a smartphone, and results are obtained within 15 min [82]. Smartphone colorimetric detection of lactate dehydrogenase as a biomarker for cellular damage for early diagnosis of serious illness in neonates was also recently shown, as illustrated in Fig. 8 [83]. The PoC platform consists of a plastic cartridge holding disposable filter papers for whole blood filtration, plasma separation, and colorimetric reaction. The cartridge is mounted in a box (Fig. 8b), which also holds the smartphone at a fixed distance for automatic imaging. A dedicated application is used for analyzing the RGB values of the acquired images, and comparable results to standard laboratory analysis are obtained in only 4 min [83]. Colorimetric-based detection using a multichannel smartphone spectrometer as an optical biosensor was recently used to detect protein content and a cancer biomarker within human serum [84]. Images captured by the phone camera were converted to transmission and absorbance spectra in the visible light range with high resolution, and the performance of the setup was comparable to benchtop instruments.

To increase the sensitivity of the assay, fluorescence-based detection is also frequently employed. For such systems, an optomechanical modulus containing excitation and/or emission filter and laser diodes for excitation are required [76]. For example, a compact multimodal microscope was integrated on a smartphone for targeted DNA sequencing and in situ point mutation analysis in

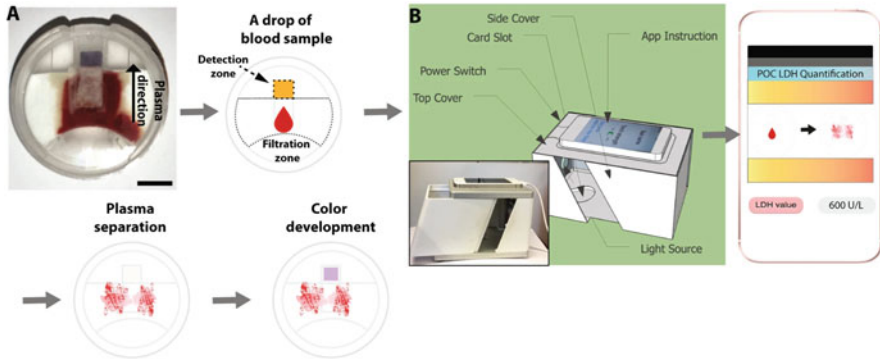


Fig. 8 (a) Schematics of a PoC lateral flow assay system for analysis of lactate dehydrogenase (LDH) in whole blood, consisting of a plastic cartridge holding filter papers. Scale bar: 0.4 cm. (b) The cartridge is placed on a designated slot inside a box; the latter keeps a fix distance between the phone camera and the cartridge for the imaging while ensuring similar light conditions between different batches. An app is used to guide the user in the assay and analyze the results. Reprinted from Ref. [83] (Halvorsen C.P., et al. A rapid smartphone-based lactate dehydrogenase test for neonatal diagnostics at the point-of-care. *Scientific Reports*. 2019;9(1):9301). Copyright © 2019, Springer Nature

tumor samples [85]. A 3D-printed lightweight optomechanical modulus is integrated on the smartphone and contains two laser diodes for multicolor fluorescence imaging, as well as a white light-emitting diode (LED) for bright-field transmission imaging. DNA sequencing and point mutation analysis are achieved via rolling circle amplification, and the results are comparable to regular benchtop microscopes. Such technology is applicable for genotyping cancer patient biopsies directly in the pathologist office at PoC. Similar concept was shown for multiplexed detection of Zika, chikungunya, and dengue viruses (belonging to the Flaviviridae family) directly in human blood, saliva, and urine samples (see Fig. 9) [86]. This platform is comprised of three components: a heating module, a reaction module, and an optical-detection and image analysis module. The latter contains multicolored LED coupled with a multi-pass band filter for fluorescence measurement. The entire platform is fitted with a smartphone, and the camera is utilized for the imaging. A dedicated application is used for fluorescence signal analysis by a novel algorithm, improving the discrimination between positive and negative signals by fivefold, compared to a naked eye. Target virus RNAs are detected by reverse-transcription loop-mediated isothermal amplification coupled with quenching of unincorporated amplification signal reporters. Recently, microfluidic-based immunoassay based on a smartphone fluorescence detection was used to conduct troponin I analysis in human serum in clinically relevant concentrations within 12 min [87]. Although fluorescence-based detection improves the sensitivity of the assay, it also requires the addition of complex and costly optical components to the system. Time-gated photoluminescence-based detection may offer one economical alternative. This concept is demonstrated for human chorionic gonadotropin quantification in a lateral

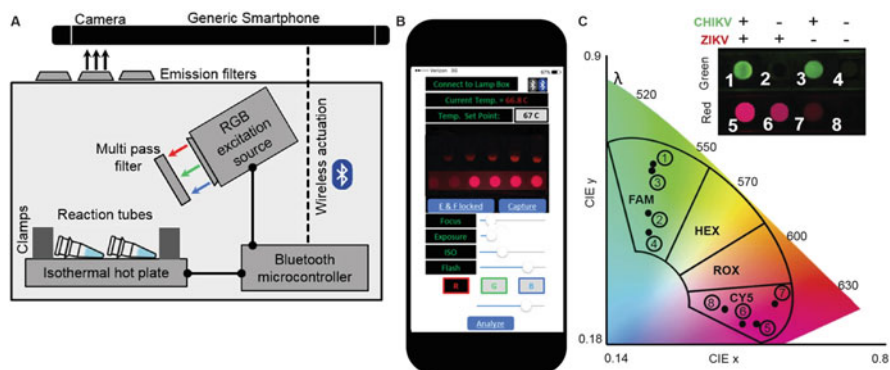


Fig. 9 (a) Schematic illustration of the smartphone-based fluorescence detection of Zika, chikungunya, and dengue virus's RNA platform, based on reverse-transcription loop-mediated isothermal amplification assay. The system comprises isothermal heating unit with reaction tubes, LED excitation source and Bluetooth microcontroller. (b) An app is used to wirelessly actuate the isothermal heater and excitation source. The smartphone camera with an emission filter captures the images, analyzed subsequently by the app. (c) Duplex detection of Zika and chikungunya viruses. The images are mapped over predefined fluorophore emission islands to distinguish between different viral targets. Adapted with changes from Ref. [86]. (Priye A. et al. A smartphone-based diagnostic platform for rapid detection of Zika, chikungunya, and dengue viruses. *Scientific Reports*. 2017;7(1):44778). Copyright © 2017, Springer Nature

flow assay with a persistent luminescent phosphor reporter [88]. A smartphone's flash is used to excite the nanophosphors, which are then imaged using the smartphone camera. A 10- to 100-fold enhancement in sensitivity is achieved compared to commercial lateral flow assays – without the need for any additional complex optical components.

6 Conclusions and Outlook

Significant research efforts have already been directed towards the development of simple and low-cost devices for LoC-based medical diagnostics at PoC. Nevertheless, commercialization of such technologies remains limited, and the following aspects must be considered:

- Real PoC application (in terms of sample in – results out) requires the integration and automation of *all* assay steps – yet most assays still require extensive user intervention, mainly in terms of sample preparation and/or reagent addition. For certain applications, this bottleneck can perhaps be solved by the integration of reagent moduli and, where possible, simple reagent storage on the chip.
- The need to improve the sensitivity, selectivity, and stability of sensing moduli is increasingly leading researchers to explore robust recognition elements – such as

aptamers, antibody fragments, and molecularly imprinted polymers. Various nanomaterials are also being incorporated for signal amplification and to improve the total assay performance.

- Scalability is an essential requirement for commercialization, and it continues to pose profound challenges for complex microfluidic structures. As a result, scalability considerations must direct the materials, design, and fabrication methods that are employed for such devices. For example, PDMS (which is commonly used for microfluidic fabrication in the academy) is not suitable for mass production, since it is fabricated mostly via soft lithography techniques. As a result, gold-standard paper-based assays continue to rule the field of PoC diagnostics by dint of the fact that they can be mass-produced at a very low-cost. Advancements in 3D-printing technology will likely begin to close that gap in the near future, at least with respect to plastic-based microfluidics.
- Smartphone technology has expanded the analytical power and increased the accessibility of many platforms. But hygiene considerations – including both contamination and disposal issues – must be carefully considered if smartphones will be deployed.
- Because multiplexing for the simultaneous detection of several biomarkers is extremely valuable in the context of medical diagnostics, the authors anticipate that research efforts in this direction will continue to increase exponentially.
- Clinical validation of all platforms is required. Many of the published works utilize human biological samples spiked with the analyte; although this is sufficient for a proof-of-concept, real clinical samples from different patients should always be tested in order to validate a platform's design integrity.
- Finally, the social impact of this emerging technology – as well as corresponding regulatory policies and concerns – should be considered when designing an assay, in order to facilitate (or at least preserve) its commercialization potential.

References

1. Sorger PK (2008) Microfluidics closes in on point-of-care assays. *Nat Biotechnol* 26 (12):1345–1346
2. Sanjay ST, Fu G, Dou M, Xu F, Liu R, Qi H et al (2015) Biomarker detection for disease diagnosis using cost-effective microfluidic platforms. *Analyst* 140(21):7062–7081
3. Lee J, Lee S-H (2013) Lab on a chip for in situ diagnosis: from blood to point of care. *Biomed Eng Lett* 3(2):59–66
4. Gubala V, Harris LF, Ricco AJ, Tan MX, Williams DE (2012) Point of care diagnostics: status and future. *Anal Chem* 84(2):487–515
5. Jung W, Han J, Choi J-W, Ahn CH (2015) Point-of-care testing (POCT) diagnostic systems using microfluidic lab-on-a-chip technologies. *Microelectron Eng* 132:46–57
6. Kost GJ (1995) Guidelines for point-of-care testing. Improving patient outcomes. *Am J Clin Pathol* 104(4 Suppl 1):S111–S127
7. Lippa PB, Müller C, Schlichtiger A, Schlebusch H (2011) Point-of-care testing (POCT): current techniques and future perspectives. *TrAC Trends Anal Chem* 30(6):887–898
8. Whitesides GM (2006) The origins and the future of microfluidics. *Nature* 442(7101):368–373

9. Zhang Z, Nagrath S (2013) Microfluidics and cancer: are we there yet? *Biomed Microdevices* 15(4):595–609
10. Volpatti LR, Yetisen AK (2014) Commercialization of microfluidic devices. *Trends Biotechnol* 32(7):347–350
11. Haeblerle S, Zengerle R (2007) Microfluidic platforms for lab-on-a-chip applications. *Lab Chip* 7(9):1094–1110
12. Schumacher S, Nestler J, Otto T, Wegener M, Ehrentreich-Förster E, Michel D et al (2012) Highly-integrated lab-on-chip system for point-of-care multiparameter analysis. *Lab Chip* 12(3):464–473
13. Eicher D, Merten CA (2011) Microfluidic devices for diagnostic applications. *Expert Rev Mol Diagn* 11(5):505–519
14. Koczula Katarzyna M, Gallotta A (2016) Lateral flow assays. *Essays Biochem* 60(1):111–120
15. Anfossi L, Di Nardo F, Cavalera S, Giovannoli C, Baggiani C (2018) Multiplex lateral flow immunoassay: an overview of strategies towards high-throughput point-of-need testing. *Biosensors* 9(1):2
16. Hemmig E, Temiz Y, Gökçe O, Lovchik RD, Delamarche E (2020) Transposing lateral flow immunoassays to capillary-driven microfluidics using self-coalescence modules and capillary-assembled receptor carriers. *Anal Chem* 92(1):940–946
17. Carrell C, Kava A, Nguyen M, Menger R, Munshi Z, Call Z et al (2019) Beyond the lateral flow assay: a review of paper-based microfluidics. *Microelectron Eng* 206:45–54
18. Yetisen AK, Akram MS, Lowe CR (2013) Paper-based microfluidic point-of-care diagnostic devices. *Lab Chip* 13(12):2210–2251
19. Gong MM, Sinton D (2017) Turning the page: advancing paper-based microfluidics for broad diagnostic application. *Chem Rev* 117(12):8447–8480
20. Channon RB, Nguyen MP, Scorzelli AG, Henry EM, Volckens J, Dandy DS et al (2018) Rapid flow in multilayer microfluidic paper-based analytical devices. *Lab Chip* 18(5):793–802
21. Magro L, Escadafal C, Garneret P, Jacquelin B, Kwasiborski A, Manuguerra J-C et al (2017) Paper microfluidics for nucleic acid amplification testing (NAAT) of infectious diseases. *Lab Chip* 17(14):2347–2371
22. Tian T, Bi Y, Xu X, Zhu Z, Yang C (2018) Integrated paper-based microfluidic devices for point-of-care testing. *Anal Methods* 10(29):3567–3581
23. Gervais L, de Rooij N, Delamarche E (2011) Microfluidic chips for point-of-care immunodiagnosics. *Adv Mater* 23(24):H151–HH76
24. Song Y, Lin B, Tian T, Xu X, Wang W, Ruan Q et al (2019) Recent progress in microfluidics-based biosensing. *Anal Chem* 91(1):388–404
25. Apple FS, Christenson RH, Valdes Jr R, Andriak AJ, Berg A, Duh S-H et al (2020) Simultaneous rapid measurement of whole blood myoglobin, creatine kinase MB, and cardiac troponin I by the triage cardiac panel for detection of myocardial infarction. *Clin Chem* 45(2):199–205
26. Clark TJ, McPherson PH, Buechler KF (2002) The triage cardiac panel: cardiac markers for the triage system. *Point Care* 1(1):42–46
27. Wang J, Ahmad H, Ma C, Shi Q, Vermesh O, Vermesh U et al (2010) A self-powered, one-step chip for rapid, quantitative and multiplexed detection of proteins from pinpricks of whole blood. *Lab Chip* 10(22):3157–3162
28. Gökçe O, Castonguay S, Temiz Y, Gervais T, Delamarche E (2019) Self-coalescing flows in microfluidics for pulse-shaped delivery of reagents. *Nature* 574(7777):228–232
29. Liu H, Crooks RM (2011) Three-dimensional paper microfluidic devices assembled using the principles of origami. *J Am Chem Soc* 133(44):17564–17566
30. Chen C-A, Yeh W-S, Tsai T-T, Li Y-D, Chen C-F (2019) Three-dimensional origami paper-based device for portable immunoassay applications. *Lab Chip* 19(4):598–607
31. Liu L, Yang D, Liu G (2019) Signal amplification strategies for paper-based analytical devices. *Biosens Bioelectron* 136:60–75
32. Bishop JD, Hsieh HV, Gasperino DJ, Weigl BH (2019) Sensitivity enhancement in lateral flow assays: a systems perspective. *Lab Chip* 19(15):2486–2499

33. Moghadam BY, Connelly KT, Posner JD (2014) Isotachophoretic preconcentration on paper-based microfluidic devices. *Anal Chem* 86(12):5829–5837
34. Guo S, Schlecht W, Li L, Dong W-J (2019) Paper-based cascade cationic isotachopheresis: multiplex detection of cardiac markers. *Talanta* 205:120112
35. Arshavsky-Graham S, Massad-Ivanir N, Paratore F, Scheper T, Bercovici M, Segal E (2017) On chip protein pre-concentration for enhancing the sensitivity of porous silicon biosensors. *ACS Sensors* 2(12):1767–1773
36. Vilensky R, Bercovici M, Segal E (2015) Oxidized porous silicon nanostructures enabling electrokinetic transport for enhanced DNA detection. *Adv Funct Mater* 25(43):6725–6732
37. Moerland CP, van Ijzendoorn LJ, Prins MWJ (2019) Rotating magnetic particles for lab-on-chip applications – a comprehensive review. *Lab Chip* 19(6):919–933
38. Chircov C, Grumezescu AM, Holban AM (2019) Magnetic particles for advanced molecular diagnosis. *Materials* 12(13):2158
39. van Reenen A, de Jong AM, den Toonder MJM, Prins MWJ (2014) Integrated lab-on-chip biosensing systems based on magnetic particle actuation – a comprehensive review. *Lab Chip* 14(12):1966–1986
40. Ríos Á, Zougagh M (2016) Recent advances in magnetic nanomaterials for improving analytical processes. *TrAC Trends Anal Chem* 84:72–83
41. Masud MK, Na J, Younus M, Hossain MSA, Bando Y, Shiddiky MJA et al (2019) Superparamagnetic nanoarchitectures for disease-specific biomarker detection. *Chem Soc Rev* 48(24):5717–5751
42. Hernández-Neuta I, Pereiro I, Ahlford A, Ferraro D, Zhang Q, Viovy J-L et al (2018) Microfluidic magnetic fluidized bed for DNA analysis in continuous flow mode. *Biosens Bioelectron* 102:531–539
43. Lacharme F, Vandevyver C, Gijs MAM (2008) Full on-chip nanoliter immunoassay by geometrical magnetic trapping of nanoparticle chains. *Anal Chem* 80(8):2905–2910
44. Xiong Q, Lim CY, Ren J, Zhou J, Pu K, Chan-Park MB et al (2018) Magnetic nanochain integrated microfluidic biochips. *Nat Commun* 9(1):1743
45. Hwang H, Choi E, Han S, Lee Y, Choi T, Kim M et al (2019) MESIA: magnetic force-assisted electrochemical sandwich immunoassays for quantification of prostate-specific antigen in human serum. *Anal Chim Acta* 1061:92–100
46. Sebba D, Lastovich AG, Kuroda M, Fallows E, Johnson J, Ahouidi A et al (2018) A point-of-care diagnostic for differentiating Ebola from endemic febrile diseases. *Sci Trans Med* 10(471):eaat0944
47. Kim MS, Kweon SH, Cho S, An SSA, Kim MI, Doh J et al (2017) Pt-decorated magnetic nanozymes for facile and sensitive point-of-care bioassay. *ACS Appl Mater Interfaces* 9(40):35133–35140
48. Jacinto MJ, Trabuco JRC, Vu BV, Garvey G, Khodadady M, Azevedo AM et al (2018) Enhancement of lateral flow assay performance by electromagnetic relocation of reporter particles. *PLoS One* 13:e0186782
49. Tamanaha CR, Mulvaney SP, Rife JC, Whitman LJ (2008) Magnetic labeling, detection, and system integration. *Biosens Bioelectron* 24(1):1–13
50. Kojima T, Takei Y, Ohtsuka M, Kawarasaki Y, Yamane T, Nakano H (2005) PCR amplification from single DNA molecules on magnetic beads in emulsion: application for high-throughput screening of transcription factor targets. *Nucl Acids Res* 33(17):e150-e
51. Berensmeier S (2006) Magnetic particles for the separation and purification of nucleic acids. *Appl Microbiol Biotechnol* 73(3):495–504
52. Zhao Y, Chen F, Li Q, Wang L, Fan C (2015) Isothermal amplification of nucleic acids. *Chem Rev* 115(22):12491–12545
53. Duan R, Lou X, Xia F (2016) The development of nanostructure assisted isothermal amplification in biosensors. *Chem Soc Rev* 45(6):1738–1749
54. Deng H, Gao Z (2015) Bioanalytical applications of isothermal nucleic acid amplification techniques. *Anal Chim Acta* 853:30–45

55. Ali MM, Li F, Zhang Z, Zhang K, Kang D-K, Ankrum JA et al (2014) Rolling circle amplification: a versatile tool for chemical biology, materials science and medicine. *Chem Soc Rev* 43(10):3324–3341
56. Nilsson M, Gullberg M, Dahl F, Szuhai K, Raap AK (2002) Real-time monitoring of rolling-circle amplification using a modified molecular beacon design. *Nucl Acids Res* 30(14):e66–e
57. Garbarino F, Minero GAS, Rizzi G, Fock J, Hansen MF (2019) Integration of rolling circle amplification and optomagnetic detection on a polymer chip. *Biosens Bioelectron* 142:111485
58. Minero GAS, Cangiano V, Garbarino F, Fock J, Hansen MF (2019) Integration of microbead DNA handling with optomagnetic detection in rolling circle amplification assays. *Microchim Acta* 186(8):528
59. Gorkin R, Park J, Siegrist J, Amasia M, Lee BS, Park J-M et al (2010) Centrifugal microfluidics for biomedical applications. *Lab Chip* 10(14):1758–1773
60. Tang M, Wang G, Kong S-K, Ho H-P (2016) A review of biomedical centrifugal microfluidic platforms. *Micromachines* 7(2):26
61. Burger R, Amato L, Boisen A (2016) Detection methods for centrifugal microfluidic platforms. *Biosens Bioelectron* 76:54–67
62. Strohmeier O, Keller M, Schwemmer F, Zehnle S, Mark D, von Stetten F et al (2015) Centrifugal microfluidic platforms: advanced unit operations and applications. *Chem Soc Rev* 44(17):6187–6229
63. Piccolo Xpress: Abaxis Inc (2019) <https://www.abaxis.com/medical/piccolo-xpress>
64. Zhu Y, Meng X, Chen Y, Li J, Shao H, Lu Y et al (2020) Self-served and fully automated biochemical detection of finger-prick blood at home using a portable microfluidic analyzer. *Sensors Actuators B Chem* 303:127235
65. Amasia M, Cozzens M, Madou MJ (2012) Centrifugal microfluidic platform for rapid PCR amplification using integrated thermoelectric heating and ice-valving. *Sensors Actuators B Chem* 161(1):1191–1197
66. Czilwik G, Messenger T, Strohmeier O, Wadle S, von Stetten F, Paust N et al (2015) Rapid and fully automated bacterial pathogen detection on a centrifugal-microfluidic LabDisk using highly sensitive nested PCR with integrated sample preparation. *Lab Chip* 15(18):3749–3759
67. Oh SJ, Seo TS (2019) Combination of a centrifugal microfluidic device with a solution-loading cartridge for fully automatic molecular diagnostics. *Analyst* 144(19):5766–5774
68. Cao X, de Mello AJ, Elvira KS (2016) Enhanced versatility of fluid control in centrifugal microfluidic platforms using two degrees of freedom. *Lab Chip* 16(7):1197–1205
69. Zhu Y, Chen Y, Meng X, Wang J, Lu Y, Xu Y et al (2017) Comprehensive study of the flow control strategy in a wirelessly charged centrifugal microfluidic platform with two rotation axes. *Anal Chem* 89(17):9315–9321
70. Li L, Miao B, Li Z, Sun Z, Peng N (2019) Sample-to-answer hepatitis B virus DNA detection from whole blood on a centrifugal microfluidic platform with double rotation axes. *ACS Sensors* 4(10):2738–2745
71. Kanchi S, Sabela MI, Mdluli PS, Inamuddin, Bisetty K (2018) Smartphone based bioanalytical and diagnosis applications: a review. *Biosens Bioelectron* 102:136–149
72. Liu J, Geng Z, Fan Z, Liu J, Chen H (2019) Point-of-care testing based on smartphone: the current state-of-the-art (2017–2018). *Biosens Bioelectron* 132:17–37
73. Vashist SK, Mudanyali O, Schneider EM, Zengerle R, Ozcan A (2014) Cellphone-based devices for bioanalytical sciences. *Anal Bioanal Chem* 406(14):3263–3277
74. Contreras-Naranjo JC, Wei Q, Ozcan A (2016) Mobile phone-based microscopy, sensing, and diagnostics. *IEEE J Sel Top Quantum Electron* 22(3):1–14
75. Dutta S (2019) Point of care sensing and biosensing using ambient light sensor of smartphone: critical review. *TrAC Trends Anal Chem* 110:393–400
76. Xu D, Huang X, Guo J, Ma X (2018) Automatic smartphone-based microfluidic biosensor system at the point of care. *Biosens Bioelectron* 110:78–88

77. Vashist SK, Luong JHT (2019) Smartphone-based point-of-care technologies for mobile healthcare. In: Vashist SK, Luong JHT (eds) *Point-of-care technologies enabling next-generation healthcare monitoring and management*. Springer, Cham, pp 27–79
78. Hernández-Neuta I, Neumann F, Brightmeyer J, Ba Tis T, Madaboosi N, Wei Q et al (2019) Smartphone-based clinical diagnostics: towards democratization of evidence-based health care. *J Intern Med* 285(1):19–39
79. Arumugam S, Colburn DAM, Sia SK Biosensors for personal mobile health: a system architecture perspective. *Adv Mater Technol*:1900720
80. Kanakasabapathy MK, Pandya HJ, Draz MS, Chug MK, Sadasivam M, Kumar S et al (2017) Rapid, label-free CD4 testing using a smartphone compatible device. *Lab Chip* 17(17):2910–2919
81. Kanakasabapathy MK, Sadasivam M, Singh A, Preston C, Thirumalaraju P, Venkataraman M et al (2017) An automated smartphone-based diagnostic assay for point-of-care semen analysis. *Sci Trans Med* 9(382):eaai7863
82. Brangel P, Sobarzo A, Parolo C, Miller BS, Howes PD, Gelkop S et al (2018) A serological point-of-care test for the detection of IgG antibodies against Ebola virus in human survivors. *ACS Nano* 12(1):63–73
83. Halvorsen CP, Olson L, Araújo AC, Karlsson M, Nguyễn TT, Khu DTK et al (2019) A rapid smartphone-based lactate dehydrogenase test for neonatal diagnostics at the point of care. *Sci Rep* 9(1):9301
84. Wang L-J, Chang Y-C, Sun R, Li L (2017) A multichannel smartphone optical biosensor for high-throughput point-of-care diagnostics. *Biosens Bioelectron* 87:686–692
85. Kühnemund M, Wei Q, Darai E, Wang Y, Hernández-Neuta I, Yang Z et al (2017) Targeted DNA sequencing and in situ mutation analysis using mobile phone microscopy. *Nat Commun* 8(1):13913
86. Priye A, Bird SW, Light YK, Ball CS, Negrete OA, Meagher RJ (2017) A smartphone-based diagnostic platform for rapid detection of Zika, chikungunya, and dengue viruses. *Sci Rep* 7(1):44778
87. Liang C, Liu Y, Niu A, Liu C, Li J, Ning D (2019) Smartphone-app based point-of-care testing for myocardial infarction biomarker cTnI using an autonomous capillary microfluidic chip with self-aligned on-chip focusing (SOF) lenses. *Lab Chip* 19(10):1797–1807
88. Paterson AS, Raja B, Mandadi V, Townsend B, Lee M, Buell A et al (2017) A low-cost smartphone-based platform for highly sensitive point-of-care testing with persistent luminescent phosphors. *Lab Chip* 17(6):1051–1059

Microfluidics for Environmental Applications



Ting Wang, Cecilia Yu, and Xing Xie

Contents

1	Introduction	268
2	Applications of Microfluidics in Environmental Science and Engineering	269
2.1	Microfluidics Used for Contaminant Analysis	269
2.2	Microfluidics Used for Microorganism Detection	273
2.3	Microfluidics Used as Research Platforms	275
3	Perspectives on Microfluidics' Applications in Environmental Science and Engineering	283
	References	284

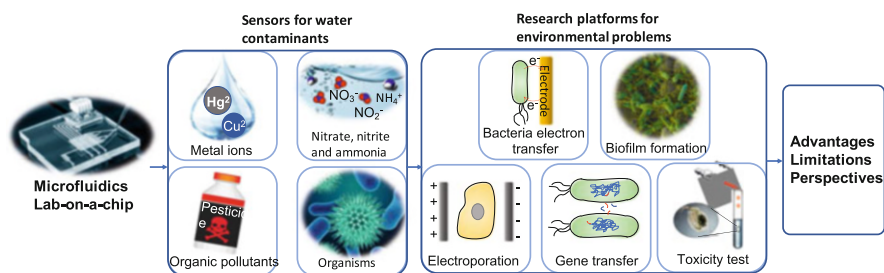
Abstract Microfluidic and lab-on-a-chip systems have become increasingly important tools across many research fields in recent years. As a result of their small size and precise flow control, as well as their ability to enable in situ process visualization, microfluidic systems are increasingly finding applications in environmental science and engineering. Broadly speaking, their main present applications within these fields include use as sensors for water contaminant analysis (e.g., heavy metals and organic pollutants), as tools for microorganism detection (e.g., virus and bacteria), and as platforms for the investigation of environment-related problems (e.g., bacteria electron transfer and biofilm formation). This chapter aims to review the applications of microfluidics in environmental science and engineering – with a particular focus on the foregoing topics. The advantages and limitations of microfluidics when compared to traditional methods are also surveyed, and several perspectives on the future of research and development into microfluidics for environmental applications are offered.

T. Wang, C. Yu, and X. Xie (✉)

School of Civil and Environmental Engineering, Georgia Institute of Technology, Atlanta, GA, USA

e-mail: xing.xie@ce.gatech.edu

Graphical Abstract



Keywords Bacterial electron transfer, Biofilm formation, Contaminant analysis, Environmental science and engineering, Lab-on-a-chip, Microfluidics, Microorganism detection

1 Introduction

Microfluidics, or “lab-on-a-chip”, is the science and technology of systems that are made using integrated circuits and/or miniaturized fluidic channels designed to realize different functions via electrical signals and/or flow manipulation [1]. When feature size and flow volume are shrunk down to microscale, surface area dramatically increases – which significantly improves the efficiency of molecular diffusion and heat transfer [1, 2]. As a result of their properties, microfluidics are increasingly finding applications in disparate areas of multidisciplinary research, including chemical [3, 4], biological [5, 6], medical (e.g., drug delivery) [2], and engineering (e.g., material synthesis) [7] fields.

Environmental science and engineering is a discipline for understanding environment-related processes and dealing with environment-related issues – such as understanding the conditions of environmental contamination and/or finding ways to affect environment remediation and protection. Some of the most widely studied environmental topics currently include pollution monitoring and analysis, research into the effects of pollutants on ecologies and human health, technologies of pollution treatment and removal, and microorganism-related challenges (such as the spread of antibiotic resistance).

Microfluidic and lab-on-a-chip devices are gaining increasing attention in this field due to their usefulness as tools for (by way of example) pollutant sensing, microorganism detection, and general environment-related process investigation (Fig. 1). Microfluidic devices offer several remarkable advantages over more conventional methods: for instance, they can more readily be used as portable detectors or analyzers due to their small size, thereby enabling on-site pollution detection and monitoring. Lab-on-a-chip devices have also provided research platforms for in situ and real-time observation of microorganisms and for visualization of other

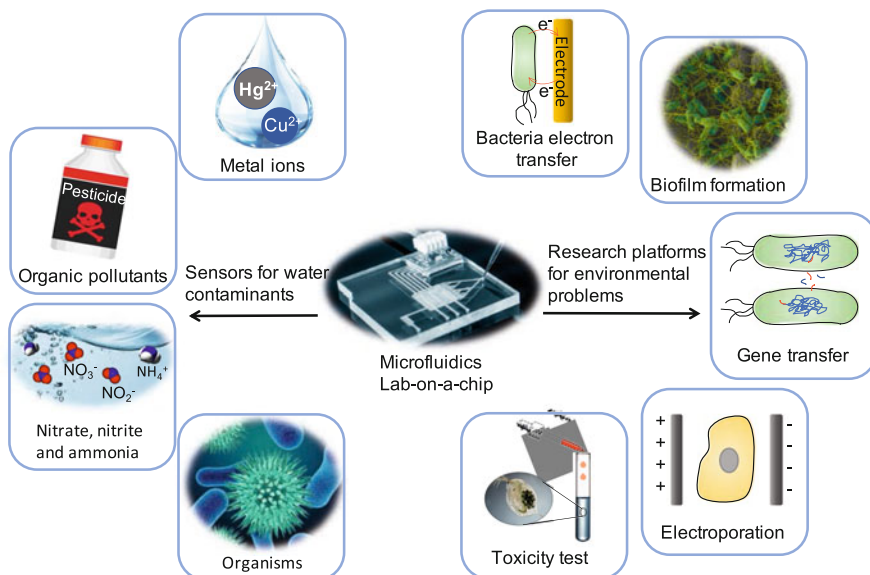


Fig. 1 Environmental applications of microfluidic and lab-on-a-chip devices (some images are from the Internet)

environmental processes. In this chapter, we will review some of the primary applications of microfluidic and lab-on-a-chip devices in environmental science and engineering. Finally, advantages, limitations, and perspectives on future development in this area will be discussed.

2 Applications of Microfluidics in Environmental Science and Engineering

2.1 Microfluidics Used for Contaminant Analysis

Conventional methods for conducting water pollutant analysis use advanced and complex instruments, such as inductively coupled plasma mass spectrometry (ICP-MS) for metal ions detection; high-performance liquid chromatography (HPLC) and gas chromatography-mass spectrometry (GC-MS) for organic compounds detection; and ultraviolet-visible spectroscopy (UV-Vis) for nitrate or nitrite detection. Compared to these traditional analytical techniques, microfluidic systems and lab-on-a-chip sensors possess several significant advantages, namely, greater portability for on-site monitoring, smaller required sample volume, shorter reaction time, and better process control. Optical and electrochemical methods are the two main approaches that are typically used for pollutant detection in

microfluidic devices and sensors [8]. Common optical methods include fluorescent, colorimetric, surface plasmon resonance, and surface-enhanced Raman scattering (SERS) [8]. The detection techniques used in electrochemical sensors consist of amperometry, voltammetry, conductometry, and potentiometry [9]. With the sensing device miniaturization and sample volume decrease, electrochemical methods offer an inherent advantage over optical approaches. Since electrochemical methods rely on the concentration instead of absolute amount of the analyte, the sensitivity is independent of the sample volume, and more accurate determinations could be achieved due to the higher surface-area-to-volume ratios of the small probes [10].

2.1.1 Heavy Metal Ion Analysis

Water contamination by heavy metals is a severe environmental problem with significant implications for public health. Indeed, many lab-on-a-chip-based sensors have been developed specifically to facilitate the detection of a variety of metal ions, including Hg (II) ions [11], Pd (II) ions [12], Cd (II) ions [13, 14], Cu (II) ions [15, 16], and other metal ions [17, 18].

Wang et al. have developed a microfluidic device for quantitative analysis of trace Hg (II) ions (Hg^{2+}) based on surface-enhanced Raman scattering (SERS) [19]. A sample containing Hg^{2+} was mixed with gold nanoparticles while flowing through a wandering channel (Fig. 2a, b). The gold nanoparticles had rhodamine B dye molecules attached on the surface. Due to the strong affinity between Hg^{2+} and gold nanoparticles, the rhodamine B attached on the gold particles could be replaced by Hg^{2+} (Fig. 2c), causing a change in the SERS signal of rhodamine B in a function of the concentration of Hg^{2+} . The SERS changing was characterized by a Raman microscope system. The concentration analysis range of Hg^{2+} was estimated to be between 0.1 and 0.5 $\mu\text{g}/\text{L}$.

Another microfluidic device has been developed for continuous and on-site monitoring of Pb (II) ions (Pb^{2+}) [20]. The device is composed of cyclic olefin copolymer microfluidic channels, with silver working and counter-electrodes. The Pb^{2+} measurement was achieved by square-wave anodic stripping voltammetry (SWASV) technique. Specifically, water sample containing Pb^{2+} was first injected into the channel through an inlet. Under a certain voltage, Pb (II) ions were deposited

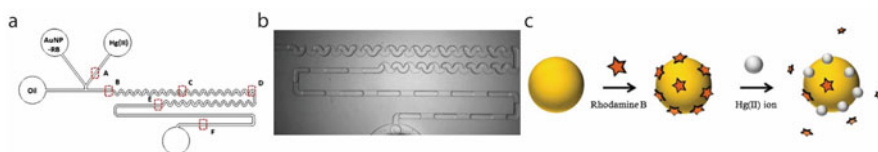


Fig. 2 Schematics of the microfluidic system for Hg ions detection. **(a)** Schematic of the microfluidic device for Hg^{2+} detection. **(b)** Photograph of the channel during operation. **(c)** Schematic of Hg^{2+} sensing mechanism based on the replacement of RB dye molecules through the reduction of Hg^{2+} on the surface of Au nanoparticles (reprinted by permission from Springer Nature Customer Service Centre GmbH: Springer, [19]. Copyright (2009))

onto the Ag electrode via electrodeposition, and then plated metal was oxidized off from the Ag electrode using a square-wave anodic potential sweep. The whole electrochemical reaction is presented by $\text{Pb}^{2+} + 2e^- \leftrightarrow \text{Pb}$. The current generated during the stripping process was measured to identify and quantify Pb (II) ions. The detection limit was 0.55 ppb, and the correlation coefficient is 0.998 within the concentration range of 1–1,000 ppb. Furthermore, the detection performance remained stable after 43 consecutive measurements, demonstrating the sensor's reusability and great potential for real-world applications.

Microfluidic systems for water arsenic detection using both colorimetric methods and electrochemical methods have also been developed [10]. In addition, biological detection methods have been pioneered as well. A strain of genetically modified *Escherichia coli* (*E. coli*) was used as reporter bacteria for arsenic detection in a microfluidic device [21]. Polydimethylsiloxane (PDMS) was used to fabricate the microchannels. The bacteria were encapsulated in agarose beads and packed into small cages in the microchannels. When water sample containing arsenic flowed through the cages, the bacteria exposed to arsenic could produce green fluorescent proteins. The fluorescence was imaged with a microscope and processed for intensity analysis. The rate of fluorescence signal increase was linearly proportional to the arsenic concentration within the range of 0–50 $\mu\text{g/L}$. More microfluidic systems for arsenic detection were reviewed in [10].

In addition to standard silicon-based sensors, paper-based microfluidics have also been developed for metal analysis (reviewed in [22]). Paper-based microfluidics are paper substrates patterned as channels and barriers to realize different functions. Compared to traditional PMDS and glass or silicon-based microfluidics, the paper-based microfluidic devices are more cost-efficient [22]. By combining eight pyridylazo compounds, a paper-based microfluidic device could discriminate eight different heavy-metal ions (Hg^{2+} , Cd^{2+} , Pb^{2+} , Ag^+ , Ni^{2+} , Cu^{2+} , Zn^{2+} , and Co^{2+}) at concentrations as low as 50 μM [23].

2.1.2 Organic Compound Analysis

Potentially toxic organic compounds – such as phenolic compounds and pesticides – are widely used across many industries. Unfortunately, some of these organic compounds may also cause water contamination, due to wastewater discharge or leaching from soil. Microfluidic sensors for organic matter have been developed based on different detection mechanisms, including amperometry [24], enzyme-based techniques [25–27], and electrophoresis [28, 29]. A lab-on-a-chip device with layer-by-layer printing of quantum dot (QD)/enzyme microarrays was fabricated for organophosphorus pesticide (OP) detection [30]. Layer-by-layer microarrays of QDs/poly (dimethyldiallyl ammonium chloride) (PDDA) and acetylcholinesterase enzyme (AChE) were fabricated on a glass slide using inkjet (Fig. 3). Water samples and acetylthiocholine (ATCh) were added to the chip for OPs detection. AChE catalyzes the hydrolysis of ATCh, generating thiocholine (TCh), which can dissociate the electron-hole pair of QDs and quench the fluorescence.

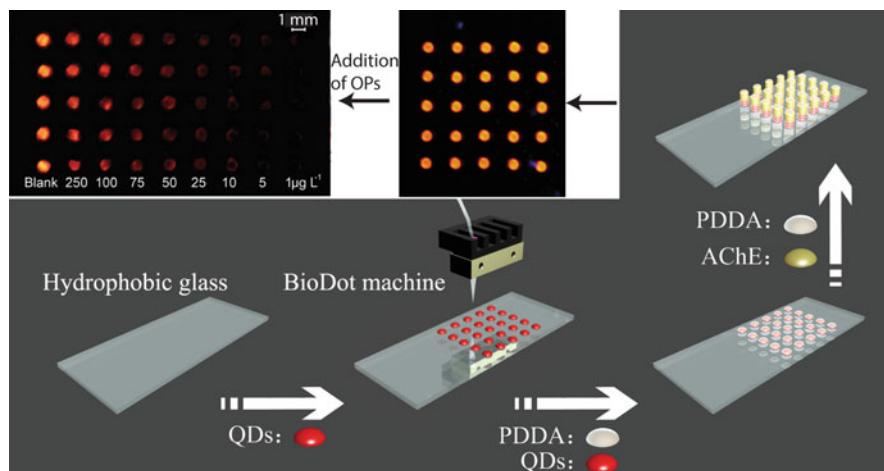


Fig. 3 The schematic of the fabrication process of the OPs detection chip and the image of QDs after OPs are added. (Reprinted from [30]. Copyright (2016), with permission from Elsevier)

When OPs are present, the activity of AChE was inhibited; thus the fluorescence of QDs will not be quenched. A detection limit of $1 \mu\text{g/L}$ of Ops was achieved with this device, which was much lower than levels specified by standard tests and other colorimetric detection methods.

2.1.3 Nitrate and Ammonia Analysis

Nitrate and nitrite are ubiquitous water contaminants in both surface and groundwater, and they each can impose harmful effects on human health. A miniaturized microfluidic sensor has been developed to facilitate nitrate determination using a double-potential-step chronocoulometry (DPSC) method [31]. Two potential steps, E_1 and E_2 , were applied sequentially to obtain oxygen reduction charge Q_1 and both nitrate and oxygen reduction charge Q_2 . The nitrate reduction charge was calculated by subtracting Q_1 from Q_2 , which is directly related to nitrate concentration in the sample. A silver sensing electrode, silver oxide reference electrode, and platinum counter electrode were then deposited on a silicon substrate. A polyimide passivation layer was also deposited to prevent short circuit and improve reliability. The microchannels were fabricated via deep reactive ion etching, which enabled the flow-through analysis. The lower and upper detection limit for nitrate were $4\text{--}75 \mu\text{M}$ and $500\text{--}2,000 \mu\text{M}$, and the linearity (R^2) was >0.99 . Other microfluidic-based sensors for nitrate [32, 33] and ammonia [34, 35] analysis were also reported.

Lab-on-a-chip systems have also found applications in a wide variety of disparate environments, including marine pollution analysis [36–39], air pollutant detection [40, 41], and bioaerosol monitoring [42–44].

2.2 *Microfluidics Used for Microorganism Detection*

Pathogen contamination of drinking water remains a serious public health concern worldwide, especially in less developed areas. Waterborne pathogens can include bacteria, viruses, and some protozoa. Some of these biological agents are highly infectious and resistant to water treatment processes and accordingly pose a severe risk to human health. Different detection approaches have been developed to facilitate pathogen detection on-chip, such as nanomechanical cantilever sensing [45, 46]; surface-enhanced Raman spectroscopy [47]; impedance-based sensing [48]; amplification-based sensing, including PCR [49–56] and loop-mediated isothermal amplification [52]; and quartz crystal microbalance-based sensing [57]. Both optical signals [58–61] and electrical signals [62, 63] are used in microorganism sensing techniques. The applications of microfluidics in waterborne pathogen detection are reviewed in [64]. Microfluidics for pathogen detection are also being developed as point-of-care devices, for diagnostic purpose [65]. Although the samples analyzed in diagnostic devices (e.g., saliva and blood) are different from environmental samples, the detection techniques and approaches are still valuable as references.

2.2.1 **Virus Detection**

An ultrasensitive virus detection sensor based on the Young interferometer has been reported [66]. The sensor is a silicon chip consisting of four light channels. Si_3N_4 and SiO_2 layers were deposited on a silicon substrate via chemical vapor deposition. The SiO_2 layers were etched to form windows for antibody functionalization and virus detection. The Si_3N_4 layer beneath served as a pathway for light (Fig. 4a). Monochromatic light from a laser source was coupled to an optical channel and guided into the four parallel channels (Fig. 4b). Antibodies for different viruses' detection were coated onto the channels. The light interfered on a screen after exiting from the four waveguide channels, generating an interference pattern. Virus binding to the antibody would be probed by the evanescent field of the guided modes, thus causing a phase change which could be measured as a change in the interference pattern. The pattern reflects the amount of the viruses bonded on the antibodies. Figure 4c shows the specific detection of herpes simplex virus type 1 (HSV-1) realized by the specific reaction between HSV-1 and the antibodies. The sensor specifically and sensitively detected HSV-1 with the concentration as low as 850 particles/mL and the detection sensitivity of the sensor was estimated to approach one single HSV-1 particle.

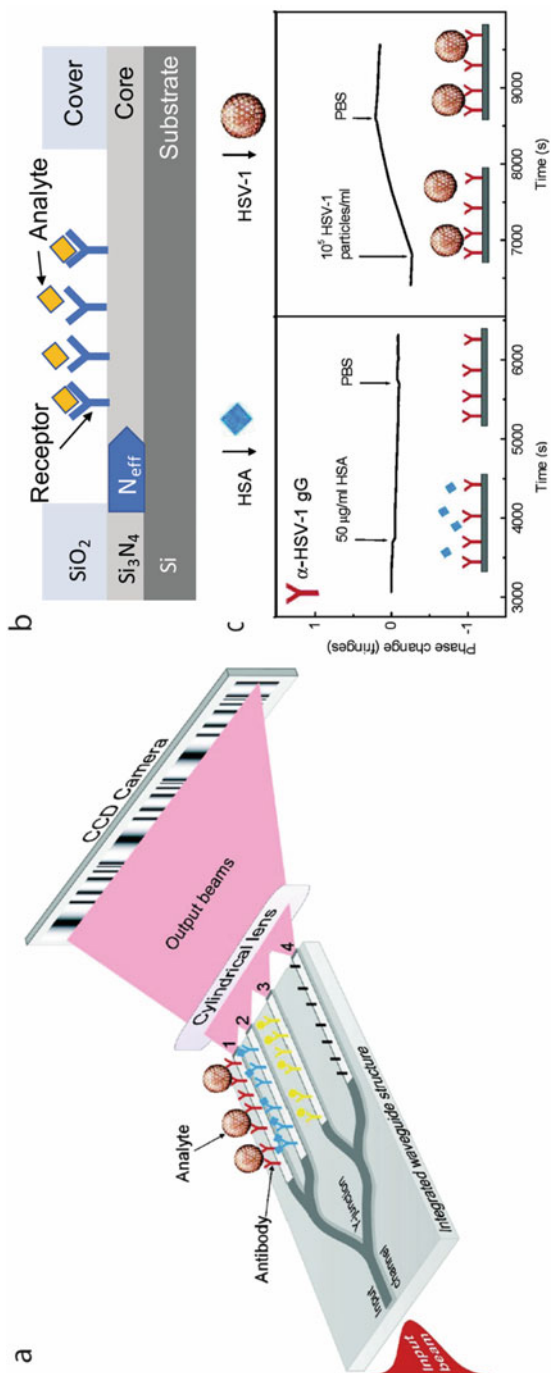


Fig. 4 (a) Schematic of the sensor for virus detection. 1, 2, and 3 are the measuring channels, and 4 is the reference channel (reprinted with permission from [66]). Copyright (2007) American Chemical Society]. (b) Cross section of the chip along the direction of the channels (Adapted from [67]). (c) Specific and selection detection of HSV-1. The figures indicate phase changes as a function of time. The phase change does not increase when human serum albumin (HSA) is added but increases only after HSV-1 is added, which is due to the specific interactions between HSV-1 and α -HSV-1 gG (reprinted with permission from [66]). Copyright (2007) American Chemical Society)

2.2.2 Bacteria Detection

Bacteria are another kind of major waterborne pathogen that poses risk to human health. Mannoor et al. have reported a microfluidic system for real-time on-chip bacteria detection using impedance spectroscopy [68]. A gold electrode array was deposited onto a silicon substrate via standard microfabrication methods. The flow channel for real-time monitoring was fabricated using PDMS and bonded to the substrate. The electrode surface was functionalized with magainin I, which is a kind of antimicrobial peptide (AMPs) used for bacteria binding. When the bacteria contained in water samples were recognized by the AMPs and bonded to the electrode surface, the impedance of the electrode array changed, which was analyzed by a spectrum analyzer. Since the binding activity was directly proportional to the variation of impedance, the bacteria concentration could be analyzed. The detection limit of *E. coli* was about 1 bacterium/ μL . The system showed sufficient selectivity toward pathogenic and Gram-negative bacteria, and also maintained broad detection capability for other bacteria. Furthermore, the flow system enabled real-time bacteria monitoring for a continuous water sample.

2.2.3 Protozoa Detection

In addition to viruses and bacteria, protozoa – especially some parasites – can pose a significant risk to human health. *Cryptosporidium* is one of the parasites of greatest concern on this front, due to its low infection dose and resistance to common water treatment approaches [69]. Several techniques have been integrated to miniaturized fluidic chips for *Cryptosporidium* detection, including optical methods such as target trapping combined with immunofluorescence or microscopy detection; mass-based methods such as quartz crystal microbalance sensing and cantilever sensing; and electrical techniques such as bioimpedance and dielectrophoresis methods. The detection of cryptosporidium in microfluidic devices is reviewed in [69].

2.3 Microfluidics Used as Research Platforms

Understanding environmental-related natural processes is another important component of environmental science and engineering. These widely studied processes are encompassed within, but certainly not restricted to, the fields of environmental microbiology, ecotoxicology, and contaminant transportation. Microfluidic and lab-on-a-chip devices are increasingly being used in environmental research laboratories, since they provide ideal research platforms for in situ and real-time observation. The combination of lab-on-a-chip devices and observation techniques (such as microscopy) enables in situ visualization, characterization, and simulation of a wide

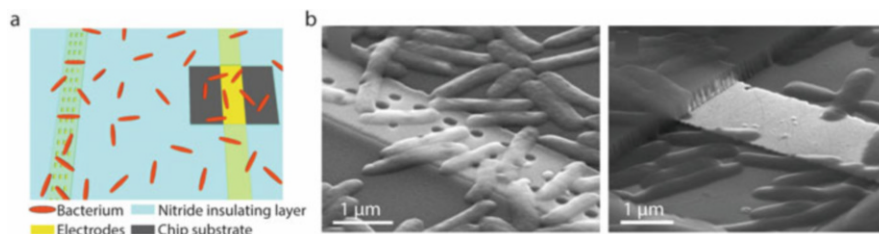


Fig. 5 Schematic of the design of the electrodes for *Shewanella* electron transfer study. (a) The silicon nitride insulating layer (blue) with nanoholes or large window openings is deposited over electrodes (yellow) to prevent or enable direct contact with bacteria (orange). (b) SEM images of the bacteria cells on the electrodes with nanoholes (left) and large window openings (right). (Reprinted with permission from [73], Proceedings of the National Academy of Sciences)

range of environment-related processes, thus becoming a valuable investigation approach in environmental studies.

2.3.1 Mechanisms of Bacteria Electron Transfer

Microbial fuel cells, which use microorganisms colonizing electrodes to catalyze electrochemical reactions and convert chemical energy into electrical power, are being intensively studied in the environmental technology field since they possess the potential capability of converting organic or inorganic waste into power via an environmentally friendly microbiological process [70, 71]. Understanding the mechanisms of electron transfer from bacteria to electrode is accordingly imperative for the further development of potential microbial fuel cells.

Three possible electron transfer pathways have been proposed: via direct contact, via conduct pili, and via diffusion of soluble redox-active molecules serving as “electron shuttles” [72]. Jiang et al. have reported a lab-on-a-chip device with microelectrodes as a platform to investigate the electron transfer between *Shewanella oneidensis* and electrodes [73]. Finger-shape electrodes were defined by photolithography and deposited onto a cover glass using metal evaporation and lift-off methods. A passive Si_3N_4 layer was deposited by chemical vapor deposition and patterned to have nanoscale openings on one electrode and a big opening on the other electrode (Fig. 5a, b). The nanoholes were small enough to prevent direct contact between bacteria and the electrode but allowed the indirect contact through pili or diffusion of extracellular redox-active molecules. A SU-8 (a commonly used epoxy-based negative photoresist) chamber was fabricated to improve reliability and environmental control. In situ cell image/tracking with a microscope and current recording revealed that the currents could be detected even without direct contact between bacteria and electrodes, suggesting that electron transfer was realized by pili or a mediator’s diffusion. In addition, the removal of the diffusible mediators caused a rapid drop of the current, which further supported that electron transfer occurs predominantly by diffusion of mediators.

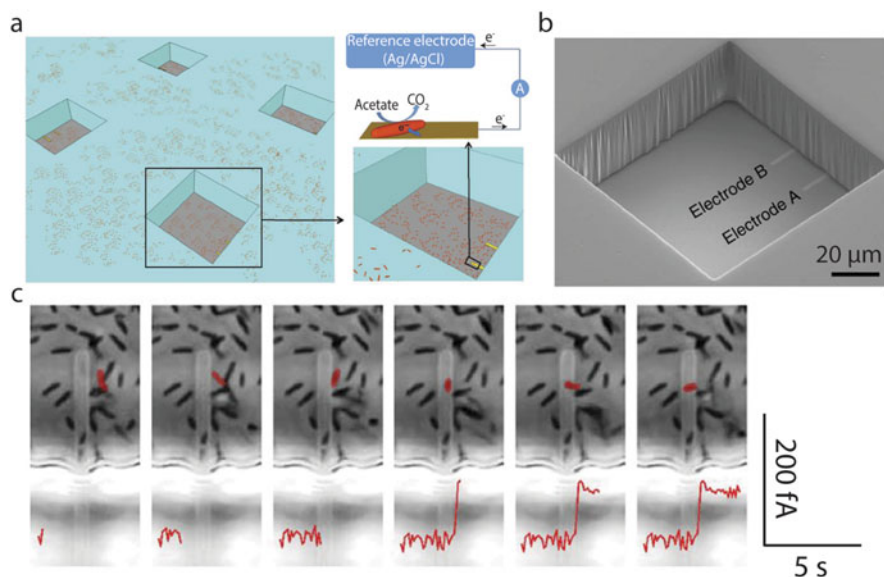


Fig. 6 (a) Schematic of experimental design for *Geobacter sulfurreducens* electron transfer. (b) SEM image of a well containing two finger electrodes. (c) In situ microscopy images of *Geobacter* cells around and on the measured electrode and the current changes at the same time. The cell that contacts the electrode at the same time with the current increases is marked in red. (Reprinted by permission from Springer Nature Customer Service Centre GmbH: Springer, [74]. Copyright (2013))

For other kinds of bacteria, however, the electron transfer mechanism may need to be altered. A similar lab-on-a-chip device was fabricated to probe the charge transport from *Geobacter sulfurreducens* to electrode [74]. Gold electrodes were deposited via metal evaporation and lift-off. Thick SU-8 was then fabricated to form wells around the electrodes to allow direct contact between bacteria and electrodes (Fig. 6a, b). Simultaneous recording of cell position and currents indicated that the contact of a cell to the electrode directly caused a stepwise increasing of current (Fig. 6c). The current of a single *Geobacter* was 92 fA, and the current density was estimated to be $\sim 10^6 \text{ A m}^{-3}$. In addition, when the diffusible redox mediators were removed, the current was not affected. These measurements together indicated that, different from *Shewanella*, the electron transfer between *Geobacter* and electrode was mainly due to direct contact. Ding et al. reported a nanoelectronics lab-on-a-chip system to investigate the electrical conductivity of both *Shewanella* and *Geobacter* and indicated that electrochemical electron transfer at the cell/electrode interface was the origin of the conductive current for both microbes [75].

As researchers have started to gain a deeper understanding of bacterial electron transfer, the role of bacterial self-assembled nanostructures for extracellular electron transfer has also garnered increased attention. For example, to elucidate the effects of microenvironment on the intercellular microbial nanostructures (nanowires)

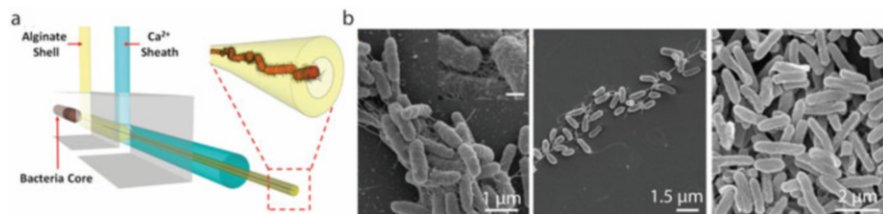


Fig. 7 (a) Schematics of the flow-focusing device for core/shell bacterial fiber generation. The bacteria-containing core stream (brown) is focused before entering the alginate shell stream (yellow), and then a CaCl_2 sheath flow is introduced to cross-link the alginate to form the cord. (b) SEM images of high (left) and low (middle) bacteria density networks as well as high-density networks cultured in electron acceptor rich conditions (right). (Reprinted with permission from [76]. Copyright (2018) American Chemical Society)

formation, a one-dimensional core/shell bacterial cable has been developed – which allows rational control of the microenvironments [76]. The fabrication method of this cable was different from common microfluidics fabrication processes. The cable was generated through a flow-focusing device with coaxially aligned glass capillaries and multiple inlets for different solutions. Bacteria solution flow was focused into a narrow stream, and alginate was injected to the device to form the scaffolding for bacteria encapsulation. A Ca^{2+} containing sheath flow was exploited to cross-link alginate to become a solid hydrogel (Fig. 7a). The results revealed that the formation of intercellular structures is closely related to the fiber diameters. More densely and closely packed bacteria produced more self-assembling microbial nanowires, which directly increased the extracellular electron transfer efficiency (Fig. 7b). Furthermore, lack of electron acceptors can enhance the production of the nanowires (Fig. 7b).

2.3.2 Biofilm Formation

Biofilm formation is a natural process that occurs during bacteria growth. On one hand, biofilms play important roles in some environmental engineering processes, including in wastewater biological treatment and microbial fuel cells. However, biofilm can also cause environmental and public health problems – including by contaminating or clogging drinking water pipelines or fouling water treatment systems. As a result, the process of biofilm formation is gaining more attention in environmental science and engineering. Drescher et al. have developed a microfluidic device to investigate biofilm formation in fluidic channels [77]. A meandering microfluidic channel was fabricated with PDMS and sealed with a cover glass. *Pseudomonas aeruginosa* bacterial solution flowed through the microfluidic channel and the biofilm formation process in the channel was observed with a microscope. This work demonstrated that the 3D biofilm streamers that bridged the space between obstacles and corners caused major clogging of the channel, instead of the biofilm attached on the inner surface. The 3D biofilm streamer was first

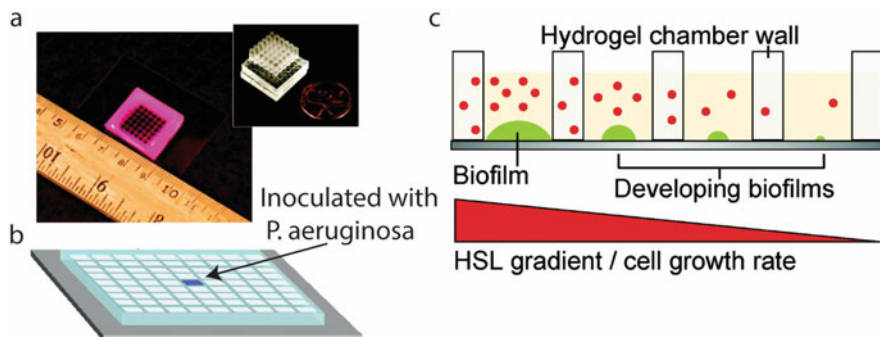


Fig. 8 (a) An image of the chamber for quorum sensing study with hydrogel chamber wall (stained with red dye) on a glass coverslip (upper). An image of the PDMS stamp used to make the chamber (lower). (b) The center chamber was inoculated with *P. aeruginosa*. (c) Schematic of the experiment. HSL diffuse through the hydrogel chamber wall, which is detected by biofilm in each chamber. (Reprinted with permission from [78]. Copyright (2011) American Chemical Society)

formed by the extracellular matrix shed from the attached bacteria and then worked as a network to catch the flowing bacteria and biomass, leading to a rapid clogging. With this microfluidic chip that enabled in situ observation of the biofilm formation, this work demonstrated a biofilm formation process which is independent of and much faster than bacteria growth. The results also suggested that the biofilm streamers may contribute more to the clogging of flow through systems such as water pipelines.

During biofilm formation, the bacteria within microbial communities can sense chemical signals from other cells and regulate their own gene expression as a response. This process is referred to as quorum sensing, and it is an important factor in regulating biofilm formation that is a current subject of intense study in the environmental microbial field. Flickinger et al. have reported a lab-on-a-chip platform to study quorum sensing between microbial communities [78]. The lab-on-a-chip device contained an array of spatially confined chambers fabricated with poly (ethylene glycol) diacrylate (PEGDA) on a silanized cover glass using a PDMS mold (Fig. 8a). *Pseudomonas aeruginosa* (*P. aeruginosa*) was used as a model bacterial strain and inoculated in the center chambers for biofilm growth (Fig. 8b). The molecule regulators secreted from the biofilm for quorum sensing, homoserine lactones (HSLs), can diffuse inside (filled with 15% PEGDA) and between the PEGDA chamber to form spatial and temporal gradients, thus enabling analysis of the relationship between the diffusion of HSLs and formation of nascent new biofilm (Fig. 8c). The results showed that HSL was detected by the bacteria cells within a distance of 8 mm. The new biofilm growth within 3 mm away from the existing biofilm, where the HSL concentration was higher than $1 \mu\text{M}$, was enhanced due to the detection of HSL, while further biofilms were not affected. In addition to regular on-chip chambers, 3D cavities with various geometries were fabricated using 3D printing strategy to study the mechanisms of community regulation [79].

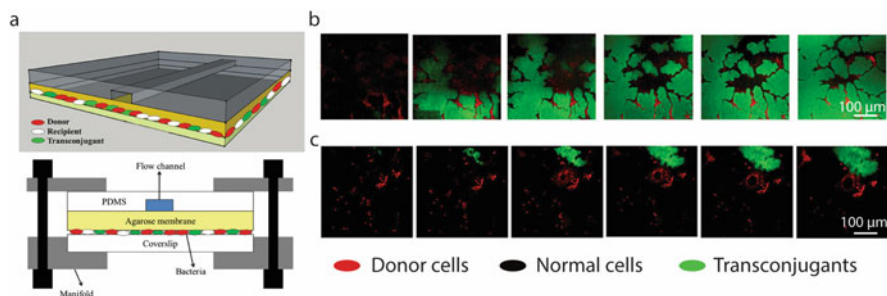


Fig. 9 (a) Schematic of the device to study antibiotic resistant genes transfer (upper) and the device setup (lower). (b) Gene spread in pure *E. coli* culture. (c) Gene spread in activated sludge community. For both (b) and (c), the donor cells *P. putida* KT2440 are red; normal *E. coli* or active sludge cells are colorless, while transconjugants emit green fluorescence. (Reprinted with permission from [80], <https://pubs.acs.org/doi/abs/10.1021/acs.est.8b03281>. Copyright (2018) American Chemical Society. Further permissions related to the material excerpted should be directed to the ACS)

2.3.3 Antibiotic Resistance Gene Transfer

It is now known that horizontal gene transfer is an important pathway by which antibiotic resistance spreads from one organism to another. Microfluidic devices are promising platforms for facilitating gene transfer study, since they enable the in situ and real-time monitoring of the process dynamics. A microfluidic device was reported to investigate the plasmid-mediated horizontal gene transfer within the same species and between different species [80]. The microfluidic chip consisted of a cover glass with a layer of agarose and a PDMS cover on top (Fig. 9a). A drop of mixed bacteria solution containing the gene donor strain (*Pseudomonas putida* harboring an antibiotic resistance plasmid) and recipient strain (*E. coli* or bacteria extracted from activated sludge) was sandwiched between the agarose and cover glass. The PDMS cover had a channel in it for broth delivery and waste removal for bacteria growth (Fig. 9a). The gene donor bacteria carried plasmid RP4, which was labeled with GFP, but also tagged with red fluorescent genes that repress the expression of GFP. So, the donor bacteria emitted red fluorescence. When the plasmids were transferred to acceptors, the acceptors would emit green fluorescent from GFP carried with the plasmids. The gene horizontal transfer process on the chip was monitored with a fluorescence microscope. The results showed that the horizontal gene transfer was highly dependent on the structure and composition of the biofilm. The plasmids were first successfully transferred from donor species *Pseudomonas putida* to acceptor *E. coli*. Within the pure *E. coli* colony, the transfer from the first transconjugants to other cells was very efficient, leading to a cascading gene spread within the single-strain biofilms (Fig. 9b). In comparison, for the activated sludge biofilm consisting of different species, vertical gene transfer appeared to be the dominant route instead of horizontal transfer (Fig. 9c). It is also found that many species that showed horizontal gene transfer were associated with human pathogens.

Other microfluidic systems for gene transfer and antimicrobial resistance related studies were also reported, including using microfluidic devices to study gene transfer on the single-cell level [81], dissect horizontal and vertical gene transfer [82], test antimicrobial susceptibility [83], and investigate the modulation of antibiotics on horizontal gene transfer [84]. More studies are reviewed in [85].

2.3.4 Electroporation

Electroporation is the phenomenon whereby pores form on a cell membrane when the cell is exposed to an external electric field. It is commonly used to control cell membrane permeability when molecular intracellular transfer is desired. In addition, electroporation is also a widely used method for cell inactivation and lysis. Researchers in environmental fields are also increasingly exploring the possibility of using electroporation as a bacteria inactivation approach for drinking water disinfection [86–89] and hazardous wastewater decontamination [90]. Understanding the electroporation process has therefore become another important environmental study topic. Since the actual formation of these pores is difficult to observe, Sengel et al. have developed a lab-on-a-chip device to image the dynamics of individual electropores [91]. The experimental setups are shown in Fig. 10a. A cover glass was coated with agarose and placed in a recess. Lipid solution was added and associated with the agarose to form a lipid monolayer. An aqueous droplet with lipid monolayer was brought onto the cover glass. Two monolayers at the contact area formed a lipid bilayer, which is similar to cell membrane. Two electrodes were placed at the two sides of the lipid bilayer to monitor the current, and the pore formation was labeled by a fluorescent dye and recorded with a fluorescence microscope (Fig. 10b). With this platform, researchers found several interesting phenomena of electroporation. When the potential difference across the bilayer reached 100 mV, the membrane permeability started to change. With higher

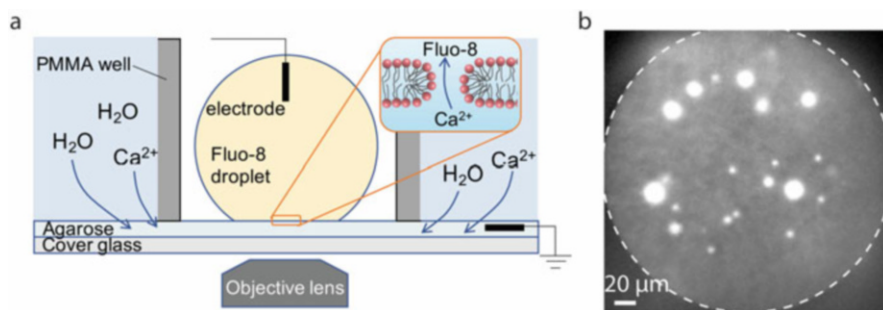


Fig. 10 Schematic of the experimental setup. (a) A lipid bilayer is formed on the interface of the droplet and the substrate. When a pore is formed due to electroporation, Ca²⁺ ions flow into the drop, which could be detected by the Ca²⁺ sensitive dye fluo-8 and visualized by a microscopy. (b) A microscopy image of pores formed on lipid bilayer. (Adapted and reprinted with permission from [91], Proceedings of the National Academy of Sciences)

transmembrane potential, larger pores formed, but a large number of small pores still existed. In addition, the pores fluctuated (opened and closed) in a variety of modes, and higher potential did not lead to more stable pores. Two adjacent pores did not tend to combine, while anti-combination was found since the potential across the lipid bilayer would be released when a nearby pore gets larger. A lab-on-a-chip device to rapidly determine the electroporation threshold for bacteria inactivation was also reported [92].

2.3.5 On-Chip Toxicity Test

Ecotoxicology focuses on identifying the toxicity level and impact of environmental pollutants on creatures and human health. Compared to traditional toxicity testing approaches, the emerging on-chip toxicity tests enabled by microfluidics are significantly more compact, convenient, and labor-efficient – and as a result they are quickly gaining substantial attention in this field.

Fine particles are major pollutants in the air, which makes them crucial indicators of general air quality. A microfluidic device aiming at recognizing the toxicity of fine particle matter ($PM_{2.5}$) on human lung epithelial cells was reported [93]. A porous membrane was bonded to the PDMS chamber, and the human lung epithelial cell line (BEAS-2B) was cultured on the membrane. Medium flowed under the membrane to replenish nutrient for cell growth (Fig. 11). The cell viability remained above 98% after 21 days of culturing, which demonstrated that this lab-on-a-chip is capable of retaining the viability of cells for the toxicity test. The air liquid interface mimicked the pulmonary natural microenvironment, which enabled the *in vitro* cytotoxicity test. Particles were added to the cells using an aerosol nebulizer, and the cytotoxicity was analyzed by several different approaches after exposure. The results showed that some metabolic pathways of the cells contributing to inflammation reactions were activated after the exposure. The cell apoptosis rate was also increased from 3.8% to 66.7% after 24 h of exposure. This configuration is also applicable for cytotoxicity test of other pollutants.

Engineered metal nanoparticles are being used for a variety of applications in many different fields. However, the potential hazards of these nanoparticles to human health and environment remain topics of hot debate and active research. To investigate the effects of silver nanoparticles on microorganisms' behavior, a

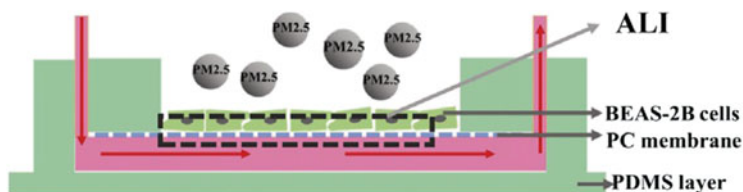


Fig. 11 Schematic of the designed microfluidic chip for ambient particle toxicity test. (Reprinted from [93]. Copyright (2019) with permission from Elsevier)

microfluidic device was reported to study the swimming response of algae to silver nanoparticles [94]. PDMS containing microchannels was fabricated via soft lithography and bonded to a glass slide, forming the microfluidic device. The microfluidic device used in this study was previously designed for a bacterial chemotaxis test, which contained a concentration-gradient generator and a chemotaxis observation channel [95]. Solution with and without silver nanoparticles were added to the two inlets, respectively. After flowing through the mixing part, nanoparticle concentration gradient was created and maintained in the observation channel. Algae was then added to the observation channel and exposed to the nanoparticle gradient. The algae swimming response was observed and recorded with a microscope. The results showed that algae moved away from the area containing 10^8 silver particles/mL, but no significant aversive swimming was found to gold nanoparticles at the same concentration. The toxicity of the released Ag ions may be the main reason leading to the avoidance behavior.

Microfluidics also have applications in aquatic toxicity tests on bacteria [96, 97], nematodes [98], crustacea [99, 100], and fish embryo [101]. More applications and future perspective were discussed in the review paper [102].

3 Perspectives on Microfluidics' Applications in Environmental Science and Engineering

Microfluidic and lab-on-a-chip devices are increasingly being used as tools in the fields of environmental science and engineering. Miniaturized microfluidic or lab-on-a-chip devices evidence remarkable sensing abilities, because sensing electrodes can be miniaturized without losing sensitivity and the configurations are compatible with thin layer operations [9]. Flow manipulation and compound separation can also be enabled by incorporating additional electrodes in existing channels, without adding additional parts. When used as detection equipment, lab-on-a-chip systems offer several comparative advantages over traditional mechanisms – including shorter analysis time, smaller sample volume, and online and real-time monitoring. All of these benefits are attributable to their small size, precise flow control, and low cost compared to traditional instruments. Some sensors have already been commercialized, such as test strips based on electrochemistry for arsenic detection [103] and sensors based on stripping square-wave voltammetry for metal analysis [104]. A DNA electrochemical biosensor has been combined with sample processing platforms for online pathogens monitoring in natural water [105]. IBM is also working on the development of sensors for environmental pollution detection, such as methane leakage [106]. Since real-world samples are often complex and signal characterization systems are still required for the systems, real-world implementation of these detection devices remains limited in some instances. In addition to further improving the performance of sensors, future studies will undoubtedly focus on developing more integrated systems that combine

sampling, pre-treatment, and signal interpretation on a single chip – which will increase the viability of on-site, real-time applications across a wide variety of real-world settings. Furthermore, exploring cost-efficient materials (e.g., paper-based devices), simpler fabrication processes and easier operation approaches will also undoubtedly continue to bring the cost associated with these devices down, which will also further facilitate the feasibility of on-site and point-of-use applications.

But compared to their use as sensors and analyzers, microfluidic devices offer even more remarkable advantages as research platforms for environment-related process investigation. Their miniaturized size and the flexible configurations for realizing various functions provide them with unique capabilities for visualizing and unveiling the secrets of numerous environmental-related processes, which are not comparable by other approaches. Therefore, we believe the future growth of lab-on-a-chip devices as research platforms will be focused on exploring novel and clever designs to realize more functions based on different investigation purposes. Nano structures, such as nanoholes, nanoparticles, nanowires, and coating layers with nanoscale thickness, are providing lab-on-a-chip devices with more features and functions. Nanofabrication techniques, including electron beam lithography and atomic layer deposition, are becoming widely used for chip fabrication. In addition, more and more lab-on-chip devices for research purpose are not restricted to standard chamber or channel on-chip configurations. Various 3D geometries are enabled by thriving 3D fabrication techniques, such as 3D printing, two photon polymerization, and micron/submicron stereolithography. To improve the capabilities of lab-on-a-chip devices, the performance of their basic functions, such as flow control, cell manipulation, cell culturing, and target tracking, is also worth improving. Finding the environmental problems and processes that could be investigated using lab-on-a-chip platforms is also important. In addition to visualizing small-scale process, such as bacterial-related phenomena mentioned in Sect. 2.3, lab-on-a-chip systems are also ideal for mimicking and simulating large-scale ecological processes, such as fate and transport of nanoparticles in soil and groundwater [107, 108]. The findings of the on-chip simulations could provide valuable experimental data for modeling and further on-site studies.

Acknowledgments The authors would like to acknowledge the US National Science Foundation [grant numbers CBET 1845354]. The authors would like to thank Dr. Janina Bahnmann for her contribution to this chapter.

References

1. Shang L, Cheng Y, Zhao Y (2017) Emerging droplet microfluidics. *Chem Rev* 117 (12):7964–8040
2. Dittrich PS, Manz A (2006) Lab-on-a-chip: microfluidics in drug discovery. *Nat Rev Drug Discov* 5(3):210–218
3. Demello AJ (2006) Control and detection of chemical reactions in microfluidic systems. *Nature* 442(7101):394–402

4. Janasek D, Franzke J, Manz A (2006) Scaling and the design of miniaturized chemical-analysis systems. *Nature* 442(7101):374–380
5. Craighead H (2010) Nanoscience and technology: a collection of reviews from nature journals. World Scientific, Singapore, pp 330–336
6. El-Ali J, Sorger PK, Jensen KF (2006) Cells on chips. *Nature* 442(7101):403–411
7. Shih SC, Mufti NS, Chamberlain MD, Kim J, Wheeler AR (2014) A droplet-based screen for wavelength-dependent lipid production in algae. *Energy Environ Sci* 7(7):2366–2375
8. Li M, Gou H, Al-Ogaidi I, Wu N (2013) Nanostructured sensors for detection of heavy metals: a review. ACS Publications, Washington
9. Kudr J, Zitka O, Klimanek M, Vrba R, Adam V (2017) Microfluidic electrochemical devices for pollution analysis—a review. *Sensors Actuators B Chem* 246:578–590
10. Yogarajah N, Tsai SS (2015) Detection of trace arsenic in drinking water: challenges and opportunities for microfluidics. *Environ Sci Water Res Technol* 1(4):426–447
11. Chen K, Lu G, Chang J, Mao S, Yu K, Cui S, Chen J (2012) Hg (II) ion detection using thermally reduced graphene oxide decorated with functionalized gold nanoparticles. *Anal Chem* 84(9):4057–4062
12. Gao S, Koshizaki N, Koyama E, Tokuhisa H, Sasaki T, Kim J-K, Cho Y, Kim D-S, Shimizu Y (2009) Innovative platform for transmission localized surface plasmon transducers and its application in detecting heavy metal Pd (II). *Anal Chem* 81(18):7703–7712
13. Jang A, Zou Z, Lee KK, Ahn CH, Bishop PL (2010) Potentiometric and voltammetric polymer lab chip sensors for determination of nitrate, pH and Cd (II) in water. *Talanta* 83(1):1–8
14. Zou Z, Jang A, MacKnight E, Wu P-M, Do J, Bishop PL, Ahn CH (2008) Environmentally friendly disposable sensors with microfabricated on-chip planar bismuth electrode for in situ heavy metal ions measurement. *Sensors Actuators B Chem* 134(1):18–24
15. Devadhasan JP, Kim J (2018) A chemically functionalized paper-based microfluidic platform for multiplex heavy metal detection. *Sensors Actuators B Chem* 273:18–24
16. Forzani ES, Zhang H, Chen W, Tao N (2005) Detection of heavy metal ions in drinking water using a high-resolution differential surface plasmon resonance sensor. *Environ Sci Technol* 39(5):1257–1262
17. Li S, Zhang C, Wang S, Liu Q, Feng H, Ma X, Guo J (2018) Electrochemical microfluidics techniques for heavy metal ion detection. *Analyst* 143(18):4230–4246
18. Sudibya HG, He Q, Zhang H, Chen P (2011) Electrical detection of metal ions using field-effect transistors based on micropatterned reduced graphene oxide films. *ACS Nano* 5(3):1990–1994
19. Wang G, Lim C, Chen L, Chon H, Choo J, Hong J, DeMello AJ (2009) Surface-enhanced Raman scattering in nanoliter droplets: towards high-sensitivity detection of mercury (II) ions. *Anal Bioanal Chem* 394(7):1827–1832
20. Jung W, Jang A, Bishop PL, Ahn CH (2011) A polymer lab chip sensor with microfabricated planar silver electrode for continuous and on-site heavy metal measurement. *Sensors Actuators B Chem* 155(1):145–153
21. Buffi N, Merulla D, Beutier J, Barbaud F, Beggah S, van Lintel H, Renaud P, van der Meer JR (2011) Development of a microfluidics biosensor for agarose-bead immobilized *Escherichia coli* bioreporter cells for arsenite detection in aqueous samples. *Lab Chip* 11(14):2369–2377
22. Lin Y, Gritsenko D, Feng S, Teh YC, Lu X, Xu J (2016) Detection of heavy metal by paper-based microfluidics. *Biosens Bioelectron* 83:256–266
23. Feng L, Li X, Li H, Yang W, Chen L, Guan Y (2013) Enhancement of sensitivity of paper-based sensor array for the identification of heavy-metal ions. *Anal Chim Acta* 780:74–80
24. Scampicchio M, Wang J, Mannino S, Chatrathi MP (2004) Microchip capillary electrophoresis with amperometric detection for rapid separation and detection of phenolic acids. *J Chromatogr A* 1049(1–2):189–194
25. Mayorga-Martinez CC, Cadevall M, Guix M, Ros J, Merkoçi A (2013) Bismuth nanoparticles for phenolic compounds biosensing application. *Biosens Bioelectron* 40(1):57–62

26. Sekretaryova AN, Volkov AV, Zozoulenko IV, Turner AP, Vagin MY, Eriksson M (2016) Total phenol analysis of weakly supported water using a laccase-based microband biosensor. *Anal Chim Acta* 907:45–53
27. Song Y, Chen J, Sun M, Gong C, Shen Y, Song Y, Wang L (2016) A simple electrochemical biosensor based on AuNPs/MPS/Au electrode sensing layer for monitoring carbamate pesticides in real samples. *J Hazard Mater* 304:103–109
28. Castañeda R, Vilela D, González MC, Mendoza S, Escarpa A (2013) SU-8/P yrex microchip electrophoresis with integrated electrochemical detection for class-selective electrochemical index determination of phenolic compounds in complex samples. *Electrophoresis* 34 (14):2129–2135
29. Ding Y, Ayon A, García CD (2007) Electrochemical detection of phenolic compounds using cylindrical carbon-ink electrodes and microchip capillary electrophoresis. *Anal Chim Acta* 584(2):244–251
30. Luan E, Zheng Z, Li X, Gu H, Liu S (2016) Inkjet-assisted layer-by-layer printing of quantum dot/enzyme microarrays for highly sensitive detection of organophosphorous pesticides. *Anal Chim Acta* 916:77–83
31. Kim D, Goldberg IB, Judy JW (2009) Microfabricated electrochemical nitrate sensor using double-potential-step chronocoulometry. *Sensors Actuators B Chem* 135(2):618–624
32. Aravamudhan S, Bhansali S (2008) Development of micro-fluidic nitrate-selective sensor based on doped-polypyrrole nanowires. *Sensors Actuators B Chem* 132(2):623–630
33. Nightingale AM, Hassan S-U, Warren BM, Makris K, Evans GW, Papadopoulou E, Coleman S, Niu X (2019) A droplet microfluidic-based sensor for simultaneous in situ monitoring of nitrate and nitrite in natural waters. *Environ Sci Technol* 53(16):9677–9685
34. Fornells E, Murray E, Waheed S, Morrin A, Diamond D, Paull B, Bredmore M (2020) Integrated 3D printed heaters for microfluidic applications: ammonium analysis within environmental water. *Anal Chim Acta* 1098:94–101
35. Gallardo-Gonzalez J, Baraket A, Boudjaoui S, Metzner T, Hauser F, Rößler T, Krause S, Zine N, Strelkas A, Alcácer A (2019) A fully integrated passive microfluidic lab-on-a-chip for real-time electrochemical detection of ammonium: sewage applications. *Sci Total Environ* 653:1223–1230
36. Fernández-Gavela A, Herranz S, Chocarro B, Falke F, Schreuder E, Leeuwis H, Heideman RG, Lechuga LM (2019) Full integration of photonic nanoimmunosenors in portable platforms for on-line monitoring of ocean pollutants. *Sensors Actuators B Chem* 297:126758
37. Geißler F, Achterberg EP, Beaton AD, Hopwood MJ, Clarke JS, Mutzberg A, Mowlem MC, Connelly DP (2017) Evaluation of a ferrozine based autonomous in situ lab-on-chip analyzer for dissolved iron species in coastal waters. *Front Mar Sci* 4:322
38. Grand MM, Clinton-Bailey GS, Beaton AD, Schaap AM, Johengen TH, Tamburri MN, Connelly DP, Mowlem MC, Achterberg EP (2017) A lab-on-chip phosphate analyzer for long-term in situ monitoring at fixed observatories: optimization and performance evaluation in estuarine and oligotrophic coastal waters. *Front Mar Sci* 4:255
39. Han S, Zhang Q, Zhang X, Liu X, Lu L, Wei J, Li Y, Wang Y, Zheng G (2019) A digital microfluidic diluter-based microalgal motion biosensor for marine pollution monitoring. *Biosens Bioelectron* 143:111597
40. Ke S, Liu Q, Deng M, Zhang X, Yao Y, Shan M, Yang X, Sui G (2018) Cytotoxicity analysis of indoor air pollution from biomass combustion in human keratinocytes on a multilayered dynamic cell culture platform. *Chemosphere* 208:1008–1017
41. Sun H, Jia Y, Dong H, Fan L (2019) Graphene oxide nanosheets coupled with paper microfluidics for enhanced on-site airborne trace metal detection. *Microsyst Nanoeng* 5 (1):1–12
42. Liu Q, Zhang X, Li X, Liu S, Sui G (2018) A semi-quantitative method for point-of-care assessments of specific pathogenic bioaerosols using a portable microfluidics-based device. *J Aerosol Sci* 115:173–180

43. Moon H-S, Nam Y-W, Park JC, Jung H-I (2009) Dielectrophoretic separation of airborne microbes and dust particles using a microfluidic channel for real-time bioaerosol monitoring. *Environ Sci Technol* 43(15):5857–5863
44. Shen F, Tan M, Wang Z, Yao M, Xu Z, Wu Y, Wang J, Guo X, Zhu T (2011) Integrating silicon nanowire field effect transistor, microfluidics and air sampling techniques for real-time monitoring biological aerosols. *Environ Sci Technol* 45(17):7473–7480
45. Burg TP, Godin M, Knudsen SM, Shen W, Carlson G, Foster JS, Babcock K, Manalis SR (2007) Weighing of biomolecules, single cells and single nanoparticles in fluid. *Nature* 446(7139):1066–1069
46. Ndieyira JW, Watari M, Barrera AD, Zhou D, Vögltli M, Batchelor M, Cooper MA, Strunz T, Horton MA, Abell C (2008) Nanomechanical detection of antibiotic–mucopeptide binding in a model for superbug drug resistance. *Nat Nanotechnol* 3(11):691
47. Premasiri W, Moir D, Klemmner M, Krieger N, Jones G, Ziegler L (2005) Characterization of the surface enhanced Raman scattering (SERS) of bacteria. *J Phys Chem B* 109(1):312–320
48. Pandya HJ, Kanakasabapathy MK, Verma S, Chug MK, Memic A, Gadjeva M, Shafiee H (2017) Label-free electrical sensing of bacteria in eye wash samples: a step towards point-of-care detection of pathogens in patients with infectious keratitis. *Biosens Bioelectron* 91:32–39
49. Ahmad F, Hashsham SA (2012) Miniaturized nucleic acid amplification systems for rapid and point-of-care diagnostics: a review. *Anal Chim Acta* 733:1–15
50. Azizi M, Zaferani M, Cheong SH, Abbaspourrad A (2019) Pathogenic bacteria detection using RNA-based loop-mediated isothermal-amplification-assisted nucleic acid amplification via droplet microfluidics. *ACS Sens* 4(4):841–848
51. Leung K, Zahn H, Leaver T, Konwar KM, Hanson NW, Pagé AP, Lo C-C, Chain PS, Hallam SJ, Hansen CL (2012) A programmable droplet-based microfluidic device applied to multiparameter analysis of single microbes and microbial communities. *Proc Natl Acad Sci* 109(20):7665–7670
52. Lin X, Huang X, Zhu Y, Urmann K, Xie X, Hoffmann MR (2018) Asymmetric membrane for digital detection of single bacteria in milliliters of complex water samples. *ACS Nano* 12(10):10281–10290
53. Ottesen EA, Hong JW, Quake SR, Leadbetter JR (2006) Microfluidic digital PCR enables multigenic analysis of individual environmental bacteria. *Science* 314(5804):1464–1467
54. Tsougeni K, Kastania A, Kaprou G, Eck M, Jobst G, Petrou P, Kakabakos S, Mastellos D, Gogolides E, Tserepi A (2019) A modular integrated lab-on-a-chip platform for fast and highly efficient sample preparation for foodborne pathogen screening. *Sensors Actuators B Chem* 288:171–179
55. Xie X, Wang S, Jiang SC, Bahnemann J, Hoffmann MR (2016) Sunlight-activated propidium monoazide pretreatment for differentiation of viable and dead bacteria by quantitative real-time polymerase chain reaction. *Environ Sci Technol Lett* 3(2):57–61
56. Zhu Y, Huang X, Xie X, Bahnemann J, Lin X, Wu X, Wang S, Hoffmann MR (2018) Propidium monoazide pretreatment on a 3D-printed microfluidic device for efficient PCR determination of ‘live versus dead’ microbial cells. *Environ Sci Water Res Technol* 4(7):956–963
57. Bao L, Deng L, Nie L, Yao S, Wei W (1996) Determination of microorganisms with a quartz crystal microbalance sensor. *Anal Chim Acta* 319(1–2):97–101
58. Lay C, Teo CY, Zhu L, Peh XL, Ji HM, Chew B-R, Murthy R, Feng HH, Liu W-T (2008) Enhanced microfiltration devices configured with hydrodynamic trapping and a rain drop bypass filtering architecture for microbial cells detection. *Lab Chip* 8(5):830–833
59. Urmann K, Arshavsky-Graham S, Walter J-G, Scheper T, Segal E (2016) Whole-cell detection of live *Lactobacillus acidophilus* on aptamer-decorated porous silicon biosensors. *Analyst* 141(18):5432–5440
60. Wang C-H, Wu J-J, Lee G-B (2019) Screening of highly-specific aptamers and their applications in paper-based microfluidic chips for rapid diagnosis of multiple bacteria. *Sensors Actuators B Chem* 284:395–402

61. Yamaguchi N, Torii M, Uebayashi Y, Nasu M (2011) Rapid, semiautomated quantification of bacterial cells in freshwater by using a microfluidic device for on-chip staining and counting. *Appl Environ Microbiol* 77(4):1536–1539
62. Mandal HS, Su Z, Ward A, Tang XS (2012) Carbon nanotube thin film biosensors for sensitive and reproducible whole virus detection. *Theranostics* 2(3):251
63. Piekarz I, Górka S, Odrobina S, Drab M, Wincza K, Gamian A, Gruszczynski S (2020) A microwave matrix sensor for multipoint label-free *Escherichia coli* detection. *Biosens Bioelectron* 147:111784
64. Bridle H, Miller B, Desmulliez MP (2014) Application of microfluidics in waterborne pathogen monitoring: a review. *Water Res* 55:256–271
65. Nasserri B, Soleimani N, Rabiee N, Kalbasi A, Karimi M, Hamblin MR (2018) Point-of-care microfluidic devices for pathogen detection. *Biosens Bioelectron* 117:112–128
66. Ymeti A, Greve J, Lambeck PV, Wink T, van Hövell SW, Beumer TA, Wijn RR, Heideman RG, Subramaniam V, Kanger JS (2007) Fast, ultrasensitive virus detection using a young interferometer sensor. *Nano Lett* 7(2):394–397
67. Ymeti A, Kanger JS, Greve J, Lambeck PV, Wijn R, Heideman RG (2003) Realization of a multichannel integrated Young interferometer chemical sensor. *Appl Opt* 42(28):5649–5660
68. Mannoor MS, Zhang S, Link AJ, McAlpine MC (2010) Electrical detection of pathogenic bacteria via immobilized antimicrobial peptides. *Proc Natl Acad Sci* 107(45):19207–19212
69. Bridle H, Kersaudy-Kerhoas M, Miller B, Gavriilidou D, Katzer F, Innes EA, Desmulliez MP (2012) Detection of *Cryptosporidium* in miniaturised fluidic devices. *Water Res* 46(6):1641–1661
70. Logan BE, Rabaey K (2012) Conversion of wastes into bioelectricity and chemicals by using microbial electrochemical technologies. *Science* 337(6095):686–690
71. Xie X, Criddle C, Cui Y (2015) Design and fabrication of bioelectrodes for microbial bioelectrochemical systems. *Energy Environ Sci* 8(12):3418–3441
72. Lovley DR (2012) Electromicrobiology. *Annu Rev Microbiol* 66:391–409
73. Jiang X, Hu J, Fitzgerald LA, Biffinger JC, Xie P, Ringeisen BR, Lieber CM (2010) Probing electron transfer mechanisms in *Shewanella oneidensis* MR-1 using a nanoelectrode platform and single-cell imaging. *Proc Natl Acad Sci* 107(39):16806–16810
74. Jiang X, Hu J, Petersen ER, Fitzgerald LA, Jackan CS, Lieber AM, Ringeisen BR, Lieber CM, Biffinger JC (2013) Probing single-to multi-cell level charge transport in *Geobacter sulfurreducens* DL-1. *Nat Commun* 4(1):1–6
75. Ding M, Shiu H-Y, Li S-L, Lee CK, Wang G, Wu H, Weiss NO, Young TD, Weiss PS, Wong GC (2016) Nanoelectronic investigation reveals the electrochemical basis of electrical conductivity in *shewanella* and *geobacter*. *ACS Nano* 10(11):9919–9926
76. Hsu L, Deng P, Zhang Y, Jiang X (2018) Core/shell bacterial cables: a one-dimensional platform for probing microbial electron transfer. *Nano Lett* 18(7):4606–4610
77. Drescher K, Shen Y, Bassler BL, Stone HA (2013) Biofilm streamers cause catastrophic disruption of flow with consequences for environmental and medical systems. *Proc Natl Acad Sci* 110(11):4345–4350
78. Flickinger ST, Copeland MF, Downes EM, Braasch AT, Tuson HH, Eun Y-J, Weibel DB (2011) Quorum sensing between *Pseudomonas aeruginosa* biofilms accelerates cell growth. *J Am Chem Soc* 133(15):5966–5975
79. Connell JL, Ritschdorff ET, Whiteley M, Shear JB (2013) 3D printing of microscopic bacterial communities. *Proc Natl Acad Sci* 110(46):18380–18385
80. Li B, Qiu Y, Zhang J, Huang X, Shi H, Yin H (2018) Real-time study of rapid spread of antibiotic resistance plasmid in biofilm using microfluidics. *Environ Sci Technol* 52(19):11132–11141
81. Burmeister A, Hilgers F, Langner A, Westerwalbesloh C, Kerkhoff Y, Tenhaef N, Drepper T, Kohlheyer D, von Lieres E, Noack S (2019) A microfluidic co-cultivation platform to investigate microbial interactions at defined microenvironments. *Lab Chip* 19(1):98–110

82. Li B, Qiu Y, Song Y, Lin H, Yin H (2019) Dissecting horizontal and vertical gene transfer of antibiotic resistance plasmid in bacterial community using microfluidics. *Environ Int* 131:105007
83. Sun H, Chan C-W, Wang Y, Yao X, Mu X, Lu X, Zhou J, Cai Z, Ren K (2019) Reliable and reusable whole polypropylene plastic microfluidic devices for a rapid, low-cost antimicrobial susceptibility test. *Lab Chip* 19(17):2915–2924
84. Lopatkin AJ, Huang S, Smith RP, Srimani JK, Syssoeva TA, Bewick S, Karig DK, You L (2016) Antibiotics as a selective driver for conjugation dynamics. *Nat Microbiol* 1(6):1–8
85. Liu Z, Banaei N, Ren K (2017) Microfluidics for combating antimicrobial resistance. *Trends Biotechnol* 35(12):1129–1139
86. Huo Z-Y, Liu H, Wang W-L, Wang Y-H, Wu Y-H, Xie X, Hu H-Y (2019) Low-voltage alternating current powered polydopamine-protected copper phosphide nanowire for electroporation-disinfection in water. *J Mater Chem A* 7(13):7347–7354
87. Huo Z-Y, Zhou J-F, Wu Y, Wu Y-H, Liu H, Liu N, Hu H-Y, Xie X (2018) A Cu 3 P nanowire enabling high-efficiency, reliable, and energy-efficient low-voltage electroporation-inactivation of pathogens in water. *J Mater Chem A* 6(39):18813–18820
88. Zhou J, Wang T, Chen W, Lin B, Xie X (2020) Emerging investigator series: locally enhanced electric field treatment (LEEFT) with nanowire-modified electrodes for water disinfection in pipes. *Environ Sci Nano* 7:397–403
89. Zhou J, Wang T, Xie X (2019) Rationally designed tubular coaxial-electrode copper ionization cells (CECICs) harnessing non-uniform electric field for efficient water disinfection. *Environ Int* 128:30–36
90. Gusbeth C, Frey W, Volkmann H, Schwartz T, Bluhm H (2009) Pulsed electric field treatment for bacteria reduction and its impact on hospital wastewater. *Chemosphere* 75(2):228–233
91. Sengel JT, Wallace MI (2016) Imaging the dynamics of individual electropores. *Proc Natl Acad Sci* 113(19):5281–5286
92. Wang T, Chen H, Yu C, Xie X (2019) Rapid determination of the electroporation threshold for bacteria inactivation using a lab-on-a-chip platform. *Environ Int* 132:105040
93. Dong H, Zheng L, Duan X, Zhao W, Chen J, Liu S, Sui G (2019) Cytotoxicity analysis of ambient fine particle in BEAS-2B cells on an air-liquid interface (ALI) microfluidics system. *Sci Total Environ* 677:108–119
94. Mitzel MR, Lin N, Whalen JK, Tufenkji N (2017) *Chlamydomonas reinhardtii* displays aversive swimming response to silver nanoparticles. *Environ Sci Nano* 4(6):1328–1338
95. Englert DL, Manson MD, Jayaraman A (2010) Investigation of bacterial chemotaxis in flow-based microfluidic devices. *Nat Protoc* 5(5):864
96. Kim M, Lim JW, Kim HJ, Lee SK, Lee SJ, Kim T (2015) Chemostat-like microfluidic platform for highly sensitive detection of heavy metal ions using microbial biosensors. *Biosens Bioelectron* 65:257–264
97. Sun P, Liu Y, Sha J, Zhang Z, Tu Q, Chen P, Wang J (2011) High-throughput microfluidic system for long-term bacterial colony monitoring and antibiotic testing in zero-flow environments. *Biosens Bioelectron* 26(5):1993–1999
98. Lockery SR, Hulme SE, Roberts WM, Robinson KJ, Laromaine A, Lindsay TH, Whitesides GM, Weeks JC (2012) A microfluidic device for whole-animal drug screening using electrophysiological measures in the nematode *C. elegans*. *Lab Chip* 12(12):2211–2220
99. Cartlidge R, Nugegoda D, Wlodkowic D (2017) Millifluidic lab-on-a-chip technology for automated toxicity tests using the marine amphipod *Allorchestes compressa*. *Sensors Actuators B Chem* 239:660–670
100. Huang Y, Persoone G, Nugegoda D, Wlodkowic D (2016) Enabling sub-lethal behavioral ecotoxicity biotests using microfluidic lab-on-a-chip technology. *Sensors Actuators B Chem* 226:289–298
101. Zhu F, Wigh A, Friedrich T, Devaux A, Bony S, Nugegoda D, Kaslin J, Wlodkowic D (2015) Automated lab-on-a-chip technology for fish embryo toxicity tests performed under continuous microperfusion (μ FET). *Environ Sci Technol* 49(24):14570–14578

102. Campana O, Wlodkovic D (2018) Ecotoxicology goes on a chip: embracing miniaturized bioanalysis in aquatic risk assessment. *Environ Sci Technol* 52(3):932–946
103. BioNanoConsulting (2020) Bio nano consulting product development page. <http://www.bio-nano-consulting.com/product-developmentdrinksafe>
104. PalmSens (2020) PalmSens ItalSensI S-C page. <https://www.palmsens.com/product/italsens-is-c/>
105. EarlyWarning (2009) Early warning biohazard water analyzer. <https://www.earlywarninginc.com/products.php>
106. IBM (2017) IBM 5 in 5: smart sensors will detect environmental pollution at the speed of light. <https://www.research.ibm.com/5-in-5/environmental-pollutants/>
107. Gigault J, Balaesque M, Tabuteau H (2018) Estuary-on-a-chip: unexpected results for the fate and transport of nanoparticles. *Environ Sci Nano* 5(5):1231–1236
108. Seyedpour S, Janmaleki M, Henning C, Sanati-Nezhad A, Ricken T (2019) Contaminant transport in soil: a comparison of the theory of porous media approach with the microfluidic visualisation. *Sci Total Environ* 686:1272–1281

Microfluidic Systems for Antimicrobial Susceptibility Testing



Ann-Kathrin Klein and Andreas Dietzel

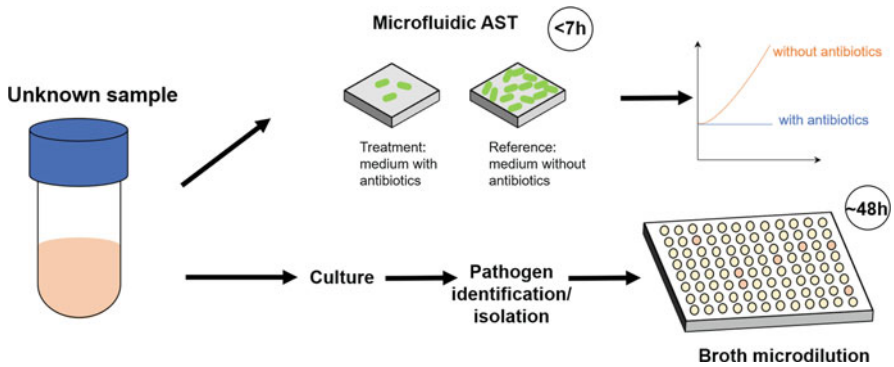
Contents

1	Introduction	292
2	Antimicrobial Susceptibility Testing (AST)	293
3	Microfluidic AST	294
3.1	Optical Detection	295
3.2	Electrical Detection	300
3.3	Biochemical Detection	301
3.4	Mechanical Detection	302
4	Conclusion	304
	References	305

Abstract Human health is threatened by the spread of antimicrobial resistance and resulting infections. One reason for the resistance spread is the treatment with inappropriate and ineffective antibiotics because standard antimicrobial susceptibility testing methods are time-consuming and laborious. To reduce the antimicrobial susceptibility detection time, minimize treatments with empirical broad-spectrum antibiotics, and thereby combat the further spread of antimicrobial resistance, faster and point-of-care methods are needed. This requires many different research approaches. Microfluidic systems for antimicrobial susceptibility testing offer the possibility to reduce the detection time, as small sample and reagent volumes can be used and the detection of single cells is possible. In some cases, the aim is to use human samples without pretreatment or pre-cultivation. This chapter first provides an overview of conventional detection methods. It then presents the potential of and various current approaches in microfluidics. The focus is on microfluidic methods for phenotypic antimicrobial susceptibility testing.

A.-K. Klein and A. Dietzel (✉)
Institute of Microtechnology Technische Universität Braunschweig, Braunschweig, Germany
e-mail: a.dietzel@tu-braunschweig.de

Graphical Abstract



Keywords Antibiotic resistance test, Antibiotic susceptibility tests (AST), Antimicrobial resistance, Microfluidics, Point-of-care systems

1 Introduction

According to the WHO, the spread of antimicrobial-resistant (AMR) infections is a leading global threat to human health. Today, about 700,000 people worldwide die annually from infections with multi-resistant pathogens [1]. Current forecasts predict ten million deaths worldwide in 2050 if the current situation is not changed [1]. This number would exceed the number of cancer-related deaths. The spread of AMR threatens the ability of modern medicine to use well-established procedures such as complex surgery, organ transplants, or chemotherapy in its fight against disease [2]. As an example for the spread of AMR, Fig. 1 shows the increase in antibiotic resistance of the most common sepsis-causing bacteria in Europe in the past few years.

One reason for the emergence of multi-resistant bacteria strains is the unnecessary use of antibiotics, as it is a common practice in animal fattening [4]. The increase in



Fig. 1 Escherichia coli resistant to third-generation cephalosporins across Europe in (a) 2009 and (b) 2019 (adapted from [3])

AMR can also be attributed to the long detection times and the resultant early non-specific therapy typical in the treatment of humans infected with such pathogens. Conventional detection methods require about 48–72 h after sample collection until antibiotic resistance is confirmed [5, 6]. However, the mortality risk of infected people increases the longer the patients do not receive appropriate therapy (7% per hour) [5]. For this reason, empirical broad-spectrum antibiotic treatments are already used in cases of suspected infection with AMR pathogens, especially in sepsis [7–9]. In such cases, this problem is exacerbated by the use of reserve antibiotics in treatment, although they may not be strictly necessary or may not have the desired effects. As a consequence, these reserve antibiotics may also lose their effectiveness.

Thus, the challenge is to extend access to antibiotics while at the same time limiting inappropriate use, in particular of broad-spectrum antibiotics and reserve antibiotics [10]. Rapid antibiotic susceptibility tests (AST) can be essential for the correct and economically efficient use of antibiotics. Besides preventing AMR development by adequate drug prescription, rapid resistance diagnostics can help to initiate appropriate antibiotic treatment promptly. Thus, rapid AST improves therapy outcomes and saves lives [11].

2 Antimicrobial Susceptibility Testing (AST)

The methods currently available for AST can be divided into genotypic and phenotypic methods [4]. Figure 2 shows an overview of phenotypic and genotypic AST methods and their assay times. Genotypic methods examine the genetic nature of the bacteria. However, one limitation of these methods is that they cannot detect unknown resistance genes [12]. For known genotypes associated with antibiotic resistance, the result is available after about 90 min. Since only known mechanisms of resistance can be proven, this may lead to false-negative results and thus to the wrong medication for the patient. When testing uncultured blood, false-positive results can be caused by even the slightest contamination of the sample if unrelated DNA is detected [13]. The disadvantages of genotypic tests make phenotypic assays more suitable for AST. These culture-based methods, such as broth microdilution or disk diffusion, are the gold standard AST methods.

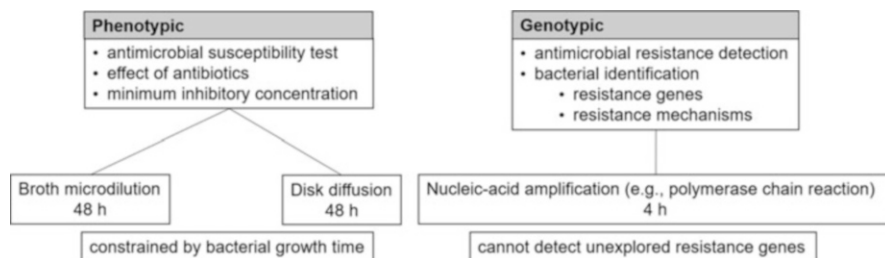


Fig. 2 Overview of phenotypic and genotypic antimicrobial susceptibility testing [13, 18, 19]

Phenotypic methods are used to investigate the growth behavior of bacterial strains in the presence of different antibiotics [4]. This method also allows a direct assessment of whether an antibiotic has stopped bacterial growth. Thus, a decision can be made about the optimal therapeutic measures. For conventional phenotypic AST, the patient sample has to be isolated and then pre-cultured, which takes between 24 and 48 h [14, 15]. In the case of broth microdilution, the growth of the bacterial culture in the presence of various antibiotic concentrations is determined by measuring the optical density (OD) [16]. This phenotypic method can also be used to determine the minimum antibiotic concentration which prevents bacterial growth, otherwise referred to as minimum inhibitory concentration (MIC) [16]. False-positive results of the phenotypic AST may be caused when, for example, bacteria form thread-like structures in the presence of antibiotics without dividing [14]. A further disadvantage of this phenotypic method is the low sensitivity of about 10^7 colony-forming units (CFU) per mL [16]. In addition, phenotypic methods require inoculum sizes of $\sim 5 \times 10^5$ CFU/ml [17]. The associated lead time for cultivation is another disadvantage [14]. The advantage, however, is that resistances can be determined directly and without prior knowledge of the resistance mechanisms.

3 Microfluidic AST

New phenotypic AST based on microfluidics have been developed in recent years to shorten the detection time and increase sensitivity [20]. With microfluidic techniques, the assay time of AST can be reduced to 1–3 h [21].

Microfluidic systems have the advantage of [4, 16, 22]:

- small sample and reagent volumes,
- detection of single cells,
- combining several sample processing steps,
- potentially accelerating biochemical reactions.

Thus, microfluidic systems can achieve high sensitivity and allow for automation and high-throughput analysis [23]. The use of small volumes at the single-cell level can also prevent cross-contamination [16].

As a basis for this novel AST, standard principles used in microfluidics were developed further. Microfluidic channel systems are therefore widely used [24]. Different detection methods are used to measure physiological or biochemical changes during or after bacterial growth [22]. In the following, selected microfluidic AST methods are described and classified according to their detection principles.

3.1 Optical Detection

3.1.1 Single-Cell Imaging

Single-cell imaging describes a group of microscopy techniques that allow imaging and single-cell detection. It is used to study cell dynamics and usually based on fluorescent molecules. In the case of AST, single-cell imaging is used to monitor bacterial growth with different antibiotic treatments. For this purpose, the bacterial cells are immobilized in various microfluidic systems. [21, 25, 26].

Balteskin et al. use the mother-machine design, a multichannel system widely used in microfluidics to test for urinary tract infections (shown in Fig. 3a). The microfluidic chip is made of a PDMS base structured by soft lithography with microchannels and closed with a cover glass bonded to the PDMS [21]. The system consists of a feeding channel through which the bacteria are first loaded, and which then ensures the culture medium supply. Several parallel growth channels branch off from this feeding channel. During loading, bacteria enter the growth channels. These so-called mother cells are where the subsequent bacterial growth originates. A sample with a low bacteria content of 10^4 CFU/ml can be used for loading (shown in Fig. 3b) [21]. The culture medium supply is achieved via a 300 nm gap [21]. The growth in each microchannel is detected separately by taking phase-contrast images using a microscope [21]. The average growth rate is calculated across all channels. Antimicrobial resistance can be detected by determining the growth rate after treatment with different antibiotics. With this system, the detection time of bacterial growth including loading can be reduced to 30 min [21].

A similar system was developed by Li et al. [27], which also permits the sorting of bacteria of different sizes from polymicrobial clinical samples by applying different pressures and incubating them separately. Lu et al. also use a microchannel system to immobilize the bacteria. It consists of 68 parallel channels with one inlet and one outlet. By integrating two microelectrodes in the PDMS system, the bacteria can be positioned in the microchannels. A sample with a bacterial content of 10^5 CFU/ml can be used for loading [28].

Choi et al. use a microfluidic agarose channel system for immobilization and bacterial cell incubation. The microfluidic chip consists of a centered inlet for cell loading and six channels running outwards in a star arrangement for bacterial incubation. The microfluidic chip is composed of a PDMS base structured by soft lithography with microchannels and closed with a cover PDMS coated by bonding. When loaded through the inlet, an agarose-bacteria solution is distributed evenly over all six channels and cures there [24]. At the six side-branched channels, different antibiotics or antibiotic concentrations can be added to the culture medium. By monitoring the individual bacterial growth and calculating the area occupied by bacteria in a microfluidic channel, antimicrobial susceptibility can be determined [24]. An automatic analysis can be performed using image-based single-cell morphological analysis (SCMA). Here, morphological changes in individual bacterial cells are automatically analyzed and categorized under different antimicrobial conditions [29]. Thus, antimicrobial sensitivity can be determined by SCMA in less than 4 h [29].

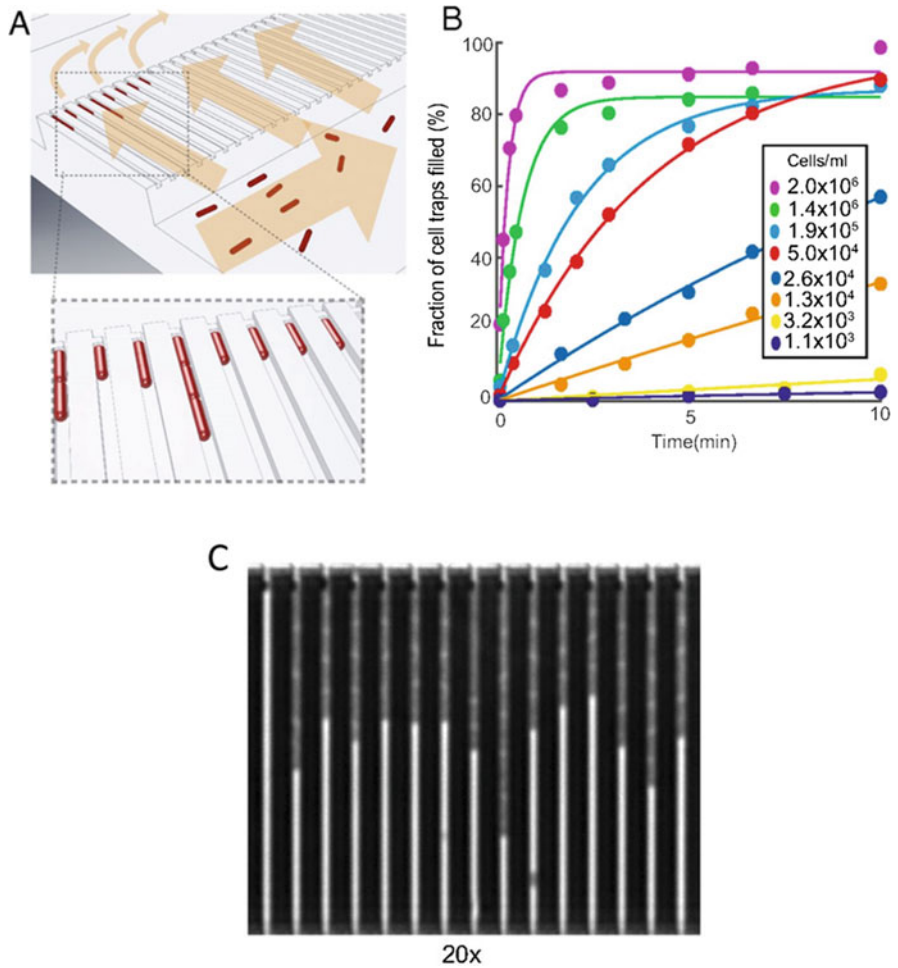


Fig. 3 Microchannel system for immobilization (a) Schematic illustration of the channel system (red: captured cells); (b) Bacterial loading of different density cell cultures at different points in time; (c) Phase contrast image of *E.coli* (lighter regions) in the system using a 20× objective (adapted with permission from [21])

3.1.2 Time-Lapse Microscopy

Using a combination of a liquid bacterial culture and agarose, alternative microfluidic approaches can achieve an assay time between 2.5 and 4 h [30–32]. Here, bacterial density is determined by grayscale intensity changes in the images (from black to white) resulting from bacterial growth [30].

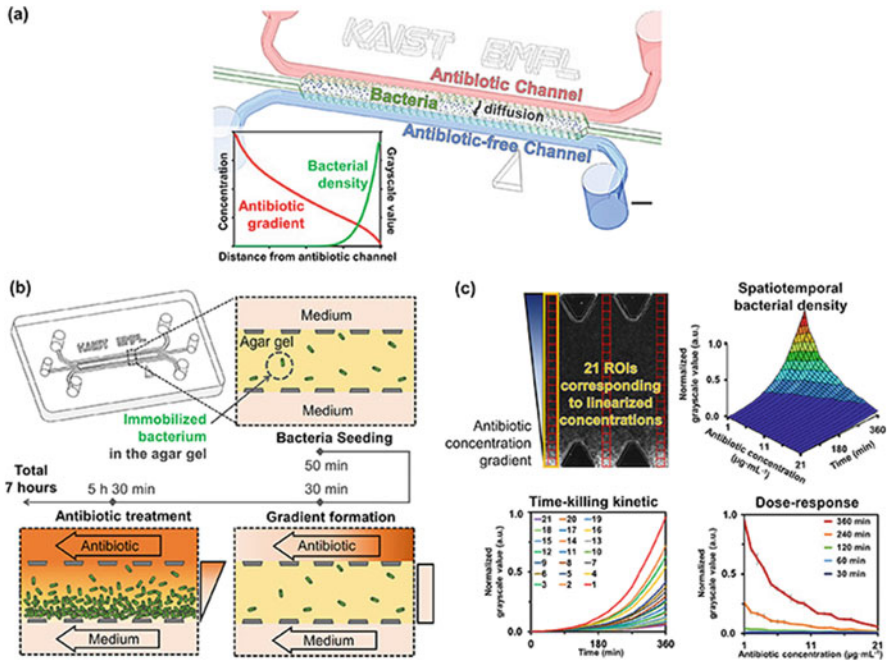


Fig. 4 Microchannel system with agarose-bacteria solution: (a) Schematic illustration of antibiotic treatment using diffusion process; (b) Experimental process using the microfluidic chip: (1) Agarose-bacteria solution is introduced. (2) The antibiotic concentration gradient is formed (30 min). (3) Changes in local bacteria growth are observed; (c) Analyzing gray intensity changes of images along with linearized antibiotic concentrations (reproduced from [32], with permission of AIP Publishing)

Kim et al. use a microfluidic system of two parallel PDMS channels sealed with a cover glass (shown in Fig. 4) [32]. An agarose-bacteria solution is fed in between the two parallel microchannels (see Fig. 4a). The medium flows through one channel and medium, the antibiotic through the other. Due to the different antibiotic concentrations of the two parallel channels, the antibiotic molecules diffuse into the agarose-bacteria solution (shown in Fig. 4b). A concentration gradient forms within 30 min. As a result of treatment under antibiotic gradients, changes in local bacterial growth can be observed [32]. Dose-effect diagrams can be reconstructed from the gray intensity changes in the images (see Fig. 4c). 2×10^8 CFU/ml was used. The changes in local bacterial growth were determined after 6 h.

3.1.3 Interferometry

Other approaches use interferometry to measure bacterial growth [33, 34]. The approach of Busche et al. is shown in Fig. 5a. Here an optofluidic microchip is used, which is fabricated by etching nanochannels into a thin silicon oxide layer and

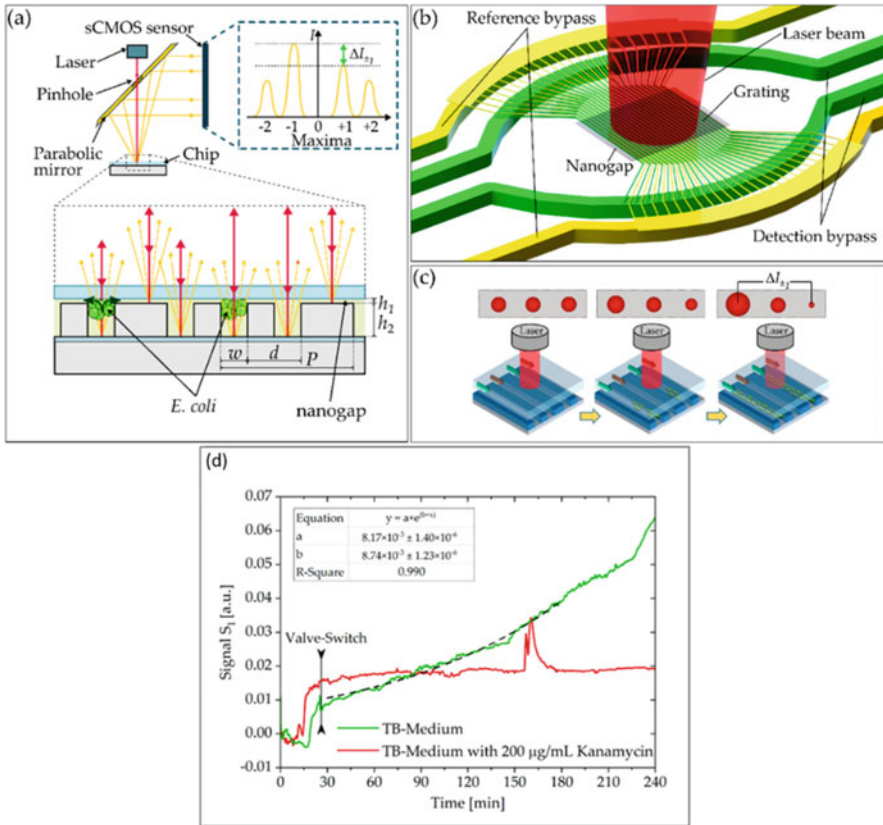


Fig. 5 Optofluidic chip for bacterial growth detection. Schematic illustrations: (a) Detection method; (b) Microchannel system as an optical grating (green: detection channels, yellow: reference channels; red: collimated laser beam); (c) Intensity distribution during bacterial growth; (d) Diffraction signal during bacterial growth with and without antibiotics (adapted from [34])

then closed by anodic bonding of a structured glass. The nanochannels, connected by a nanogap, create an optical grating (shown in Fig. 5b). This combines a nanofluidic bacterial cell trap with an optical asymmetric grating [34]. The channel system consists of detection channels and reference channels, which can be pressurized and supplied with bacteria and a culture medium via bypass channels. The bacteria are first loaded into the detection channels and immobilized at the nanogap by bypass cross-flow [35]. Then culture medium flows through all channels. The refractive index in the detection channels is changed by bacterial growth. Using a collimated laser beam, a change in the intensity distribution can be measured, as shown in Fig. 5c [36]. By treating the bacteria with and without antibiotics, the effect of the antibiotic on bacterial growth can be determined (shown in Fig. 5d).

3.1.4 Fluorescence Imaging

Fluorescence imaging is the visualization of fluorescence dyes or proteins as markers for molecular processes or structures [4]. Using a green fluorescent protein (GFP) requires genetic modification of the bacteria, so this detection method is not suitable for the analysis of clinical samples [38, 39]. GFP is suitable for real-time observation of bacterial growth due to the high correlation between fluorescence intensity and cell density.

Mohan et al. have developed a channel/chamber system made from PDMS that is filled using negative pressure (shown in Fig. 6a) [37]. One antibiotic channel and one bacterial channel lead to a set of eight chambers (2.4 nl each), as shown in Fig. 6b [39]. When all chambers are filled, a mixing valve is used to achieve a homogeneous mixture within the culture chambers (shown in Fig. 6c, d). The bacterial count can be determined by fluorescence imaging [37], which requires the bacteria used to express GFP. This system is suitable as a multiplex microfluidic system since parallel tests can be carried out with high throughput. In the research work presented in this paragraph, a 48-well array was used, in which 12 different antibiotics or antibiotic concentrations can be tested in parallel. This takes less time than a conventional phenotypic test, as there is no need for pre-cultivation [37]. For the

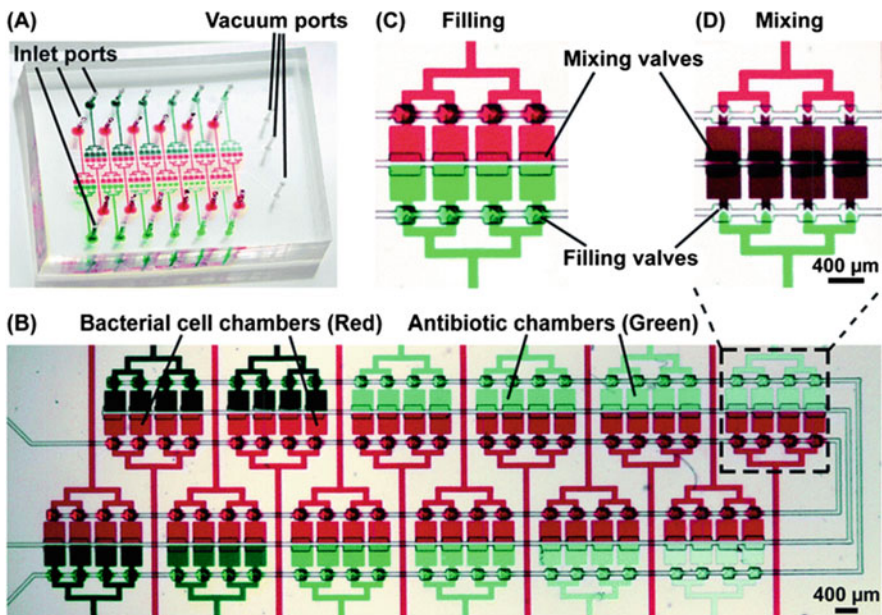


Fig. 6 Multiplex microfluidic AST system with bacteria immobilization in nanoliter arrays: (a) Entire array with inlet ports for bacteria and antibiotics and vacuum ports for filling using negative pressure; (b) Close-up of the 48 wells; each well can be loaded with bacteria concentration (red) or antibiotics (green); (c) Set of eight chambers during filling; (d) Set of eight chambers during mixing (reproduced with permission from [39])

MIC determination of polymicrobial samples, initial cell counts of ~100 to 300 cells were set [39]. Bacterial growth was observed over 16 h. A decision regarding antibiotic susceptibility including the determination of MIC could be made after 2–4 h [39].

In droplet microfluidics, discrete microdroplets (volumes from pL to mL) are generated and analyzed in an immiscible phase [40]. Each microdroplet is separated by a liquid–liquid interface, usually stabilized by amphiphilic surfactants.

In AST, the droplets serve as incubators for the encapsulated bacterial cells, allowing both antibiotics and viability dyes to be added. The fluorescent dye resazurin is used to demonstrate the viability of the bacteria treated with antibiotics [41–43]. It is a metabolism marker. Resazurin reacts irreversibly to resofurin, which has strong fluorescent properties, through the cellular reaction potential [42]. This reaction occurs at a rate that is proportionate to the aerobic respiration of the cells in a bacterial culture [42].

Derzsi et al. have developed a passive-dilution platform generating droplets using five different pipettes. They measured the fluorescence intensity of resofurin after a 4 h droplet incubation. With different concentrations of antibiotics, they were able to determine the MIC [44].

3.1.5 Relative Optical Density

Liu et al. use high-throughput screening of antibiotic-resistant bacteria in picodroplets [45]. The microfluidic system is based on PDMS structured with microchannels using soft lithography [45]. The detection is carried out using a system for light scattering without bacteria labeling [45]. This method is used to study the relative optical density of droplets. It allows distinguishing between droplets with growth and those with inhibited growth/resistance. Bacterial concentrations of 10^5 CFU/ml have been measured. In other approaches, the droplet microfluidics was used to treat bacteria with combinations of antibiotics [40, 47].

Another approach combines optical density measurement with hydrodynamic immobilization in traps [46]. The system consists of cup-shaped structure arrangements that are used as mechanical barriers to capture bacteria flowing in a microchannel. The structure dimensions are designed to trap exactly one bacterial cell. Based on this, the bacterial growth rate under the influence of antibiotics can be determined at a bacterial concentration of 10^7 CFU/ml [46].

3.2 Electrical Detection

3.2.1 Measuring the Electrical Resistance Change

Yang et al. [48] use a microfluidic channel system as reported in [21, 27] to capture and incubate the bacteria in microchannels ($2\ \mu\text{m} \times 2\ \mu\text{m}$ with a gap of 800 nm)

[48]. In contrast to the systems mentioned earlier, the detection is completely electrical. As the bacteria grow, the electrical resistance in the channel increases while the electrical current decreases. The change in the bacteria population is proportionate to the electrical resistance. Thus, bacterial growth can be tested directly with antibiotic treatment. With this microfluidic system, small urine samples can be tested without pretreatment [48].

3.2.2 Electrochemical Detection

Besant et al. use a system of 2.5 nl wells in which microbeads with a diameter of 5 μm are immobilized in stacks and thus serve as a bacterial filter [49]. For detection, an electrochemical approach is used. By adding resazurin, a shrinking of a redox-active molecule is reached, which is directly related to the number of metabolically active bacteria. Antibiotic-resistant bacteria reduce resazurin to resorufin, while antibiotic-sensitive bacteria do not reduce it [49]. The two molecular states can be distinguished by measurement using electrodes integrated into the well. A minimum cell concentration of 10^5 CFU/ml can be used [49]. In this phenotypic approach, growth is measured over 100 min in the presence of an antibiotic [49].

3.3 Biochemical Detection

One common marker to measure the metabolic activities of bacteria is the adenosine triphosphate (ATP). Using this marker, the efficient emission photons (550–570 nm; of which the luciferin substrate is catalyzed by luciferase in the presence of ATP) and oxygen is measured [50]. This measurement process requires sensitive microplate readers, able to capture the photons. The detection method using ATP is known as ATP bioluminescence.

Dong et al. have developed a multilayer system consisting of a culture layer with 384 reaction chambers and culture medium veins made of polystyrene; a membrane layer made of fiberglass membrane filter; and a sample layer with sample and air veins made of polystyrene (shown in Fig. 7a). The system is covered by two glass layers. On the reaction chamber side, the fiberglass membrane filter is coated with antibodies for bacteria immobilization. Figure 7b shows the standard process for using this system. The metabolism of a bacterial concentration generates an ATP bioluminescence signal. The antimicrobial effect of an antibiotic can be determined directly from a urine sample after 3–6 h if the bacterial concentration is above 1,000 CFU/ml [51].

Dong et al. also use antibody binding to membranes for label-free optical detection [52]. However, antibodies are not available for all bacteria.

Further biochemical approaches use Raman spectroscopy of biomarkers [53, 54], DNA samples [55–57], or RNA markers [58, 59]. These are genotypic tests.

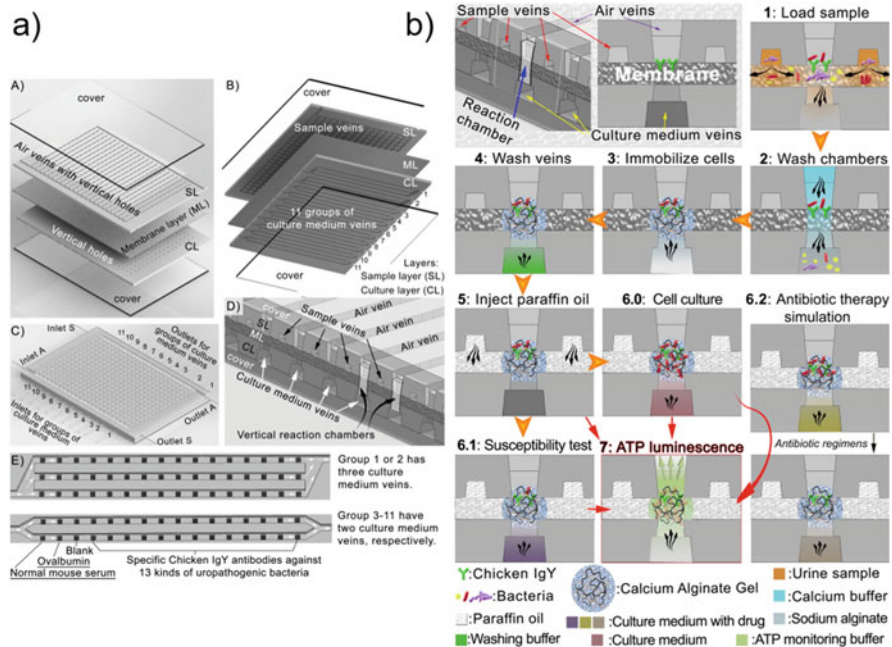


Fig. 7 Microfluidic AST using ATP bioluminescence for detection and antibody binding for bacteria immobilization: **(a)** Multilayer system design; **(b)** Schematic illustration of the standard AST process: (1) the urine sample is loaded into the sample veins, and the bacteria cells are captured by antibodies; (2) unbound bacterial cells are removed; (3) the bound cells are encapsulated by calcium alginate gel; (4) the alginate solution is washed away; (5) paraffin oil is introduced to isolate each reaction chamber; the bound cells (6.0) can then be reproduced, (6.2) inhibited by series of antibiotics, or (6.1) inhibited by a single antibiotic; (7) the cells are quantified using ATP bioluminescence in a microplate reader. (Adapted with permission from [51]. Copyright 2015 American Chemical Society)

3.4 Mechanical Detection

Mechanical detection methods are based, for example, on a mechanical cantilever signal to determine antimicrobial susceptibility. For immobilization, the cantilever surface is functionalized with bacteria-specific receptors such as antibodies. The binding results in either a cantilever deflection or a resonance frequency change [60–62].

Other cantilever-based systems use cantilevers with embedded microchannels, also known as suspended microchannel resonators [62, 63]. Etayash et al. use a bi-material cantilever with a 50-pL volume microchannel, which can provide three signals (adsorbed mass, adsorption stress, and mid-infrared spectroscopy of the adsorbates; shown in Fig. 8a, b, e) [62]. For the immobilization of the bacteria, the microfluidic channel surfaces are functionalized with chemical or physical receptors

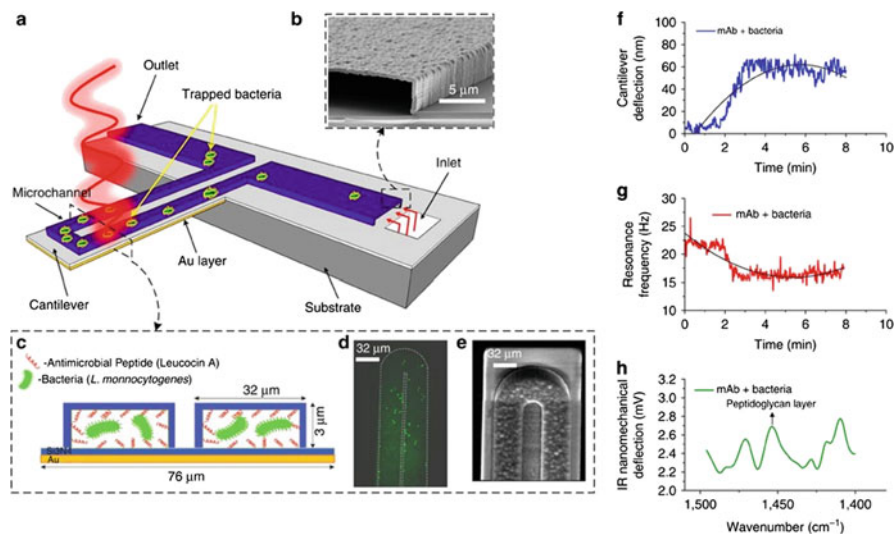


Fig. 8 Bi-material cantilever with embedded microchannel: (a) Schematic illustration of the system. The cantilever is made of silicon nitride coated with gold, which is fixed on a silicon substrate. The microchannel surface is functionalized with specific receptors. Additionally, the cantilever is irradiated with infrared light. (b) Cross-section of the inlet at the bottom of the system using scanning electron microscopy. (c) Cross-section of the cantilever with the embedded microfluidic channel. (d) Fluorescent image of the microchannel with immobilized bacteria. (e) Scanning electron microscopy image of the cantilever tip. (f) Nanomechanical cantilever deflection resulting from infrared absorption of the bacteria. (g) Change in the resonance frequency due to adsorption of bacteria in the microchannel. (h) The wavelength at which the bacteria absorb infrared light depends on the nanomechanical cantilever deflection resulting from irradiation with a certain range of infrared light. (Reprinted with permission from [62])

capturing the bacteria selectively, as shown in Fig. 8c, d. The bacteria accumulation within the microchannel leads to a change in the cantilever resonance frequency and a cantilever deflection (shown in Fig. 8f, g), where the cantilever resonance frequency is caused by the absorbed mass and the cantilever deflection is caused by the adsorption stress. Additional irradiation with infrared light stimulates the captured bacteria and causes deflection proportionate to the infrared absorption of the bacteria. Thus, a nanomechanical infrared spectrum can be generated for selective identification of dead and living bacteria. Bacteria that are treated with antibiotics show a significant nanomechanical reaction [62]. Cell concentrations between 10^2 and 10^5 CFU/ml were tested [62]. In initial experiments, when captured *E. coli* were treated with antibiotics and exposed, a deflection of the cantilever and a shift in resonance frequency were observed after 30 min.

4 Conclusion

This chapter provides a review of different research approaches for microfluidic AST, which are mainly used to detect antibiotic susceptibility based on bacterial cultures (phenotypic). Basic microfluidic concepts were further developed to provide suitable solutions for microfluidic AST. The different microfluidic systems found in the literature can be classified by their detection methods: optical, electrical, biochemical, and mechanical. Table 1 lists the detection and immobilization methods covered in this chapter.

In all microfluidic systems mentioned, the bacterial cells are physically trapped, and their mobility is thus restricted. The nutrients/culture medium required for growth are supplied via channels or by diffusion.

It seems preferable to use systems that allow on-chip cultivation, as it requires no time-consuming pre-cultivation. However, one fundamental difficulty is the cell loading at very low bacterial concentrations, which can impede the accumulation of a sufficient number of bacterial cells. A solution for loading uncultivated and therefore low-concentration samples into a microfluidic system for analysis is an on-chip filtration of the bacteria in small volumes to increase the concentration.

The systems used for optical detection are transparent and often consist of PDMS or PDMS and glass. While PDMS are easy to fabricate and air permeable, they cannot be used to test small MIC values of antibiotics, as small molecules and drugs are absorbed during testing [64–66].

Some detection methods seem complex and expensive, so they are only partially suitable for use as AST. This is particularly the case with some optical detection methods. Another issue arises when using dead-end systems, which tend to clog.

In conclusion, several microfluidic AST have been shown to provide faster results than conventional AST (<7 h) and thus support clinical decisions on the correct use of antibiotics. The analysis of morphology and the number of single cells by minimizing the incubation area significantly improve the resolution. Reducing the analysis size, in turn reducing the number of samples and reagents used, allows the

Table 1 Detection and immobilization methods

Types	Detection methods	Immobilization methods
Optical	Imaging without labeling <ul style="list-style-type: none"> • Single-cell imaging • Time-lapse microscopy • Interferometry Fluorescence imaging <ul style="list-style-type: none"> • Fluorescent viability dyeing • Fluorescence signal by using resazurin 	<ul style="list-style-type: none"> • Microchannel system • Confined microchannels • Agarose gel • Nanoliter arrays • Microdroplets
Electrical	Electrical resistance Electrochemical	<ul style="list-style-type: none"> • Microchannel system • Stacked microbeads
Biochemical	<ul style="list-style-type: none"> • ATP bioluminescence • pH changes • Redox potential 	<ul style="list-style-type: none"> • Antibodies
Mechanical	<ul style="list-style-type: none"> • Cantilever 	<ul style="list-style-type: none"> • Antibodies

integration of several parallel tests on one microfluidic device. Due to their size and the intended ease of use, microfluidic approaches for novel AST can contribute to the development of point-of-care systems. However, steps still need to be taken to develop microfluidic AST, to provide a cost-effective, portable, accurate, and time-efficient device.

Microfluidic devices can also simplify and accelerate sample pretreatment (cleaning and isolation) for the subsequent AST. Besides the use as microfluidic AST, microfluidic devices can also be used for antibiotic development or research on the mechanisms of AMR development [45].

References

1. World Health Organization (2016) United Nations meeting on antimicrobial resistance. *Bull World Health Organ* 94(9):638–639. <https://doi.org/10.2471/BLT.16.020916>
2. Friedman ND, Temkin E, Carmeli Y (2016) The negative impact of antibiotic resistance. *Clin Microbiol Infect* 22(5):416–422. <https://doi.org/10.1016/j.cmi.2015.12.002>
3. European Centre for Disease Prevention and Control (2017) Surveillance atlas of infectious diseases. <https://www.ecdc.europa.eu/en/surveillance-atlas-infectious-diseases>. Accessed 3 Nov 2020
4. Khan ZA, Siddiqui MF, Park S (2019) Progress in antibiotic susceptibility tests: a comparative review with special emphasis on microfluidic methods. *Biotechnol Lett* 41(2):221–230. <https://doi.org/10.1007/s10529-018-02638-2>
5. Stürenburg E, Junker R (2009) Point-of-care testing in microbiology: the advantages and disadvantages of immunochromatographic test strips. *Dtsch Arztebl Int* 106(4):48–54. <https://doi.org/10.3238/arztebl.2009.0048>
6. Mach KE, Mohan R, Baron EJ, Shih M-C, Gau V, Wong PK, Liao JC (2011) A biosensor platform for rapid antimicrobial susceptibility testing directly from clinical samples. *J Urol* 185(1):148–153. <https://doi.org/10.1016/j.juro.2010.09.022>
7. Ferrer R, Martin-Loeches I, Phillips G, Osborn TM, Townsend S, Dellinger RP, Artigas A, Schorr C, Levy MM (2014) Empiric antibiotic treatment reduces mortality in severe sepsis and septic shock from the first hour: results from a guideline-based performance improvement program. *Crit Care Med* 42(8):1749–1755. <https://doi.org/10.1097/CCM.0000000000000330>
8. Karam G, Chastre J, Wilcox MH, Vincent J-L (2016) Antibiotic strategies in the era of multidrug resistance. *Crit Care* 20(1):136. <https://doi.org/10.1186/s13054-016-1320-7>
9. Kollef MH (2008) Broad-spectrum antimicrobials and the treatment of serious bacterial infections: getting it right up front. *Clin Infect Dis* 47(Suppl 1):S3–S13. <https://doi.org/10.1086/590061>
10. Laxminarayan R, Matsoso P, Pant S, Brower C, Røttingen J-A, Klugman K, Davies S (2016) Access to effective antimicrobials: a worldwide challenge. *Lancet* 387(10014):168–175. [https://doi.org/10.1016/S0140-6736\(15\)00474-2](https://doi.org/10.1016/S0140-6736(15)00474-2)
11. Bhattacharyya RP, Bandyopadhyay N, Ma P, Son SS, Liu J, He LL, Wu L, Khafizov R, Boykin R, Cerqueira GC, Pironti A, Rudy RF, Patel MM, Yang R, Skerry J, Nazarian E, Musser KA, Taylor J, Pierce VM, Earl AM, Cosimi LA, Shores N, Beechem J, Livny J, Hung DT (2019) Simultaneous detection of genotype and phenotype enables rapid and accurate antibiotic susceptibility determination. *Nat Med* 25(12):1858–1864. <https://doi.org/10.1038/s41591-019-0650-9>
12. Hou HW, Bhattacharyya RP, Hung DT, Han J (2015) Direct detection and drug-resistance profiling of bacteremias using inertial microfluidics. *Lab Chip* 15(10):2297–2307. <https://doi.org/10.1039/c5lc00311c>

13. Khan ZA, Siddiqui MF, Park S (2019) Current and emerging methods of antibiotic susceptibility testing. *Diagnostics (Basel)* 9(2). <https://doi.org/10.3390/diagnostics9020049>
14. Murray C, Adeyiga O, Owsley K, Di Carlo D (2015) Research highlights: microfluidic analysis of antimicrobial susceptibility. *Lab Chip* 15(5):1226–1229. <https://doi.org/10.1039/c5lc90017d>
15. Garcia-Prats JA, Cooper TR, Schneider VF, Stager CE, Hansen TN (2000) Rapid detection of microorganisms in blood cultures of newborn infants utilizing an automated blood culture system. *Pediatrics* 105(3 Pt 1):523–527. <https://doi.org/10.1542/peds.105.3.523>
16. Zhang K, Qin S, Wu S, Liang Y, Li J (2020) Microfluidic systems for rapid antibiotic susceptibility tests (ASTs) at the single-cell level. *Chem Sci* 11(25):6352–6361. <https://doi.org/10.1039/D0SC01353F>
17. Smith KP, Kirby JE (2018) The inoculum effect in the era of multidrug resistance: minor differences in inoculum have dramatic effect on MIC determination. *Antimicrob Agents Chemother* 62(8). <https://doi.org/10.1128/AAC.00433-18>
18. van Belkum A, Burnham C-AD, Rossen JWA, Mallard F, Rochas O, Dunne WM (2020) Innovative and rapid antimicrobial susceptibility testing systems. *Nat Rev Microbiol* 18(5):299–311. <https://doi.org/10.1038/s41579-020-0327-x>
19. Vasala A, Hytönen VP, Laitinen OH (2020) Modern tools for rapid diagnostics of antimicrobial resistance. *Front Cell Infect Microbiol* 10:308. <https://doi.org/10.3389/fcimb.2020.00308>
20. Mishra P, Mishra KP, Singh D, Ganju L, Kumar B, Singh SB (2018) Advances in rapid detection and antimicrobial susceptibility tests: a review. *Def Life Sci J* 4(1):12–20. <https://doi.org/10.14429/dlsj.4.12572>
21. Baltekin Ö, Boucharin A, Tano E, Andersson DI, Elf J (2017) Antibiotic susceptibility testing in less than 30 min using direct single-cell imaging. *Proc Natl Acad Sci U S A* 114(34):9170–9175. <https://doi.org/10.1073/pnas.1708558114>
22. S-u H, Zhang X (2020) Microfluidics as an emerging platform for tackling antimicrobial resistance (AMR): a review. *Curr Anal Chem* 16(1):41–51. <https://doi.org/10.2174/1573411015666181224145845>
23. Lee W-B, Fu C-Y, Chang W-H, You H-L, Wang C-H, Lee MS, Lee G-B (2017) A microfluidic device for antimicrobial susceptibility testing based on a broth dilution method. *Biosens Bioelectron* 87:669–678. <https://doi.org/10.1016/j.bios.2016.09.008>
24. Choi J, Jung Y-G, Kim J, Kim S, Jung Y, Na H, Kwon S (2013) Rapid antibiotic susceptibility testing by tracking single cell growth in a microfluidic agarose channel system. *Lab Chip* 13(2):280–287. <https://doi.org/10.1039/c2lc41055a>
25. Hiratsuka T, Komatsu N (2019) Single-cell live imaging. *Methods Mol Biol* 1979:409–421. https://doi.org/10.1007/978-1-4939-9240-9_24
26. Mullassery D, Horton CA, Wood CD, White MRH (2008) Single live-cell imaging for systems biology. *Essays Biochem* 45:121–133. <https://doi.org/10.1042/BSE0450121>
27. Li H, Torab P, Mach KE, Surrette C, England MR, Craft DW, Thomas NJ, Liao JC, Puleo C, Wong PK (2019) Adaptable microfluidic system for single-cell pathogen classification and antimicrobial susceptibility testing. *Proc Natl Acad Sci U S A* 116(21):10270–10279. <https://doi.org/10.1073/pnas.1819569116>
28. Lu Y, Gao J, Zhang DD, Gau V, Liao JC, Wong PK (2013) Single cell antimicrobial susceptibility testing by confined microchannels and electrokinetic loading. *Anal Chem* 85(8):3971–3976. <https://doi.org/10.1021/ac4004248>
29. Choi J, Yoo J, Lee M, Kim E-G, Lee JS, Lee S, Joo S, Song SH, Kim E-C, Lee JC, Kim HC, Jung Y-G, Kwon S (2014) A rapid antimicrobial susceptibility test based on single-cell morphological analysis. *Sci Transl Med* 6(267):267ra174. <https://doi.org/10.1126/scitranslmed.3009650>
30. Hou Z, An Y, Hjort K, Hjort K, Sandegren L, Wu Z (2014) Time lapse investigation of antibiotic susceptibility using a microfluidic linear gradient 3D culture device. *Lab Chip* 14(17):3409–3418. <https://doi.org/10.1039/C4LC00451E>

31. Li B, Qiu Y, Glidle A, McIlvenna D, Luo Q, Cooper J, Shi H-C, Yin H (2014) Gradient microfluidics enables rapid bacterial growth inhibition testing. *Anal Chem* 86(6):3131–3137. <https://doi.org/10.1021/ac5001306>
32. Kim S, Lee S, Kim J-K, Chung HJ, Jeon JS (2019) Microfluidic-based observation of local bacterial density under antimicrobial concentration gradient for rapid antibiotic susceptibility testing. *Biomicrofluidics* 13(1):14108. <https://doi.org/10.1063/1.5066558>
33. Leonard H, Halachmi S, Ben-Dov N, Nativ O, Segal E (2017) Unraveling antimicrobial susceptibility of bacterial networks on micropillar architectures using intrinsic phase-shift spectroscopy. *ACS Nano* 11(6):6167–6177. <https://doi.org/10.1021/acsnano.7b02217>
34. Busche JF, Möller S, Klein A-K, Stehr M, Purr F, Bassu M, Burg TP, Dietzel A (2020) Nanofluidic immobilization and growth detection of *Escherichia coli* in a Chip for antibiotic susceptibility testing. *Biosensors (Basel)* 10(10). <https://doi.org/10.3390/bios10100135>
35. Busche JF, Möller S, Stehr M, Dietzel A (2019) Cross-flow filtration of *Escherichia coli* at a Nanofluidic gap for fast immobilization and antibiotic susceptibility testing. *Micromachines (Basel)* 10(10). <https://doi.org/10.3390/mi10100691>
36. Purr F, Bassu M, Lowe RD, Thürmann B, Dietzel A, Burg TP (2017) Asymmetric nanofluidic grating detector for differential refractive index measurement and biosensing. *Lab Chip* 17(24):4265–4272. <https://doi.org/10.1039/c7lc00929a>
37. Mohan R, Mukherjee A, Sevgen SE, Sanpitakseree C, Lee J, Schroeder CM, Kenis PJA (2013) A multiplexed microfluidic platform for rapid antibiotic susceptibility testing. *Biosens Bioelectron* 49:118–125. <https://doi.org/10.1016/j.bios.2013.04.046>
38. Kim S, Masum F, Jeon JS (2019) Recent developments of Chip-based phenotypic antibiotic susceptibility testing. *Biochip J* 13(1):43–52. <https://doi.org/10.1007/s13206-019-3109-7>
39. Mohan R, Sanpitakseree C, Desai AV, Sevgen SE, Schroeder CM, Kenis PJA (2015) A microfluidic approach to study the effect of bacterial interactions on antimicrobial susceptibility in polymicrobial cultures. *RSC Adv* 5(44):35211–35223. <https://doi.org/10.1039/C5RA04092B>
40. Kaminski TS, Scheler O, Garstecki P (2016) Droplet microfluidics for microbiology: techniques, applications and challenges. *Lab Chip* 16(12):2168–2187. <https://doi.org/10.1039/c6lc00367b>
41. Boedicker JQ, Li L, Kline TR, Ismagilov RF (2008) Detecting bacteria and determining their susceptibility to antibiotics by stochastic confinement in nanoliter droplets using plug-based microfluidics. *Lab Chip* 8(8):1265–1272. <https://doi.org/10.1039/b804911d>
42. Avesar J, Rosenfeld D, Truman-Rosentsvit M, Ben-Arye T, Geffen Y, Bercovici M, Levenberg S (2017) Rapid phenotypic antimicrobial susceptibility testing using nanoliter arrays. *Proc Natl Acad Sci U S A* 114(29):E5787–E5795. <https://doi.org/10.1073/pnas.1703736114>
43. Churski K, Kaminski TS, Jakiela S, Kamysz W, Baranska-Rybak W, Weibel DB, Garstecki P (2012) Rapid screening of antibiotic toxicity in an automated microdroplet system. *Lab Chip* 12(9):1629–1637. <https://doi.org/10.1039/c2lc21284f>
44. Derzsi L, Kaminski TS, Garstecki P (2016) Antibigrams in five pipetting steps: precise dilution assays in sub-microliter volumes with a conventional pipette. *Lab Chip* 16(5):893–901. <https://doi.org/10.1039/C5LC01151E>
45. Liu X, Painter RE, Enesa K, Holmes D, Whyte G, Garlisi CG, Monnsma FJ, Rehak M, Craig FF, Smith CA (2016) High-throughput screening of antibiotic-resistant bacteria in picodroplets. *Lab Chip* 16(9):1636–1643. <https://doi.org/10.1039/c6lc00180g>
46. Pitruzzello G, Thorpe S, Johnson S, Evans A, Gadêlha H, Krauss TF (2019) Multiparameter antibiotic resistance detection based on hydrodynamic trapping of individual *E. coli*. *Lab Chip* 19(8):1417–1426. <https://doi.org/10.1039/C8LC01397G>
47. Shang L, Cheng Y, Zhao Y (2017) Emerging droplet microfluidics. *Chem Rev* 117(12):7964–8040. <https://doi.org/10.1021/acs.chemrev.6b00848>
48. Yang Y, Gupta K, Ekinci KL (2020) All-electrical monitoring of bacterial antibiotic susceptibility in a microfluidic device. *Proc Natl Acad Sci U S A* 117(20):10639–10644. <https://doi.org/10.1073/pnas.1922172117>

49. Besant JD, Sargent EH, Kelley SO (2015) Rapid electrochemical phenotypic profiling of antibiotic-resistant bacteria. *Lab Chip* 15(13):2799–2807. <https://doi.org/10.1039/c5lc00375j>
50. Mirasoli M, Guardigli M, Michelini E, Roda A (2014) Recent advancements in chemical luminescence-based lab-on-chip and microfluidic platforms for bioanalysis. *J Pharm Biomed Anal* 87:36–52. <https://doi.org/10.1016/j.jpba.2013.07.008>
51. Dong T, Zhao X (2015) Rapid identification and susceptibility testing of uropathogenic microbes via immunosorbent ATP-bioluminescence assay on a microfluidic simulator for antibiotic therapy. *Anal Chem* 87(4):2410–2418. <https://doi.org/10.1021/ac504428t>
52. Rostova E, Ben Adiba C, Dietler G, Sekatskii SK (2016) Kinetics of antibody binding to membranes of living Bacteria measured by a photonic crystal-based biosensor. *Biosensors (Basel)* 6(4). <https://doi.org/10.3390/bios6040052>
53. Liu C-Y, Han Y-Y, Shih P-H, Lian W-N, Wang H-H, Lin C-H, Hsueh P-R, Wang J-K, Wang Y-L (2016) Rapid bacterial antibiotic susceptibility test based on simple surface-enhanced Raman spectroscopic biomarkers. *Sci Rep* 6:23375. <https://doi.org/10.1038/srep23375>
54. Han Y-Y, Lin Y-C, Cheng W-C, Lin Y-T, Teng L-J, Wang J-K, Wang Y-L (2020) Rapid antibiotic susceptibility testing of bacteria from patients' blood via assaying bacterial metabolic response with surface-enhanced Raman spectroscopy. *Sci Rep* 10(1):12538. <https://doi.org/10.1038/s41598-020-68855-w>
55. Rolain JM, Mallet MN, Fournier PE, Raoult D (2004) Real-time PCR for universal antibiotic susceptibility testing. *J Antimicrob Chemother* 54(2):538–541. <https://doi.org/10.1093/jac/dkh324>
56. Schoepp NG, Khorosheva EM, Schlappi TS, Curtis MS, Humphries RM, Hindler JA, Ismagilov RF (2016) Digital quantification of DNA replication and chromosome segregation enables determination of antimicrobial susceptibility after only 15 minutes of antibiotic exposure. *Angew Chem Int Ed Engl* 55(33):9557–9561. <https://doi.org/10.1002/anie.201602763>
57. Hindson CM, Chevillet JR, Briggs HA, Gallichotte EN, Ruf IK, Hindson BJ, Vessella RL, Tewari M (2013) Absolute quantification by droplet digital PCR versus analog real-time PCR. *Nat Methods* 10(10):1003–1005. <https://doi.org/10.1038/nmeth.2633>
58. Khazaei T, Barlow JT, Schoepp NG, Ismagilov RF (2018) RNA markers enable phenotypic test of antibiotic susceptibility in *Neisseria gonorrhoeae* after 10 minutes of ciprofloxacin exposure. *Sci Rep* 8(1):11606. <https://doi.org/10.1038/s41598-018-29707-w>
59. Halford C, Gonzalez R, Campuzano S, Hu B, Babbitt JT, Liu J, Wang J, Churchill BM, Haake DA (2013) Rapid antimicrobial susceptibility testing by sensitive detection of precursor rRNA using a novel electrochemical biosensing platform. *Antimicrob Agents Chemother* 57(2):936–943. <https://doi.org/10.1128/AAC.00615-12>
60. Mader A, Gruber K, Castelli R, Hermann BA, Seeberger PH, Rädler JO, Leisner M (2012) Discrimination of *Escherichia coli* strains using glycan cantilever array sensors. *Nano Lett* 12(1):420–423. <https://doi.org/10.1021/nl203736u>
61. Wang J, Morton MJ, Elliott CT, Karoonuthaisiri N, Segatori L, Biswal SL (2014) Rapid detection of pathogenic bacteria and screening of phage-derived peptides using microcantilevers. *Anal Chem* 86(3):1671–1678. <https://doi.org/10.1021/ac403437x>
62. Etayash H, Khan MFR, Kaur K, Thundat T (2016) Microfluidic cantilever detects bacteria and measures their susceptibility to antibiotics in small confined volumes. *Nat Commun* 7:12947. <https://doi.org/10.1038/ncomms12947>
63. Godin M, Delgado FF, Son S, Grover WH, Bryan AK, Tzur A, Jorgensen P, Payer K, Grossman AD, Kirschner MW, Manalis SR (2010) Using buoyant mass to measure the growth of single cells. *Nat Methods* 7(5):387–390. <https://doi.org/10.1038/nmeth.1452>
64. van Meer BJ, de Vries H, Firth KSA, van Weerd J, Tertoolen LGJ, Karperien HBJ, Jonkheijm P, Denning C, IJzerman AP, Mummery CL (2017) Small molecule absorption by PDMS in the context of drug response bioassays. *Biochem Biophys Res Commun* 482(2):323–328. <https://doi.org/10.1016/j.bbrc.2016.11.062>

65. Toepke MW, Beebe DJ (2006) PDMS absorption of small molecules and consequences in microfluidic applications. *Lab Chip* 6(12):1484–1486. <https://doi.org/10.1039/B612140C>
66. Shirure VS, George SC (2017) Design considerations to minimize the impact of drug absorption in polymer-based organ-on-a-chip platforms. *Lab Chip* 17(4):681–690. <https://doi.org/10.1039/C6LC01401A>

Organ-on-a-Chip



Ilka Maschmeyer and Sofia Kakava

Contents

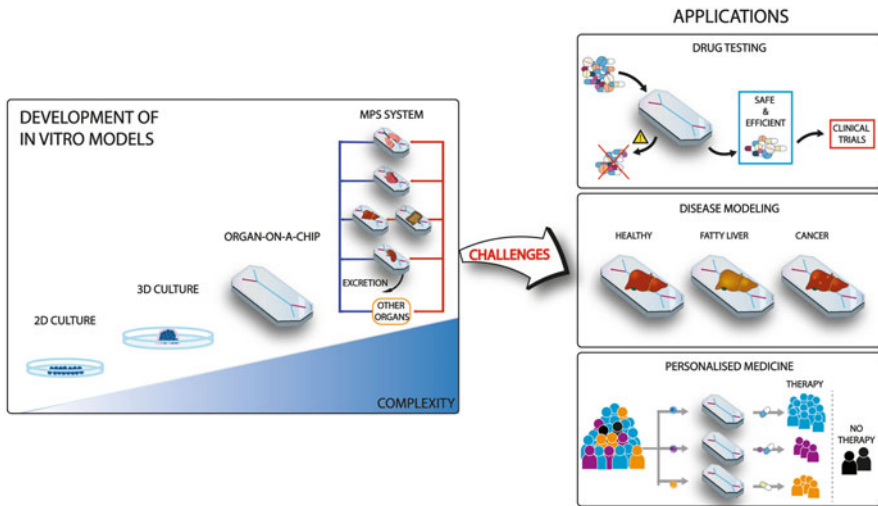
1	Introduction	312
1.1	A Global Health Challenge	312
1.2	What Is an Organ-on-a-Chip?	314
2	Multi-organ-Chips and Humans-on-a-Chip	317
2.1	Potentials of the Platform	317
2.2	Design Considerations and Challenges	319
2.3	Generated Multi-organ Platforms	329
2.4	Commercialization	332
2.5	Ongoing Research	333
3	Conclusion and Outlook	333
	References	335

Abstract Limitations of the current tools used in the drug development process, cell cultures, and animal models have highlighted the need for a new powerful tool that can emulate the human physiology *in vitro*. Advances in the field of microfluidics have made the realization of this tool closer than ever. Organ-on-a-chip platforms have been the first step forward, leading to the combination and integration of multiple organ models in the same platform with human-on-a-chip being the ultimate goal. Despite the current progress and technological developments, there are still several unmet engineering and biological challenges curtailing their development and widespread application in the biomedical field. The potentials, challenges, and current work on this unprecedented tool are being discussed in this chapter.

I. Maschmeyer (✉)
TissUse GmbH, Berlin, Germany
e-mail: ilka.maschmeyer@tissuse.com

S. Kakava
Utrecht University, Utrecht, The Netherlands

Graphical Abstract



Keywords Bioengineering, Disease modeling, Drug development, Human-on-a-chip, Microfluidics, Organ-on-a-chip

1 Introduction

1.1 A Global Health Challenge

We are currently facing a global health challenge stemming from the high cost and long runway time currently associated with the process of drug discovery and development. According to a report issued by the Pharmaceutical Research and Manufacturers of America (“PhRMA”) as of 2015, the average drug is estimated to cost 2.6 billion dollars to develop and take 10 years to complete [1]. Drug manufacturing is characterized by low efficiency, with failures being much more common than successful attempts (less than 12% of possible candidates in clinical trials are ultimately approved) [2, 3] (Fig. 1). These stark realities place the pharmaceutical industry under intense economic, ethical, and scientific pressure to find ways to accelerate the drug development process and to develop drugs that are safer and more effective in humans at a lower cost. The tools currently used to test the safety and efficacy of new drugs, animal models, and cells in dishes constitute one of the key bottlenecks that currently prevent the accurate prediction of human responses and halt the efficient development of new therapies [2, 5]. Although these tools have immensely contributed to delineating mechanisms underlying basic biological processes and the initiation and causes of a number of diseases,

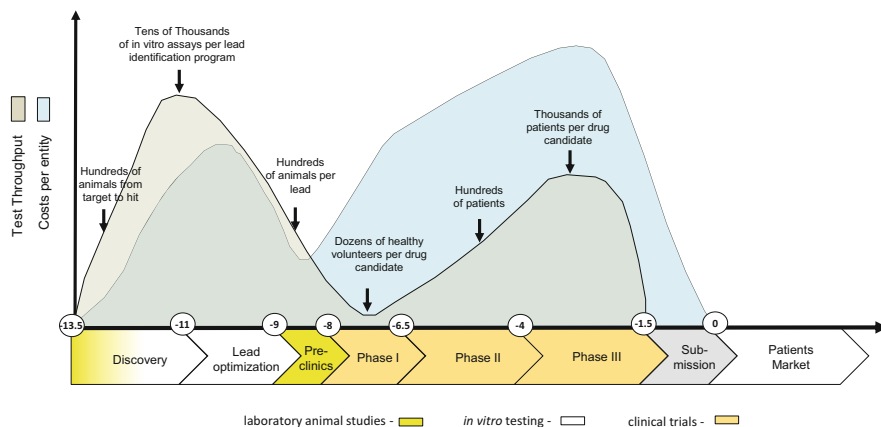


Fig. 1 Drug development: a lengthy and costly process. The vertical axis shows the number of tests performed (grey) and the corresponding cost (blue) (costly process). The horizontal axis shows the time in years that is required to a drug to be developed (lengthy process). From “Biology-inspired microphysiological system approaches to solve the prediction dilemma of substance testing” by [4], ALTEX, 33(3), 272–321. Reprinted under the terms of the Creative Commons Attribution 4.0 International license

they nevertheless fail to fully capture the complexities of human biology and physiology.

The current gold standard for preclinical studies is *in vivo* experiments using animal models. Yet conventional *in vitro* cell cultures are not able to recapitulate interactions between the different organs and tissues – a prerequisite for studying pharmacokinetic processes. As a result, animals are used to test for the safety, non-targeted drug toxicity, and efficacy of new drugs [6]. In many cases, animal studies lead to inaccurate data extrapolation [7] because they fail to accurately predict human responses (mainly due to interspecies differences in the genome, biological pathways, and cell physiology) [5]. One characteristic and illustrative example is the case of the clinical trial of TGN1412 by TeGenero Pharmaceuticals in 2006. Preclinical trials had demonstrated the safety and efficacy of an immunomodulatory drug in both rodents and monkeys. However, upon administration to humans during Phase I clinical studies, six otherwise healthy individuals demonstrated multiple organ failure [8] due to a 4% difference in the targeted sequence between humans and monkeys [9]. Moreover, in the recent years, there is a movement toward the reduction of the number of animals used which might further affect the drug development [6].

Alternatively, *in vitro* assays with human-derived cells can be performed for the preliminary screening of new drugs [6]. Next to conventional 2D cultures, 3D cell cultures have been extensively developed in the last 50 years. For example, by applying hydrogel technology, cell-cell interaction, polarization, and lumen formation are achieved with tissue hallmarks being present *in vitro* [10, 11].

Conventional 3D cell cultures have certain limitations, however. Components such as tissue architecture, tissue-tissue communication, dynamic fluid flow, and the normal mechanical cues which cells are constantly exposed to in vivo are usually not present in these culturing systems. Exposure of cells to all the above is highly important, since these factors influence both the development and function of a tissue or organ [12]. Great advances in microfluidics (namely, organ-on-a-chip systems) have recently started to allow researchers to overcome these limitations.

Advances in the tissue engineering research field since the early 2000s [13] have also opened up new avenues toward the development of such a system. The organ-on-a-chip technology applies a microfluidic approach to the human cell culture, to replicate tissue and organ physiology (i.e., structures, networks, and mechanical cues) and functions [5, 14, 15]. Multi-organ-chip systems and the development of a human-on-a-chip system could similarly help to tackle the abovementioned problems in the drug screening process [4] and pave the way for truly personalized drug testing (patient-on-a-chip), laying the groundwork for clinical-trial-on-a-chip.

1.2 *What Is an Organ-on-a-Chip?*

An organ-on-a-chip is a biomimetic microscale cell culture device that combines 3D tissue engineered constructs with a microfluidic network of continuously perfused micrometer-sized chambers. The development of such a device requires a multidisciplinary approach, combining the engineering aspect with biological functionality [4]. These platforms are designed to recapitulate in vitro – in a controlled and scale relevant manner – the basic mechanical (blood flow, air pressure) and extracellular cues, the physiochemical environment, the multicellular architecture, physiology, and functions of a given tissue or organ [16]. Mechanical stimuli to the cells – generated by the fluid flow, spatial liquid conditions, and concentration gradients – are among the parameters that can be controlled with the microfluidics technology maintaining an organ-specific physical and biochemical environment [14, 15]. In this fashion, these devices establish a functional unit of an organ in a tridimensional environment which cannot be achieved with conventional 2D culture systems. Each unit is a simplified, yet still realistic, mock-up of a human organ of interest that recapitulates in vivo-like responses and can capture the wide diversity among individuals [5, 10, 17, 18] (Fig. 2 left).

Huh et al. [14] have undertaken groundbreaking work in this field by developing a structurally complex lung-on-a-chip that allows gas exchange between microvascular endothelial and alveolar epithelial cells by mimicking inhalations and exhalation through mechanical forces. Indeed, a great number of single organ-on-a-chip platforms have been developed for many different organs and applications as shown in Table 1. More can be found in a number of reviews about organ-on-a-chip [1, 6, 18, 50]. Their applications include disease modeling and personalized tissue models

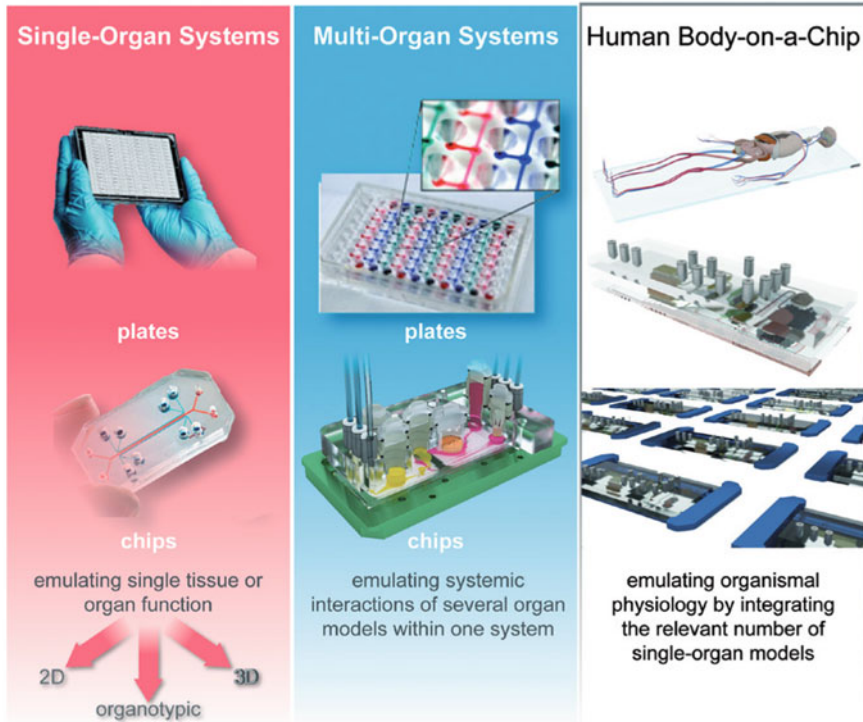


Fig. 2 Tools that can emulate the human biology in vitro. Left: Single organ-on-a-chip systems that emulate a single organ. On top showing the MIMETAS OrganoPlate for 3D perfused cell culture in microtiter format, in the middle the lung-on-a-chip developed by the Wyss Institute, Center: Multi-organ systems that emulate the systemic interaction of several organs. On top showing the hanging drop microtiter plate by ETH Basel with microfluidic channel connecting multiple spheroids and at the bottom an impression of the four-organ system developed by TissUse, Right: Shows an impression of a human body-on-a-chip platform. (Courtesy of MIMETAS, The Netherlands; Wyss Institute, USA; ETH, Switzerland; and TissUse GmbH, Germany, respectively). From “Biology-inspired microphysiological system approaches to solve the prediction dilemma of substance testing” by Marx et al. [4], ALTEX, 33(3), 272–321. Reprinted under the terms of the Creative Commons Attribution 4.0 International license

using human-induced pluripotent stem cells (hiPSCs) and cell-based assays for drug discovery [6]. Some researchers are also incorporating different organ-on-a-chip modules in a dynamic microfluidic device that recapitulates even more complex physiological functions [1].

Table 1 Examples of single organ-on-a-chip platforms

Organ	Incorporated cell types	References
Adipose tissue	Cell line	[19]
Bone	hiPSCs	[20]
	MSCs	[21]
Brain	Primary cells, cell line, and hiPSCs	[22]
	Human brain organoids (hiPSCs)	[23]
Bone marrow	Cell lines and primary cells	[24]
Colon	Primary human cells	[25]
Gut	Cell line and microbial flora	[26]
	Human enteroids	[27]
Heart	hiPSCs	[28]
	Rat primary cells or hiPSCs	[29]
Kidney	Human kidney tissue	[30]
	Cell lines	[31]
Liver	Primary human cells and cell lines	[32]
	Bioprinted hepatic spheroids (HepG2/C3A)	[33]
	Rat, dog, or human primary hepatocytes, liver sinusoidal endothelial cells, with or without Kupffer cells	[34]
Lung	Cell lines	[14]
	Primary human endothelial and epithelial (health and diseased) cells	[35]
	Primary human lung alveolar epithelial cells	[36]
Muscle	Cell line	[37]
Pancreas	Primary mouse tissue	[38]
Reproductive	Human and mice primary tissue	[39]
Eye	Retinal organoids derived from hiPSCs	[40]
Skin	Primary human tissue	[41]
	Primary and induced pluripotent stem cell (iPSC)-derived endothelial stem cells	[42]
Stomach	hiPSCs (human gastric organoids)	[43]
Vascular	iPSCs	[44]
	Cell lines	[45]
	Primary human endothelial cells	[46]
Uterus	Primary mouse tissue	[47]
Cancer	Patient-derived organotypic tumor spheroids	[48]
	Human pancreatic cancer cell lines	[49]

2 Multi-organ-Chips and Humans-on-a-Chip

Generating a tool that can emulate the human biology *in vitro* is a formidable goal. Multi-organ microfluidic microdevices and human-on-a-chip (or body-on-a-chip) platforms help to meet this goal by interconnecting different organ models with a fluidic stream to create a physiologically realistic system [51, 52]. This unprecedented tool – commonly referred to as micro-cell culture analogs (μ CCA) [53] – was first suggested by Shuler in 1996 [54], and many names have since been used to describe it, including microphysiological systems (MPS) [4, 16], body-on-a-chip [55], human-on-a-chip [56], and physiome-on-a-chip [57].

Using microfabricated devices, various organ combinations have been developed for both disease modeling [51] and drug toxicity [58]. Sophisticated and dynamic multi-organ platforms consist of human cells growing on opposite sides of a thin permeable planar scaffold that is placed either in a transwell geometry [59] or between microfluidic channels [60] and employs active flow from onboard or external pumps to achieve system perfusion (Fig. 2). Such a system can constitute a powerful tool, with immense possibilities in the biomedical field – particularly with respect to drug discovery and development processes [16]. Human-on-a-chip platforms can mimic the way in which drugs and their metabolites are consumed, produced, and exchanged [2]. But developing a human-on-a-chip platform that authentically models human physiology (and associated biochemical and biological responses) presents a series of engineering and biological challenges: To start with, different organs must be cultured at the same time, in the same device, and with the same circulating liquid phase – all while remaining fully functional and physiologically relevant. These threshold challenges must all be adequately addressed in order to facilitate truly widespread application of human-on-a-chip in research and development contexts [61].

2.1 *Potentials of the Platform*

A successful multi-organ-chip device has to appropriately mimic key aspects of the human physiology. To that end, it must constitute a complex and dynamic system in which the different organs or tissues are all connected and interact in a physiologically relevant manner, to facilitate the simulation and modeling of human metabolism *in vitro*. The obvious complexity – yet, paradoxically, the simultaneously simplicity – of this platform is precisely what makes it such a potentially powerful tool in the drug discovery process [2, 10, 18].

Using small volumes of reagents, microfluidics can incorporate the required mechanical cues in microfabricated miniaturized platforms – including accounting for physiologically relevant levels of fluid shear stress, cyclic strain, and mechanical compression. The ability to successfully mimic dynamic systems at a small scale is essential for the development of the multi-organ and human-on-chip platforms.

Another equally important advantage of multi-organ-chip platforms is their ability to recapitulate and study the crosstalk of the different organs. Imitating *in vivo* blood distributions, the connection of fluid channels across such a platform allows researchers to study the communication of different compartments and crosstalk between the incorporated organ tissues. This interplay allows for more realistic modeling of a human system in terms of hormonal control [62] and organ interplay and regulation through molecular crosstalk (e.g., cytokines and growth factors) in physiological or pathological conditions [51, 63]. Various diseases can thus be studied – which is particularly critical for those currently lacking a representative and accurate animal model [64]. The mechanisms of various diseases and the systemic interactions that they induce can also be assessed and monitored in different stages of the disease, helping to shed light on onset mechanisms that may presently remain unknown to science. The discovery of unknown interactions between organs observed only in real time is yet another tantalizing prospect.

Using these systems, for the first time, metabolism, efficacy, toxicity, and bioactivation of a drug can all be studied within the same human-simulating system [53]. The response of both the targeted and non-targeted organs, as well as the interaction and influence of a drug upon the whole system, can be assessed in one fell swoop. This will allow researchers to assess the toxicity and efficacy of a drug with far greater accuracy prior to entering the clinical phase, which will both lower the cost and increase the speed of drug development.

This tool can also be directly adopted in the clinical phase (clinical trial-on-a-chip), with platforms generated from patients of different genetic identity (i.e., mimicking different ages, sexes, and ethnicities). Instead of being conducted monolithically, subtle but potentially medically important differences can actually be taken into consideration during this critical phase. Subpopulations of “responders” and “nonresponders” can also be identified, with different metabolic rates and genetic makeup being identified to elucidate the mechanism underlying this divergent drug response [18, 65] (Fig. 3).

Taken to its extreme, the applications of multi-organ-chip devices in the drug discovery process can be extended even further, to the field of truly personalized medicine. By using biopsies or hiPSCs from patients, human-on-a-chip tailored *to a single patient* could revolutionize personalized medicine and the healthcare system as a whole. The so-called patient-on-a-chip platform could be generated using cells directly from a patient [2, 16, 66, 67]. A drug could thereafter be screened before administration to a patient while monitoring for adverse effects. This would allow doctors to determine ideal dosage on a truly individual level – a particularly important development in cases of vulnerable or rare populations and polypharmacy [68]. For example, “at-risk” groups such as children, the elderly, and pregnant individuals rarely enter clinical trials – which means that most drug toxicity and efficacy testing is derived from the relatively healthy adult subpopulation [69] and prescriptions are necessarily made based on a generalized success rate in such individuals [67].

Finally, toxicity assessment of chemicals (i.e., chemical exposure) and environmental toxicants, and the study of their mechanism of action, represents yet another

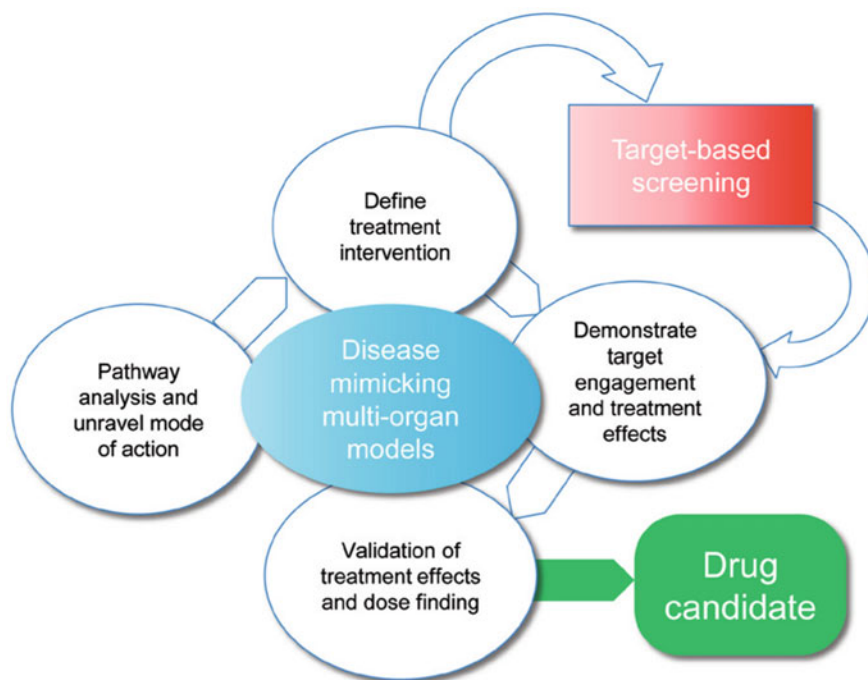


Fig. 3 How multi-organ systems can influence the drug discovery. Disease mimicking multi-organ system can – among others – be used to analyze and unravel disease mechanisms and validate treatment effects, thus transforming drug discovery screening strategies. From “Biology-inspired microphysiological system approaches to solve the prediction dilemma of substance testing” by Marx et al. [4], ALTEX, 33(3), 272–321. Reprinted under the terms of the Creative Commons Attribution 4.0 International license

possible application of this technology [17]. For example, the tobacco industry could apply this platform to more closely study the health hazards and the systemic effect of tobacco inhalation and potentially develop future products that minimize these effects [4, 23, 70].

2.2 Design Considerations and Challenges

The human body is a complex and dynamic system composed of organs and tissues that are in constant interaction with each other. If the emerging technology of organ-on-a-chip and human-on-a-chip can accurately capture this complexity, it will become an extremely powerful tool for drug development. Developing such a complex and sophisticated system poses a number of hugely demanding engineering and biological challenges, however.

2.2.1 Required Functions

Determining the safety and efficacy of a therapeutic drug candidate is critical during its development. This safety profile is primarily determined by four different synergic and sequential functions – absorption, distribution, metabolism, and excretion (ADME) – that are frequently carried out by different organs within the human body. Briefly, systemic absorption of a drug to the bloodstream depends on the route of administration and can be either direct as in case of intravenous (IV) injection or indirect including via the small intestine (oral application), skin (topical dermal application), or lungs (inhalative application). In all instances, a drug is then systemically distributed and metabolized by the liver to create new compounds, called metabolites. The metabolism of a drug may be required for it to exert its pharmacological activity (prodrug – bioactivation). The drug and its metabolites will eventually reach other organs and tissues in the body, where they will either exert therapeutic or toxic effects (e.g., nephrotoxicity) before ultimately being excreted.

To be able to precisely determine the human response to a therapeutic drug candidate, multi-organ-chip platforms must be able to incorporate organ tissues that can reflect the *in vivo* pharmacokinetics/pharmacodynamics and end use of the relevant parts of a human body [71]. Based on the disposition of a compound described by ADME, in most cases this means that at least three main organs must be adequately represented. These would be the relevant tissue responsible for the absorption, the organ where the drug is metabolized (liver), and the organ through which the compounds are ultimately excreted (i.e., kidneys or intestines). Although the representation of these ADME functions is crucial, the combination of organs is not universal, but rather depends on the route of administration and characteristics of each specific compound. Since most drugs are orally administered, the most common organ combination can be considered that of small intestine, liver, and kidney. However, the lungs (for example) may have to replace small intestine as the organ responsible for absorption in the case of an inhaled drug. Furthermore, multi-organ-chips must include the organs in which the efficacy and toxicity of a compound is evaluated [71]. The number of these organs varies, depending on the number of targeted organs and the predictability of the toxicity exerted by the compound. Testing of a new compound with limited data or extrapolation problems may require the incorporation of as many organs as possible to identify and assess the breadth of physiological responses and side effects. The latter is essential to increase the efficiency and decrease of costs in the drug development process. Especially when drug-induced toxicity is being assessed, the liver [72] and kidney (nephrotoxicity) [73] must be meticulously monitored, since they represent the two most commonly affected organs (Fig. 4).

Although a given organ may not be present in a study, its function must not be completely neglected. For example, hormones produced by thyroid gland or insulin produced by the pancreas may need to be added to a system in order to ensure proper function.

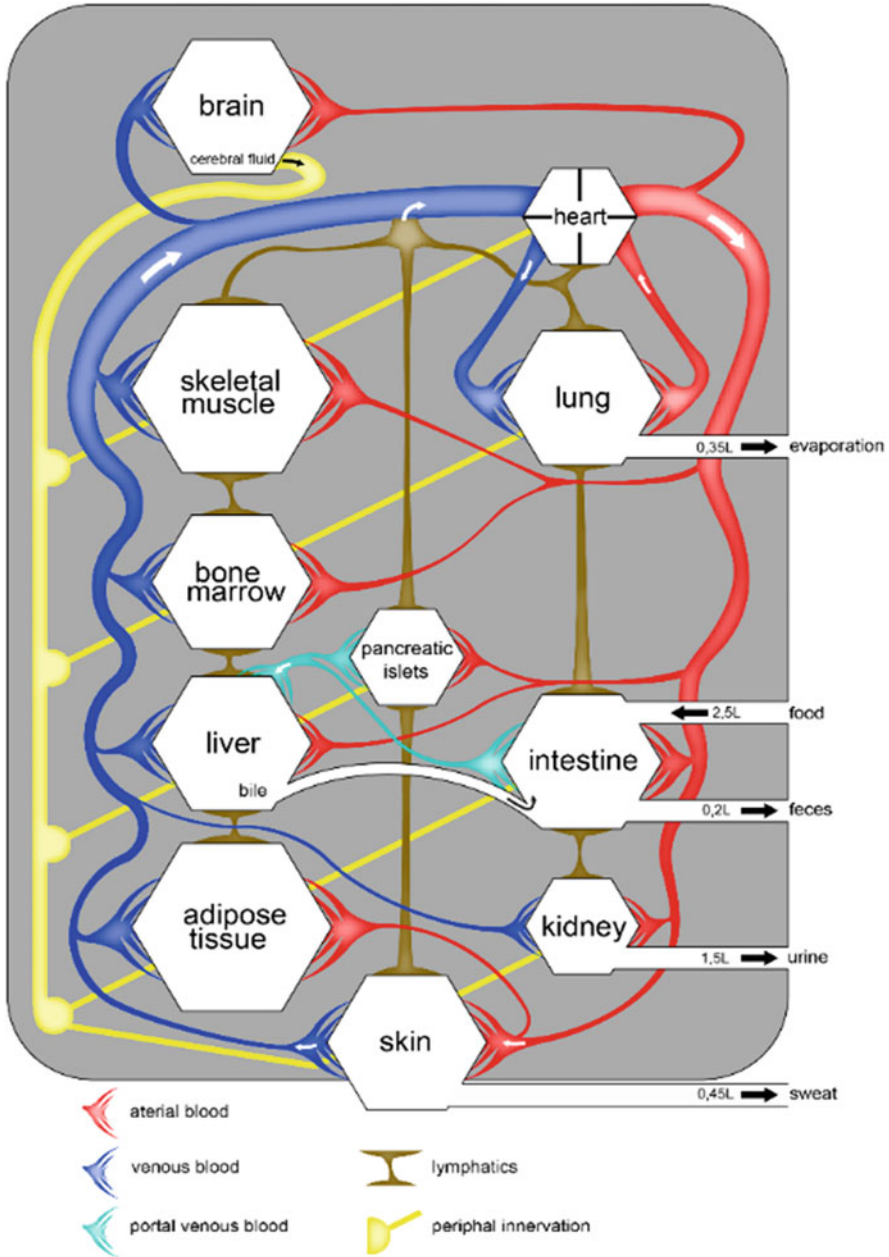


Fig. 4 Human-on-a-chip-template. The figure illustrates the minimal set of human organs, their physiological connection through blood vessels and nerves, and system input and output. All these are required and need to be properly scaled to create a universal and physiological human-on-a-chip template. From “Biology-inspired microphysiological systems to advance medicines for patient benefit and animal welfare” by Marx et al. [74], *ALTEX*, 37, 1–30. Reprinted under the terms of the Creative Commons Attribution 4.0 International license

2.2.2 Materials

Employing the right material with the right properties for the construction of organ-on-chip systems is equally important. Currently, the most commonly used material in microfluidic organ-on-chip devices is PDMS (polydimethylsiloxane) [28, 58, 75–77]. Its wide use in the microfluidics can be attributed to a number of key characteristics, including being (1) optically transparent, (2) highly compliant, and (3) tunable material that is nevertheless relatively (4) cheap, (5) easy, and (6) quick to fabricate [78–80]. But there are several drawbacks in implementing PDMS in biomedical research that have increasingly highlighted the need to evaluate other options. As reviewed by Sackmann et al., one of its disadvantages is that it nonspecifically absorbs small, hydrophobic molecules – which can severely compromise the study of pharmacological compounds and signaling dynamics [78, 80]. Moreover, PDMS also has a strong tendency for surface rearrangement, shows leakage of uncrosslinked oligomers to the media, and is highly gas permeable – which can potentially harm the tissue cells being used to facilitate experiments. Although some of these issues can be partially mitigated, all of them impose additional variability and complicate the comparison between platforms and the obtained results [77, 81, 82].

The limitations of PDMS have prompted the exploration of other materials. Thermoplastic materials, such as polystyrene and cyclic olefin copolymer, could potentially be used in microfluidic devices [80, 83–85]. Polystyrene – a material which has long been used in cell biology applications – is another promising candidate, since it lacks properties such as nonspecific molecule absorption, favoring its use in quantitative pharmacology applications. Challenges in the fabrication of this material continue to prevent its widespread employment, however [78].

Another promising suggestion comes from a recent publication by Edington et al., exploiting a different format than what is usually used – that of an open microfluidic system [59]. This novel design allows for gas exchange at the air-liquid interface and accordingly does not require the use of an oxygen-permeable material.

Many other candidate materials are currently being explored. The ideal material needs to meet the strict requirements of the biological community while simultaneously being amenable to easy practical fabrications. Therefore, this is a particularly daunting slot to fill.

2.2.3 Design Principles and Scaling Rules

To generate a human-on-a-chip platform that accurately emulates human biology and the interaction between the organs, several design parameters and operational strategies have to be considered. Some of these parameters refer to the general characteristics of each organ and can thus easily be found in the literature. These include the cardiac output of an organ (CO), the rate of blood flow in it (Q), the number of cells per organ (n), the ratio that exists between the different types of cells,

and the residence time of each organ (τ). For example, the kidney receives $\approx 20\%$ of the cardiac output, has a flow rate of 1.2 L min^{-1} , $\approx 2 \times 10^9$ cells, and has a residence time of 0.148 min [56].

The same parameters must also be considered systemically in a multi-organ-chip platform. For example, the cardiac output directed to each organ should be represented by a percentage of the systemic flow rate (Q_{sys}), mimicking the human physiology while avoiding shear stress [86]. At the same time, the perfusion rate and perfusion frequency (f) must be such in order to support and provide sufficient nutrients and oxygen to each and every system without washing away secreted factors, metabolites, and/or drugs (e.g., concentrations of compounds in tissue (Ct) and blood (Cb)) [61, 72, 87]. Liquid-to-cell ratios and liquid residence time can be employed to control oxygen delivery [65], providing the right oxygen concentration for each microenvironment [88] while maintaining oxygen tension at physiological levels [85]. Capillary length and diameter can also affect all of the above parameters [52]. Moreover, within multi-organ-chips, the surface area of each organ is another important designing parameter. It must be relevant to the function of each organ and comparable to that of the other organs in the platform in order to ensure accurate metabolic representation. Cell metabolism may also change during culture as cell maturity develops, which is a factor that needs to be determined prior to the specification of the other principles noted above [89].

On the other hand, there are several parameters that typically remain comparatively obscure, since they relate instead to the characteristics of a specific drug's ADME function. The main parameters that must be considered (to the extent possible) on this front are drug's rate of partitioning into each organ (K), the unbound fraction of a drug (f), intrinsic reaction rate per cell and per drug concentration in tissue (R), blood to plasma partitioning (B:P), and, finally, the drug's intrinsic clearance rate (C). Moreover, the absorption of a molecule, its solubility (S), and permeability (P) through various relevant barriers within the human body (skin, lungs, gut), particle size, $\text{Log}P$, $\text{p}K_a$, and dose all need to be defined [1, 56]. For this purpose, *in vitro* assays or mathematical models can be used.

The success of human-on-a-chip is significantly dependent on the proper scaling of each individual organ so that it remains physiologically relevant to the corresponding *in vivo* organ. For example, if the design of the liver compartment is not in accordance with the other organ compartments, this will lead to an under- or overproduction of metabolites – resulting in a mischaracterization of biological responses and a failure to accurately predict human physiology. Both engineering and biological aspects need to be taken into account in the design and construction of organ-on-a-chip systems. [89].

Although human-on-a-chip represents a powerful tool that can closely mimic human physiology, it still fundamentally remains an *in vitro* system. Therefore, acquired data must always be interpreted within the context of the platform and is not directly scalable in the *in vivo* context. In other words, scaling of the human-on-a-chip must be split into two distinct yet closely associated activities: first, “on-platform scaling” based on functional scaling and only then followed by *in vitro*-*in vivo* translation (IVIVT). In other words, the use of pharmacological models

during the “on-platform scaling” phase aims to identify key specification of the platform (PK and PD) in order to facilitate observations relative to, but not identical to, each organ and the human body – which will then be translated to the *in vivo* context [57]. A step forward on this point was made by Maass et al., using a mechanistic model-based multifunctional scaling method to manufacture single and multi-organ-on-a-chip platforms [90].

Quantitative systems pharmacology (QSP) is a pharmacological model used for the analysis and comprehension of interactions between drugs and a biological system as a whole. Compared to the traditional pharmacokinetic/pharmacodynamics (PKPD) model, which is not directly translatable to multi-organ platform, QSP can integrate mechanistic information from a wide range of data sources – including preclinical data, genetic information, drug properties, and human physiology and pathology – while simultaneously testing hypothesis and extending our understanding to multiple patient populations [59, 91]. This means that organ-on-a-chip-QSP models could potentially be used to predict the PK and PD of a drug, discover disease biomarkers for the use in clinical trials, and help to understand the mechanism of a disease or a drug and its response even for a single individual patient [91]. To cite one example, Edington et al. have recently created a multi-organ-chip platform of up to ten different organs using QSP and PBPK modeling to establish the design of the platform and the interpretation of the data [59]. More about MPS-QSP modeling can be found in an illustrative review by Cirit and Strokes [91].

2.2.4 Cell Sources

One of the key requirements for these systems to be implemented as new screening paradigms is the identification of the optimal source of phenotypically mature and stable cells with the same genetic profile that exhibit the main relevant functions of each original tissue and accurately reproduce human *in vivo* responses [65]. This is much easier said than done – interspecies differences in the genome, drug metabolism, and clearance in many tissues make the extrapolation of the data from an animal to a human population extremely challenging [92, 93]. Therefore, the use of human cells is a functional prerequisite (Fig. 5).

A source widely used in many organ-on-a-chip studies is established human cell lines (either cancer-derived or immortalized) to model complex functions within single organs (e.g., lungs [14] or muscle [94]) or observe multi-organ interactions. However, the use of such established cell lines prevents the study of personalized platforms and ignores the potential for strong genetic variations in drug responses that could highlight toxic responses to certain drugs within certain subpopulations. Moreover, in many cases the expression of key components in such cell lines differs substantially from that seen in primary tissue. For example, the most commonly used hepatocyte lines (HepG2, Huh7, and Hep3B) all derive from tumors that exhibit lower or variable expression of many important CYP450 functions when compared with the primary human hepatocytes [95]. Since the liver is the main organ for the

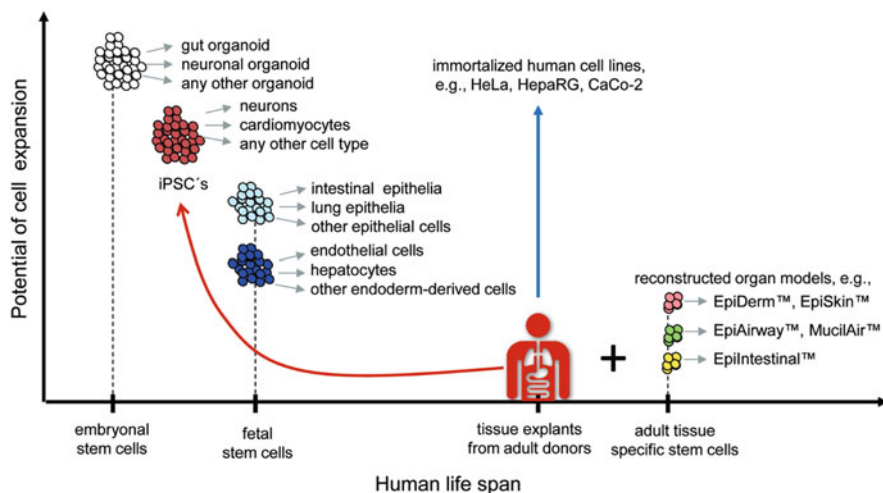


Fig. 5 Human cell and tissue sources to be used in multi-organ systems. The vertical axis illustrates the expansion potential of different human cell and tissue sources compared plotted against their appearance in the human life span, as illustrated in the horizontal axis. Grey arrows illustrate the differentiation potential of each stem cell pool. Red arrow illustrates the induction back to pluripotency (iPSCs). Blue arrow indicates the unlimited expansion potential that immortalized cell lines have. From “Biology-inspired microphysiological system approaches to solve the prediction dilemma of substance testing” by Marx et al. [4], ALTEX, 33(3), 272–321. Reprinted under the terms of the Creative Commons Attribution 4.0 International license

metabolism of drugs, the need for complementary approaches under these circumstances is clear.

One alternative approach is to use primary cells, isolated through biopsies and/or tissue explants, to provide cultures with a phenotype that is very close to the tissue of origin in its mature state. Tissue biopsies from donors and primary cell lines have also been used for the establishment of multi-organ-chip platforms [58, 96]. One issue with these cell lines is that their functional (i.e., protein and gene expression) and structural characteristics are frequently altered shortly after their isolation and establishment of culture, because of the extreme changes their microenvironment has undergone [97]. A solution might be to instead use organoids isolated from human adult stem cells or established from hiPSCs. A combination of the microfluidic organ-on-a-chip and organoid technology could potentially be adopted to develop disease models with tissues directly isolated from patients. One example of an autologous multi-organ-chip has recently been published by Ramme et al. and features interconnecting miniaturized human intestine, liver, brain, and kidney equivalents. All four organ models were pre-differentiated from induced pluripotent stem cells obtained from the same healthy donor, before being successfully reintegrated into a microphysiological system and cultured in a common medium for 14 days [66].

2.2.5 Medium

For the proper function of the multi-organ-chip, there is also an indisputable need for a common media that can perfuse the different organ-on-a-chips [16, 76]. The role of this medium is to serve as a blood surrogate. To accomplish this task, the medium must be able to deliver sufficient oxygen to the different cellular compartments while simultaneously removing CO₂ using oxygen carriers such as hemoglobin or a perfluorocarbon oxygen carrier. And an equally important role is that of providing the required transport proteins for the communication between the different organs while promoting the maintenance of intracellular ions and transport proteins. It also needs to be able to maintain the osmolarity, pH, and salinity of the entire system at the proper levels [16].

Suffice to say, combining all of these complex functions in a single material is no easy task – particularly because different cells can have radically different needs. A particularly compelling example is TGF- β 1 (transforming growth factor beta-1), since it is important for the proliferation and growth of A549 lung cells but inhibits that of hepatocellular carcinoma cells. To overcome this, Zhang et al. managed to create an isolated cell-specific microenvironment in the A549 compartment of their platform where TGF- β 1 was controlled-released by gelatin microspheres mixed with cells [98]. Nevertheless, endothelial (vascular) and epithelial barriers may promote the establishment of such isolated cellular microenvironments controlling the release of factors. Moreover, as far as the concentration of factors in the medium is concerned, the frequency of changing medium and replenishing of water to account for evaporation and consumption must be carefully evaluated, so as not to cause any unwanted dilution of secreted metabolites. Special care must also be taken when choosing the right concentration of a drug or toxin where the active compound is a product of cell metabolism or signaling. In such a case, dilution is determined by the number of cells and must be carefully evaluated to avoid excess dilution that could affect the readout of the experiment [16].

An alternative solution to the common medium problem is based on the hypothesis that by first conditioning the cells in their established organ medium, components that are fundamental for the growth of one tissue but toxic for another can be sufficiently metabolized before the media is ever exchanged [99].

To date, different approaches have been adopted from different groups to overcome the common medium problem. Vascularization of the microchannels of the platform with endothelial cells forming a barrier corresponding to that found in the human body represents an important advancement in surmounting this problem. A tissue-blood separation can allow each organ to be conditioned and cultured on its tissue-specific medium while still permitting organ crosstalk through the vascular connections. In this approach, tissue-specific molecules are isolated and consumed by the targeted tissue while communications remain possible via secreted biomarker, cytokines, or secreted vesicles (e.g., exosomes). Notably, however, endothelial barriers can substantially contribute to drug absorption, distribution, metabolism, excretion, and toxicity – meaning that their absence could significantly affect PK

studies [100, 101]. Recently, a vascular endothelium was incorporated in an eight-organ platform by Novak et al., to create a tissue-tissue interface. Specifically, two parallel and continuously perfused microchannels were separated by a porous membrane that was seeded with human organ-specific parenchymal and vascular endothelial cells on each side. A common medium (blood substitute) was used for the perfusion of the vascular channel, while an organ-specific medium was used for the parenchymal channel except of lung and skin when it was exposed to an air-liquid interface [102]. More about the importance and current models of the vasculature-on-chip can be found in a recent review by Pollet and den Toonder [103].

2.2.6 Sensory Systems (Instrumentation)

As the development of organ-on-a-chip platforms advances, there has been increasing recognition of the need for an integrated multi-sensor to monitor changes in the system in real time [52, 89]. Monitoring a large number of functions and variables (structure and function) that characterize the microenvironment parameters as a response to pharmaceutical compounds in a continuous, automated, and noninvasive manner is critical [77]. The ability to conduct long-term in situ assessment of both biochemical and biophysical parameters continues to pose substantial challenges. Biofouling (especially when electrodes are used) and inconsistent functional reading affects many sensing components that are maintained for long-term use. Their use is also fundamentally limited by biocompatibility and system integration issues [1].

Until analytical chemistry becomes possible to conduct in low volumes, determining the best trade-off between sampling frequency, sampling volume, and the number of analytes that can be quantified will continue to impose yet another challenge. Many approaches used in cell culture (e.g., ELISA, western blot, fluorescence- or label-free assays such as RT-PCR, mRNA arrays) to capture and quantify soluble factors, capillary electrophoresis, and mass spectrometry (MS) represent examples of existing off-chip sensor technology that can be used to characterize the dynamic state of organ-on-a-chips [52].

Optical sensors are one of the most popular integrated sensors within organ-on-chips, since they are highly sensitive, are easily miniaturized, can precisely detect changes using near-neglectable amounts of analytes, and can reliably perform even under a dynamic range of flow rates [85]. The broad category of optical sensors can be subdivided into absorbance-, fluorescence intensity-, and surface plasmon-based sensors [1]. Drawbacks associated with the use of optical sensors include the fact that the dyes used may influence the metabolism of the cells, and serial measurement can also lead to photobleaching and phototoxicity [16]. Moreover, the number of dyes that can be monitored simultaneously is inherently limited as a result of spectral overlap [104]. To date, however, optical imaging has successfully been designed to detect alteration in oxygen and pH indicators [85].

Electrical and electrochemical sensors can also be deployed to measure key parameters such as pH, glucose, lactate, and oxygen concentrations, as well as

secreted biomarkers [105]. Electrochemical sensors have the advantage of directly and rapidly detecting a biological event as an electrical signal and being able to specifically quantify metabolites. Despite their high sensitivity and miniaturization capabilities, however, they can easily be affected by electrode position or size and biofouling, and they too can potentially interfere with biochemical species in the culture medium and flow rate. Electrochemical-based sensors have been extended to transepithelial electrical resistance (TEER) sensors – a nondestructive, real-time, and label-free method [1] that has been integrated to organ-on-a-chip platforms to measure the integrity of tissue junction dynamics of endothelial and epithelial cells. Another type of electrical sensors is the biochemical biosensors for monitoring of secreted biomarkers. Microfluidic immunoassays capable of detecting multiple proteins at low concentrations in small volumes [106] have found application in many organ-on-a-chip devices for the in situ monitoring of a number of secreted biomarkers [77, 107, 108].

Considering the small volume of the organ-on-chip platforms, the risk of interference between the different sensing methods should not be ignored [52]. Ideally, the different sensors should be harmoniously integrated within a multi-sensor system, so that electrical and electrochemical sensors are used wherever possible to free up the optical bandwidth for measurements that cannot be done electrochemically – such as fluorescent measurements taken via optical sensors [52, 104]. This approach was recently applied in a study by Zhang et al. that successfully integrated a microfluidic controlling breadboard for timed routing of fluids, physical sensors for monitoring extracellular microenvironment parameters (e.g., pH, oxygen, temperature), regenerating electrochemical sensors for measuring soluble protein biomarkers, and miniature microscopes for observation of organoid morphologies [77].

Potential morphological changes of the cellular compartment must also be carefully monitored. Impedance sensors, quartz crystal microbalance (QCM) systems, surface plasmon resonance (SPR) systems, and surface acoustic wave (SAW) systems can be used. Furthermore, when modeling a pathophysiological condition on a chip, an endpoint analysis should include the assessment of the restoration of the physiological organ function and pathohistology [4]. The tissue can then be histologically sectioned for immunostaining and in situ hybridization after the termination of the experiment (if allowed by its thickness).

Finally, in a dynamic platform connecting a collection of organs, it is challenging to constantly remain at a stable equilibrium. Therefore, for homeostasis to be maintained, there is a need for an automated dynamic regulatory multisensory system responsible to precisely monitor the physicochemical changes in the platform, while actuators control and stabilize the system. The “Emerging Biosensor Trends in Organs-on-a-Chip” will be further discussed in the chapter (this volume) by Rothbauer and Ertl [109].

2.3 *Generated Multi-organ Platforms*

The interconnection of different organ-on-a-chip through microfluidics on the same platform (i.e., a multi-organ platform) has been reported several times with different organ combinations, aims (e.g., disease modeling or drug toxicity assessment), and design principles (e.g., single-pass perfusion or recirculating microfluidic flow) (Table 2). In single-pass perfusion platforms, multiple organs may be unidirectionally connected in parallel, in series, or both. Multi-organ platforms have been developed using this design approach and can be used to model drug transport from one organ to the other while mimicking crosstalk between the organs [45, 118]. However, the design of these systems currently limits the crosstalk of an organ or a drug to only those organs that are located “downstream” within the system.

On the other hand, multi-organ platforms connected with a recirculating perfusion system are much closer to actual human physiology (i.e., mimicking true blood circulation) and thus enable the communication of the various organs both downstream and upstream within a system. Shuler’s group pioneered the development of a chip-based micro-cell culture analog (μ CCA) that was subsequently used by Sin et al., in pharmacokinetic/pharmacodynamic (PK/PD) modeling with real-time oxygen sensors [119]. This μ CCA system has also been further developed since by Esch et al., who have used a two-organ chip (liver-gut) based on the μ CCA platform to test the effect of the ingested carboxylated polystyrene nanoparticles in the system, showing potential liver injury [112]. Oleaga et al. have even expanded this system to a four-organ chip, consisting of human cardiac, liver, skeletal muscle, and neuronal tissues. All of these different tissues were perfused with a common serum-free medium that was able to maintain functional cultures for a period of 2 weeks. The platform was used for toxicity testing, to assess the multi-organ toxicity response after exposure to several well-known cytotoxic compounds including doxorubicin, atorvastatin, valproic acid, acetaminophen, and N-acetylaminophenol [117]. A variety of other systemic arrangements have also been attempted by different groups. Of note, Zhang et al. have developed a five-organ platform with four separate channel-based cell culture space creating isolated cell-specific microenvironments [98]. Using a different approach, Zhang et al. have also developed a liver-heart and liver-cancer-heart modular platform with integrated sensors for measurements of environmental parameters, immune biosensors, and miniature microscopes that was used for toxicity testing [77].

A very different approach was pioneered by the group of Uwe Marx, which developed a multi-organ-on-a-chip (MOC) prototype with robust peristaltic on-chip micropumps in order to avoid nonphysiological fluid-to-tissue ratios. 3D cell spheroids, reconstructed tissue equivalents, and donor-derived tissue explants or biopsies can all be cultured in this platform [4]. Human liver spheroids (hepatocytes and stellate cells) and skin biopsies have also been successfully cultured on this MOC platform, evidencing tissue crosstalk that revealed a dose-dependent toxic response to exposure to troglitazone [120]. A further step forward was made by Maschmeyer et al. when they incorporated barrier tissues (intestine and skin) with parenchymal

Table 2 Examples of multi-organ-on-a-chip platforms

Organ combination	Perfusion	Tested drug/toxin	References
<i>Two-organ platform</i>			
Heart-liver-vascular tissue	High-pressure pulsatile flow	None	[110]
Liver-tumor	External peristaltic pump	Cyclophosphamide	[111]
GI tract-liver-other organs' system	Peristaltic pump for two fluidic circuits	Carboxylated polystyrene nanoparticles	[112]
Liver-intestine and liver-skin	On-chip micropump	Troglitazone	[76]
Liver-neurospheres	On-chip micropump	Hexanedione	[113]
Liver-pancreas	On-chip micropump	None	[51]
Gut-liver	Onboard pneumatic microfluidic pumping	None	[63]
Gut-liver	On-chip pumps	Diclofenac, hydrocortisone	[86]
Liver-heart and liver-cancer-heart	Microfluidics-controlling breadboard	Capecitabine, acetaminophen, doxorubicin	[77]
Skin-tumor (lung)	Peristaltic micropump	Anti-EGFR antibody cetuximab	[114]
Heart-liver body-on-a-chip system with a skin surrogate	Pumpless, flow driven by a rocking platform	Diclofenac, ketocozazole, hydrocortisone, acetaminophen	[115]
Liver-testis equivalents with hepatic stellate cells	On-chip peristaltic pump	Cyclophosphamide	[116]
<i>Four-organ platforms</i>			
Liver-lung-kidney-fat	Peristaltic pump	None	[98]
Intestine-liver-skin-kidney	On-chip micropump	None	[58]
Cardiac-muscle-neuronal-liver	Pumpless, gravity-driven flow	Doxorubicin, atorvastatin, valproic acid, acetaminophen	[117]
Intestine-liver-kidney-BBB	Manual transfer of media supernatant	None	[118]
Intestine, liver, brain-kidney	On-chip micropumps	None	[66]
<i>Up to ten-organ platform</i>			
Ovary-fallopian tube-uterus-cervix-liver	Four-port peristaltic pump structure	None	[62]

(continued)

Table 2 (continued)

Organ combination	Perfusion	Tested drug/toxin	References
4-MPS: Liver-gut-endometrium-lung 7-MPS: 4-MPS-pancreas-heart-brain 10-MPS: 7-MPS-muscle-skin-kidney	A high degree-of-freedom (DOF) onboard pumping system with separate high-capacity recirculation pumps for each MPS, flow-through microperfusion, and a system of spillway channels	Diclofenac (DCF)	[59]
Intestine-liver-kidney-heart-lung-skin-brain (vascularized)	Automatic and regular robotic transfer of liquid samples between individual organ chips that are each continuously perfused Perfusion pumps assigned to each of the organ chips to ensure that they experience continuous fluid flow independently of the action of the robotic fluid transfer system	Inulin-FITC distribution	[102]

organ (liver) in a platform with entirely endothelialized microfluidic channels, to mimic vasculature [76]. Using different routes of administration (i.e., systemic, oral, or dermal), repeated dose testing for troglitazone was performed for 9–11 days. The same platform was thereafter used to co-culture human artificial liver microtissues and human neurospheres (neuronal spheroids) for long-term exposure to hexanedione (xenobiotic) and showed increased sensitivity when compared to respective single-tissue cultures [113]. The integration of a biological vasculature with physiological fluid-to-tissue ratios allowed the use of the platform for long-term repeated dose substance evaluation at homeostatic conditions [81]. Human small intestine, liver spheroids, skin biopsy, and a proximal tubule cell monolayer barrier (kidney) were interconnected and remained functional thereafter for 28 days [58]. This means that a 28-day co-culture of four-organ chip could be established for *in vitro* ADMET testing and repeated dose toxicity testing of drug candidates. Furthermore, a two-organ chip interconnecting pancreatic islets and liver spheroid was successfully established to study the organ crosstalk based on insulin and glucose regulation for up to 15 days, in an experiment aimed at modeling human type 2 diabetes mellitus [51] (Fig. 6).

Yet another approach involves using alternate materials (i.e., other than PDMS) that show no drug absorption, small volumes, and an open platform configuration to enable media sampling and high-content measurements and computational models for experimental designing [59, 63, 86]. A gut-liver platform with these characteristics has been successfully deployed for quantitative pharmacokinetic studies [86] and inflammation interactions [63]. The system has since been further extended to four-organ, seven-organ, and ten-organ chip devices [59].

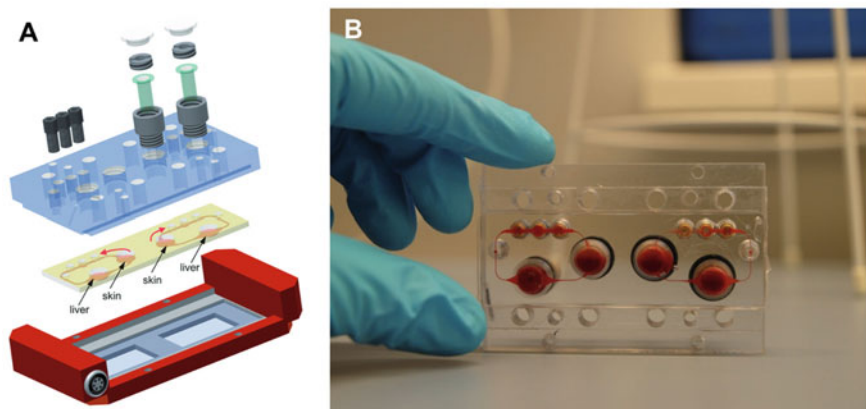


Fig. 6 A multi-organ-chip platform. **(a)** A PDMS chip (yellow), with two independent microcircuits each connecting two tissue culture compartments. The platform supports the integration of 3D tissues, such as cell spheroids, and standard 96-well inserts for reconstructed barrier organ models. A peristaltic on-chip micropump (black) enables pulsatile unidirectional fluid flow at physiological frequencies. **(b)** Two blood-perfused circuits (worm’s-eye view). From “Biology-inspired microphysiological system approaches to solve the prediction dilemma of substance testing” by Marx et al. [4], *ALTEX*, 33(3), 272–321. Reprinted under the terms of the Creative Commons Attribution 4.0 International license

2.4 Commercialization

It is widely acknowledged that the current cost of drug development is commercially unsustainable in the long run [80]. In an effort to mitigate this problem, significant and growing attention has been focused on organ-on-chip platforms, and many large pharmaceutical companies, including Roche [40], Pfizer [70], Bayer [114], and AstraZeneca [51, 121], have entered into collaborations aimed at developing and using this emerging technology in the R&D space. More can be found at a recent review by Marx et al. [74]. Apart from single organ-on-chip units, a multi-organ-chip platform mimicking human physiology would be extremely useful not only in the pharmaceutical sphere but also with respect to environmental toxicants [17] in the cosmetics industry [4] and for the future development of products that involve tobacco inhalation [4, 23, 35]. Multi-organ-chip platforms have already been made commercially available by TissUse GmbH, Germany; CN Bio, UK; InSphero AG, Switzerland; Draper, USA; and Hesperos Corporation, USA. A more in-depth overview of commercialization attempts to date can be found on a review by Zhang et al. [122].

Considering all the promising potential applications for a sophisticated human-on-a-chip platform, it is perhaps not surprising that no single specialized design will be the right “fit” for all experiments. Yet this raises an important question: How can a sophisticated yet complex platform be commercialized if it is not suitable for a wide range of experiments? It is clear that the ideal system must be flexible and modular,

allowing for easy physical reconfigurability and reprogrammable organ configuration within a dynamic system in which fluid paths and rates can be carefully monitored and controlled. Moreover, it goes without saying that any commercially viable system will require a substantial amount of scientific data and cross-pharma testing and validation to ensure reliability, robustness, and reproducibility. This will be no easy feat to achieve.

2.5 Ongoing Research

Over the past few years, a number of sophisticated multi-organ platforms have been successfully developed. The next goal must be the successful integration, within the same platform, of a minimum of ten interconnected organs that collectively emulate minimal organismal functionality across the human body, i.e., the circulatory, endocrine, gastrointestinal, immune, integumentary, musculoskeletal, nervous, reproductive, respiratory, and urinary functions [4]. The precise number has yet to be defined by the scientific community and regulatory bodies – but to date, a combination of up to 13 organ compartments on one chip (including barrier and non-barrier tissues) by Miller and Shuler represents the highest number attempted. The culture of five different cell lines for 7 days has also been successfully demonstrated [84].

A number of recent initiatives have emerged that are aimed at advancing organ-on-a-chip platforms to a human-on-a-chip model, with an initial focus on emulating the normal physiology of nonpregnant adulthood. The first prototypes of these initiatives currently remain in the experimental evaluative phase (Fig. 7). More about the aims and state-of-art of each of these exciting initiatives can be found in a review by Marx et al. [4].

3 Conclusion and Outlook

The complex nature of human physiology and organ system structure has been a major hurdle in studying the different processes of the human body in a truly systemic manner. The lack of a physiologically relevant model continues to significantly impact the cost and pace of drug development. Nevertheless, although the technology still remains in its infancy, the emergence of organ-on-a-chip tools has increasingly started to open up new and promising avenues in this direction. Owing to great recent advances of the field, the integration of multiple organs into one platform has now been achieved, and various combinations, designs, and end-goals are increasingly being explored by researchers.

The ultimate goal in this field is the development of a biomimetic, sophisticated, and reliable platform – namely, the “human-on-a-chip” – which accurately emulates the complexity of human physiology and can be successfully used in drug

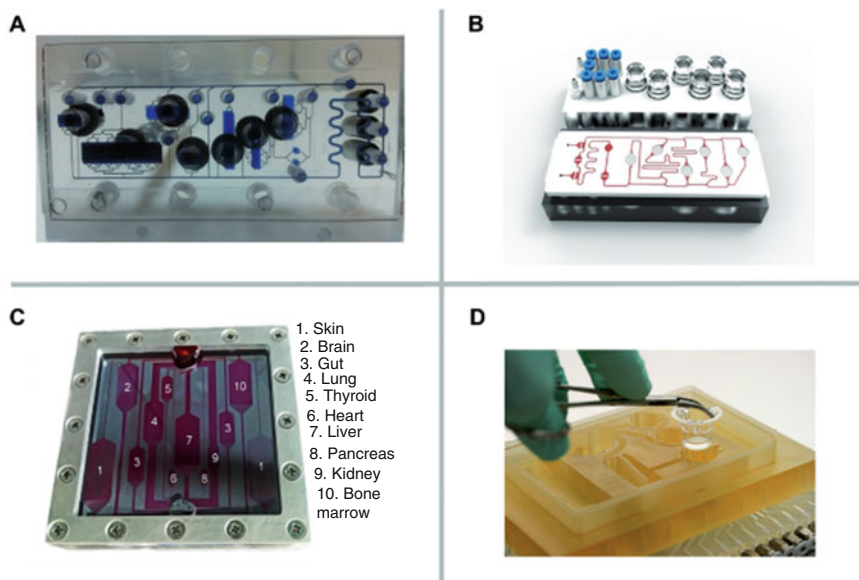


Fig. 7 Prototypes of human-on-a-chip platforms. Images illustrate four multi-organ prototypes in experimental evaluation that by increasing the level of complexity and number of organs involved aim to the development of a human-on-a-chip platform. (a) The ten-organ prototype of TissUse GmbH, Germany (“GO-Bio-MOC” program); (b) the six-organ prototype of Bioclinicum, Russia (“Homunculus” program); (c) the ten-organ prototype of Cornell University, USA; and (d) a four-way PhysioMimetics prototype of MIT, USA (“Human Physiome on a Chip Program,” US DARPA/NIH/FDA MPS initiative). From “Biology-inspired microphysiological system approaches to solve the prediction dilemma of substance testing” by Marx et al. [4], *ALTEX*, 33 (3), 272–321. Reprinted under the terms of the Creative Commons Attribution 4.0 International license

development. Such a powerful tool would immediately find application across many different fields. Nevertheless, the unprecedented complexity of this ideal system continues to pose major engineering and biological challenges that must be overcome by future research. The development of a modular platform, and a “plug-and-play” architecture, can potentially help in speeding up the commercialization of a multi-organ or human-on-chip platform.

Notwithstanding the promising advances discussed above in various aspects of the organ-on-a-chip field, the development of a platform that successfully integrates a multi-sensor or actuator system that can monitor (in real-time) the responses of more than ten different physiologically interconnected and fully functional organ tissues with accurate crosstalk for more than a month remains far out of reach. Nevertheless, the pace of recent progress in pursuit of this ideal has been stunning. The authors fully anticipate that more sophisticated systems will continue to be developed in the coming years, as new innovations become available and pave the way for new targeted therapeutics and ever-more-personalized approaches.

References

1. Ahadian S, Civitarese R, Bannerman D, Mohammadi MH, Lu R, Wang E, Davenport-Huyer L, Lai B, Zhang B, Zhao Y, Mandla S, Korolj A, Radisic M (2018) Organ-on-a-chip platforms: a convergence of advanced materials, cells, and microscale technologies. *Adv Healthc Mater* 7 (2):1–53. <https://doi.org/10.1002/adhm.201700506>
2. Esch MB, Smith AST, Prot J-M, Oleaga C, Hickman JJ, Shuler ML (2014b) How multi-organ microdevices can help foster drug development. *Adv Drug Deliv Rev* 69–70(1):158–169. <https://doi.org/10.1016/j.addr.2013.12.003>
3. PhRMA (2015) Biopharmaceutical research & development: the process behind new medicines. http://phrma-docs.phrma.org/sites/default/files/pdf/rd_brochure_022307.pdf
4. Marx U, Andersson TB, Bahinski A, Beilmann M, Beken S, Cassee FR, Cirit M, Daneshian M, Fitzpatrick S, Frey O, Gaertner C, Giese C, Griffith L, Hartung T, Heringa MB, Hoeng J, Roth A (2016) Biology-inspired microphysiological system approaches to solve the prediction dilemma of substance testing. *ALTEX* 33(3):272–321. <https://doi.org/10.14573/altex.1603161>
5. Bhise NS, Ribas J, Manoharan V, Zhang YS, Polini A, Massa S, Dokmeci MR, Khademhosseini A (2014) Organ-on-a-chip platforms for studying drug delivery systems. *J Control Release* 190:82–93. <https://doi.org/10.1016/j.jconrel.2014.05.004>
6. Kimura H, Sakai Y, Fujii T (2018) Organ/body-on-a-chip based on microfluidic technology for drug discovery. *Drug Metab Pharmacokinet* 33(1):43–48. <https://doi.org/10.1016/j.dmpk.2017.11.003>
7. Balijepalli A, Sivaramakrishnan V (2017) Organs-on-chips: research and commercial perspectives. *Drug Discov Today* 22(2):397–403. <https://doi.org/10.1016/j.drudis.2016.11.009>
8. Suntharalingam G, Perry MR, Ward S, Brett SJ, Castello-Cortes A, Brunner MD, Panoskaltis N (2006) Cytokine storm in a phase 1 trial of the anti-CD28 monoclonal antibody TGN1412. *N Engl J Med* 355(10):1018–1028. <https://doi.org/10.1056/NEJMoa063842>
9. Hansen S, Leslie RGQ (2006) TGN1412: scrutinizing preclinical trials of antibody-based medicines drug giants hamstrung by supporting the use of. *Nature* 441(May):2006–2006. <https://doi.org/10.1038/441282a>
10. Bhatia SN, Ingber DE (2014) Microfluidic organs-on-chips. *Nat Biotechnol* 32(8):760–772. <https://doi.org/10.1038/nbt.2989>
11. van Duinen V, Trietsch SJ, Joore J, Vulto P, Hankemeier T (2015) Microfluidic 3D cell culture: from tools to tissue models. *Curr Opin Biotechnol* 35:118–126. <https://doi.org/10.1016/j.copbio.2015.05.002>
12. Mammoto T, Mammoto A, Ingber DE (2013) Mechanobiology and developmental control. *Annu Rev Cell Dev Biol* 29(1):27–61. <https://doi.org/10.1146/annurev-cellbio-101512-122340>
13. Park TH, Shuler ML (2003) Integration of cell culture and microfabrication technology. *Biotechnol Prog* 19(2):243–253. <https://doi.org/10.1021/bp020143k>
14. Huh D, Matthews BD, Mammoto A, Montoya-Zavala M, Hsin HY, Ingber DE (2010) Reconstituting organ-level lung functions on a chip. *Science* 328(5986):1662–1668. <https://doi.org/10.1126/science.1188302>
15. Valencia PM, Farokhzad OC, Karnik R, Langer R (2012) Microfluidic technologies for accelerating the clinical translation of nanoparticles. *Nat Nanotechnol* 7(10):623–629. <https://doi.org/10.1038/nnano.2012.168>
16. Wikswo JP (2014) The relevance and potential roles of microphysiological systems in biology and medicine. *Exp Biol Med* 239(9):1061–1072. <https://doi.org/10.1177/1535370214542068>
17. Cho S, Yoon JY (2017) Organ-on-a-chip for assessing environmental toxicants. *Curr Opin Biotechnol* 45(January):34–42. <https://doi.org/10.1016/j.copbio.2016.11.019>
18. Ronaldson-Bouchard K, Vunjak-Novakovic G (2018) Organs-on-a-chip: a fast track for engineered human tissues in drug development. *Cell Stem Cell* 22(3):310–324. <https://doi.org/10.1016/j.stem.2018.02.011>

19. Zhu J, He J, Verano M, Brimmo AT, Glia A, Qasaimeh MA, Chen P, Aleman JO, Chen W (2018) An integrated adipose-tissue-on-chip nanoplasmonic biosensing platform for investigating obesity-associated inflammation. *Lab Chip* 18(23):3550–3560. <https://doi.org/10.1039/C8LC00605A>
20. de Peppo GM, Marcos-Campos I, Kahler DJ, Alsalman D, Shang L, Vunjak-Novakovic G, Marolt D (2013) Engineering bone tissue substitutes from human induced pluripotent stem cells. *Proc Natl Acad Sci* 110(21):8680–8685. <https://doi.org/10.1073/pnas.1301190110>
21. Lozito TP, Alexander PG, Lin H, Gottardi R, Cheng A, Tuan RS (2013) Three-dimensional osteochondral microtissue to model pathogenesis of osteoarthritis. *Stem Cell Res Ther* 4(Suppl 1):S6. <https://doi.org/10.1186/scrt367>
22. Brown JA, Pensabene V, Markov DA, Allwardt V, Diana Neely M, Shi M, Britt CM, Hoillett OS, Yang Q, Brewer BM, Samson PC, McCawley LJ, May JM, Webb DJ, Li D, Bowman AB, Reiserer RS, Wikswa JP (2015) Recreating blood-brain barrier physiology and structure on chip: a novel neurovascular microfluidic bioreactor. *Biomicrofluidics* 9(5):1–15. <https://doi.org/10.1063/1.4934713>
23. Wang Y, Wang L, Zhu Y, Qin J (2018) Human brain organoid-on-a-chip to model prenatal nicotine exposure. *Lab Chip* 18(6):851–860. <https://doi.org/10.1039/C7LC01084B>
24. Chou DB, Frisimantas V, Milton Y, David R, Pop-Damkov P, Ferguson D, MacDonald A, Vargel Bölükbaşı Ö, Joyce CE, Moreira Teixeira LS, Rech A, Jiang A, Calamari E, Jalili-Firoozinezhad S, Furlong BA, O'Sullivan LR, Ng CF, Choe Y, Marquez S et al (2020) On-chip recapitulation of clinical bone marrow toxicities and patient-specific pathophysiology. *Nat Biomed Eng*. <https://doi.org/10.1038/s41551-019-0495-z>
25. Sontheimer-Phelps A, Chou DB, Tovaglieri A, Ferrante TC, Duckworth T, Fadel C, Frisimantas V, Sutherland AD, Jalili-Firoozinezhad S, Kasendra M, Stas E, Weaver JC, Richmond CA, Levy O, Prantil-Baun R, Breault DT, Ingber DE (2019) Human colon-on-a-chip enables continuous *in vitro* analysis of colon mucus layer accumulation and physiology. *Cell Mol Gastroenterol Hepatol*. <https://doi.org/10.1016/j.jcmgh.2019.11.008>
26. Kim HJ, Huh D, Hamilton G, Ingber DE (2012) Human gut-on-a-chip inhabited by microbial flora that experiences intestinal peristalsis-like motions and flow. *Lab Chip* 12(12):2165–2174. <https://doi.org/10.1039/c2lc40074j>
27. Foulke-Abel J, In J, Yin J, Zachos NC, Kovbasnjuk O, Estes MK, de Jonge H, Donowitz M (2016) Human Enteroids as a model of upper small intestinal ion transport physiology and pathophysiology. *Gastroenterology* 150(3):638–649e8. <https://doi.org/10.1053/j.gastro.2015.11.047>
28. Mathur A, Loskill P, Shao K, Huebsch N, Hong SG, Marcus SG, Marks N, Mandegar M, Conklin BR, Lee LP, Healy KE (2015) Human iPSC-based cardiac microphysiological system for drug screening applications. *Sci Rep* 5:1–7. <https://doi.org/10.1038/srep08883>
29. Lind JU, Busbee TA, Valentine AD, Pasqualini FS, Yuan H, Yadid M, Park SJ, Kotikian A, Nesmith AP, Campbell PH, Vlassak JJ, Lewis JA, Parker KK (2017) Instrumented cardiac microphysiological devices via multimaterial three-dimensional printing. *Nat Mater* 16(3):303–308. <https://doi.org/10.1038/nmat4782>
30. Weber EJ, Chapron A, Chapron BD, Voellinger JL, Lidberg KA, Yeung CK, Wang Z, Yamaura Y, Hailey DW, Neumann T, Shen DD, Thummel KE, Muczynski KA, Himmelfarb J, Kelly EJ (2016) Development of a microphysiological model of human kidney proximal tubule function. *Kidney Int* 90(3):627–637. <https://doi.org/10.1016/j.kint.2016.06.011>
31. Vedula EM, Alonso JL, Arnaut MA, Charest JL (2017) A microfluidic renal proximal tubule with active reabsorptive function. *PLoS One* 12(10):1–15. <https://doi.org/10.1371/journal.pone.0184330>
32. Verneti LA, Senutovitch N, Boltz R, DeBiasio R, Ying Shun T, Gough A, Taylor DL (2016) A human liver microphysiology platform for investigating physiology, drug safety, and disease models. *Exp Biol Med* 241(1):101–114. <https://doi.org/10.1177/1535370215592121>

33. Bhise NS, Manoharan V, Massa S, Tamayol A, Ghaderi M, Miscuglio M, Lang Q, Zhang YS, Shin SR, Calzone G, Annabi N, Shupe TD, Bishop CE, Atala A, Dokmeci MR, Khademhosseini A (2016) A liver-on-a-chip platform with bioprinted hepatic spheroids. *Biofabrication* 8(1):014101. <https://doi.org/10.1088/1758-5090/8/1/014101>
34. Jang KJ, Otieno MA, Ronxhi J, Lim HK, Ewart L, Kodella KR, Petropolis DB, Kulkarni G, Rubins JE, Conegliano D, Nawroth J, Simic D, Lam W, Singer M, Barale E, Singh B, Sonee M, Streeter AJ, Manthey C et al (2019) Reproducing human and cross-species drug toxicities using a liver-Chip. *Sci Transl Med* 11(517). <https://doi.org/10.1126/scitranslmed.aax5516>
35. Benam KH, Villenave R, Lucchesi C, Varone A, Hubeau C, Lee HH, Alves SE, Salmon M, Ferrante TC, Weaver JC, Bahinski A, Hamilton GA, Ingber DE (2016b) Small airway-on-a-chip enables analysis of human lung inflammation and drug responses in vitro. *Nat Methods* 13(2):151–157. <https://doi.org/10.1038/nmeth.3697>
36. Zamprogno P, Wüthrich S, Achenbach S, Stucki JD, Hobi N, Schneider-Daum N, Lehr C-M, Huwer H, Geiser T, Schmid RA, Guenat OT (2019) Second-generation lung-on-a-chip array with a stretchable biological membrane. *BioRxiv*, 608919. <https://doi.org/10.1101/608919>
37. Agrawal G, Aung A, Varghese S (2017) Skeletal muscle-on-a-chip: an in vitro model to evaluate tissue formation and injury. *Lab Chip* 17(20):3447–3461. <https://doi.org/10.1039/c7lc00512a>
38. Silva PN, Green BJ, Altamentova SM, Rocheleau JV (2013) A microfluidic device designed to induce media flow throughout pancreatic islets while limiting shear-induced damage. *Lab Chip* 13(22):4374–4384. <https://doi.org/10.1039/c3lc50680k>
39. Xu Z, Li E, Guo Z, Yu R, Hao H, Xu Y, Sun Z, Li X, Lyu J, Wang Q (2016) Design and construction of a multi-organ microfluidic Chip mimicking the in vivo microenvironment of lung cancer metastasis. *ACS Appl Mater Interfaces* 8(39):25840–25847. <https://doi.org/10.1021/acsami.6b08746>
40. Achberger K, Probst C, Haderspeck JC, Bolz S, Rogal J, Chuchuy J, Nikolova M, Cora V, Antkowiak L, Haq W, Shen N, Schenke-Layland K, Ueffing M, Liebau S, Loskill P (2019) Merging organoid and organ-on-a-chip technology to generate complex multi-layer tissue models in a human retina-on-a-chip platform. *elife* 8:1–26. <https://doi.org/10.7554/eLife.46188>
41. Ataç B, Wagner I, Horland R, Lauster R, Marx U, Tonevitsky AG, Azar RP, Lindner G (2013) Skin and hair on-a-chip: in vitro skin models versus ex vivo tissue maintenance with dynamic perfusion. *Lab Chip* 13(18):3555–3561. <https://doi.org/10.1039/c3lc50227a>
42. Abaci HE, Guo Z, Coffman A, Gillette B, Lee WH, Sia SK, Christiano AM (2016) Human skin constructs with spatially controlled vasculature using primary and iPSC-derived endothelial cells. *Adv Healthc Mater* 5(14):1800–1807. <https://doi.org/10.1002/adhm.201500936>
43. Lee KK, McCauley HA, Broda TR, Kofron MJ, Wells JM, Hong CI (2018) Human stomach-on-a-chip with luminal flow and peristaltic-like motility. *Lab Chip* 18(20):3079–3085. <https://doi.org/10.1039/C8LC00910D>
44. Belair DG, Whisler JA, Valdez J, Velazquez J, Molenda JA, Vickerman V, Lewis R, Daigh C, Hansen TD, Mann DA, Thomson JA, Griffith LG, Kamm RD, Schwartz MP, Murphy WL (2015) Human vascular tissue models formed from human induced pluripotent stem cell derived endothelial cells. *Stem Cell Rev Rep* 11(3):511–525. <https://doi.org/10.1007/s12015-014-9549-5>
45. Phan DTT, Wang X, Craver BM, Sobrino A, Zhao D, Chen JC, Lee LYN, George SC, Lee AP, Hughes CCW (2017) A vascularized and perfused organ-on-a-chip platform for large-scale drug screening applications. *Lab Chip* 17(3):511–520. <https://doi.org/10.1039/c6lc01422d>
46. Poussin C, Kramer B, Lanz HL, Van den Heuvel A, Laurent A, Olivier T, Vermeer M, Peric D, Baumer K, Dulize R, Guedj E, Ivanov NV, Peitsch MC, Hoeng J, Joore J (2020) 3D human microvessel-on-a-chip model for studying monocyte-to-endothelium adhesion under flow - application in systems toxicology. *Altex* 37(1):47–63. <https://doi.org/10.14573/altex.1811301>

47. Li WX, Liang GT, Yan W, Zhang Q, Wang W, Zhou XM, Liu DY (2013) Artificial uterus on a microfluidic chip. *Fenxi Huaxue/Chin J Anal Chem* 41(4):467–472. [https://doi.org/10.1016/S1872-2040\(13\)60639-8](https://doi.org/10.1016/S1872-2040(13)60639-8)
48. Aref AR, Campisi M, Ivanova E, Portell A, Larios D, Piel BP, Mathur N, Zhou C, Coakley RV, Bartels A, Bowden M, Herbert Z, Hill S, Gilhooley S, Carter J, Cañadas I, Thai TC, Kitajima S, Chiono V et al (2018) 3D microfluidic ex vivo culture of organotypic tumor spheroids to model immune checkpoint blockade. *Lab Chip* 18(20):3129–3143. <https://doi.org/10.1039/C8LC00322J>
49. Nguyen DHT, Lee E, Alimperti S, Norgard RJ, Wong A, Lee JJK, Eyckmans J, Stanger BZ, Chen CS (2019) A biomimetic pancreatic cancer on-chip reveals endothelial ablation via ALK7 signaling. *Sci Adv* 5(8):1–10. <https://doi.org/10.1126/sciadv.aav6789>
50. Wang Z, He X, Qiao H, Chen P (2020) Global trends of organoid and organ-on-a-chip in the past decade: a bibliometric and comparative study. *Tissue Engineering Part A*. <https://doi.org/10.1089/ten.tea.2019.0251>
51. Bauer S, Wennberg Huldt C, Kanebratt KP, Durieux I, Gunne D, Andersson S, Ewart L, Haynes WG, Maschmeyer I, Winter A, Åmmälä C, Marx U, Andersson TB (2017) Functional coupling of human pancreatic islets and liver spheroids on-a-chip: towards a novel human ex vivo type 2 diabetes model. *Sci Rep* 7(1):1–11. <https://doi.org/10.1038/s41598-017-14815-w>
52. Wikswo JP, Block FE, Cliffel DE, Goodwin CR, Marasco CC, Markov DA, McLean DL, McLean JA, McKenzie JR, Reiserer RS, Samson PC, Schaffer DK, Seale KT, Sherrod SD (2013a) Engineering challenges for instrumenting and controlling integrated organ-on-chip systems. *IEEE Trans Biomed Eng* 60(3):682–690. <https://doi.org/10.1109/TBME.2013.2244891>
53. Sung JH, Shuler ML (2009) A micro cell culture analog (μ CCA) with 3-D hydrogel culture of multiple cell lines to assess metabolism-dependent cytotoxicity of anti-cancer drugs. *Lab Chip* 9(10):1385–1394. <https://doi.org/10.1039/b901377f>
54. Shuler ML, Ghanem A, Quick D, Wong MC, Miller P (1996) A self-regulating cell culture analog device to mimic animal and human toxicological responses. *Biotechnol Bioeng* 52(1):45–60. [https://doi.org/10.1002/\(SICI\)1097-0290\(19961005\)52:1<45::AID-BIT5>3.0.CO;2-Z](https://doi.org/10.1002/(SICI)1097-0290(19961005)52:1<45::AID-BIT5>3.0.CO;2-Z)
55. Sung JH, Srinivasan B, Esch MB, McLamb WT, Bernabini C, Shuler ML, Hickman JJ (2014) Using physiologically-based pharmacokinetic-guided “body-on-a-chip” systems to predict mammalian response to drug and chemical exposure. *Exp Biol Med* 239(9):1225–1239. <https://doi.org/10.1177/1535370214529397>
56. Abaci HE, Shuler ML (2015) Human-on-a-chip design strategies and principles for physiologically based pharmacokinetics/pharmacodynamics modeling. *Integr Biol* 7(4):383–391. <https://doi.org/10.1039/C4IB00292J>
57. Stokes CL, Cirit M, Lauffenburger DA (2015) Physiome-on-a-Chip: the challenge of “scaling” in design, operation, and translation of microphysiological systems. *CPT Pharm Syst Pharmacol* 4(10):559–562. <https://doi.org/10.1002/psp4.12042>
58. Maschmeyer I, Lorenz AK, Schimek K, Hasenberg T, Ramme AP, Hübner J, Lindner M, Drewell C, Bauer S, Thomas A, Sambo NS, Sonntag F, Lauster R, Marx U (2015b) A four-organ-chip for interconnected long-term co-culture of human intestine, liver, skin and kidney equivalents. *Lab Chip* 15(12):2688–2699. <https://doi.org/10.1039/c5lc00392j>
59. Edington CD, Chen WLK, Geishecker E, Kassis T, Soenksen LR, Bhushan BM, Freake D, Kirschner J, Maass C, Tsamandouras N, Valdez J, Cook CD, Parent T, Snyder S, Yu J, Suter E, Shockley M, Velazquez J, Velazquez JJ et al (2018) Interconnected microphysiological Systems for Quantitative Biology and Pharmacology Studies. *Sci Rep* 8(1):1–18. <https://doi.org/10.1038/s41598-018-22749-0>
60. Bein A, Shin W, Jalili-Firoozinezhad S, Park MH, Sontheimer-Phelps A, Tovaglieri A, Chalkiadaki A, Kim HJ, Ingber DE (2018) Microfluidic organ-on-a-chip models of human intestine. *CMGH* 5(4):659–668. <https://doi.org/10.1016/j.jcmgh.2017.12.010>

61. Cooper M, Charest JL, Coppeta J (2019) Design principles for dynamic microphysiological systems. In: *Microfluidic cell culture systems* 2nd edn. Elsevier, Amsterdam, pp 1–29. <https://doi.org/10.1016/B978-0-12-813671-3.00001-3>
62. Xiao S, Coppeta JR, Rogers HB, Isenberg BC, Zhu J, Olalekan SA, McKinnon KE, Dokic D, Rashedi AS, Haisenleder DJ, Malpani SS, Arnold-Murray CA, Chen K, Jiang M, Bai L, Nguyen CT, Zhang J, Laronda MM, Hope TJ et al (2017) A microfluidic culture model of the human reproductive tract and 28-day menstrual cycle. *Nat Commun* 8:1–13. <https://doi.org/10.1038/ncomms14584>
63. Chen WLK, Edington C, Suter E, Yu J, Velazquez JJ, Velazquez JG, Shockley M, Large EM, Venkataraman R, Hughes DJ, Stokes CL, Trumper DL, Carrier RL, Cirit M, Griffith LG, Lauffenburger DA (2017) Integrated gut/liver microphysiological systems elucidates inflammatory inter-tissue crosstalk. *Biotechnol Bioeng* 114(11):2648–2659. <https://doi.org/10.1002/bit.26370>
64. Holmes AM, Creton S, Chapman K (2010) Working in partnership to advance the 3Rs in toxicity testing. *Toxicology* 267(1–3):14–19. <https://doi.org/10.1016/j.tox.2009.11.006>
65. Huh D, Hamilton GA, Ingber DE (2011) From 3D cell culture to organs-on-chips. *Trends Cell Biol* 21(12):745–754. <https://doi.org/10.1016/j.tcb.2011.09.005>
66. Ramme AP, Koenig L, Hasenberg T, Schwenk C, Magauer C, Faust D, Lorenz AK, Krebs AC, Drewell C, Schirrmann K, Vladetic A, Lin GC, Pabinger S, Neuhaus W, Bois F, Lauster R, Marx U, Dehne EM (2019) Autologous induced pluripotent stem cell-derived four-organ-chip. *Future Sci OA* 5(8). <https://doi.org/10.2144/fsoa-2019-0065>
67. Skardal A, Shupe T, Atala A (2016) Organoid-on-a-chip and body-on-a-chip systems for drug screening and disease modeling. *Drug Discov Today* 21(9):1399–1411. <https://doi.org/10.1016/j.drudis.2016.07.003>
68. Guthrie B, Makubate B, Hernandez-Santiago V, Dreischulte T (2015) The rising tide of polypharmacy and drug-drug interactions: population database analysis 1995–2010. *BMC Med* 13(1):74. <https://doi.org/10.1186/s12916-015-0322-7>
69. Anderson GD (2002) Children versus adults: pharmacokinetic and adverse-effect differences. *Epilepsia* 43(s3):53–59. <https://doi.org/10.1046/j.1528-1157.43.s.3.5.x>
70. Benam KH, Novak R, Nawroth J, Hirano-Kobayashi M, Ferrante TC, Choe Y, Prantil-Baun R, Weaver JC, Bahinski A, Parker KK, Ingber DE (2016a) Matched-comparative modeling of Normal and diseased human airway responses using a microengineered breathing lung chip. *Cell Syst* 3(5):456–466.e4. <https://doi.org/10.1016/j.cels.2016.10.003>
71. Ishida S (2018) Organs-on-a-chip: current applications and consideration points for in vitro ADME-Tox studies. *Drug Metab Pharmacokinet* 33(1):49–54. <https://doi.org/10.1016/j.dmpk.2018.01.003>
72. Knowlton S, Tasoglu S (2016) A bioprinted liver-on-a-chip for drug screening applications. *Trends Biotechnol* 34(9):681–682. <https://doi.org/10.1016/j.tibtech.2016.05.014>
73. Li Z, Jiang L, Zhu Y, Su W, Xu C, Tao T, Shi Y, Qin J (2018) Assessment of hepatic metabolism-dependent nephrotoxicity on an organs-on-a-chip microdevice. *Toxicol In Vitro* 46(March 2017):1–8. <https://doi.org/10.1016/j.tiv.2017.10.005>
74. Marx U, Akabane T, Andersson TB, Elizabeth B, Beilmann M, Beken S, Brendler-Schwaab S, Cirit M, David R, Dehne E-M, Durieux I, Ewart L, Fitzpatrick SC, Frey O, Fuchs F, Griffith LG, Hamilton GA, Hartung T, Hoeng J et al (2020) Biology-inspired microphysiological systems to advance medicines for patient benefit and animal welfare. *ALTEX* 37:1–30. <https://doi.org/10.14573/altex.2001241>
75. Huh D, Leslie DC, Matthews BD, Fraser JP, Jurek S, Hamilton GA, Thorneloe KS, McAlexander MA, Ingber DE (2012) A human disease model of drug toxicity–induced pulmonary edema in a lung-on-a-chip microdevice. *Sci Trans Med* 4(159):159ra147. <https://doi.org/10.1126/scitranslmed.3004249>
76. Maschmeyer I, Hasenberg T, Jaenicke A, Lindner M, Lorenz AK, Zech J, Garbe L-AA, Sonntag F, Hayden P, Ayehunie S, Lauster R, Marx U, Materne E-MM (2015a) Chip-based human liver-intestine and liver-skin co-cultures - a first step toward systemic repeated dose substance testing in vitro. *Eur J Pharm Biopharm* 95:77–87. <https://doi.org/10.1016/j.ejpb.2015.03.002>

77. Zhang YS, Aleman J, Shin SR, Kilic T, Kim D, Mousavi Shaegh SA, Massa S, Riahi R, Chae S, Hu N, Avci H, Zhang W, Silvestri A, Sanati Nezhad A, Manbohi A, De Ferrari F, Polini A, Calzone G, Shaikh N et al (2017) Multisensor-integrated organs-on-chips platform for automated and continual in situ monitoring of organoid behaviors. *Proc Natl Acad Sci* 114 (12):E2293–E2302. <https://doi.org/10.1073/pnas.1612906114>
78. Berthier E, Young EWKK, Beebe D (2012) Engineers are from PDMS-land, biologists are from Polystyrenia. *Lab Chip* 12(7):1224. <https://doi.org/10.1039/c2lc20982a>
79. Chan CY, Huang P-H, Guo F, Ding X, Kapur V, Mai JD, Yuen PK, Huang TJ (2013) Accelerating drug discovery via organs-on-chips. *Lab Chip* 13(24):4697. <https://doi.org/10.1039/c3lc90115g>
80. Sackmann EK, Fulton AL, Beebe DJ (2014) The present and future role of microfluidics in biomedical research. *Nature* 507(7491):181–189. <https://doi.org/10.1038/nature13118>
81. Schimek K, Busek M, Brincker S, Groth B, Hoffmann S, Lauster R, Lindner G, Lorenz A, Menzel U (2013) Integrating biological vasculature into a multi-organ-chip microsystem. *Lab Chip*:3588–3598. <https://doi.org/10.1039/c3lc50217a>
82. Zhang W, Zhang YS, Bakht SM, Aleman J, Shin SR, Yue K, Sica M, Ribas J, Duchamp M, Ju J, Sadeghian RB, Kim D, Dokmeci MR, Atala A, Khademhosseini A (2016) Elastomeric free-form blood vessels for interconnecting organs on chip systems. *Lab Chip* 16 (9):1579–1586. <https://doi.org/10.1039/c6lc00001k>
83. Esch MB, Ueno H, Applegate R, Shuler ML (2016) Modular, pumpless body-on-a-chip platform for the co-culture of GI tract epithelium and 3D primary liver tissue. *Lab Chip*. <https://doi.org/10.1039/C6LC00461J>
84. Miller PG, Shuler ML (2016) Design and demonstration of a pumpless 14 compartment microphysiological system. *Biotechnol Bioeng* 113(10):2213–2227. <https://doi.org/10.1002/bit.25989>
85. Shaegh SAM, De Ferrari F, Zhang YS, Nabavinia M, Mohammad NB, Ryan J, Pourmand A, Laukaitis E, Sadeghian RB, Nadhman A, Shin SR, Nezhad AS, Khademhosseini A, Dokmeci MR (2016) A microfluidic optical platform for real-time monitoring of pH and oxygen in microfluidic bioreactors and organ-on-chip devices. *Biomicrofluidics* 10(4):1–14. <https://doi.org/10.1063/1.4955155>
86. Tsamandouras N, Chen WLK, Edington CD, Stokes CL, Griffith LG, Cirit M (2017) Integrated gut and liver microphysiological systems for quantitative in vitro pharmacokinetic studies. *AAAPS J* 19(5). <https://doi.org/10.1208/s12248-017-0122-4>
87. Giobbe GG, Michielin F, Luni C, Giulitti S, Martewicz S, Dupont S, Floreani A, Elvassore N (2015) Functional differentiation of human pluripotent stem cells on a chip. *Nat Methods* 12 (7):637–640. <https://doi.org/10.1038/nmeth.3411>
88. Radisic M, Malda J, Epping E, Geng W, Langer R, Vunjak-Novakovic G (2006) Oxygen gradients correlate with cell density and cell viability in engineered cardiac tissue. *Biotechnol Bioeng* 93(2):332–343. <https://doi.org/10.1002/bit.20722>
89. Wikswo JP, Curtis EL, Eagleton ZE, Evans BC, Kole A, Hofmeister LH, Matloff WJ (2013b) Scaling and systems biology for integrating multiple organs-on-a-chip. *Lab Chip* 13(18):3496. <https://doi.org/10.1039/c3lc50243k>
90. Maass C, Stokes CL, Griffith LG, Cirit M (2017) Multi-functional scaling methodology for translational pharmacokinetic and pharmacodynamic applications using integrated microphysiological systems (MPS). *Integr Biol* 9(4):290–302. <https://doi.org/10.1039/C6IB00243A>
91. Cirit M, Stokes CL (2018) Maximizing the impact of microphysiological systems with in vitro – in vivo translation. *Lab Chip* 18(13):1831–1837. <https://doi.org/10.1039/C8LC00039E>
92. Beckwitt CH, Clark AM, Wheeler S, Taylor DL, Stolz DB, Griffith L, Wells A (2018) Liver organ on a chip. *Exp Cell Res* 363(November 2017):15–25. <https://doi.org/10.1016/j.yexcr.2017.12.023>
93. Martignoni M, Groothuis GMM, de Kanter R (2006) Species differences between mouse, rat, dog, monkey and human CYP-mediated drug metabolism, inhibition and induction. *Expert Opin Drug Metab Toxicol* 2(6):875–894. <https://doi.org/10.1517/17425255.2.6.875>

94. Grosberg A, Nesmith AP, Goss JA, Brigham MD, McCain ML, Parker KK (2012) Muscle on a chip: in vitro contractility assays for smooth and striated muscle. *J Pharmacol Toxicol Methods* 65(3):126–135. <https://doi.org/10.1016/j.yascn.2012.04.001>
95. Guo L, Dial S, Shi L, Branham W, Liu J, Fang J, Green B, Deng H, Kaput J, Ning B (2011) Similarities and differences in the expression of drug-metabolizing enzymes between human hepatic cell lines and primary human hepatocytes. *Drug Metabol Dispos* 39(3):528–538. <https://doi.org/10.1124/dmd.110.035873>
96. Zhu J, Xu Y, Rashedi AS, Pavone ME, Julie Kim J, Woodruff TK, Burdette JE (2016) Human fallopian tube epithelium co-culture with murine ovarian follicles reveals crosstalk in the reproductive cycle. *Mol Hum Reprod* 22(11):756–767. <https://doi.org/10.1093/molehr/gaw041>
97. Stacey G (2006) Primary cell cultures and immortal cell lines. *Encycl Life Sci*:1–6. <https://doi.org/10.1038/npq.els.0003960>
98. Zhang C, Zhao Z, Abdul Rahim NA, Van Noort D, Yu H (2009) Towards a human-on-chip: culturing multiple cell types on a chip with compartmentalized microenvironments. *Lab Chip* 9(22):3185–3192. <https://doi.org/10.1039/b915147h>
99. Coppeta JR, Mescher MJ, Isenberg BC, Spencer AJ, Kim ES, Lever AR, Mulhern TJ, Prantil-Baun R, Comolli JC, Borenstein JT (2017) A portable and reconfigurable multi-organ platform for drug development with onboard microfluidic flow control. *Lab Chip* 17(1):134–144. <https://doi.org/10.1039/C6LC01236A>
100. Poisson J, Lemoigne S, Boulanger C, Durand F, Moreau R, Valla D, Rautou PE (2017) Liver sinusoidal endothelial cells: physiology and role in liver diseases. *J Hepatol* 66(1):212–227. <https://doi.org/10.1016/j.jhep.2016.07.009>
101. Yu F, Selva Kumar ND, Choudhury D, Foo LC, Ng SH (2018) Microfluidic platforms for modeling biological barriers in the circulatory system. *Drug Discov Today* 23(4):815–829. <https://doi.org/10.1016/j.drudis.2018.01.036>
102. Novak R, Ingram M, Marquez S, Das D, Delahanty A, Herland A, Maoz BM, Jeanty SSF, Somayaji MR, Burt M, Calamari E, Chalkiadaki A, Cho A, Choe Y, Chou DB, Crounce M, Dauth S, Divic T, Fernandez-Alcon J et al (2020) Robotic fluidic coupling and interrogation of multiple vascularized organ chips. *Nat Biomed Eng*. <https://doi.org/10.1038/s41551-019-0497-x>
103. Pollet AMAO, den Toonder JMJ (2020) Recapitulating the vasculature using organ-on-chip technology. *Bioengineering* 7(1):17. <https://doi.org/10.3390/bioengineering7010017>
104. Eklund SE, Snider RM, Wikswo J, Baudenbacher F, Prokop A, Cliffel DE (2006) Multianalyte microphysiometry as a tool in metabolomics and systems biology. *J Electroanal Chem* 587(2):333–339. <https://doi.org/10.1016/j.jelechem.2005.11.024>
105. Eklund SE, Taylor D, Kozlov E, Prokop A, Cliffel DE (2004) A Microphysiometer for simultaneous measurement of changes in extracellular glucose, lactate, oxygen, and acidification rate. *Anal Chem* 76(3):519–527. <https://doi.org/10.1021/ac034641z>
106. Diercks AH, Ozinsky A, Hansen CL, Spotts JM, Rodriguez DJ, Aderem A (2009) A microfluidic device for multiplexed protein detection in nano-liter volumes. *Anal Biochem* 386(1):30–35. <https://doi.org/10.1016/j.ab.2008.12.012>
107. Riahi R, Shaegh SAM, Ghaderi M, Zhang YS, Shin SR, Aleman J, Massa S, Kim D, Dokmeci MR, Khademhosseini A (2016) Automated microfluidic platform of bead-based electrochemical immunosensor integrated with bioreactor for continual monitoring of cell secreted biomarkers. *Sci Rep* 6(December 2015):1–14. <https://doi.org/10.1038/srep24598>
108. Shin SR, Zhang YS, Kim DJ, Manbohi A, Avci H, Silvestri A, Aleman J, Hu N, Kilic T, Keung W, Righi M, Assawes P, Alhadrami HA, Li RA, Dokmeci MR, Khademhosseini A (2016) Aptamer-based microfluidic electrochemical biosensor for monitoring cell-secreted trace cardiac biomarkers. *Anal Chem* 88(20):10019–10027. <https://doi.org/10.1021/acs.analchem.6b02028>
109. Rothbauer M, Ertl P (2020) Emerging biosensor trends in organ-on-a-chip. *Adv Biochem Eng Biotechnol*. https://doi.org/10.1007/10_2020_129

110. Vunjak-Novakovic G, Bhatia S, Chen C, Hirschi K (2013) HeLiVa platform: integrated heart-liver-vascular systems for drug testing in human health and disease. *Stem Cell Res Ther* 4 (Suppl 1):S8. <https://doi.org/10.1186/scri369>
111. Frey O, Misun PM, Fluri DA, Hengstler JG, Hierlemann A (2014) Reconfigurable microfluidic hanging drop network for multi-tissue interaction and analysis. *Nat Commun* 5 (May):1–11. <https://doi.org/10.1038/ncomms5250>
112. Esch MB, Mahler GJ, Stokol T, Shuler ML (2014a) Body-on-a-chip simulation with gastro-intestinal tract and liver tissues suggests that ingested nanoparticles have the potential to cause liver injury. *Lab Chip* 14(16):3081–3092. <https://doi.org/10.1039/c4lc00371c>
113. Materne E-M, Ramme AP, Terraso AP, Serra M, Alves PM, Brito C, Sakharov DA, Tonevitsky AG, Lauster R, Marx U (2015) A multi-organ chip co-culture of neurospheres and liver equivalents for long-term substance testing. *J Biotechnol* 205:36–46. <https://doi.org/10.1016/j.jbiotec.2015.02.002>
114. Hübner J, Raschke M, Rüttschle I, Gräßle S, Hasenberg T, Schirrmann K, Lorenz A, Schnurre S, Lauster R, Maschmeyer I, Steger-Hartmann T, Marx U (2018) Simultaneous evaluation of anti-EGFR-induced tumour and adverse skin effects in a microfluidic human 3D co-culture model. *Sci Rep* 8(1):1–12. <https://doi.org/10.1038/s41598-018-33462-3>
115. Pires de Mello CP, Carmona-Moran C, McAleer CW, Perez J, Coln EA, Long CJ, Oleaga C, Riu A, Note R, Teissier S, Langer J, Hickman JJ (2020) Microphysiological heart–liver body-on-a-chip system with a skin mimic for evaluating topical drug delivery. *Lab Chip* 15(2): 391–398. <https://doi.org/10.1039/C9LC00861F>
116. Baert Y, Ruetschle I, Cools W, Oehme A, Lorenz A, Marx U, Goossens E, Maschmeyer I (2020) A multi-organ-chip co-culture of liver and testis equivalents: a first step toward a systemic male reprotoxicity model. *Hum Reprod*:1–16. <https://doi.org/10.1093/humrep/deaa057>
117. Oleaga C, Bernabini C, Smith AST, Srinivasan B, Jackson M, McLamb W, Platt V, Bridges R, Cai Y, Santhanam N, Berry B, Najjar S, Akanda N, Guo X, Martin C, Ekman G, Esch MB, Langer J, Ouedraogo G et al (2016) Multi-organ toxicity demonstration in a functional human in vitro system composed of four organs. *Sci Rep* 6(December 2015):1–17. <https://doi.org/10.1038/srep20030>
118. Vernetti L, Gough A, Baetz N, Blutt S, Broughman JR, Brown JA, Foulke-Abel J, Hasan N, In J, Kelly E, Kovbasnjuk O, Repper J, Senutovitch N, Stabb J, Yeung C, Zachos NC, Donowitz M, Estes M, Himmelfarb J et al (2017) Functional coupling of human microphysiology systems: intestine, liver, kidney proximal tubule, blood-brain barrier and skeletal muscle. *Sci Rep* 7(October 2016):1–14. <https://doi.org/10.1038/srep42296>
119. Sin A, Chin KC, Jamil MF, Kostov Y, Rao G, Shuler ML (2004) The design and fabrication of three-chamber microscale cell culture analog devices with integrated dissolved oxygen sensors. *Biotechnol Prog* 20(1):338–345. <https://doi.org/10.1021/bp034077d>
120. Wagner I, Materne EM, Brincker S, Süßbier U, Frädrich C, Busek M, Sonntag F, Sakharov DA, Trushkin EV, Tonevitsky AG, Lauster R, Marx U (2013) A dynamic multi-organ-chip for long-term cultivation and substance testing proven by 3D human liver and skin tissue co-culture. *Lab Chip* 13(18):3538–3547. <https://doi.org/10.1039/c3lc50234a>
121. Foster AJ, Chouhan B, Regan SL, Rollison H, Amberntsson S, Andersson LC, Srivastava A, Darnell M, Cairns J, Lazic SE, Jang KJ, Petropolis DB, Kodella K, Rubins JE, Williams D, Hamilton GA, Ewart L, Morgan P (2019) Integrated in vitro models for hepatic safety and metabolism: evaluation of a human liver-chip and liver spheroid. *Arch Toxicol* 93(4): 1021–1037. <https://doi.org/10.1007/s00204-019-02427-4>
122. Zhang B, Radisic M (2017) Organ-on-a-chip devices advance to market. *Lab Chip* 17(14): 2395–2420. <https://doi.org/10.1039/c6lc01554a>

Emerging Biosensor Trends in Organ-on-a-Chip



Mario Rothbauer and Peter Ertl

Contents

1	Introduction	344
2	Bipolar and Tetrapolar Electrode Approaches for Transepithelial and Endothelial Resistance (TEER) Measurements at Human In Vitro Barriers	346
3	Bipolar and Tetrapolar Impedance Spectroscopy Approaches for Integrity Monitoring of Human In Vitro Organ and Barrier Models	347
4	Monitoring of Organ Function Using Electrochemical Analysis Techniques: Straight Through the Heart	348
5	Monitoring Organ/Tissue Metabolism Using Electrochemical Analysis Techniques	350
6	Monitoring of Organ Metabolism and Architecture Using Optical Sensors	350
7	Conclusion	351
	References	352

Abstract Organ-on-a-chip technology is ideally suited to cultivate and analyze 2D/3D cell cultures, organoids, and other tissue analogues in vitro, because these microphysiological systems have been shown to generate architectures, structural organization, and functions that closely resemble their respective human tissues and organs. Although great efforts have been undertaken to demonstrate organotypic cell behavior, proper cell-to-cell communication, and tissue interactions in recent years, the integration of biosensing strategies into organ-on-a-chip platforms is still in its infancy. While a multitude of micro-, nano-, and biosensors are well established and could be easily adapted for organ-on-a-chip models, to date only a handful of

M. Rothbauer

Department of Orthopedics and Trauma Surgery, Karl Chiari Lab for Orthopedic Biology, Medical University of Vienna, Vienna, Austria

Faculty of Technical Chemistry, Vienna University of Technology, Vienna, Austria

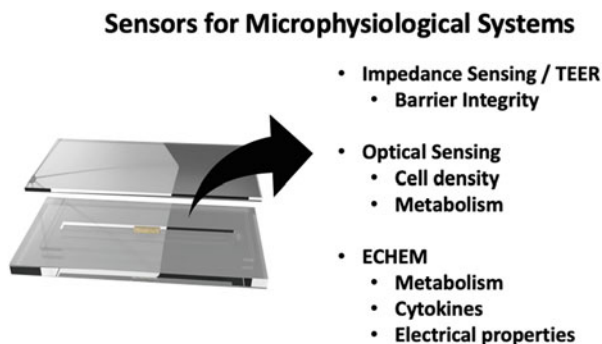
P. Ertl (✉)

Faculty of Technical Chemistry, Vienna University of Technology, Vienna, Austria

e-mail: Peter.ertl@tuwien.ac.at

analytical approaches (aside from microscopical techniques) have been combined with organ-on-a-chip technology. This chapter aims to summarize current efforts and survey the progress that has been made in integrating analytical techniques that are being implemented for organ-, multi-organ-, and body-on-a-chip systems based on electrochemical and optical sensors.

Graphical Abstract



Keywords Biosensing, Microphysiological systems, Organs-on-a-chip, Sensor integration

1 Introduction

Two decades ago, George Whitesides and his colleagues introduced soft lithography to biomedical engineers, chemists, and biologists as a simple and fast method to develop microfluidic devices – thereby paving the way for the development of microfluidic cell-based assays made from poly-dimethylsiloxane [1]. Over the course of the last 23 years, the technology that started using simple microchannels and two-dimensional cells monolayers (so-called cell-based microfluidics) has rapidly progressed into more complex cell culture systems [2] (Fig. 1). For instance, the integration of microfluidic components – including valves, micropumps, mixers, actuators, and microsensors – has provided controlled liquid handling routines and analytical power of true lab-on-a-chip systems [3]. However, it was only in the last decade that the first microphysiological system for lung tissue (lung-on-a-chip) was developed that was capable of simulating breathing motions of the lung [1, 2]. For the first time, the scientific community witnessed a groundbreaking concept of actuating lung epithelial cell layers using flexible porous membranes to emulate a key biomechanical function of the lung. The last decade has seen a global trend toward more physiologically relevant cell cultures systems, with the aim of reengineering in vivo-like cellular microenvironments for 2D and 3D cell cultures

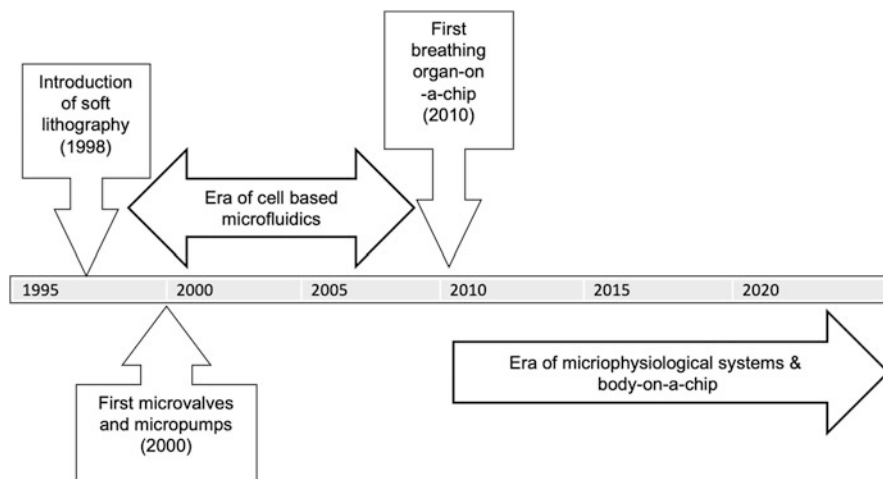


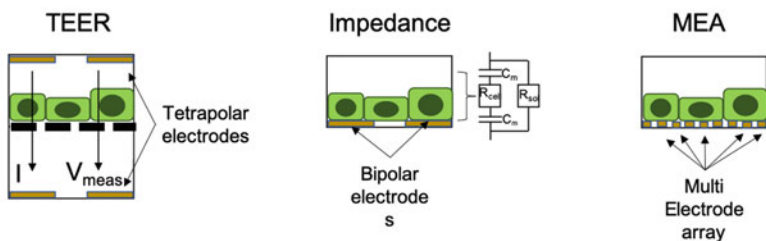
Fig. 1 Timeline for the emergence of organ-on-a-chip systems and microphysiological systems

that truly resemble actual human tissue architecture and organ function and physiology *in vitro* [4]. Yet notwithstanding recent biological advancements using patient-derived primary cell and iPSC-culture systems, little progress has been made to date in improving the functionality and analytic capabilities of these microphysiological systems. Even though a variety of sensors based on electrochemical, acoustic, optical, and magnetic readouts have been developed and integrated into cell-based microfluidic devices [5], only a few analytical sensing methods have actually been used in microphysiological systems so far. Among these, bipolar and tetrapolar electric cell impedance (ECIS) and resistance measurements (TEER) are mainly used to assess the integrity of human epithelial and endothelial barrier models – while multielectrode arrays (MEAs) are employed to detect electrophysiological activities of cells and electrochemical and optochemical sensors to study metabolic parameters and biomarker release such as oxygen demand, pH levels, and release of, for example, cytokines. Most organ-on-a-chip systems heavily depend on microscopy and off-chip analytical techniques, due in part to the familiarity of laboratory staff with standard techniques such as ELISA, PCR, metabolic plate-reader assays, and staining techniques for fluorescence microscopy and histology. The previous chapters by Szita highlighted how microfluidic technology can help to improve *in vitro* cell cultures, whereas in their chapter, Maschmeyer and Kakava elaborated on how organ-on-a-chip systems help to create a cellular microenvironment that recreates human tissue and organ responses *in vitro*. Accordingly, the current chapter focuses solely on the question how to make microphysiological systems (such as organs-, multi-organ-, and body-on-a-chip systems) more functional via the integration of micro- and biosensors.

2 Bipolar and Tetrapolar Electrode Approaches for Transepithelial and Endothelial Resistance (TEER) Measurements at Human In Vitro Barriers

Transepithelial/endothelial resistance (TEER) measurements as shown in Fig. 2a are considered the golden standard for analyzing barrier model integrity without the need for invasive dye leakage assays based on fluorescein or fluorescence-labelled dextran molecules. Jeong et al. integrated a TEER sensor array using etched 200 nm gold thin films within a PDMS and polycarbonate hybrid biochip to study barrier integrity of primary murine BMVECs in the absence and presence of astrocyte co-culture using a commercial EVOM2 Volt-ohm meter in combination with a multiplexer [6]. Using this setup, the authors demonstrated improved barrier integrity when using Matrigel instead of fibronectin – achieving a near doubling in resistance values at day 4. Interestingly, however, exposure to histamine resulted in loss of barrier integrity only in the presence of a monolayer culture – highlighting the protective function of astrocytes in a co-culture system. Using a similar measurement setup, Walter et al. established several tissue barrier models including intestine, blood-brain, and lung barriers within a single microfluidic device containing embedded integrated TEER electrodes fabricated either from gold or transparent indium tin oxide thin films [7]. Similar to the EVOM2, a Millicell[®]

a) Electrochemical sensing techniques



b) Optical sensing techniques

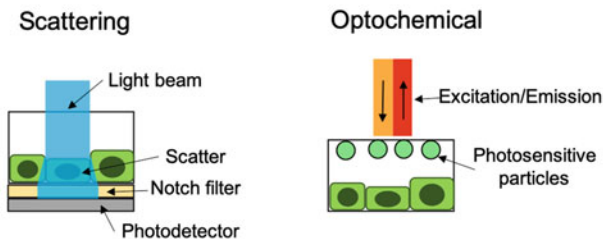


Fig. 2 Sensing principles for (a) electrochemical and (b) optical including TEER, impedance spectroscopy, MEAs, light scattering, and optochemical cell-based analysis

ERS-2 Volt-ohm meter in combination with a single integrated Ag/AgCl electrode pair was used by Ramadan et al. to establish bipolar TEER recordings for HacaT/U937 co-culture as a model for immune competent skin in the presence and absence of an air-liquid interface and toxicants [8]. A more refined measurement approach was also recently demonstrated by Henry et al., who employed a tetrapolar electrode TEER setup using a PGstat128N potentiostat to assess primary human airway epithelial cells (hAECs) over a 60-day long-term culture at the air-liquid interface (ALI) and human Caco-2 intestinal epithelial cells up to 12 days [9]. The inherent flexibility and analytical power of potentiostats enabled continuous impedance spectroscopy recordings at high temporal resolution at multiple frequencies and defined amplitudes to monitor multiple parameters such as impedance and capacitance of cell barriers. In a follow-up study, a similar TEER approach was also used by Park et al. to elucidate the influence of hypoxia on transport of drugs and antibodies at the human blood-brain barrier (BBB). Here, an increasing barrier tightness by fivefold and more was observed following exposure of iPS-derived endothelial cells to either oxygenated or hypoxic culture conditions prior seeding and differentiation into the BBB [10].

3 Bipolar and Tetrapolar Impedance Spectroscopy Approaches for Integrity Monitoring of Human In Vitro Organ and Barrier Models

A more general electrochemical approach that provides similar information to direct TEER readings is called electric cell impedance spectroscopy (ECIS; see also Fig. 2a) and involves a system wherein complex electric impedance of a cell culture system in contact with the working electrode is monitored in a time-resolved way over a broad range of frequencies ranging from a few Hz (similar frequency as TEER) to kHz, or even MHz, regimes. Depending on the applied frequency, different electrical properties of cell-based barrier models are detected – thus providing information on changes in (a) capacity of cell membranes, (b) conductivity of medium, and (c) resistive components caused by increase in tight junctions or cellular movements. In its simplest implementation, a pair of wire or thin film electrodes can be used to measure changes in impedance over time as a function of barrier integrity. By way of one illustrative example: a tetrapolar TEER measurement setup has been used to analyze on-chip μ BBB integrity by inserting four platinum wires into small electrode channels and sealed with photocurable [11, 12]. Between the four platinum electrodes, a total of six different impedance values could be derived for a single chip by recording impedance values between the upper and lower electrode pair (E1 + E3/E2 + E4) for blank medium measurements or through the BBB for the remaining four electrode combinations. The results of this study showed a distinct dependence electrode pairing and obtained signal variance, suggesting the need for signal processing by averaging the four cellular

values and baseline subtracting the acellular medium recordings for an individual experiment in order to generate an average impedance curve for hCMEC/D3 cells. This approach eliminates an acellular control measurement as blank values needed for signal normalization, since control values are simultaneously recorded with the cell barriers. Moreover, Mermoud et al. have tracked of membrane deflection during the breathing motion of an actuated flexible PDMS membrane in a breathing lung-on-chip system employing coplanar impedance biosensors in a microimpedance tomography (MITO) sensing approach based on printed circuit board (PCB)-technology [13]. Furthermore, the authors showed that membrane permeabilization events (buildup and breakdown) of A549 type II alveolar epithelial cells during breathing motion can be monitored. Another bioimpedance application involves nanoparticle risk assessment at human barrier models, where, e.g., Schuller et al. [14] have developed a highly integrated placenta-on-a-chip system containing an array of embedded membrane-bound thin film impedance microsensors capable of non-invasively monitoring placental barrier integrity. Using an optimized plasma-assisted liftoff procedure, high-resolution coplanar interdigitated electrode structures with 15 μm resolution were fabricated on a porous membrane without clogging the pores [15]. Barrier integrity was continuously monitored using a cell-culture treated PET membrane that acted as a growth surface for a placental barrier of trophoblast-derived BeWo cells. Using a bipolar impedance spectroscopy approach in the absence and presence of standardized silicon dioxide (SiO_2), titanium dioxide (TiO_2), and zinc oxide (ZnO) nanoparticles, the authors demonstrated a high degree of similarity to standard tetrapolar TEER approaches. The benefits of employing membrane-based impedance biosensors include higher temporal resolution, the elimination of complex electrode pair positioning at top and bottom of the microchannel, and the removal of unwanted stray resistance originating from the porous polymer membrane (which shows high variance due to the pore fabrication process).

4 Monitoring of Organ Function Using Electrochemical Analysis Techniques: Straight Through the Heart

Electrochemical analysis techniques are well established for a variety of biological models, including neuronal and muscular *in vitro* models where activity of neuronal networks and beating of cardiac muscles/bodies are monitored using multielectrode arrays (MEAs; see also Fig. 2a). For instance, Oleaga et al. have presented a multi-tissue-on-a-chip platform which performed long-term analysis up to 1 month culture duration of cardiomyocyte and hepatocyte co-culture as well as a muscle and motoneuronal unit for multi-organ studies [16, 17]. Using a MEA for potentiometric measurements (electrical activity) in combination with a cantilever array, cardiac beating was evaluated after exposure with well-known drug metabolites generated by hepatic metabolism. Boudou et al. used a similar cantilever-based method for drug screening of electro-stimulated cardiac microtissues made from fibrin/collagen

3D matrices [18]. A similar approach was also used by Caluori et al. to analyze cardiac bodies derived from a patient-derived dystrophin-deficient cell line, which were reprogrammed from fibroblasts for Duchenne muscular dystrophy (DMD) studies [19]. To improve the sensitivity of electrochemical beating rate analysis, Inácio et al. applied PEDOT:PSS conductive polymer instead of metallic electrodes – which can be printed very easily using a common material inkjet printer [20]. In contrast to the pristine and tiny electrodes of MEAs, the bigger footprints of the printed MEAs enabled efficient monitor beating rates of whole embryoid bodies with enhanced signal quality. Another tetrapolar ECIS using MEAs was used by Maoz et al. to enhance analysis outcome of endothelial barrier integrity using a myocardial barrier model comprising of IPS-derived cardiomyocyte cultures and a primary human endothelium [21]. Dynamic and time-resolved alterations in the electrical activity of the cardiac model were detected following the treatment with tumor necrosis factor alpha and the cardioactive drug isoproterenol. Another modular approach was introduced by Gaio et al. using their modular “Cytostretch” platform, which combines MEA sensors with strain gauges [22]. Yet another way to measure mechanical deformation of 3D myocyte tissues using integrated copper force probes was reported by Chan et al. [23]. Additional modular modules have also incorporated porous membranes and 3D patterned microgrooves to allow for analysis of a variety of aspects important to organ and multi-organ chips including immune cell migration; measurement of electrical field potential of cardiac cells; improved cell/sarcomere orientation; and real-time monitoring of membrane stretch as a function of electrical resistance changes using a 2×2 arrayed plug and play chip. Overall, a number of reports have now demonstrated that impedance spectroscopy is not only useful to assess barrier integrity but also to monitor, for example, cardiac contraction status using high-speed impedance setup to monitor efficacy of cardioactive drugs such as verapamil and doxorubicin [24].

In addition to the abovementioned approaches, electrochemical techniques have also been used in combination with biorecognition elements (e.g., antibodies or aptamers) as ELISA-type assays to monitor on-chip secretion of cytokines. For instance, Shin et al. developed an aptamer-functionalized gold microelectrode for sensitive detection of secreted cardiac damage-associated biomarkers, which was evaluated against doxorubicin cardiotoxicity resulting in good correlation to complementary viability and beating analyses [25]. A similar sensing approach, using a more complex biological system, was presented by Zhang et al., who combined liver and cardiac organoids to detect cardiac biomarker secretion following the addition of acetaminophen (paracetamol) and doxorubicin [26]. A combination of impedimetric TEER, ELISA-like impedimetric biomarker analysis, and cardiac beating monitoring was established by Skardal et al. using a heart-liver-lung multi-organ-on-a-chip system [27]. The individual organ models printed from primary human cells were used to analyze the side effects of drugs by detecting cardiac beating using real-time microscopy, impedimetric affinity sensors to detect antibody-binding events, and transendothelial electrical resistance measurements to assess barrier integrities. The authors demonstrated that organ-organ interplay between lung tissue and a heart model can trigger severe adverse effects.

5 Monitoring Organ/Tissue Metabolism Using Electrochemical Analysis Techniques

For decades, electrochemical techniques such as amperometry and voltammetry have been extensively used to detect metabolic parameters such as respiration rate, lactate levels, and glucose consumption. Sensor performance of electroanalytical techniques is constantly improving, and, with the integration of electrodes in microdevices, the rate of their application in microphysiological systems is steadily increasing. It is important to note in microphysiological cell culture systems, highly sensitive and selective analysis of metabolic parameters is a key metric for evaluating (a) an organoid's proper physiologic function, (b) the toxicity of biochemical stimuli, and (c) the onset, progression, and remission of pathophysiological processes. Yet despite the inherent advantages of employing embedded electrical biosensors, to date, the Seahorse assay system remains the dominant method employed to monitor organoid cell metabolism *in vitro* [28]. Although widely accepted, in its current configuration (as an external inset for microtiter plate-based analysis approach), this setup is not suitable for stand-alone *in situ* analysis of complex cell cultures, since it cannot be integrated. To address the demands of time-resolved analysis of key physiological parameters with high spatial resolution in co-cultures and multi-organ-chip devices, a number of innovative approaches have been reported in recent years. As an example, Moya et al. presented a chronoamperometric approach to monitor oxygen consumption using inkjet printing of multiple sensors into an extremely thin, porous membrane for liver oxygen respiration monitoring using two-dimensional cultures of primary freshly isolated hepatocyte cultures [29]. Similarly, Misun et al. have measured the current density at a constant voltage of 0.65 V (e.g., amperometry) using either glucose oxidase (GOx) or lactate oxidase (LOx)-modified working electrodes to study the dynamic cellular metabolism. Using a plug and play biosensing unit that can be clicked onto a microfluidic hanging drop when sensing is initiated, lactate accumulation and glucose consumption were detected in a spheroidal HCT116 human colon carcinoma organoid model [30].

6 Monitoring of Organ Metabolism and Architecture Using Optical Sensors

Optical sensing principles as shown in Fig. 2b hold great potential for organ-on-a-chip application due to the straightforward integration and ease of use. A variety of non-invasive optochemical sensor approaches have also been developed to study cell and tissue metabolism using sensitive optochemical tracer molecules. Among these, porphyrin-based optical oxygen sensors have proven particularly useful in cell analysis applications [31]. For instance, Ungerboeck et al. have implemented a ratiometric imaging system to quantify oxygen levels with high spatial resolution

in microfluidic systems [32]. Using a simple CCD camera set up, a global image of the microfluidic device was taken, and variations of local oxygen tension calculated using two different wavelengths. Additionally, Sticker et al. have demonstrated the ability to monitor hypoxic conditions in a microfluidic stroke-on-a-chip (BBB) model to emulate *in vivo* conditions during stroke using embedded oxygen sensor spots consisting of opto-chemical oxygen-sensitive microbeads. Importantly, the authors showed precise control over apparent oxygen levels inside a microfluidic device fabricated from oxygen-scavenging OSTEmer thiol-ene epoxies by adjusting the microfluidic flow velocities [33]. Furthermore, Zirath et al. used a similar opto-chemical sensing approach based on immobilized microbeads impregnated with porphyrin-based oxygen indicator dye to study oxygen gradients across the cultivation chambers of 2D and 3D microfluidic organ models. The authors also demonstrated the ability to tune oxygen gradients by changing flow profiles and chip materials for a three-dimensional vascular barrier model based on human adipose-derived mesenchymal stem cells in co-culture with HUVEC endothelial cells in a fibrin hydrogel scaffold [34]. An alternative optical approach to monitor morphological changes of 3D-tissue structures is predicated on using light scattering measurements to detect structural changes within on-chip 3D *in vitro* synovium using organic photodiodes [35]. In this approach, perpendicular 480 nm light is directed through an organoid – but only light scattered at greater than a 20° angle to the incident light beam actually passes through the notch filter and is detected by an organic photodiode. Using this simple optical setup, the authors demonstrated the ability to readily detect the onset of structural changes in the synovium that take place during inflammatory arthritic processes. Following TNF- α stimulation of the 3D synovial organoids, dynamic cellular matrix reorganization events were detected in a non-invasive manner with only a few days. Moreover, this setup was used as a quality control tool to assess cross-linking processes of natural hydrogels including Matrigel, collagen, and fibrin, which are known to change optical densities in the presence of uncontrolled or failed cross-linking events.

7 Conclusion

The global trend toward *in vitro* biological systems of increased complexity that are capable of mimicking (patho)physiology of tissue *in vivo* has created a renewed demand for microdevices that permit analysis of key biochemical parameters. The integration of non-invasive micro- and biosensors, therefore, presents a real opportunity to establish organs- and multi-body-on-a-chip with improved organo-typic functionality. In the last decade, a number of optical and electrochemical sensing approaches have been employed to monitor important organ functions, including barrier integrity (TEER/ECIS); metabolic parameters (e.g., porphyrin-based oxygen sensing, amperometry, and voltammetry); organ activity such as cardiac beating (e.g., cantilevers and MEAs); and as biomarker secretion (amperometry coupled with biorecognition elements). However, results obtained from a Scopu[®] search

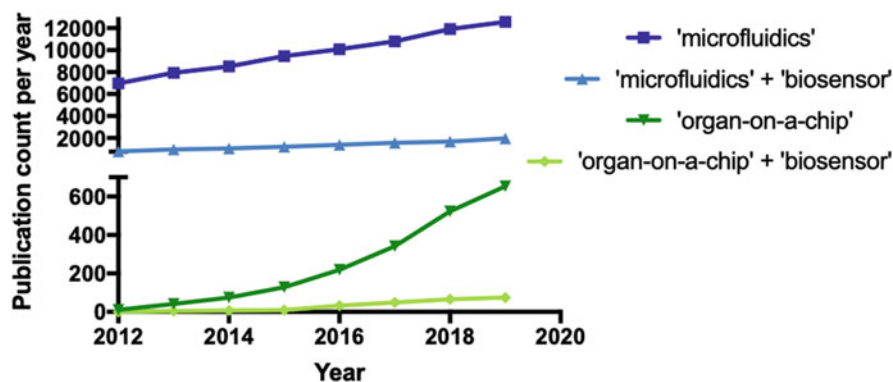


Fig. 3 Results of the Scopus research on annual publication output for the search terms “microfluidics,” “microfluidics + biosensor,” “organ-on-a-chip,” and “organ-on-a-chip + biosensor”

seen in Fig. 3 highlight that the integration of biosensing strategies into microphysiological organ-on-a-chip systems remains in its infancy. Out of the 12,570 microfluidic papers that were published in 2019, only 13% reported embedded sensors – which is surprisingly similar to the rate of organ-on-a-chip applications (seen in 75 out of 654 papers published in 2019). These relatively low percentages underscore the need for additional technical skills and engineering expertise, costly clean room facilities, and infrastructure that all remain unfortunate predicates for sensor microfabrication. To date, improvement in microphysiological systems is mainly associated with recent progress seen in biofabrication techniques and iPSC technology to generate advanced in vitro organ models. Nevertheless, looking ahead, the authors anticipate that more and more well-established sensing techniques will be incorporated into this game-changing technology in an attempt to standardize miniaturized microphysiological systems.

References

1. Xia Y, Whitesides GM (1998) Soft lithography. *Angew Chem Int Ed Engl* 37:550–575
2. Charwat V et al (2014) Monitoring cellular stress responses using integrated high-frequency impedance spectroscopy and time-resolved ELISA. *Analyst* 139:5271–5282
3. Rothbauer M et al (2019) Monitoring transient cell-to-cell interactions in a multi-layered and multi-functional allergy-on-a-chip system. *Lab Chip* 19:1916–1921
4. Rothbauer M, Rosser JM, Zirath H, Ertl P (2019) Tomorrow today: organ-on-a-chip advances towards clinically relevant pharmaceutical and medical in vitro models. *Curr Opin Biotechnol* 55:81–86. <https://doi.org/10.1016/j.copbio.2018.08.009>
5. Wartmann D et al (2015) Automated, miniaturized, and integrated quality control-on-chip (QC-on-a-chip) for cell-based cancer therapy applications. *Front Mater* 2:60. <https://doi.org/10.3389/fmats.2015.00060>

6. Jeong S et al (2018) A three-dimensional arrayed microfluidic blood-brain barrier model with integrated electrical sensor array. *IEEE Trans Biomed Eng* 65(2):431–439. <https://doi.org/10.1109/TBME.2017.2773463>
7. Walter FR et al (2016) A versatile lab-on-a-chip tool for modeling biological barriers. *Sensors Actuators B Chem* 222:1209–1219. <https://doi.org/10.1016/j.snb.2015.07.110>
8. Ramadan Q, Ting FCW (2016) In vitro micro-physiological immune-competent model of the human skin. *Lab Chip* 16(10):1899–1908. <https://doi.org/10.1039/c6lc00229c>
9. Henry OYF et al (2017) Organs-on-chips with integrated electrodes for trans-epithelial electrical resistance (TEER) measurements of human epithelial barrier function. *Lab Chip* 17:2264–2271
10. Park TE et al (2019) Hypoxia-enhanced Blood-Brain Barrier Chip recapitulates human barrier function and shuttling of drugs and antibodies. *Nat Commun* 10(1):1–12. <https://doi.org/10.1038/s41467-019-10588-0>
11. van der Helm MW et al (2016) Direct quantification of transendothelial electrical resistance in organs-on-chips. *Biosens Bioelectron* 85:924–929. <https://doi.org/10.1016/j.bios.2016.06.014>
12. van der Helm MW et al (2017) Fabrication and validation of an organ-on-chip system with integrated electrodes to directly quantify transendothelial electrical resistance. *J Vis Exp* 127:e56334. <https://doi.org/10.3791/56334>
13. Mermoud Y, Felder M, Stucki JD, Stucki AO, Guenat OT (2018) Microimpedance tomography system to monitor cell activity and membrane movements in a breathing lung-on-chip. *Sensors Actuators B Chem* 255:3647–3653. <https://doi.org/10.1016/j.snb.2017.09.192>
14. Schuller P et al (2020) A lab-on-a-chip system with an embedded porous membrane-based impedance biosensor array for nanoparticle risk assessment on placental Bewo trophoblast cells. *Sensors Actuators B Chem* 312:127946. <https://doi.org/10.1016/j.snb.2020.127946>
15. Schuller P et al (2019) Optimized plasma-assisted bi-layer photoresist fabrication protocol for high resolution microfabrication of thin-film metal electrodes on porous polymer membranes. *MethodsX* 6:2606–2613. <https://doi.org/10.1016/j.mex.2019.10.038>
16. Oleaga C et al (2018) Investigation of the effect of hepatic metabolism on off-target cardiotoxicity in a multi-organ human-on-a-chip system. *Biomaterials* 182:176–190
17. Oleaga C et al (2016) Multi-organ toxicity demonstration in a functional human in vitro system composed of four organs. *Sci Rep* 6:20030
18. Boudou T et al (2011) A microfabricated platform to measure and manipulate the mechanics of engineered cardiac microtissues. *Tissue Eng A* 18:910–919
19. Caluori G et al (2019) Non-invasive electromechanical cell-based biosensors for improved investigation of 3D cardiac models. *Biosens Bioelectron* 124:129–135
20. Inácio PMC et al (2017) Bioelectrical signal detection using conducting polymer electrodes and the displacement current method. *IEEE Sensors J* 17:3961–3966
21. Maoz BM et al (2017) Organs-on-Chips with combined multi-electrode array and transepithelial electrical resistance measurement capabilities. *Lab Chip* 17:2294–2302
22. Gaio N et al (2018) A multiwell plate Organ-on-Chip (OOC) device for in-vitro cell culture stimulation and monitoring. In: 2018 IEEE micro electro mechanical systems (MEMS). IEEE, Belfast, pp 314–317
23. Chan V et al (2015) Fabrication and characterization of optogenetic, multi-strip cardiac muscles. *Lab Chip* 15:2258–2268
24. Zhang X, Wang T, Wang P, Hu N (2016) High-throughput assessment of drug cardiac safety using a high-speed impedance detection technology-based heart-on-a-chip. *Micromachines* 7:122
25. Shin SR et al (2016) Aptamer-based microfluidic electrochemical biosensor for monitoring cell-secreted trace cardiac biomarkers. *Anal Chem* 88:10019–10027
26. Zhang YS et al (2017) Multisensor-integrated organs-on-chips platform for automated and continual in situ monitoring of organoid behaviors. *Proc Natl Acad Sci* 114:E2293–E2302
27. Skardal A et al (2017) Multi-tissue interactions in an integrated three-tissue organ-on-a-chip platform. *Sci Rep* 7:8837

28. Dauth S et al (2017) Neurons derived from different brain regions are inherently different in vitro: a novel multiregional brain-on-a-chip. *J Neurophysiol* 117:1320–1341
29. Moya A et al (2018) Online oxygen monitoring using integrated inkjet-printed sensors in a liver-on-a-chip system. *Lab Chip* 18:2023–2035
30. Misun PM, Rothe J, Schmid YRF, Hierlemann A, Frey O (2016) Multi-analyte biosensor interface for real-time monitoring of 3D microtissue spheroids in hanging-drop networks. *Microsyst Nanoeng* 2(1):1–9. <https://doi.org/10.1038/micronano.2016.22>
31. Vollmer AP, Probst RF, Gilbert R, Thorsen T (2005) Development of an integrated microfluidic platform for dynamic oxygen sensing and delivery in a flowing medium. *Lab Chip* 5(10):1059–1066. <https://doi.org/10.1039/b508097e>
32. Ungerböck B, Mistlberger G, Charwat V, Ertl P, Mayr T (2010) Oxygen imaging in microfluidic devices with optical sensors applying color cameras. *Procedia Eng* 5:456–459. <https://doi.org/10.1016/j.proeng.2010.09.145>
33. Sticker D et al (2019) Oxygen management at the microscale: a functional biochip material with long-lasting and tunable oxygen scavenging properties for cell culture applications. *ACS Appl Mater Interfaces* 11:9730–9739
34. Zirath H et al (2018) Every breath you take: non-invasive real-time oxygen biosensing in two- and three-dimensional microfluidic cell models. *Front Physiol* 9:815. <https://doi.org/10.3389/fphys.2018.00815>
35. Rothbauer M et al (2020) Monitoring tissue-level remodelling during inflammatory arthritis using a three-dimensional synovium-on-a-chip with non-invasive light scattering biosensing. *Lab Chip* 20(8):1461–1471. <https://doi.org/10.1039/C9LC01097A>

Microfluidics in Biotechnology: Quo Vadis



Steffen Winkler, Alexander Grünberger, and Janina Bahnemann

Contents

1	Introduction	356
2	Main Fields of Microfluidics in Biotechnology and Their Realized Potential	357
3	Challenges and Solutions for Microfluidic Proof-of-Concept Systems in Biotechnology	362
3.1	Design and Fabrication	362
3.2	Handling	363
3.3	Standardization	365
4	Emerging LOCs: From the Lab to the Chip	366
4.1	Directed Evolution and Adapted Laboratory Evolution	366
4.2	“CRISPR-on-a-Chip” (COC)	367
4.3	Organisms-on-a-Chip	368
5	Future LOC Technologies: From Lab Applications to Point-of-Use Solutions	369
5.1	Advanced Microfluidic Technologies	369
5.2	Advanced Miniaturized Analytics	370
5.3	Digitalization: Machine Learning, Neuronal Networks, and Artificial Intelligence ..	371
6	Integrated Point-of-Use Devices for Monitoring, Understanding, and Controlling Bioprocesses	371
7	Concluding Remarks	373
	References	374

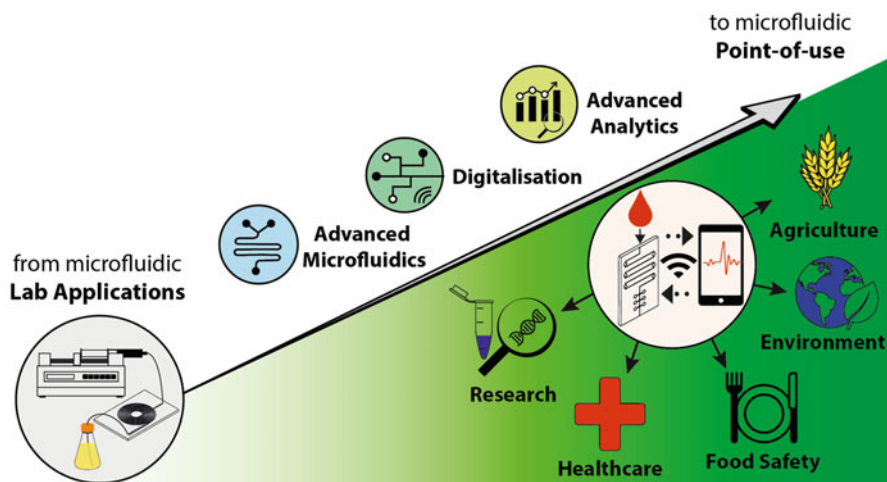
Abstract The emerging technique of microfluidics offers new approaches for precisely controlling fluidic conditions on a small scale, while simultaneously facilitating data collection in both high-throughput and quantitative manners. As such, the so-called lab-on-a-chip (LOC) systems have the potential to revolutionize the field of biotechnology. But what needs to happen in order to truly integrate them

S. Winkler and J. Bahnemann (✉)
Institute of Technical Chemistry, Leibniz University Hannover, Hannover, Germany
e-mail: jbahnemann@iftc.uni-hannover.de

A. Grünberger (✉)
Multiscale Bioengineering, Technical Faculty, Bielefeld University, Bielefeld, Germany
e-mail: alexander.gruenberger@uni-bielefeld.de

into routine biotechnological applications? In this chapter, some of the most promising applications of microfluidic technology within the field of biotechnology are surveyed, and a few strategies for overcoming current challenges posed by microfluidic LOC systems are examined. In addition, we also discuss the intensifying trend (across all biotechnology fields) of using point-of-use applications which is being facilitated by new technological achievements.

Graphical Abstract



Keywords Biochemical engineering, Industrial biotechnology, Lab-on-a-chip, Medical biotechnology, Microfluidic screening, Microfluidics, Nanofluidics, Organ-on-a-chip, Point-of-care, Point-of-use

1 Introduction

The application of microfluidic systems in biotechnology has recently become a subject of intense research interest [1, 2]. Emerging research and industrial applications include point-of-care medical diagnostics [3], organ-on-a-chip [4], and multiresistant bacteria testing [5] via microbioreactors [6] in red biotechnology. In white biotechnology, current approaches include catalysis, single-cell culture [7, 8], and droplet-based screening [9] through integrated biosensors and other analytics in miniaturized devices. Nevertheless, many microfluidic applications still depend on proof-of-concept systems, which have not yet realized their full potential. Accordingly, one of the most pressing challenges that will need to be addressed over the next few years is how to efficiently and effectively transform these systems into

routine applications that can actually be advanced into the market and, ideally, exceed the “gold standards” that currently exist in the field.

But how does this process look like? What, exactly, does it entail? In this review, the current state of the art of microfluidic systems is surveyed, with the aim of highlighting some of the most promising applications that have been developed to date. Furthermore, we identify and consider a number of pressing challenges that must be addressed before the full potential of this emerging technology can be realized within the field of biotechnology – and a few emerging applications and technologies are also highlighted to illustrate how (taken together) they might be leveraged to create superior microfluidic devices in the near future. Finally, we offer a few cautious predictions regarding how microfluidic systems might shape biotechnology in the future.

2 Main Fields of Microfluidics in Biotechnology and Their Realized Potential

There is an enormous variety of microfluidic systems currently being deployed in the field of biotechnology research – although lab-on-a-chip (LOC) is frequently employed as an umbrella term to broadly describe all of these microfluidic-based biotechnologies. By way of example, some of these systems include PCR-, genomics-, proteomics-, diagnosis-, catalysis-, transfection-, organ-, human-, tumor-, electrophoresis-, differentiation-, microscopy-, and bioreactors-on-a-chip. While most LOCs remain locked in the proof-of-concept phase, over the last decade a few have made advancements into the broader market. The commercial potential of LOCs has thus already been partially realized, in the form of aspiring start-ups and commercially available devices – although the present state of affairs only hits at the tremendous future potential for deploying LOCs within routine biotechnological applications. In this review, we have identified 350 companies that have begun to explore incorporating microfluidics into biotechnological applications (Fig. 1), with the particular focus on microfluidic devices in the following application areas in biotechnology: clinical applications, including point-of-care (POC) devices and other devices for clinical diagnosis; screening techniques; cell manipulation and analysis, such as single-cell sorting; genetics and genomics, with established technologies like PCR-on-a-chip; bioanalytics and biosensors; and organ-on-a-chip (OOC), among others.

The number of companies developing microfluidic systems for biotechnological application is now growing significantly. The first companies in this field primarily focused on diagnostic devices and gene analysis systems (see Fig. 1, “Clinical Applications (POC/Diagnosis)” and “Genetics and Genomics”). This is not surprising, taking into account that the first microfluidic breakthroughs in the world of biotechnology were achieved in these fields. Driven by the human genome project, capillary electrophoresis technology (a predecessor to the electrophoresis-on-a-chip)

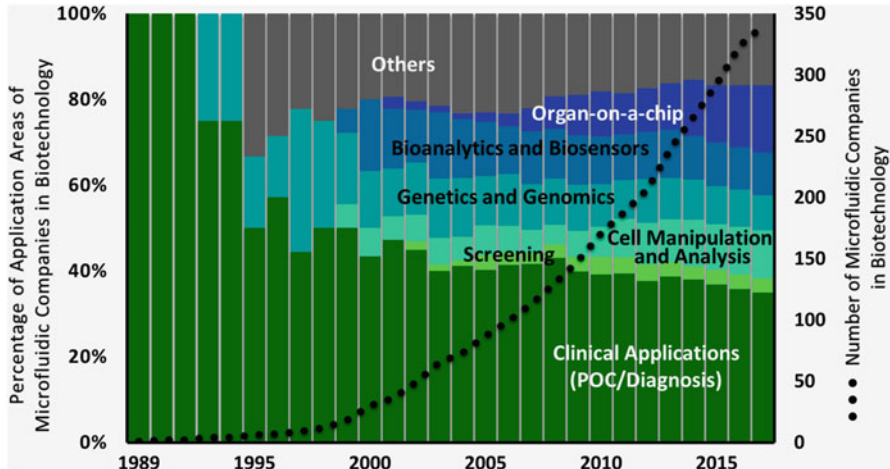


Fig. 1 Overview of the development of companies offering microfluidics for application in biotechnology over the past 20 years. This figure is based on an extensive market research, which the authors have carried out consistently (based on the references [10–12]) in 2020 and reflects only a trend in company development. The authors provide no guarantee for the exact number of existing companies focusing on microfluidics for biotechnological applications

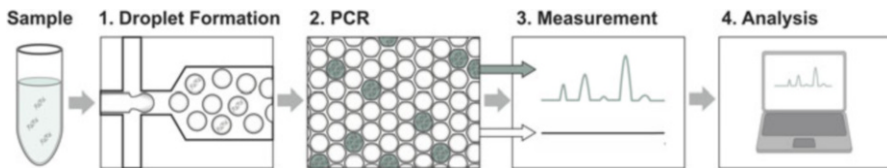


Fig. 2 The principle of digital PCR. In the first step, droplet microfluidics is used to distribute the DNA molecules in independent droplets. After the PCR, only droplets containing DNA are detected by fluorescence measurements. The distribution of DNA in the droplets follows a Poisson’s distribution that is finally used to calculate the DNA quantity. Translated with permission from J. Bahemann and A. Grünberger [15], Copyright (2021), Zukunftsforum Biotechnologie (Hrsg.), DECHEMA e.V. Frankfurt/M. (2021)

was invented to increase DNA sequencing speed and throughput [13]. Not only the sequencing, but also the powerful technology of PCR has been successfully miniaturized [14]. PCR-on-a-chip technology has developed rapidly in recent years, and these days more advanced technologies that build on this foundation – such as the digital PCR (dPCR) (Fig. 2) [16, 17] – are actually beginning to replace longstanding non-microfluidic “gold standards” such as quantitative PCR (qPCR).

Companies have also increasingly started to deploy these technologies in more commercially profitable endeavors, that is the development of POC diagnostics (Fig. 3). The potent combination of advanced liquid handling features – such as pumping, mixing, and separation – with gene analysis techniques, and the potential

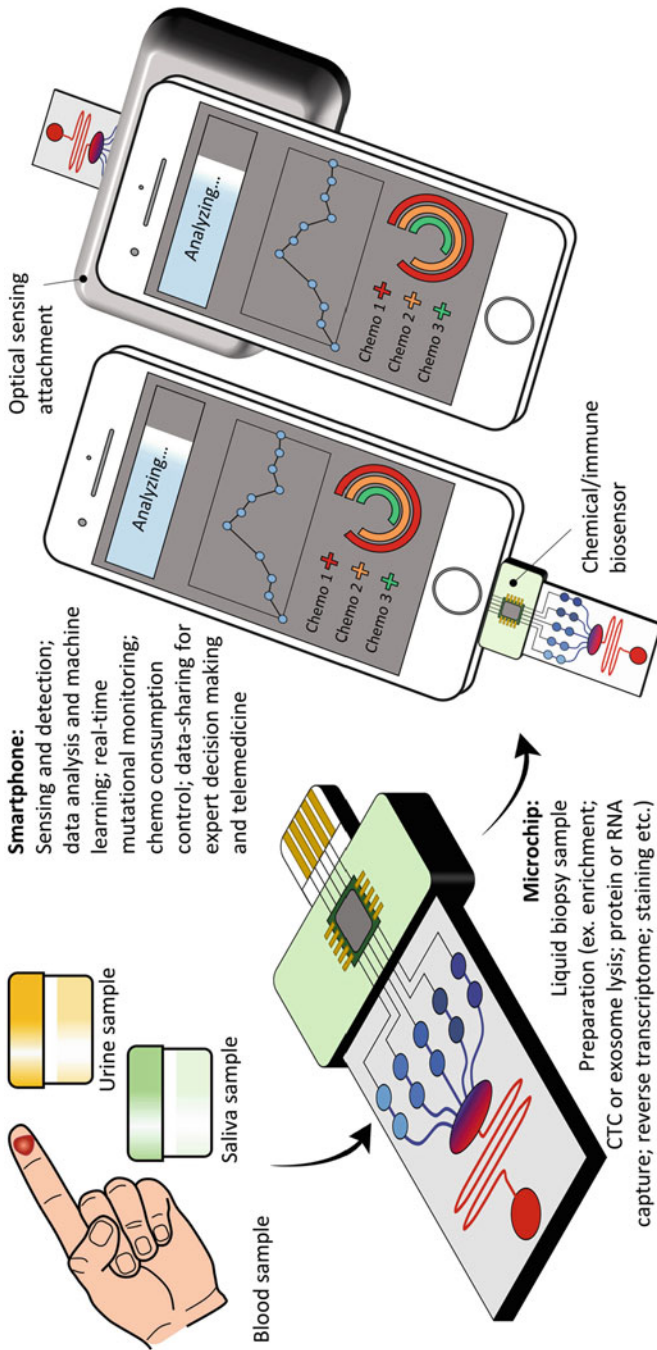


Fig. 3 Example of a microfluidic point-of-care device. A patient sample, such as blood, saliva, or urine, is processed and analyzed using a microfluidic chip. The chip contains a biosensor for detection of biologic markers and is read out and analyzed by a connected smartphone. Reprinted from Samandari et al. [18] (Copyright (2018), with permission from Elsevier)

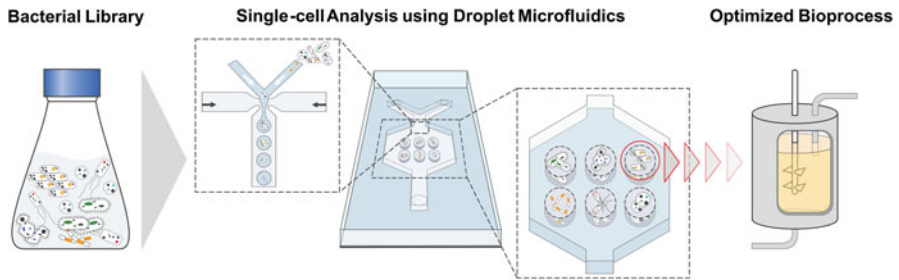


Fig. 4 Principle of single-cell analysis using droplet microfluidics. Herein, droplet microfluidics is used to singularize different types or strains of bacteria of a library in droplets followed by single-cell analysis and identification of potent cells for optimization of a specific bioprocess. Translated with permission from J. Bahnemann and A. Grünberger [15], Copyright (2021), Zukunftsforum Biotechnologie (Hrsg.), DECHEMA e.V. Frankfurt/M. (2021)

for usage in highly rentable clinical studies, has led to a veritable explosion of microfluidic POC start-up companies. Indeed, POC devices (see chapter: “Lab-on-a-Chip Devices for Point-of-Care Medical Diagnostics” [3]) currently constitute the single largest market for LOCs in biotechnologies.

The discovery of droplet microfluidics has facilitated the emerging field of single-cell analytics (Fig. 4). In the last years, droplet microfluidics has been applied to cell sorting [19], mammalian cell analysis [20, 21], microorganism analysis [22], and single-cell drug screening [23]. In addition, developments in the field of droplet microfluidics have also led to advancements in microfluidic ultra-high-throughput screening [24]. One major push on this front is to replace the current well-plate drug screening process commonly used in the pharmaceutical industry by droplet microfluidics.

As illustrated in the chart shown in Fig. 1, there are also companies working in the field of bioanalytics and biosensors. These companies offer an ever-increasing set of diverse analytical tools – from biosensors for environmental or animal applications to novel microfluidic modulation spectrometers [25], microfluidic resistive pulse sensing [26], sub-terahertz (THz) vibrational spectroscopy [27], optical microcavity technologies [28], to name but a few.

OOC applications represent perhaps the latest – and certainly the most advanced – application of this technology. OOCs combine tissue engineering with microfluidics to achieve complex 2D or 3D cellular systems [4]. Due to their exciting potential to revolutionize drug testing protocols and minimize costs associated with drug failure in the clinical stages (which is unfortunately extremely common), multiple start-ups have charged into the market in this area [29]. Furthermore, these systems can also be further refined into disease-on-a-chip (DOC) systems, which may be able to provide researchers entirely new insights into pathological processes. Even human-on-a-chip systems are now being developed. In principle, these systems combine several OOCs containing different human cells in a single chip to simulate even the most complex human physiological processes (Fig. 5).

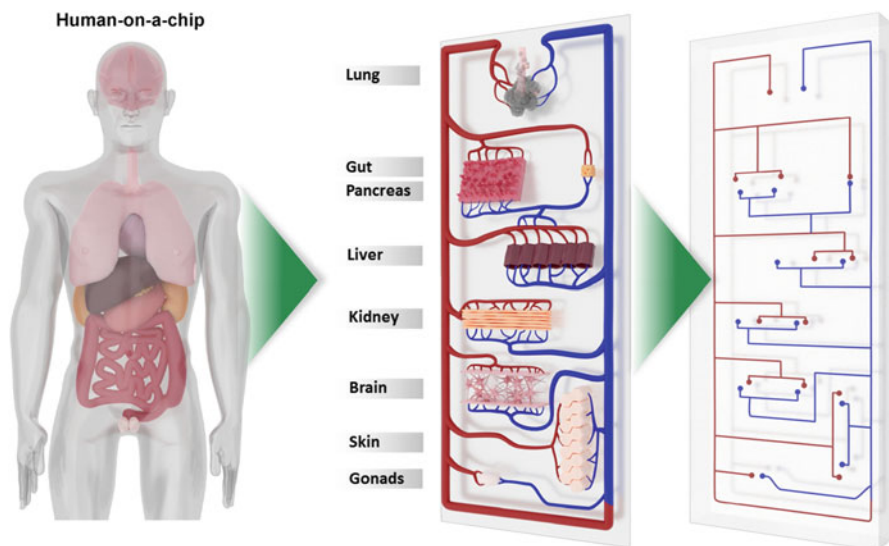


Fig. 5 Principle of the human-on-a-chip. The human-on-a-chip mimics human physiological processes by connecting and maintaining several different organ-on-a-chip systems in a single microfluidic chip. With permission from *Springer International Publishing: Bahnmann et al.* [30], Copyright (2021)

As the illustrated examples demonstrate, microfluidics is currently experiencing a significant breakthrough period within the field of biotechnology. The sheer scope and diversity of the adoption of this technology in this field is perhaps most starkly underlined by the fact that the fraction of “unassignable” companies (see Fig. 1, “Others”) is increasing rapidly. At the same time, however, microfluidics unquestionably still remains in its infancy – indeed, many LOCs exist only in the form of proof-of-concept systems [31]. With inconvenient handling requirements, comparatively low robustness, complex standards, and bulky hardware, LOCs are often derided as complicated “chip-in-a-lab” systems [32]. Accordingly, beyond the few commercially available systems, most published microfluidic devices still suffer from a low technological readiness level (TRL) of just 3–4 points out of a 12-point scale [32]. Even comparatively established technologies in this area – such as POC testing – have a long way to go before their full potential will be realized. Critical challenges continue to plague researchers and developers, and must be adequately addressed before microfluidic routine applications can truly replace the current “gold standards” in biotechnology.

3 Challenges and Solutions for Microfluidic Proof-of-Concept Systems in Biotechnology

In the last 20–30 years, the applications of microfluidic technologies have been pioneered in research areas such as microsystems engineering, physics, chemistry, and biology. This has led to the development of a wide array of promising proof-of-concept systems, which primarily seek to miniaturize and automatize existing lab procedures in a LOC format. But the central question now faced by this maturing industry is whether these systems actually confer any true advantage over the “gold standards” that are currently being used in these areas. Three major challenges – summarized in Fig. 6 – that continue to plague microfluidic proof-of-concept systems and early commercialized devices are identified and discussed below.

3.1 Design and Fabrication

The first key obstacle for the development and deployment of microfluidic devices for biotechnological applications has been the relatively limited access that researchers actually have to microfluidic fabrication facilities [33–35]. As reported by Kotz et al. [36], a number of fabrication techniques have been developed for manufacturing microfluidic devices. Perhaps the most widely used are molding

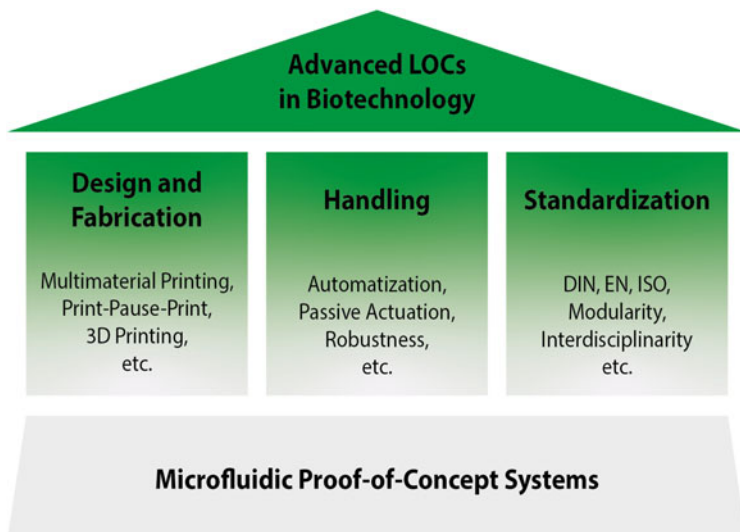


Fig. 6 Towards advanced microfluidic devices in biotechnology. Microfluidic proof-of-concept systems are currently facing great challenges, such as the design and fabrication, handling and standardization of microfluidic devices, to become advanced LOCs for real-world applications in biotechnology

techniques – including, for example, hot embossing, injection molding, and soft lithography – and laminates. While these techniques represent a solid foundation for the production of three-dimensional microfluidic structures, they are also extremely laborious and costly [31]. As a result, only engineers and microsystems technicians who are already experts in the field of microfluidics tend to be comfortable deploying them, whereas experts in the fields of their intended substantive application – such as biologists and biochemists – can generally contribute little to their development. In addition, the complicated and time-consuming developmental process of these fabrication techniques creates an understandable reluctance to implement many small, but often useful, improvements. One potential solution is showcased in the latest advances in additive manufacturing [31, 37–40].

Design and fabrication through these methods are comparatively much simpler, and 3D printers are far more affordable than classic clean room facilities. Furthermore, one early concern with respect to this method – that the printing resolution would be too low – has effectively been mitigated through recent advancements in multijet printing [41], stereolithography, and two-photon laser techniques (which are now reaching the micrometer and even nanometer scale). As the number of 3D printers is increasing, so are the number of different 3D printing materials that can be used.

Especially for biological applications, materials (such as acrylates or silicones) that are biocompatible are increasingly being brought onto the market [42–44]. Although many high-resolution 3D printers remain limited for fabrications employing just a single material, in the last few years, tremendous efforts have been made to achieve multimaterial 3D printing [45] or multiprocess 3D printing (as well as print-pause-print (PPP) 3D printing) [46]. The successful integration of sealing connections (e.g., elastic silicones), movable functional units (e.g., microvalves or micropumps [47]), porous barriers (e.g., porous membranes [48]), electronic components (e.g., electrochemical sensors [49, 50], heating/cooling elements [51], magnetic elements [52], and copper fibers for dielectrophoresis [53]) – and even the implementation of chemical reagents [54, 55] solely by 3D printing – has already been well demonstrated in the literature. Because multimaterial 3D printing is of significant interest for many other industries, we will likely see further advances within this field in the years to come.

3.2 *Handling*

As one might expect, realizing the vision of miniaturizing very complex multi-step lab procedures into a simple LOC has also turned out to be a very challenging endeavor. At the micro- or nano-scale, even the smallest disturbances – such as dust particles, air bubbles, vibrations, leaking interconnections, leachables, etc. – can lead to dysfunction of the whole chip, necessitating time-consuming and expensive repair (or even replacement) efforts. The robustness of any LOC is thus a crucial component of consideration [56], and this is only all the more true when the system in

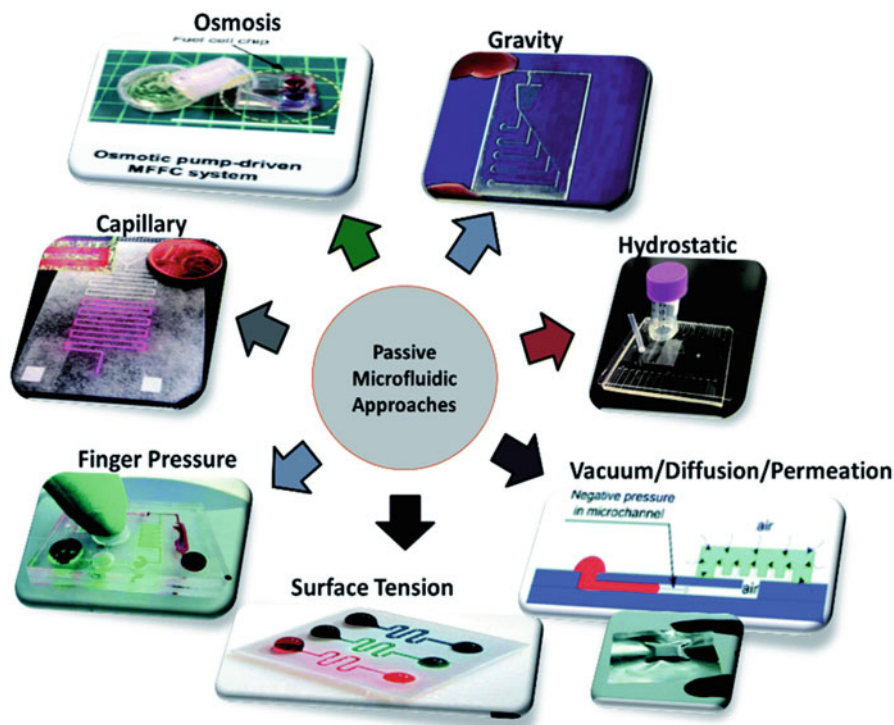


Fig. 7 Different approaches employed in passively driven microfluidics and LOC devices. All techniques are actuated by a single driving force that is controlled by specific structural elements for precise control of flow, mixing events, and other LOC operations. Reproduced from Ref. [57] with permission from The Royal Society of Chemistry

question will be used not by a trained scientist, but rather by untrained people (such as students or even patients) as in the so-called easy-to-use POC devices.

Improving the robustness of future LOC devices can be best achieved by replacing actively controlled units, such as pumps and valves, with passively controlled elements that are incorporated directly into the design of the chip itself (Fig. 7). Paper-based POC devices have already illustrated how this can be realized by using microcapillary forces that induce a passively controlled flow [58]. These flow speeds depend on the kind of adsorption material used, which can be determined during the design process. Similarly, centrifugal POC devices use predefined channel sizes to convert centrifugal forces into well-defined liquid flow. The so-called passive check and burst valves allow a more complex design of the fluid circuit. And complex processes can also be completely controlled by either the chip design or by a few external actuators. The concept of passive control can be transferred into any application where easy handling and automatization is needed –

and since many protocols for preparative or analytical applications in biotechnology follow predictable steps that are always the same, this is a logical fit.

Adoption of this principle is currently a prime focus of the so-called microfluidic circuits or microfluidic networks [59]. These networks seek to transfer Ohm's law ($U = I \cdot R$) of electric resistance into the field of microfluidics, where the resistance R corresponds to the microfluidic channel resistance, the intensity I to the flow-rate, and the potential U to the pressure [60]. In theory, this means that the flow can be controlled by the channel resistance, the channel resistance in turn by the channel geometry, and the channel geometry by the chip design and fabrication. Using these built-in control features, a manufacturer can theoretically exert maximum control of the process – to the point where, at least ideally, an unexperienced end user may only need to push a start-button. This principle can also be further extended to achieve time-dependent LOC control (e.g., where a specific valve only opens when an increasing pressure gradient reaches a critical value, etc.). Duncan et al. have already used a constant and single vacuum source in combination with microvalves and resistors to achieve oscillating microvalves, which, in principle, could function as a membrane-based micropump [61]. Furthermore, slower or faster oscillations could certainly be achieved by adaptation of the resistors, leading to different pump speeds. Just like in electronic chips, these oscillators could theoretically be further used to induce rhythms that activate several LOC procedures after a specific time or after a single externally controlled event (such as a simple valve opening).

None of the above-mentioned methods can currently control complete LOC procedures. However, although they are still in their infancy, these methods already demonstrate the high potential of passively controlled microfluidics for easy-to-use but fully automated LOCs – as illustrated by the possibility that a sophisticated design of a microfluidic chip could (for example) be harnessed to upgrade a microvalve to a micropump without losing robustness. In contrast, classic pneumatic micropumps are controlled by at least two pressure or vacuum sources [62], which are in turn controlled by external valves constituting a serious additional risk for device dysfunctions.

3.3 *Standardization*

In principle, the primary purpose of LOC technologies is to transfer research in the fields of biology and chemistry into our modern world of machines, computers, and data. This requires tremendous interdisciplinary input from scientists across a wide range of fields, all leveraging and combining their specific areas of substantive knowledge to design, manufacture, functionalize, automatize, and deploy sophisticated LOCs. On the one hand, this interdisciplinarity push has led to a huge variety in LOC devices while, on the other hand, it has also led to veritable confusion in the form of a seemingly endless number of different fabrication techniques, design concepts, ways of flow control, integration techniques, etc. Successful mass-market incorporation of microfluidics technology into biotechnological applications will

ultimately require the adoption of *standardization concepts* (e.g., ISO standards, protocols and guidelines to organize the pioneered knowledge into a common microfluidic language, etc.) in order to allow researchers from all fields to meaningfully understand and contribute to future LOC development by adopting high level good manufacturing practice (GMP) standards in most fields of biotechnology. This standardization will also allow biologists to consider fabrication and design rules (such as material properties and microchannel characteristics), and engineers to consider biological demands (such as maximal shear flow, biocompatibility and more), and to allow both groups to effectively communicate their own needs using a common language of sorts [63].

For very basic operations (such as pumping, mixing, and separation), microfluidic solutions have already been developed that can be further characterized and classified to develop a database of microfluidic operators. This modularity is crucial to facilitate faster design and configuration via plug-and-play processes [31]. Once again, drawing on analogies to the field of mechanics, these modules could be saved as 3D computer-aided design (CAD) files – although, of course, new software must still be developed to enable the proper and efficient use of these files. 3D printing of microfluidic devices, in particular, could further push the standardization of LOC modules. Additionally, there is a need for standardization efforts regarding the chip-to-world interface [64]. Currently, many proof-of-concept systems use diverse kinds of tube connections, pumps, control units, and more. For industrial applications (such as drug screening), however, LOCs must be easily implementable into existing processes and standards.

4 Emerging LOCs: From the Lab to the Chip

One focus of current microfluidics development aims to miniaturize biotechnological workflows “to the chip,” in order to take advantage of greatly improved workflows that are realizable via miniaturization and/or automatization. In principle, this holds true not just for classical LOCs procedures (such as the PCR), but also for newer biotechnological methods (see following subchapters). The huge variety of possible LOCs cannot be summed up in a single book chapter; therefore, in this section, we focus only on a subset of novel LOCs that show a high potential for further revolutionizing biotechnologies.

4.1 *Directed Evolution and Adapted Laboratory Evolution*

In 2018, the Nobel Prize in Chemistry was awarded to Frances H. Arnold for her pioneering achievements in directed evolution. The techniques that she spearheaded have helped to optimize reactions by developing faster, more specific, more stable, and/or more sensitive enzymes [65]. These advances are of particular interest for

large industries focused on improving or streamlining the performance of bioprocesses. Using the phenomenon of mutagenesis, enzymes can be either specifically or randomly modified to create mutant libraries, which can then be subsequently screened to identify improved enzyme abilities. The last step remains a challenging task – and LOC platforms that make use of droplet screening, in combination with advanced droplet sorting systems, are ideal tools for efficiently screening mutant libraries to identify enzymes with enantio-selectivity or high catalytic activity in ultrahigh-throughput [66]. Organisms (such as *Escherichia coli*) that express the mutant enzymes may also be singularized in droplets, lysed, analyzed, and sorted. Such systems could even be further extended by LOC-based transformation or transfection, to re-cultivate promising mutants. It also bears noting that the high-throughput and automatization properties of directed evolution on-chip would contribute to a greater understanding of enzyme mechanisms and evolution processes in general.

4.2 “CRISPR-on-a-Chip” (COC)

Emmanuelle Charpentier and Jennifer A. Doudna were honored with the Nobel Prize for Chemistry in 2020 for their outstanding scientific achievement in developing the CRISPR-Cas (Clustered Regularly Interspaced Short Palindromic Repeats) method for gene editing. The discovery of the so-called gene scissor represents a fundamental breakthrough in the field of molecular biology, and is expected to tremendously change life sciences in the years to come [67, 68] – just like DNA sequencing and PCR have done in previous decades. Indeed, researchers have already started to use this technique in microfluidic platforms [69], predominantly for on-chip point-of-care gene detection with CRISPR-based gene biosensors or automated gene editing in LOCs.

One recently developed chip uses a graphene field-effect transistor, in combination with a deactivated CRISPR-Cas9 protein complexed with a specific single-guide RNA, to achieve the unmediated detection of a specific gene on-chip (Fig. 8a) [70]. In contrast to PCR, this system can abstain from gene amplification and leverage CRISPR technology to create gene biosensors. By implementing biosensors into future COCs, this technique could potentially be used to screen large numbers of mutations for detecting diseases in a microarray – and the quantification of gene expression could also be applied to clusters of genes for a completely new molecular understanding of gene regulation and other basic mechanisms (such as cell differentiation), which in turn might be used for the development of novel drugs.

In combination with microfluidics, the CRISPR-Cas9 system may also be used to automatize gene editing. A recent approach combines digital microfluidics with the CRISPR-Cas9 technique for on-chip gene editing of cell cultures (Fig. 8b) [71]. Similar platforms could enable multiplexing and high-throughput gene editing in future, opening up theoretically endless application possibilities across many diverse sub-fields in the biotechnology sphere.

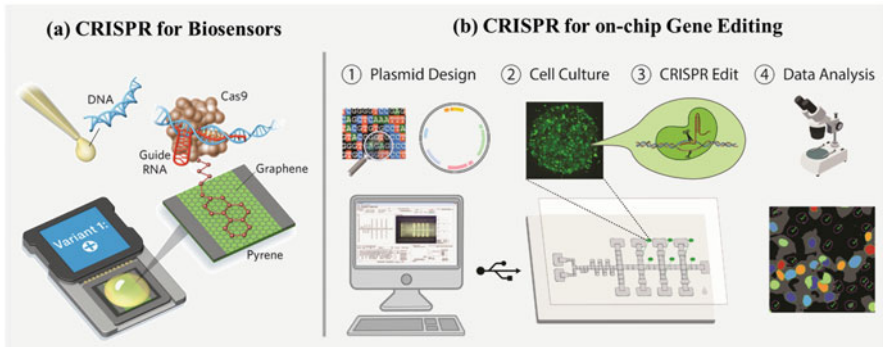


Fig. 8 CRISPR-on-a-chip. **(a)** CRISPR-Cas9 for unamplified gene detection in biosensors. The Cas9 complexed with a target-specific guide RNA is immobilized on the surface of the graphene within a graphene field-effect transistor. The complex identifies and binds to the target gene, resulting in an electrical signal output. Adapted by permission from Springer Nature: Nature Biomedical Engineering, Hajian et al. [70], copyright, 2020. **(b)** An automated CRISPR-based gene editing platform. Designed plasmids (1) are used for gene editing of cell cultures inside a microfluidic chip (2, 3) and results are analyzed by microscopy (4). The computer-controlled chip is based on digital microfluidics for dispersion, merging, mixing, and splitting of droplets. Reproduced from Ref. [71] with permission from The Royal Society of Chemistry

4.3 Organisms-on-a-Chip

After single-cell analysis and organs-on-a-chip, the “next level of life” is represented in the emerging “organisms-on-a-chip” technology. Similar to organs-on-a-chip, organisms-on-a-chip can be used for drug testing, diagnosis, or simply to understand biochemical and physiological processes. Prominent examples thereof are the nematode *Caenorhabditis elegans* [72], the malaria parasite *Plasmodium falciparum* [73], and the zebrafish [74]. Plants-on-a-chip [75] and roots-on-a-chip [76] have also been developed in the field of green biotechnology, while for blue biotechnology corals-on-a-chip are being developed [77]. It can simply be stated that the opportunities for future organisms-on-a-chip systems are essentially endless – although to date, few avenues have truly been explored in this emerging field. One challenge is the difficulty of adequately emulating natural as well as defined artificial environments [78, 79] to enable detailed fundamental insights regarding an organism’s overall behavioral pattern.

5 Future LOC Technologies: From Lab Applications to Point-of-Use Solutions

The dawning of the twenty-first century has ushered in the so-called information age, and the immediate access to comprehensive information enabled by this incredible technological revolution in computing will only become increasingly important in the years to come. Industrial applications are already promoting on-demand and easy-to-use technologies. Smartphones, for example, have demonstrated the enormous benefit of immediate information exchange. POC devices remain perhaps the best examples, to date, of similar efforts to leverage microfluidic biotechnologies for rapid extraction of information via implemented analytics – however, in the future, this trend will not be limited to POC and other red biotechnological analytic devices, but will instead almost certainly expand to all biotechnology fields in the form of point-of-use applications (Fig. 9). Accordingly, in the following we will discuss three central LOC technologies representing advancements of current microfluidic lab applications to point-of-use analytics in all aspects of biotechnology.

5.1 Advanced Microfluidic Technologies

Point-of-use applications require robust LOCs based on easy-to-use working principles. As described above, passively actuated LOCs (such as paper, centrifugal, and

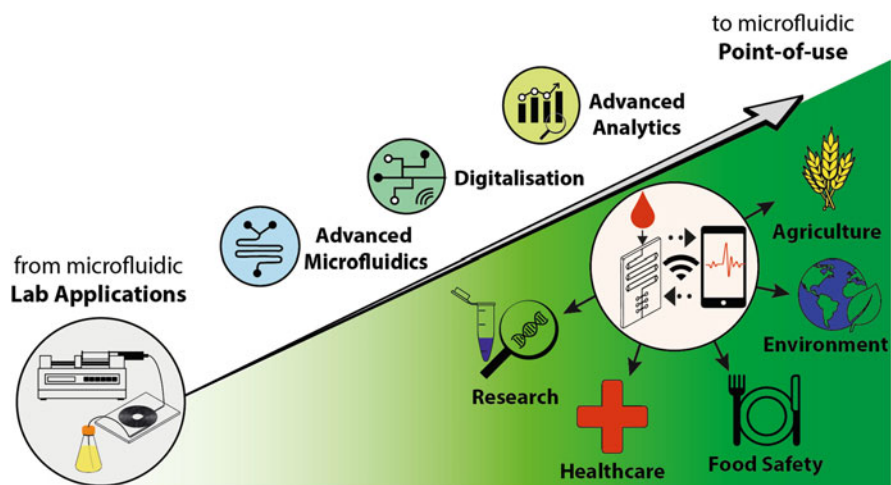


Fig. 9 Microfluidic devices in biotechnology: From microfluidic lab applications to microfluidic point-of-use. Advances in microfluidics, analytics, and digitalization will accelerate the trend to advanced microfluidic devices – available at the point-of-use. These point-of-use systems will rapidly expand to large biotechnological application fields, such as research, healthcare, food safety, environment protection, and agriculture

capillary microfluidics) further these goals by increasing the level of automatization within the system. Another emerging technology that also exhibits great potential to automate actively controlled LOCs is digital microfluidics based on the concept of electrowetting. Electrowetting – originally developed for displays and lenses – uses electrodes that, when activated, increase hydrophilicity. Consequently, droplets of liquids can be freely controlled in two dimensions and mixed, incubated, or divided using digital commands [80]. These very basic operations in turn facilitate greater automatization of lab procedures. In addition, the electronic (i.e., digital) control of droplets also makes it easier to connect and control electrowetting-based LOCs with smartphones. Because LOCs always benefit from advances in liquid handling within the system, this technique is increasingly being leveraged within new microfluidic applications [80].

LOCs must also offer as many functionalities as possible to meet the complex demands of endless possible point-of-use applications – and the nascent field of nanofluidics offers even greater promise for further expansion of microfluidic functions [81, 82]. Due to substantial recent improvements in device fabrication, LOCs have now reached the nanometer and even sub-nanometer scale. This does not simply result in advantages such as the further increase in throughput; it also introduces both molecular and quantum effects, as well as special fluid phenomena not seen in macroscale systems [82]. These effects include (for example) faster flow of water in nanotubes and faster ion transport, both of which can be used for biological or biotechnological purposes. For example, nanochannels have already been designed to mimic the high water permeability and selectivity of aquaporins [83], and artificial carbon nanotube molecular transport systems have been designed that mimic the process seen in proteins transported across cell membranes [84].

5.2 *Advanced Miniaturized Analytics*

Aside from microfluidic technologies, implementable analytics are also essential for advancing to omnifarious point-of-use systems. Biosensors are currently the analytical tools of choice in this regard [44, 85]. They typically contain biological catalytic recognition elements (such as enzymes, antibodies, aptamers [86], peptides, cells, or molecularly imprinted polymers) and a transducer (which is typically electrochemical, optical, acoustic, or gravimetric in nature) [87, 88]. Transducer technology in particular has been rapidly advancing, to the point where nanoresonators, localized surface plasmon resonance (LSPR) [89], surface acoustic waves (SAW) [90], optical fibers [91], photonic crystals [92], and quartz crystal microbalances (QCM) [93] are now all being miniaturized into an on-chip format. But biosensors may not be the tool of choice in the future – emerging analytics such as microscopy-on-a-chip [94, 95], terahertz spectroscopy [96], and field asymmetric ion mobility spectrometry (FAIMS) all show tremendous promise on this front [97]. As soon as it comes to identification and quantification of analytes in complex samples, however, state-of-the-art analytics such as mass spectrometry, Raman-, NMR-, or IR-spectroscopy

remain indispensable. Although attempts have been made to miniaturize mass spectrometers [98], NMR- [99], IR- [100], and Raman spectrometers [99], miniaturized building components are often not commercially available yet. Nevertheless, the current trend to point-of-use applications may well create a market for such parts, which would thereby facilitate the future miniaturization of high-end analytics.

5.3 Digitalization: Machine Learning, Neuronal Networks, and Artificial Intelligence

The capacity for high-throughput analysis within microfluidic devices, in combination with advanced analytics, can quickly generate a veritable mass of data which can itself become very difficult to evaluate and visualize. This is particularly true when the raw data is tough to quantify as, for example, is the case for microscopic images of cells or complex sequence analysis. Machine learning, neuronal networks, and artificial intelligence have all been suggested as tools for efficiently combing through such data [101]. Possible microfluidic applications include cell classification [102], signal processing [103], DNA base calling for DNA sequencing [104], flow sculpting for microchannel design [105], and cell segmentation [106]. Moving forward, it will only become increasingly important to set up systems that facilitate the global sharing and evaluation of large data sets in real-time. For example, environmental pollution of the air might 1 day be tracked by smartphone compatible LOCs – which would then feed the data generated into cloud saving and deep learning tools that can be used to immediately identify possible causes, direct further measurements, and make useful predictions.

6 Integrated Point-of-Use Devices for Monitoring, Understanding, and Controlling Bioprocesses

Currently, the primary benefit of point-of-use devices is mostly seen in their portability, time efficiency, cost efficiency, and easy-to-use handling [107, 108]. But all of these abilities are really just basic requirements that will ultimately help to enable integrated point-of-use devices that facilitate unprecedented opportunities to constantly monitor important parameters and immediately react to alterations. Wherever there are processes which will benefit from creating such a real-time monitoring and feedback control loop, integrated point-of-use devices point the way towards an even more efficient and integrated future.

One prominent example of this phenomenon from the field of biotechnology is the bioreactor. Monitoring bioprocess parameters like pH, biomass, oxygen, glucose, and product concentration – and, in turn, controlling these parameters via a live feed – is the key to maximize product yields and purities [109]. While some basic

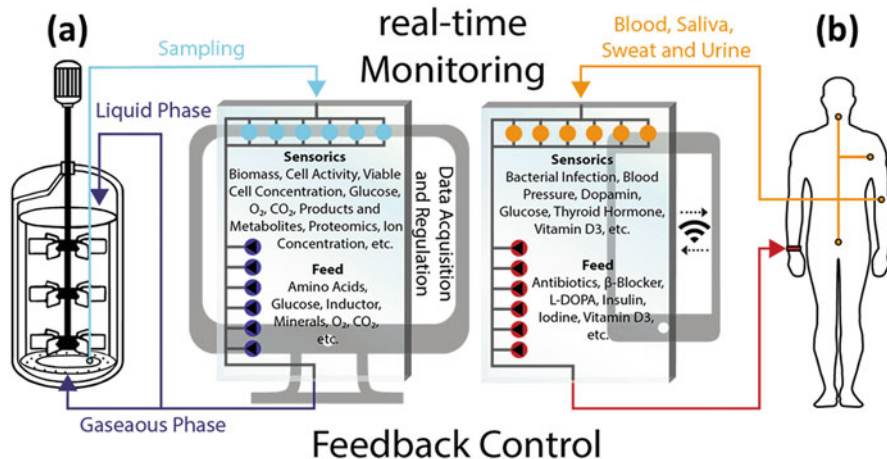


Fig. 10 The use of integrated point-of-use microfluidic devices for optimizing bioprocesses. The concept is illustrated using the example of a bioreactor (a) and a human being (b). These two bioprocesses can be monitored, analyzed, and controlled to improve either an industrial production or the state of health. Therefore, each LOC contains a sensor system, a connection to modern data analysis with computers or smartphones and an integrated feed. This results in a fully automatable control loop for permanent optimization, which in principle could be transferred to any bioprocess in all areas of life

parameters such as pH, temperature, and dissolved oxygen concentration are already being monitored on-line, various parameters still remain dependent on sampling for off-line detection. There is thus a clear need for novel on-line or at-line microfluidic, analytical, and data processing techniques that can be implemented within a single or multiple LOCs for multi-parameter monitoring. As illustrated in Fig. 10a, at-line LOCs could allow for the delivery and processing of samples and feedback-controlled feeding in a quasi on-line process with minimal dead volumes, dead time, and without unwanted influence on the process. Future advances in analytics will undoubtedly offer a wide variety of on-chip biosensors, spectrometers, microscopes, and other elements all aimed at measuring and calibrating an endless array of parameters with minimal time or sample requirements. In addition, LOCs could also exceed current feeding methods due to their ability to facilitate the precise mixing and distribution of a variety of independently controlled substances, enabling even the most complex feeding strategies for any kind of bioreactor. Finally, digitalization (including machine learning and neuronal networks) could foreseeably be used to interpret complex changes in bioprocess parameters and correlate them with a feedback control – effectively creating a full-automated bioreactor.

Similar to bioreactors, the objective of current POC devices is to understand, optimize, and control the human physiological (and in particular, pathological) processes. At present, most microfluidic POC devices obtain body fluids used for off-line analysis and subsequent therapy via drugs or other therapeutic strategies. But with miniaturized biosensors and micropumps, online monitoring and instantaneous

feedback-controlled drug therapy may foreseeably become available in the future. Exciting current examples of this young technology are implantable or on-skin glucose sensors in combination with insulin pumps [110, 111], dopamine monitoring [112], and online supplementation by infusion pumps [113]. Completely integrated point-of-use LOC devices for monitoring and feedback control could, in principle, be applied for nearly every biomarker in body fluids (Fig. 10b). This would create an invaluable tool in the fight against public health scourges like diabetes and hypertension – and it would also help physicians to recognize serious conditions (like lactate acidosis) as they are in the process of actively developing. To go even one step further, in the distant future, LOCs may 1 day become key tools in enhancing human physiology; for example, extracorporeal membrane oxygenation (ECMO) has already been intensively used to increase oxygenation in the blood of premature neonates [114] and COVID-19 patients [115]. And recently developed ECMO-on-a-chip systems [116, 117] may not only replace current ECMO devices – they could even be applied to increase athletic performance. Novel cancer treatment approaches are already exploring LOCs for on-chip immunotherapy [118]. Immunotherapy-on-a-chip could theoretically extract, sort, genetically modify, and return immune cells to the blood in a faster, less toxic, and more reproducible manner. Genetic modifications may also increase the effectiveness of immune cells against tumor cells [119] – and, in principle, other cells and other cell properties could also be modified, as well. In short, within our lifetimes LOCs may well become a valuable tool not only to develop a whole host of novel disease treatments, but also to optimize what even a healthy human being is capable of doing.

7 Concluding Remarks

Spearheaded by LOCs, microfluidics technology is an increasingly important tool across the field of biotechnology. Many successful proof-of-concept studies have already demonstrated the high potential for its application, and enterprising companies have already started to further realize this potential by introducing commercially available LOCs for routine applications (with a predominant focus, to date, on POC, screening, single-cell analytics, and novel organ-on-a-chip devices). Like with any emerging technology, significant challenges still block the path to full realization – including laborious and costly fabrication, inconvenient handling, and unsatisfactory standardization. Fast and easy fabrication by novel multimaterial 3D-printing, higher robustness via passively actuated chips as well as modularity, and the adoption of a unified and common biomicrofluidic language represent promising – but, as yet, not-fully-realized – solutions to these challenges. When these problems have been addressed and this technology is further buttressed via advanced microfluidic handling, advanced analytics, and digitalization, the practical applications promised by fully-mature microfluidic systems are nearly limitless: for example, the overwhelming number of analytical instruments currently used for monitoring and controlling processes could be simplified into a single, fully integrated point-of-use LOC. These

new opportunities will undoubtedly raise a whole host of thorny ethical considerations, up to and including the question of whether these new advances actually make our lives easier and better or instead threaten to fundamentally alter our very physical existence. In closing, such is the promise of this exciting field that it may not ultimately be a question of what we can do with microfluidics – but rather, what we *want* to do with it.

Acknowledgements The authors would like to thank Niklas M. Epping (Institute of Technical Chemistry, Leibniz University Hannover, Germany) and Dr. Natalie Rotermund (Institute of Zoology, University of Hamburg, Germany) for their contribution in creating the illustrations.

References

- Scheler O, Postek W, Garstecki P (2019) Recent developments of microfluidics as a tool for biotechnology and microbiology. *Curr Opin Biotechnol* 55:60–67. <https://doi.org/10.1016/j.copbio.2018.08.004>
- Bai Y, Gao M, Wen L et al (2018) Applications of microfluidics in quantitative biology. *Biotechnol J* 13:e1700170. <https://doi.org/10.1002/biot.201700170>
- Arshavsky-Graham S, Segal E (2020) Lab-on-a-chip devices for point-of-care medical diagnostics. *Adv Biochem Eng Biotechnol*. https://doi.org/10.1007/10_2020_127
- Maschmeyer I, Kakava S (2020) Organ-on-a-chip. Springer, Berlin, pp 1–32
- Khan ZA, Siddiqui MF, Park S (2019) Progress in antibiotic susceptibility tests: a comparative review with special emphasis on microfluidic methods. *Biotechnol Lett* 41:221–230. <https://doi.org/10.1007/s10529-018-02638-2>
- Frey LJ, Krull R (2020) Microbioreactors for process development and cell-based screening studies. Springer, Berlin
- Dusny C, Grünberger A (2020) Microfluidic single-cell analysis in biotechnology: from monitoring towards understanding. *Curr Opin Biotechnol* 63:26–33. <https://doi.org/10.1016/j.copbio.2019.11.001>
- Matula K, Rivello F, Huck WTS (2020) Single-cell analysis using droplet microfluidics. *Adv Biosyst* 4:1900188. <https://doi.org/10.1002/adbi.201900188>
- Payne EM, Holland-Moritz DA, Sun S et al (2020) High-throughput screening by droplet microfluidics: perspective into key challenges and future prospects. *Lab Chip* 20:2247–2262. <https://doi.org/10.1039/D0LC00347F>
- Fluidicmems (2020) Microfluidic companies | fluidicmems. <https://www.fluidicmems.org/microfluidic-companies>. Accessed 5 Dec 2020
- Google My Maps (2020) FluidicMEMS.com’s list of microfluidics/lab-on-a-chip companies – Google My Maps. <https://www.google.com/maps/d/u/0/viewer?ie=UTF8&hl=en&msa=0&z=2&mid=1e7udQ19Wyzaq4RVk48vWv8P59GM&ll=16.911338356870246%2C-6.3215279999999865>. Accessed 5 Dec 2020
- The MicroFluidic Circle (2020) Emerging microfluidic companies – the microfluidic circle. <https://www.ufluidix.com/circle/microfluidic-companies/>. Accessed 6 Dec 2020
- Swerdlow H, Gesteland R (1990) Capillary gel electrophoresis for rapid, high resolution DNA sequencing. *Nucleic Acids Res* 18:1415–1419. <https://doi.org/10.1093/nar/18.6.1415>
- Northrup MA, Gonzalez C, Hadley D et al (1995) A mems-based miniature DNA analysis system. In: Proceedings of the international solid-state sensors and actuators conference – TRANSDUCERS’95. IEEE, pp 764–767
- Bahnemann J, Grünberger A (2021) Biotechnologie ganz klein. *Zukunftsforum Biotechnologie* (Hrsg.), DECHEMA e.V., Frankfurt. [ISBN] 978-3-89746-232-8

16. Quan P-L, Sauzade M, Brouzes E (2018) dPCR: a technology review. *Sensors* 18:1271. <https://doi.org/10.3390/s18041271>
17. Samiei E, Tabrizian M, Hoorfar M (2016) A review of digital microfluidics as portable platforms for lab-on-a-chip applications. *Lab Chip* 16:2376–2396. <https://doi.org/10.1039/c6lc00387g>
18. Samandari M, Julia MG, Rice A et al (2018) Liquid biopsies for management of pancreatic cancer. *Transl Res* 201:98–127. <https://doi.org/10.1016/j.trsl.2018.07.008>
19. Cheng Z, Wu X, Cheng J et al (2017) Microfluidic fluorescence-activated cell sorting (μ FACS) chip with integrated piezoelectric actuators for low-cost mammalian cell enrichment. *Microfluid Nanofluid* 21:9. <https://doi.org/10.1007/s10404-017-1847-1>
20. Manak MS, Varsanik JS, Hogan BJ et al (2018) Live-cell phenotypic-biomarker microfluidic assay for the risk stratification of cancer patients via machine learning. *Nat Biomed Eng* 2:761–772. <https://doi.org/10.1038/s41551-018-0285-z>
21. Nimir M, Ma Y, Jeffreys SA et al (2019) Detection of AR-V7 in liquid biopsies of castrate resistant prostate cancer patients: a comparison of AR-V7 analysis in circulating tumor cells, circulating tumor RNA and exosomes. *Cell* 8:688. <https://doi.org/10.3390/cells8070688>
22. Mahler L, Du G, Dajkovic A et al (2020) Rethinking culture-based microbiology – deep insights into any microbiota. *Biomillenia, Romainville*
23. Josephides D, Davoli S, Whitley W et al (2020) Cyto-mine: an integrated, picodroplet system for high-throughput single-cell analysis, sorting, dispensing, and monoclonality assurance. *SLAS Technol* 25:177–189. <https://doi.org/10.1177/2472630319892571>
24. Hengoju S, Tovar M, Man DKW et al (2020) Droplet microfluidics for microbial biotechnology. *Adv Biochem Eng Biotechnol*. https://doi.org/10.1007/10_2020_140
25. Mirasol F (2020) Shaping IR spectroscopy into a powerful tool for biopharma characterizations. *BioPharm Int* 33:42–47
26. Vaclavek T, Prikryl J, Foret F (2019) Resistive pulse sensing as particle counting and sizing method in microfluidic systems: designs and applications review. *J Sep Sci* 42:445–457. <https://doi.org/10.1002/jssc.201800978>
27. Globus T, Ferrance J, Moskaluk C et al (2018) Sub-terahertz spectroscopic signatures from micro-rna molecules in fluid samples for ovarian cancer analysis. *Case Rep Liter Rev* 2(2):1–3
28. Tsai A (2019) Ultra-sensitive chemical and nanoparticle sensing with optical microcavities. *Periodic* 7:16. <http://www.chem.ox.ac.uk/periodic2019/>
29. Zhang B, Radisic M (2017) Organ-on-a-chip devices advance to market. *Lab Chip* 17:2395–2420. <https://doi.org/10.1039/c6lc01554a>
30. Bahnemann J, Enders A, Winkler S (2021) Microfluidic systems and organ (human) on a chip. In: *Basic concepts on 3D cell culture*. Springer, Heidelberg. ISBN: 978-3-030-611 66749-8. <https://doi.org/10.1007/978-3-030-66749-8>
31. Chiu DT, deMello AJ, Di Carlo D et al (2017) Small but perfectly formed? Successes, challenges, and opportunities for microfluidics in the chemical and biological sciences. *Chem* 2:201–223. <https://doi.org/10.1016/j.chempr.2017.01.009>
32. Dekker S, Isgor PK, Feijten T et al (2018) From chip-in-a-lab to lab-on-a-chip: a portable Coulter counter using a modular platform. *Microsyst Nanoeng* 4:34. <https://doi.org/10.1038/s41378-018-0034-1>
33. Andersson H, van den Berg A (2006) Where are the biologists? *Lab Chip* 6:467–470. <https://doi.org/10.1039/b602048h>
34. Kandelousi MS (2018) *Microfluidics and nanofluidics*. InTech, London
35. Nguyen H-T, Thach H, Roy E et al (2018) Low-cost, accessible fabrication methods for microfluidics research in low-resource settings. *Micromachines* 9:461. <https://doi.org/10.3390/mi9090461>
36. Kotz F, Helmer D, Rapp BE (2020) Emerging technologies and materials for high-resolution 3D printing of microfluidic chips. *Adv Biochem Eng Biotechnol*. https://doi.org/10.1007/10_2020_141

37. Rupal BS, Garcia EA, Ayranci C et al (2019) 3D printed 3D-microfluidics: recent developments and design challenges. *JID* 22:5–20. <https://doi.org/10.3233/jid-2018-0001>
38. Preuss J-A, Nguyen GN, Berk V et al (2020) Miniaturized free-flow electrophoresis – production, optimization and application using 3D printing technology. *Electrophoresis*. <https://doi.org/10.1002/elps.202000149>
39. Enders A, Siller IG, Urmann K et al (2019) 3D printed microfluidic mixers—a comparative study on mixing unit performances. *Small* 15:e1804326. <https://doi.org/10.1002/smll.201804326>
40. Siller IG, Preuss J-A, Urmann K et al (2020) 3D-printed flow cells for aptamer-based impedimetric detection of *E. coli* crooks strain. *Sensors* 20:4421. <https://doi.org/10.3390/s20164421>
41. Lavrentieva A, Fleischhammer T, Enders A et al (2020) Fabrication of stiffness gradients of GelMA hydrogels using a 3D printed micromixer. *Macromol Biosci* 20:e2000107. <https://doi.org/10.1002/mabi.202000107>
42. Siller IG, Enders A, Gellermann P et al (2020) Characterization of a customized 3D-printed cell culture system using clear, translucent acrylate that enables optical online monitoring. *Biomed Mater* 15:55007. <https://doi.org/10.1088/1748-605X/ab8e97>
43. Siller IG, Epping N-M, Lavrentieva A et al (2020) Customizable 3D-printed (co-)cultivation systems for in vitro study of angiogenesis. *Materials* 13:4290. <https://doi.org/10.3390/ma13194290>
44. Siller IG, Enders A, Steinwedel T et al (2019) Real-time live-cell imaging technology enables high-throughput screening to verify in vitro biocompatibility of 3D printed materials. *Materials* 12:2125. <https://doi.org/10.3390/ma12132125>
45. Li F, Macdonald NP, Guijt RM et al (2018) Increasing the functionalities of 3D printed microchemical devices by single material, multimaterial, and print-pause-print 3D printing. *Lab Chip* 19:35–49. <https://doi.org/10.1039/c8lc00826d>
46. MacDonald E, Wicker R (2016) Multiprocess 3D printing for increasing component functionality. *Science* 353:aaf2093. <https://doi.org/10.1126/science.aaf2093>
47. Begolo S, Zhukov DV, Selck DA et al (2014) The pumping lid: investigating multi-material 3D printing for equipment-free, programmable generation of positive and negative pressures for microfluidic applications. *Lab Chip* 14:4616–4628. <https://doi.org/10.1039/c4lc00910j>
48. Li F, Smejkal P, Macdonald NP et al (2017) One-step fabrication of a microfluidic device with an integrated membrane and embedded reagents by multimaterial 3D printing. *Anal Chem* 89:4701–4707. <https://doi.org/10.1021/acs.analchem.7b00409>
49. O’Neil GD, Ahmed S, Halloran K et al (2019) Single-step fabrication of electrochemical flow cells utilizing multi-material 3D printing. *Electrochem Commun* 99:56–60. <https://doi.org/10.1016/j.elecom.2018.12.006>
50. Duarte LC, Chagas CLS, Ribeiro LEB et al (2017) 3D printing of microfluidic devices with embedded sensing electrodes for generating and measuring the size of microdroplets based on contactless conductivity detection. *Sensors Actuators B Chem* 251:427–432. <https://doi.org/10.1016/j.snb.2017.05.011>
51. Fornells E, Murray E, Waheed S et al (2020) Integrated 3D printed heaters for microfluidic applications: ammonium analysis within environmental water. *Anal Chim Acta* 1098:94–101. <https://doi.org/10.1016/j.aca.2019.11.025>
52. Scotti G, Nilsson SME, Haapala M et al (2017) A miniaturised 3D printed polypropylene reactor for online reaction analysis by mass spectrometry. *React Chem Eng* 2:299–303. <https://doi.org/10.1039/C7RE00015D>
53. Yuan R, Lee J, Su H-W et al (2018) Microfluidics in structured multimaterial fibers. *Proc Natl Acad Sci U S A* 115:E10830–E10838. <https://doi.org/10.1073/pnas.1809459115>
54. Sanchez D, Nordin G, Munro T (2020) Microfluidic temperature behavior in a multi-material 3D printed chip. American Society of Mechanical Engineers Digital Collection, New York

55. Kitson PJ, Rosnes MH, Sans V et al (2012) Configurable 3D-printed millifluidic and microfluidic ‘lab on a chip’ reactionware devices. *Lab Chip* 12:3267–3271. <https://doi.org/10.1039/c2lc40761b>
56. Kaminski TS, Scheler O, Garstecki P (2016) Droplet microfluidics for microbiology: techniques, applications and challenges. *Lab Chip* 16:2168–2187. <https://doi.org/10.1039/c6lc00367b>
57. Narayanamurthy V, Jeroish ZE, Bhuvaneshwari KS et al (2020) Advances in passively driven microfluidics and lab-on-chip devices: a comprehensive literature review and patent analysis. *RSC Adv* 10:11652–11680. <https://doi.org/10.1039/D0RA00263A>
58. Carrell C, Kava A, Nguyen M et al (2019) Beyond the lateral flow assay: a review of paper-based microfluidics. *Microelectron Eng* 206:45–54. <https://doi.org/10.1016/j.mee.2018.12.002>
59. Case DJ, Liu Y, Kiss IZ et al (2019) Braess’s paradox and programmable behaviour in microfluidic networks. *Nature* 574:647–652. <https://doi.org/10.1038/s41586-019-1701-6>
60. Zaidon N, Nordin AN, Ismail AF (2015) Modelling of microfluidics network using electric circuits. In: 2015 IEEE regional symposium on micro and nanoelectronics (RSM). IEEE, pp 1–4
61. Duncan PN, Nguyen TV, Hui EE (2013) Pneumatic oscillator circuits for timing and control of integrated microfluidics. *Proc Natl Acad Sci U S A* 110:18104–18109. <https://doi.org/10.1073/pnas.1310254110>
62. Lee Y-S, Bhattacharjee N, Folch A (2018) 3D-printed quake-style microvalves and micropumps. *Lab Chip* 18:1207–1214. <https://doi.org/10.1039/C8LC00001H>
63. Ortseifen V, Viefhues M, Wobbe L et al (2020) Microfluidics for biotechnology: bridging gaps to foster microfluidic applications. *Front Bioeng Biotechnol* 8:1324. <https://doi.org/10.3389/fbioe.2020.589074>
64. Mohammed MI, Haswell S, Gibson I (2015) Lab-on-a-chip or chip-in-a-lab: challenges of commercialization lost in translation. *Proc Technol* 20:54–59. <https://doi.org/10.1016/j.protcy.2015.07.010>
65. Arnold FH (2018) Directed evolution: bringing new chemistry to life. *Angew Chem Int Ed Engl* 57:4143–4148. <https://doi.org/10.1002/anie.201708408>
66. Ma F, Chung MT, Yao Y et al (2018) Efficient molecular evolution to generate enantioselective enzymes using a dual-channel microfluidic droplet screening platform. *Nat Commun* 9:1030. <https://doi.org/10.1038/s41467-018-03492-6>
67. Waddington SN, Privolizzi R, Karda R et al (2016) A broad overview and review of CRISPR-Cas technology and stem cells. *Curr Stem Cell Rep* 2:9–20. <https://doi.org/10.1007/s40778-016-0037-5>
68. McNutt M (2015) Breakthrough to genome editing. *Science* 350:1445. <https://doi.org/10.1126/science.aae0479>
69. Ahmadi F, Quach ABV, Shih SCC (2020) Is microfluidics the “assembly line” for CRISPR-Cas9 gene-editing? *Biomicrofluidics* 14:61301. <https://doi.org/10.1063/5.0029846>
70. Hajian R, Balderston S, Tran T et al (2019) Detection of unamplified target genes via CRISPR-Cas9 immobilized on a graphene field-effect transistor. *Nat Biomed Eng* 3:427–437. <https://doi.org/10.1038/s41551-019-0371-x>
71. Sinha H, Quach ABV, Vo PQN et al (2018) An automated microfluidic gene-editing platform for deciphering cancer genes. *Lab Chip* 18:2300–2312. <https://doi.org/10.1039/c8lc00470f>
72. Mondal S, Ben-Yakar A (2020) *Caenorhabditis elegans*-on-a-chip: microfluidic platforms for high-resolution imaging and phenotyping. In: *Organ-on-a-chip*. Elsevier, Amsterdam, pp 363–390
73. Kolluri N, Klapperich CM, Cabodi M (2017) Towards lab-on-a-chip diagnostics for malaria elimination. *Lab Chip* 18:75–94. <https://doi.org/10.1039/c7lc00758b>
74. Yang F, Gao C, Wang P et al (2016) Fish-on-a-chip: microfluidics for zebrafish research. *Lab Chip* 16:1106–1125. <https://doi.org/10.1039/c6lc00044d>

75. Jiang H, Xu Z, Aluru MR et al (2014) Plant chip for high-throughput phenotyping of *Arabidopsis*. *Lab Chip* 14:1281–1293. <https://doi.org/10.1039/c3lc51326b>
76. Grossmann G, Guo W-J, Ehrhardt DW et al (2011) The RootChip: an integrated microfluidic chip for plant science. *Plant Cell* 23:4234–4240. <https://doi.org/10.1105/tpc.111.092577>
77. Shapiro OH, Kramarsky-Winter E, Gavish AR et al (2016) A coral-on-a-chip microfluidic platform enabling live-imaging microscopy of reef-building corals. *Nat Commun* 7:10860. <https://doi.org/10.1038/ncomms10860>
78. Stanley CE, Grossmann G, i Solvas XC et al (2016) Soil-on-a-Chip: microfluidic platforms for environmental organismal studies. *Lab Chip* 16:228–241. <https://doi.org/10.1039/c5lc01285f>
79. Täuber S, Golze C, Ho P et al (2020) dMSCC: a microfluidic platform for microbial single-cell cultivation of *Corynebacterium glutamicum* under dynamic environmental medium conditions. *Lab Chip* 20:4442–4455. <https://doi.org/10.1039/d0lc00711k>
80. Wang H, Chen L, Sun L (2017) Digital microfluidics: a promising technique for biochemical applications. *Front Mech Eng* 12:510–525. <https://doi.org/10.1007/s11465-017-0460-z>
81. Edel JB, Ivanov A, Kim M (eds) (2017) *Nanofluidics: nanoscience and nanotechnology*. In: *RSC nanoscience & nanotechnology*, vol 41, 2nd edn. Royal Society of Chemistry, Cambridge
82. Bocquet L (2020) Nanofluidics coming of age. *Nat Mater* 19:254–256. <https://doi.org/10.1038/s41563-020-0625-8>
83. Barboiu M (2016) Artificial water channels--incipient innovative developments. *Chem Commun* 52:5657–5665. <https://doi.org/10.1039/c6cc01724j>
84. Ghasemi A, Amiri H, Zare H et al (2017) Carbon nanotubes in microfluidic lab-on-a-chip technology: current trends and future perspectives. *Microfluid Nanofluidics* 21:151. <https://doi.org/10.1007/s10404-017-1989-1>
85. Serra PA (2011) New perspectives in biosensors technology and applications. InTech, London
86. Prante M, Segal E, Scheper T et al (2020) Aptasensors for point-of-care detection of small molecules. *Biosensors* 10:108. <https://doi.org/10.3390/bios10090108>
87. Bhalla N, Jolly P, Formisano N et al (2016) Introduction to biosensors. *Essays Biochem* 60:1–8. <https://doi.org/10.1042/EBC20150001>
88. Preuß J-A, Reich P, Bahner N et al (2020) Impedimetric aptamer-based biosensors: applications. *Adv Biochem Eng Biotechnol* 174:43–91. https://doi.org/10.1007/10_2020_125
89. Aćimović SS, Šipová H, Emilsson G et al (2017) Superior LSPR substrates based on electromagnetic decoupling for on-a-chip high-throughput label-free biosensing. *Light Sci Appl* 6:e17042. <https://doi.org/10.1038/lsa.2017.42>
90. Liu B, Chen X, Cai H et al (2016) Surface acoustic wave devices for sensor applications. *J Semicond* 37:21001. <https://doi.org/10.1088/1674-4926/37/2/021001>
91. Zhao Y, Tong R-J, Xia F et al (2019) Current status of optical fiber biosensor based on surface plasmon resonance. *Biosens Bioelectron* 142:111505. <https://doi.org/10.1016/j.bios.2019.111505>
92. Inan H, Poyraz M, Inci F et al (2017) Photonic crystals: emerging biosensors and their promise for point-of-care applications. *Chem Soc Rev* 46:366–388. <https://doi.org/10.1039/c6cs00206d>
93. Montagut Y, Garcia J, Jimenez Y et al (2011) QCM technology in biosensors. In: Serra PA (ed) *Biosensors – emerging materials and applications*. InTech, London
94. Paiè P, Bragheri F, Bassi A et al (2016) Selective plane illumination microscopy on a chip. *Lab Chip* 16:1556–1560. <https://doi.org/10.1039/c6lc00084c>
95. Pimstall CW, Coté GL (2015) Malaria diagnosis using a mobile phone polarized microscope. *Sci Rep* 5:13368. <https://doi.org/10.1038/srep13368>
96. Tang Q, Liang M, Lu Y et al (2016) Microfluidic devices for terahertz spectroscopy of live cells toward lab-on-a-chip applications. *Sensors* 16:476. <https://doi.org/10.3390/s16040476>
97. Costanzo MT, Boock JJ, Kemperman RHJ et al (2017) Portable FAIMS: applications and future perspectives. *Int J Mass Spectrom* 422:188–196. <https://doi.org/10.1016/j.ijms.2016.12.007>

98. Zhai Y, Feng Y, Wei Y et al (2015) Development of a miniature mass spectrometer with continuous atmospheric pressure interface. *Analyst* 140:3406–3414. <https://doi.org/10.1039/c5an00462d>
99. Zaleskiy SS, Danieli E, Blümich B et al (2014) Miniaturization of NMR systems: desktop spectrometers, microcoil spectroscopy, and “NMR on a chip” for chemistry, biochemistry, and industry. *Chem Rev* 114:5641–5694. <https://doi.org/10.1021/cr400063g>
100. Bomers M, Charlot B, Barho F et al (2020) Microfluidic surface-enhanced infrared spectroscopy with semiconductor plasmonics for the fingerprint region. *React Chem Eng* 5:124–135. <https://doi.org/10.1039/C9RE00350A>
101. Riordon J, Sovilj D, Sanner S et al (2019) Deep learning with microfluidics for biotechnology. *Trends Biotechnol* 37:310–324. <https://doi.org/10.1016/j.tibtech.2018.08.005>
102. Heo YJ, Lee D, Kang J et al (2017) Real-time image processing for microscopy-based label-free imaging flow cytometry in a microfluidic chip. *Sci Rep* 7:11651. <https://doi.org/10.1038/s41598-017-11534-0>
103. Han S, Kim T, Kim D et al (2018) Use of deep learning for characterization of microfluidic soft sensors. *IEEE Robot Autom Lett* 3:873–880. <https://doi.org/10.1109/LRA.2018.2792684>
104. Boža V, Brejová B, Vinař T (2017) DeepNano: deep recurrent neural networks for base calling in MinION nanopore reads. *PLoS One* 12:e0178751. <https://doi.org/10.1371/journal.pone.0178751>
105. Stoecklein D, Lore KG, Davies M et al (2017) Deep learning for flow sculpting: insights into efficient learning using scientific simulation data. *Sci Rep* 7:46368. <https://doi.org/10.1038/srep46368>
106. Zaimi A, Wabartha M, Herman V et al (2018) AxonDeepSeg: automatic axon and myelin segmentation from microscopy data using convolutional neural networks. *Sci Rep* 8:3816. <https://doi.org/10.1038/s41598-018-22181-4>
107. Vashist SK, Luong JHT (2019) An overview of point-of-care technologies enabling next-generation healthcare monitoring and management. In: Vashist SK, Luong JHT (eds) *Point-of-care technologies enabling next-generation healthcare monitoring and management*. Springer, Cham, pp 1–25
108. Vashist SK, Luong JHT (eds) (2019) *Point-of-care technologies enabling next-generation healthcare monitoring and management*. Springer, Cham
109. Stanke M, Hitzmann B (2013) Automatic control of bioprocesses. *Adv Biochem Eng Biotechnol* 132:35–63. https://doi.org/10.1007/10_2012_167
110. Vettoretti M, Facchinetti A (2019) Combining continuous glucose monitoring and insulin pumps to automatically tune the basal insulin infusion in diabetes therapy: a review. *Biomed Eng Online* 18:1–17. <https://doi.org/10.1186/s12938-019-0658-x>
111. Kim J, Campbell AS, Wang J (2018) Wearable non-invasive epidermal glucose sensors: a review. *Talanta* 177:163–170. <https://doi.org/10.1016/j.talanta.2017.08.077>
112. Godinho C, Domingos J, Cunha G et al (2016) A systematic review of the characteristics and validity of monitoring technologies to assess Parkinson’s disease. *J Neuroeng Rehabil* 13:24. <https://doi.org/10.1186/s12984-016-0136-7>
113. Kim HJ, Jeon BS, Jenner P (2017) Hallmarks of treatment aspects: Parkinson’s disease throughout centuries including l-dopa. *Int Rev Neurobiol* 132:295–343. <https://doi.org/10.1016/bs.im.2017.01.006>
114. Fletcher K, Chapman R, Keene S (2018) An overview of medical ECMO for neonates. *Semin Perinatol* 42:68–79. <https://doi.org/10.1053/j.semperi.2017.12.002>
115. Bartlett RH, Ogino MT, Brodie D et al (2020) Initial ELSO guidance document: ECMO for COVID-19 patients with severe cardiopulmonary failure. *ASAIO J* 66:472–474. <https://doi.org/10.1097/MAT.0000000000001173>

116. Dabaghi M, Saraei N, Fusch G et al (2018) An ultra-thin highly flexible microfluidic device for blood oxygenation. *Lab Chip* 18:3780–3789. <https://doi.org/10.1039/c8lc01083h>
117. Gimbel AA, Flores E, Koo A et al (2016) Development of a biomimetic microfluidic oxygen transfer device. *Lab Chip* 16:3227–3234. <https://doi.org/10.1039/c6lc00641h>
118. Lagae L (2018) Boosting cell therapy production. *Genet Eng Biotechnol News* 38:20. <https://doi.org/10.1089/gen.38.09.08>
119. Li D, Li X, Zhou W-L et al (2019) Genetically engineered T cells for cancer immunotherapy. *Signal Transduct Target Ther* 4:35. <https://doi.org/10.1038/s41392-019-0070-9>